DE LA MACROEVOLUTION A LA MICROEVOLUTION CHEZ LE PHYTOPLANCTON : LE CAS DES ISOCHRYSIDALES

El Mahdi Bendif

▶ **To cite this version:**

El Mahdi Bendif. DE LA MACROEVOLUTION A LA MICROEVOLUTION CHEZ LE PHYTOPLANCTON : LE CAS DES ISOCHRYSIDALES. Ecologie, Environnement. Paris 6, 2011. Français. NNT : . tel-01180722

HAL Id: tel-01180722

https://hal.sorbonne-universite.fr/tel-01180722v1

Submitted on 28 Jul 2015

HAL is a multi-disciplinary open access archive for the deposit and dissemination of scientific research documents, whether they are published or not. The documents may come from teaching and research institutions in France or abroad, or from public or private research centers.

L'archive ouverte pluridisciplinaire **HAL**, est destinée au dépôt et à la diffusion de documents scientifiques de niveau recherche, publiés ou non, émanant des établissements d'enseignement et de recherche français ou étrangers, des laboratoires publics ou privés.

THESE DE DOCTORAT DE L'UNIVERSITE PIERRE ET MARIE CURIE

Spécialité

Diversité du Vivant

Présentée par

M. Bendif El Mahdi

Pour obtenir le grade de

DOCTEUR de l'UNIVERSITÉ PIERRE ET MARIE CURIE

Sujet de la thèse :

DE LA MACROEVOLUTION A LA MICROEVOLUTION CHEZ LE PHYTOPLANCTON : LE CAS DES ISOCHRYSIDALES

soutenue le

devant le jury composé de :

Dr. Colomban de Vargas, UPMC/CNRS	Directeur de thèse
Dr. Probert Ian, UPMC/CNRS	Directeur de thèse (membre invité)
Pr. Bente Edvardsen, UIO	Rapporteur
Pr. Jeremy Young, UCL	Rapporteur
Dr. Nathalie Simon, UPMC/CNRS	Examinateur
Dr. Declan Schroeder, MBA	Examinateur
Pr. Bruno de Reviers, UPMC/MNHN	Examinateur

« La Nature, mélange singulier d'agencements merveilleux et de mécanismes inutilement compliqués, de beautés et de misères, tour à tour maternelle et cruelle, brise tous les cadres dans lesquels on essaie de l'enfermer »

Lucien Cuenot

Remerciements

Je tiens vivement à exprimer ma reconnaissance et ma gratitude aux personnes qui m'auront accompagné de près ou de loin dans cette riche aventure.

Je remercie avant tous les instigateurs de ce projet pour la confiance qu'ils m'ont accordé, et le soutien des « coccologues » en premier lieu Colomban de Vargas, pour m'avoir accueilli au sein de l'équipe EPPO, et de m'avoir permis de travailler en me donnant des moyens d'avancer dans mes recherches. Je ne cache pas nos difficultés à interagir, mais le temps à montrer de belles améliorations pour lesquelles je te suis reconnaissant,

et Ian Probert, la force tranquille, merci pour m'avoir particulièrement aidé dans l'élaboration d'un questionnement scientifique, et surtout pour ton soutien pendant ces cinq dernières années. Dans un autre contexte, j'aurais bien raconté les anecdotes de notre rencontre à Caen en avril 2006… ou de l'invitation à Roscoff en 2007 lors du meeting BOOM…

Ce fut avec plaisir que je répondis à votre appel en 2007, et c'est avec ce même plaisir (avec tous les hauts et les bas☺) que finalement, nous avons réussit à produire ces travaux... Merci à vous deux pour la passion des « algues de pierres ».

Merci à Declan Schroeder, mon co-encadrant d'outre manche, présent sans l'être par nos échanges électroniques riches en questions et en aide, d'autant plus lors de ces derniers mois où nos questionnements s'intensifiaient. Au plaisir de continuer cette collaboration.

Merci à Jeremy Young, pour m'avoir accueilli dans son laboratoire à Londres le temps d'une semaine de réflexion sur les Noëlaerhabdaceae, et d'une soirée au pub... mais surtout merci d'avoir répondu patiemment à toutes mes questions ennuyeuses ou pas sur les coccolithophores. Je remercie aussi Martine Couapel qui m'aura hébergé lors de ce séjour.

De l'autre coté du globe, je remercie vivement Kyoko Hagino qui du Japon m'a aussi soutenu. Je la remercie d'autant plus pour m'avoir permit de partager les prémices de cette étude et de m'avoir orienté sur la direction de mes recherches.

Je remercie Bente Edvardsen non seulement d'avoir accepté de participer à mon jury de thèse mais aussi de m'avoir particulièrement remonté le moral par ses conseils avisés peu avant la fin.

Merci à Luc Beaufort pour m'avoir intégrer à son projet et pour les échanges que nous avons partagé avec tous les collaborateurs précités et aussi pour son soutien.

Toute ma sympathie à l'énergie des EPPOistes, à qui je dois une part de ma réflexion et de mon énergie. Merci à mes amis portugais, Miguel et Antonio. Vous m'avez beaucoup appris, vous m'apprenez encore, merci pour toute votre aide et votre bienveillance. Merci Peter, le roi de la salsa, pour les idées que nous partageons et celles que nous allons faire aboutir prochainement. Yoshi et Yurika, je vous remercie tout aussi profondément, pour nos moments passés à Roscoff et au Japon, merci pour ce bel échange culturel. Margaux, je te remercierai toujours pour cette énergie toujours positive et curieuse, et la vague de motivation que tu apportes à chacune de nos rencontres, merci beaucoup pour ton aide. Un grand merci à Sarah sans qui je n'aurai pas su commencer quoique ce soit lors de ma thèse et bravo encore pour ce que tu continues de donner à l'équipe. Merci aux « symbiologues » Fabrice et Johan, je reconnais en vous une grande motivation par votre sourire à toute épreuve, au travers des échanges que nous avons pu avoir, d'autant plus depuis ma migration dans le bureau de Johan, merci pour toute cette émulation. Si je dis « Give me Five »... je remercie la « perfect team » : Angélique, ma voisine normande, merci pour toute ton aide et tout ton soutien, Lucie, Raphael et Noan, pour la cool attitude en station et surtout hors station... Merci pour ces superbes soirées... l'activité du labo n'étant pas la seule que nous avons partagée...

Merci à Frédéric, Stéphane, Nathalie, Christophe, Sebastien et Marie Jo, et au dynamisme de tout le groupe Plankton : Fabienne, Roseline, Priscilla, Florence, Domi, Daniel, Estelle, Laure, Nathalie, Christophe 6, Anne Claire, Aliou, Frédérique L, Domi B, Florian, Marine, Alexia, Daniella, Catharina, Laurence, Frederique P, Christian, en espérant n'oublier personnes... ... Fabien, Elodie, Aurelie, Sylvie pour ceux qui étaient là...

Merci à tous les STATIONAUTES.

Mes vives amitiés à mes disciples boxeurs Eric (et à toute la familia) et Sergio,

Et à Matt, Sophie, Natty, JB, Pouline, Zophia,Vivi, Alex, Vlad, Amel, Dada, Tania, Nathalie, Greg, Julie, Fred, Kevin, Rémi, Renan, les Janiseries et les Poucheries.

Merci au collectif normand, Jean Bob, MSB, les Moutons, Biboule, Biboulette, Bidass, Petitpapanoëlus, Arnouille, le Duk, la Duchesse, la prêtresse de Vaas, Foret d'Automne, Salsa du démon, Goyo, Quentine, la Chine, les Decks, Anaïs, Chinois, Krugman, les Baudeaux, Tomasi

Et tous ceux que je n'ai pas eu le temps de citer, merci beaucoup...

Merci Joana, pour toute ta patience, ton aide, ta compréhension, ton soutien ... de nos coins perdus respectifs...

Je dédie ces travaux à mes parents, et mes frères, Saïd, Ryad et Nadir, pour tout ce qu'ils m'ont apporté et tout leur soutien.

Table des matières

INTRODUCTION

Importance biogéochimique et rôle écologique des coccolithophores

Les coccolithophores, membres du phytoplancton marin, ont eu un impact considérable dans les grands cycles biogéochimiques et la régulation du climat global au cours des derniers ~200 millions d'années (Fig. 1). De part leur capacité photosynthétique, ils participent à l'incorporation du dioxide de carbone (CO_2) dans la matière organique du plancton océanique, tout en produisant de l'oxygène (O_2 ; Fig. 1A)

$$CO_2 + H_2O \longrightarrow CH_2O \text{ (matière organique)} + O_2$$

La photosynthèse océanique contribue au maintien du CO_2 atmosphérique à des concentrations relativement faible. En effet ~25% du carbone fixé par le phytoplancton est exporté vers les profondeurs océaniques pour un total de 11 à 16 Gt par an (Falkowski et al. 2000). Cette séquestration du carbone, un processus complexe a l'interface des systèmes biologiques et physico-chimiques, porte le nom de « pompe a carbone organique » (Volk and Hoffert, 1985).

Etant a la fois photosynthétiques et calcifiant, les coccolithophores jouent un rôle d'autant plus complexe dans cette régulation des flux de carbones aux interfaces atmosphère/océan/lithosphère. Leur capacité à produire les coccolithes (écailles de carbonate de calcium), organises en coccosphere, est une fonction primordiale du plancton marin. En effet la sédimentation et dissolution dans la colonne d'eau de ces carbonates biogéniques serait à l'origine du maintien d'un gradient vertical de l'alcalinité marine.

$$Ca^{2+} + 2HCO_3^- \longrightarrow CaCO_3 + CO_2 + H_2O$$

Les coccolithes sédimentées sont parmi les contributeurs majeurs de l'accumulation du calcaire sur les fonds marins, la plus importante séquestration de carbone inorganique sur terre au cours des temps géologiques. Environ 35% des fonds marins mondiaux sont ainsi recouverts de carbonates, , les coccolithes contribuant à ~25% du du transport vertical total de carbone vers les fonds océaniques. Ce processus de pompe biologique agissant sur les carbonates et à l'origine d'une production de CO_2 porte le nom de « contre-pompe des (Fig. 1B) et quatre fois moins de carbone transiterait à travers cette pompe que par la pompe organique.

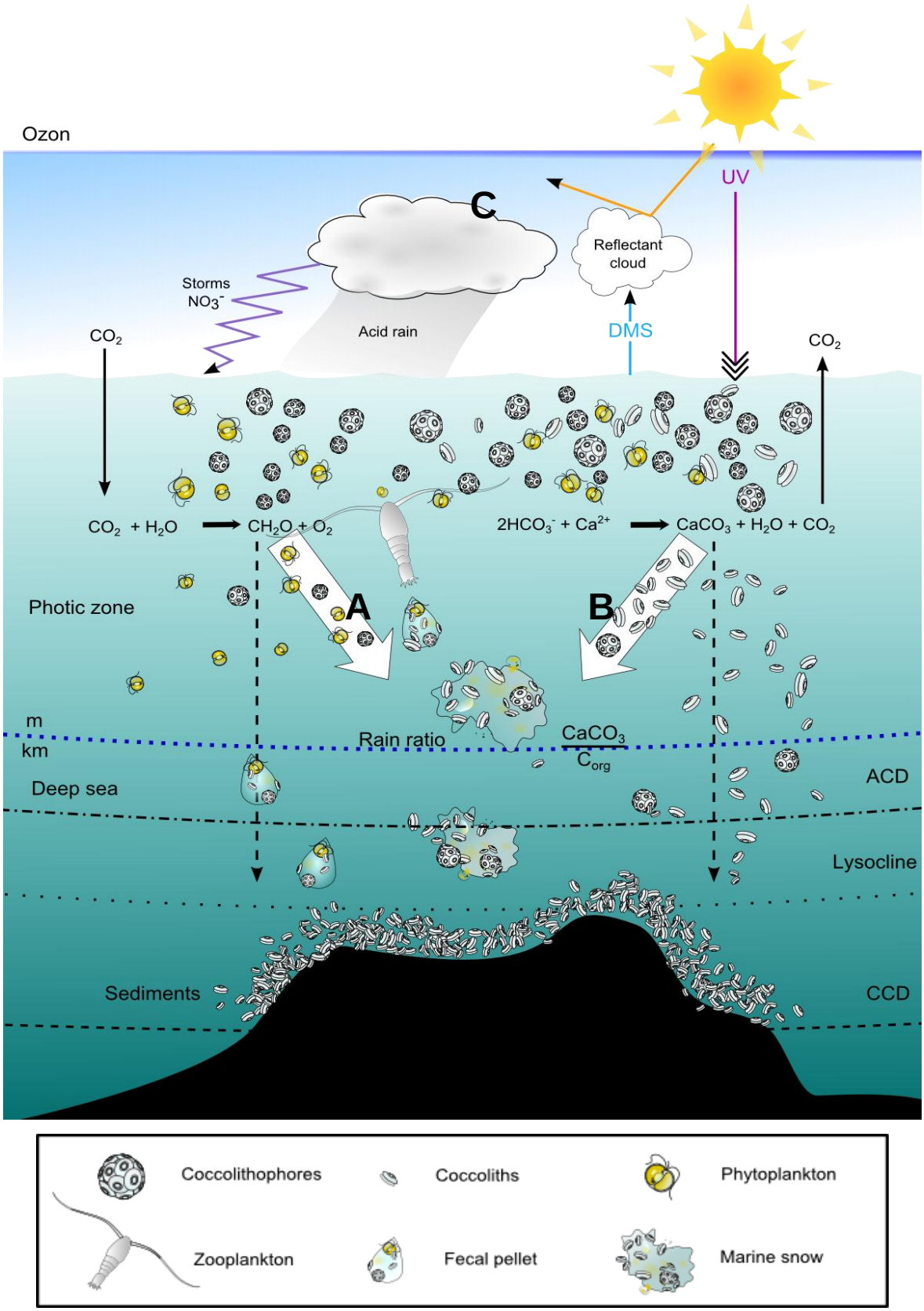

Figure 1. Participation du phytoplancton et des coccolithophores dans le cycle du carbone (pompes biologiques organique –A- et inorganique –B-) et dans le cycle du soufre et la régulation du climat (C). A. Production photosynthétique de matière organique dans les eaux de surfaces à l'origine du transport du carbone vers le fond de l'océan ; B. Production et sédimentation du $CaCO_3$ et libération du CO_2 vers la surface de l'océan,; C. Action des efflorescences de phytoplancton sur le cycle du soufre par la production de DMS (dimethylsulfure), un gaz qui serait important pour la nucléation des nuages. Modifié a partir de de Vargas et al. 2007.

Les coccolithophores ont commencé à impacter de manière significative le cycle du carbone lors de leur prolifération dans les océans dès la fin du Jurassique (environ 150 Ma) comme en témoignent les bassins sédimentaires et les falaises de craie (Fig. 2 ; Morse et Mackenzie 1990). Leur expansion, leur diversification, et l'occupation de nouvelles niches lors de cette période ont provoqué des changements significatifs au niveau de la distribution du carbone dans les océans (voir évolution des Haptophytes). Ainsi, ces processus qui auraient été limités aux régions côtières jusqu'alors, furent déplacés et généralisés à l'océan global pour la première fois dans l'histoire de la terre (Hay, 2004), provoquant une révolution de la régulation chimique du carbone océanique (Ridgwell and Zeebe, 2005).

Figure 2. Falaise de calcaire datant du crétacé supérieur (Etretat, Normandie, France). Les stratifications sont le résultat de couches de $CaCO_3$ biogénique successivement accumulées pendant des millions d'années.

Par ailleurs, les efflorescences des espèces phytoplanctoniques *Emiliania huxleyi* (coccolithophore) et *Phaeocystis pouchetii* peuvent avoir un impact important sur le climat global. Ces deux espèces d'haptophytes sont connues pour la production de larges efflorescences océaniques émettant de quantités considérables de diméthylsufures ($(CH_3)_2S$; DMS), un métabolite volatile augmentant les pluies acides ainsi que la formation de nuages à haut pouvoir réflecteur (Fig. 1C). D'une part, les UV et la lumière se retrouvent filtrés, protégeant les algues et favorisant leur développement tout en limitant la croissance de l'efflorescence. D'autre part, l'augmentation de l'albédo entraine un réchauffement au dessus de la couche de nuage provoquant des tempêtes et de fortes pluies. Ces pluies apportent des

nutriments dus à la formation de nitrates par les éclairs, réactivant la prolifération des algues. Ces phénomènes auraient donc un double rôle de régulation du climat et des proliférations micro-algales.

Le CO_2 est le gaz à effet de serre le plus important dans l'atmosphère après la vapeur d'eau et contribue de manière significative aux phénomènes de réchauffement de la planète. Aussi, les variations globales des températures entre les âges glaciaires et interglaciaires ont été en partie attribuées à la variabilité des niveaux de CO_2 atmosphériques (Fig. 3).

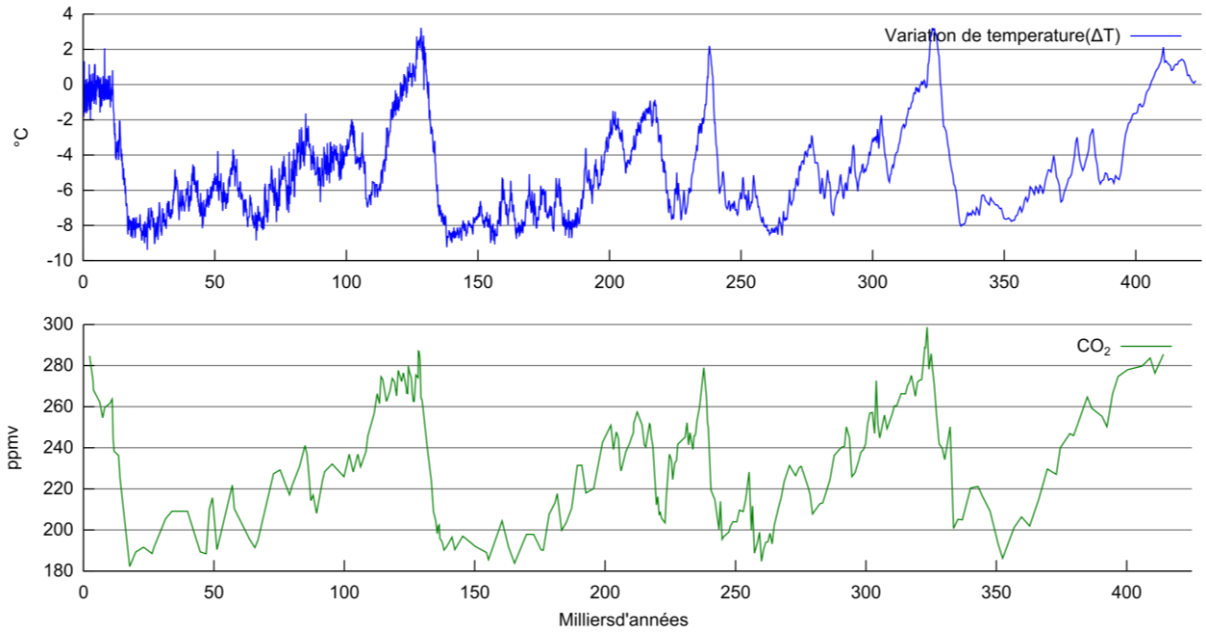

Figure 3. Analyse des sédiments des glaces de la station Vostok (Antarctique). Les graphes représentent les variations des températures et de la teneur en CO_2 atmosphérique lors des 400 000 ans, les baisses de températures coïncident avec les glaciations de l'hémisphère nord. (Source : http://www.usgcrp.gov/usgcrp/images/Vostok.jpg)

Actuellement, nous observons une augmentation exceptionnellement rapide du CO_2 atmosphérique causée par l'utilisation humaine des combustibles fossiles terrestre (charbon) et océanique (pétrole). Ce CO_2 anthropogénique est en parti dissout dans les océans, un phénomène appelé 'acidification des océans' qui aurait commence a modifier la chimie des carbonates dès la révolution industrielle au 19ème siècle. Pour la fin du XXIème siècle, certains scenario prédisent un triplement de [CO_2] des eaux de surfaces par rapport aux valeurs préindustrielles provoquant un baisse du pH des eaux marines d~0.4 unités (Fig. 4). Ces changements vont certainement affecter les communautés planctoniques et leur contribution au cycle du carbone (Fig. 5; Rost et Riebsell 2004).

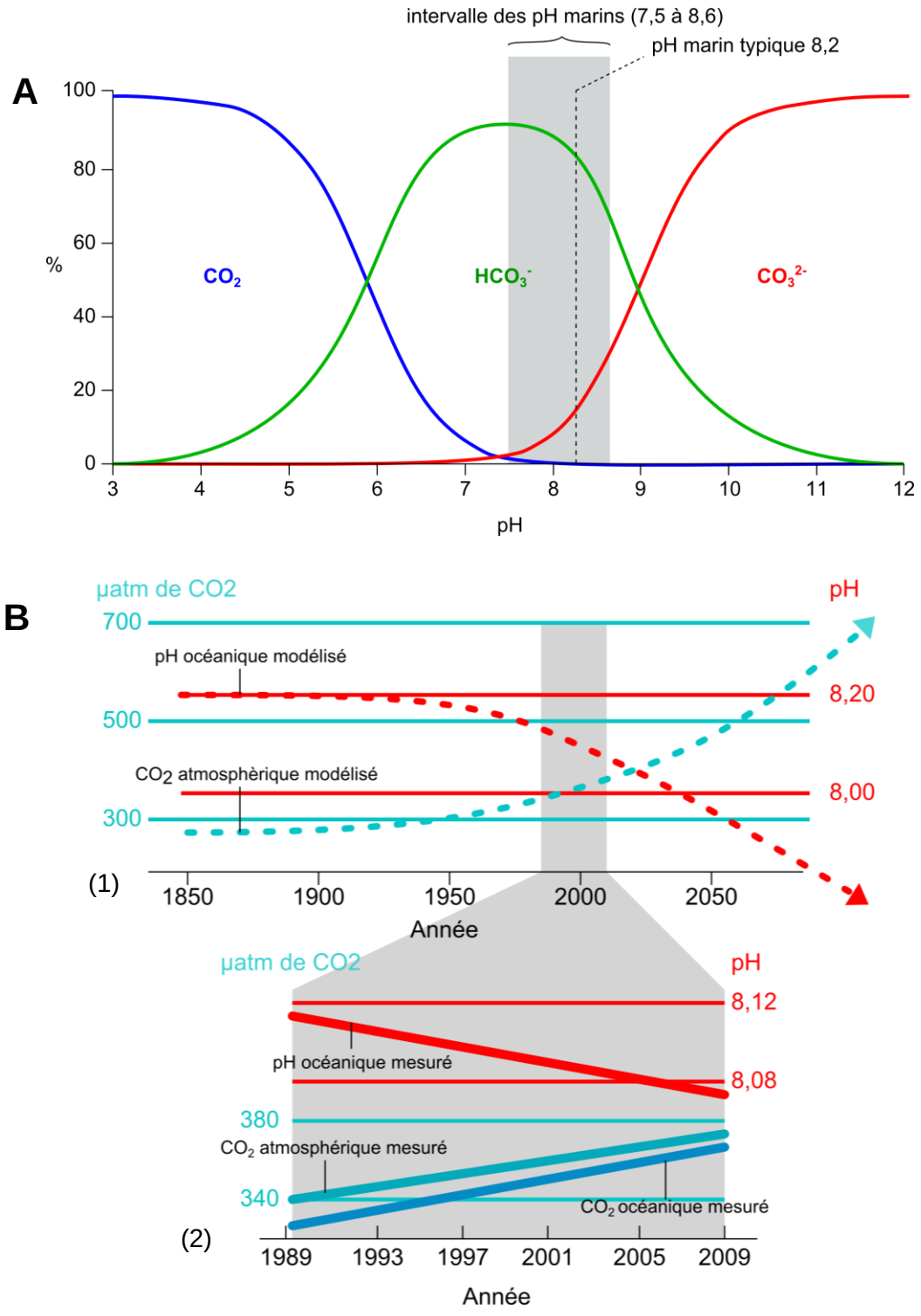

Figure 4. Relation entre le CO_2 et le pH dans l'océan : A. Proportions relatives des espèces inorganiques de carbones (CO_2, HCO_3^- et CO_3^{2-}) dans l'eau de mer en fonction du pH (15°C à la salinité de 35) ; B. Prédictions du pH océanique selon les modèles climatiques (1), et mesures enregistrées entre 1989 et 2009 à la station ALOHA (océan Pacifique) (2). Les corrélations indiquent que si l'élévation du CO2 continue, le pH diminuerait significativement (d'après Houghton et al. 1995 et Hardt et Safina 2010).

La question cruciale de l'adaptation du phytoplancton face à ces changements se pose d'autant plus chez les coccolithophores qui fabriquent un exosquelette calcaire particulièrement sensible à la corrosion de l'acidification. La compréhension de ces potentiels traits d'adaptation chez les coccolithophores actuels est fondamentale. Du mode de spéciation (macroévolution) à la structuration des populations actuelles et de leurs traits de vie (microévolution), la surveillance des espèces les plus cosmopolites de coccolithophores relèvent de questions encore mal connues sur leur plasticité écologique et leur diversité génétique. Ces points essentiels peuvent être étendus aux autres espèces phytoplanctoniques ainsi qu'à l'ensemble des protistes pélagiques.

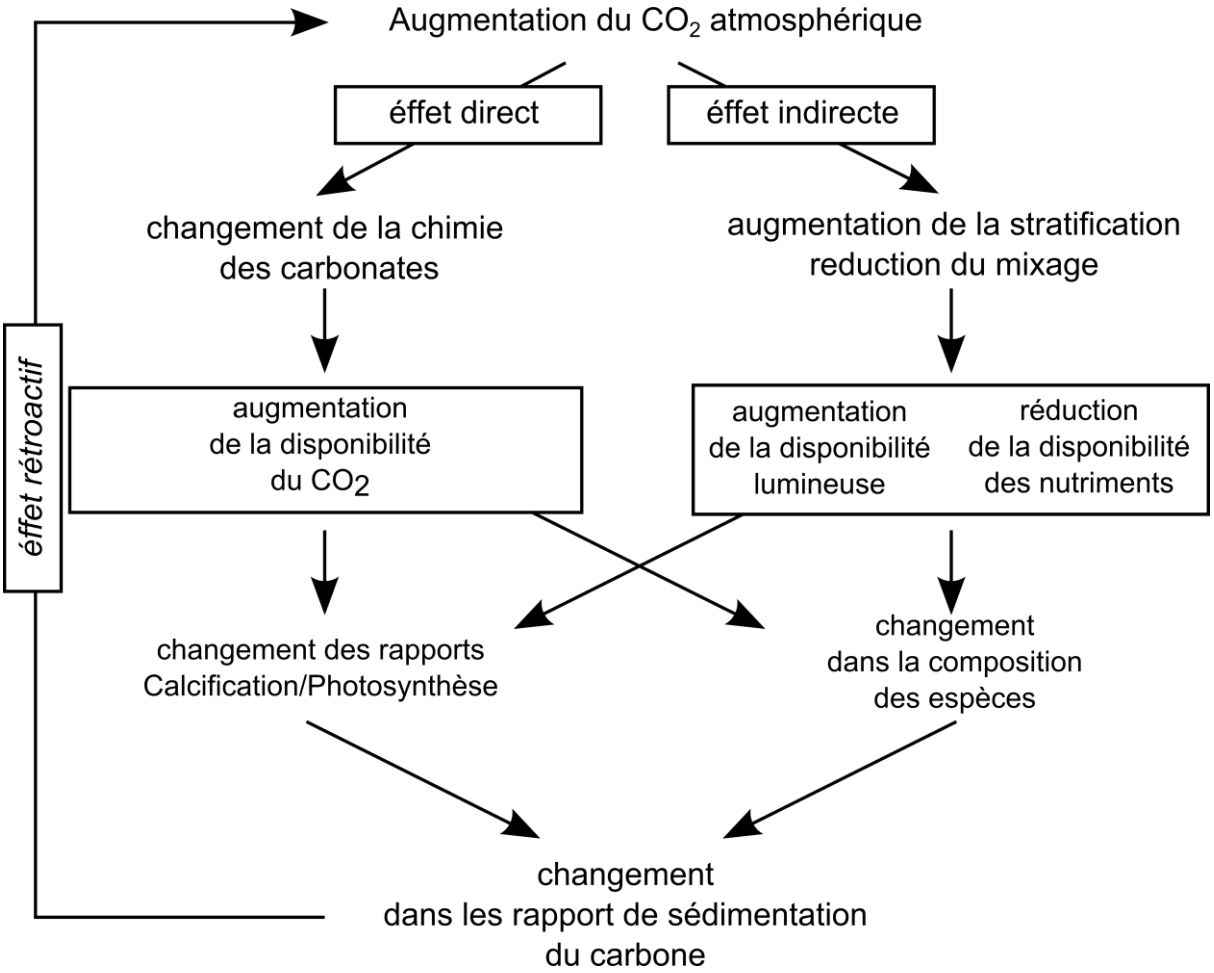

Figure 5. Effets de l'élévation du CO_2 atmosphérique sur l'océan et son impact sur le phytoplancton. Cette élévation du CO_2 cause directement des changements de la chimie des carbonates. Les effets indirects sont liés à l'augmentation de la stratification au cours du temps. Ces effets directs et indirects affecteraient la physiologie des coccolithophores et la structure des communautés phytoplanctoniques avec de possibles conséquences sur la balance des pompes biologiques.

De la pierre à l'algue, considérations historiques sur les coccolithophores

Les premières observations de coccolithes remontent au 19ème siècle, lorsque Christian Gottfried Ehrenberg -aujourd'hui considéré comme le « Fondateur de la Micropaléontologie »- décrit en 1836 de microscopiques objets elliptiques au niveau des craies de l'île de Rugen dans la mer Baltique. Après 14 années d'études sur divers échantillons, il les distingue d'autres organismes elliptiques potentiellement vivants leur attribuant une origine minérale et les appelle « *morpholithes calcaires* ». En 1858, peu après l'expédition de l'HMS Cyclops explorant les sédiments des fonds marins, Thomas Henry Huxley décrit sur des échantillons profonds « *une multitude de très curieux corps arrondis, en toute apparence constituées de plusieurs couches concentriques… et ressemblant … plus ou moins à la plante unicellulaire Protococcus… je vais, par souci de commodité, simplement les appelées coccolithes* », pierres arrondies (du grec κοκκος « rond » mais aussi « grain », λιθος « pierre »). Il fait le rapprochement entre ses observations et celles d'Ehrenberg et en attribue aussi une origine inorganique.

Puis en 1861, Georges Charles Wallich rapporte avoir observé non seulement des coccolithes à l'état libre mais aussi des associations de coccolithes formant de petites sphères, qu'il nomme « *coccosphères* » et propose l'hypothèse que les coccosphères seraient des larves de foraminifères (Fig. 6). Au courant de la même année, Henry Clifton Sorby, après avoir décrit plus en détail les coccolithes, leur confère aussi une origine biogénique. Il confirme leur composition calcaire, tout comme les thèques des foraminifères, mais en propose une origine indépendante, se basant sur les propriétés optiques de la calcite les constituant.

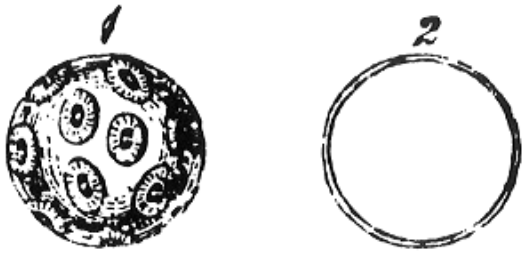

Figure 6. Première illustration d'une coccosphère (Wallich 1861)

A partir de ces nouvelles considérations, Huxley réexamine en 1868 les échantillons de *l'HMS Cyclops* préservés dans l'alcool depuis 1857. Il y trouve de nombreuses masses gélatineuses transparentes associées à des coccolithes et des coccosphères et conclut que ces masses gélatineuses constituent un protoplasme duquel les coccolithes et les coccosphères en sont des éléments squelettiques. Se basant sur la classification phylogénétique d'Ernst Haeckel (1866), il définit cette masse protoplasmique de monère, la décrivant comme une nouvelle espèce nommée *Bathybius haeckelii* en l'honneur du célèbre biologiste allemand

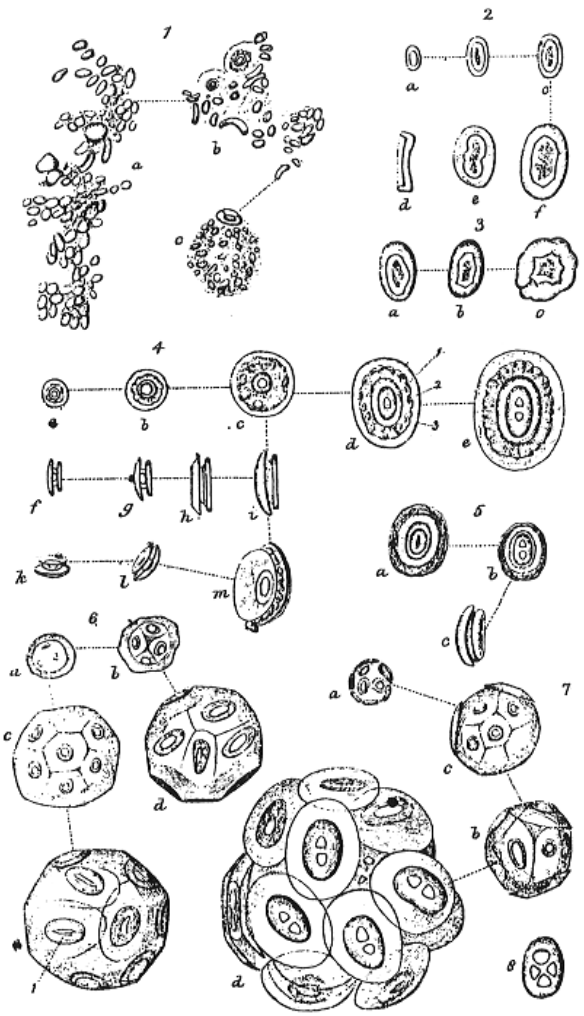

Figure 7. Coccolithes et coccosphères selon Huxley (1868). La figure 1 représente la masse gélatineuse de *Bathybius* dans laquelle sont logées les coccolithes. Nous pouvons remarquer aussi la fine représentation des coccolithes des figures 4e, 5b et 7d, rappelant celles du genre *Coccolithus*.

(Fig. 7). Ce dernier voit un intérêt naturel à l'étude de cette espèce qu'il considère très vite comme étant la forme de vie la plus primitive.

Connaitre la distribution de *Bathybius* devient alors l'un des objectifs de la campagne du *Challenger* (1872-1876), qui, après 2 ans et demi d'intenses recherches, n'en décèle la présence nulle part. Néanmoins, les scientifiques de l'expédition remarquent que les échantillons préservés dans l'alcool présentaient des précipités sous forme de gelée, rappelant *Bathybius* ; gelée absente des échantillons non préservés dans l'alcool. En 1875, des analyses révèlent que ces précipités sont constitués de sulfates de calcium associés à de petites quantités de matière organique. Huxley reconnait alors avoir fait une erreur et invalide sa théorie, contrairement à Haeckel qui la soutiendra jusqu'en 1883.

Après l'observation de formes pélagiques, Wallich soutient alors en 1877 l'hypothèse que les coccospheres sont des formes vivantes libres et décrit deux espèces *Coccosphaera pelagica* et *Coccosphaera carterii*. Bien plus tard, John Murray et ses collaborateurs du Challenger établissent fermement que les coccosphères forment l'exosquelette de petites algues calcaires (Tizard et al. 1885 ; Murray et Blackmann 1898). Dès lors de nombreuses observations de coccosphères mais aussi de rhabdosphères (ραβδος « bâton » ; coccosphères composées de rhabdolithes) sont reportées. Les observations se succèdent précisant au fur et à mesure la nature biologique de ces « curieux organismes » en tant qu'algue unicellulaire.

Au début du 20ème siècle, Lohmann observe des flagelles pour la première fois chez certaines formes (1902) et classe les coccosphères dans les Chrysomonades en se basant sur la couleur des plastes. Il décrit pour la première fois le polymorphisme des coccosphères en détail établissant la première étude extensive sur sa diversité définissant le taxon des Coccolithophorideae (φερω « porter »; « les porteurs de coccolithes »), groupe qu'il associe à sa définition du « nannoplancton » pour les organismes planctoniques inférieurs à 45 µm (Fig. 8).

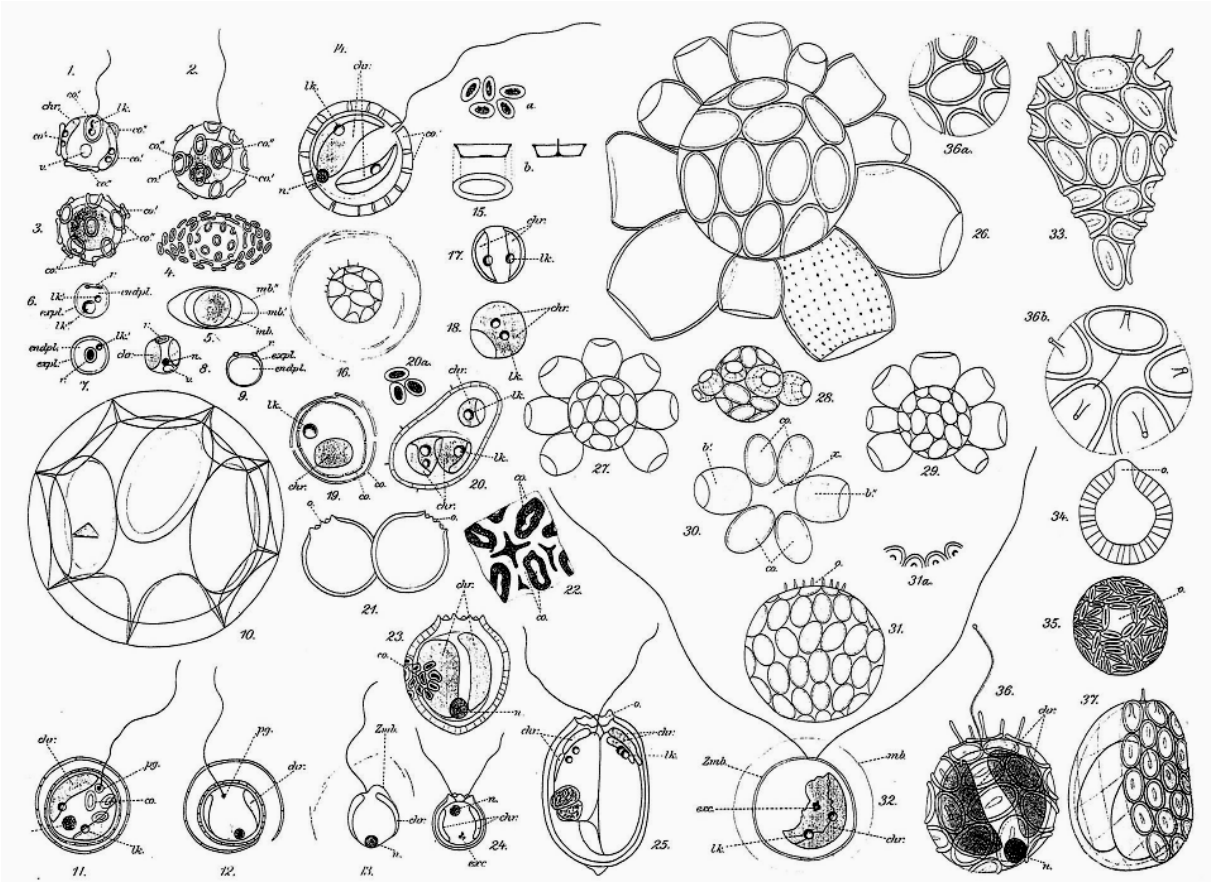

Figure 8. Planche 4 de Lohmann (1902) présentant différentes espèces de *Pontosphaera* (Fig. 1-20), *Syracosphaera* (Fig. 21-25 ; 31-37) et *Scyphosphaera* (Fig. 26-30). Nous pouvons remarquer l'attention particulièrement de Lohmann aux contenus cellulaires de cellules ainsi qu'aux flagelles des espèces vivantes.

Dès lors, de nombreuses espèces vivantes et fossiles de coccolithophores sont décrites, à travers des observations en microscopie optique et l'investigation des caractères physiologiques, jusqu'aux premiers essais de mise en culture de ces microalgues dans les années 50. Les coccolithophores fossiles se révèlent être de bons marqueurs stratigraphiques pour définir les ères géologiques, des investigations facilitées par l'avènement de la microscopie électronique en transmission au début des années 50, mais aussi et surtout par la microscopie électronique à balayage vers la fin des années 60. De programmes internationaux

de forage et datation des sédiments océaniques se mettent en place, encore à l'œuvre de nos jours, qui permettent de déterminer les zones à sédiments biogéniques caractérisant les principales ères de l'histoire de notre planète.

La microscopie électronique permet une description fine des espèces, et notamment la démonstration de l'affinité des coccolithophores avec d'autres algues unicellulaires non-coccolithophores bien connues possédant un « *troisième flagelle* ». Cet appendice, détecté en 1900 chez *Phaeocystis globosa* par Scherffel et puis observé chez d'autres algues tel *Prymnesium saltans* (Massart 1920) et *Chrysochromulina parva* (Lackey 1939), semble permettre aux cellules de se fixer. En 1955, Mary Parke et Irène Manton décrivent en détail cet appendice grâce à la microscopie électronique et démontrent qu'il ne s'agit pas d'un « *troisième flagelle* » mais d'un nouvel organite qu'elles nomment « haptonème » (απτω « toucher » ou « fixer », νημα « fil » ; « le filament qui touche» ; *cf partie 3*). La reconnaissance de cet organite par Stosch en 1958 chez *Pleurochrysis scherffelii* a permit la définition des Haptophyceae en 1962 par Christensen, la classe d'algue incluant tous les organismes possédant un haptonème incluant les coccolithophores et d'autres algues non coccolithophores. Aussi, la première caractérisation de phases holococcolithe et hétérococcolithe est rapportée en 1960 par Parke et Adams chez *Coccolithus pelagicus* supposant la possible alternance de ces deux phases dans son cycle de vie ; la reconnaissance et l'étude de l'alternance de ce type de formes continue d'être un champ d'exploration de la biologie des coccolithophores (Frada 2009).

Le concept d'haptophytes en tant que lignée indépendante d'algues (Haptophyta) est proposé en 1972 par Hibberd puis accepté en 1976 sur la base de caractères morphologiques et ultrastructuraux propres. Ce concept a été confirmé par les études en phylogénie moléculaire. Celles-ci apportent de nouvelles précisions et de nouveaux paradigmes, au niveau de la classification du groupe et de son origine encore non définie (Edvardsen et al. 2000, Fujiwara et al. 2001, Yoon et al. 2004 ; voir « Origine et évolution des haptophytes »), et de manière plus général, sur notre connaissance de l'évolution des eucaryotes. Les données moléculaires (Saez et al. 2004) et les études sur l'homologie de la biominéralisation des coccolithes (Young et Henriksen, 2003; Young et al. 2005) supportent l'idée que les coccolithophores forment un clade monophyletique dans la classe des Prymnesiophyceae. Un ancêtre commun aurait probablement développé la capacité à contrôler la précipitation intracellulaire de la calcite, et l'agencement des écailles calcaires matures à la surface de la

cellule (de Vargas et al. 2007; Leadbeater, 1994). Dans ce groupe monophylétique majoritairement coccolithophore, les espèces connues qui ne produisent pas de coccolithes (comme les Isochrysidaceae) ou bien qui n'en produisent que lors d'une phase dans leur cycle de vie (telles les Noealaerhabdaceae et les Pleurochrysidaceae) auraient alors perdu totalement ou partiellement leur capacité de biominéralisation (Billard and Inouye, 2004; de Vargas and Probert, 2004). Ainsi la présence ou l'absence de coccolithes ne peut être l'unique caractère de classification des cellules coccolithophores. Sur la base de cette monophylie et de phylogénies des gènes ribosomiques des haptophytes, de Vargas et al. (2007) intègrent tous les haptophytes potentiellement calcifiants dans la sous classe des Calcihaptophycideae (Fig. 9).

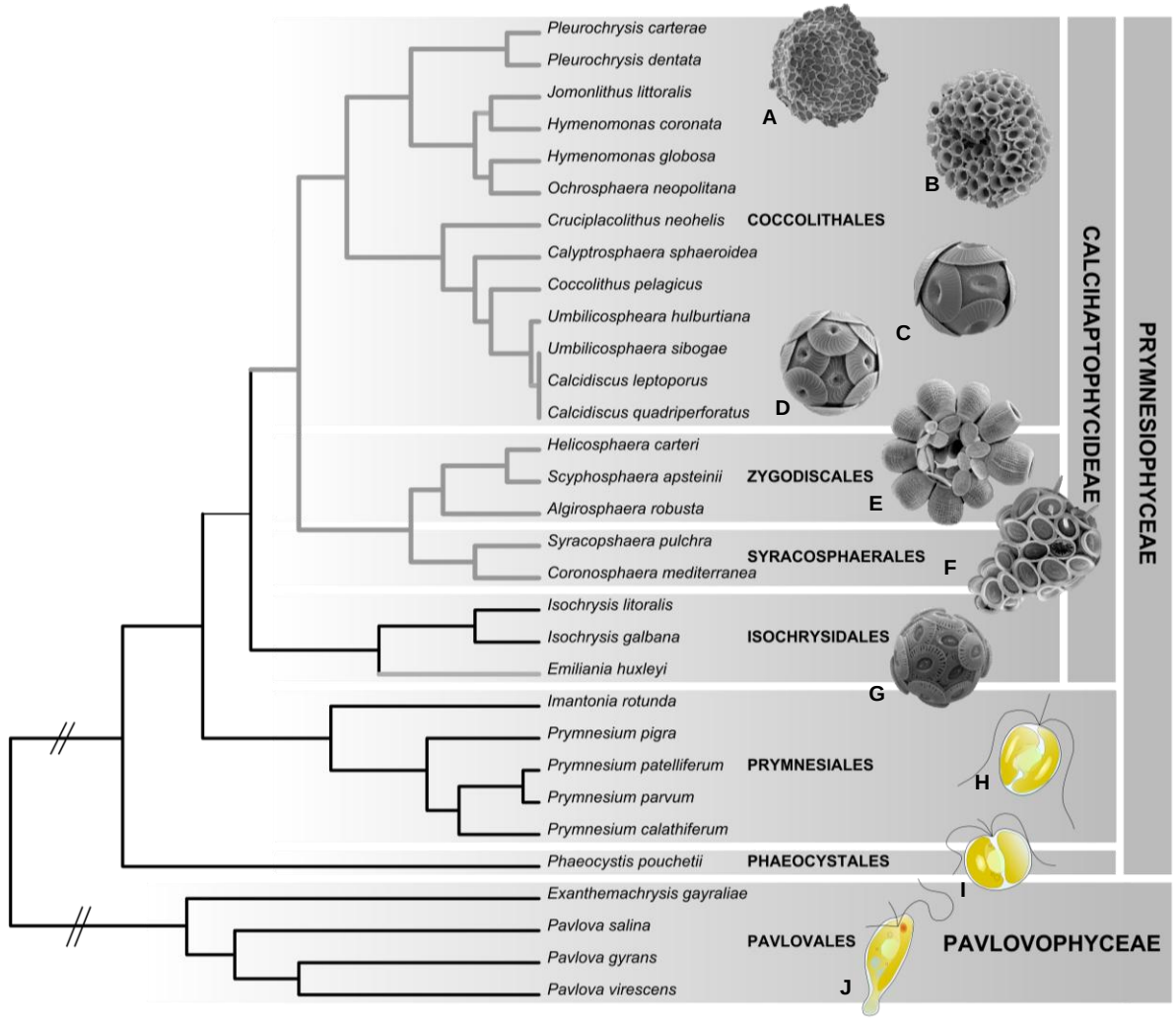

Figure 9. Phylogénie actuelle des Haptophytes inférée à partir de séquences ribosomiques (d'après de Vargas et al. 2007). Les branches grises correspondent aux haptophytes calcifiants. A. *Pleurochrysis carterae*; B. *Hymenomonas globosa*; C. *Coccolithus pelagicus*; D. *Calcidiscus pelagicus*; E. *Scyphosphaera apsteinii*; F. *Syracosphaera pulchra*; G. *Emiliania huxleyi*; H. *Prymnesium parvum*; I. *Phaeocystis pouchetii*; J. *Pavlova gyrans*. (Auteurs : Jeremy Young (A-D) ; Margaux Carmichael et Noan Le Bescot (E-G)).

Aspects de la biologie structurale et évolutive des haptophytes

Très répandus dans tous les océans, les haptophytes forment une lignée de protistes majoritairement photosynthétiques, et probablement largement mixotrophes. Les haptophytes seraient actuellement représentés par ~300 espèces dont ~200 chez les coccolithophores. Ces derniers comporteraient >4000 espèces fossiles, les haptophytes possédant le bilan fossile le plus riche du monde algal (cette estimation serait à revoir à la hausse du fait de la perte de fossiles par la haute dissolution des coccolithes dans la colonne d'eau lors de la sédimentation (Andruleit et al. 2004)). De nombreuses espèces sont tropicales et quelques unes vivent en eau douce pouvant présenter des phases émergées fixées à un substrat. La principale caractéristique de ces protistes est l'haptonème, un appendice filiforme inséré entre les deux flagelles. Différent des flagelles par sa composition microtubulaire, sa taille varie selon les espèces et il est parfois même absent. Il permettrait l'adhésion à un substrat, le déplacement de particules voire la capture de proies (Fig. 10; Inouye et Kawashi 1994).

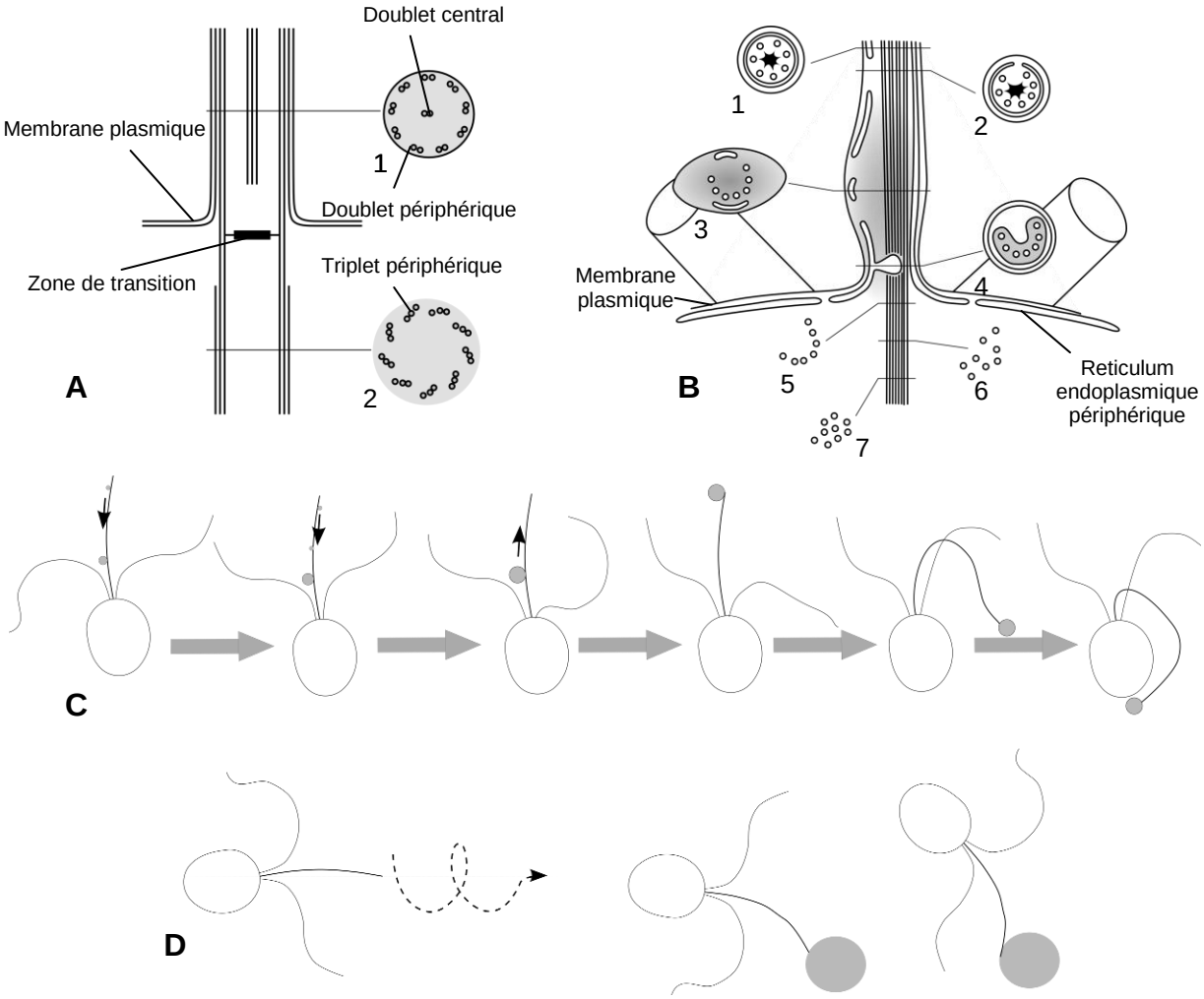

Figure 10. Structure et fonction de l'haptonème : A. Organisation du flagelle haptophyte (1: organisation microtubulaire du flagelle, 2: organisation microtubulaire de la base flagellaire); B. Organisation microtubulaire de l'haptonème (1-7 : sections démontrant les niveaux d'organisations microtubulaires de l'haptonème ; d'après Billard et Inouye 2004; C. Haptonème accumulant des particules avant phagocytose; D. Haptonème se fixant à un substrat. (D'après Inouye et Kawashi 1994).

Les espèces d'haptophytes sont essentiellement basées sur l'observation de plusieurs caractères morphologiques dont la combinaison est souvent mise en perspective d'une trame évolutive et/ou écologique. Des grands types structuraux aux cycles de vie des haptophytes, la description des structures et du comportement des espèces dans leur environnement a mené à une connaissance exceptionnellement précise pour un groupe de phytoplancton. La compréhension de l'évolution des coccolithophores ne peut ainsi passer que par la connaissance de la biologie des haptophytes en général.

1 Typologie structurale

Deux grands types structuraux séparent la lignée des haptophytes: les Pavlovophyceae, et les Prymnesiophyceae. Ces deux types structuraux correspondent surtout à deux organisations flagellaires différentes, les Prymnesiophyceae possèdent deux flagelles isokontes (de longueurs égales) contrairement aux Pavlovophyvoceae qui sont anisokontes (de longueurs inégales). Chez ces derniers, le flagelle long porte parfois des poils fins sans structures tubulaires (mastigonèmes). D'autres caractères les distinguent aussi, comme la présence d'un stigma chez les Pavlovophyceae ou la manière de stocker les glucides sous forme de granules de paramylon (une étude taxonomique est présentée dans l'annexe 2 montrant une description détaillée des espèces types de cette classe).

De manière générale, les haptophytes contiennent des formes individuelles mobiles, flagellées possédant deux flagelles, égaux ou inégaux, avec un haptonème inséré entre eux; des formes individuelles immobiles; des formes immobiles pélagiques ou benthiques incluses dans du mucilage; des formes coloniales, voire des formes amiboïdes, cellules mobiles grâce à des pseudopodes (Fig. 11; Edvardsen et al. 2000).

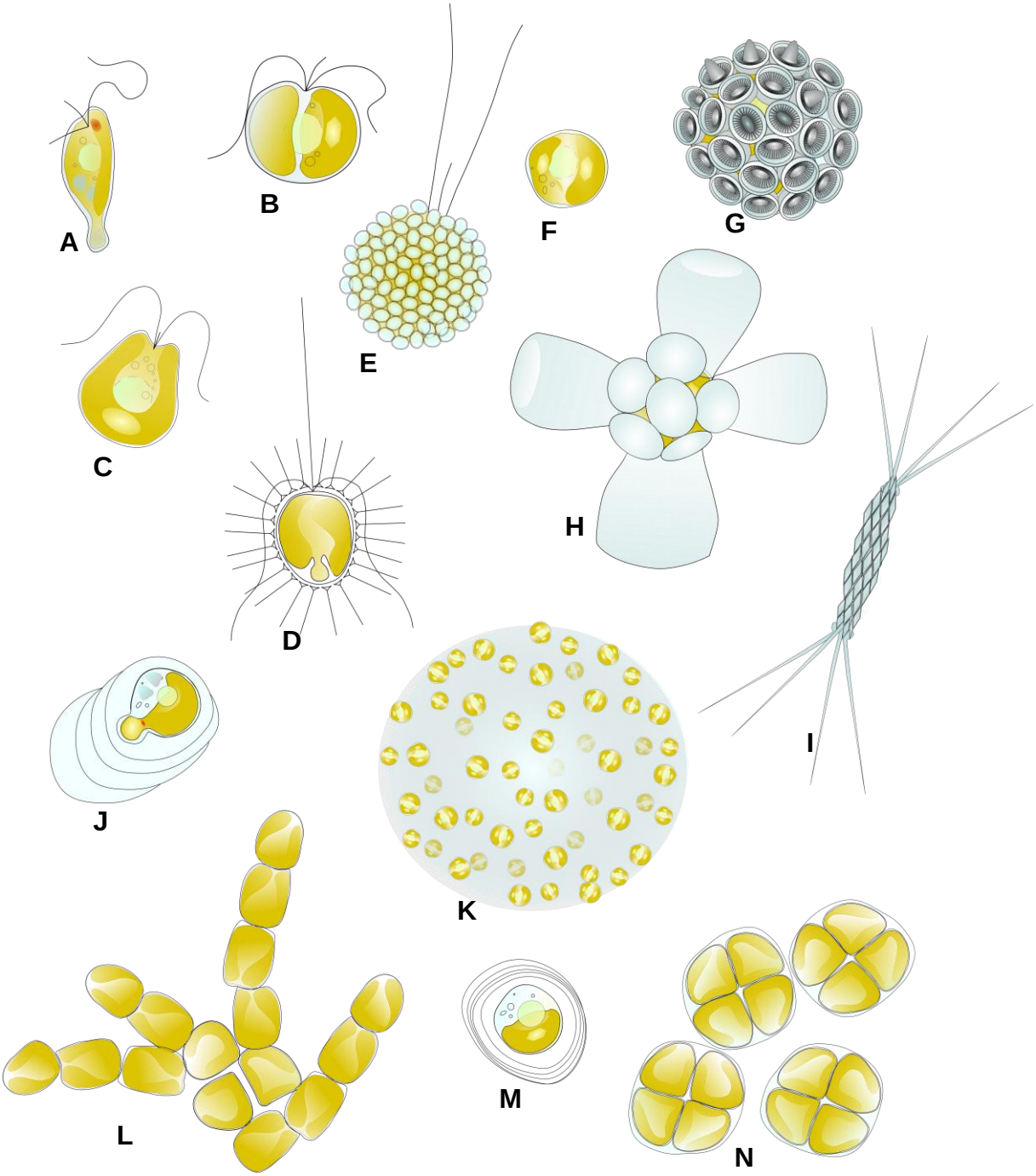

Figure 11. Variétés des formes chez les haptophytes. Formes mobiles : A. *Pavlova gyrans* ; B. *Phaeocystis globosa* ; C. *Isochrysis galbana* ; D. *Haptolina ericina*; E. *Pleurochrysis carterae* ; formes individuelles immobiles : F. *Dicrateria inornata* ; G. *Coronosphaera mediterranea* ; H. *Scyphosphaera apsteinii* ; I. *Calciosolenia murrayi* ; formes mucifères immobiles : J. *Exanthemachrysis gayraliae* (benthique à mucilage stratifié); K. *Phaeocystis globosa* (colonie pélagique) ; L. *Pleurochrysis sp.* (colonie benthique filamenteuse) ; M. *Chrysotila lamellosa* (benthique à mucilage stratifié) ; N. *Chrysotila lamellosa* (colonies benthiques)

2 Organisation ultrastructurale

Les cellules haptophytes possèdent un réticulum endoplasmique sous la membrane plasmique qui entoure le cytoplasme (réticulum endoplasmique périphérique). Les mitochondries possèdent des crêtes tubulaires. Le noyau et les plastes sont enveloppés par un reticulum périplastidial (ou membrane nucléoplastidiale). Dans les plastes, les thylakoïdes sont assemblés par trois, sans lamelle périphérique et ne forment pas de grana. Un pyrénoïde peut parfois être présent montrant diverses morphologies, protubérant, interne mais aussi sous la forme d'un cristal lenticulaire traversé par une lamelle de thylacoïdes (Fig. 12). Ces caractères permettent de distinguer les cellules haptophytes des autres eucaryotes, et certaines variations de caractères comme le pyrénoïde peuvent distinguer certains rangs taxonomiques.

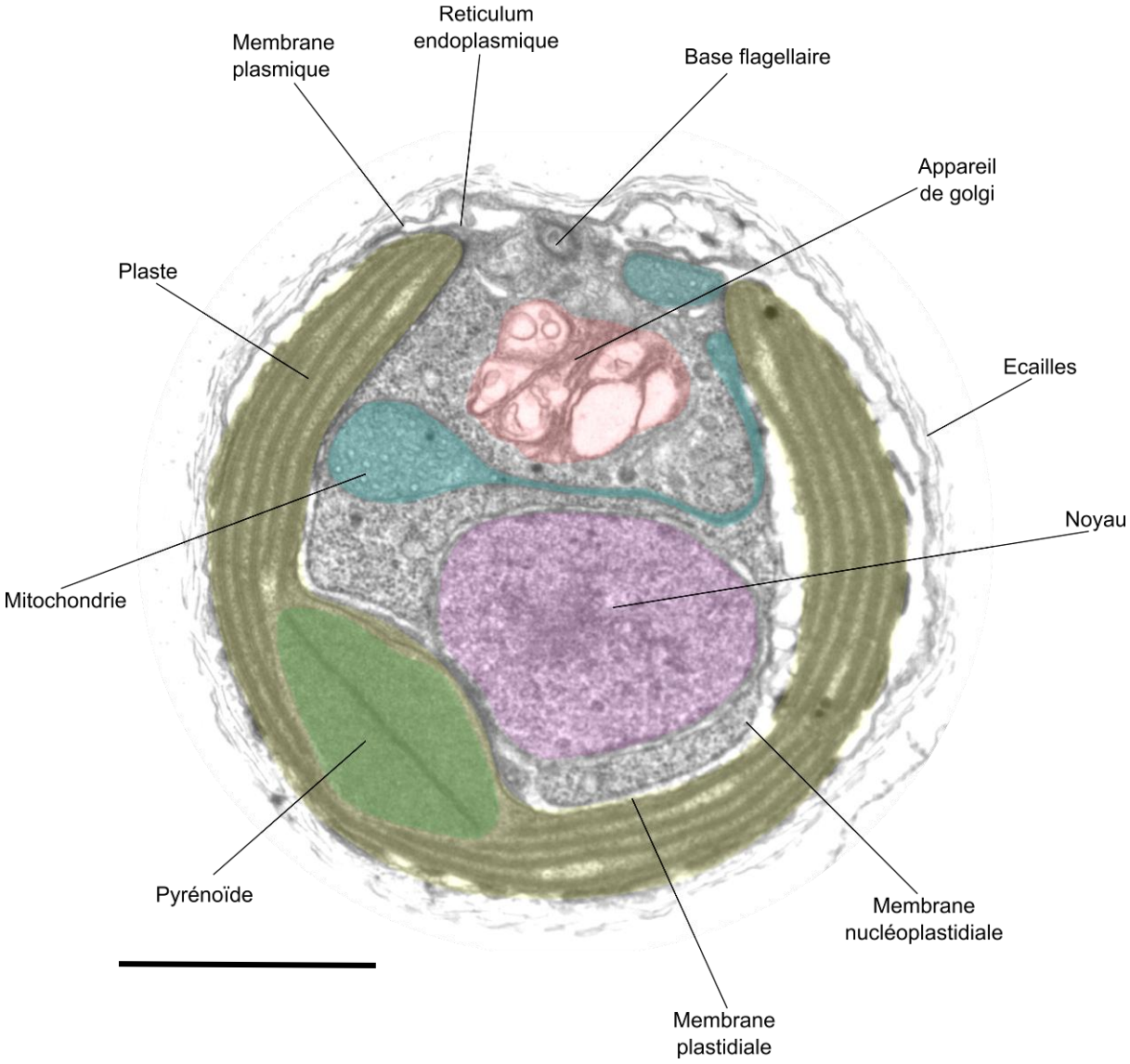

Figure 12. Section d'une cellule d'*Isochrysis galbana* en microscopie électronique en transmission. Les organelles sont artificiellement colorées. Echelle : 1 µm.

3 Pigments

Les plastes des haptophytes présentent généralement des colorations jaunes dorées. Avant tout, les pigments composent les éléments essentiels à la photosynthèse par leur capacité à capter l'énergie lumineuse. Les principaux pigments haptophytes sont les chlorophylles a (chl a) et c (chl c), et les caroténoïdes, comme la fucoxanthine (Tab. 1). La collecte de l'énergie lumineuse est effectué par les chlorophylles a, c et quelques fucoxanthines. La chl a absorbe la lumière rouge et bleue alors que les chl c absorbent dans le bleu, avec une affinité moindre pour le rouge et le vert. Les caroténoïdes présentent divers pigments qui peuvent être impliqués dans la collecte d'énergie lumineuse montrant des spectres d'absorptions pour la lumière bleu et verte, complétant la couverture d'absorption du spectre lumineux des chlorophylles. D'autres caroténoïdes ont une fonction photoprotectrice comme les diatoxanthines ou les diadinoxanthines. La modulation de ces affinités est assurée par la capacité des pigments à s'associer à d'autres molécules. L'ensemble des différentes formes dérivées de ces pigments (pigments accessoires) produisent des signatures pigmentaires qui peuvent correspondre à des adaptations à certaines conditions lumineuses. Ainsi les conditions lumineuses détermineraient en partie la présence des espèces dans l'environnement, selon leur composition pigmentaire.

Tableau 1. Liste de pigments communément observés chez les haptophytes

Pigments	Abbreviations	
Chlorophylle a	chl a	
Divinyl Protochlorophyllide	MgDVP	
Monovinyl Chlorophylle c1	chl c1	c1
Divinyl Chlorophylle c2	chl c2	c2
Chl c2-monogalactosyldiacylglyceride E.hux-type	chl c2-MGDG Ehux	c2E
Chl c2-monogalactosyldiacylglyceride C.pol-type	chl c2-MGDG Cpoly	c2C
Divinyl chlorophylle c3	chl c3	DVc3
Monovinyl chlorophylle c3	MVc3	
Fucoxanthine	Fx	Fx
19'-Butanoyloxyfucoxanthine	BFx	BFx
19'-Hexanoyloxyfucoxanthine	HFx	HFx
4-keto-Fucoxanthine	4kFx	4kFx
4-keto-Hexanoyloxyfucoxanthine	4kHFx	4kHFx
Diadinoxanthine	Ddx	
Diatoxanthine	Dtx	
β,ε-Carotene	α-Carotene βε	
β,β-Carotene	β-Carotene	

Il existe des formes spécifiques parmi ces pigments accessoires. Par exemple, les formes dérivées de la fucoxantine 19' hexanoyloxyfucoxanthine (Hfx ; Norgard et al. 1977)) et 19' butanoyloxyfucoxanthine (Bfx; Vesk et Jeffrey 1987) semblent être spécifiques d'un

bon nombre d'haptophytes. Ces pigments sont souvent utilisés en océanographie comme marqueurs des haptophytes. Même si d'autres pigments accessoires ont été caractérisés, leur utilisation n'a pas toujours été validée dans un cadre global de détection environnementale. Aussi, l'habitat, la distribution phylogénétique et la composition pigmentaire des espèces haptophytes semblent avoir un lien fort (Van Lenning et al 2004). Il a été démontré que la distribution des pigments chl c1 et HFx coïncident avec la taxinomie au niveau des familles et la phylogénie des haptophytes (Fig.13) excepté chez les Prymnesiaceae. Les espèces se retrouvant exclusivement en milieu côtier, comme les espèces calcifiantes de la famille des Pleurochrysidaceae et du genre *Cruciplacolithus*, les espèces non calcifiantes de la famille des Isochrysidaceae, certaines du genre *Prymnesium* ou celles de la classe des Pavlovophyceae, semblent synthétiser le pigment chl c1. Il est aussi important de noter que les Isochrysidales et les Pavlovophyceae ne produisent pas de pigments accessoires caroténoïdes à part la fucoxanthine. Les autres espèces, plus océaniques et à large spectre biogéographique, synthétisent le pigment HFx et d'autres pigments accessoires caroténoïdes. Cette dichotomie claire indique une sélection de ces pigments en tant que caractères spécifiques dans les différents environnements. Cependant l'avantage fonctionnel que représentent ces deux modes pigmentaires pour leur environnement respectif reste mal compris, rendant la signification évolutive de ces caractères spéculative. La comparaison dans d'autres phyla pourrait permettre en partie d'en comprendre la portée évolutive et une étude plus approfondie des affinités de ces pigments dans différents contextes permettraient d'en comprendre les avantages fonctionnels.

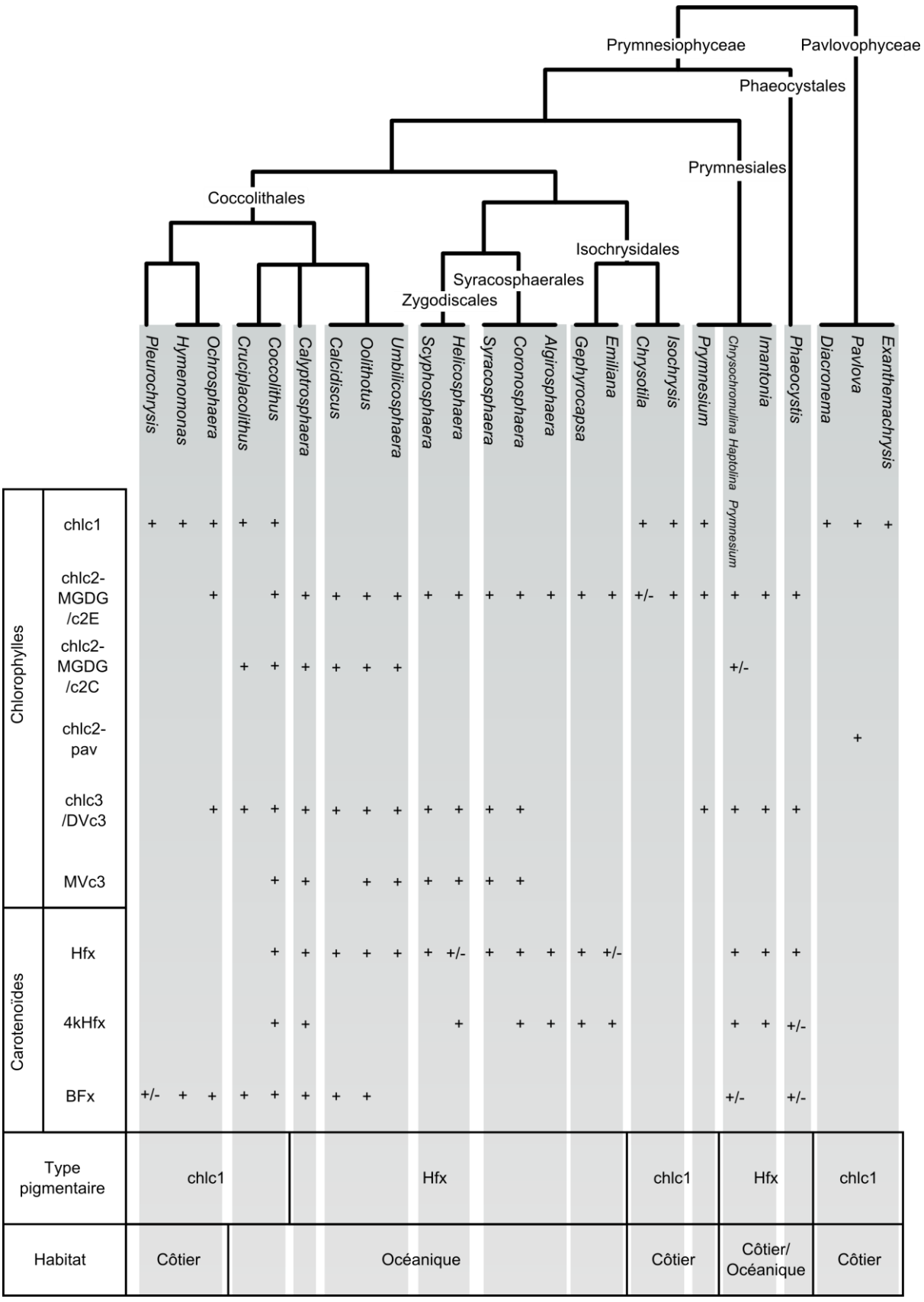

Figure 13. Distribution des pigments accessoires sur une phylogénie consensuelle des haptophytes (van Lenning et al. 2004; Zapata et al. 2004). Les pigments communs MgDVP, chl a, chl c2, Fx, Ddx, Dtx, β-Carotene ont été omis de ce tableau. Le genre Prymnesium est divisé en deux groupes pigmentaires, le groupe contenant le chlc1 est composé des espèces *P. parvum* and *P. patelliferum*.

4 Ecailles organiques et biominéralisées

Les ornementations cellulaires forment un caractère fondamental des haptophytes. La plupart des Prymnesiophyceae sont recouverts d'écailles microfibrillaires organiques. Observable par les méthodes de microscopie électronique de coloration négative ou d'ombrages, la structure générale de ces écailles est particulièrement distinctive au niveau taxinomique servant parfois à la définition de l'espèce mais aussi à la définition du stade de vie (voir partie 5; Billard 1994 ; Billard et Inouye 2004).

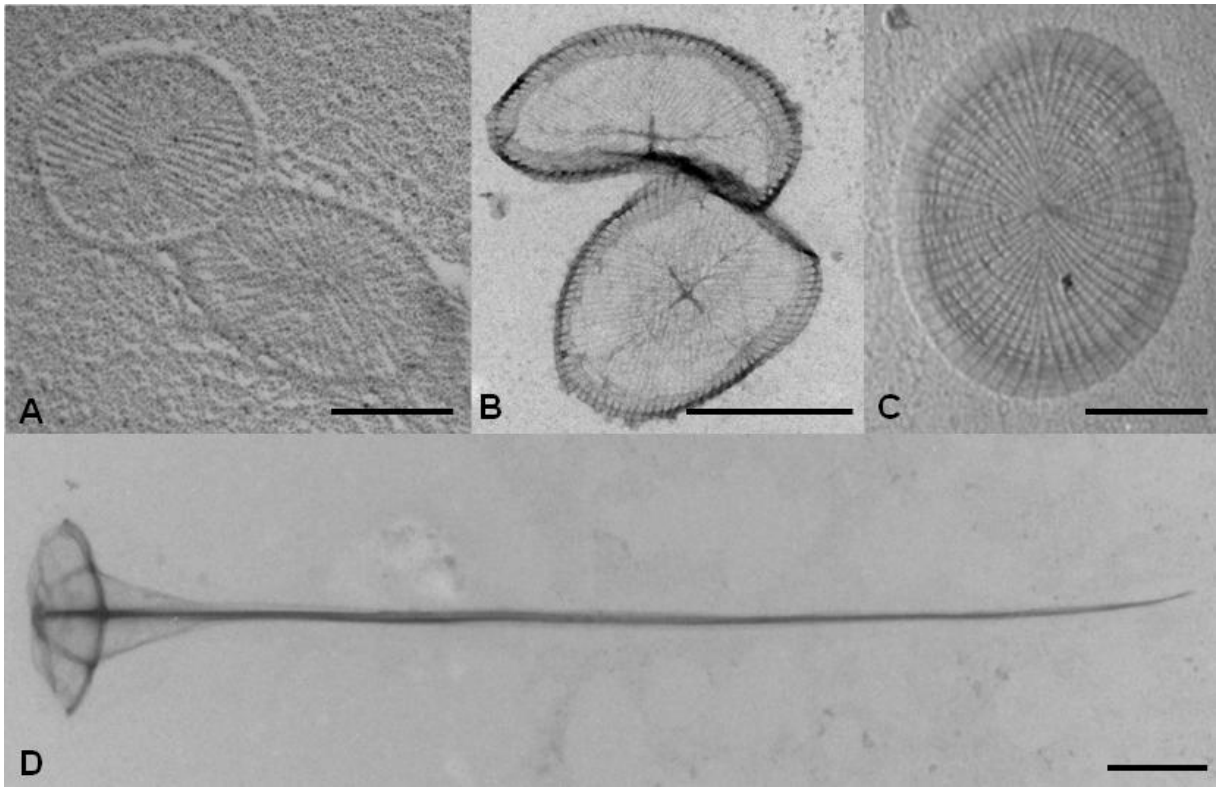

Figure 14. Exemples d'écailles organiques chez les prymnésiophycées: A. Face indifférenciée des écailles chez *Isochrysis sp.* en ombrage; B. Face proximale d'une écaille chez *Haptolina hirta* en coloration négative; C. Face distal d'une écaille de *Chrysochromulina sp.* en ombrage; D. Face distale en épine chez *Haptolina hirta* en coloration négative. Echelle : A, C : 200 µm ; B, D : 500 µm (auteur : Ian Probert).

La face proximale (surface proche de la membrane plasmique) est toujours organisée par l'agencement de microfibres en radiales sur quatre quadrants (Fig. 14A, B). Le nombre de ces radiales est variable selon l'espèce, 5-6 chez *Chrysotila lamellosa* à plus de 40 chez *Chrysochromulina mactra*. La taille aussi varie montrant alors des espaces plus importants entre les microfibrilles radiaires. L'agencement de la surface proximale peut parfois être le seul patron de microfibrilles de l'écaille comme chez les Isochrysidales, chez *Phaeocystis pouchetii* ou *Imantonia rotunda*. La surface distale (surface externe à la cellule)

quant à elle peut démontrer des variations importantes. Des microfibrilles sont arrangées en bande spirales formant 4 à 5 tours (Fig. 14C). Des projections élaborées ainsi que différents niveaux d'ornementations peuvent se retrouver sur cette surface de l'écaille telles les épines chez certaines *Haptolina* (Fig. 14D).

La composition chimique de ces écailles déterminée chez *Pleurochrysis scherffelii* (Brown et al. 1969) et *Prymnesium chiton* (Allen et Nothcote 1975) suggère un assemblage de glycoproteines dont la base polysaccharidique serait assimilable à de la cellulose. Ces écailles sont synthetises dans l'appareil de golgi et excrétés par exocytose (Leadbeater 1994).

Chez certaines espèces, les écailles microfibrillaires sont utilisées comme matrice permettant la biominéralisation des coccolithes comme chez *Pleurochrysis carterae* et *Coccolithus pelagicus*. Ces espèces se retrouvent généralement avec une couche externe de coccolithes couvrant une couche d'écailles organiques. Cette organisation ne se retrouve pas chez tous les coccolithophores, *Emiliania huxleyi* et *Umbilicosphaeara foliosa* produiraient leurs coccolithes à partir d'une matrice glycoprotéique différente de l'écaille microfibrillaire qu'ils produisent (Leadbeater 1994).

Parmi les coccolithes, trois types morphologiques majeurs ont été décrits : les hétérococcolithes, les holococcolithes et les nannolithes (Fig. 15A, B ; Young et al. 2003). Les hétérococcolithes et les holococcolithes peuvent coexister au sein d'une même espèce et correspondent à l'alternance du cycle de vie diplo-haploide (voir partie 5). La biominéralisation des hétérococcolithes comprend la précipitation et le façonnement, en agencement radial, de cristaux de calcite dans des vacuoles intracellulaires (Fig. 15C, D. Les holococcolithes, faits d'un amoncèlement organisé de petits cristaux de $CaCO_3$ hexahedriques, seraient précipités extracellulairement. Quant aux nannolithes, ils présentent des structures très diverses et leur mode de biomineralisation est encore très mal connu. Chez les coccolithophores, le concept morphologique d'espèce est principalement basé sur la reconnaissance des cristaux qui structurent les coccolithes. Leur variabilité et la complexité de leur agencement définit les morpho-espèces. Ce concept est appliqué autant en biologie qu'en micropaléontologie.

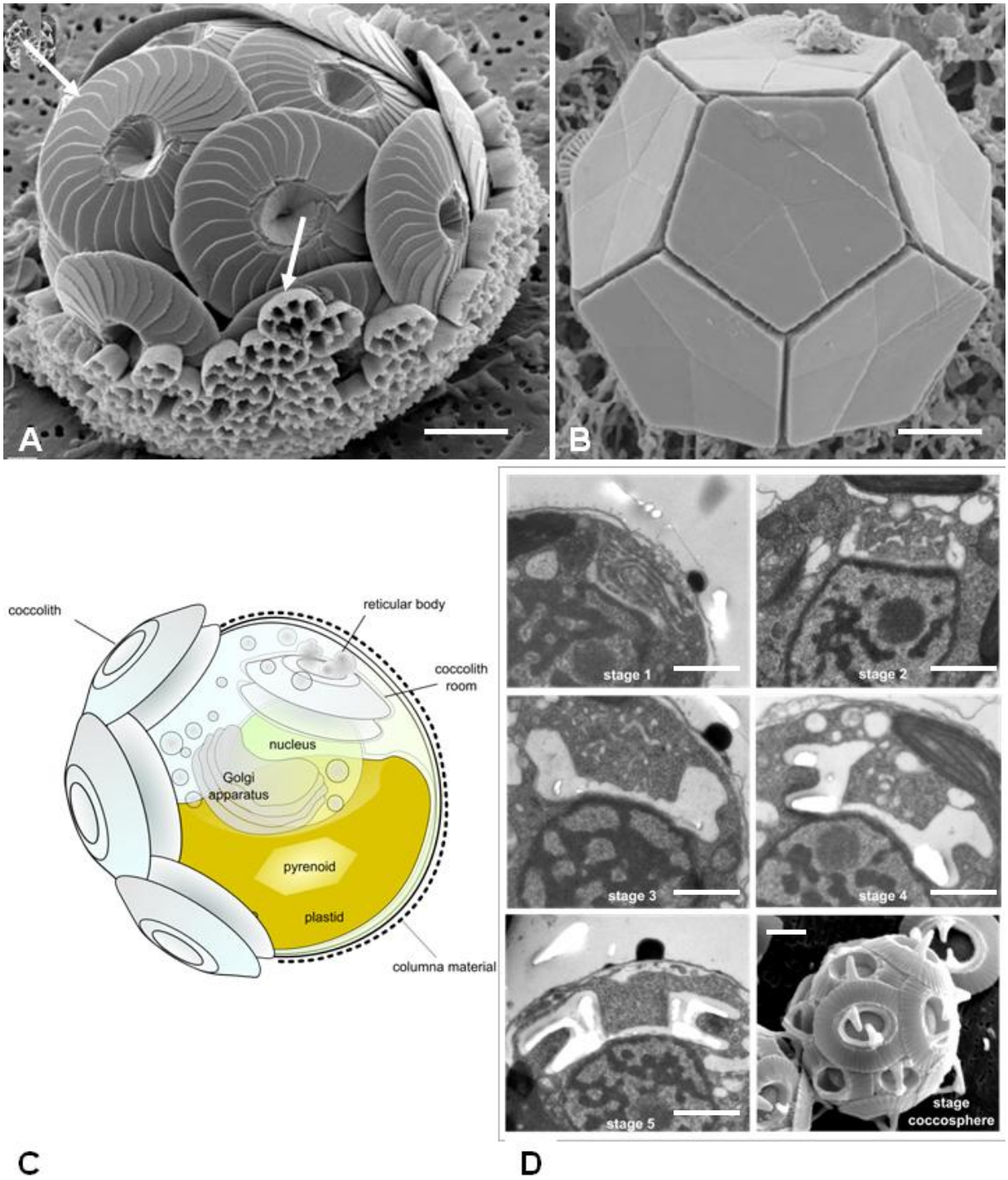

Figure 15. Différents types de coccolithes et coccolithogénèse. A. Combinaison hétérococcolithes (flèche de gauche)/holococcolithes (flèche du milieu) sur une coccosphère de *Calcidiscus leptoporus*. B. Organisation des nannolithes chez *Braarudosphaera bigelowii*. C. Schéma récapitulatif du processus de coccolithogénèse ; D. Différentes étapes dans la coccolithogénèse chez *Gephyrocapsa oceanica* : la vacuole contenant le coccolithe montre une relation forte avec le noyau, la base glycoprotéique montre un aplanissement à la zone de contact avec le noyau et la concentration des corps réticulés contenant les ions Ca^{2+} et CO_3^{2-} permettrait leur concentration et précipitation dans la vacuole. Echelle : A- D: 1 µm. (auteur des clichés A-B : Young et al. 2003)

D'autres structures externes biominéralisées ont été identifiés chez l'espèce *Prymnesium neolepsis*. Cette espèce serait l'unique représentant des haptophyte à produire des écailles de silices.

Chez les Pavlovophyceae, alors que l'absence d'écailles est notable, de petits corps denses peuvent recouvrir le flagelle long (Fig. 16A) et la cellule (Fig. 16B). Assimilés à des écailles, ces corps denses sont formés dans l'appareil de Golgi et leur mode de déposition et d'agencement sur la membrane plasmique reste inconnu (Fig. 16C).

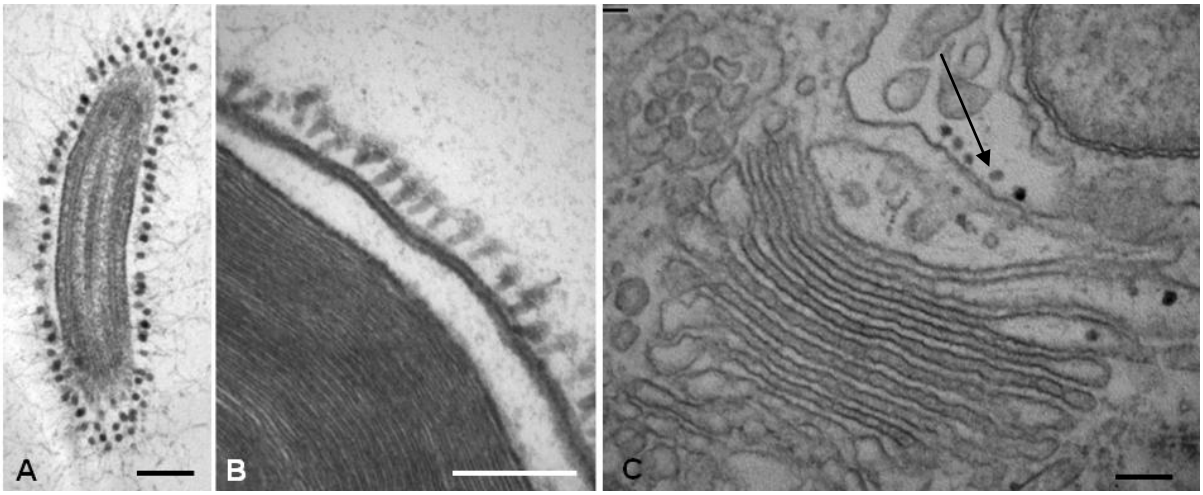

Figure 16. Corps denses chez les Pavlovophyceae. A. Corps denses sur le flagelle de *Pavlova pinguis* ; B. Corps denses apposés à la membrane plasmique des cellules de *Rebecca salina* ; C. Appareil de Golgi possédant des corps denses en formation (flèche). Echelle : A- C: 100 nm.

La ou les fonctions des écailles et des coccolithes restent encore peu définies, souvent spéculatives (Fig. 17). Néanmoins, les écailles semblent avoir une signification profonde sur le cycle de vie et l'évolution des haptophytes, comme chez l'espèce *Emiliania huxleyi*, qui présente une phase haploïde insensible aux virus, insensibilité probablement due à la présence d'écailles organiques que l'on ne retrouve pas dans la phase diploïde (Frada et al. 2008; cf partie 5).

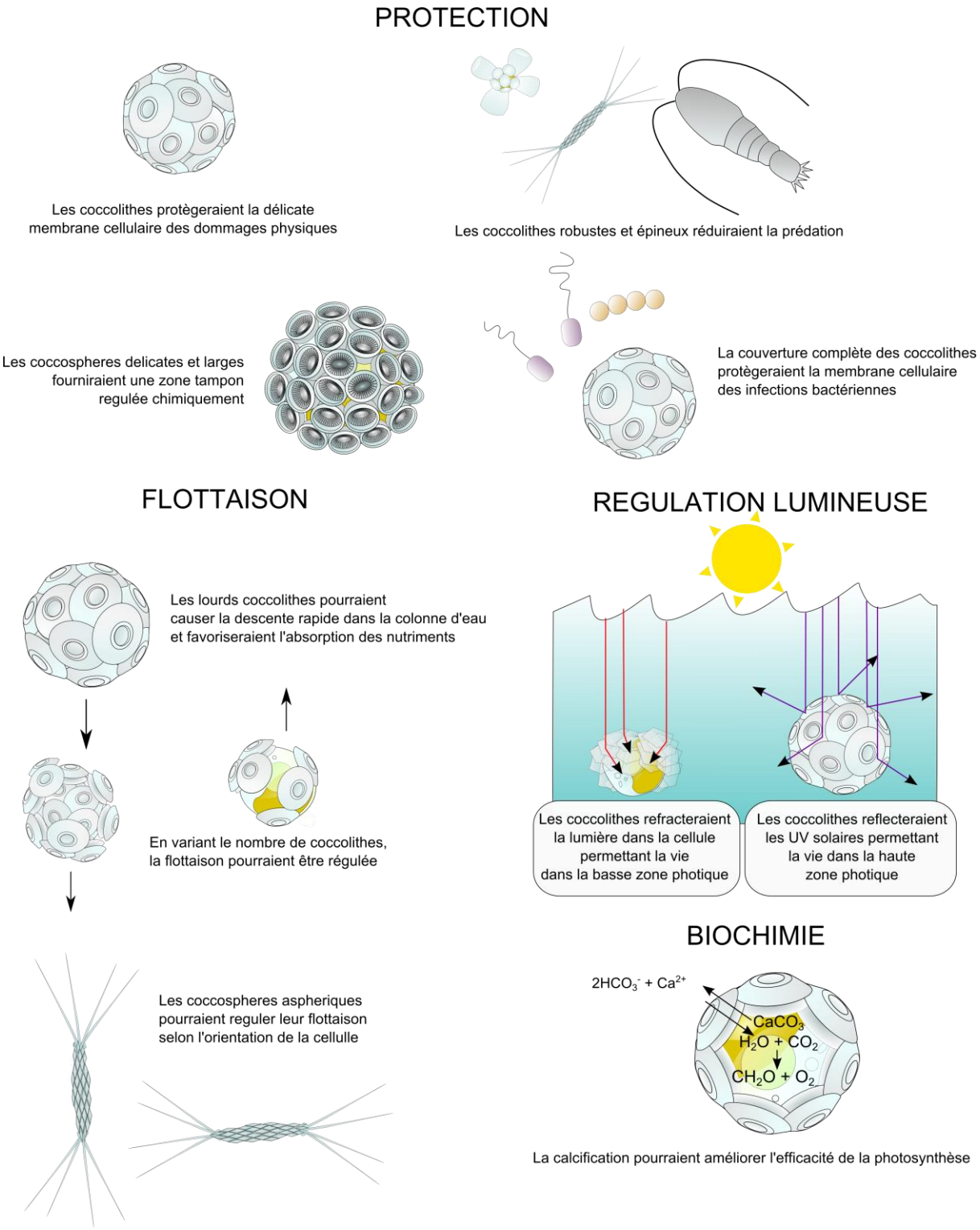

Figure 17. Fonctions hypothétiques des coccolithes (d'après Young 1994)

5 Reproduction et cycle de vie

Les haptophytes se reproduisent le plus souvent asexuellement, par multiplication végétative. Chez les coccolithophores, les coccolithes sont redistribuées sur les cellules filles et le même procédé semble s'opérer pour les écailles organiques (Billard and Inouye, 2004). L'alternance de stades de vie aux morphologies distinctes est particulièrement fréquente chez les haptophytes. Bien que la sexualité reste inconnue, ces alternances sont le plus souvent liées au niveau de ploïdie des cellules, ce qui suggère un cycle de vie sexué et haplo-diplobiontique (Green et al. 1996 ; Houdan et al. 2004). Fréquemment rencontré dans le monde eucaryote unicellulaire, ce type de cycle peut parfois être complexe, et chaque phase du cycle de vie peut être capable de multiplication végétative.

En règle générale, les stades de vie se distinguent au niveau des écailles organiques et/ou des coccolithes. Selon le modèle proposé par Billard en 1994 (Fig. 18A), si l'écaille haptophyte présente deux

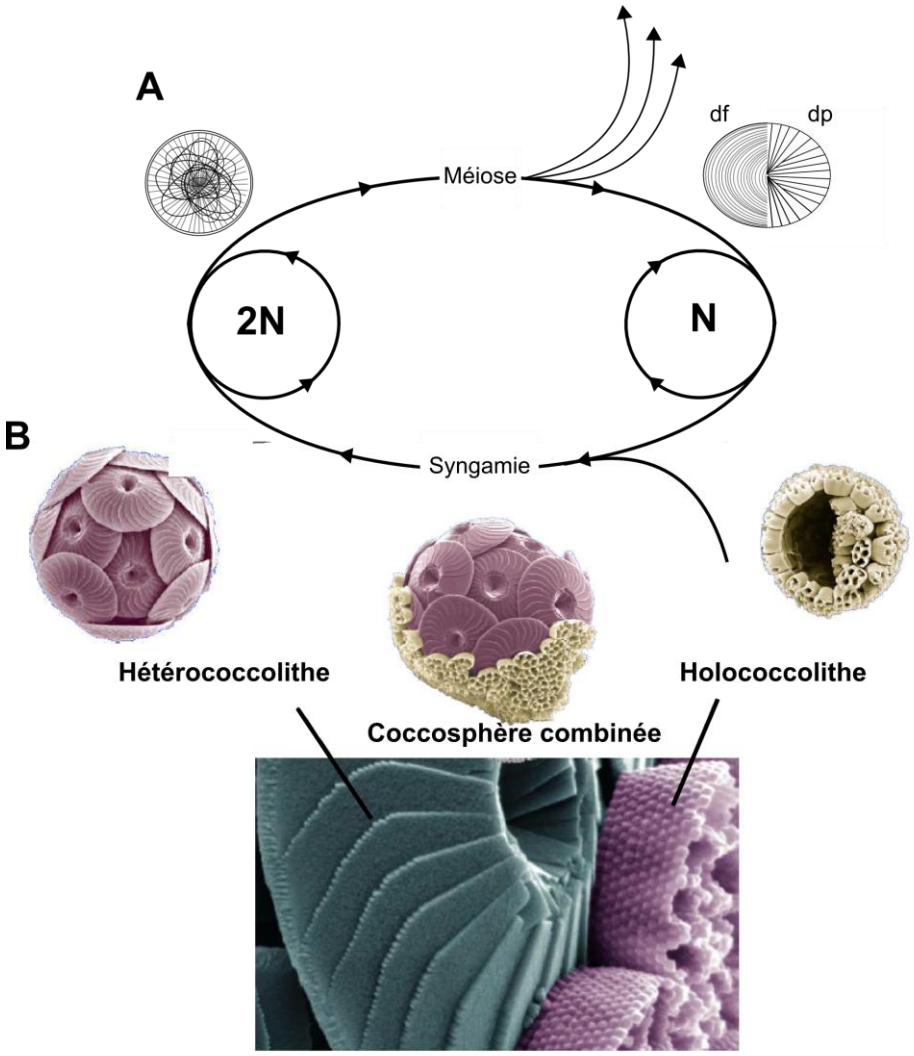

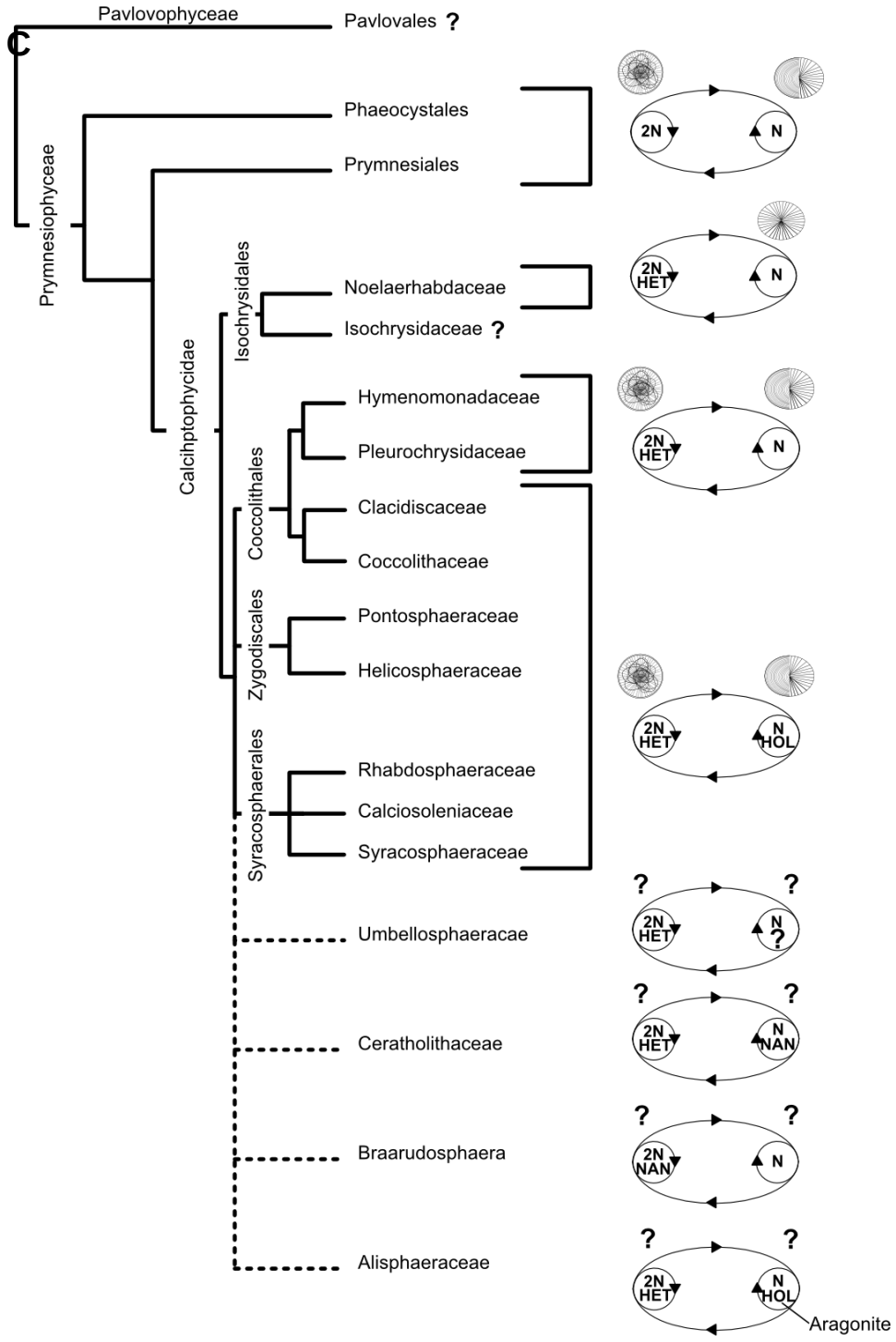

Figure 18. Représentation schématique du cycle de vie des haptophytes : A. Modélisation du cycle haplodiplobiontique des haptophytes selon Billard (1994). Le processus dominant de reproduction est la multiplication asexuée qui a lieu lors des phases haploïdes et diploïdes. Les transitions entre les phases sont la méiose et la syngamie qui semblent rares ou occasionnelles et les conditions provoquant ces transitions sont le plus souvent inconnues. B. Illustration d'un cycle de vie hétéro-/holo-coccolithophore typique, avec *Calcidiscus quadriperforatus* en exemple (adapté de Billard 1994 et Young et al. 2005) : la combinaison des types de coccolithes correspond à l'une ou l'autre des transitions, et s'observent occasionnellement dans les échantillons naturels. Ici les hétéroccolithes sont disposés sous les holococcolithes, ce qui logiquement résulterait d'une syngamie). C. Arbre phylogénétique consensus des familles majeures d'haptophytes (d'après Houdan et al. 2004, et Frada 2009). Les lignes pointillées représentent les groupes pour lesquelles la phylogénie reste incertaine. Les points d'interrogations indiquent la méconnaissance d'un cycle de vie sexué ou du type d'écailles organiques. La distribution phylogénétique du cycle haplo diplobiontique chez les haptophytes en démontre l'ancestralité au sein de la classe des Prymnesiophyceae. HET : Hétérococcolithe, HOL : Holococcolithe ; NAN : Nannolithe.

ornementations distinctes sur sa face distales et proximale, il s'agit d'un stade haploïde. A l'opposé, le stade diploïde présente la même ornementation sur les deux faces, et l'ornementation correspond à celle de la face distale de l'écaille haploïde. Dans le cas des coccolithophores, cette alternance des deux types d'écailles organiques est souvent accompagnée de l'alternance des deux types de coccolithes, hétérococcolithes et holococcolithes pour les stades diploïde et haploïde, respectivement (voir partie 4 ; Fig. 18B).

La stratégie haplo-diploïde implique un cout à la valeur adaptative de chaque phase de vie et doit donc être compensée par des avantages d'importance évolutive et/ou écologique. L'idée suggérée par de Vargas et al. (2007) supporte une stratégie permettant de répondre aux contraintes sélectives qui peuvent s'exercer lors d'une phase de vie, telles la prédation, le parasitisme, une infection virale, ou des variations environnementales. Bien que les conditions déclenchant le passage d'une phase à une autre restent peu connues, l'exemple d'*Emiliania huxleyi* et de l'infection de son stade diploïde par un virus (*Emiliania huxleyi* virus (*EhV*)) illustrent ce propos (Frada et al 2008). Chez *E. huxleyi*, la pression virale imposée sur la phase de vie diploïde peut être considéré comme une force évolutive majeure pour le maintien du cycle haplo-diploïde. Par ailleurs, les physiologies distinctes des deux stades de vie d *E. huxleyi* suggèrent des adaptations differentielles à des nichesécologiques (Houdan et al 2004). Un même constat a été fait chez des Prymnesiophyceae non calcifiant, dont chacune des phases présentent des physiologies bien distinctes (*Prymnesium polylepis*, Billard et al 1994). Ainsi les coccolithophores auraient hérités des Prymnesiophyceae non calcifiants cette stratégie adaptative fondamentale qu'est le cycle haplodiplobiontique (Fig. 18C). A l'instar des hétérococcolithophores, les holococcolithophores semblent être particulièrement adaptées aux eaux oligotrophes, suggérant l'exploitation de différentes niches (Kleijne 1991 ; Cros et al 2000).

Cependant, le cycle haplodiplobiontique semble absent chez certains groupes. Les Pavlovophyceae et les Isochrysidaceae représentent deux cas particuliers illustrant ce problème (Fig. 18C). Ces deux groupes présentent des alternances de phases entre cellules flagellées et colonies benthiques selon les conditions environnementales (Fig. 19). L'activité mitotique des phases benthiques et flagellées varie selon l'espèce et la dominance d'une des phases. Par exemple, les souches des espèces *Exanthemachrysis gayraliae* (Pavlovophyceae) et *Chrysotila lamellosa* (Isochrysidaceae) ont une phase benthique dominante se reproduisant asexuellement et libèrent des cellules flagellées très rapidement après un changement de milieu. Ces cellules flagellées ne semblent pas pouvoir se multiplier. *C. lamellosa* qui porte

des écailles organiques fibrillaires semblent posséder le même type d'écailles tout le long de ce processus (voir partie 4). Les espèces *Pavlova gyrans* (Pavlovophyceae) et *Isochrysis galbana* (Isochrysidaceae), quant à elles, se multiplient asexuellement lors de leur phase flagellée dominante et éjectent leurs flagelles avant de commencer une vie benthique où elles se multiplient aussi lorsque les nutriments viennent à manquer.

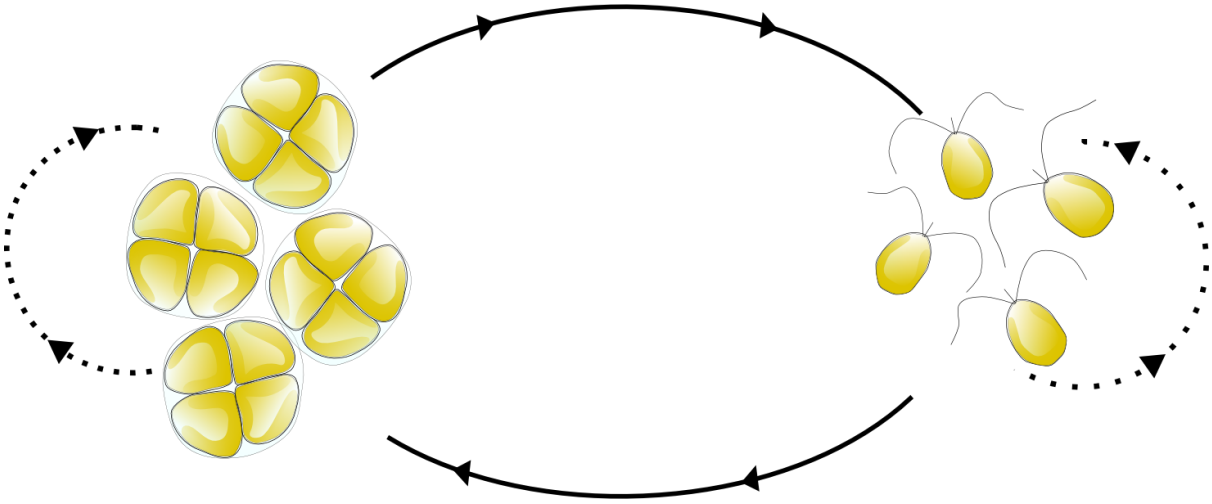

Figure 19. Représentation du cycle de vie bentho-pélagique chez la plupart des espèces de Pavlovophyceae et Isochrysidaceae. Selon l'espèce, la phase de vie considérée peut ou non se multiplier végétativement.

Bien que ces groupes pourraient avoir un cycle haplo-diplobiontique encore inconnu, ils pourraient aussi l'avoir perdu et ne présenter actuellement qu'un type de ploïdie, Dans tous les cas, les espèces exclusivement côtières et benthiques de ces deux groupes (comme *E. gayralie* et *C. lamellosa*) présentent deux phases de vies alternatives pouvant être considéré comme une adaptation aux changements environnementaux rapides qui caractérisent les milieux côtiers (Fig. 13). Certains éléments morphologiques favorisent l'hypothèse de la persistence d'un stade haploïde chez les Isochrysidaceae. Selon le modèle de Billard, la perte de l'agencement distal aurait été commun à tout l'ordre des Isochrysidales (ordre contenant les deux familles Isochrysidaceae et Noelaerhabdaceae) et les Isochrysidaceae auraient perdu le cycle haplo-diplobiontique. Le seul type d'écaille microfibrillaire retrouvé chez les Isochrysidales, présente un type d'agencement en quatre quadrants caractéristique de la face proximal pour la majorité des Prymnesiophyceae. Or *Emiliania huxleyi*, représentant des Noelaerhabdaceae, est connue pour ne présenter d'écailles organiques que lors de son stade haploïde. Par homologie, nous pouvons suggérer que la possession de ce type d'écaille chez les Isochrysidaceae correspond à un stade haploïde. Malgré cette hypothèse, la reproduction sexuée reste néanmoins un mystère chez cette famille.

6 De l'origine des haptophytes à l'évolution des coccolithophores

L'origine des haptophytes est sujette à de nombreux débats. Le phylum des haptohytes présente quelques affinités avec les hétérokontes, les cryptophytes (ces trois lignées formant le règne des Chromistes, Cavalier-Smith 1994) et les alvéolés. Ces lignées partagent la chlorophylle c et les chromistes ont un reticulum périplastidial en continuité avec les membranes nucléaires. Mais à l'instar des haptophytes, les hétérokontes possèdent deux flagelles anisokontes portant des mastigonèmes que l'on retrouve aussi chez les cryptophytes. La composition pigmentaire ainsi que la continuité du plaste et du noyau s'expliqueraient par l'hypothèse d'évènements endosymbiotiques commun à ces lignées, liés à l'acquisition de matériel plastidial d'une algue rouge, antérieure à leur radiation. Ces éléments participent aux arguments d'une origine commune de ces quatre lignées formant le super règne des chromalvéolés (Cavalier-Smith 2002).

Cependant, la monophylie de ce super-groupe ne semble pas être supportée par les études phylogénétiques selon l'origine génomique des gènes utilisés (Baurain et al. 2010). Alors que l'utilisation de gènes plastidiaux la conforte tout en associant les hétérokontes aux alvéolés (Hackett et al. 2007), les analyses phylogénomiques de gènes nucléaires ne permettent pas de positionner robustement les haptophytes et les cryptophytes (Burki et al. 2007). Ces études amènent les débats actuels à redéfinir les hypothèses des endosymbioses à l'origine de ces lignées. De plus, l'hypothèse d'un ancêtre haptophyte dépourvu de plaste reste plausible.

La première trace fiable de fossiles d'haptophytes (coccolithophores) remonte à ~220 millions d'années (Bown et al. 2005). L'apparition des haptophytes non-calcifiant serait donc bien antérieure à cette date. Seules les méthodes de datation par la phylogénie moléculaire peuvent aider à approximer la période d'origine des haptophytes, bien qu'elles ne permettent pas de déterminer la date de l'acquisition du plaste (Fig. 20). Différentes études s'accordent sur une date comprise entre 1100 et 637 millions d'années (Yoon et al. 2004 ; Berney et Pawlowski 2006 ; Liu et al. 2009), la date la plus vraisemblable proposée étant ~830 millions d'années (Liu et al. 2009) L'hypothèse probable serait que la divergence de l'hôte aurait débuté dès l'incorporation du plaste. La forme ancestrale haptophyte aurait été vraisemblablement un protiste côtier mixotrophe, pourvu d'un haptonème développé à la

prédation[1], de deux flagelles[2], d'un stigma[3], d'écailles[4], capable de biominéralisation[5] et ayant un cycle diplo-haplobiontique. La scission majeure entre les Pavlovophyceae et les Prymnesiophyceae aurait eu lieu à l'aube du Phanerozoique (~543 millions d'années). La capacité des Prymnesiophyceae à produire des écailles biominéralisées (calcite) aurait été acquise durant le Carbonifère, entre 391 et 291 millions d'années, en même temps que la transition entre le régime mixotrophe et autotrophe chez les coccolithophores. Cette transition précède leur expansion des milieux côtiers vers les milieux océaniques. L'émergence des coccolithophores semble avoir suivi la plus grande crise biologique que la terre ait connue, la crise Permien-Trias (250 million d'années) où 85% de la diversité marine fut perdue. L'intensification du volcanisme libérant de fort taux de CO_2, les pluies acides résultantes et les refroidissements climatiques causés par les cendres de cette période auraient été les conditions de l'évolution des coccolithophores et l'origine de leur grande diversification dès ~220 millions d'année (Bown 2005; Bowring et al. 1998 ; Godderis et al. 2007). Cette diversification aurait été accentuée par les nouvelles ouvertures océaniques et la colonisation de ces nouveaux milieux durant le Trias et le Jurassique (de Vargas et al. 2007). L'apparition des holococcolithes à ~185 millions d'années (cf partie 3.5 ; Bown et al. 2005) semble congruente avec cette colonisation des milieux océaniques suggérant une affinité héritée des milieux oligotrophes. La transition des coccolithophores depuis les environnements côtiers

[1] L'origine de l'haptonème est inconnue; l'hypothèse suggérée par Cavalier Smith (1994) considère une origine commune de l'hôte haptophyte avec les hôtes cryptophytes et hétérokontes. Il propose l'idée que l'haptonème serait à l'origine une racine flagellaire composée de 8 microtubules qui aurait subit une duplication et une extension (Cavalier Smith 1994). D'autres spéculations peuvent être formulées telle que la dégénérescence d'un flagelle anciennement dupliqué ou l'acquisition d'un flagelle bactérien par d'autres épisodes endosymbiotiques au cours de la genèse de la cellule haptophyte,.

[2] Les Pavlovophyceae possèdent deux flagelles inégaux à l'instar des Prymnesiophyceae. Le caractère anisokonté est souvent perçu comme ancestral, or la simplification de l'appareil basale des Pavlovophyceae suggère une possible régression d'un appareil flagellaire plus complexe tel que celui des Prymnesiophyceae. A l'heure actuelle, nous ne pouvons encore statuer de l'état ancestral de ce caractère chez les haptophytes (Cavalier Smith 2002 ; Annexe2). Une forme amiboïde peut aussi être suggérée si on considère que les caractères flagellaires ont été acquis des endosymbioses.

[3] Le stigma est un organe récepteur impliqué dans le phototactisme, il est généralement lié à un pigment photorécepteur localisé sur un flagelle. Il n'est présent que chez les Pavlovophyceae et est considéré comme un organite ancestral probablement hérité de l'épisode endosymbiotique. Si on considère cet épisode commun à tous les Haptophytes, les Prymnesiophyceae auraient alors perdu cette structure qui serait compensé par une épifluorescence détectable sur un des flagelles (Kawai et al 1991).

[4] Pour l'ancestralité des corps denses (Pavlovophyceae) ou écailles plates (Prymnesiophyceae) deux hypothèses existent, la complexification des corps denses en écailles microfibrillaires (Cavalier-Smith 1994) ou la simplification / perte des écailles microfibrillaires en corps denses (Liu et al 2009).

[5] Les Pavlovophyceae précipitent intracellulairement des cristaux de sulfates de baryum (Fesnel et Gayral 1979) et de nombreuses structures biominéralisées sont observées voire suspectées chez les Prymnesiales (Silva et al 2001 ; Edvardsen et al 2011). Ces mécanismes de biominéralisation sont encore peu connus au niveau physiologique, les structures impliquées étant dissimilaires entre les espèces impliquées. Nous ne pouvons que spéculer de leur lien potentiel avec la biominéralisation propre aux coccolithophores.

vers l'océan fut un pas remarquable dans leur évolution, et un événement crucial qui transforma le système biogéochimique de la terre.

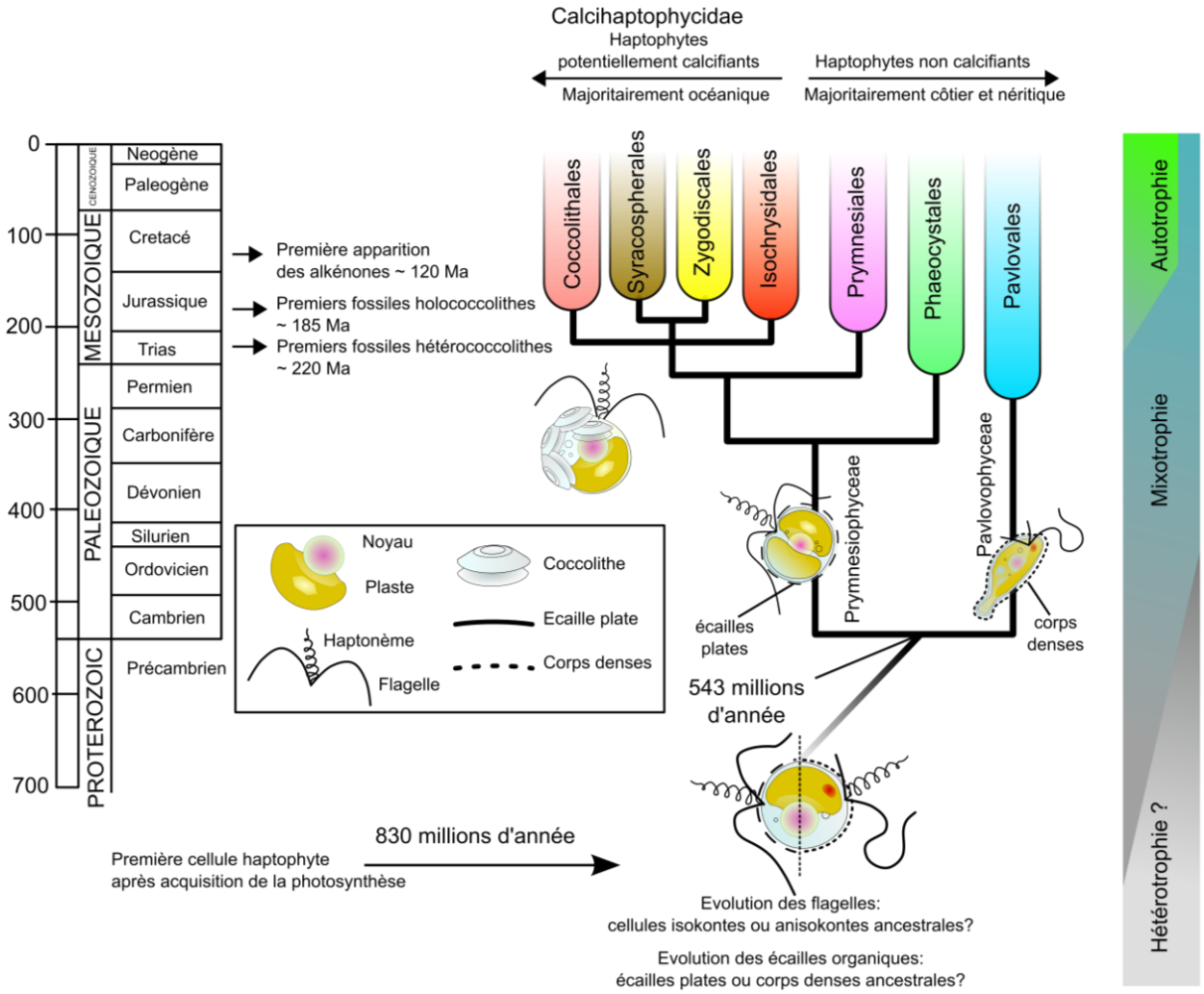

Figure 20. Histoire évolutive des haptophytes (modifiée d'après de Vargas et al. 2007 et Liu et al. 2009). Les traces fossiles des innovations majeures sont présentées le long de l'échelle des temps géologiques (à gauche) en perspective d'un arbre phylogénétique synthétique montrant les principaux ordres du phylum.

La radiation des coccolithophores est à l'origine de quatre ordres distincts au sein des Calcihaptophycideae : les Coccolithales, Syracosphaerales, Zygodiscales et Isochrysidales (Fig. 9, 20). Chacun de ces groupes présente une morphostructure distincte des coccolithes, dont les variations sont la base de clefs de détermination pour l'identification des genres et morpho-espèces. La filiation attribuée au caractère se rapproche des filiations déduites moléculairement. La résolution de ces reconstructions morpho-moléculaires semble limitée par la crise Crétacé/Paléogène (~65 ma), au cours de laquelle la diversité morpho-spécifique des coccolithophores a connu une réduction d'~80% (Fig. 21).

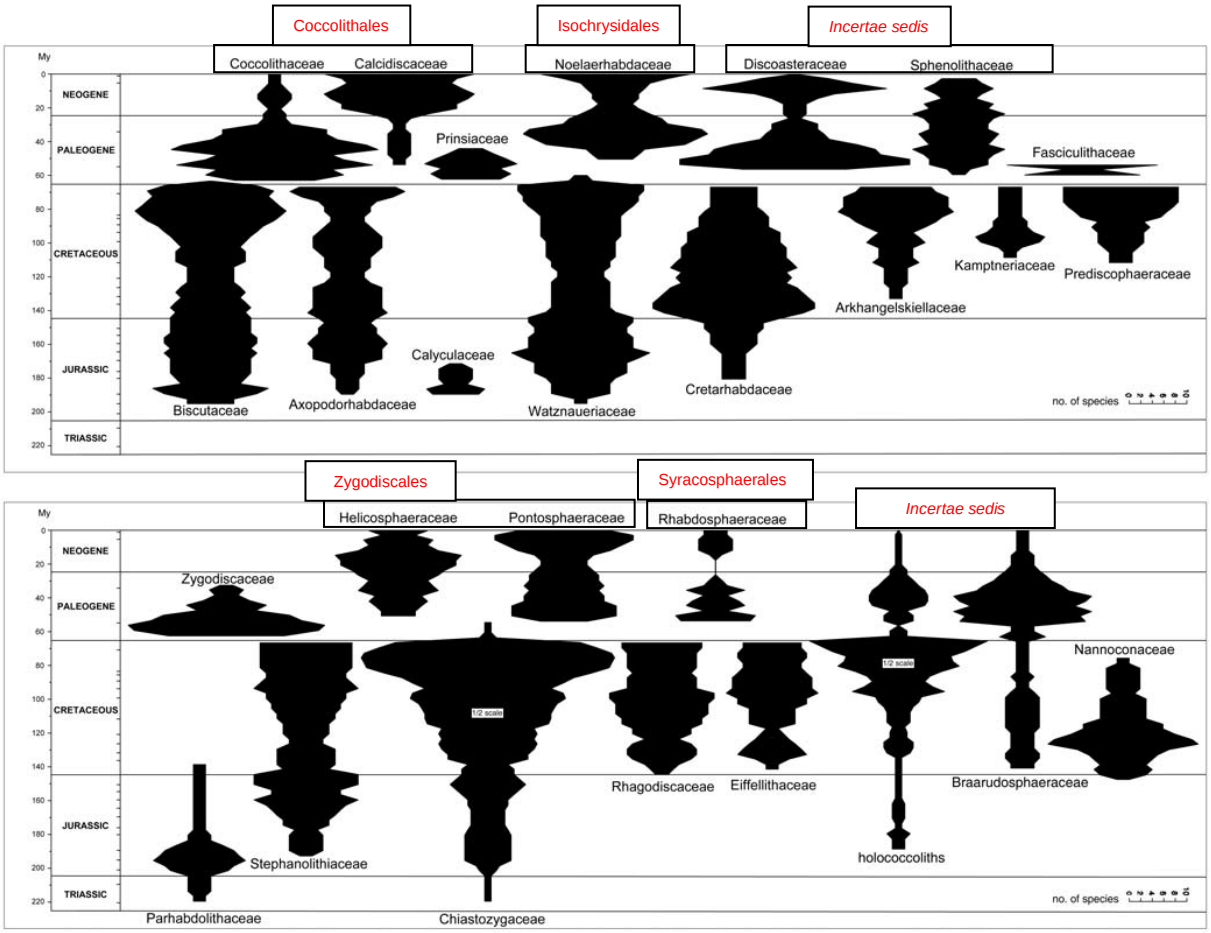

Figure 21. Diagramme en broche indiquant le nombre de morpho-espèces par famille par trois millions d'année d'intervalle. La composition des familles suit les schémas taxinomiques proposés par Bown et Young (1997) et Young et Bown (1997), congruente avec les classifications phylogénétiques d'Edvardsen et al. 2000, Saez et al. 2004 et Liu et al. 2009 des familles actuelles.

Les successions de ces groupes morphologiques coïncident souvent avec les grandes variations environnementales des ères géologiques. Malgré la succession des crises biologiques, les espèces vivants aujourd'hui représentent tous les grands ordres de coccolithophores. Les morpho-espèces *Coccolithus pelagicus* (ex *Coccosphaera pelagica* Wallich 1877) représentant des Coccolithales et *Helicosphaera carterii* (ex *Coccosphaera carterii* Wallich 1877) représentant des Zygodiscales, sont les premières espèces décrites officiellement (en faisant abstraction du cas de *Bathybius haeckelii*). Comme la plupart des espèces modernes, elles ont une répartition biogéographique large. La morpho-espèce *Emiliania huxleyi* de la famille des Isochrysidales est probablement l'espèce cosmopolite la plus jeune, avec un succès évolutif et écologique notable.

Originalité écologique et évolution de l'espèce *Emiliania huxleyi*

Emiliania huxleyi est de loin l'espèce la plus abondante et cosmopolite des coccolithophores vivant dans les océans modernes. Présente dans les eaux côtières et pélagiques de l'océan planétaire, Sous sa forme diploïde, *E. huxleyi* a la capacité de générer des efflorescences printanières massives dans les provinces tempérées et subpolaires des deux hémisphères, à l'origine de masses d'eau "laiteuses" détectables par satellites (Fig. 22). La terminaison de ces efflorescences est contrôlée par la prolifération d'un virus lytique (*EhV*) qui infecte les cellules diploïdes. Alors que la majeure partie des cellules meurt, des transitions méiotiques permettraient de constituer un pool de cellules haploïdes résistantes aux infections virales. L'export massif de coccolithes issus de ces efflorescences vers les fonds marins est un mécanisme fondamental pour la pompe à carbone biologique (Fig. 1).

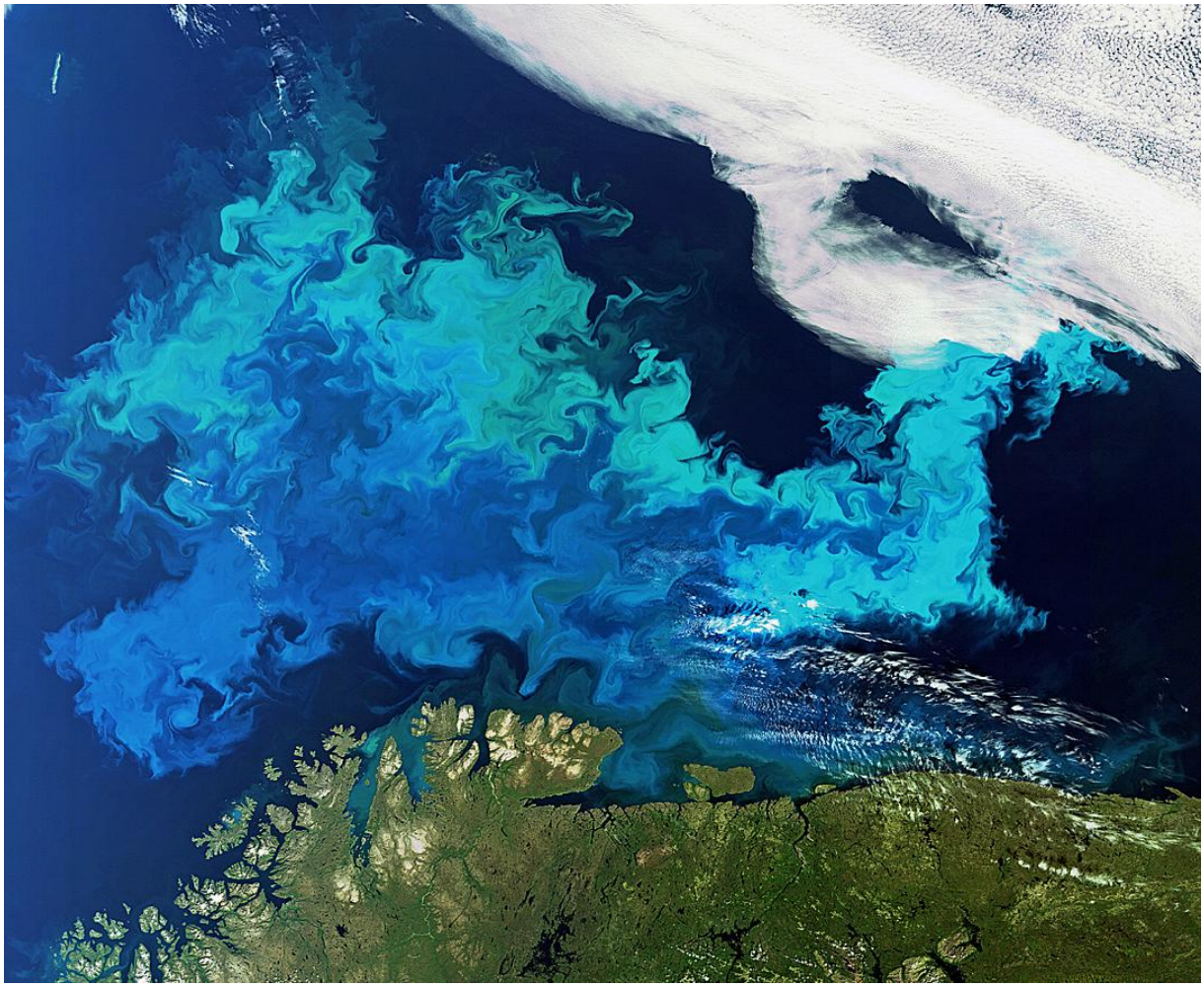

Figure 22. Efflorescence d'*Emiliania huxleyi* au niveau de la mer des Barents (Extrait d'une image acquise *par* le satellite Envisat le 17 août 2011 à 9h25 UTC (ESA))

Comme toutes les autres espèces de coccolithophores, *E. huxleyi* est définie sur des critères morphologiques. Cette morpho-espèce est issue d'un bilan fossile bien documenté sur les 65 dernier millions d'année (Fig. 23A). La plupart des morpho-espèces ancestrales sont éteintes, mais trois genres proches vivant dans l'océan moderne en aurait dérivé: (1) *Reticulofenestra* apparu il y a ~55 millions d'années, avec au moins 4 morpho-espèces connues, (2) *Gephyrocapsa* apparu il y a ~4 millions d'année, comprenant ~5 morpho-espèces et (3) *Emiliania* apparue il y a 291 000 ans (Raffi et al. 2006 ; Fig. 23C), avec 4 morphotypes connus. Ces trois genres forment la famille des Noëlaerhabdaceae au sein de l'ordre des Isochrysidales (voir chapitre 1). Au niveau structural, on dénote l'absence d'un haptonème chez *E. huxleyi,* ainsi que des écailles microfibrillaires en phase haploïde semblables à celles des espèces *Isochrysis galbana* et *Chrysotila lamellosa*.

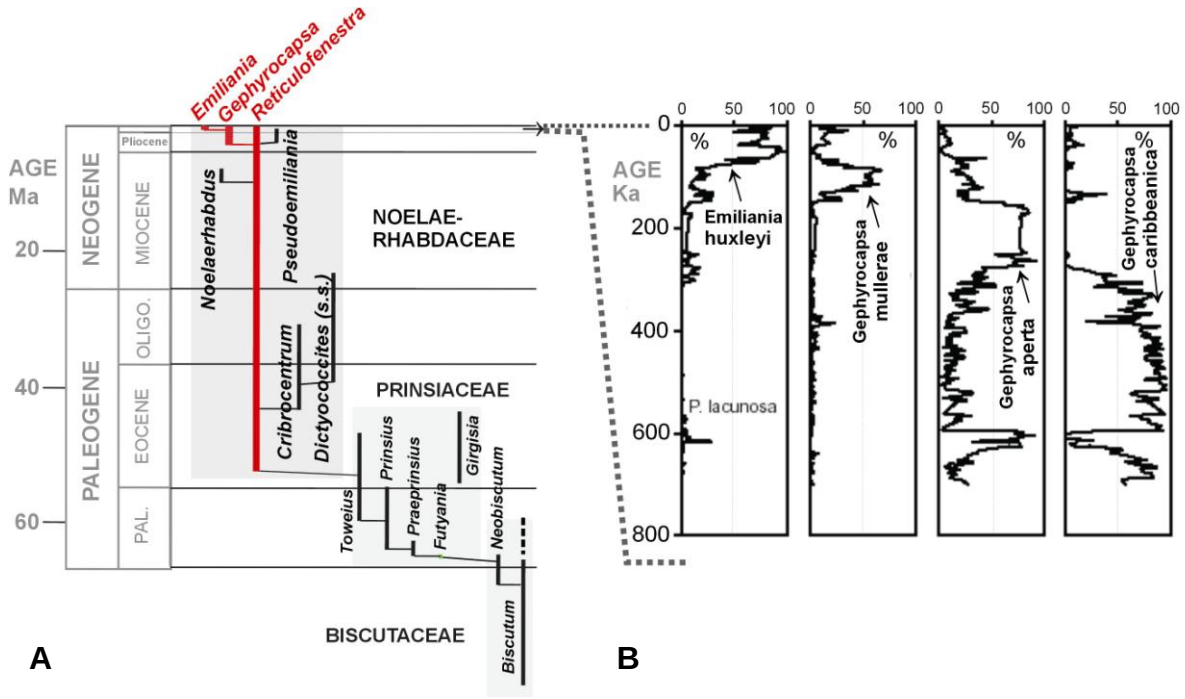

Figure 23. Evolution des Noëlaerhabdaceae et d'*Emiliania huxleyi*. A. Succession des morpho-espèces fossiles à l'origine d'*E. huxleyi*; B. Bilan fossile montrant la succession des dominances aux sein du genre *Gephyrocapsa* et chez l'espèce *E. huxleyi* au cours des derniers 800 000 ans (sédiements de l'Atlantique Nord ; Hine et Weaver 1998).

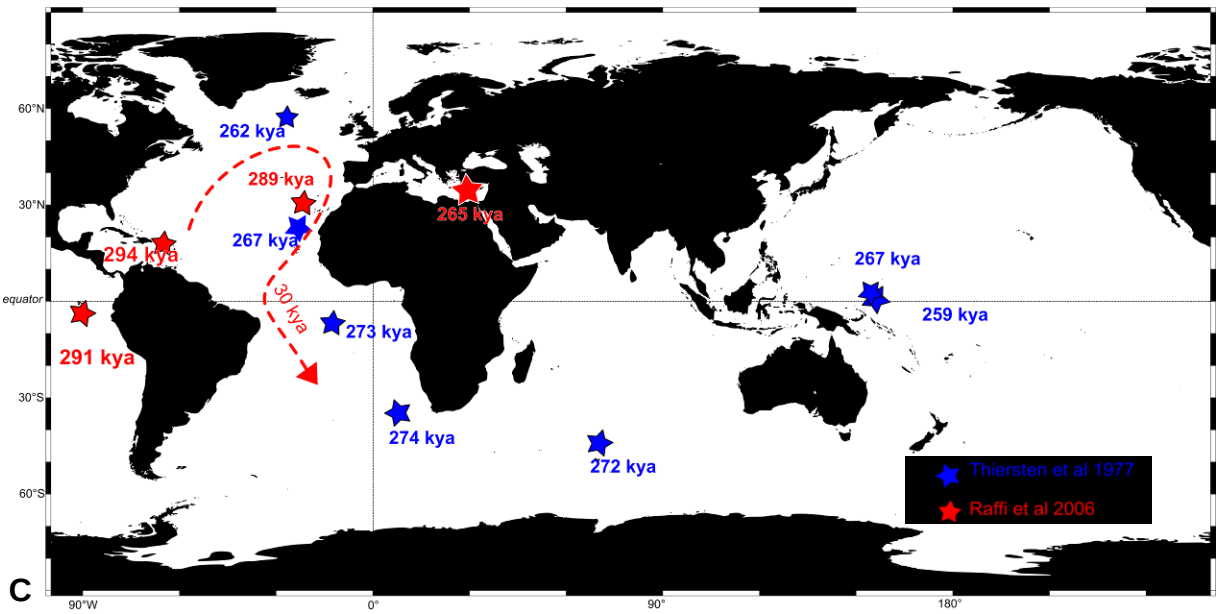

Figure 23 bis. C. Emplacement et dates des carottes sédimentaires présentant les premières occurrences d'*E. huxleyi*. L'occurrence serait synchrone selon Thiersten (1977) et daté à 277 000 ans (bleu), Hine et Weaver (1998) proposent une apparition à 294 000 ans suivie pendant 30 000 ans par une colonisation de l'Atlantique Sud en accord avec Raffi et al. (2006) qui proposent une colonisation du bassin est de la mer Méditerranée à 265 000 ans (rouge).

Les données sédimentaires indiquent que différentes espèces morphologiques du genre *Gephyrocapsa* auraient largement dominé, numériquement, les assemblages nannoplanctoniques du Pléistocène, jusqu'à l'apparition d'*E. huxleyi* ~ 291 000 (Fig. 23B, C). Les analyses morphologiques des échantillons divers d'*E. huxleyi* en microscopie électronique à balayage montrent que cette morpho-espèce, malgré son très jeune âge, se serait diversifiée en au moins 4 variétés morphologiques (morphotypes; Fig. 24), et pourrait même contenir d'autres variants (Young et al. 2003). Le statut biologique et taxonomique de ces morphotypes est peu connu, comme le sont leurs niches écologiques, et leur distribution horizontale (biogéographie) et verticale (hydrographie).

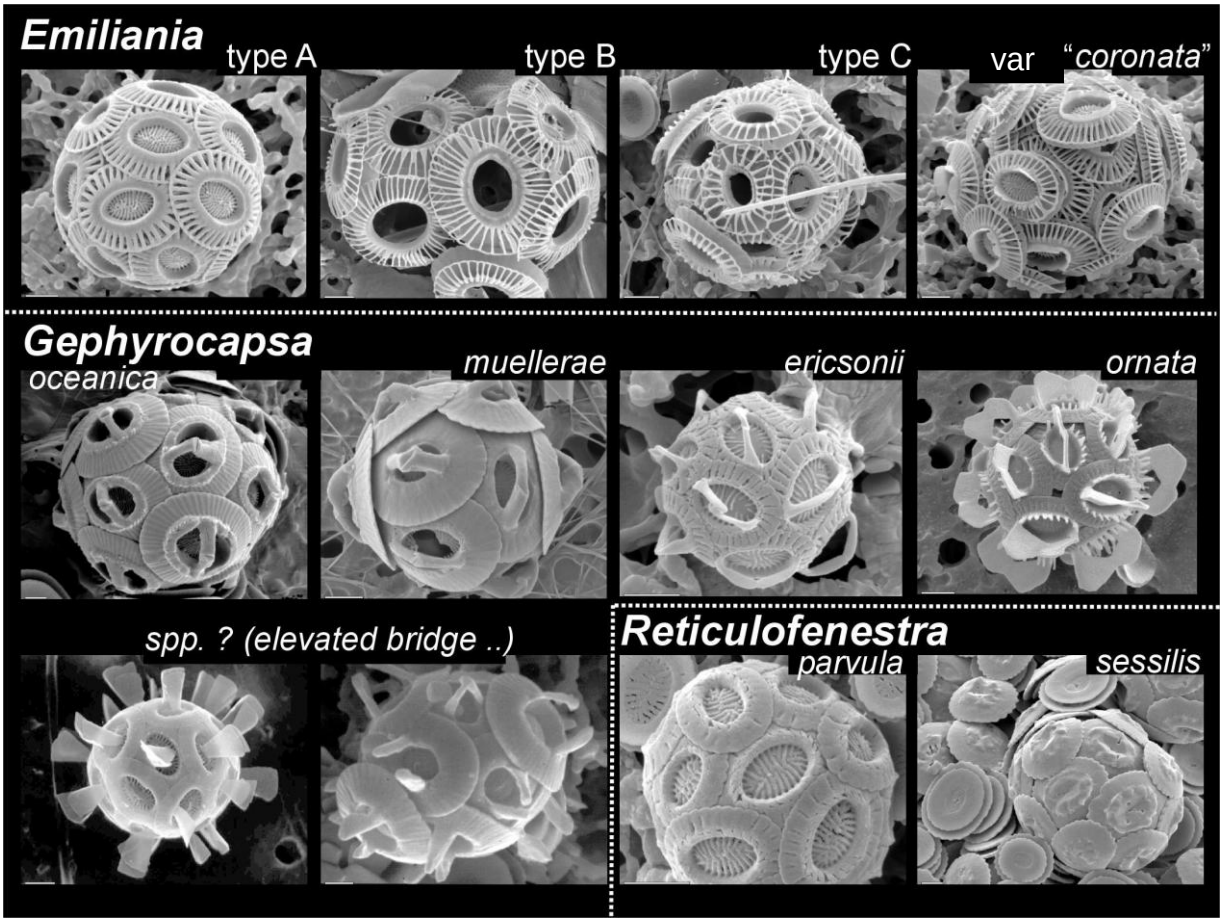

Figure 24. Exemple de variations morphologiques chez *Emiliania huxleyi* et les espèces apparentées. Bien que résultant d'une radiation récente, tous les genres actuels de Noëlaerhabdaceae présentent des morphologies remarquablement différentes qui ont été classifiées en espèces, sous-espèces, variétés ou types différents, selon les auteurs (Photos: Young et al. 2003).

Jusqu'à présent, les analyses génétiques des souches d'*E. huxleyi* n'ont apporté que peu de réponse quant aux facteurs influençant leur diversification morphologique et leur adaptation écologique à l'origine de leur ubiquité. D'une part les marqueurs génétiques traditionnellement utilisés pour discriminer les taxa de microalgues, tels le *18S* nucléaire (Edvardsen et al. 2000), le *16S* chloroplastique ou le gène *rbcL* ne distinguent pas *E. huxleyi* de *G. oceanica* (Fujiwara et al. 2001). Les taux de substitution de l'ADN de ces marqueurs nucléaires et chloroplastiques sont trop lents pour analyser cette radiation évolutive récente. D'autre part, une tentative d'analyse de souches d'*E. huxleyi* de différentes origines géographiques par RAPD (Random Amplification of Polymorphic DNA; Medlin et al. 1996) a généré d'importantes variations génétiques sans distinction d'isolats, particulièrement difficile d'interprétation. Des essais d'analyse par AFLP (Amplified Fragment-Length Polymorphism ; Iglesias-Rodriguez et al. 2002) et marqueurs microsatellites (Iglesias Rodriguez et al. 2006) ont également échoués dans leur capacité de résoudre les patrons

micro-évolutifs chez *E. huxleyi*. La question de la singularité d'*E. huxleyi* par rapport au genre *Gephyrocapsa* persiste. Et si *E. huxleyi* est bien une espèce distincte, est-elle une espèce unique avec une très grande plasticité écologique et phénotypiques, ou plutôt un assemblage d'espèces ou de sous-espèces en cours radiation?

Le manque de discrimination des marqueurs génétiques traditionnels avait déjà été démontré chez d'autres espèces de coccolithophores comme *Calcidiscus leptoporus* et *Coccolithus pelagicus*. *C. leptoporus* et *C. pelagicus* présentent deux morphotypes distincts dont la divergence remonte respectivement à 320 000 ans et à 2 150 000 ans et présentent dans chacun des cas, des séquences 18S identiques (Saez et al. 2003). L'utilisation du gène plastidial *tufa* (codant pour un facteur d'élongation), à taux de substitutions plus élevé, a permit de confirmer la distinction des morphotypes chez ces espèces, morphotypes qualifiés alors d'espèces pseudocryptiques (Saez et al. 2003). Ces exemples montrent qu'au sein d'une morpho-espèce peut exister une diversité génétique et que celle-ci peut être révélée par des marqueurs génétiques évoluant plus vite que les marqueurs conservés. L'utilisation de gènes codant d'origine cytoplasmique est connue pour présentée des avantages sur les gènes ribosomiques nucléaires, sur lesquels la fonction primordiale de traduction imposerait une forte pression de sélection stabilisatrice (purification ; Avise et al. 2000). Les génomes de mitochondrie ou de plaste sont moins régulés et d'avantages soumis aux phénomènes d'oxydations causées par les métabolismes opérant dans ces organelles. Ces génomes fixent plus de substitutions et la conservation de la fonctionnalité des gènes semble assumée par les contraintes sélectives que supposent de tel changement. De plus, la transmission des organelles peut être assurée de manière monoparentale, ce qui accroit la probabilité de fixation d'une mutation. Chez de nombreux protistes, la dégénérescence d'un des organelles surnuméraires s'effectue peu après la formation du zygote. Les génomes organellaires présentent peu de recombinaison et de par leur sensibilité à l'environnement, leur évolution permet de témoigner de la structuration de populations au niveau biogéographique pouvant représenter des événements d'isolement reproductif à l'origine des espèces. Ainsi ces marqueurs semblent intéressants pour l'étude de la microévolution lorsque les marqueurs traditionnels n'apportent aucunes résolutions. Dans le cas d'*E. huxleyi*, l'utilisation du gène chloroplastique *tufA* a démontré une incapacité à la séparer de *G. oceanica*, tout en démontrant un découpage au sein de l'espèce, correspondant en partie a la typologie morphologique classique (Cook et al 2011).

A l'autre extrémité du spectre évolutif, l'isolement et la caractérisation du gène codant pour la protéine *gpa*, potentiellement impliquée dans la calcification chez *E. huxleyi*, a permit de définir un marqueur coïncidant avec les morphotypes. Ce marqueur définit les « Calcification Morphotype Motifs», ou CMMs, qui présentent une certaine distribution selon les morphotypes (Schroeder et al 2005).

Tableau 2. Distribution des CMM selon les morphotypes d'*E. huxleyi*

Morphotypes d'*E. huxleyi*	CMM
A	I III IV
Type R	?
var. *corona*	?
Type B	II
Type B/C	?
Type C	?

Le profil CMM reste inconnu pour certains morphotypes dont les représentants sont peu présents dans les isolats des collections de cultures. Ceci illustre un autre problème : la difficulté à isoler et cultiver certaines souches d'*E. huxleyi*. L'utilisation de ce marqueur sur des extractions d'ADN environnemental a démontré que d'autres CMMs existent, sans que l'on puisse leur attribuer un morphotype (Ripley et al 2007). Les connaissances restent encore limitées sur ce gène. La recherche de nouveaux isolats représentant les morphotypes manquant pourrait permettre d'estimer la diversité et l'évolution des CMMs. Il faudrait aussi comprendre la fonction de ce gène, qui pourrait coder pour une protéine servant de support a la nucléation des ions Ca2+ au cours de la coccolithogénèse (Cortjens et al 1998). Quoi qu'il en soit, les données *gpa* et *tufa* suggèrent que la polymorphie de l'espèce *E. huxleyi* est l'expression d'une variabilité génétique potentiellement assimilable à un pseudocrypticisme. L'isolement reproductif de ces catégories morphologiques reste néanmoins à tester ou à confirmer afin de statuer de leur définition d'espèce ou de sous espèces, ceci entre et dans les genres *Emiliania* et *Gephyrocapsa*.

Problématique et objectif :

De part son importance écologique, le coccolithophore *Emiliania huxleyi* est une espèce modèle, quasi-emblématique du phytoplancton océanique. L'acidification des océans liée à l'augmentation du CO2 atmosphérique, et l'impact que ce phénomène pourrait avoir sur

le phytoplancton, la calcification et les cycles biogéochimiques sont particulièrement étudiés à partir de cette espèce (Riebsell et al. 2000 ; Iglesias Rodrigez et al. 2007). Les données polémiques suggèrent que nos connaissances sur les réponses physiologiques et les adaptations d'*E. huxleyi* face aux changements environnementaux sont limitées par la méconnaissance évolutive du modèle lui-même (Langer et al. 2009). Quelle est la définition de l'espèce chez *E. huxleyi*? Peut-elle être limitée à son concept morphologique ou être démultipliée par ces morphotypes/CMMs ou par une structuration génétique indépendante? Dès lors, quelle valeur et consequence évolutive et adaptative pouvons-nous accorder aux démultiplications du concept *E. huxleyi* ?

Le concept biologique d'espèce étant peu applicable pour la plupart des coccolithophores, le concept typologique (englobant le concept morphologique) a souvent été adopté. L'utilité paléontologique des coccolithophores a combiné l'utilisation de ce concept à celui d'espèces évolutives : « une espèce évolutive est une lignée, une séquence de populations ancêtres-descendants, qui se développe séparément des autres, avec son propre rôle évolutif unitaire et ses tendances » (Simpson 1961). Ce concept définit l'espèce en tant que lignée phylétique et s'applique facilement aux populations isolées sans pour autant expliciter le « rôle unitaire » ni pourquoi les lignées phylétiques ne se croiseraient pas entre elles. L'avènement des phylogénies moléculaires et la génétique des populations a permis une nette amélioration de ce concept, qui peut rejoindre l'assomption clef du concept biologique de l'espèce, définissant la lignée en tant qu'entité conservant son pool de gènes, dont la distribution des variations allèliques témoigne de l'hybridation au sein des espèces.

Le concept typologique classiquement utilisé chez les Noëlaerhabdaceae a produit de nombreuses descriptions morphologiques fossiles qui semblent se confondre chez certaines espèces de *Gephyrocapsa.* Ces confusions seraient dues à l'utilisation arbitraire de certains caractères morphologiques et surtout à l'apparition et à la disparition de morphostructures similaires au cours du temps évolutif. Le concept morphologique trouve donc ses limites dans l'arbitraire de l'observateur et de l'observation, contraints par la technique parfois peu résolutive, ainsi que les connaissances et les concepts en vigueur. L'historique des coccolithophores souligne cette assomption qui reflète la difficulté à définir les espèces de protistes tout en étudiant leur importance écologique et évolutive (cf. partie 2). Au vue des cas précité de *C. leptoporus* et *C. pelagicus*, il est fort probable que le concept morphologique des *Gephyrocapsa* soit dépassé par les données génétiques. Tel que Bollmann en 1997 le conçoit, les différenciations au sein de ce genre démontrent des variations qui semblent continues sur

l'ensemble des caractères étudiées, pouvant refléter une variabilité génétique bien plus elevée que l'on ne le pense (de Vargas et al. 2004).

Dans ce travail, nous avons cherche à redéfinir le concept de lignée évolutive et d'espèce chez *Emiliania huxleyi*, par une approche macro- a micro-évolutive, basée sur l'étude de caractères morphogénétiques. Nous présenterons les résultats en six chapitres, ayant fait l'objet d'articles scientifiques publiés, soumis, ou en préparation.

Chapitre 1 : Nous y proposons une phylogénie compréhensive de l'ordre contenant *Emiliania huxleyi*, à savoir, les Isochrysidales. Cette phylogénie oriente la révision des caractères morphologiques de l'ordre, mettant en perspective les concepts d'espèces classiquement mis en œuvre pour l'établissement d'une taxinomie compréhensive. La question de la distinction des genres *Emiliania* et *Gephyrocapsa* y est posée. L'histoire taxinomique complexe de ces espèces, doublée des données phylogénétiques et ultrastructurales démontrant une singulière similarité entre les deux espèces, suggère que la nomination *Emiliania huxleyi* serait synonyme de *Gephyrocapsa huxleyi*. (Article soumis dans la revue Protist)

Chapitre 2 : La mise en place des outils nécessaires à l'étude de la microévolution chez *E. huxleyi* requiert l'évaluation de divers marqueurs génétiques à taux de substitution rapide. La comparaison des marqueurs nécessite leur séquençage chez un nombre suffisant de souches de Noëlaerhabdaceae, afin de mesurer leur taux de substitution relatifs et leur phylogénie moléculaire respective. Suivant leur capacité discriminative et leur facilite d'utilisation, ces nouveaux marqueurs peuvent jouer le rôle de 'barcodes', des outils simples pour la détection et quantification des espèces dans leur milieu naturel, favorisant la mutation d'une taxinomie nominative vers une taxinomie moléculaire. (Article en préparation)

Chapitre 3 : L'utilisation du gène mitochondrial *cox1* permet de définir une structuration biogéographique de souches d'Emiliania huxleyi en provenance de l'océan global. Cette trame eco-évolutive permet la définition d'un nouveau morphotype, « O » proche du morphotype B, et exclusivement present dans les zones tempéré et polaires. (Article publié dans *Journal of Phycology*)

Chapitre 4 : La variabilité de la calcification d' *E. huxleyi* sur la fin des glaciations est mesurée par la comparaison des morphologies de l'espèce et démontre une tendance générale

des Noëlaerhabdaceae à la décalcification en liaison avec l'augmentation du CO_2 atmosphérique. Paradoxalement, certaines formes semblent plus calcifiées dans les zones les plus acides de l'océan mondial. La proportion de ces formes augmente en fonction de l'acidité du milieu. Cette hyper-calcification semble être liée à des profils génétiques particuliers, suggérant un phénomène d'adaptation aux milieux les plus acidifiés. (Article publié dans *Nature*)

Chapitre 5 : La comparaison des génomes et des transcriptômes de certaines souches de E. huxleyi a permit de mettre en évidence la perte de gènes fondamentaux à l'établissement de la phase haploïde. Ceux-ci concernent la fonction flagellaire nécessaire à la syngamie. La recherche de ces gènes a pu mettre en évidence le fait que ces gènes seraient absents en majorité chez les souches provenant de milieux oligotrophes. La faible pression biologique ne permettrait pas de maintenir au fil des générations la reproduction sexuées chez ces individus. Il est résulterait une potentielle baisse de l'adaptabilité sur le long terme chez ces populations. (Article en préparation)

Chapitre 6 : L'analyse des marqueurs mitochondriaux sur les espèces sœurs au sein des gephyrocapsides permet l'établissement d'un scenario de spéciation d'*Emiliania huxleyi* au sein des Noëlaerhabdaceae. Une analyse phylogénétique par horloge moléculaire semblent démontrer la sensibilité des espèces au changement climatiques rapides causés par les cycles de glaciations sur les derniers 400 000 ans. Le couplement de ces marqueurs aux CMMs dévoile l'esquisse d'une trame évolutive complexe des morphotypes, supposant une évolution rapide de ces derniers. (Article en préparation)

Annexe 1: Cette etude présente le projet de Master 2 de Julien Laurent sur la phylogéographie des Noëlaerhabdaceae en Mer Mediterranée. La construction de librairie de clones basées sur le gène *cox1* nous a permit d'en tester la validiter dans le cadre de la detection moleculaire environnementale des Noëlaerhabdaceae. Le cas de la mer Mediterranée démontre une diversité génétique associée à des préférences trophiques potentielles. L'utilisation prometteuse de cet outil moleculaire permettrait d'établir une surveillance environnementale des populations à une plus grande echelle.

Annexe 2 : La révision taxonomique de la classe des Pavlovophyceae intégre les approches cytomorphologiques et moléculaires (phylogénie et pigments photosynthétiques). L'apport de

cette étude à la compréhension de l'évolution des Prymnesiophyceae et donc des haptophytes est fondamental. Cette étude est présentée ici en annexe comme un écho à l'introduction et au chapitre 1, la problematique qu'il pose étant liée aussi au probleme du concept d'espèce chez les protistes. La classe des Pavlovophyceae a souvent aussi été décriée comme étant proche des Isochrysidales pour différents traits comme nous l'avons mentionné dans l'introduction. Nous avons préferé maintenir la position de cette article en annexe par soucis de cohérence avec le cadre général des Isochrysidales. (Article publié dans *Protist*)

CHAPITRE 1

SYSTEMATICS OF THE HAPTOPHYTE ORDER ISOCHRYSIDALES

El Mahdi Bendif[1], Ian Probert[2], Jeremy R. Young[3], Declan C. Schroeder[4] and Colomban de Vargas[1]

[1]CNRS-UPMC (Université Paris-06), UMR 7144, Groupe Plancton, Station Biologique de Roscoff, 29682 Roscoff cedex, France

[2]CNRS-UPMC (Université Paris-06), FR2424, Station Biologique de Roscoff, 29682 Roscoff cedex, France

[3]Paleontology Department, The Natural History Museum, London SW7 5BD, UK

[4]Marine Biological Association of the United Kingdom, Citadel Hill, Plymouth, Devon, PL1 2PB, UK

Abstract

The Isochrysidales is a haptophyte order which contains some well-known species, most notably the bloom-forming *Emiliania huxleyi* which is the model organism for coccolithophore research and the non-calcifying *Isochrysis galbana* which is widely used as a food source in aquaculture. The order contains two extant families, the Isochrysidaceae and the Noëlaerhabdaceae, each containing three extant genera. The existing taxonomy within this order is based exclusively on morphological and ultrastructural characters of the cell, and in the case of the Noëlaerhabdaceae of the coccoliths covering the cell. In order to assess the validity of the existing taxonomic scheme, a phylogeny based on sequences of nuclear SSU and LSU rDNA and mitochondrial cytochrome oxidase 1 (cox1) genes of a range of culture strains (including authentic strains when available) was constructed and compared with cytological and ultrastructural observations. The isochrysidaceaen culture strain *Isochrysis* affinis *galbana* (Tahiti isolate), commonly known as T-Iso, is clearly genetically distinct from *I. galbana*, despite effectively being identical in terms of morphology. By contrast, within the Noëlaerhabdaceae, the SSU rDNA sequences of *Emiliania huxleyi* and *Gephyrocapsa oceanica* are identical and the LSU rDNA sequences differ by a single nucleotide. No significant ultrastructural differences were found between the two species, either in the calcifying diploid stage or the non-calcifying haploid phase. The taxonomic revision of this order requires an unusual mix of compromises in order to reflect both genetic and morpho-structural differentiation while remaining of practical utility. One new genus (*Tisochrysis* gen. nov.) is erected and two new species (*T. lutea* sp. nov., *Isochrysis nuda* sp. nov.) are described. *Dicrateria inornata* is shown to be a member of the Prymnesiales and *Imantonia rotunda* transferred into this genus (*D. rotunda* comb. nov.).

Key words: coccolithophores, *Emiliania huxleyi, Gephyrocapsa oceanica*, Isochrysidales, *Isochrysis galbana*, phylogeny, taxonomy, ultrastructure

Introduction

The coccolithophore *Emiliania huxleyi* is one of the most abundant and widely distributed unicellular photosynthetic eukaryotes in modern oceans (Brown and Yoder 1994). Coccolithophores (Prymnesiophyceae, Haptophyta) produce composite cell coverings of minute calcite platelets (coccoliths) and consequently have been key contributors to both the oceanic carbon pump and counter-pump, and thus to the flux of CO_2 between the atmosphere and oceans (Rost and Riebesell 2004), since their origin in the Triassic. The impact of predicted anthropogenically-induced ocean acidification on coccolithophores, and particularly on *E. huxleyi*, is a subject of intense debate, with culture experiments demonstrating variable, strain-specific response patterns to CO_2 perturbation (e.g. Iglesias-Rodriguez et al. 2008; Langer et al. 2009; Riebesell et al. 2000). Despite the fact that understanding of the genetic basis of calcification is in its infancy (Mackinder et al. 2010), focus is now turning to attempting to predict future evolutionary adaptability through the study of genotypic variability within and between extant populations and/or morphotypes, a field in which metagenomic surveys will likely become increasingly predominant in coming years. The existence of a robust taxonomic framework should be considered to be a prerequisite for any such study of environmental diversity. Often, however, existing taxonomic schemes were established decades ago based on morphological and ultrastructural comparison of organisms and are yet to be updated in the light of molecular genetic data from cultured representatives. This is the case in the Isochrysidales, the prymnesiophycean order to which *E. huxleyi* and related coccolithophores belong.

The Prymnesiophyceae contains six described extant orders, four of which are grouped within the sub-class Calcihaptophycideae, a clade in which all prymnesiophytes that use organic plate scales as a substrate for calcification (i.e. the coccolithophores) are found (de Vargas et al. 2007). While the vast majority of known calcihaptophytes calcify in at least one life cycle phase, the order Isochrysidales is unusual in being composed of both calcifying species and species with no known calcifying stage. The order, a monophyletic clade that branches early in the evolution of the Calcihaptophycideae (e.g. Sáez et al. 2004; Medlin et al. 2008), contains two families: the Isochrysidaceae that contains exclusively non-calcifying organisms, and the Noëlaerhabdaceae that contains taxa that calcify in one life cycle phase, including the widespread coccolithophores *E. huxleyi* and *Gephyrocapsa oceanica*. The current taxonomy of extant Isochrysidales is shown in Table 1.

Table 1. Current taxonomy of extant Isochrysidales (bold = type genus or type species; * The type for the family Noëlaerhabdaceae is the fossil genus *Noëlaerhabdus* Jerkovic. ** The type for *Reticulofenestra* is the fossil species *R. caucasica* Hay, Mohler et Wade.

Order	ISOCHRYSIDALES (Pascher 1910) Edvardsen and Eikrem 2000		
	Family	ISOCHRYSIDACEAE (Bourrelly 1957) Edvardsen and Eikrem 2000	
		Genus	*Chrysotila* (Anand 1937) Green and Parke 1975
			Chrysotila lamellosa (Anand 1937) Green and Parke 1975
			***Chrysotila stipitata* (Anand 1937) Green and Parke 1975**
		Genus	*Dicrateria* Parke 1949
			Dicrateria gilva Parke 1949
			***Dicrateria inornata* (Parke 1949) Green and Pienaar 1977**
		Genus	***Isochrysis* (Parke 1949) Green and Pienaar 1977**
			***Isochrysis galbana* (Parke 1949) Green and Pienaar 1977**
			Isochrysis litoralis Billard et Gayral 1972
	Family	NOËLAERHABDACEAE * (Jerkovic 1970) Young and Bown 1997	
		Genus	*Emiliania* Hay and Mohler 1967
			***Emiliania huxleyi* (Lohmann 1902) Hay and Mohler 1967**
		Genus	*Gephyrocapsa* Kamptner 1943
			Gephyrocapsa crassipons Okada and McIntyre, 1977
			Gephyrocapsa ericsonii McIntye and Bé 1967
			Gephyrocapsa muellerae Bréhéret 1978
			***Gephyrocapsa oceanica* Kamptner 1943**
			Gephyrocapsa ornata Heimdal 1973
		Genus	*Reticulofenestra* ** Hay, Mohler and Wade 1966
			Reticulofenestra maceria (Okada and McIntyre, 1977) Young 2003
			Reticulofenestra parvula (Okada and McIntyre, 1977) Biekart, 1989
			Reticulofenestra punctata (Okada and McIntyre, 1977) Jordan and Young, 1990
			Reticulofenestra sessilis (Lohmann, 1912) Jordan and Young, 1990

The Isochrysidales are unique in producing alkenones (Marlowe et al. 1984), a suite of long-chain (C_{37}-C_{39}) unsaturated methyl and ethyl ketones that are resistant enough to be retained in ancient sediments. The chemical structure of these lipids varies as a function of growth temperature (Conte et al. 1994): the ratio of the diunsaturated C_{37} methyl ketone ($C_{37:2}$) versus the triunsaturated homologue ($C_{37:3}$) (expressed as $U^{K'}_{37}$ = [$C_{37:2}$] / [$C_{37:3}$ + $C_{37:2}$]) linearly correlates with growth temperature and can be used as a paleothermometer (Brassell et al. 1986; Marlowe et al. 1984). Sedimentary coretop $U^{K'}_{37}$ has been widely adopted by geochemists as a proxy for past sea surface temperature (e.g. Müller et al. 1998). The first appearance of alkenones in the sediment archive extends down to the mid-Cretaceous at ca. 120 Ma (Brassell and Dumitrescu 2004), suggesting that the evolutionary origin of the Isochrysidales occurred at or before this period, a theory supported by molecular clock studies that have dated the divergence of this order within the Calcihaptophycideae

within the range 203-119 Ma (Liu et al. 2010).

While there are no obvious synapomorphic structural characters of the order as a whole, in comparison with other prymnesiophytes, members of the order Isochrysidales typically have relatively simple flagellar roots, a haptonema that is reduced, and organic scales with simple ornamentation. In certain species currently classified as isochrysidaleans, one or other of the latter two characters (haptonema, scales) may even be absent.

The non-calcifying Isochrysidaceae contains species known mainly from near-shore coastal and estuarine environments. Members of this family occur as motile biflagellate and/or non-motile mucilage-covered forms, the former being dominant in the genera *Isochrysis* and *Dicrateria*, and the latter dominating in *Chrysotila*. Strains of *Isochrysis galbana*, the type species of the genus *Isochrysis*, as well as a widespread culture isolate from Tahiti designated *I.* affinis *galbana* (commonly named "T-Iso"), are widely used as feedstocks in bivalve aquaculture (Bougaran et al. 2003; Brown et al. 1993; Jeffrey et al. 1994) and have consequently been the focus of studies on the ecophysiology of lipid production (Conte et al. 1994; O'Shea et al. 2010). In contrast to *I. galbana* and T-Iso, other isochrysidaceaen species have received little attention since their original descriptions. Culture isolates of several taxa have been included in screening for alkenones (Marlowe et al. 1984) and extracellular calcification has been described in *Chrysotila* (Green and Course 1983).

The other extant isochrysidalean family, the Noëlaerhabdaceae, comprises exclusively pelagic species that typically inhabit open ocean environments. This family includes the extant genera *Emiliania*, *Gephyrocapsa* and *Reticulofenestra*. Coccolith-bearing cells of these three genera are non-motile and have placolith-shaped coccoliths with a distinctive structure in which both the proximal and distal shields are composed of a single cycle of elaborately modified calcite crystals with sub-radially oriented *c* axes, i.e. R-units in the terminology of Young (1992). V-units, calcite crystals characterized by sub-vertically oriented *c* axes, are present in the proto-coccolith ring but are not developed in the fully formed coccolith (Young 1992; Young et al. 2004; Fig. 1). *Emiliania huxleyi* is known to undergo a haplo-diplontic life cycle, the diploid coccolith-bearing cells alternating with haploid cells that are motile and covered by non-mineralized organic scales (Green et al. 1996; Klaveness 1972a, 1972b). *Emiliania huxleyi* has long been a model species for culture-based ecophysiological studies (Westbroek et al. 1993; Paasche 2002) and this status has recently been reinforced by establishment of genetic resources including EST libraries (von Dassow et al. 2009; Wahlund et al. 2004) and a full genome sequence (http://genome.jgi-

psf.org/Emihu1/Emihu1.home.html). From morphological evidence it has been hypothesised that *Emiliania* evolved from the *Gephyrocapsa* complex via *G. protohuxleyi* (McIntyre 1970), a taxon often considered to be a con-specific variant of the extant species *G. ericsonii* (e.g. Cros and Fortuno 2002; Young et al. 2004). The first occurrence of *Gephyrocapsa* in the fossil assemblage is estimated at around 3.6 Ma and members of this genus frequently dominated coccolithophore assemblages from about 1.7 Ma. *Emiliania huxleyi* first occurred around 270 ka and dominates most nannofossil assemblages from about 85 ka (Thierstein et al. 1977). *Gephyrocapsa* and *Emiliania* are distinguished on the basis of coccolith morphology (presence/absence of a bipartite bridge across the central area of the coccolith), but genetic studies have revealed that *G. oceanica* and *E. huxleyi* have identical sequences for the SSU rDNA gene (Edvardsen et al. 2000) and the rbcL gene (Fujiwara et al. 2001). *Emiliania huxleyi* has a number of apparently unique or unusual ultrastructural features (e.g. in the diploid phase a characteristic reticular body of Golgi origin involved in coccolithogenesis and lack of non-mineralized body scales underlying coccoliths; in the haploid phase a refractive body termed the 'X-body', see Paasche 2002 and references therein). Since the cytology and ultrastructure of other members of the Noëlaerhabdaceae has never been reported, it is not clear whether these features are unique to the genus or common to the family.

In this study, a taxonomic reassessment of the order Isochrysidales is proposed, based on a combination of new morphological and ultrastructural observations and a molecular phylogenetic reconstruction based on sequences of the ribosomal SSU and LSU genes and the mitochondrial cytochrome oxidase 1 (cox1) gene. Where possible, this study was based on the use of authentic (including type) culture strains. The study revealed notable inconsistencies in the existing taxonomic scheme and the existence of taxa that we believe should represent one new genus and two new species that are described here. The proposed taxonomy provides a phylogenetic scheme of evolution that can form the framework for future studies on the biodiversity, biogeography and microevolution of members of this order.

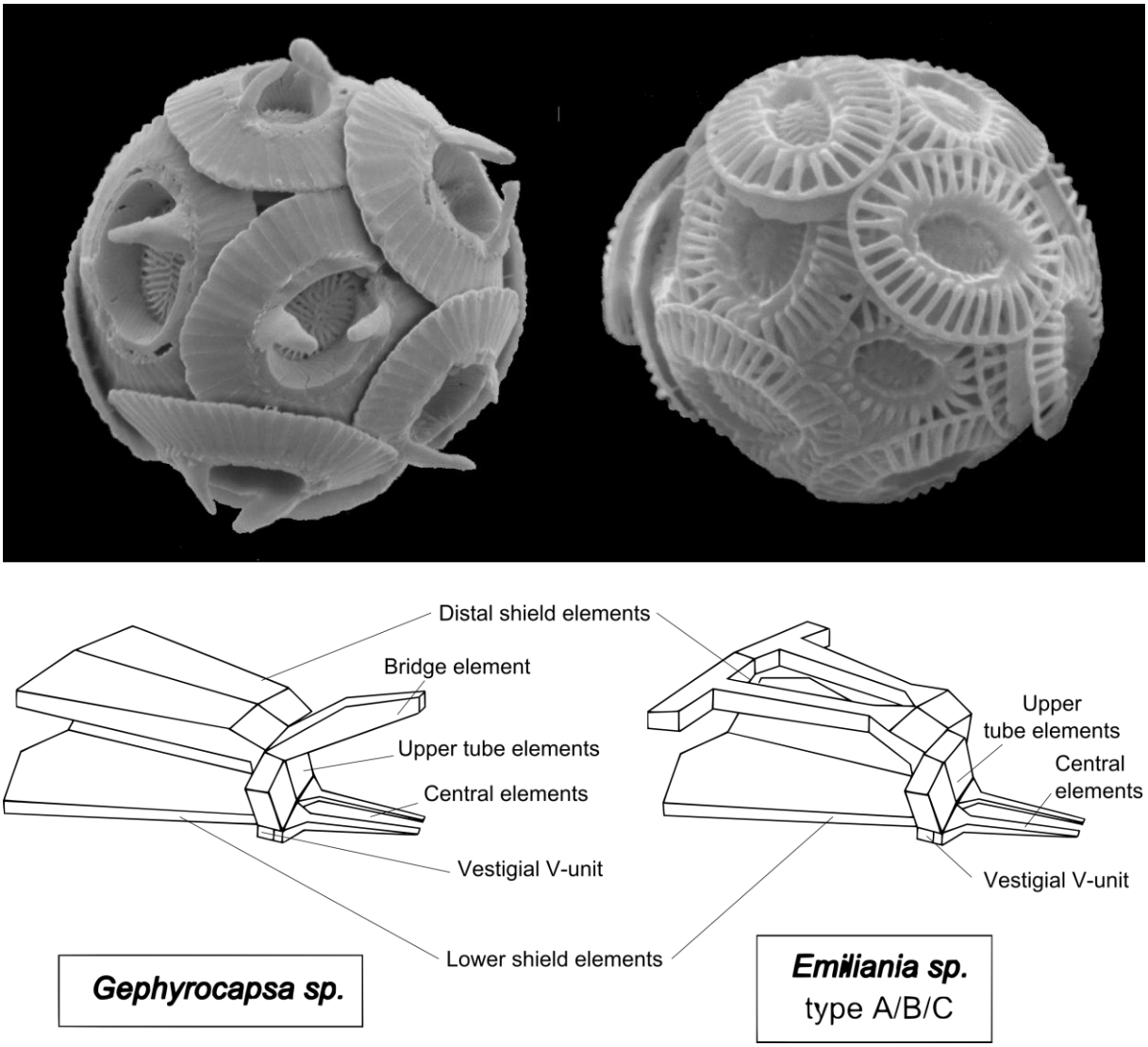

Figure 1. Coccolith structure of Noëlaerhabdaceae redrawn from Young (1992).

Results

Molecular phylogenies

The topology of the maximum likelihood tree inferred from concatenated sequences of the three genes (SSU and LSU rDNA, cox1) was similar to the phylogenetic reconstructions inferred from each individual gene. Bayesian analyses yielded the same overall topology. The tree consists of two strongly supported clusters corresponding to the family level separation of the Isochrysidaceae and Noëlaerhabdaceae (Fig. 2).

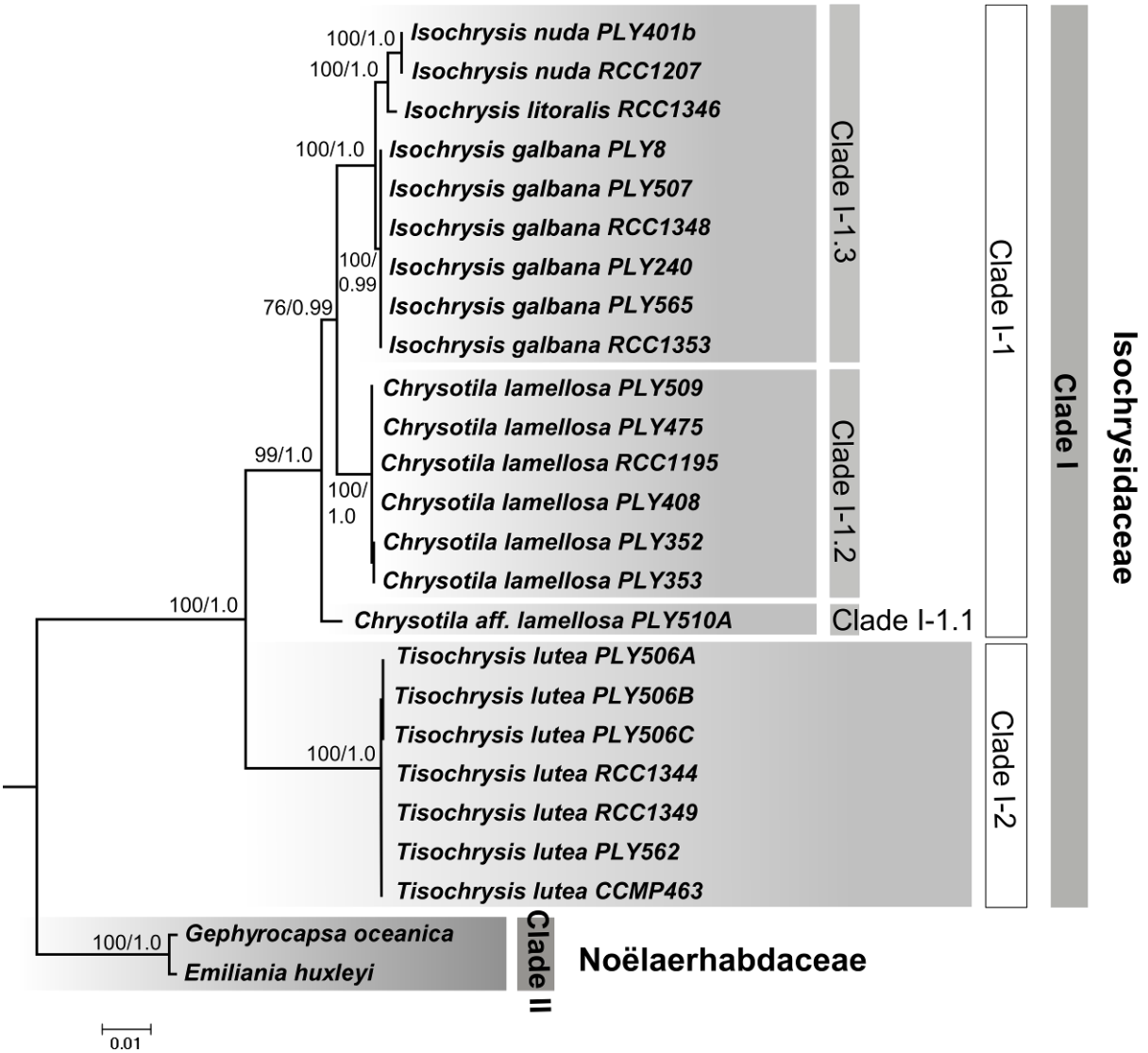

Figure 2. Phylogenetic tree of the Isochrysidales, inferred from concatenated sequences of SSU rDNA, LSU rDNA and cox1 genes. Bootstrap values and posterior probabilities for Maximum Likelihood and Bayesian analyses, respectively, are given at each node of the tree. Sequences of *Phaeocystis globosa* were used as the outgroup. The original species name and strain codes are given in Table 2.

Within the Isochrysidaceae, two main clades, I-1 and I-2, are statistically strongly supported. Clade I-1 is subdivided into three sub-clades with high bootstrap support: clade I-

1.1 composed of the uncharacterized strain PLY510A; clade I-1.2 regrouping sequences from several strains of *Chrysotila lamellosa* and *Chrysotila* sp., and clade I-1.3 with all *Isochrysis galbana* strains, *Pseudoisochrysis paradoxa* RCC1353, *Isochrysis litoralis* RCC1346, *Dicrateria* sp. RCC1207 and *Isochrysis* sp. PLY401B. Clade I-2 consists of the *Isochrysis* affinis *galbana* Tahiti isolate (RCC1349) which had sequences identical to three other T-Iso-like strains (PLY562, RCC1344 and CCMP463), and a short branch supported by a bootstrap value and posterior probability of 70% and 0.98 (not shown), respectively, defining three undescribed strains (PLY506A, PLY506B, PLY506C). Of the three genes sequenced, these latter strains differed from the T-Iso strains by a single nucleotide substitution in the SSU rDNA sequence. In trees constructed using distance methods (SFig. 1), *Chrysotila* sp. PLY510A grouped with *C. lamellosa*, introducing a degree of doubt as to the phylogenetic position of this sub-clade. The clustering of the PLY510A strain was tested by comparing the best ML tree without constraint versus a ML tree constrained with an alternative topology, where PLY510A was part of Clade I-1.2. In the constrained ML tree, the bootstrap support value was very low (19%) for the tested hypothetical clade (SFig. 2), with no support from the likelihood and topology test values (table 3). The SSU rDNA sequence of strain PLY564, the authentic culture of *Dicrateria inornata*, falls outside the Isochrysidales, being nearly identical to sequences of *Imantonia rotunda* (Prymnesiales; Fig. 3). The SSU rDNA sequences of all three strains designated as *Chrysotila stipitata* (including the two strains PLY377 and PLY432 studied by Green and Parke 1975 and considered to be authentic) had closest BLAST hits (97% similarity) to the pinguiophyte *Glossomastix* and are not included in Fig. 2.

The Noëlaerhabdaceae is composed of sequences from *E. huxleyi* and *G. oceanica*. While SSU rDNA sequences of the two genera were identical, one single position varied between them in the LSU rDNA gene sequences. The cox1 gene sequences exhibited up to 2.1% divergence between *Emiliania* and *Gephyrocapsa*, with clear delineation of the two taxa.

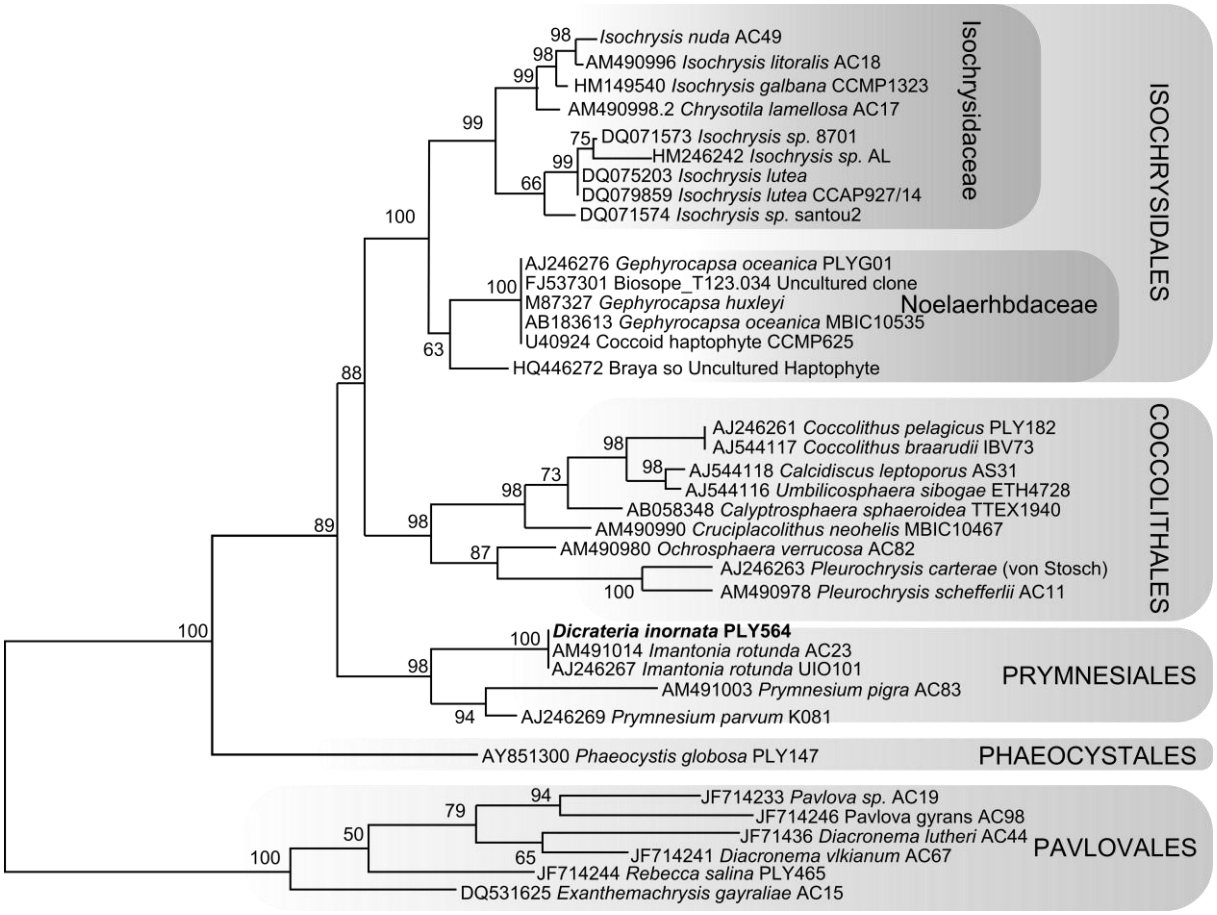

Figure 3. Maximum likelihood tree inferred from haptophytes SSU rDNA sequences. Bootstrap values are given at each node of the tree. As indicated in bold, the sequence of *Dicrateria inornata* PLY564 clusters with sequences of *Imantonia* in the Prymnesiales. Pavlovales sequences were used as the outgroup.

Morphological observations

***Chrysotila* affinis *lamellosa* PLY510A (Fig. 4):** The shape and size of the golden brown cells of this strain varies depending on culture conditions. In old cultures, cells are typically spherical, measure between 6 - 7 µm, and are solitary and non-motile. After inoculating these cells into fresh medium, they divide into four pyriform cells (3 x 6 µm) forming morulae-like colonies (Fig. 4A). Colonies typically remain embedded in a thick layer of homogeneous mucilage (Fig. 4B). Between two to four days after inoculation into fresh medium, cell

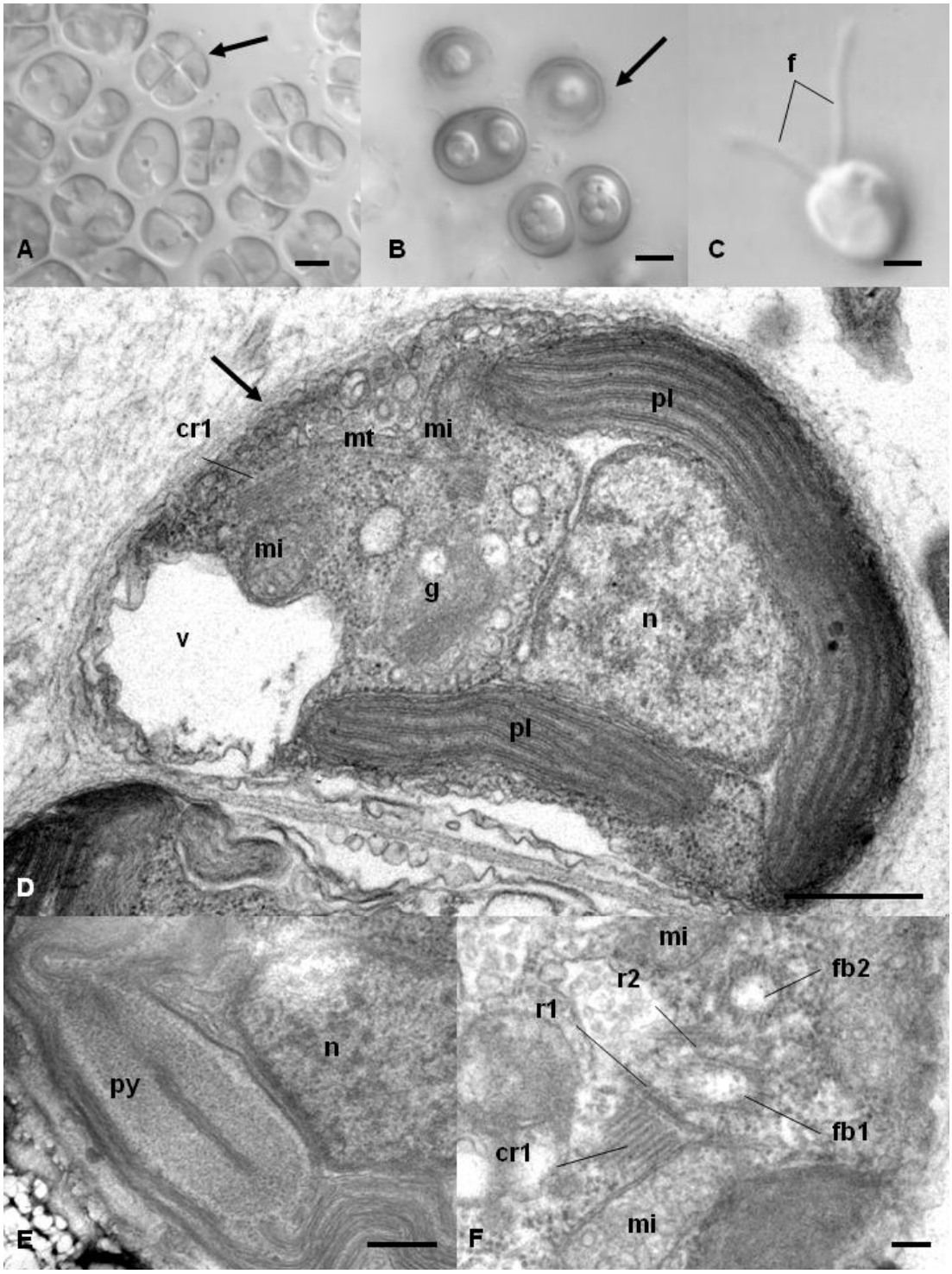

Figure 4. *Chrysotila* affinis *lamellosa* (PLY510A): A. LM micrograph of non-motile colony of cells in mucilage, organised in quartets of four cells resulting from two mitotic divisions (arrow); B. LM micrograph of non-motile cells in mucilage with toluidine blue coloration, arrow showing mucilage stratification; C. LM micrograph of motile cell with flagella; D. TEM. micrograph of motile cell in longitudinal section showing the nucleus, a parietal plastid, a Golgi apparatus, a mitochondrion and homogenous mucilage (arrow); E. TEM micrograph of pyrenoid crossed by a thylakoid lamellum in transverse section; F. TEM micrograph of basal body in transverse section, showing the two flagellar bases and the flagellar roots (r1, cr1 and r2). Scale bars: A: 5 µm, B: 2 µm, C: 1 µm, D: 200 nm, E: 500 nm, F: 200 nm. (Abbrev: cr1: accessory compound components of root 1; f: flagellum; fb1 and 2: left and right flagellar base; g: Golgi apparatus; mi: mitochondrion; mt: microtubule; n: nucleus; pl: plastid; py: pyrenoid; r1 and 2: microtubular roots 1 and 2).

colonies release motile swarmers that remain present for less than four days in the culture. These spherical cells (3 x 4.5-5 µm) have isokont flagella (6 - 8 µm), but no emergent haptonema (Fig. 4C). These cells eventually shed their flagella, settle to the bottom of the culture flask and continue to divide, forming homogeneous mucilage-covered colonies. Cells increase in size as the culture ages. Observation of thin sections revealed a single plastid enclosed within a nucleoplastidial membrane, a mitochondrion and a Golgi apparatus (Fig. 4D) and a pyrenoid traversed by a single thylakoid lamella (Fig. 4E). Components of the flagellar appartus include root 1 (R1) and its accessory compound root (CR1) and root R2 between the flagellar bases (Fig. 3F).

***Isochrysis nuda* sp. nov. RCC1207, PLY401b (Fig. 5):** Cells are predominantly non-motile and non-benthic, mostly spherical (around 4 µm diameter) with a single golden yellow plastid (Fig. 5A). Motile cells exhibit two isokont flagella measuring between 7.5 µm and 9 µm (Fig. 5B). Details of the basal body revealed two flagellar bases between which a reduced haptonema without scales is inserted (Fig. 5C). The flagella are abbreviated suggesting their release during fixation (Fig. 5C-D). Thin sections revealed that the cell membrane is not surrounded by organic scales. The cell ultrastructure shows the presence of a mitochondrion, a Golgi apparatus and a single plastid per cell enclosed within a nucleoplastidial membrane and with an immersed pyrenoid, traversed by thylakoid lamella (Fig. 5D).

***Isochrysis galbana* RCC1348 (Fig. 6):** Motile cells possess a single golden yellow plastid and two flagella with a reduced haptonema. Cell shape varies from ellipsoidal to spherical and cell size is from 3.5 – 6.5 µm (Fig. 6A). Multiple layers of thin organic scales measuring around 100 nm cover the cell, each scale exhibiting a pattern of 4 quadrants composed of around 10 radial ridges and a central swelling (Fig. 6B-E). A dense layer of smaller scales (10 nm), exhibiting a superficial pattern of 12 radial ridges, covers the haptonema (Fig. 6C-D). Observation of cell infrastructure revealed a pyrenoid traversed by a single thylakoid lamella within the plastid that is enclosed within a nucleoplastidial membrane. A mitochondrion and a Golgi apparatus were also observed (Fig. 6E).

***Tisochrysis lutea* (ex. *Isochrysis* affinis *galbana* (T-Iso)) RCC1349 (Fig. 7) :** Cells of this species are predominately motile, golden brown in colour, with cell shape varying from spherical to ovate or oblong (3.5 - 6 µm) with an apical depression into which the flagella are inserted (Fig. 7A). The two flagella are equal in length (around 7 µm) and a short haptonema

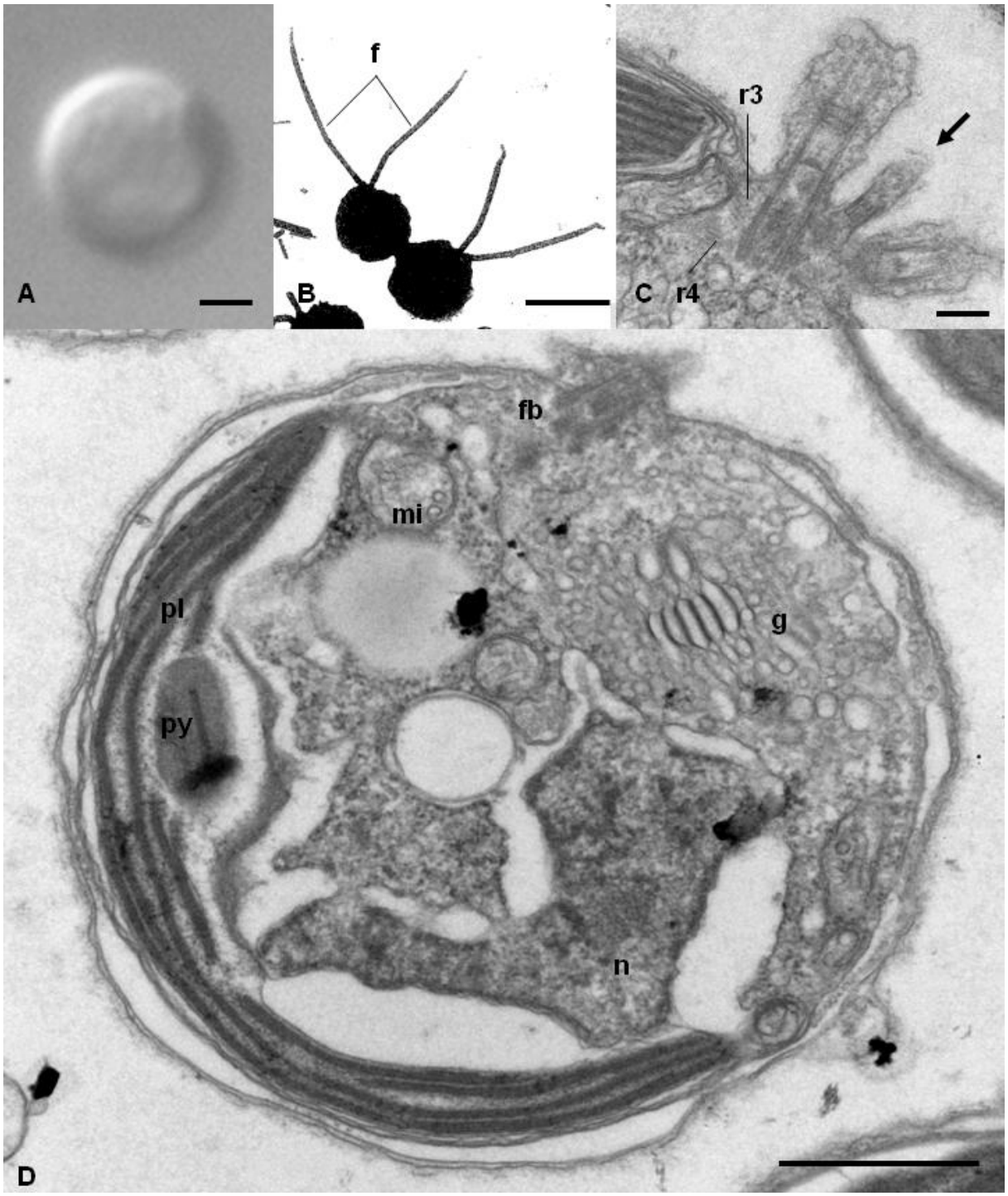

Figure 5. *Isochrysis nuda* (RCC1207). A. LM micrograph of a non-flagellated cell ; B. TEM micrograph of whole mounted flagellated cells; C. TEM micrograph of basal body in transverse section showing flagellar base and abbreviated haptonema (arrow); D. TEM micrograph of a cell displaying a flagellar base, a Golgi apparatus, a mitochondrion, a nucleus, a parietal plastid and a pyrenoid crossed by a thylakoid lamella in lonigtudinal section. Scale bars: A: 1 µm, B: 5 µm, C: 200 µm, D: 1 µm. (Abbrev: f: flagellum; fb: flagellar base; g: Golgi apparatus; mi: mitochondrion; n: nucleus; pl: plastid; py: pyrenoid; r3 and 4: microtubular roots 3 and 4).

is present (around 100 nm; Fig. 7A,D). The cell is covered by a dense layer of thin organic scales identical to those of *Isochrysis galbana*, measuring around 100 nm with a superficial pattern of around 40 radial ridges and a central swelling (Fig. 7E). Smaller scales measuring around 100 nm with a superficial pattern of 12 radial ridges are abundantly present on the haptonema and on the cell membrane in the vicinity of the flagellar insertion (Fig. 7C, D, F). The emergent part of the haptonema is composed of 3 or 4 microtubules within a sheath of endoplasmic reticulum (Fig. 7D, F). Thin sections reveal the presence of one or two parietal plastids linked to the nucleus within a nucleoplastidial membrane (Fig. 7E). A prism-shaped pyrenoid traversed by a single thylakoid lamella is present in the plastid. The basal body components include root 1 adjacent to the left flagellum and its accessory component (CR1), root 2 seemingly composed of two microtubules, and roots 3 and 4 originating on either side of the right flagellar base (Fig. 7F, G, H). In the late stationary phase of culture, most cells lose their flagella and become non-motile. These cells are mostly spherical, ranging in diameter between 4 and 6 µm, and sometimes produce a mucilage covering. In such old cultures, the colour of cells typically becomes brownish-orange to orange.

***Gephyrocapsa oceanica* (Figs 8 and 9):** *Gephyrocapsa oceanica* exhibits a life cycle identical to that of *E. huxleyi*, a non-motile coccolith bearing phase alternating with a motile, non-calcifying phase, with both phases capable of independent asexual reproduction.

Motile cells (5.5 x 6 µm) are ellipsoidal in shape (Fig. 8A). The two flagella (around 7 µm) emerge from an apical insertion and no emergent haptonema is present. Parietal plastids are brownish in colour and a refractive body can be observed within the cell in LM. A layer of organic scales organised in staggered rows covers the entire cell membrane (Fig. 8B, C). Thin sections show cells with an ellipsoidal shape containing one or two plastids enclosed within the nucleoplastidial membrane. Each plastid contains a pyrenoid with a three cornered or trapezoidal shape traversed by a thylakoid lamella (Fig. 8D, E). Lipid droplets are often observed. An unusual vacuole sometimes occurs which may be related to the refractive body (x-body). Flagellar roots were found with R1 and R3 adjacent to the left and right flagellar bases, respectively (Fig. 8F). No haptonematal root was observed.

Coccolith-bearing cells are non-motile and contain a brownish coloured plastid (Fig. 9A). Coccoliths are characterised by the presence of a prominent bridge over the central area of a heavy calcified placolith (Fig. 9A, B). Thin sections show that a layer of columnar material is present between the coccoliths and the cell membrane and that no non-mineralized body scales are present (Fig. 9D). The parietal plastid is enclosed within a nucleopastidial

membrane and contains a trapezoidally-shaped pyrenoid (Fig. 9D). The coccolith-producing vesicle directly abuts the nucleus and is linked to a reticular body of Golgi origin that is structurally identical to that reported for *E. huxleyi* (Fig. 9D, E).

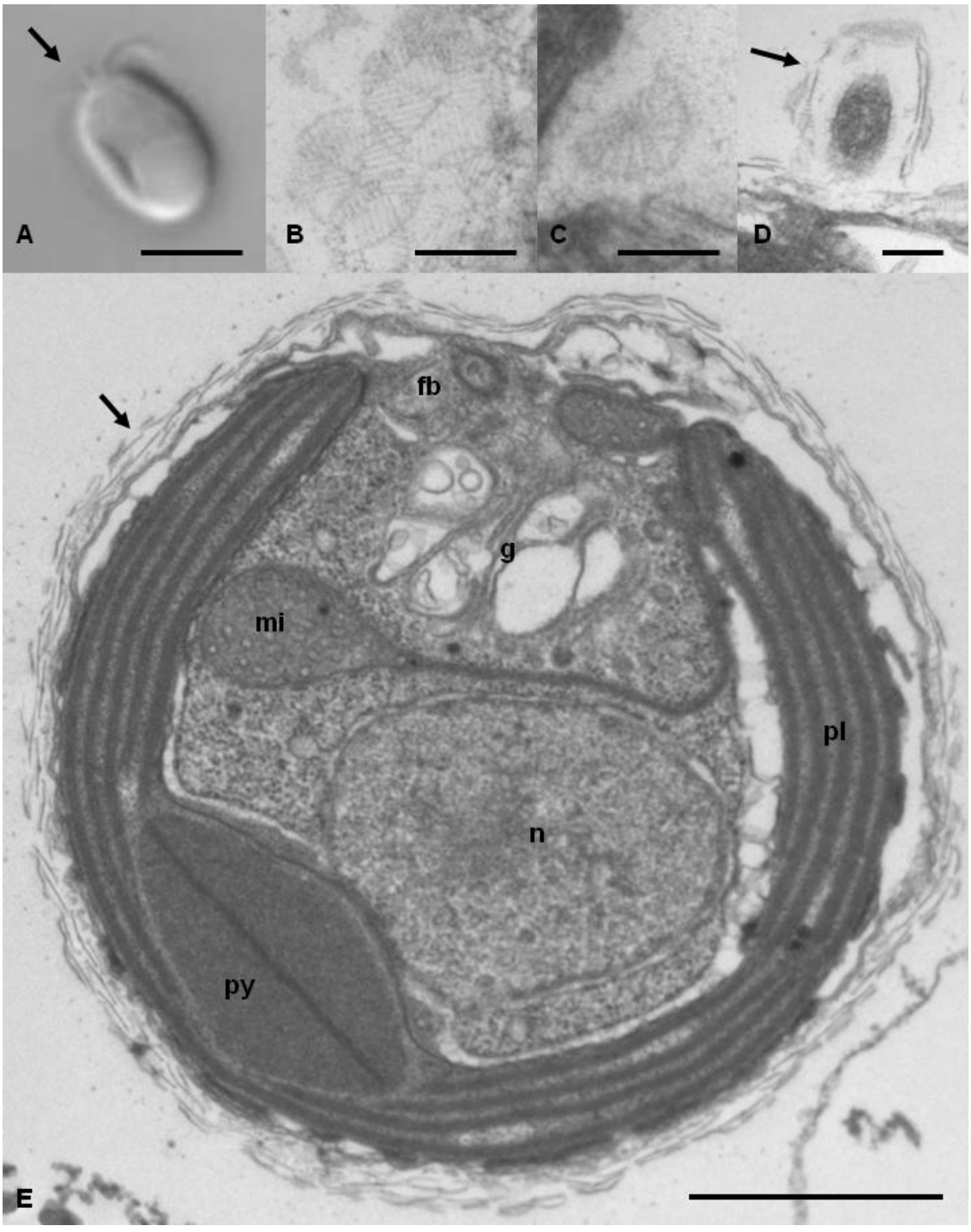

Figure 6. *Isochrysis galbana* (RCC1348): A. LM micrograph of a motile cell with two flagella and the haptonema (arrow); B. TEM micrograph of body scales in glancing section; C. TEM micrograph of haptonematal scale (arrow) in glancing section; D. TEM micrograph of the haptonema in longitudinal section, showing scales (arrow); E. TEM micrograph of a cell displaying multilayer scales (arrow), a flagellar base, a Golgi apparatus, a mitochondrion, a nucleus, a parietal plastid and a pyrenoid crossed by a thylakoid lamella in lonigtudinal section. Scale bars: A: 4 µm, B: 200 nm, C, D: 100 nm, E: 1 µm. (Abbrev: fb: flagellar base; g: Golgi apparatus; mi: mitochondrion; n: nucleus; pl: plastid; py: pyrenoid).

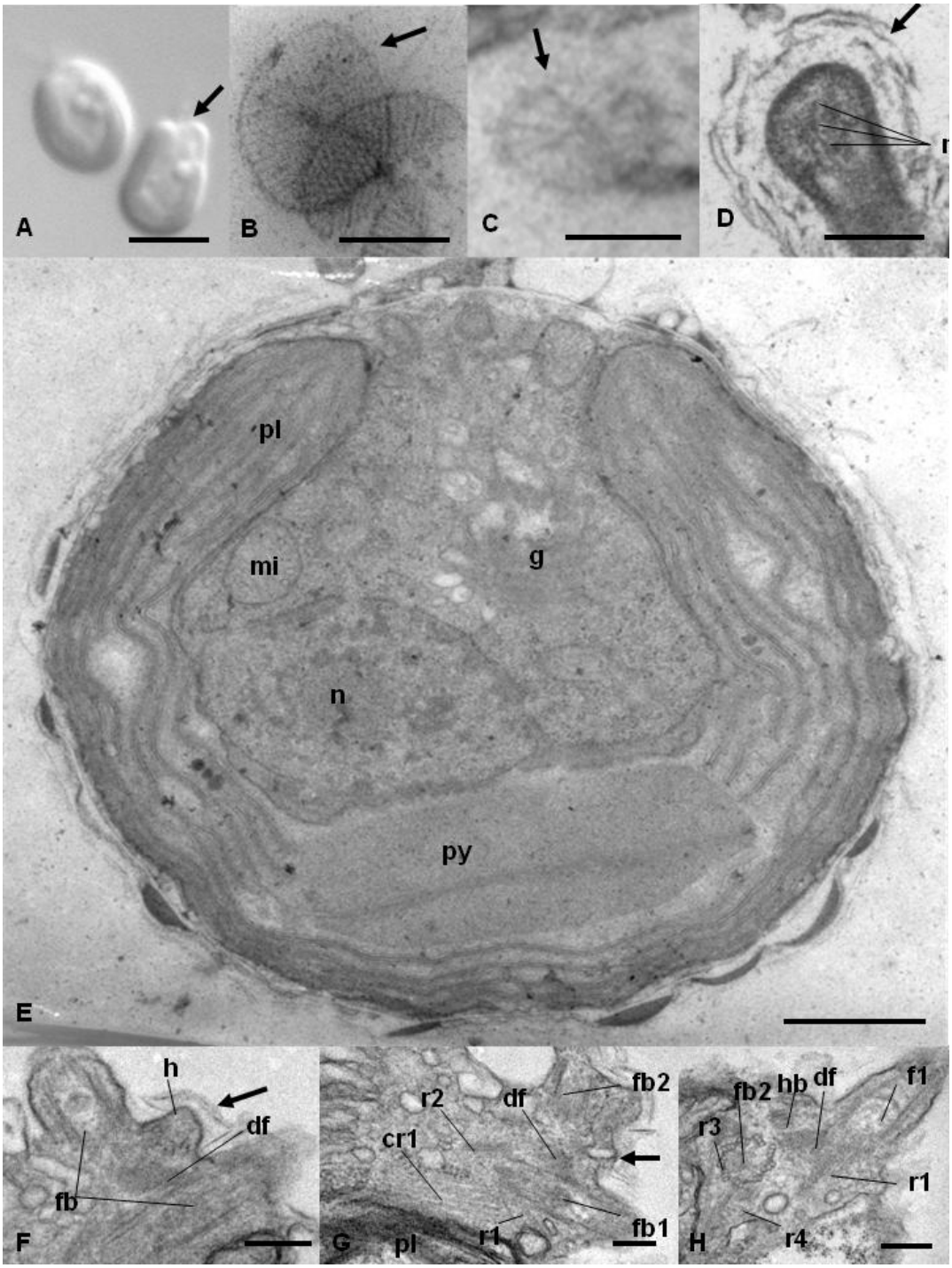

Figure 7. *Tisochrysis lutea* (RCC1349): A. LM micrograph of two motile cells with apical depression (arrow); B. TEM micrograph of body scales (arrow) in transverse section; C. TEM micrograph of haptonematal scale (arrow) in glancing section; D. TEM micrograph of the haptonema in longitudinal section, showing scales (arrow) and three constitutive microtubules; E. TEM micrograph of a cell displaying a nucleus, a Golgi apparatus, a parietal plastid and a pyrenoid crossed by a thylakoid lamella in longitudinal section; F. TEM micrograph of basal body in transverse section showing flagellar base and distal fibre, abbreviated haptonema composed of 4 microtubules and adjacent haptonematal scales (arrow); G. TEM micrograph of basal body in longitudinal section, showing flagellar base, a distal fibre, roots 1 and 2 and the accessory compound component of root 1, haptonematal scales (arrow); H. TEM micrograph of basal body in transverse section, showing flagellar and haptonematal bases, a distal fibre and roots 1, 3 and 4; Scale bars: A: 5 µm, B: 200 nm, C, D: 100 nm, E: 1 µm, F, G, H: 100 nm. (Abbrev: cr1: accessory compound component of root 1; df: distal fibre; f1: flagella; fb: flagellar base; fb1 and 2: left and right flagellar base; g: Golgi apparatus; h: haptonema; mi: mitochondrion; mt: microtubule; n: nucleus; pl: plastid; py: pyrenoid; r1, 2, 3 and 4: microtubular root 1, 2, 3 and 4)

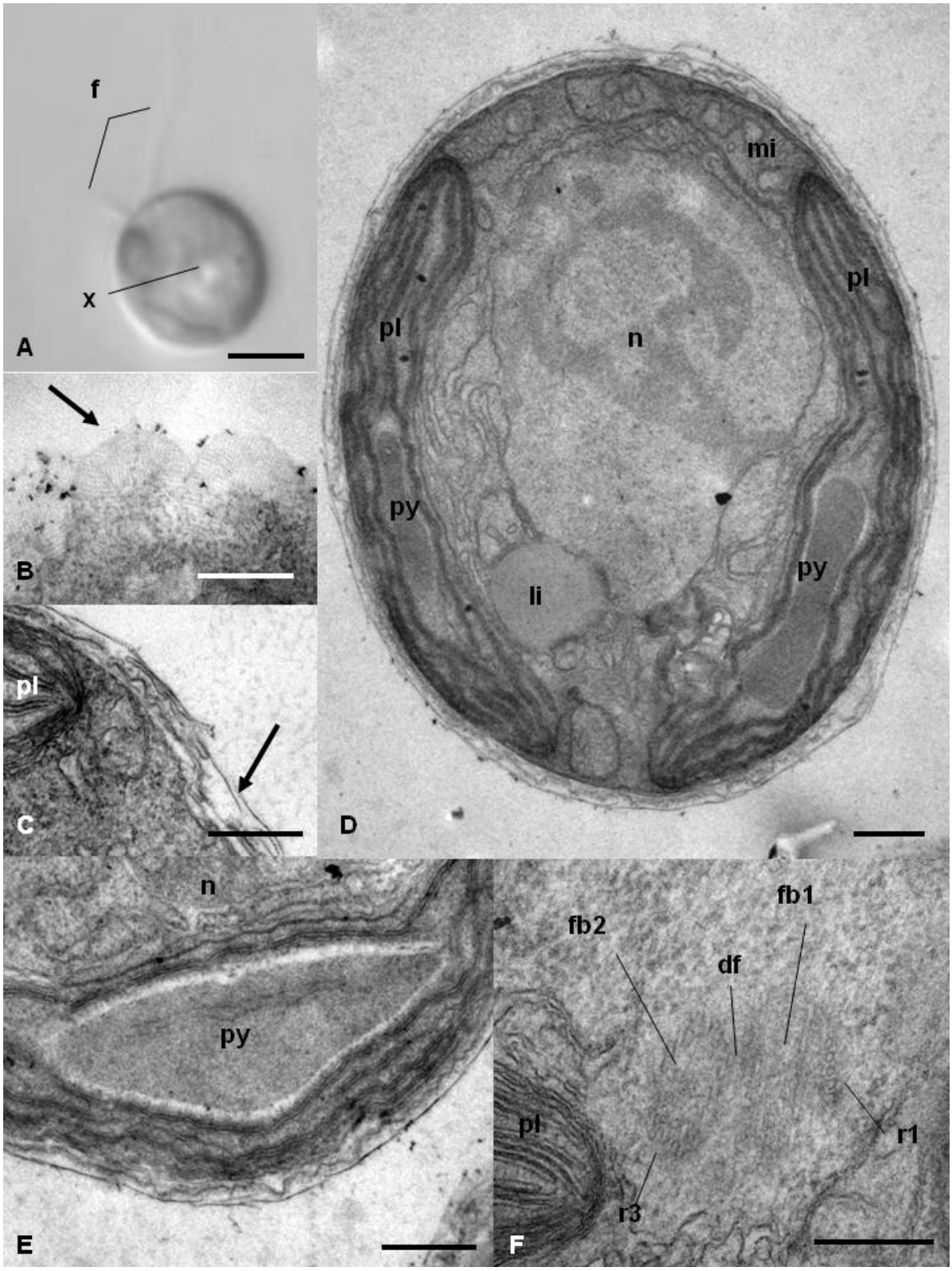

Figure 8. *Gephyrocapsa oceanica* haploid phase (RCC1315): A. LM micrograph of a motile cell; B. TEM micrograph of body scales (arrow) in glancing section; C. TEM micrograph of body scales (arrow) in transversal section; D. TEM micrograph of a cell in transverse section; E. TEM micrograph of a pyrenoid crossed by a thylakoid lamellum in transverse section; F. TEM micrograph of basal body in transverse section, showing flagellar bases with the distal fibre and flagellar roots 1 and 3; Scale bars A: 5 µm, B, C: 1 µm, D: 500 nm, E, F: 200 nm. (Abbrev: df: distal fibre; f: flagellum; fb1 and 2: left and right flagellar base; g: Golgi apparatus; li: lipidic droplet; mi: mitochondrion; n: nucleus; pl: plastid; py: pyrenoid; r1-3: flagellar root 1 and 3; x: refractive x-body)

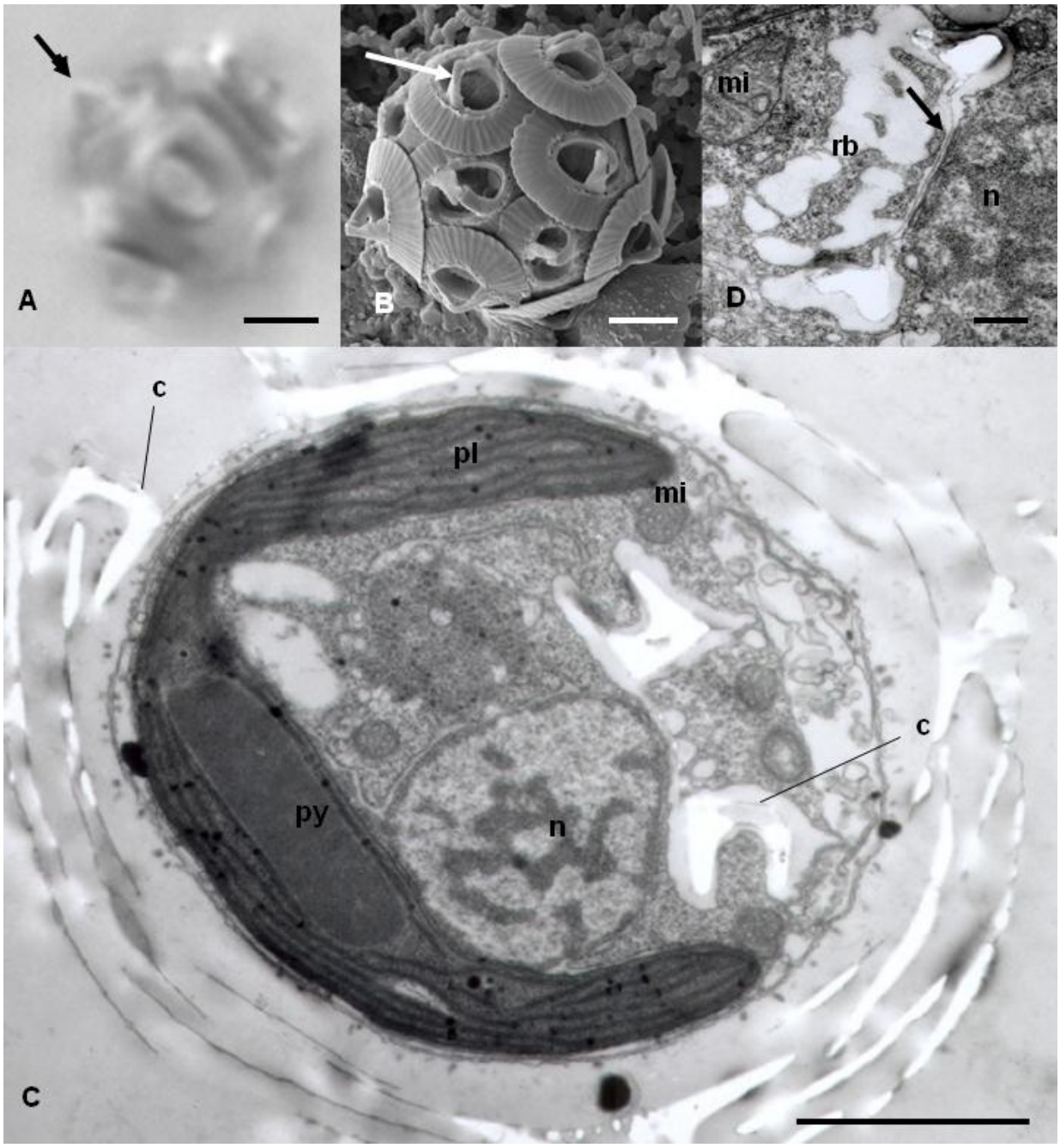

Figure 9. *Gephyrocapsa oceanica* diploid phase (RCC1314): A. LM micrograph of a non-motile cell covered by coccoliths with bridge (arrow); B. SEM micrograph of a coccosphere displaying coccoliths with bridge over the central area (arrow); C. TEM micrograph of cell in transverse section showing detail of coccolith adhesion on cell membrane with columnar material and the intracellular production of a coccolith in close proximity to the nucleus and a parietal plastid; D. TEM micrograph of early stage of coccolithogenesis showing the basal structure (arrow) of the coccolith between the nucleus and the reticular body ; Scale bars: A, B: 2 µm, B: 200 nm, C: 1 µm D: 500 nm. (Abbrev: c: coccolith; mi: mitochondrion; n: nucleus; pl: plastid; py: pyrenoid; rb: reticular body).

Discussion

This culture-based morpho-molecular review of the systematics of the prymnesiophyte order Isochrysidales reveals notable inconsistencies in the existing taxonomic scheme and the existence of two new species that are described here. The two families that comprise the Isochrysidales are well separated in the multi-gene molecular phylogeny (~2% genetic distance in combined SSU and LSU rDNA sequences), confirming that the calcifying Noëlaerhabdaceae and non-calcifying Isochrysidaceae are related, but distinct clades. Within each family, however, the new data presented here highlight issues with the actual taxonomy at the generic level. Resolution of these issues is not straightforward since there are cases of either conserved (or convergent) morphology amongst genetically divergent taxa and morphological divergence between taxa that are extremely closely related at the genetic level. Below we firstly discuss and present our conclusions on the taxonomic issues within each family, then we discuss what insights the new data provide about the evolution of the Isochrysidales as a whole.

Isochrysidaceae

Clade I-1: This clade is composed of (1) strain PLY510A (previously designated as *Chrysotila* sp.), (2) several strains with identical sequences including the two *C. lamellosa* strains considered representative of authentic material by Green and Parke (1975), (3) *Isochrysis galbana*, also represented by several strains with identical sequences including the authentic strain, (4) the authentic strain of *I. litoralis* (RCC1346, and (5) two strains designated as *Dicrateria* sp. (RCC1207) and *Isochrysis* sp. (PLY401B).

The taxonomic history within the Isochrysidaceae is somewhat complicated. *Chrysotila stipitata* and *C. lamellosa* were first described from wild material collected in the 'Chrysophyceae belt' of the intertidal zone below chalk cliffs in southern England by Anand (1936, 1937). At the time, *Chrysotila* was erected as a new genus with *C. stipitata* as the type species. Shortly afterwards, Geitler (1943) described another new genus, *Ruttnera*, containing *R. spectabilis*, an organism with a dominant palmelloid phase and motile cells having two equal flagella. The new genera *Isochrysis* (containing *I. galbana*) and *Dicrateria* (containing the type species *D. inornata* as well as *D. gilva*) were described by Parke (1949). A second *Ruttnera* species, *R. chadefaudii*, was described by Bourrelly and Magne (1953) and a third, *R. pringsheimii*, by Subrahmanyan (1962). Later, the two species *Gloeochrysis maritima* and *G. litoralis*, which were originally described by Anand (1937) at the same time as the formal descriptions of *C. stipitata* and *C. lamellosa*, were transferred to *Ruttnera* by Parke and Dixon

(1964). Billard and Gayral (1972) described two new *Isochrysis* species, *I. maritima* and *I. litoralis*, the species names chosen to reflect their similarity to *R. maritima* and *R. litoralis*, respectively, to which they could not however be assigned due to differences in flagellar type (equal for *I. maritima* and *I. litoralis*, very unequal (anisokont) for *R. maritima* and *R. litoralis*). Billard and Gayral (1972) concluded that the transfer of *G. maritima* and *G. litoralis* to *Ruttnera* by Parke and Dixon (1964) was not warranted since *Ruttnera* is characterised by organisms with equal flagella. In 1974, a culture strain from the type locality of *R. spectabilis* (the type strain no longer existed) was concluded to be con-specific with *C. lamellosa* (Green and Parke 1974) and both of these genera were shown to have affinities with the recently erected class Haptophyceae (Christensen 1962). The diagnoses of the genus *Chrysotila* and of the species *C. stipitata* and C. *lamellosa* were subsequently revised by Green and Parke (1975) following new observations on these organisms based on cultures (two strains of each species) held to be representative of these species (since no type cultures existed). These four strains (PLY353 and PLY408 for *C. lamellosa* and PLY377 and PLY432 for *C. stipitata*) were used in the present study. These authors concluded that *I. maritima* and *R. spectabilis* were synonymous with *C. lamellosa* and stated that other *Ruttnera* species (*R. chadefaudii* and *R. pringsheimii*) were of uncertain taxonomic position. *R. chadefaudii* was considered to be comparable to *R. spectabilis* (= *C. lamellosa*) in most respects, the most important difference being the lack of lamellations and stalks in the mucilage surrounding the cells (Green and Parke 1974). *R. pringsheimii* was suggested by Green and Parke (1974) to have affinity with *Phaeocystis* due to the form of swarmers and colonies. The single taxon of the genus *Imantonia*, *I. rotunda*, was described by Reynolds (1974) and included in the Isochrysidales due to morphological similarities with *Dicrateria inornata* (notably lack of haptonema), but later transferred to the Prymnesiales by Edvardsen et al. (2000) based on evidence from SSU rDNA sequences. Edvardsen et al. (2000) predicted that *D. inornata* would also be proved to belong to the Prymnesiales once gene sequences became available to corroborate the morphological / ultrastructural similarity of these two genera.

As it stands, therefore, the genus *Chrysotila* contains the type species *C. stipitata* as well as *C. lamellosa* (= *R. spectabilis*, = *I. maritima*) and should possibly also contain *R. chadefaudii* either as a synonym of *C. lamellosa* or as a discrete species. *Isochrysis* contains *I. galbana* and *I. litoralis*, and *Dicrateria* contains *D. inornata* as well as *D. gilva*. *Gloeochrysis* still exists, but has an uncertain taxonomic position, probably being related to the Chrysophyceae.

The fact that all three strains designated as *C. stipitata* had SSU rDNA sequences similar to those of members of the heterokont class Pinguiophyceae was surprising. In the palmelloid mucous-covered phase, *Chrysotila* species can resemble certain chrysophytes *sensu lato*. However, it appears certain that the strains of *C. stipitata* isolated and studied by Green and Parke (1975), a priori the same as two of the strains included in the present study, were indeed haptophytes given the fact that isokont flagella with no mastigonemes, body scales, and a haptonematal base were illustrated. We have not observed the non-lamellated mucous stalks typical of *C. stipitata* in any of the three strains and attempts to provoke formation of motile cells (which are more easily distinguished) were not successful. The ultrastructure of the three strains was clearly that of heterokont organisms (results not shown) and clearly different from that reported for the two Plymouth strains by Green and Parke (1975). It would thus appear that either a mislabelling occured at some point since Green and co-workers studied these strains in the 1970s or that PLY377 and PLY432 contained both *C. stipitata* and the pinguiophyte when they were established and that the latter species came to dominate the cultures over time. The same scenario might have occurred in the strain originally from the University of Caen collection, the surprising point if this was the case being the coincidental occurrence of the same pinguiophyte (the sequence from RCC1196 being identical to those of PLY377 and PLY432). Alternatively, RCC1196 may have been misidentified when it was isolated in 1968 and thus never have contained *C. stipitata*, in which case, however, the surprising coincidence remains. It is interesting to note that Marlowe et al. (1984) reported that alkenones were not present in PLY377, suggesting that *C. stipitata* had already disappeared from the culture by this time. We recently obtained the same result for RCC1196 (unpublished data). Had *C. stipitata* turned out to be a pinguiophyte, the genus *Chrysotila* would have had to have been transferred since it is the type species of the genus, but we conclude that *C. stipitata* is really a haptophyte, and that the cultures held to be representative of this species no longer exist in their original form. No gene sequences and, to our knowledge, no cultures of this taxon currently therefore exist, but it remains as the type species of the genus.

Chrysotila sp. PLY 510A is very similar to *C. lamellosa* in terms of morphology and ultrastructure but is genetically distinct. The two taxa form colonies of cells embedded in thick stratified mucilage that may form short stalks. Emission of flagellate cells seems to be more predictable in *Chrysotila* sp. PLY510A than described in *C. lamellosa* PLY352 and PLY408 (Green and Parke 1974). Both taxa are euryhaline. Epilithic isolates of *C. lamellosa* from terrestrial environments exist, for example the strain of *Ruttnera spectabilis* that was

thoroughly described by Green and Parke (who related it to *C. lamellosa*) that was isolated by Geitler from a sample scraped from a wall in Vienna, Austria (Green and Parke 1975). We have successfully cultured *Chrysotila* sp. PLY510A in freshwater medium over multiple growth cycles. *Chrysotila* sp. PLY510A cannot be assigned to *C. stipitata* (or *R. chadefaudii*) due to the presence of lamellations in the mucilage covering. The 0.6% divergence in ribosomal gene sequences between PLY510A and the representative cultures of *C. lamellosa* provides strong evidence that it is a distinct cryptic entity. Examples can be found in all other haptophyte orders of distinct species with clear morphological differences exhibiting a similar or lesser degree of genetic divergence in ribosomal gene sequences. In some cases, notably the genera *Emiliania* and *Gephyrocapsa,* taxa with less genetic divergence are distinguished at the genus level. While we consider that this organism warrants description at least at the species level given the level of genetic divergence from *C. lamellosa*, in the absence of sequences of the type species of the genus, *C. stipitata* (see above), it is not possible to be certain (despite the apparent morphological distinction) that this is indeed a new species. We therefore do not formally describe the species represented by strain PLY510A (designated *Chrysotila* affinis *lamellosa*) awaiting future genetic comparison with *C. stipitata*.

The other cultured species in clade I-1 are *I. galbana*, *I. litoralis* and a taxon represented by two strains designated as *Dicrateria sp.* (RCC1207) and *Isochrysis* sp. (PLY401B). Several culture isolates have sequences identical to the authentic culture of *I. galbana*. One of these, strain RCC1353 (equivalent to AC80, UTEX1988 and CCAP949/1), was designated as *Pseudoisochrysis paradoxa*, a *nomen nudum* applied provisionally to a culture by the isolator F. Ott, the paradox being that the organism resembled *Isochrysis* in morphology but was greenish in colour (Jordan et al. 2005). The culture was subsequently studied in detail by Pennick (1977) and shown to be a prasinophyte and formally described as *Pyramimonas virginica*. However, the original name was still used for copies of this culture maintained in certain culture collections and Farmer (1993) reported this strain to be an alkenone producer. Our results, as well as those of Sàez et al. (2004), confirm that RCC1353 is morphologically and genetically identical to *I. galbana*. It seems highly likely, therefore, that the original culture was a mixture of *I. galbana* and the prasinophyte *P. virginica* and that one or the other organism has come to dominate different copies of the strain. The name *Pseudoisochrysis paradoxa* was never formally proposed and so is invalid, and we consider it synonymous with *Isochrysis galbana*. Strains RCC1207 and PLY401B differ from *I. galbana* and *I. litoralis* in not possessing body scales, a character that links them to *Dicrateria inornata*. However, the SSU rDNA sequence of the authentic strain of *D. inornata* (PLY564)

does not match those of RCC1207 and PLY401B, but rather is almost identical to that of the prymnesialian species *Imantonia rotunda*. This genetic similarity corroborates published information that shows that *D. inornata* and *I. rotunda* are very similar in ultrastructure (Green and Pienaar 1977), pigment signatures (Jeffrey and Wright 1994; Zapata et al 2004), and the fact that neither produces alkenones (Marlowe et al 1984). The only clear morphological distinction between these two taxa is the presence (*I. rotunda*) or absence (*D. inornata*) of body scales. Based on these results, we transfer *Dicrateria* to the Prymnesiales and include *D. rotunda* comb. nov. in this genus which is emended to include organisms with and without scales. A new species, *Isochrysis nuda* sp. nov., is described for the taxon represented by the culture strains RCC1207 and PLY401B. In contrast to *I. galbana*, the palmelloid phase is prominent in cultures of both *I. litoralis* and *I. nuda.* and the haptonema is reduced to such an extent that it is only visible in electron microscopy in the latter two species that cluster together in the molecular phylogeny. *Isochrysis nuda* is distinguished from *I. litoralis* by the lack of body scales. The genus *Isochrysis* is emended to reflect the inclusion of organisms with and without scales.

We consider that there are sufficient morpho-structural differences between the *Chrysotila* and *Isochrysis* species (notably dominance of palmelloid versus flagellate stages) to usefully maintain these as separate genera despite the fact that the inclusion of sequences of *Chrysotila* affinis *lamellosa* PLY510A in the molecular phylogeny makes *Chrysotila* a paraphyletic genus (Fig. 2).

Clade I-2: The second clade is a congruent group composed of the culture strain informally known as *Isochrysis* aff. *galbana* "Tahiti isolate", alias T-Iso, together with other strains that are genetically identical to T-Iso. This is the first time that the phylogenetic relationships of T-Iso with other members of the Isochrysidales have been presented. The morphological and ultrastructural characters of T-Iso are extremely similar to those of *I. galbana*, even for characters that are often phylogenetically discriminant such as scale morphology and the structure of the flagellar/haptonematal basal body. We noted a minor difference in plastid coloration (orange for T-Iso vs yellow-green for *I. galbana*) that is most marked in stationary phase cultures. One other character defining both T-Iso and *Isochrysis* is excretion of a thin mucilage layer by non-motile cells, well characterised by toluidine blue staining. Despite this morpho-structural similarity, the genetic distance between the *Isochrysis* and T-Iso clusters is in excess of 1% in SSU rDNA sequences, i.e. equal to or greater than the genetic distance between most closely related genera for which genetic data exists within the haptophytes (cf. Edvardsen et al. 2000). Should the T-Iso clade be retained within the genus *Isochrysis*, the

genus would clearly be polyphyletic. Thus we conclude that the definition of a new genus for clade I-2 is warranted and we propose the name *Tisochrysis* for this genus in reference to the well known T-Iso strain. Within this new genus, we describe the species represented by the T-Iso strain as *Tisochrysis lutea* sp. nov..

Noëlaerhabdaceae

Emiliania huxleyi and *Gephyrocapsa oceanica* have previously been shown to be genetically identical in both ribosomal (SSU rDNA) and plastidial (RbcL) gene markers (Edvardsen et al. 2000; Fujiwara et al. 2001) and the ultrastructure of both coccolith-bearing and non-mineralized phases in the life cycle of *E. huxleyi* were described several decades ago (Klaveness 1972a-b). In addition to SSU rDNA, we sequenced another ribosomal gene (LSU rDNA) and a relatively rapidly evolving mitochondrial barcode marker, the cox1 gene. We also studied the ultrastructure of both life cycle phases of *G. oceanica* and present the first ultrastructural comparison of *Gephyrocapsa* and *Emiliania*.

Our analyses confirmed that the two taxa are identical in SSU rDNA sequences and revealed a consistent 1 nucleotide substitution (~0.1% divergence) in LSU rDNA sequences. Cox1 gene sequences provided greater resolution, the two taxa diverging by up to 2.1 % in this mitochondrial marker. Hagino et al. (2011) reported that the cox1 gene can even solve two distinct, biogeographically isolated clades within the morphospecies *E. huxleyi*. The phylogenetic analysis based on concatenation of the three genes sequenced in our study confirms that *E. huxleyi* and *G. oceanica* are distinct, but genetically very closely related species. In terms of ultrastructure and life cycle, the two genera are also strikingly similar. Their life cycle consists of a non-motile placolith-bearing phase ('C-cells'), a motile phase that bears non-mineralized organic scales ('S-cells'), and non-calcified coccoid or amoeboid cells ('N cells'), the latter being relatively infrequently observed in *G. oceanica* cultures. All of the ultrastructural features that distinguish *E. huxleyi* from other coccolithophores (reticular body involved in coccolithogenesis, lack of non-mineralized body scales underlying coccoliths in the coccolith-bearing phase, 'X-body' in the flagellate phase) were also observed in *G. oceanica*. As reported by Klaveness (1972b) for *E. huxleyi*, the flagellar basal body of *G. oceanica* was very rarely observed in thin sections. Both species appear to have relatively simple flagellar roots with no trace of a haptonematal base, but in the absence of detailed reconstruction of the basal body of either species it is not possible to define whether there are any minor distinguishing features.

These two species that are highly similar in both their genetic and ultrastructural characters were classified in different genera exclusively based on coccolith morphology, specifically the presence (*Gephyrocapsa*) or absence (*Emiliania*) of a bipartite bridge spanning the central area of the placolith. This is a very visible feature, even in light microscopy, but in structural terms the bridge is simply a conjunct extension of a set of crystals of the inner tube (one to six crystals on either side of the inner tube), i.e. the bridge is formed by variation of the growth pattern of certain existing crystal units, without nucleation of any additional crystals. Such variation of growth pattern is frequently observed in coccolith evolution, for instance in *E. huxleyi* var. *corona* the inner tube elements extend upwards to form an irregular collar around the central area. Bridge formation in *Gephyrocapsa* is rather unusual in that only a limited set of rim elements are involved and the bridge is invariably oriented at an angle rotated clockwise from the long axis of the coccolith in distal view, i.e. it is a chiral structure that is preserved throughout the geological range of the genus.

The palaeontological, morphostructural, and molecular genetic data all indicate that *Emiliania* diverged very recently from *Gephyrocapsa*. Distinction of the genera undoubtedly makes *Gephyrocapsa* paraphyletic and the only character that reliably separates the two genera is loss of bridge formation in *Emiliania*. The phylogenetic approach applied here challenges this concept and does not support the generic level significance of this morphological character. Loss and gain of characters is the basis of evolution and the case of *E. huxleyi* highlights that maintenance of the bridge is not necessarily stable through time. Even if the palaeontological evidence indicates that the *Gephyrocapsa* bridge structure has evovled only once, the possible occurrence of multiple events of bridge gains in pre-*Gephyrocapsa* lineages and of other cases of bridge loss in distinct *Gephyrocapsa* lineages cannot be excluded, meaning that reliance on this character for taxonomy at the generic level may well lead to polyphyly.

First described by Lohmann (1902) as *Pontosphaera huxleyi*, *E. huxleyi* has undergone several taxonomic changes through the 20th century (Tab. 5). Following technological limitations and the state of knowledge of coccolithophore classification at the time, these taxonomic changes have also reflected the thematic and practical interests of different scientific communities. The two last changes (*Coccolithus* to *Emiliania*, *Emiliania* to *Gephyrocapsa*) represent the crux of the taxonomic question posed by the new comparative data presented here. Hay and Mohler (Hay et al. 1967) integrated *Coccolithus huxleyi* into a newly erected genus *Emiliania,* even though Kamptner (1956) had noted the high degree of homology of the structure of coccolith elements between *E. huxleyi* and *G. oceanica*.

Kamptner (1941) in fact suggested that the two species might be capable of hybridizing due to observation of confusing combinations of both coccolith types on single coccospheres occurring in some sediment samples (Clocchiati 1971). Such anomalous coccospheres containing coccoliths normally regarded as forming on discrete species were termed "xenospheres", on the basis that they are probably artefactually-formed coccospheres, as discussed in detail by Young and Geisen (2002). The doubt introduced by these structures and particularly the similarity between the coccolith structure of the two species led Reinhardt (1972) to formally propose the transfer of *E. huxleyi* into the genus *Gephyrocapsa*. This proposition has not been widely followed, mainly because, in practice, discrimination of bridge-forming Noëlaerhabdaceae as *Gephyrocapsa* has proven useful, notably for palaeontologists but also for marine biologists. From a purist's point of view, taxonomy exists to provide tools for species denomination, and, in the frame of a phyletic classification, to integrate this denomination into an evolutionary context, i.e. to provide *consistent* information on the relatedness of organisms. In this context, it can be argued that taxonomic choices should not be made according merely to considerations of practical convenience and the large majority of morpho-genetic data obtained and reviewed in this study argue for the transfer of *Emiliania* into the genus *Gephyrocapsa*. Since the combinations *Emiliania huxleyi* and *Gephyrocapsa huxleyi* have both been validly proposed, we conclude that the choice of which name to use remains the responsibility of individual scientists studying these organisms and that this choice can be informed by the data presented here.

Table 5. Genus level taxonomic changes in the morphospecies *E. huxleyi*.

Changes		Author	Date	Discipline	Methodology/taxonomic concept
Pontosphaera	*huxleyi*	Lohmann	1902	Biology	Light microscope/Morphological concept
Pontosphaera/Hymenomonas	*huxleyi*	Kamptner	1930	Biology/Paleontology	Light microscope/Morphological concept
Hymenomonas/Coccolithus	*huxleyi*	Kamptner	1943	Biology/Paleontology	Light microscope/Morphological concept
Coccolithus/Emiliania	*huxleyi*	Hay and Mohler	1967	Paleontology	Electron microscopy/Coccolith concept
Emiliania/Gephyrocapsa	*huxleyi*	Reinhardt	1972	Paleontology	Electron microscopy/Coccolith concept

Finally, note that of the Noëlaerhabdaceae, only *E. huxleyi* and *G. oceanica* were included in this study, these two species being relatively easy to isolate and culture. Other *Emiliania, Gephyrocapsa* and *Reticulofenestra* morphological species and varieties, all sharing the same basic coccolith structure, are obvious targets for future isolation into culture as this would permit more detailed assessment of phylogenetic affiliations. In combination with paleontological calibrations of molecular phylogenetic reconstructions, this would also

help to refine understanding of modes and rates of morpho-genetic evolution in this important group.

Evolutionary history of the Isochrysidales

The overall evolutionary scheme of the Isochrysidales is one in which successive loss of characters is the predominant pattern (Fig. 10). There is some doubt as to the phylogenetic position of the Isochrysidales within the Calcihaptophycidaeae (de Vargas et al. 2007, Liu et al. 2010), but it nevertheless appears probable that the earliest Isochrysidalean was a pelagic organism that exhibited a haplo-diploid life cycle, calcifying in at least one life cycle stage (diploid), with relatively well-developed flagella/haptonema and relatively ornate body scales. Prior to the divergence of the two extant families within the order, alkenones evolved and there was in all probability already an ultrastructural simplification (e.g. reduction in complexity of flagellar/haptonematal structure and scales). The suggested roles of alkenones as a novel and unique means of metabolic storage (Epstein et al. 2001) potentially associated with the function of the coccolith-producing vesicle (Sawada and Shiraiwa 2004) indicate that their evolution might have been a key factor in a fundamental ecological change towards the fast growing, opportunistic strategy that distinguishes most Noëlaerhabdaceans (both extant and extinct) from other coccolithophores. Structural simplification might be considered a logical consequence of adoption of such a strategy.

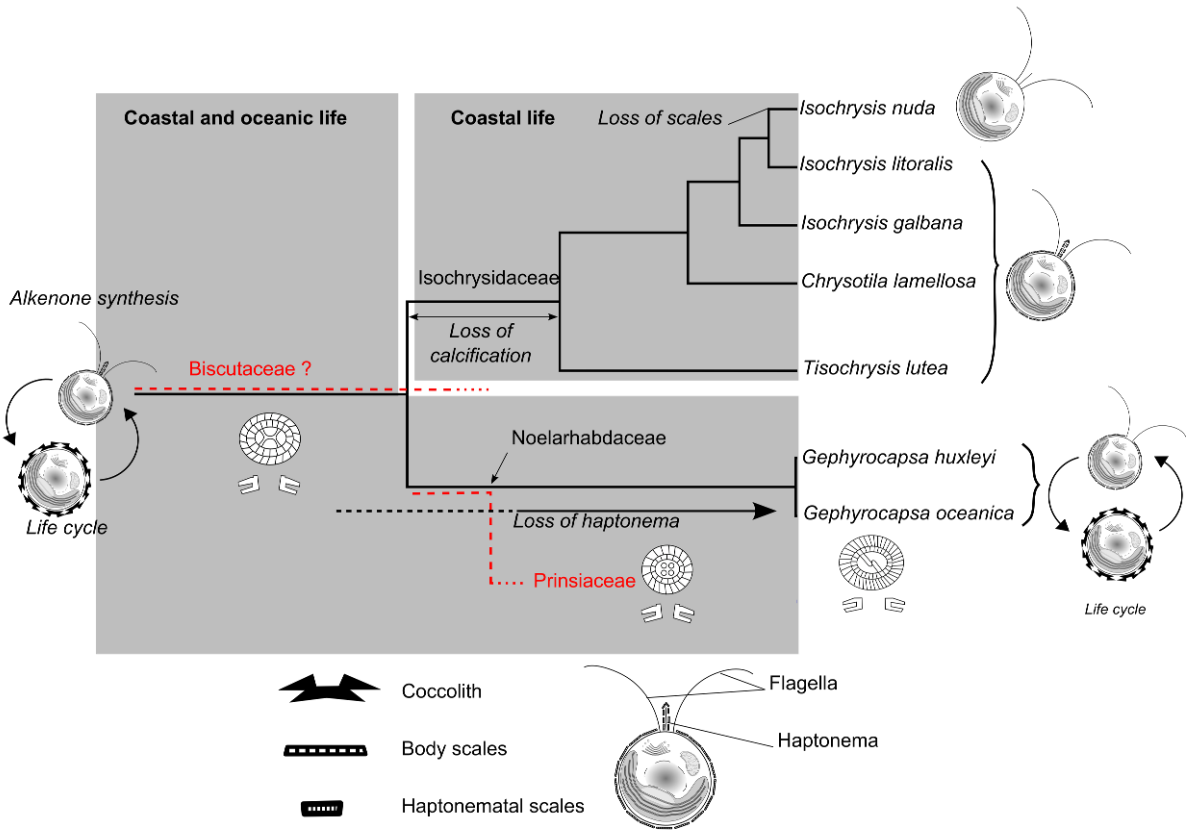

Figure 10. Hypothetical traits of evolution in the Isochrysidales.

Following the main divergence within the order that has been suggested to have occurred in the Early Cretaceous from molecular clock data (Liu et al. 2010), the two modern families evidently emerged from very different evolutionary histories. The Noëlaerhabdaceae form large pelagic populations throughout their geological range (Eocene to recent), as do their putative ancestors the Prinsiaceae (Paleocene-Eocene) and Biscutaceae (Early Jurassic to Palaeocene), as outlined in Bown (1998) and Young et al. (1999). This implies a potentially high rate of sexual reproduction. By contrast, the Isochrysidaceae lost the ability to form coccoliths and possibly also the ability to reproduce asexually in one or other of the life cycle phases (haplo-diploidy has never been demonstrated in this family), as they adapted to life in coastal environments. The Noëlaerhabdaceae would therefore be expected to exhibit a high rate of genetic evolution since large populations have a higher chance of producing beneficial mutations, but this would not necessarily correspond to high rates of speciation given the possibility for genetic exchange. Genetic evolution might be expected to be slower in smaller, coastal populations of Isochrysidaceae, but could nevertheless result in higher levels of speciation given the more heterogeneous nature of the environment and thus increased likelihood of ecological and geographical isolation of populations.

Table 4. Summary of morphological and ultrastructural characters within the Isochrysidales. The data, from previous studies and the current work, support the novel, morpho-genetic framework presented herein.

Family		**Isochrysidaceae**						**Noëlaerhabdaceae**	
Genus		***Chrysotila***		***Isochrysis***			***Tisochrysis***	***Gephyrocapsa***	
Species		***C. lamellosa***	*C.* affinis *lamellosa*	***I. galbana***	*I. litoralis*	*I. nuda*	***T. lutea***	***G. oceanica***	*G. huxleyi*
Habitats	zonation	**littoral. terrestrial**	littoral	**coastal**	littoral	coastal	**coastal**	**oceanic**	oceanic
	climate (or latitude)	**temperate**	temperate?	**temperate**	temperate	temperate / tropical	**tropical**	**tropical**	cold, temperate, tropical
Motile stage	description	**Pyriform and rather compressed, slightly metabolic, sub equal flagella**	Oblong, ovate, slightly compressed with equal flagella	**Dominant stage, ellipsoid, variable morphology**	Elongated with subequal flagella	Dominant stage, spherical or subovate, not metabolic, with subequal flagella	**Dominant stage, ovate, oblong, round (variable morphology)**	**Haploid S-Cell stage, round, ovate or ellipsoid**	Haploid S-Cell stage, round, ovate or ellipsoid
	cell size (µm)	**4.5-8 x 3-6**	4 x 3	**5-6 x 2-4 x 2.5-3**	4 x 7	3-5.5	**4.5-7.5 x 3.5-6**	**5.5 x 6**	3.5-5.5 x 5
Non-motile stage	description	**Dominant stage, cells embedded in thick stratified mucilage, hemispherical or spherical cells**	Dominant stage, cells embedded in thick stratified mucilage, hemispherical or spherical cells	**Round cell with homogenous mucilage**	Dominant stage hemispherical or round, no sarcinoid condition	Spherical and large	**Various morphologies, mostly round or ovate cells with homogenous thin mucilage or coccoid**	**Dominant stage, round and coccolith bearing, diploid C-Cell; sometimes naked round (N-cell)**	Dominant stage, round and coccolith bearing, diploid C-Cell; sometimes naked round (N-cell)
	cell size (µm)	**4.5-11 (Green and Parke 1975); 3-7 (Billard and Gayra 1972l)**	4 x 6	**5 x 6**	4-6 x 6-8; 5	4.5 -5	3-6 x 3-6.5	**04-juin**	3.5-5
Body scales	size (µm)	**0.2 x 0.14 (Green and Parke 1975); 0.16 x 0.14 (Billard and Gayral 1972)**	**not observed**	**0.3-0.4 x 0.2-0.3**	0.3 x 0.18	absent	**0.35 x 0.25**	**1.3 x 1**	1.3 x 1
Coccoliths	size (µm)	-	-	-	-	-	-	**3-4 x 3.5-5**	2.5-3 x 3.5-4
Insertion of appendages		**apical**	apical	**apical**	apical	apical	**apical**	**apical**	apical
Flagella	length (µm)	**6-7 and 4-5 (Green and Parke 1975); 8 and 6 (Billard and Gayral 1972)**	approx. 4	**approx. 7**	7-8 x 8-9	approx. 7	**approx. 7**	**7**	6.5-7
	flagellar action	**heterodynamic (Green and Parke 1975); homodynamic (Billard and Gayral 1972)**	homodynamic	**homodynamic**	homodynamic	homodynamic	**homodynamic**	homodynamic	homodynamic
Haptonema	presence/absence	+	**?**	+	-	+	+	-	-

	microtubule composition	**2-3 MT (Green and Parke 1975)**	**?**	**3 MT**	?	**3 MT**	**3MT**	**-**	-
	organisation	**?**	**?**	**4 MT base**	?	-	**3-4MT**	**-**	-
	special feature	**-**	**-**	**scales (0.08-0.10 x 0.05-0.08)**	?	-	**scales (0.10 x 0.07)**	**-**	-
Plastid	caracteristics	**1-2 yellow green**	1 golden green	**1 yellow brown parietal**	1-2 golden yellow parietal	1 yellow brown	**1-2 golden yellow parietal**	**1 yellow green**	1 golden yellow parietal
	pyrenoid	**1**	1	**1**	1/plastid	1	**1**	**1**	1
Strains		**PLY353, PLY408, AC17, PLY475, PLY352, PLY489, PLY509**	PLY510A, PLY510B, PLY510C	**RCC1349, RCC1353, PLY507, PLY240**	RCC1346	RCC1207, PLY401B	**RCC1349, PLY562, CCMP463, S-1, PLY506A, PLY506B, PLY506C**	**RCC1314**	RCC1216, PLY92
Basionym		***Chrysotila lamellosa* Anand 1937**		***Isochrysis galbana* Parke 1949**	*Isochrysis litoralis* Billard et Gayral 1972	*Isochrysis nuda* Bendif and Probert 2011	***Tisochrysis lutea* Bendif and Probert 2011**	***Gephyrocapsa oceanica* Kamptner 1943**	Pontosphaera *huxleyi* Lohmann 1902

With 10 extant taxa now formally described, the known diversity within the Isochrysidales remains low compared to most other haptophyte orders. With current knowledge, the two families within the order contain roughly equivalent numbers of species. There are some indications that microdiversity is high within the Noëlaerhabdaceae. A number of studies have demonstrated intraspecific genetic diversity in cultured (e.g. Medlin et al. 1996) and natural populations (e.g. Iglesias-Rodriquez et al. 2006) of *E. huxleyi*. Both *E. huxleyi* and *G. oceanica* exhibit several more or less distinct morphological variants (morphotypes, see Young and Westbroek 1991) and while there are some indications that this may have a genetic basis (e.g. Schroeder et al. 2005), it is not clear whether this corresponds to biologically independent taxa. Hagino et al. (2011) revealed the existence of two distinct, biogeographically isolated mitochondrial haplotypes of *E. huxleyi* with no clear relationship to morphotype, leading to the suggestion that morphotype may be an inherited polymorphism in these two lineages. Our study provides a first indication that species are genetically more clearly delineated within the Isochrysidaceae, but that morpho-structural characters are rather conserved (presence of cryptic taxa). As a consequence of this, it would be predicted that significant levels of biological (but probably not morphological) diversity remain to be discovered in this family.

Concluding remarks

The dichotomous evolutionary pathways of the two families within the Isochrysidales represents an interesting case study of the difficulty of defining a unified taxonomic concept for protists, even when comparing relatively closely related organisms. Molecular schemes challenge morphological assumptions in different ways in the two families of the order. It is clear that defining reference levels to estimate taxonomic rank based solely on molecular divergence, as is increasingly applied to microbial and metazoan diversity, remains a difficult task in protistan systematics, but our study demonstrates that the same applies to definition based solely on morphological criteria, upon which the overwhelming majority of protistan taxonomy remains based. We applied a case-by-case taxonomic treatment, attempting to take into account the need for overall taxonomic consistency, but also the difficulty of assigning a standardized taxonomic value to characters that evolve at different rates, as well as the pragmatic need for a scheme that is applicable at the practical level. In both families, suggested taxonomic changes impact the scientific and societal use of these widely-known organisms, a factor that tends to lead to resistance to adopt taxonomic changes. In this context, we simply note that the taxonomic history of both families illustrates that taxonomy is by nature an evolutionary process based on advances in the state of knowledge of groups of organisms and that carefully chosen taxonomic names are a powerful means to convey a subset of the state-of-the-art of this knowledge.

Finally, we note that the effort made to maintain type or authentic strains is invaluable for this type of study. Discovery of new features or accidental changes in cultures can only be verified by the existence of, and open-access to, this reference material. The case of the *C. stipitata* strains reported here demonstrates the importance of independently verifying strain identity of cultures obtained from collections.

This study provides a framework for proposing evolutionary scenarios linked to the important role of coccolithophores in global biogeochemical dynamics and for interpreting future environmental monitoring by gene sequencing efforts.

Taxonomic summary

Chrysotila Anand

Type species: *Chrysotila stipitata* Anand

BASIONYM: *Chrysotila stipitata* Anand 1937 *Journal of Botany* 7: 289–297

Chrysotila lamellosa Anand

BASIONYM: *Chrysotila lamellosa* Anand 1937*Journal of Botany* 7: 289–297

SYNONYMS: *Ruttnera spectabilis* Geitler 1943 *In Rev Gesamten Hydrobio Hydrogr* 43: 100-109; *Isochrysis maritima* Billard and Gayral 1972 *Br Phycol J***:** 289–297

REVISED DIAGNOSIS OF *Isochrysis* Parke **emend Bendif and Probert**:

Cells solitary, usually motile, 3-7 µm in diameter, sometimes metabolic. Scales present or absent; when present, in several layers with 10 radiating ribs arranged in each of four quadrants. Flagella two, more or less equal (around 7 µm), inserted apically. Abbreviated haptonema present between flagella; when emergent, approximately three microtubules in emergent part and covered with small round scales with 12 radial ridges. Plastid 1-2, parietal, yellow-brown with an immersed pyrenoid. Asexual reproduction by division in the motile and non-motile stages.

TYPE SPECIES: *Isochrysis galbana* Parke

BASIONYM: *Isochrysis galbana* Parke 1949 *J mar biol Ass UK* 28: 255-286

Isochrysis litoralis Billard and Gayral 1972

BASIONYM: *Isochrysis litoralis* Billard and Gayral 1972 *Br Phycol J***:** 289–297

***Isochrysis nuda* sp. nov. Bendif et Probert**

DIAGNOSIS :

Cellulae solitariae mobiles (4 µm) non squamae. Bina flagella aequalia (7.5 - 9 µm) in apical iter insertae, haptonema brevia (100 nm). Uno plastid parietale flavi vel flavirenti quisque pyrenoides unicum immersum fivens. Propagatio vegetativa duplicatione cellularum mobilum.

Cells solitary, motile, 4 µm in diameter, without scales. Flagella two, equal (7.5 - 9 µm) inserted apically with an abbreviated haptonema (100 nm) between; the latter with three to four microtubules in the emergent part. Plastid single, parietal, yellow-brown with an immersed pyrenoid. Asexual reproduction by division in the motile stages.
HOLOTYPE: Cryopreserved strain RCC1207 in the Roscoff Culture Collection
ETYMOLOGY: *nuda* to highlight the lack of body scales in this species of *Isochrysis*.

Tisochrysis **Bendif et Probert gen. nov.**
DIAGNOSIS :
Cellulae solitariae mobiles squamae multistratus vestitum. Bina flagella aequalia in apical iter insertae, haptonema brevia et squamae orbicularis, 12 porcatus radiates. Uno plastid parietale flavi vel flavirenti quisque pyrenoides unicum immersum fivens. Propagatio vegetativa duplicatione cellularum mobilum et immobilum. Sequentiae geneticae rerum nominibus 18S, 28S rRNA gene et cox1 gene pro genus propiae.

Cells solitary, motile, covered by several layers of scales with 10 radiating ribs arranged in each of four quadrants. Flagella two, equal, inserted apically with an abbreviated haptonema between, bearing small round scales with 12 radial ridges. Plastid single, parietal, yellow-brown with an immersed pyrenoid. Asexual reproduction by division in the motile and non-motile stages. Nucleotide sequences of 18S rRNA, 28 rRNA and cox1 genes distinctive from previously described isochrysidalean taxa.
ETYMOLOGY: combination of 'T' from Tahiti and *Isochrysis*.

TYPE SPECIES: ***Tisochrysis lutea*** **Bendif et Probert sp. nov.**
DIAGNOSIS :
Cellulae solitariae mobiles (3-7.5 µm) squamae multistratus vestitum 10 radiantibus in quattuor quadrantes dispositis instructae. Bina flagella aequalia in apical iter insertae, haptonema brevia 3-4 microtubulae et squamae orbicularis, 12 porcatus radiates. Uno plastid parietale flavi vel flavirenti quisque pyrenoides unicum immersum fivens. Propagatio vegetativa duplicatione cellularum mobilum et immobilum. Cellulae immobiles cum mucilagines stratum.

Cells solitary, motile, 3-7.5 µm in diameter, metabolic, covered by several layers of scales with a superficial pattern of around 40 radial ridges. Flagella two, equal (around 7 µm) inserted apically with an abbreviated haptonema (100 nm) between; the latter with three to four microtubules in the emergent part and bearing small oval scales with a central swelling and around 12 radial ridges. Plastid single, parietal, yellow-brown with an immersed pyrenoid. Asexual reproduction by division in the motile and non-motile stages. Non-motile cells embedded in thin layer of mucilage.
HOLOTYPE: Cryopreserved strain RCC1349 in the Roscoff Culture Collection.
ETYMOLOGY: *lutea* in latin refers to the orange color of old cultures of the species.

REVISED DIAGNOSIS OF *Dicrateria* Parke **emend Bendif and Probert**:
Cells motile, more or less spherical, 2-5.5 µm in diameter, not metabolic. Flagella two, subequal, 4.5-9 µm in length, smooth, arising from a papilla, the bases widely divergent; the papilla elongated in the plane at right-angles to that containing the flagellar bases. Haptonema absent with sometimes a proboscis containing endoplasmic reticulum between the flagella. Body scales absent or present; when present, 0.45-0.68 µm in diameter with 16-23 superficial radiating ridges; a second scale type, 0.72-0.8 µm in diameter with upturned rims, sometimes present. Plastids two, golden-brown, parietal, sometimes four in older cells, each with an immersed pyrenoid. Asexual reproduction by division in the motile and non-motile condition.
BASIONYM: Dicrateria Parke 1949
SYNONYM: *Imantonia* Reynolds 1974 *British Phycological Journal* 9: 429-434.

TYPE SPECIES: *Dicrateria inornata* Parke
BASIONYM: *Dicrateria inornata* Parke 1949 *J mar biol Ass UK* 28: 255-286;

***Dicrateria rotunda* comb. nov. Bendif and Probert**
BASIONYM: *Imantonia rotunda* Reynolds 1974 J Phycol Br 9: 429-434.
SYNONYM: *Imantonia rotunda* Reynolds 1974 J Phycol Br 9: 429-434.

Material and methods

Origin and morphological characterisation of analysed strains: Isochrysidales strains (Table 2) from the Roscoff Culture Collection (RCC), the Plymouth culture collection (PLY) and the Provasoli-Guillard Center for Culture of Marine Phytoplankton (CCMP) were maintained in K/2(-Si,-Tris,-Cu) medium (Keller et al. 1987) at 17°C with 50µmol-photons.m^{-2}.s^{-1} illumination provided by daylight neon tubes with a 14:10h L:D cycle.

Living cells were observed with an Olympus BX51 light microscope equipped with differential interference contrast (DIC) optics. Polysaccharide excretions from cultured cells were stained with 1% toluidine blue. For transmission electron microscopy (TEM), cells were collected by gentle centrifugation and fixed with a 2.5% glutaraldehyde solution with 0.25M sucrose in 0.1M sodium cacodylate buffer at pH 7.2 for two hours. After three rinses in 0.1M cacodylate buffer with decreasing sucrose concentration (0.25M, 0.1M, 0M), cells were post-fixed for one hour with 1% osmium tetroxide and washed once in 0.1M cacodylate buffer. Dehydration was performed by transfer through a graded ethanol series (30, 50, 70, 85, 90, 95 and 100%) for 10 min each. The dehydrated cells were suspended in a 50:50 mixture of Epon's resin and ethanol for one hour and then embedded in 100% epon's resin. The embedded samples were polymerized at 60°C for twenty-four hours and sectioned using a Leica ultramicrotome with a diamond knife. Thin sections were placed on formvar covered copper grids. Sections were stained with uranyl acetate followed by post staining with lead citrate according to Reynold's protocol (1963). The sections were examined under a JEOL 1011 and a JEOL JEM 1400 transmission electron microscope at an accelerating voltage of 80 kV. For scanning electron microscopy (SEM), coccolithophore cells were grown until early exponential phase and then filtered onto nitrocellulose filters that were dried in a desiccator before being sputter coated with a thin layer of Au/Pd. Observations were made with a Philips XL 30 FEG.

Table 2. List and sequence accession numbers of the 26 Isochrysidales strains used in this study (* indicates authentic strains; Algobank-Caen (AC and HAP), Culture Collection of Algae and Protozoa (CCAP), Provasoli-Guillard Center for Culture of Marine Phytoplankton (CCMP), Commonwealth Scientific and Industrial Research Organisation (CS), North East Pacific Culture Collection (NEPCC), Plymouth Culture Collection (PLY), Roscoff Culture Collection (RCC), and, University of Texas (UTEX)).

Name	Strain codes	Equivalent strain codes	Origin	GenBank accession number (18S+28S+cox1)
*Chrysotila lamellosa**	PLY353		SW England; estuarine	
*Chrysotila lamellosa**	PLY408	CCAP 918/1, CS272	England; terrestrial	
Chrysotila lamellosa	RCC1195	AC17, HAP17	English Channel; coastal	
Chrysotila lamellosa	PLY475		Terrestrial	
Chrysotila lamellosa	PLY489		UK; terrestrial	
*Chrysotila stipitata**	PLY377		SW England; coastal	
*Chrysotila stipitata**	PLY432	CCAP 918/2	English Channel; coastal	
Chrysotila stipitata	RCC1196	AC4, HAP4	English Channel; coastal	
Chrysotila sp.	PLY509		S. Wales; coastal	
Chrysotila sp.	PLY510A		England; E. coast	
Dicrateria inornata	PLY564	CS267	English channel ; coastal	
Dicrateria sp.	RCC1207	AC49, HAP49	Atlantic (Morocco); coastal	
Emiliania huxleyi	RCC1216	TQ26	South Pacific,	
Gephyrocapsa oceanica	RCC1292	PR3F1	North Atlantic	
Isochrysis aff. galbana	RCC1349	T.ISO, AC102, HAP34T, CCAP927/14, CCMP1324, NEPCC 601, CS-177;	Pacific (tropical): coastal	
Isochrysis sp.	RCC1344	AC620, S-1	Atlantic (spain); coastal	
*Isochrysis galbana**	RCC1348	RCC1347, PLY I, AC34, AC101, HAP34, HAP34bis, CCAP927/1, UTEX987, CCMP1323, NEPCC2, NEPCC633, PLY565	Irish Sea	
*Isochrysis litoralis**	RCC1346	AC18, HAP18	English Channel; coastal	
Isochrysis sp.	RCC1350	CCMP463	Atlantic ocean	
Isochrysis sp.	PLY8		Irish Sea	
Isochrysis sp.	PLY240		Irish Sea	
Isochrysis sp.	PLY352		SW England; estuarine	
Isochrysis sp.	PLY401B		English Channel; coastal	
Isochrysis sp.	PLY506A		Pacific (tropical)	
Isochrysis sp.	PLY506B		Pacific (tropical)	
Isochrysis sp.	PLY506C		Pacific (tropical)	
Isochrysis sp.	PLY507		Eastern USA; estuarine	
Isochrysis sp.	PLY562		North Sea; coastal	
*Pseudoisochrysis paradoxa**	RCC1353	AC80, HAP80, CCAP949/1, UTEX1988	North Atlantic USA; estuarine	

Genetic analyses: Genomic DNA was extracted using the DNeasy Plant mini kit (Qiagen). SSU, LSU and cox1 genes were amplified by PCR using different couples of primers listed in the supplementary table 1. PCRs were performed in a total reaction volume of 25 µL using the *GoTaq* Polymerase kit (Promega). A standard PCR protocol was used with a T1 thermal cycler (Biometra): 2 min initial denaturation at 95°C, followed by 35 cycles of 30s at 95°C, 30s annealing at 55°C and 1 min extension at 72°C. A final 5 min extension step at 72°C was conducted to complete the amplification. Amplification products were controlled by electrophoresis on a 1% agarose gel. The PCR products were sequenced directly on an ABI PRISM 3100 xl DNA auto sequencer (Perkin-Elmer) using the ABI PRISM BigDye Terminator Cycle Sequencing Kit (Perkin-Elmer).

For each gene, an alignment including sequences from other haptophytes was first performed with the online version of the multiple alignment program MAFFT (Katoh et al. 2007). Alignements were double-checked *de visu* in the sequence editor BIOEDIT (Hall 1999). Excessively variable regions were automatically removed using the Gblocks software (Castresana 2000) with optimised parameters for rRNA alignments (minimum length of a block = 5; allowing gaps in half of positions) for both SSU and LSU rDNA. The Gblocks software retained 1720 nucleotide positions for phylogenetic analyses from the initial 1820 positions in the SSU rDNA, and 514 out of the initial 550 positions for LSU rDNA. For the cox1 gene, a fragment of around 400 nucleotides was sequenced; 330 nucleotides were retained for sequences alignment that was checked by hand after codons translation.

Appropriate models of DNA substitution were detected with TREEFINDER (Jobb et al. 2004), using the three proposed statistics (AIC, AICc and BIC), and the partition-wise option. For SSU rDNA, a TN substitution model (Tamura and Nei 1993) was selected taking into account a gamma-shaped distribution of the rates of substitution among sites (G= 0.10) optimised with the following rate parameters: TC= 0.50, TA= 0.11, TG= 0.11, CA= 0.11, CG= 0.11, AG= 0.08 and the following nucleotide frequency parameters: T= 0.25, C= 0.22, A= 0.25, G= 0.28. For the LSU rDNA, a J2 substitution model (Jobb et al. 2004) was selected, with a gamma-shaped distribution of the rates of substitution among sites (G= 0.20) optimised with the following rate parameters: TC= 0.56, TA= 0.02, TG= 0.18, CA= 0.02, CG= 0.18, AG= 0.03, and the following nucleotide frequency parameters: T= 0.18, C= 0.27, A= 0.22, G= 0.34. For cox1, a J1 substitution model (Jobb et al. 2004) was proposed taking into account a gamma-shaped distribution of the rates of substitution among sites (G= 0.30) optimised with the following rate parameters: TC= 0.27, TA= 0.14, TG= 0.14, CA= 0.02, CG= 0.02, AG= 0.42, and the following nucleotide frequency parameters: T= 0.27, C= 0.18,

A= 0.41, G= 0.14. The selected models and parameters were used to perform phylogenetic analyses. The phylogenetic reconstruction was determined using two methods: maximum likelihood (ML), as implemented in TREEFINDER (Jobb et al. 2004) and Bayesian statistics with Mr.BAYES v3.1.2 (Ronquist and Huelsenbeck 2003). The robustness of ML trees topology was tested by bootstrapping with 1000 replicates. The Bayesian analysis was conducted with two runs of four Markov chains, for at least 3 million generations, sampling every 100th generation. The burn-in option was set for discarding 25% from the 30,000 trees found. A research for distance clustering was also performed using the neighbour joining method to infer a distance tree and this analysis showed a different topology (SF1). For testing alternative topologies, comparison of likelihood scores of the competing hypotheses (best inferred tree versus alternative hypothesis) was performed using various criteria: Shimodaira-Hasegawa (SH, Shimodaira and Hasegawa 1999), Approximately Unbiased (AU, Shimodaira 2002) and Kishino-Hasegawa (KH, Kishino and Hasegawa 1989) as implemented in TREEFINDER (Jobb et al. 2004).

Table 3. Likelihood scores and likelihood-based test of tree topologies, using the Kishino-Hasegawa (KH; Kishino and Hasegawa 1989), Shimodaira-Hasegawa (SH; Shimodaira and Hasegawa 1999)) and Approximately Unbiased (AU; Shimodaira 2002)) statistics. * indicates statistical significance.

Best ML tree	Likelihood	KH	SH	AU
Without constraint	-6141,121	1	1	0,89
With constraint	-6146,836	0,14*	0,69	0,11*

Acknowledgements

We thank Richard Pipe and Maria Jutson from the Plymouth Culture Collection and Benoit Véron from the Algobank Culture Collection for providing Isochrysidales strains. From the Station Biologique de Roscoff, we thank Morgan Perennou and Gwen Tanguy from the Service GENOMER for sequencing assistance, and Sophie Le Panse from the Electron Microscopy platform. We are also grateful to Bruno de Reviers for helpful discussions on taxonomic details. This work was supported by a PhD grant from the Region Bretagne (EMB), and by the following research programs: the EC FP7–"European Project on Ocean Acidification" (EPOCA, grant agreement 211384; EMB, DCS, CdV), the EU FP7 I3 program ASSEMBLE (grant 227799), the Interreg IV program MARINEXUS (IP), and the EU EraNet BiodivERsA program “Biodiversity of Marine euKaryotes (BioMarKs; CdV).

References

Anand PL (1936). Seven new Chrysophyceae from the south-east of England. *Proceedings of the Tweny Third Indian Science Congress, Indore*. 282-283.

Anand PL (1937). A taxonomic study of the algae of British chalk-cliffs. *J Bot* 75: 1-51.

Biekart JW (1989). The distribution of calcareous nannoplankton in late Quaternary sediments collected by the Snellius II Expedition in some southeast Indonesian basins. *Proc K Ned Akad Wet* 92: 77-141.

Billard C and Gayral P (1972). Two new species of *Isochrysis* with remarks on the genus *Ruttnera*. *Br Phycol J***:** 289-297.

Bougaran G, Le Déan L, Lukomska E, Kaas R and Baron R (2003). Transient initial phase in continuous culture of *Isochrysis galbana* affinis *Tahiti*. *Aquat Living Res* 16: 389-394.

Bourrelly P and Magne F (1953). Deux nouvelles espèces de Chrysophycées marines. *Rev Gen Bot* 60: 684-687.

Bourrelly P (1957). Recherches sur les Chrysophycées. Morphologie, Phylogénie, Systématique. *Rev Algo*, mémoire hors-série 1. 414 pp.

Bown PR (1998). *Calcareous Nannofossil Biostratigraphy*. British Micropalaeontological Society Publication Series, Chapman and Hall (London). 315 pp.

Brassell SC and Dumitrescu M (2004). Recognition of alkenones in a lower Aptian porcellanite from the west-central Pacific. *Org Geochem* 35: 181-188.

Brassell SC, Eglinton G, Marlowe IT, Plaufmann U and Sarnthein M (1986). Molecular stratigraphy: a new tool for climatic assessment. *Nature* 320: 129-133.

Bréhéret J (1978). Formes nouvelles quaternaires et actuelles de la famille des Gephyrocapsaceae (Coccolithophorides). *C R Acad Sc Paris* 287: 447-449.

Brown MR, Garland CD, Jeffrey SW, Jameson ID and Leroi JM (1993). The gross and amino acid compositions of batch and semi-continuous cultures of *Isochrysis* sp. (clone T.ISO), *Pavlova lutheri* and *Nannochloropsis oculata*. *J Appl Phycol* 5: 285-296.

Brown CW and Yoder JA (1994). Coccolithophorid Blooms In The Global Ocean. *J Geo Res-Ocean* 99**:** 7467-7482.

Castresana J (2000). Selection of conserved blocks from multiple alignments for their use in phylogenetic analysis. *Mol Biol Evol* 17: 540-552.

Christensen T (1962). Alger. In Botanik Bd. 2, Systematisk Botanik, Nr. 2, (ed. Böscher TW, Lange M and Sorensen T), Munksgaard (Copenhagen). pp 1-178.

Clocchiatti M (1971). Sur l'éxistence de coccosphères portant coccolithes de *Gephyrocapsa oceanica* et de *Emiliania huxleyi* (Coccolithophoridés). *C R Acad Sc Paris* 273: 318-321.

Conte MH, Volkman JK and Eglington G (1994). Lipid biomarkers of the Haptophyta. In Green JC and Leadbeater BSC (eds) The Haptophyte algae. The Systematics Association special volume 51, Oxford University Press (Oxford, UK). pp 265-85.

Cros L and Fortuno JM (2002). Atlas of Northwestern Mediterranean Coccolithophores. *Scientia Marina*, 66 (supplement 1). 186 pp.

de Vargas C, Aubry MP, Probert I and Young J (2007). Origin and evolution of Coccolithophores: from coastal hunters to oceanic farmers, In Falkowski, P. G. and Knoll, A. [eds.], Evolution of Primary Producers in the Sea, Academic Press. pp 251-285.

Edvardsen B, Eikrem W, Green JC, Andersen RA, Moon-van der Staay SY and Medlin LK (2000). Phylogenetic reconstructions of the Haptophyta inferred from 18S ribosomal DNA sequences and available morphological data. *Phycologia* 39: 19-35.

Epstein BL, D'Hondt S and Hargraves PE (2001). The possible metabolic role of C37 alkenones in *Emiliania huxleyi. Org Geochem* 32: 867-875.

Farmer C (1993). Steroidal-diols and long-chain ketones as biomarkers of Prymnesiophyte algae. *Honours Thesis, University of Tasmania, Australia.*

Fujiwara S, Tsuzuki M, Kawachi M, Minaka N and Inouye I (2001). Molecular phylogeny of the Haptophyta based on the *rbcL* gene and sequence variation in the spacer region of the RUBISCO operon. *Phycologia* 37: 121-129.

Geitler L (1943). Eine neue atmophytische Chrysophycee, *Ruttnera spectabilis* nov. gen., nov. spec.. *Int Rev Gesamten Hydrobiol Hydrogr* 43: 100-109.

Green JC and Course PA (1983) Extracellular calcification in *Chrysotila lamellosa* (Prymnesiophyceae). *Br Phycol J* 18: 367-382.

Green JC and Parke M (1974). A reinvestigation by light and electron microscopy of *Ruttnera spectabilis* Geitler (Haptophyceae), with special reference to the fine structure of the zooids. *J mar biol Ass UK* 54: 539-550.

Green JC and Parke M (1975). New observations upon members of the genus *Chrysotila* Anand, with remarks upon their relationships within the Haptophyceae. *J mar biol Ass UK* 55: 109-121.

Green JC and Pienaar RN (1977). The taxonomy of the order Isochrysidales (Prymnesiophyceae) with special reference to the genera *Isochrysis* Parke, *Dicrateria* Parke and *Imantonia* Reynolds. *J mar biol Ass UK* 57: 7-17.

Green JC, Course PA and Tarran GA. (1996). The life cycle of *Emiliania huxleyi*: A brief review and a study of relative ploidy levels analysed by flow cytometry. *J Marin Sys* 9: 33-44.

Hagino K, Bendif EM, Young J, Kogame K, Probert I, Takano Y, Horiguchi T, de Vargas C and Okada H (2011). New evidence for morphological and genetic variation in the cosmopolitan coccolithophore *Emiliania huxleyi* (Prymnesiophyceae) from cox1b-ATP4 genes. *J Phycol* (in press).

Hall TA (1999). BioEdit: a user-friendly biological sequence alignment editor and analysis program for Windows 95/98/NT. *Nucleic Acids Sym* 41: 95-98.

Hay WW, Mohler HP and Wade ME (1966). Calcareous nannofossils from Nal'Chik (Northwest Caucasus). *Eclog Geol Helvet* 59: 379-399.

Hay WW, Mohler HP, Roth PH, Schmidt RR and Boudreaux JE (1967). Calcareous nannoplankton zonation of the Cenozoic of the Gulf Coast and Caribbean-Antillean area, and transoceanic correlation. *Trans Gulf Coast Asso Geol Soc* 17: 428-480.

Heimdal BR (1973). Two new taxa of recent coccolithophorids. *Met ForErge* 13: 70-75.

Iglesias-Rodriguez MD, Halloran PR, Rickaby REM, Hall IR, Colmenero-Hidalgo E, Gittins JR, Green DRH, Tyrrell T, Gibbs SJ, von Dassow P, Rehm E, Armbrust EV and Boessenkool KP (2008). Phytoplankton calcification in a high-CO2 world. *Science* 320: 336-340.

Iglesias-Rodriguez MD, Schofield OM, Batley J, Medlin LK and Hayes PK (2006). Intraspecific genetic diversity in the marine coccolithophore *Emiliania huxleyi* (Prymnesiophyceae): the use of microsatellite analysis in marine phytoplankton population studies. *J Phycol* 42: 526-536.

Jeffrey SW and Wright SW (1994). Photosyntheitic pigments in the Haptophyta. In Green JC and Leadbeater BSC (eds) The Haptophyte algae. The Systematics Association special volume 51, Oxford University Press (Oxford, UK). pp 113-132.

Jeffrey SW, Brown MR and Volkman JK (1994). Haptophytes as feedstocks in mariculture. In Green JC and Leadbeater BSC (eds) The Haptophyte algae. The Systematics Association special volume 51, Oxford University Press (Oxford, UK). pp 265-85.

Jerkovic L (1970). *Noelaerhabdus* nov. gen. Type d'une nouvelle famille de coccolithophoridés fossiles : Noëlaerhabdaceae du Miocène supérieur de Yougoslavie. *C R Acad Sc Paris* 270: 468-470.

Jobb G, von Haeseler A and Strimmer K (2004). TREEFINDER: A powerful graphical analysis environment for molecular phylogenetics. *BMC Evol Biol* 28: 4-18.

Jordan RW and Young JR (1990). Proposed changes to the classification system of living coccolithophorids. *INA Newsletter* 12: 15-18.

Jordan RW, Cros L and Young JR (2005). A revised classification scheme for living haptophytes. *Micropaleontology* 50 (Suppl. 1): 55-79.

Kamptner E (1930). Die Kalkflagellaten des Süsswassers und ihre Beziehungen zu jenen der Brackwassers und des Meeres. *Int Rev Gesamten Hydrobiol Hydrogr* 24: 147-163.

Kamptner E (1941). Die Coccolithineen der Südwestküste von Istrien. *Ann Naturhistor Mus Wien* 51: 54-149.

Kamptner E (1943). Zur Revision der Coccolithineen-Spezies *Pontosphaera huxleyi* Lohmann. *Anz Akad Wiss Wien Math -Naturw K* 80: 43-49.

Kamptner E (1956). Das Kalkskelett von *Coccolithus huxleyi* (Lohmann) Kamptner und *Gephyrocapsa oceanica* Kamptner (Coccolithineae). *Arch Protistenkde* 101: 171-202.

Katoh K, Kuma K, Toh H and Miyata T (2007). MAFFT version 5 : improvement in accuracy of multiple sequence alignment. *Nucleic Acids Res* 33: 511-518.

Keller MD, Selvin RC, Claus W and Guillard RRL (1987). Media for the culture of oceanic ultraphytoplankton. *J Phycol* 23: 633-638.

Kishino H and Hasegawa M (1989). Evaluation of the maximum-likelihood estimate of the evolutionary tree topologies from DNA sequence data, and the branching order in Hominoidea. *J Mol Evol* 29: 170-179.

Klaveness D (1972a). *Coccolithus huxleyi* (Lohmann) Kamptner I. Morphological investigations on the vegetative cell and the process of coccolith formation. *Protistologica* 8: 335-346.

Klaveness D (1972b). *Coccolithus huxleyi* (Lohmann) Kamptner. II. The flagellate cell, aberrant cell types, vegetative propagation and life cycles. *Br Phycol J* 7: 309-318.

Langer G, Nehrke G, Probert I, Ly J and Ziveri P (2009). Strain-specific responses of *Emiliania huxleyi* to changing seawater carbonate chemistry. *Biogeosciences* 6: 2637-2646.

Liu H, Aris-Brosou S, Probert I and de Vargas C (2010). A timeline of the environmental genetics of the haptophytes. *Mol Biol Evol* 27: 171-176.

Lohmann H (1902). Die Coccolithophoridae, eine monographie der Coccolithen bildenden flagellaten, zugleich ein Beitag zur Kenntnis des Mittelmeerauftriebs. *Arch Protistenkde* 1: 89-165.

Lohmann H (1912) Untersuchungen über das Pflanzen- und Tierleben der Hochsee. *Veroff Inst Meereskd Univ Berlin NF, Georg-Naturw Reihe* 1: 1-92.

Mackinder LCM, Wheeler G, Schroeder D, Riebesell U and Brownlee C (2010). Molecular mechanisms underlying calcification in coccolithophores. *Geomicrobiol J* 27, 585-595.

Marlowe IT, Green JC, Neal AC, Brassell SC, Eglington G and Course PA (1984). Long chain (n-C_{37}-C_{39}) Alkenones in the Prymnesiophyceae. Distribution of Alkenones and other Lipids and their Taxonomic Significance. *Br Phycol J* 19: 203-216.

McIntyre A (1970). *Gephyrocapsa protohuxleyi* sp. n. a possible phyletic link and index fossil for the Pleistocene. *Deep Sea Res* 17: 187-190.

McIntyre A and Bé AWH (1967). Modern coccolithophorids of the Atlantic Ocean - I. Placoliths and cyrtoliths. *Deep Sea Res* 14: 561-597.

Medlin LK, Barker GLA, Campbell L, Green JC, Hayes PK, Marie D, Wrieden S and Vaulot D (1996). Genetic characterisation of *Emiliania huxleyi* (Haptophyta). *J Marin Sys* 9: 13-31.

Medlin LK, Sàez AG and Young JR (2008). A molecular clock for coccolithophores and implications for selectivity of phytoplankton extinctions across the K / T boundary. *Mar Mic* 67: 69-86.

Müller PJ, Kirst G, Ruhland G, von Storch I and Rosell-Mele A (1998). Calibration of the alkenone paleotemperature index $U^{K'}37$ based on core-tops from the eastern South Atlantic and the global ocean (60°N-60°S). *Geochim. Cosmochim. Acta* 62: 1757-1772.

Okada H and McIntyre A (1977). Modern coccolithophores of the Pacific and North Atlantic Oceans. *Micropal* 23: 1-55.

O'Shea SK, Holland F and Bilodeau A (2010). Modeling the Effects of Salinity and pH on the Cadmium Bioabsorptive Properties of the Microalgae *Isochrysis galbana* (T-Iso) in Coastal Waters. *J Coast Res* 26: 56-66.

Paasche E (2002). A review of the coccolithophorid *Emiliania huxleyi* (Prymnesiophyceae), with particular reference to growth, coccolith formation, and calcification-photosynthesis interactions. *Phycologia* 40: 503-529.

Parke M (1949). Studies on marine flagellates. *J mar biol Ass UK* 28: 255-286.

Parke M and Dixon PS (1964). A revised check-list of British marine algae. *J mar biol Ass UK* 44: 499-542.

Pascher A (1910). Chrysomonaden aus dem Hirschberger Grossteiche. *Int Rev Gesamten Hydrobiol Hydrogr* 1: 1-66.

Pennick NC (1977). Studies on the external morphology of *Pyramimonas*. 4. *Pyramimonas virginica* sp.. *Archr Protistenkd* 119: 239-246.

Reinhardt P (1972). Coccolithen. Kalkiges Plankton seit Jahrmillionen. *Die neue Brehm Bücheri* 453: 1-99.

Reynolds ES (1963). The use of lead citrate at high pH as an electron-opaque stain in electron microscopy. *J Cell Biol* 17: 208-212.

Reynolds N (1974). *Imantonia rotunda* gen. et sp. nov., a new member of the Haptophyceae. *Br Phycol J* 9: 429-434.

Riebesell U, Zondervan I, Rost B, Tortell PD, Zeebe RE and Morel FMM (2000). Reduced calcification of marine plankton in response to increased atmospheric CO_2. *Nature* 407: 364-367.

Ronquist F and Huelsenbeck JP (2003). MRBAYES 3: Bayesian phylogenetic inference under mixed models. *Bioinformatics* 19: 1572-1574.

Rost B and Riebesell U (2004). Coccolithophores and the biological pump responses to environmental changes. In Thierstein, H. R. and Young, J. R. [Eds.] Coccolithophores – From Molecular Processes to Global Impact. Springer, Berlin. pp. 99-125.

Sáez AG, Probert I, Young J, Edvardsen B, Eikrem W and Medlin LK (2004). A review of the phylogeny of the Haptophyta. In Thierstein, H. R. and Young, J. R. [Eds.] Coccolithophores – From Molecular Processes to Global Impact. Springer, Berlin. pp. 251-269.

Sawada K and Shiraiwa Y (2004). Alkenone and alkenoic acid compositions of the membrane fractions of *Emiliania huxleyi*. *Phytochemistry* 65: 1299-1307.

Schroeder DC, Biggi GF, Hall M, Davy J, Martínez JM, Richardson AJ, Malin G and Wilson WH (2005). A genetic marker to separate *Emiliania huxleyi* (Prymnesiophyceae) morphotypes. *J Phycol* 41: 874-879.

Shimodaira H and Hasegawa M (1999). Multiple comparisons of log-likelihoods with applications to phylogenetic inference. *Mol Biol Evol* 16: 1114-1116.

Shimodaira H (2002). An approximately unbiased test of phylogenetic tree selection. *Syst Biol* 51: 492-508.

Subrahmanyan R (1962). On *Ruttnera pringsheimii* sp. nov. (Chrysophyceae) from the coastal waters of India. *Arch Microbiol* 42: 219-225.

Tamura K and Nei M (1993). Estimation of the number of nucleotide substitutions in the control region of mitochondrial DNA in humans and chimpanzees. *Mol Biol Evol* 10: 512-526.

Thierstein HR, Geitzenauer KR, Molfino B and Shackleton NJ (1977). Global synchroneity of late Quarternary coccolith datum levels: Validation by oxygen isotopes. *Geology* 5: 400-404.

von Dassow P, Ogata H, Probert I, Wincker P, Da Silva C, Audic S, Claverie J-M and de Vargas C (2009). Transcriptome analysis of functional differentiation between haploid and diploid cells of *Emiliania huxleyi*, a globally significant photosynthetic calcifying cell. *Genome Biol* 10: R114.

Wahlund TM, Hadaegh AR, Clark R, Nguyen B, Fanelli M and Read BA (2004). Analysis of expressed sequence tags from calcifying cells of marine coccolithophorid (*Emiliania huxleyi*). *Mar Biotech* 6: 278-290.

Westbroek P, Brown CW, van Bleijswijk J, Brownlee C, Brummer GJ, Conte M, Egge J, Fernandez E, Jordan R, Knappertsbusch M, Stefels J, Veldhuis M, van der Wal P and Young J (1993). A model system approach to biological climate forcing. An example of *Emiliania huxleyi*. *Global Planetary Change* 8: 27-46.

Young JR (1992). The description and analysis of coccolith structure. In: Harmsmid B and Young JR, *Nannoplankton Research*. ZPZ. pp 35-71.

Young JR and Bown PR (1997). Higher classification of calcareous nannofossils. *J Nanno Res* 19: 15-20.

Young JR, Davis SA, Bown PR and Mann S (1999). Coccolith ultrastructure and biomineralisation. *J Struct Biol* 126: 195-215.

Young JR and Geisen M (2002). Xenospheres-associations of coccoliths resembling coccospheres. *J Nanno Res* 24: 127-135.

Young JR, Geisen M, Cros L, Kleijne A, Probert I, Sprengel C and Østergaard JB (2003). A guide to extant coccolithophore taxonomy. *J Nanno Res* Special Issue 1. 124 pp.

Young JR, Henriksen K and Probert I (2004). Structure and morphogenesis of the coccoliths of the CODENET species. In Thierstein, H. R. and Young, J. R. [Eds.] Coccolithophores – From Molecular Processes to Global Impact. Springer, Berlin. pp.191-216.

Young JR and Westbroek P (1991). Genotypic variation in the coccolithophorid species *Emiliania huxleyi*. *Mar Micropal* 18: 5-23.

Zapata M, Jeffrey SW, Wright SW, Rodriguez F, Garrido JL and Clementson L(2004). Photosynthetic pigmentsin 37 species (65 strains) of Haptophyta: Implications for oceanography and chemotaxonomy. *Mar Eco Prog Ser* 270: 83-102.

Supplementary information

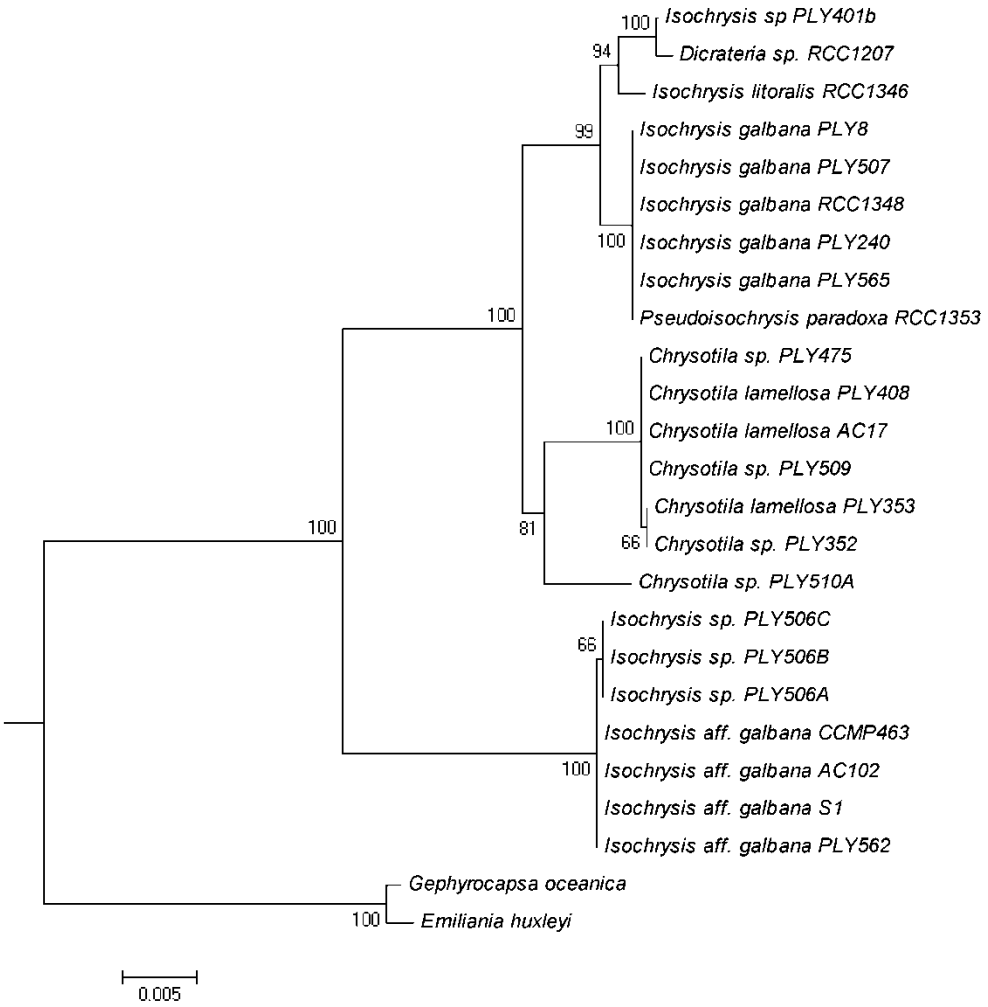

Supplementary figure 1. Neighbour joining phylogenetic tree of the Isochrysidales, inferred from concatenated sequences of SSU rDNA, LSU rDNA and cox1 genes. Bootstrap values are given at each node of the tree. Sequences of *Phaeocystis globosa* were used as an outgroup. The original species name and strain codes are given in Table 2.

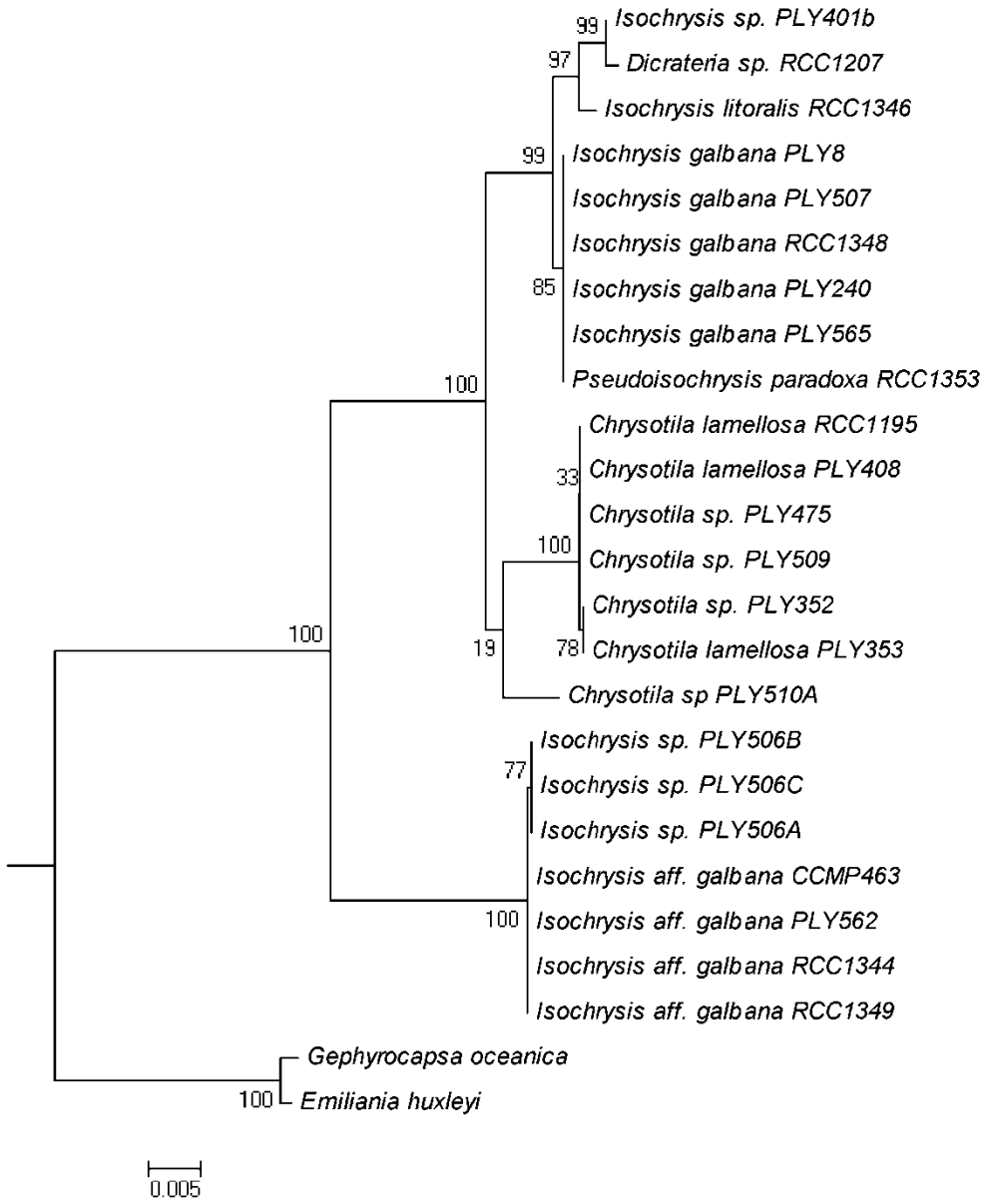

Supplementary figure 2. ML phylogenetic tree of the Isochrysidales, inferred from concatenated sequences of SSU rDNA, LSU rDNA and cox1 genes. This topology was obtained by constrained inference from the distance tree. Bootstrap values are given at each node of the tree. Sequences of *Phaeocystis globosa* were used as an outgroup. The original species name and strain codes are given in Table 2.

Supplementary table 1. primers used in this study

target gene	primer name	primer sequences 5'-3'	direction	reference	couple used in this study
SSU	A18Dir	AACCTGGTTGATCCTGCCAGT	forward	Sogin et al 1990	Prym887r
	A18Rev	TCCTTCTGCAGGTTCACCTAC	reverse		Prym429f
	Prym429f	GCGCGTAAATTGCCCGAA	forward	Coolen et al 2004	A18Dir
	Prym887r	GGAATACGAGTGCCCCTGAC	reverse		A18Rev
LSU	Hapto4	ATGGCGAATGAAGCGGGC	forward	Liu et al 2009	couple
	IspLR2	CTTCACCCTACCCAGGCATA	reverse	in this study	
cox1	igA	GCAATATCTAGTCCTGAATTTGA	forward	Hayashi-Ishimaru et al. 1997	couple
	igB	ACCAGCATTTGGAATAGTTTCAC	reverse		

Supplementary references

Coolen MJL, Muyzer G, Rijpstra, WIC, Schouten S, Volkman JK and Damste JSS (2004). Combined DNA and lipid analyses of sediments reveal changes in Holocene haptophyte and diatom populations in an Antarctic lake. *Earth Planet Sci Lett* 223: 225-239.

Hayashi-Ishimaru Y, Ehara M, Inagaki Y and Ohama T (1997) A deviant genetic code in prymnesiophytes (yellow-algae): UGA codon for tryptophan. Curr Genet 32: 296-299.

Liu H, Probert I, Uitz J, Claustre H, Aris-Brossou S, Frada M, Not F and de Vargas C (2009) Extreme oceanic biodiversity in noncalcifying haptophytes explains a major pigment paradox. *Proc Natl Acad Sci USA* 106: 12803-12808.

Sogin ML (1990) Amplification of ribosomal RNA genes for molecular evolution studies. In Innes MA, Gelfand DH, Sninsky JJ, White TJ (eds) PCR protocols. Academic Press, San Diego. pp. 307-320.

CHAPITRE 2

EVALUATION OF GENETIC MARKERS FOR THE COSMOPOLITAN COCCOLITHOPHORES *G. HUXLEYI* AND *G. OCEANICA*

El Mahdi Bendif [1], Ian Probert[2], Margaux Carmichael[1], Sarah Romac[1], Kyoko Hagino[3], Kazuhiro Kogame[4], Yoshihito Takano[5] and Colomban de Vargas[1]

[1]CNRS UMR7144/UPMC, EPPO team, Station Biologique de Roscoff, 29682 Roscoff, France

[2]CNRS /UPMC, FR2424, Station Biologique de Roscoff, 29682 Roscoff, France

[3]Institute for Study of the Earth's Interior Okayama University, 827 Yamada, Misasa, Tottori 682-0193, Japan

[4]Department of Natural History Sciences, Faculty of Science, Hokkaido University, Sapporo 060-0810, Japan

[5]Institute for East China Sea Research, Nagasaki University, Nagasaki, 1-14 Bunkyo, Nagasaki, 852-8521, Japan

Introduction

Coccolithophores are marine photosynthetic protists characterized by their covering of minute calcite platelets (the coccoliths). Playing extremely important roles in global biogeochemical cycles (Rost and Riebesell 2004) since their origin in the Triassic (Bown 2005), intense research interest has recently been focussed on attempting to predict the responses of coccolithophores to environmental changes linked to the antropogenically-induced rise in atmospheric CO_2, i.e. effects such as global warming and ocean acidification (Riebesell et al. 2000; Iglesias-Rodriguez et al 2008; Langer et al 2009). The fossil remains of coccolithophores also provide valuable proxies for paleo-environment reconstruction, both via elemental and isotopic analysis of coccoliths (e.g. Andrews and Giraudeau 2002) and via measurement of the ratio of different types of alkenone, a class of robust long-chain (C_{37}-C_{39}) esters of polyunsaturated n-C_{36} acids and C_{27}-C_{29} sterols produced uniquely by members of the coccolithophore order Isochrysidales and widely used as a proxy for sea surface temperature (Müller et al. 1998).

The two most ecologically important extant coccolithophores are *Gephyrocapsa huxleyi* Lohmann (Lohmann 1902; Reinhardt 1972) and *G. oceanica* Kamptner (Kamptner 1943), the former in particular regularly forming very extensive "white water" blooms in high latitude coastal and shelf ecosystems (Winter et al 1994). These two closely related members of the Isochrysidales are distinguished by the relative degree of calcification of coccoliths and above all by the elevation of two of the central tube crystals to form a disjunct bridge over the central area of coccoliths of *G. oceanica* (Fig. 1). The first appearance of *G. huxleyi* in the fossil record was relatively recent (291 ka, Raffi et al 2006) and the fossil record suggests that *G. huxleyi* evolved from *G. oceanica* (Samtleben 1980). In terms of calcification, different culture strains of *G. huxleyi* have been reported to respond differently to acidification of the growth medium (Riebesell et al. 2000, Iglesias-Rodriguez et al. 2008), raising the question as to whether distinct genetic entities (cryptic or pseudo-cryptic species) exist within this morphologically defined species (e.g. Langer et al. 2010). Comparison of classical ribosomal gene markers provides little or no resolution between *G. huxleyi* and *G. oceanica* (Edvardsen et al, 2001; Fujiwara et al. 2001; Liu et al 2010), but there is evidence for genetic separation between these two species and/or within *G. huxleyi* from genetic markers including the nuclear-encoded calcium binding protein *GPA* gene (Schroeder et al 2005), the plastid-encoded elongation factor *tuf*A gene (Medlin et al 2008; Cook et al 2011) and the widely used mitochondrial barcode marker, cytochrome c oxidase subunit 1 (*cox1*, Hagino et al 2011). These studies were conducted with different, and generally small, sets of culture strains, and

different markers appear to give different phylogenetic patterns in relation to morphology and biogeographical origin of strains. In addition, in some cases the two morpho-species are only partially separated by the genetic marker (e.g. the *tuf*A analysis of Medlin et al 2008).

In this context, we used a relatively large set of culture strains to test a variety of genetic markers from different cellular compartments for their ability to distinguish genotypes between and within these two morpho-species and for their suitability for performing phylogenetic reconstructions. In addition to the classical (but relatively slowly evolving) ribosomal *18S* and *28S* rDNA and plastidial *rbcL* markers, we chose to extend previous analyses of *tuf*A and *cox1* and to include a comparison of other markers such as the plastid-encoded 16S rDNA (widely used in prokaryote phylogenetics and increasingly used for photosynthetic organisms), the plastid-encoded *pet*A gene (coding for a subunit of cytochrome f), and mitochondrion-related genes including other cytochrome oxidase genes (cox2, cox3), the *rpl16* (coding for a protein involved in the ribosomal large subunit) and *dam* (coding for a DNA adenine methylase). Evaluation of these molecular tools represents an essential first step towards large-scale assessment, using next generation sequencing amongst other methods, of the biodiversity, biogeography and evolutionary dynamics of these key phytoplanktonic organisms.

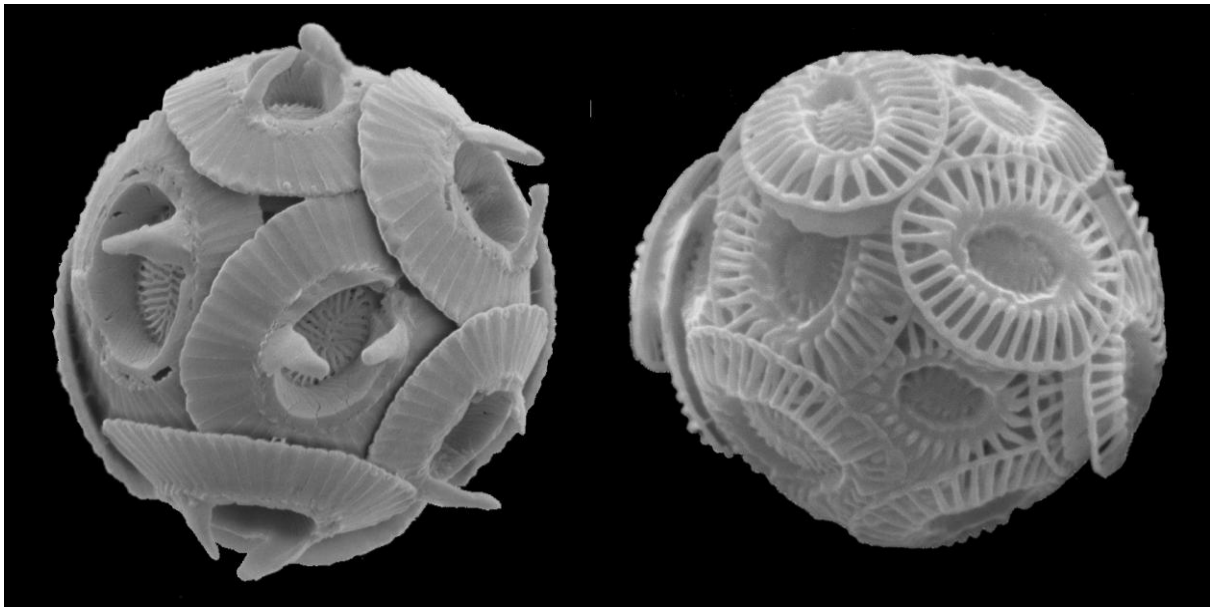

Figure 1. *Gephyrocpasa oceanica* and *Gephyrocapsa huxleyi*

Materials and Methods

Origin and morphological characterisation of culture strains. Clonal *Gephyrocapsa* strains (Supplementary Table 1) from the Roscoff Culture Collection (RCC), the Plymouth culture collection (PLY) and the Provasoli-Guillard Center for Culture of Marine Phytoplankton (CCMP) were maintained in K/2(-Si,-Tris,-Cu) medium (Keller et al. 1987) at 17°C with 50 µmol-photons.m^{-2}.s^{-1} illumination provided by daylight neon tubes with a 14:10h L:D cycle. For analysis of coccolith morphology by scanning electron microscopy (SEM), calcified cells were harvested at early exponential growth phase and filtered onto 0.22 µm nucleopore filters (Millipore), then dried for 2 hours at 55°C. Small pieces of filters were gold/palladium sputter coating and observed with a FEI Quanta SEM (FEI).

DNA extraction, amplification and sequencing. Genomic DNA was extracted from cultures harvested in the exponential phase of growth using the DNeasy Plant mini kit (Qiagen). Partial *SSU, LSU, 16S, rbcL, petA, cox1, cox2, cox3, rpl16* and *dam* genes were amplified by PCR using the primer sets listed in Table 1 (primer maps are illustrated in supplementary figure S1). PCRs were performed in a total reaction volume of 25 µL using the *Phusion* Polymerase kit (Finnzyme). A standard PCR protocol was used for all genes with a T1 thermal cycler (Biometra): 2 min initial denaturation at 98°C, followed by 35 cycles of 10s at 98°C, 30s annealing at 55°C, 30s extension at 72°C. A final 10 min extension step at 72°C was conducted to complete the amplification. Amplification products were controlled by electrophoresis on a 1% agarose gel. The PCR products were sequenced directly on an ABI PRISM 3100 xl DNA auto sequencer (Perkin-Elmer, Foster City, CA, USA) using the ABI PRISM BigDye Terminator Cycle Sequencing Kit (Perkin-Elmer). The sequences determined in this study were deposited in GenBank (Accession Nos).

Phylogenetic analyses. The nucleotide sequence datasets of each gene were aligned using the online version of the multiple alignment program MAFFT (Katoh et al. 2007). Alignments were double-checked *de visu* in the sequence editor BIOEDIT (Hall 1999) and coding region were determined from sequences held in the plastidial genome (Sanchez-Puerta et al. 2005) and in the mitochondrial genome (Sanchez Puerta et al 2004). Sequences were compared using the Kimura 2-parameter distance with the MEGA 5 software (Tamura et al. 2011). Maximum likelihood (ML) and neigbour joining (NJ) phylogenetic trees were inferred using the MEGA 5. Appropriate models of DNA substitution were detected with MEGA 5, using the three proposed statistics (AIC, AICc and BIC). The robustness of the branching of trees was tested by bootstrapping based on 1000 replicates for both methods.

Table 1. Details of genetic markers and primers used in this study

Genomic compartiment	Gene	Function	Primer name and Sequence		Reference
nucleus	*18S*	small ribosomal subunit: traduction	A18-dir A18-rev	5'-AACCTGGTTGATCCTGCCAGT-3' 5'-TGATCCTTCTGCAGGTTCACCTAC-3'	Sogin et al 1989
	28S	large ribosomal subunit: traduction	Lhapto4 Leuk20r	5'-TAATGGCGAATGAAGCGGGC-3' 5'-CTCCTTGGTCCGTGTTTCTAGACG-3'	Liu et al 2009
plastid	*16S*	small ribosomal subunit: traduction	OXY359F OXY1313R		Füller et al 2006
	rbcl	ribulose-bisphosphate carboxylase: photosynthesis			Fujiwara et el 2001
	tufA (short fragment)	elongation factor Tu: translation	tufA_815F tufA_1199R	5'- AGACTCTGGATGAAGGAATGG-3' 5'- CCTGCACCTACTGTTCTACC-3'	in this study
	tufA (long fragment)	elongation factor Tu: translation	tufA F1 tufA_1199R	5'- CAATGCCTCAAACACGTGAG - 3' 5'- CCTGCACCTACTGTTCTACC-3'	in this study
	petA	cytochrome f subunit: electron transfert	petA-F1 petA-R1	5 - CAGCAGCGGTTTGAATTGTA - 3' 5'-CAGAGGTTGAAGTGCCACAA-3'	in this study
mitochondrion	*cox1 (short fragment)*	cytochrome c oxidase subunit 1: electron transfert	EGcox1F5 EGcox1R8	5'-GCTCACCGAACTCCTTTATTTG-3' 5'-GAAGCAATTGCATTTCATTGAG-3'	in this study
	cox1 (long fragment)	cytochrome c oxidase subunit 1: electron transfert	EGcoxF5 EGatp4-16959R	5'-GCTCACCGAACTCCTTTATTTG-3' 5'-TGC CGA TTT CGC ATC AAT AAG-3'	in this study Hagino et al 2011
	cox2	cytochrome c oxidase subunit 2: electron transfert	cox2 F1 cox2 R2	5'-CCCACTTACAACTCAAGGGGC-3' 5'-CCAAACATCGCTGCATTCACCTC-3'	in this study
	cox3	cytochrome c oxidase subunit 3: electron transfert	EGcox3F1 EGcox3R1	5'-TCCTACACTTGGATATTTAG-3' 5'-TCGCATTTTTGGTTTGGAAGACC-3'	in this study
	rpl16	protein 16 large ribosomal subunit: traduction	rpl16 F rpl16 R	5'-TGTTATTAGCTCCAAAGCGTTC-3' 5'-GTTAACAAGCCAGACTTAACTGG-3'	in this study
	dam	DNA reparation	dam F1 dam R2	5'-GGGTCTGGGTCGGTTTTACT-3' 5'-AAGTCGCCTTTTTGAAGTG-3'	in this study

Results

Amplification success

In this study of multiple culture isolates of two closely related coccolithophores, *G. huxleyi* and *G. oceanica*, amplification success was very high (near 100%) for all selected genes except for 18S and 28S rDNA and cox1. Of the markers tested, the ribosomal genes from nuclear DNA (18S and 28S rDNA) exhibit the highest GC content (>60%, table 2), potentially explaining their lower amplification success rates. High GC content of haptophyte 18S rDNA has been suggested to be responsible for the consistent lack of haptophyte sequences in clone library studies of plankton diversity using universal 18S rDNA eukaryote primers (e.g. Liu et al 2009). Amplification of cox1 failed for some strains due to the presence of an approximately 2500 base pair long intron in the gene (Table S1).

Table 2. Characteristics of genes (partial fragments) used in this study

Gene	Average length (bp)	GC content (%)	Amplification Success	Codons (residues)	Nucleotide substitutions	Non-synonymous substitutions	Synonymous substitutions	Parsimonious informative site	Best model (AICc)
18S	1721	60	70%	-	0	-	-		-
28S	631	62.1	76%	-	1 (0.2%)	-	-		-
16S	700	51.2	91%	-	0	-	-		HKY
rbcL	1378	45.6	89%	70	0	-	-		-
tufA (short)	240	43.7	94%	80	6 (2.9%)	1	5	4	K2P
tufA (long)	637	37,9	95%	212	26(6.4%)	9	15	24	HKY+G
petA	417	41.2	96%	139	21 (5.3%)	3	19	10	HKY
cox1 (short)	651	30,7	90%	217	32 (5.7%)	0	32	27	HKY+G
cox1 (long)	903	32.2	83%	301	53 (4.4%)	4	49	38	HKY+I
cox2	786	31.8	94%	262	20 (1.7%)	1	19	15	HKY+I
cox3	810	34.6	96%	270	38 (4.2%)	4	34	30	HKY
rpl16	326	29.8	93%	108	14 (4.0%)	3	11	10	TN+I
dam	414	27.3	91%	138	26 (6.0%)	11	15	20	HKY

Substitution rates and specific distance

Of the different markers, the respective partial sequences of the nuclear 18S rDNA and the plastidial 16S rDNA and rbcL were identical for all strains of both morpho-species (table 2), confirming that they are not suitable for discrimination of *G. huxleyi* and *G. oceanica*. A consistent 1 base pair (0.16%) differentiation between the two taxa was recorded with 28S rDNA sequences. All other gene markers tested in this study exhibited higher relative nucleotide substitution rates, with the partial sequences of plastidial *tuf*A(long) (6.4%) and mitochondrial *dam* (6.0%) exhibiting the highest degrees of variability for the set of cultures analyzed (table 1). While several of the markers tested thus exhibited sufficient variability to be potentially suitable for barcoding and phylogenetic applications, full distinction of *G. oceanica* from *G. huxleyi* was not achieved with certain genes. The sequences of *tuf*A(long and short), *pet*A and *cox1*(short) only partially delineated the two morpho-species, each highlighting microdiversity within each morpho-species, but with interspecific overlap (i.e. polyphyly in phylogenetic reconstructions, figure 2). Previous studies using the plastid gene *tufA* also reported that microdiversity could be revealed within these morpho-species, but that *G. oceanica* and *G. huxleyi* cannot be distinguished with this marker (Medlin et al. 1996; Cook et al. 2011). By contrast, consistent interspecific delineation was attained with the

mitochondrial *cox1* (long), *cox2*, *cox3*, *rpl16* and *dam* markers. These mitochondrial markers also delineated consistent groups within *G. huxleyi*, strictly comparable to the biogeographically distinct groups distinguished within this morpho-species using a longer mitochondrial fragment spanning the *cox1-atp4* genes (Hagino et al. 2011). The highest percentage of interspecific differentiation was attained with the *dam* gene (2.6%) that also exhibited the highest level of intraspecific divergence within *G. oceanica* (1.5%, equal to the divergence within this morpho-species shown by *pet*A, table 3). *Cox3*, *rpl16* and *dam* all exhibited 0.8-0.9% intraspecific variability within *G. huxleyi*, but the largest intraspecific divergences for this morpho-species were exhibited by the plastidial *tuf*A(long) and *pet*A markers (1.2% and 1.1% respectively, table 3).

Table 3. Percentage inter- and intra-specific distances for gene markers investigated in this study

Gene	Interspecific distance	Intraspecific distance	
		G. oceanica	*G. huxleyi*
18S	-	0%	0%
28S	0.1%	0%	0%
16S	-	0%	0%
rbcl	-	0%	0%
tufA (short)	-	0.3%	0.6%
tufA (long)	-	1.2%	1.2%
petA	-	1.5%	1.1%
cox1 (short)	-	0.3%	0.4%
cox1 (long)	1%	0.6%	0.4%
cox2	1.8%	0.6%	0.4%
cox3	2.1%	0.1%	0.9%
rpl16	2.3%	1%	0.8%
dam	2.6%	1.5%	0.8%

Phylogenetic analyses

With the low rate or lack of apparent substitution, the *18S, 28S* (nuclear) and *16S* (plastidial) rDNA and the *rbcl* genes were not suitable for constructing phylogenies. Other markers exhibited a phylogenetic signal taking into account the relevant parsimonious sites, lowering for some markers the substitution signal. The substitution model designated for most marker datasets was the HKY model (Hasegawa et al. 1985) which distinguishes transversion and transition rates with unequal base frequencies. For the *tufA* short fragment dataset, the K2P substitution model (Kimura 1980) as applied, differing from the HKY model by being

based on equality of base frequencies, and for the *rpl16* dataset, the TN model (Tamura and Nei 1993) allowed different rates for two transitions (A-G and C-T) and constant rates for transversions with unequal base frequencies.

Phylogenetic trees obtained for these more variable genes were not congruent between plastidial and mitochondrial markers, with full monophyletic delineation of morpho-species only achieved with the mitochondrial markers (Fig. 2). For the plastidial markers, the *tufA* topology defined four statistically supported clades, while *petA* formed three clades, but in both cases a paraphyletic pattern was evident in the trees. For both of these genes, the phylogenies did not correspond to geographical origin of strains or morpho-species delineation. For the mitochondrial markers, three statistically supported clades were recovered in each phylogenetic tree with evidence of morphospecies delineation. The clade GO contains exclusively members of the *G. oceanica* morphospecies and is highly diverse in *cox1*. Clades I and II correlate to the two *G. huxleyi* clades identified by Hagino et al (2011; α and β in chapters 4, 5, 6 and in the discussion). The diversity within these clades differed according to the marker, for example clade II is not well defined in the rpl16 phylogeny, while cox3 shows the highest diversity within this clade.

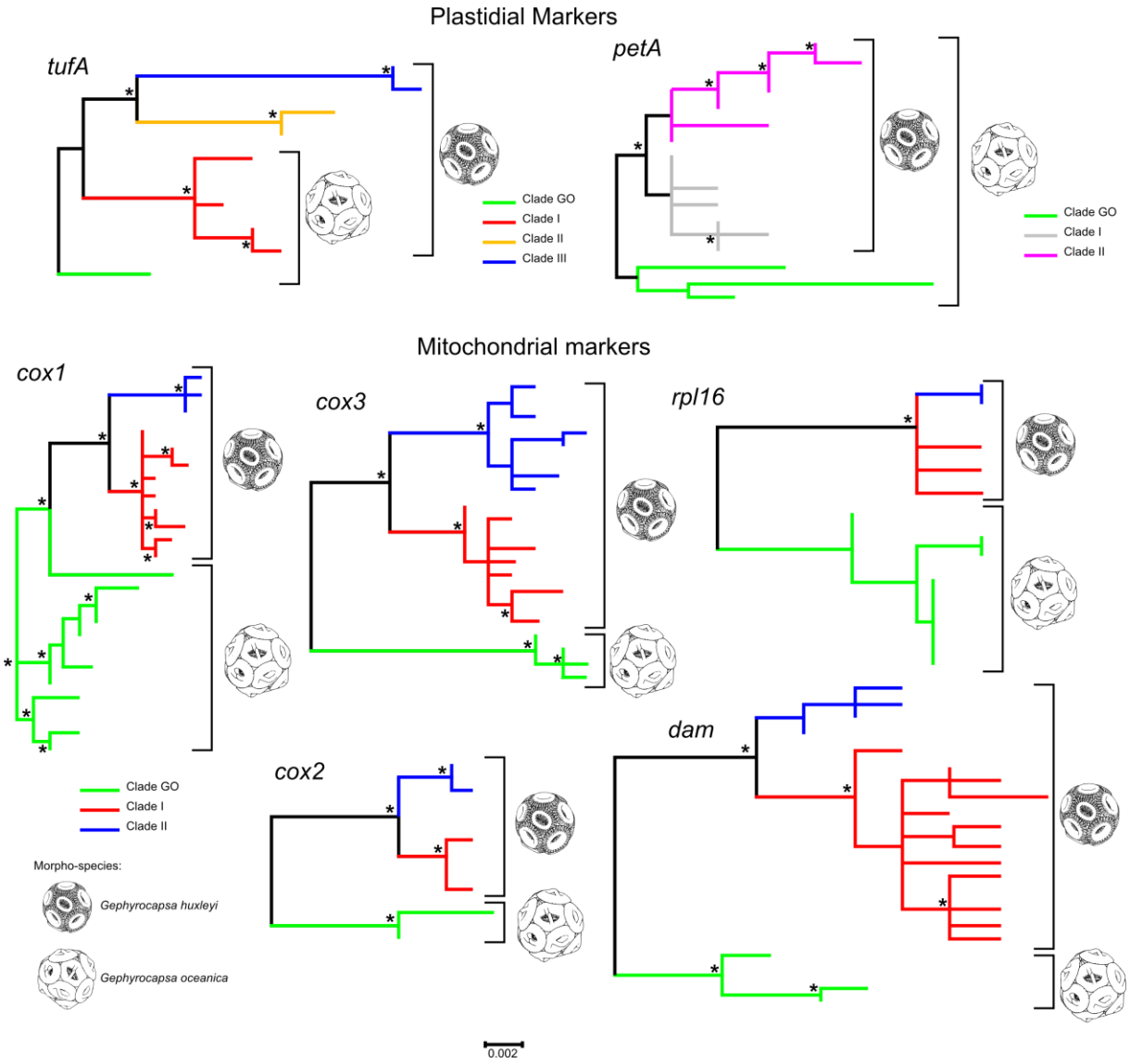

Figure 2. Unrooted phylogenetic trees inferred from the markers used in this study. The pattern of morpho-species delineation is given for each tree according to our SEM observations. For plastidial markers, clades are independantly defined for each gene; for mitochondrial markers, clades I and II correspond to clades defined by Hagino et al (2011). Strains positions are given in supplementary figures 2-5 and supplementary table 1. (*) are marked for bootstrap values higher than 70% (for more details see Fig. S2-5). Coccospheres were drawn by Kamptner (1956).

Discussion

Of the nuclear rDNA markers tested, the 28S rDNA exhibits a higher rate of substitution than 18S rDNA and is suitable for genetic distinction of the *G. huxleyi* and *G. oceanica* morpho-species, albeit not ideal due to the minimal number of substitutions (one putative substitution). The 28S rDNA marker is not, however, variable enough for

phylogenetic studies within these lineages. Ribosomal genes from the nuclear genome, implicated in the key process of translation during protein production, have been classically chosen to resolve species and higher-level phylogeny due to their high level of conservation and slow evolutionary rate (Sogin et al 1986). The implication of these molecules in vital functional gene networks also implies strong selective pressure. Ribosomal RNAs, that are highly expressed and interact with numerous partners during protein synthesis, occur in numerous copies in the nuclear genome and are subject to mechanisms of concerted evolution between the copies, meaning that fixation of mutations is very slow on these molecules. For pelagic protists, a high level of conservation of ribosomal genes is expected due to their theoretically high effective population size (Piganeau et al. 2010). Some planktonic lineages, such as the Foraminifera (Pawlowsky et al 1997), have been shown to exhibit unusually high rates of substitution in these ribosomal genes, but haptophytes seem to show evolutionary rates for these genes on a par with average rates for eukaryotes (Liu et al. 2009). From the plastid genome, the 16S rDNA, also involved in protein synthesis, is also highly conserved like the nuclear 18S rDNA, as is the rbcL gene that codes for the large subunit of RuBisCO and thus plays an important role in the metabolic pathway of carbon fixation by photosynthesis. Neither of these plastid markers are therefore suited either for identification or for evolutionary studies for *G. huxleyi* / *G. oceanica*.

All other gene markers tested in this study exhibited higher relative nucleotide substitution rates, with the partial sequences of plastidial *tuf*A(long) (6.4%) and mitochondrial *dam* (6.0%) exhibiting the highest degrees of variability for the set of cultures analyzed (table 1). The general pattern emerging from our dataset is of interspecific overlap with (the faster evolving) plastidial markers and interspecific differentiation with mitochondrial markers.

Given the recentness of this speciation, interspecific overlap in plastid marker sequences may result from the plastid genomes of the two species not having had sufficient time to accumulate independent mutations (incomplete lineage sorting which can occur when the coalescence point of a gene predates the speciation event). Incomplete lineage sorting means that genealogical histories of individual gene loci may be misleading or uninformative about the relationships among species or populations (Maddison and Knowles 2006). Since maximum substitution rates of markers from different cellular compartments were broadly equivalent (table 2), the interspecific overlap exhibited by plastidial markers might also have alternative causes, notably introgression. Coccolithophores have a haplo-diplontic sexual life cycle (Billard et al 2004) and the pattern emerging from plastidial markers could reflect past (or even potentially ongoing) hybridization of closely related sub-lineages of these morpho-

species. Introgression of plastid genes is well documented in some plant lineages. In the newly-formed zygote of many unicellular algae, the plastids from both gametes are present, but the plastid from one mating type quickly degenerates (= mono-parental inheritance). The chlorophyte *Chlamydomonas* is unusual in that the plastids from the two gametes fuse, but in spite of this (and by an unkown mechanism), inheritance of plastid DNA is still normally uniparental (Birky 2008). The mode of transmission of plastids in haptophytes is not known, but introgression of plastid genes remains a possibility. In our case, the branches in the *petA* tree have low bootstrap support, indicating that the phylogenetic signal is weak, potentially due to rapid evolution of the gene. The low level of non-synonymous substitutions in this marker might also result from purifying selection despite the relatively high level of substitutions compared to other markers. The *tufA* marker has more non-synonymous substitutions than *petA*, but relatively less substitutions overall, suggesting that selective pressure is weaker allowing fixation of more substitutions impacting the protein sequence even though the evolutionary rate is slower. The level of saturation of the third codon position is generally estimated in order to verify the validity of the phylogenetic signal of coding genes, but the low distances between lineages in this study precluded such estimation.

Mitochondrial transmission in eukaryotes is typically mono-parental (=clonal), resulting in a lack of genetic exchange (recombination) that implies that the within-species history of mitochondrial DNA can be appropriately represented by a unique tree (Avise et al 2000). Recombination of mitochondrial DNA can occur and hybrid introgression of mitochondrial DNA is relatively common in some groups, particularly arthropods and plants (Galtier et al. 2009), but these issues do not seem to be relevant in the present case. Reciprocal monophyly between *G. oceanica* and *G. huxleyi* was found for all mitochondrial phylogenies except *cox1*(short) which exhibited a paraphyletic pattern. In the study organisms, *cox1* has some unusual structural characteristics in that, on the one hand it is separated into two fragments that are distant in the mitochondrial genome (which suggests a recombination event prior to the appearance of *G. oceanica* and above all the existence of a splicing process including specific splicing for the *cox1* gene; Sanchez Puerta et al 2004), and on the other hand the presence in certain strains of a 2500bp long intron that is specific for each morpho-species. These introns appear to be similar to the introns found in the haptophyte *Pavlova lutheri* and the diatom *Thalassosira pseudonana* (Ehara et al, 2000) and are probably type 2 introns that have the characteristic of auto-splicing during mRNA maturation. The origin of these introns is not clear, but it seems possible that they are transposable elements. *Cox1* possess four non-synonymous substitutions near the 3’ terminal region of the gene seemingly shared between

G. oceanica haplotypes. Theses substitutions affect the sequence of the protein without changing its steric structure, the conformation of the protein thus being conserved, highlighting its vital importance. Changes in this molecule are thus probably more constrained than those encoded by other mitochondrial genes, as witnessed by the fact that it possesses the lowest substitution rate even though it is the most polymorphic in *G. oceanica* strains, hence the polyphyletic phylogenetic pattern. The other mitochondrial markers present more substitutions and are less polymorphic, their phylogenies exhibiting monophyletic patterns for each species. These markers potentially define two phylogenetic species within *G. huxleyi* strictly comparable to the biogeographically groups distinguished using a longer mitochondrial fragment spanning the *cox1-atp4* genes (Hagino et al. 2011).

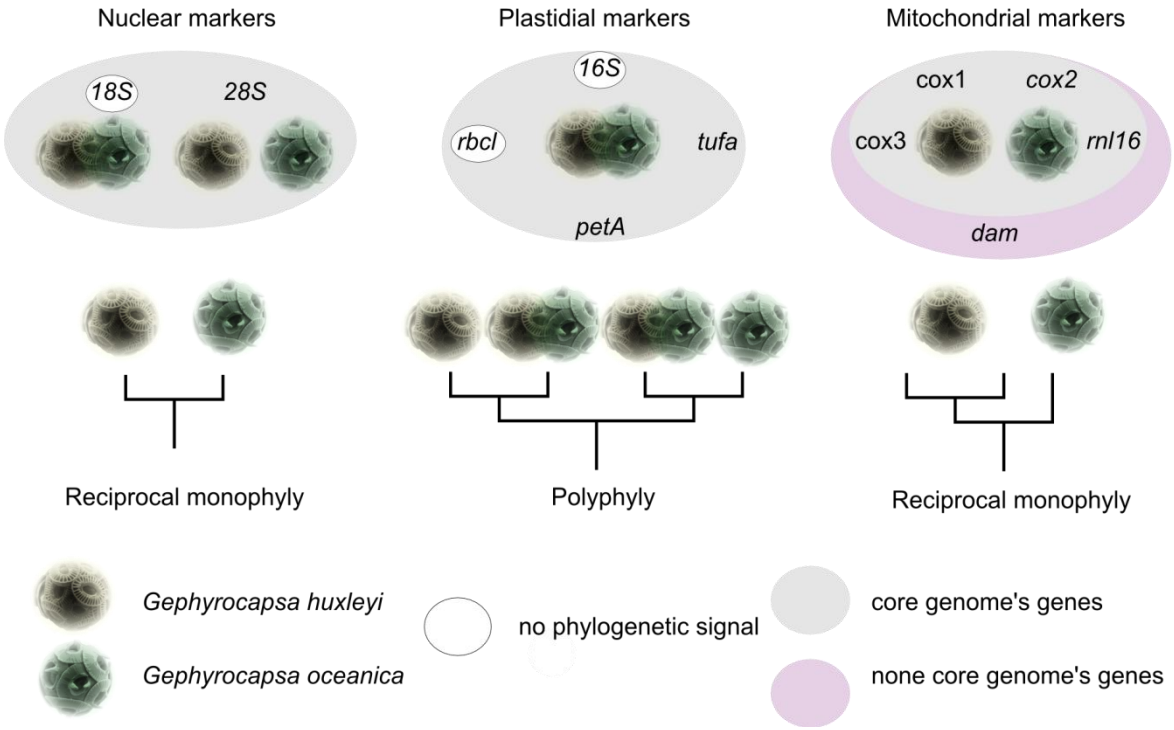

Figure 3. Synthetic view of the assessed phylogenies by each marker for the different compartment.

Concluding remarks

Of the genetic markers tested here, the mitochondrial genes combined the best amplification success, sequence quality and discriminatory power for the set of *G. oceanica* and *G. huxleyi* cultures investigated. The widely used barcoding marker *cox1* exhibits the most polymorphic pattern, other genes with higher substitution rates not exhibiting as much intra-specific pattern. Discrimination within *G. huxleyi* is achieved by all of the mitochondrial markers. *Cox1* could be suitable for discrimination of genotypes by using a fragment

excluding the intron and including the 3' extremity. This would potentially increase the amplification success rate, while maintaining sufficient phylogenetic signal. Of the nuclear markers tested, the *28S* rDNA marker was able to discriminate the two morpho-species, but more variable nuclear markers would clearly be useful. None of the chloroplast markers tested were suitable for inter-specific discrimination of *G. oceanica* and *G. huxleyi*. Analyses of alternative plastidial genes is required to test whether plastids could provide useful information on micro-evolutionary processes through the comparison of clonal culture strains. Whilst mitochondrial DNA sequence distance appears to be particularly promising as an indicator of species (and intra-morpho-species) delineation in this coccolithophore lineage, study of multiple genetic loci in a phylogenetic context, combined with careful morphological and ecological analysis will be required to establish robust and accurate species boundaries between, and notably within, these morpho-species.

References

Andersson, S. G. E. *et al.* (1998). The genome sequence of *Rickettsia prowazekii* and the origin of mitochondria. *Nature* 396, 133–143

Andrews JT and Giraudeau J (2003) Multi-proxy records showing significant Holocene environmental variability: the inner N. Iceland shelf (Húnaflói). *Quaternary Science Reviews*, 22: 175-193

Avise JC (2000) *Phylogeography: The History and Formation of Species.* Harvard University Press, Cambridge.

Billard C and Inouye I (2004) What's new in coccolithophore biology? In: Thierstein HR, Young JR (eds) *Coccolithophores: From the molecular processes to global impact*. Springer

Birky, C. William (2008), Uniparental inheritance of organelle genes, *Current Biology* 18 (16): R692–R695

Bown, P.R., 2005. Calcareous nannoplankton evolution: a tale of two oceans. Micropaleontology, 51(4): 299-308.

Cook, S.S., Whittock, L., Wright, S.W. & Hallegraeff, G.M. (2011). Photosynthetic pigment and genetic differences between two Southern Ocean morphotypes of *Emiliania huxleyi* (Haptophyta). *Journal of Phycology* 47(3): 615-626.

Edvardsen B, Eikrem W, Green JC, Andersen RA, Moon-van der Staay SY and Medlin LK (2000). Phylogenetic reconstructions of the Haptophyta inferred from 18S ribosomal DNA sequences and available morphological data. *Phycologia* 39: 19-35.

Ehara, M., Watanabe, K. I., & Ohama, T. (2000). Distribution of cognates of group II introns detected in mitochondrial cox1 genes of a diatom and a haptophyte. *Gene*, *256*(1-2), 157-167.

Fujiwara S, Tsuzuki M, Kawachi M, Minaka N and Inouye I (2001). Molecular phylogeny of the Haptophyta based on the *rbcL* gene and sequence variation in the spacer region of the RUBISCO operon. *Phycologia* 37: 121-129.

Galtier, N., Nabholz, B., Glemin, S. and Hurst, G. D. D. (2009), Mitochondrial DNA as a marker of molecular diversity: a reappraisal. *Molecular Ecology*, 18: 4541–4550.

Hall TA (1999) BioEdit: a user-friendly biological sequence alignment editor and analysis program for Windows 95/98/NT. Nucleic Acids Symposium Series 41: 95–98.

Iglesias-Rodriguez MD, Halloran PR, Rickaby REM, Hall IR, Colmenero-Hidalgo E, Gittins JR, Green DRH, Tyrrell T, Gibbs SJ, von Dassow P, Rehm E, Armbrust EV and Boessenkool KP (2008). Phytoplankton calcification in a high-CO2 world. *Science* 320: 336-340.

Kamptner E (1943). Zur Revision der Coccolithineen-Spezies *Pontosphaera huxleyi* Lohmann. *Anz Akad Wiss Wien Math -Naturw K* 80: 43-49.

Kamptner, E. (1956) Das Kalkskelett von *Coccolithus huxleyi* (Lohmann) Kamptner und *Gephyrocapsa oceanica* Kamptner (Coccolithineae).*Arch Protistenkd,* 101 **:** 99–202.

Keller MD, Selvin RC, Claus W and Guillard RRL (1987). Media for the culture of oceanic ultraphytoplankton. *J Phycol* 23: 633-638

Kimura M (1980) A simple method for estimating evolutionary rates of base substitutions through comparative studies of nucleotide sequences. Journal of Molecular Evolution 16: 111–120.

Langer G, Nehrke G, Probert I, Ly J and Ziveri P (2009). Strain-specific responses of *Emiliania huxleyi* to changing seawater carbonate chemistry. *Biogeosciences* 6: 2637-2646.

Liu, H., Probert, I., Uitz, J., Claustre, H., Aris-Brossou, S., Frada, M., Not, F. & de Vargas, C. (2009). Haptophyta rule the waves: Extreme oceanic biodiversity in non-calcifying haptophytes explains the 19-Hex paradox. *PNAS* 106:12803-12808

Liu H, Aris-Brosou S, Probert I and de Vargas C (2010). A timeline of the environmental genetics of the haptophytes. *Mol Biol Evol* 27: 171-176.

Maddison W. P., and Knowles L. L.(2006) Inferring phylogeny despite incomplete lineage sorting. Syst. Biol. 2006;55:21-30

McFadden GI (2001). "Primary and secondary endosymbiosis and the origin of plastids". *J Phycology* 37 (6): 951–9.

Medlin LK, Sàez AG and Young JR (2008). A molecular clock for coccolithophores and implications for selectivity of phytoplankton extinctions across the K / T boundary. *Mar Mic* 67: 69-86.

Müller PJ, Kirst G, Ruhland G, von Storch I and Rosell-Mele A (1998). Calibration of the alkenone paleotemperature index $U^{K'}37$ based on core-tops from the eastern South Atlantic and the global ocean (60°N-60°S). *Geochim. Cosmochim. Acta* 62: 1757-1772.

Lohmann H (1902). Die Coccolithophoridae, eine monographie der Coccolithen bildenden flagellaten, zugleich ein Beitag zur Kenntnis des Mittelmeerauftriebs. *Arch Protistenkde* 1: 89-165.

Pawlowski J, Bolivar I, Fahrni J F, de Vargas C, Gouy M and Zaninetti L (1997) Extreme differences in rates of molecular evolution of foraminifera revealed by comparison of ribosomal DNA sequences and the fossil record. *Mol Biol Evol* 14: 498-505

Piganeau G, Eyre-Walker A, Grimsley N, Moreau H (2011) How and Why DNA Barcodes Underestimate the Diversity of Microbial Eukaryotes. PLoS ONE 6(2): e16342.

Reinhardt P (1972). Coccolithen. Kalkiges Plankton seit Jahrmillionen. *Die neue Brehm Bücheri* 453: 1-99.

Riebesell U, Zondervan I, Rost B, Tortell PD, Zeebe RE and Morel FMM (2000). Reduced calcification of marine plankton in response to increased atmospheric CO_2. *Nature* 407: 364-367.

Rost B and Riebesell U (2004). Coccolithophores and the biological pump responses to environmental changes. In Thierstein, H. R. and Young, J. R. [Eds.] Coccolithophores – From Molecular Processes to Global Impact. Springer, Berlin. pp. 99-125.

Samtleben C (1980) Die evolution der coccolithophoriden-Gattung Gephyrocapsa nach Befunden im Atlantik. *PaläontologischeZeitschrift* 54, 91– 127.

Sánchez Puerta V., Bachvaroff, T. R. & Delwiche, C.F. (2004). The complete Mitochondrial genome sequence of the Haptophyte *Emiliania huxleyi* and its Relation to Heterokonts. *DNA Res.* 11:1-10.

Sanchez-Puerta MV, Bachvaroff TR, Delwiche CF (2005) The complete plastid genome sequence of the haptophyte *Emiliania huxleyi*: a comparison to other plastid genomes**.** *DNA Res*, 12: 151-156

Schroeder DC, Biggi GF, Hall M, Davy J, Martínez JM, Richardson AJ, Malin G and Wilson WH (2005). A genetic marker to separate *Emiliania huxleyi* (Prymnesiophyceae) morphotypes. *J Phycol* 41: 874-879.

Tamura K and Nei M (1993). Estimation of the number of nucleotide substitutions in the control region of mitochondrial DNA in humans and chimpanzees. *Mol Biol Evol* 10: 512-526.

Tamura K., Peterson D., Peterson N., Stecher G., Nei M., and Kumar S. (2011). MEGA5: Molecular Evolutionary Genetics Analysis using Maximum Likelihood, Evolutionary Distance, and Maximum Parsimony Methods. *Molecular Biology and Evolution*

Winter A, Jordan R, Roth P (1994) Biogeography of living coccolithophores in ocean waters. In: Winter A and Siesser WG (editors) "Coccolithophores". Cambridge University Press, Cambridge, UK.

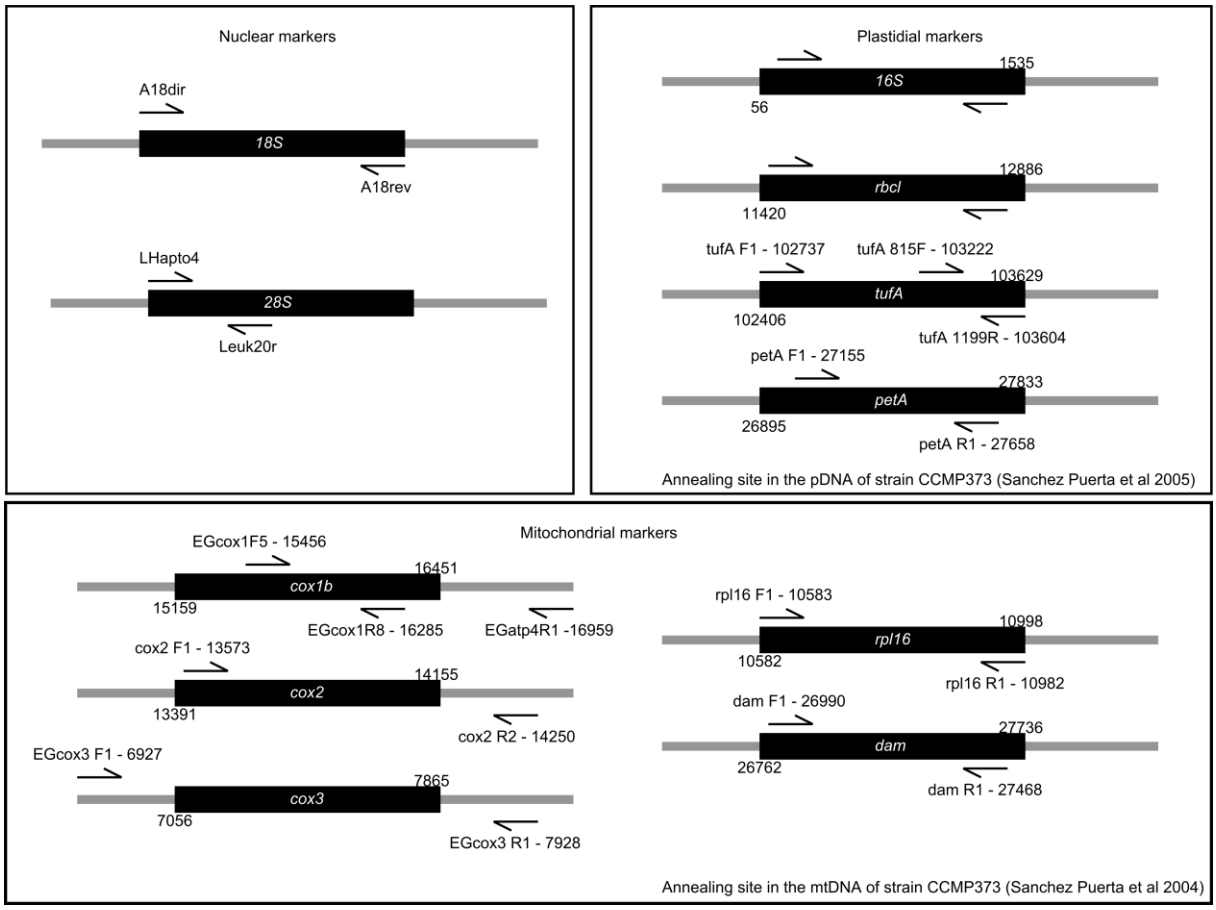

Supplementary Figure 1. Primer mapping for each markers of this study.

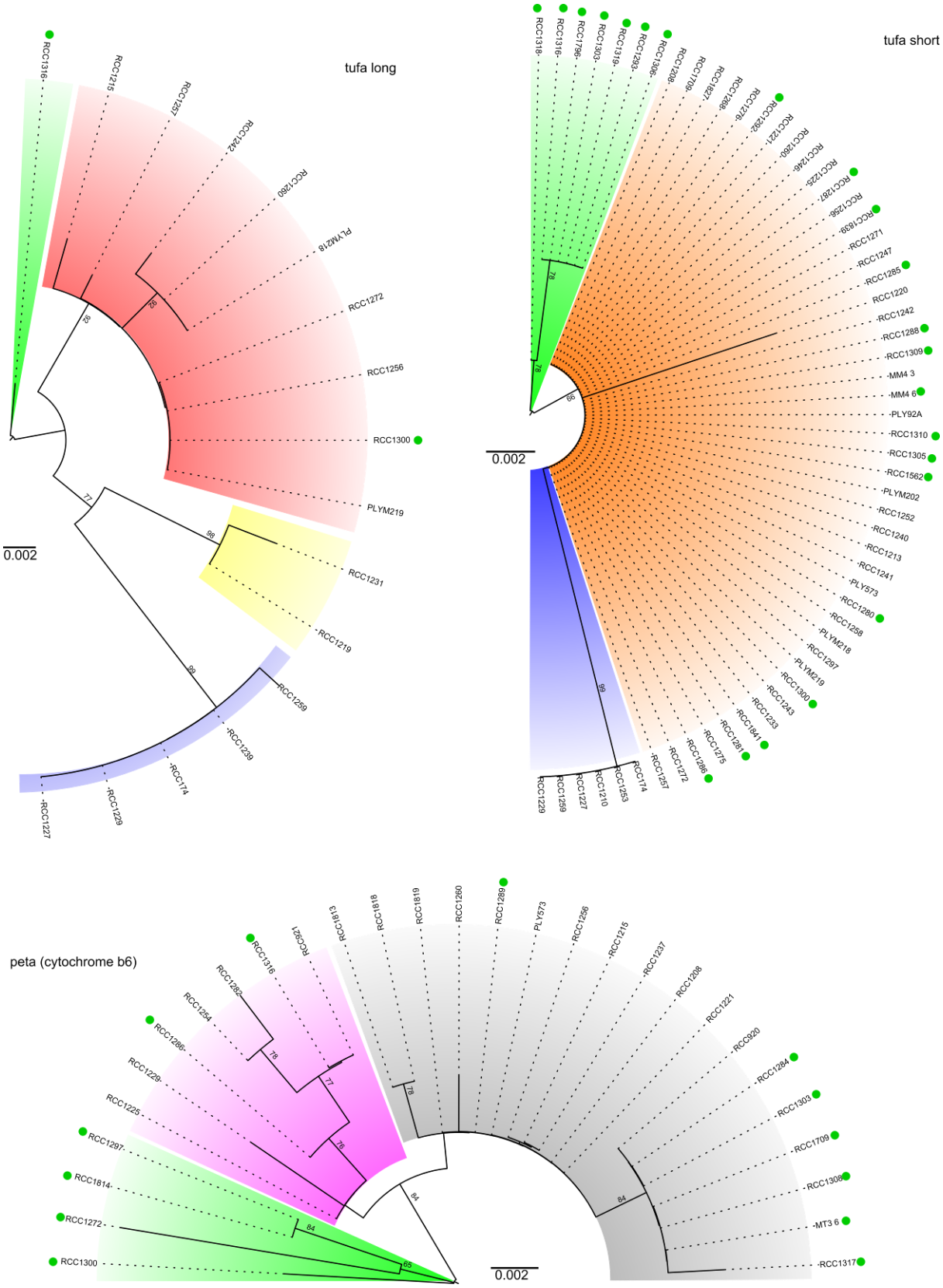

Supplementary figure 2. Phylogenetic trees inferred from plastid genes tufA and petA. In the tufA short tree, orange corresponds to a clade with strains from clade I and clade II. Green dots correspond to G. oceanica.

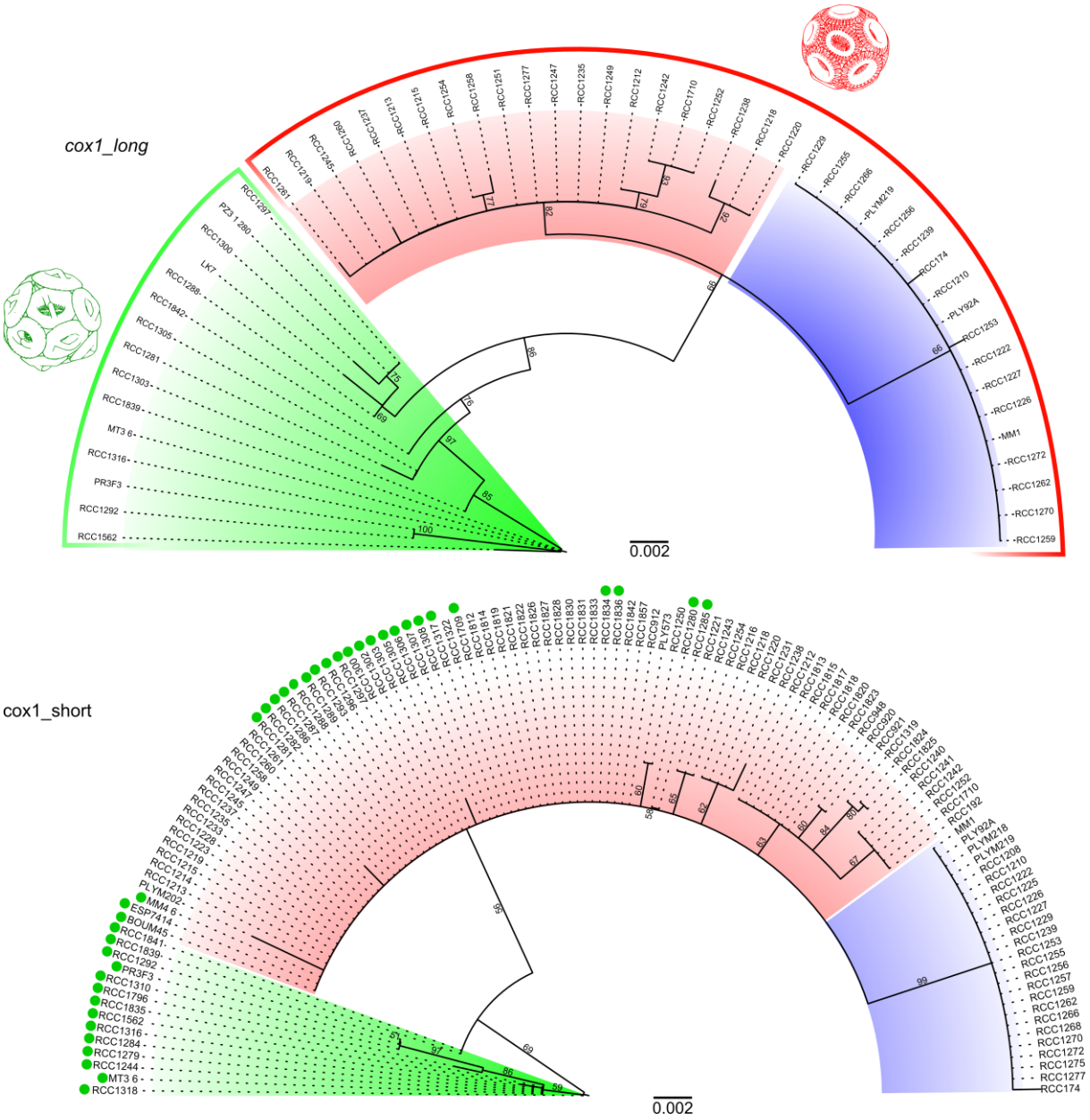

Supplementary figure 3. Phylogenetic trees inferred from mitochondrion genes cox1 (long and short fragments). In cox1 short tree, green dots corresponds to *G. oceanica*.

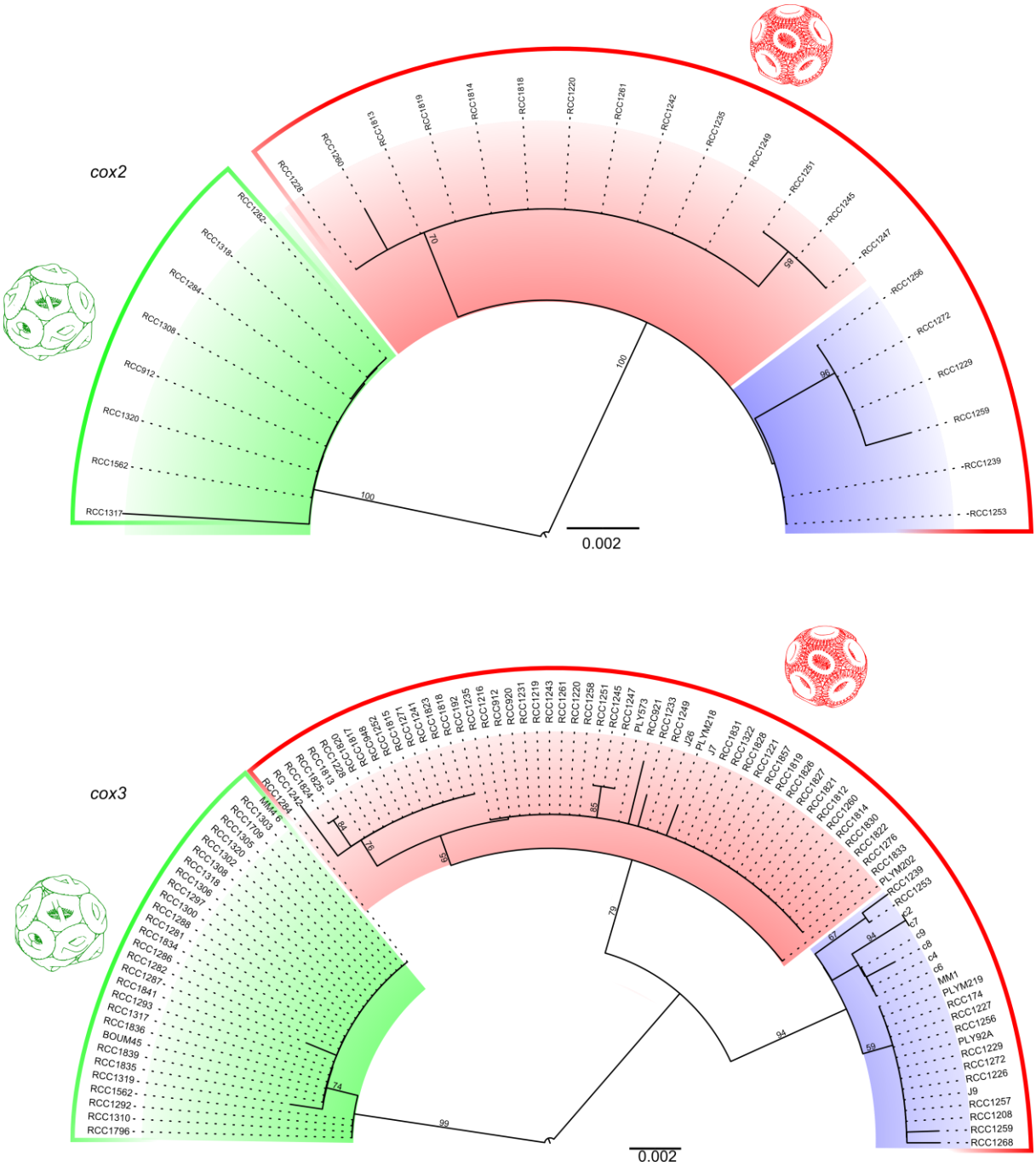

Supplementary figure 4. Phylogenetic trees inferred from mitochondrion genes cox2 and cox3.

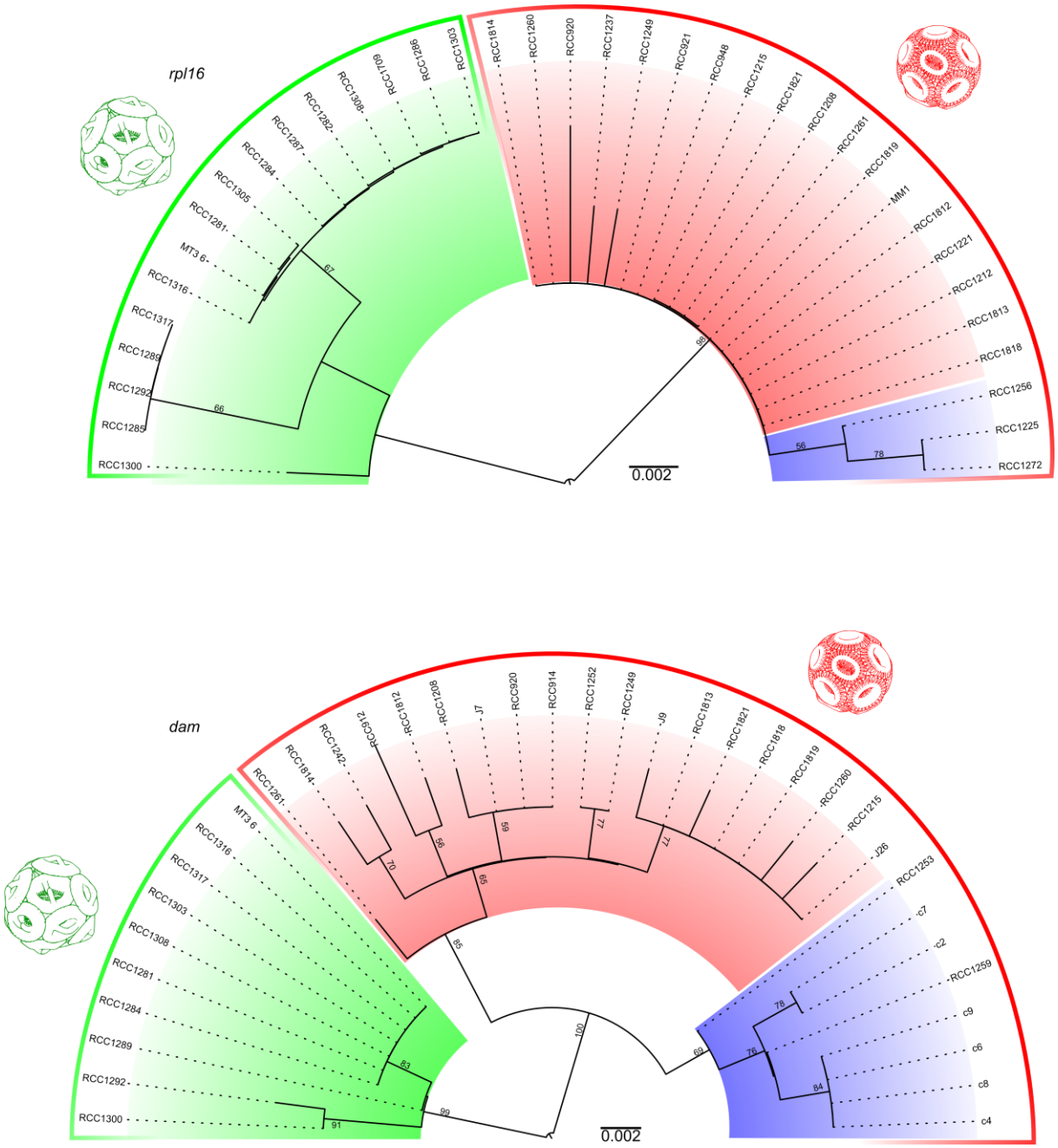

Supplementary figure 5. Phylogenetic trees inferred from mitochondrion genes *rpl16* and *dam*.

Table 2. List of strains used in this studies with their designations and genetic characterization. (GH: suspected *G. huxleyi* intron, GO: suspected *G. oceanica* intron, Av: Available)

Species		RCC #	Other Designation	Ocean Origin	Isolator	Date Isolation	Coordinate						*28S*	*cox1 short*	*cox1 long*	*intron*	*cox2*	*cox3*	*rpl16*	*dam*	*tufA short*	*tufA long*	*petA*
Gephyrocapsa	*huxleyi*	174	PLY92D	English Channel	J. C. Green	1975	50	2	N	4	22	W		Beta	Beta			Beta			Beta	Beta	
Gephyrocapsa	*huxleyi*	192	RCC192		L. Provasoli									Alpha				Alpha					
Gephyrocapsa	*huxleyi*	912	RCC912	Pacific Ocean	D. Vaulot, D. Marie	2004	8	20	S	141	15	W		Alpha			Alpha		Alpha				
Gephyrocapsa	*huxleyi*	920	RCC920	Pacific Ocean	D. Vaulot, D. Marie	2004	8	20	S	141	15	W		Alpha		GH		Alpha	Alpha				Av
Gephyrocapsa	*huxleyi*	921	RCC921	Pacific Ocean	D. Vaulot, D. Marie	2004	8	20	S	141	15	W		Alpha				Alpha	Alpha				Av
Gephyrocapsa	*huxleyi*	948	RCC948	Pacific Ocean	L. Garczarek, D. Marie	2004	33	21	S	78	6	W		Alpha		GH		Alpha	Alpha				
Gephyrocapsa	*huxleyi*	1208	AS64	Mediterranean Sea	I. Probert	1999	37	25	N	0	53	W	*G. huxleyi*	Alpha		GH		Alpha	Alpha	Alpha	Alpha		Av
Gephyrocapsa	*huxleyi*	1210	N44-20C	Baltic Sea	M. Steinke	1998	59	77	N	20	64	E	*G. huxleyi*	Beta							Beta		
Gephyrocapsa	*huxleyi*	1212	NS10Y	Atlantic Ocean	I. Probert	2000	34	28	S	17	18	E		Alpha	Alpha				Alpha				
Gephyrocapsa	*huxleyi*	1213	NAP22	Mediterranean Sea	I. Probert	2001	40	90	N	14	15	E	*G. huxleyi*	Alpha	Alpha						Alpha		
Gephyrocapsa	*huxleyi*	1214	NAP21	Mediterranean Sea	I. Probert	2000	40	90	N	14	15	E	*G. huxleyi*	Alpha									
Gephyrocapsa	*huxleyi*	1215	TW1	Mediterranean Sea	I. Probert	2001	41	40	N	2	48	E	*G. huxleyi*	Alpha	Alpha				Alpha	Alpha		Alpha	Av
Gephyrocapsa	*huxleyi*	1216	TQ26	Pacific Ocean	I. Probert	1998	42	18	S	169	50	E		Alpha				Alpha			Alpha		
Gephyrocapsa	*huxleyi*	1217	TQ26(N)	Pacific Ocean	I. Probert	1998	42	18	S	169	50	E		Alpha				Alpha			Alpha		
Gephyrocapsa	*huxleyi*	1218	TQ25	Pacific Ocean	I. Probert	1998	42	18	S	169	50	E	*G. huxleyi*	Alpha	Alpha								
Gephyrocapsa	*huxleyi*	1219	TQ23	Pacific Ocean	I. Probert	1998	42	18	S	169	50	E	*G. huxleyi*	Alpha	Alpha			Alpha				Alpha	
Gephyrocapsa	*huxleyi*	1220	TQ22	Pacific Ocean	I. Probert	1998	42	18	S	169	50	E	*G. huxleyi*	Alpha	Alpha		Alpha	Alpha			Alpha		
Gephyrocapsa	*huxleyi*	1221	ASM4-3	Mediterranean Sea	I. Probert	1999	37	14	N	1	15	W	*G. huxleyi*	Alpha				Alpha	Alpha		Alpha		Av
Gephyrocapsa	*huxleyi*	1222	N44-20D	Baltic Sea	M. Steinke	1998	59	77	N	20	64	E		Beta	Beta								
Gephyrocapsa	*huxleyi*	1225	D2303-15	North Sea	M. Steinke	1998	58	23	N	3	30	W	*G. huxleyi*	Beta				Beta	Beta		Beta		Av
Gephyrocapsa	*huxleyi*	1226	D2301-5, MS1	North Sea	M. Steinke	1998	58	23	N	3	30	W	*G. huxleyi*	Beta	Beta								
Gephyrocapsa	*huxleyi*	1227	D1902-28C	North Sea	M. Steinke	1998	58	42	N	3	21	E	*G. huxleyi*	Beta	Beta		Beta	Beta			Beta	Beta	
Gephyrocapsa	*huxleyi*	1228	BDV1	English Channel	I. Probert	2003	49	24	N	1	8	W	*G. huxleyi*	Alpha		GH	Alpha	Alpha					
Gephyrocapsa	*huxleyi*	1229	D1902-28A	North Sea	M. Steinke	1998	58	42	N	3	21	E	*G. huxleyi*	Beta	Beta		Beta	Beta			Beta	Beta	Av
Gephyrocapsa	*huxleyi*	1231	TQ21	Pacific Ocean	I. Probert	1998	42	18	S	169	50	E	*G. huxleyi*	Alpha				Alpha				Alpha	
Gephyrocapsa	*huxleyi*	1233	VF18	Mediterranean Sea	I. Probert	2007	43	41	N	7	19	E		Alpha				Alpha			Alpha		
Gephyrocapsa	*huxleyi*	1235	VF20	Mediterranean Sea	I. Probert	2007	43	41	N	7	19	E		Alpha	Alpha		Alpha	Alpha					
Gephyrocapsa	*huxleyi*	1237	VF22	Mediterranean Sea	I. Probert	2007	43	41	N	7	19	E		Alpha	Alpha				Alpha				Av
Gephyrocapsa	*huxleyi*	1238	EHJG	Pacific Ocean	I. Probert	2005	34	1	N	139	50	E		Beta	Beta								
Gephyrocapsa	*huxleyi*	1239	OS5	Pacific Ocean	K. Hagino	2003	43	13	N	141	1	E		Beta	Beta		Beta	Beta			Beta	Beta	
Gephyrocapsa	*huxleyi*	1240	MT0610A	Pacific Ocean	K. Hagino	2002	41	30	N	141	15	E		Alpha		GH		Alpha			Alpha		
Gephyrocapsa	*huxleyi*	1241	MT0610B	Pacific Ocean	K. Hagino	2002	41	30	N	141	15	E		Alpha				Alpha			Alpha		
Gephyrocapsa	*huxleyi*	1242	CCMP1516	Pacific Ocean	L. Polans	1991	2	67	S	82	72	W		Alpha	Alpha		Alpha	Alpha		Alpha	Alpha	Alpha	
Gephyrocapsa	*huxleyi*	1243	S-13	Atlantic Ocean	I. Probert	2002								Alpha				Alpha			Alpha		
Gephyrocapsa	*huxleyi*	1245	LK6	Atlantic Ocean	I. Probert	1999	44	60	N	1	5	W	*G. huxleyi*	Alpha	Alpha		Alpha	Alpha					

Gephyrocapsa	*huxleyi*	1246	ESP6CL2	Mediterranean Sea	I. Probert	1999	41	36	N	2	39	E	*G. huxleyi*								Alpha			
Gephyrocapsa	*huxleyi*	1247	ESP7410	Mediterranean Sea	I. Probert	1999	41	28	N	2	19	E	*G. huxleyi*	Alpha	Alpha		Alpha	Alpha			Alpha			
Gephyrocapsa	*huxleyi*	1249	ESP41	Mediterranean Sea	I. Probert	1998	41	28	N	2	19	E	*G. huxleyi*	Alpha	Alpha		Alpha	Alpha	Alpha	Alpha				
Gephyrocapsa	*huxleyi*	1250	ASM6	Mediterranean Sea	I. Probert	1999	37	10	N	1	13	W	*G. huxleyi*	Alpha	Alpha									
Gephyrocapsa	*huxleyi*	1251	CC21	Atlantic Ocean	I. Probert	1999	38	44	N	9	37	W	*G. huxleyi*		Alpha		Alpha	Alpha						
Gephyrocapsa	*huxleyi*	1252	MT0610E	Pacific Ocean	K. Hagino	2002	41	30	N	141	15	E		Alpha	Alpha			Alpha			Alpha			
Gephyrocapsa	*huxleyi*	1253	OS2	Pacific Ocean	K. Hagino	2002	43	13	N	141	1	E		Beta	Beta		Beta	Beta		Beta	Beta			
Gephyrocapsa	*huxleyi*	1254	AS56A	Mediterranean Sea	I. Probert	1999	37	10	N	1	13	W	*G. huxleyi*	Alpha										
Gephyrocapsa	*huxleyi*	1255	CCMP370	Atlantic Ocean	E. Paasche	2005	59	50	N	10	60	E		Beta				Beta						
Gephyrocapsa	*huxleyi*	1256	BP91	Atlantic Ocean	I. Probert	1999	63	27	N	20	14	W	*G. huxleyi*	Beta	Beta		Beta	Beta	Beta		Alpha			Av
Gephyrocapsa	*huxleyi*	1257	BP81	Atlantic Ocean	I. Probert	1999	63	27	N	20	14	W	*G. huxleyi*	Beta				Beta			Alpha			
Gephyrocapsa	*huxleyi*	1258	PC101	Atlantic Ocean	I. Probert	1998	40	35	N	10	0	W	*G. huxleyi*	Alpha	Alpha			Alpha			Alpha			
Gephyrocapsa	*huxleyi*	1259	CCMP374	Atlantic Ocean	T. Skinner	1990	42	50	N	69	0	W		Beta	Beta		Beta	Beta		Beta	Beta	Beta		
Gephyrocapsa	*huxleyi*	1260	CCMP373	Atlantic Ocean	B. Guillard	1960	32	10	N	64	30	W		Alpha	Alpha	GH	Alpha	Alpha	Alpha	Alpha	Alpha	Alpha		Av
Gephyrocapsa	*huxleyi*	1261	ESP6CG1	Mediterranean Sea	I. Probert	1999	42	16	N	3	18	E		Alpha	Alpha		Alpha	Alpha	Alpha	Alpha				
Gephyrocapsa	*huxleyi*	1262	BG10-2	Atlantic Ocean	I. Probert	2007	49	30	N	10	30	W		Beta	Beta									
Gephyrocapsa	*huxleyi*	1266	BG10-5	Atlantic Ocean	I. Probert	2007	49	30	N	10	30	W		Beta	Beta									
Gephyrocapsa	*huxleyi*	1268	BG10-8	Atlantic Ocean	I. Probert	2007	49	30	N	10	30	W		Beta	Beta			Beta			Alpha			
Gephyrocapsa	*huxleyi*	1270	BG10-9	Atlantic Ocean	I. Probert	2007	49	30	N	10	30	W		Beta	Beta									
Gephyrocapsa	*huxleyi*	1271	BGI2	Atlantic Ocean	I. Probert	2007	51	20	N	10	29	W				GH		Alpha			Alpha			
Gephyrocapsa	*huxleyi*	1272	BG10-6	Atlantic Ocean	I. Probert	2007	49	30	N	10	30	W		Beta	Beta	GH	Beta	Beta	Beta		Alpha	Alpha		Av
Gephyrocapsa	*huxleyi*	1275	BG10-1	Atlantic Ocean	I. Probert	2007	49	30	N	10	30	W		Beta		GH					Alpha			
Gephyrocapsa	*huxleyi*	1276	BGD1	Atlantic Ocean	I. Probert	2007	50	30	N	10	30	W				GH		Alpha			Alpha			
Gephyrocapsa	*huxleyi*	1277	BGC1	Atlantic Ocean	I. Probert	2007	49	30	N	10	30	W		Beta	Beta									
Gephyrocapsa	*huxleyi*	1322	JS12	Mediterranean Sea	I. Probert	1998	36	15	N	1	35	W	*G. huxleyi*	Alpha				Alpha						
Gephyrocapsa	*huxleyi*	1710	NG1	Pacific Ocean	K. Hagino	2007	32	40	N	129	7	E		Alpha	Alpha									
Gephyrocapsa	*huxleyi*	1731	CCMP2090	Pacific Ocean	L. Polans	1991	2	67	S	82	72	W		Alpha	Alpha		Alpha	Alpha		Alpha	Alpha	Alpha		
Gephyrocapsa	*huxleyi*	1812	BOUM06	Mediterranean Sea	I. Probert	2008	39	6	N	5	21	E		Alpha				Alpha	Alpha	Alpha				Av
Gephyrocapsa	*huxleyi*	1813	BOUM12	Mediterranean Sea	I. Probert	2008	33	38	N	32	39	E		Alpha		GH	Alpha	Alpha	Alpha	Alpha				Av
Gephyrocapsa	*huxleyi*	1814	BOUM13	Mediterranean Sea	I. Probert	2008	33	38	N	32	39	E		Alpha			Alpha	Alpha	Alpha	Alpha				
Gephyrocapsa	*huxleyi*	1815	BOUM14	Mediterranean Sea	I. Probert	2008	33	38	N	32	39	E		Alpha				Alpha						
Gephyrocapsa	*huxleyi*	1817	BOUM16	Mediterranean Sea	I. Probert	2008	33	38	N	32	39	E		Alpha				Alpha						
Gephyrocapsa	*huxleyi*	1818	BOUM17	Mediterranean Sea	I. Probert	2008	33	38	N	32	39	E		Alpha			Alpha	Alpha	Alpha	Alpha				Av
Gephyrocapsa	*huxleyi*	1819	BOUM18	Mediterranean Sea	I. Probert	2008	33	38	N	32	39	E		Alpha		GH	Alpha	Alpha	Alpha	Alpha				Av
Gephyrocapsa	*huxleyi*	1820	BOUM19	Mediterranean Sea	I. Probert	2008	33	38	N	32	39	E		Alpha		GH		Alpha						
Gephyrocapsa	*huxleyi*	1821	BOUM20	Mediterranean Sea	I. Probert	2008	33	38	N	32	39	E		Alpha				Alpha	Alpha	Alpha				
Gephyrocapsa	*huxleyi*	1822	BOUM21	Mediterranean Sea	I. Probert	2008	33	38	N	32	39	E		Alpha				Alpha						
Gephyrocapsa	*huxleyi*	1823	BOUM22	Mediterranean Sea	I. Probert	2008	33	38	N	32	39	E		Alpha				Alpha						
Gephyrocapsa	*huxleyi*	1824	BOUM23	Mediterranean Sea	I. Probert	2008	33	38	N	32	39	E		Alpha				Alpha						
Gephyrocapsa	*huxleyi*	1825	BOUM24	Mediterranean Sea	I. Probert	2008	33	38	N	32	39	E		Alpha				Alpha						

Gephyrocapsa	*huxleyi*	1826	BOUM25	Mediterranean Sea	I. Probert	2008	33	38	N	32	39	E		Alpha				Alpha					
Gephyrocapsa	*huxleyi*	1827	BOUM36	Mediterranean Sea	I. Probert	2008	39	6	N	5	21	E		Alpha				Alpha			Alpha		
Gephyrocapsa	*huxleyi*	1828	BOUM37	Mediterranean Sea	I. Probert	2008	39	6	N	5	21	E		Alpha				Alpha					
Gephyrocapsa	*huxleyi*	1830	BOUM39	Mediterranean Sea	I. Probert	2008	39	6	N	5	21	E		Alpha				Alpha					
Gephyrocapsa	*huxleyi*	1831	BOUM40	Mediterranean Sea	I. Probert	2008	39	6	N	5	21	E		Alpha				Alpha					
Gephyrocapsa	*huxleyi*	1833	BOUM42	Mediterranean Sea	I. Probert	2008	39	6	N	5	21	E		Alpha				Alpha					
Gephyrocapsa	*huxleyi*	1857	BOUM77	Mediterranean Sea	I. Probert	2008	34	8	N	18	27	E		Alpha		GH		Alpha					
Gephyrocapsa	*huxleyi*		C2	South Pacific	I. Probert	2011												Beta		Beta			
Gephyrocapsa	*huxleyi*		C4	South Pacific	I. Probert	2011												Beta		Beta			
Gephyrocapsa	*huxleyi*		C6	South Pacific	I. Probert	2011												Beta		Beta			
Gephyrocapsa	*huxleyi*		C7	South Pacific	I. Probert	2011												Beta		Beta			
Gephyrocapsa	*huxleyi*		C8	South Pacific	I. Probert	2011												Beta		Beta			
Gephyrocapsa	*huxleyi*		C9	South Pacific	I. Probert	2011												Beta		Beta			
Gephyrocapsa	*huxleyi*		ESP7414	Mediterranean Sea	I. Probert	1999	41	28	N	2	19	E	*G. huxleyi*	Alpha									
Gephyrocapsa	*huxleyi*		J26	Irish sea???	I. Probert	2011												Beta		Alpha			
Gephyrocapsa	*huxleyi*		J7	Irish sea???	I. Probert	2011												Beta		Alpha			
Gephyrocapsa	*huxleyi*		J9	Irish sea???	I. Probert	2011												Beta		Alpha			
Gephyrocapsa	*huxleyi*		MM1	Pacific Ocean	K. Hagino		60	50	N	4	50	E		Beta	Beta			Beta	Beta				
Gephyrocapsa	*huxleyi*		PLY573	Pacific Ocean	L. Rhodes	1991	36	16	S	174	48	E		Alpha		GH		Alpha	Alpha		Alpha		
Gephyrocapsa	*huxleyi*		PLY92A	English Channel	I. Parke	1957								Beta	Beta			Beta			Alpha		
Gephyrocapsa	*huxleyi*		PLYM202	South Pacific	I. Inouye	1990								Alpha				Alpha			Alpha		
Gephyrocapsa	*huxleyi*		PLYM218	South Indian ocean	R. N. Pienaar	1983								Beta				Alpha			Alpha	Alpha	
Gephyrocapsa	*huxleyi*		PLYM219, NZEH	South Pacific	L. Rhodes	1992								Beta	Beta			Beta			Alpha	Alpha	
Gephyrocapsa	*oceanica*	1223	ASM9	Mediterranean Sea	I. Probert	1999	37	10	N	1	13	W	*G.ocenica*	Alpha									
Gephyrocapsa	*oceanica*	1244	MM4-3	Pacific Ocean	K. Hagino									Gephy		GO					Alpha		
Gephyrocapsa	*oceanica*	1279	ESP755	Mediterranean Sea	I. Probert	1999	41	28	N	2	19	E	*G.ocenica*	Gephy		GO							
Gephyrocapsa	*oceanica*	1280	ESP752	Mediterranean Sea	I. Probert	1999	41	28	N	2	19	E	*G.ocenica*	Gephy							Alpha		
Gephyrocapsa	*oceanica*	1281	THAU1	Indian Ocean	I. Probert	2000	31	56	S	115	44	E	*G.ocenica*	Alpha	Gephy			Gephy	Gephy	Gephy	Alpha		
Gephyrocapsa	*oceanica*	1282	ESP6M11	Mediterranean Sea	I. Probert	1999	41	28	N	2	19	E	*G.ocenica*	Alpha			Gephy	Gephy	Gephy				Av
Gephyrocapsa	*oceanica*	1284	ESP6M3	Mediterranean Sea	I. Probert	1999	41	28	N	2	19	E	*G.ocenica*	Gephy		GO	Gephy	Gephy	Gephy	Gephy			Av
Gephyrocapsa	*oceanica*	1285	ESP6M2	Mediterranean Sea	I. Probert	1999	41	28	N	2	19	E	*G.ocenica*	Alpha					Alpha		Alpha		
Gephyrocapsa	*oceanica*	1286	AS62E	Mediterranean Sea	I. Probert	1999	37	17	N	0	48	W	*G.ocenica*	Alpha				Gephy	Gephy		Alpha		
Gephyrocapsa	*oceanica*	1287	AS62A	Mediterranean Sea	I. Probert	1999	37	17	N	0	48	W	*G.ocenica*	Alpha				Gephy	Gephy		Alpha		Av
Gephyrocapsa	*oceanica*	1288	JS8	Mediterranean Sea	I. Probert	1998	36	15	N	1	35	W		Alpha	Gephy			Gephy			Alpha		
Gephyrocapsa	*oceanica*	1289	ASM10	Mediterranean Sea	I. Probert	1999	37	17	N	0	48	W	*G.ocenica*	Alpha					Gephy	Gephy	Alpha		Av
Gephyrocapsa	*oceanica*	1292	PR3F1	Atlantic Ocean	I. Probert		14	49	N	67	3	W		Gephy	Gephy			Gephy	Gephy	Gephy	Alpha	???	
Gephyrocapsa	*oceanica*	1293	NS10Z	Atlantic Ocean	I. Probert	2001	34	28	S	17	18	E	*G.ocenica*	Alpha				Gephy			Gephy		
Gephyrocapsa	*oceanica*	1295	PZ1-3	Pacific Ocean	I. Probert													Gephy					
Gephyrocapsa	*oceanica*	1296	ESP56	Mediterranean Sea	I. Probert	1998	36	41	N	4	25	W	*G.ocenica*	Alpha									
Gephyrocapsa	*oceanica*	1297	PZ3-14	Pacific Ocean	I. Probert									Alpha	Gephy			Gephy					Av

Gephyrocapsa	*oceanica*	1300	PZ3-1	Pacific Ocean	I. Probert								Alpha	Gephy			Gephy	Gephy	Gephy	Alpha	Alpha	Av
Gephyrocapsa	*oceanica*	1302	JS7	Mediterranean Sea	I. Probert	1998	36	15	N	1	35	W	*G.ocenica*	Alpha				Gephy						
Gephyrocapsa	*oceanica*	1303	LK7	Atlantic Ocean	I. Probert	1999	44	60	N	1	5	W		Gephy	Gephy			Gephy	Gephy	Gephy	Gephy		Av
Gephyrocapsa	*oceanica*	1305	PC65	Atlantic Ocean	I. Probert	2001	38	14	N	9	43	W	*G.ocenica*	Alpha	Alpha			Gephy	Gephy		Alpha		
Gephyrocapsa	*oceanica*	1306	PC64	Atlantic Ocean	I. Probert	2000	38	14	N	9	43	W	*G.ocenica*	Alpha				Gephy			Gephy		
Gephyrocapsa	*oceanica*	1307	PC51	Atlantic Ocean	I. Probert	1999	38	12	N	9	38	W	*G.ocenica*	Alpha									
Gephyrocapsa	*oceanica*	1308	JS15	Mediterranean Sea	I. Probert	1998	36	15	N	1	35	W	*G.ocenica*	Alpha			Gephy	Gephy	Gephy	Gephy			Av
Gephyrocapsa	*oceanica*	1309	JS14	Mediterranean Sea	I. Probert	1998	36	15	N	1	35	W	*G.ocenica*								Alpha		
Gephyrocapsa	*oceanica*	1310	PR3S4	Atlantic Ocean	I. Probert									Gephy				Gephy			Alpha		
Gephyrocapsa	*oceanica*	1316	LK9	Atlantic Ocean	I. Probert	1999	44	60	N	1	5	W	*G.ocenica*	Gephy	Gephy				Gephy		Gephy	Gephy	Av
Gephyrocapsa	*oceanica*	1317	JS10	Mediterranean Sea	I. Probert	1998	36	15	N	1	35	W		Alpha			Gephy	Gephy	Gephy	Gephy			Av
Gephyrocapsa	*oceanica*	1318	THAU4	Indian Ocean	I. Probert	2000	31	56	S	115	44	E	*G.ocenica*	Gephy			Gephy	Gephy			Gephy		
Gephyrocapsa	*oceanica*	1319	NS6-2	Atlantic Ocean	I. Probert	2002	36	40	S	16	46	E	*G.ocenica*	Alpha				Gephy			Gephy		
Gephyrocapsa	*oceanica*	1320	ESP6M6	Mediterranean Sea	I. Probert	1999	41	28	N	2	19	E					Gephy	Gephy					
Gephyrocapsa	*oceanica*	1562	NIES1000	Pacific Ocean	M. Kawachi	1999	34	5	N	139	34	E		Gephy	Gephy		Gephy	Gephy			Alpha		
Gephyrocapsa	*oceanica*	1709	MT0610G	Pacific Ocean	K. Hagino	2002	41	30	N	141	15	E		Alpha				Gephy	Gephy		Alpha		Av
Gephyrocapsa	*oceanica*	1796	DS7	South China Sea	I. Probert	2009	20	41	N	106	48	E		Gephy				Gephy			Gephy		
Gephyrocapsa	*oceanica*	1834	BOUM43	Mediterranean Sea	I. Probert	2008	39	6	N	5	21	E		Alpha				Gephy					
Gephyrocapsa	*oceanica*	1835	BOUM44	Mediterranean Sea	I. Probert	2008	39	6	N	5	21	E		Gephy		GH		Gephy					
Gephyrocapsa	*oceanica*	1836	BOUM46	Mediterranean Sea	I. Probert	2008	39	6	N	5	21	E		Gephy				Gephy					
Gephyrocapsa	*oceanica*	1839	BOUM50	Mediterranean Sea	I. Probert	2008	39	6	N	5	21	E		Gephy	Gephy	GO		Gephy			Alpha		
Gephyrocapsa	*oceanica*	1841	BOUM53	Mediterranean Sea	I. Probert	2008	39	6	N	5	21	E		Gephy		GO		Gephy			Alpha		
Gephyrocapsa	*oceanica*	1842	BOUM54	Mediterranean Sea	I. Probert	2008	39	6	N	5	21	E		Alpha	Gephy	GO							
Gephyrocapsa	*oceanica*		BOUM45	Mediterranean Sea	I. Probert	2008	39	6	N	5	21	E		Gephy				Gephy					
Gephyrocapsa	*oceanica*		MM4_6	Pacific ocean	K. Hagino									Alpha				Gephy			Alpha		
Gephyrocapsa	*oceanica*		MT3-6	Pacific Ocean	K. Hagino	2006	41	50	N	141	25	E		Gephy	Gephy				Gephy	Gephy			Av
Gephyrocapsa	*oceanica*		PR3F3	Atlantic Ocean	I. Probert		14	49	N	67	3	W		Gephy	Gephy								

CHAPITRE 3

NEW EVIDENCE FOR MORPHOLOGICAL AND GENETIC VARIATION IN THE COSMOPOLITAN COCCOLITHOPHORE *EMILIANIA HUXLEYI* (PRYMNESIOPHYCEAE) FROM THE *COX1b-ATP4* GENES

Kyoko Hagino[1], El Mahdi Bendif[2], Jeremy R. Young[3], Kazuhiro Kogame[4], Ian Probert[2], Yoshihito Takano[5], Takeo Horiguchi[4], Colomban de Vargas[2] and Hisatake Okada[6]

[1]Institute for Study of the Earth's Interior Okayama University, 827 Yamada, Misasa, Tottori 682-0193, Japan

[2]CNRS UMR7144/UPMC, EPPO team, Station Biologique de Roscoff, 29682 Roscoff, France

[3]Palaeontology Department, The Natural History Museum, London SW7 5BD, UK

[4]Department of Natural History Sciences, Faculty of Science, Hokkaido University, Sapporo 060-0810, Japan

[5]Institute for East China Sea Research, Nagasaki University, Nagasaki, 1-14 Bunkyo, Nagasaki, 852-8521, Japan

[6]Administrative Office, Hokkaido University, N8 W5 Kita-Ku, Sapporo, 060-0808, Japan

Hagino-Tomioka K, Bendif EM, Probert I, Young J, Kogame K, Takano Y, Horiguchi T, de Vargas C and Okada, H. New evidence for morphological and genetic variation in a cosmopolitan coccolithophore *Emiliania huxleyi* (Prymnesiophyceae) from the cox1b-ATP4 genes. Journal of Phycology 47:1164-1176, 2011

Abstract

Emiliania huxleyi (Lohmann) Hay *et* Mohler is a cosmopolitan coccolithophore occurring from tropical to subpolar waters and exhibiting variations in morphology of coccoliths possibly related to environmental conditions. We examined morphological characters of coccoliths and partial mitochondrial sequences of the cytochrome oxidase 1b (*cox1b*) through adenosine triphosphate synthase 4 (*atp4*) genes of thirty-nine clonal *E. huxleyi* strains from the Atlantic and Pacific Oceans, Mediterranean Sea and their adjacent seas. Based on the morphological study of culture strains by SEM, Type O, a new morphotype characterized by coccoliths with an open central area, was separated from existing morphotypes A, B, B/C, C, R and var. *corona*, characterized by coccoliths with central area elements. Molecular phylogenetic studies revealed that *E. huxleyi* consists of at least two mitochondrial sequence groups with different temperature preferences/tolerances: a cool water group occurring in subarctic North Atlantic and Pacific and a warm water group occurring in the sub-tropical Atlantic and Pacific and in the Mediterranean Sea.

Key index words: biogeography; coccolithophore; *Emiliania huxleyi*; mitochondrial DNA; morphotype.

Abbreviations: *atp4,* adenosine triphosphate synthase 4; *cox1,* cytochrome oxidase 1b; ka, kiloannum; ky kilo-years

Introduction

Coccolithophores are single-celled marine haptophytes characterized by bearing calcareous scales called coccoliths. They play an important role as primary producers in the oceans and contribute to the global carbon cycle through photosynthesis and calcification of coccoliths (e.g. Rost and Riebesell 2004). Vast numbers of coccoliths produced in surface waters sink to the deep-sea floor where they constitute a significant part of deep-sea sediments. The evolutionary history of coccolithophores has been extensively studied based on the continuous fossil record of coccoliths preserved in marine sediments. Palaeontological studies have revealed that coccolithophore floras in the geological past were often dominated by a few cosmopolitan taxa (e.g. Young 1998, Hine and Weaver 1998). It is not known whether these cosmopolitan taxa were indeed single biological species or complexes of cryptic species with different environmental preferences.

Emiliania huxleyi (Lohmann) Hay *et* Mohler is the youngest coccolithophore morphospecies, appeared ca. 290ka (e.g., Raffi et al. 2006). It is thought that *E. huxleyi* diverged from *Gephyrocapsa oceanica* Kamptner, since *E. huxleyi* and *G. oceanica* are genetically identical in SSU rDNA and RUBISCO *rbc*L sequences (Medlin et al. 1996, Fujiwara et al. 2001), and *G. oceanica* has a longer fossil record than *E. huxleyi* (e.g., Hine and Weaver 1998). In the early part of its evolutionary history, *E. huxleyi* was initially a minor species in the coccolithophore flora but it progressively increased in relative abundance through time. The *E. huxleyi* acme, which is defined by ≥50% dominance in the total fossil coccolithophore flora, started diachronously from 85ka in low latitudes, 73ka in transitional latitudes, and 61ka in high latitudes of the North Atlantic Ocean (e.g., Thierstein et al. 1977, Gard 1986, 1989, Jordan et al. 1996). In modern oceans, *E. huxleyi* is undoubtedly the most abundant and cosmopolitan coccolithophore species, occurring in almost all assemblages from tropical to subpolar waters and frequently constituting ≥50 % of the coccolithophore flora (e.g., McIntyre and Bé 1967, Okada and Honjo, 1973).

Morphological variation in coccoliths of *E. huxleyi* that are likely related to hydrographic conditions have been reported in various biogeographic studies, although the morphotype classification, especially for morphotypes from cold water masses, has not always been consistent between authors. McIntyre and Bé (1967) classified *E. huxleyi* into warm- and cold-water types based on the morphology of the central area and proximal shield of coccoliths (Table 1, Fig. 1). They mentioned that the cold-water type has a central plate. Subsequent studies, however, also included specimens with open central area in the cold-water type (e.g., Winter

1985, Verbeek 1989) probably because the general appearance of the coccoliths with an open central area resembled the cold-water type rather than the warm-water type. Winter (1985) also mentioned that their cold-water types were not always related to low temperature. To avoid the use of morphotype names associated with temperature, Young and Westbroek (1991) renamed the warm- and cold-water types as Types A and C, respectively. They also described Type B characterized by a solid central plate and larger coccolith size than Type C (Table 1, Fig. 1). Culture strains of Type C were not available at the time, and it was not known whether the morphology of the central area was a stable character reflecting genetic differences. Therefore, Young and Westbroek (1991) included open central area morphotypes in their Type C. Later, Young et al. (2003) described Type B/C characterized by a solid/open central plate and a transitional size between that of Types B and C. Okada and Honjo (1973) described a subarctic type based on irregularly arranged distal shield elements. Hagino et al. (2005) considered this to be comparable to Type B of Young and Westbroek (1991) without consideration of central area morphology. They also reported Type B from the N.W. Pacific, illustrating specimens with an open central area. Judging from the SEM images shown in the previously published papers, all coccolithophore workers in the last three decades have classified *E. huxleyi* specimens with an open central area into either the cold-water type, Type B or Type C. Classification of *E. huxleyi* morphotypes from tropical to temperate waters has been more consistent than that of morphotypes from cold-water regimes, the following four morphotypes have been reported: *E. huxleyi* var. *corona* (Okada and McIntyre 1977), Types A and C (Young and Westbroek 1991), and Type R (Young et al. 2003) (Table 1, Fig. 1).

Table 1 Classification of morphotypes of *Emiliania huxleyi*.

Morphotype in this study	Morphology of distal shield	Morphology of central area	Length of distal shield	Comparable morphotypes in literature
Type A	moderate-heavily calcified elements	grill	< 4µm	Warm type (McIntyre and Bé, 1967)
Type B	lightly calcified elements	solid plate	≥ 4µm	Type B (Young et al. 2003)
Type B/C	lightly calcified elements	solid plate	< 4µm	Type B/C (Young et al. 2003)
Type C	lightly calcified elements	solid plate	< 3.5µm	Cold type (McIntyre and Bé, 1967) Type C (Young et al. 2003)
Type O	lightly calcified elements	open	varied in size	Subarctic type (Okada and Honjo, 1975) Type B (Hagino et al. 2005)
Type R	*Reticulofenestra*-like heavily calcified distal shield elements	grill	< 4µm	Type R (Young et al. 2003)
var. *corona*	moderately calcified elements with elevated central tube	grill	3.5-4.5 µm	var. *corona* (Okada and McIntyre, 1977)

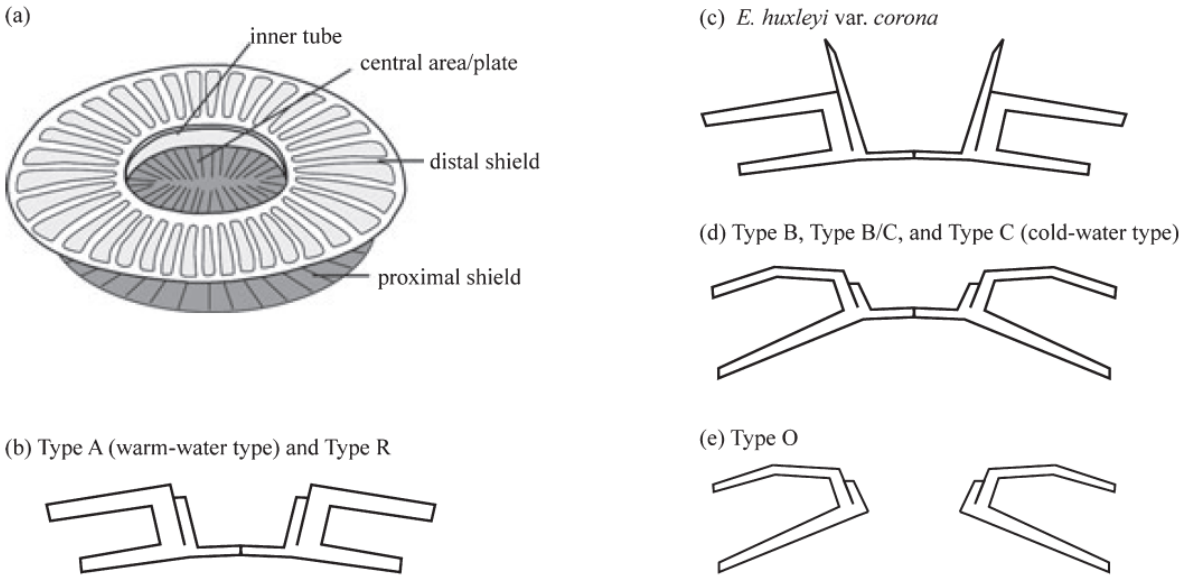

Figure. 1. (a) Schematic diagram of coccolith of *Emiliania huxleyi.* (b) cross section of Types A and R, (c) cross section of *E. huxleyi* var. *corona,* (d) cross section of Types B, B/C, and C, (e) cross section of Type O.

Inter-strain genetic variation of *E. huxleyi* has been studied since the early 1990s in order to investigate genetic relationships among morphotypes as well as genetic diversity in natural *E. huxleyi* populations. Culture strains of Types A and B were shown to be identical in SSU rDNA sequences (Medlin et al. 1996), and therefore morphotypes of *E. huxleyi* have typically been regarded as intra-specific variants rather than discrete species. Fine-scale genetic variation within *E. huxleyi* populations has been detected by Random Amplification of Polymorphic DNA (RAPD) and microsatellite analysis, although this genetic variation showed no clear relation to morphotype (Medlin et al. 1996, Iglesias-Rodriguez et al. 2002). Schroeder et al. (2005) reported a genetic marker differentiating Type A from Type B: the gene coding for the calcium binding protein GPA, which was isolated from coccolith-producing vesicles and shown to precipitate calcium (Corstjens et al. 1998). Subsequent studies have found variation in GPA sequences from environmental samples (Martínez-Martínez et al. 2007, Ripley et al. 2008). Iglesias-Rodriguez et al. (2006) provided evidence of low gene flow between *E. huxleyi* populations of the Bergen fjord and the N.E. Atlantic Ocean based on microsatellite analysis of multiple clonal culture strains. Strains/samples used in these genetic studies were almost exclusively collected from the North Atlantic Ocean and adjacent seas, and genetic relationships between *E. huxleyi* populations from the Atlantic and other oceans have not been revealed.

Mitochondrial DNA evolves relatively rapidly, and so is often used in studies of fine-scale genetic variation and phylogeography (e.g. Schwaninger 2008). The complete

mitochondrial genome sequence of *E. huxleyi* has been obtained from strain CCMP373 (Sánchez Puerta et al. 2004). In the present study, we examined, for the first time variations in partial mitochondrial sequences of *E. huxleyi*, using multiple clonal culture strains from the Atlantic Ocean, Pacific Ocean, Mediterranean Sea and their adjacent seas. This genetic variation was compared to coccolith morphology, biogeography and environmental parameters. Furthermore, we re-examined the morphology of *E. huxleyi* in field samples used for previous morphological studies in order to refine definition of morphotypes and integrate this with our new information from culture and molecular studies.

Materials and Methods

Morphological studies of clonal culture strains and field samples: The coccolith morhology of thirty-nine clonal *E. huxleyi* strains (Table S1) was studied by SEM. In addition, morphological variation of *E. huxleyi* populations in ten selected, previously studied, field samples, was re-examined by SEM (Table 2). Clonal culture strains were maintained in MNK medium (Noël et al. 2004) at 18˚C in a 18:6 h light:dark regime. 10-100 mL of cell suspension of each strain were sampled during the exponential growth phase and filtered onto mixed cellulose ester (Millipore HAWP04700) or polycarbonate filters (Whatman 7060-4710). Small pieces of dried filter samples were mounted on aluminum SEM stubs and sputter-coated with gold-palladium or platinum using an ion sputter 208HR (Cressington Scientific, Watford, England) or Hitachi E-1020 (Hitachi Corp., Hitachinaka, Japan). The morphotype of each culture strain and the morphotype composition of field samples were examined using a Phillips XL30 FEG SEM (Philips FEI, Eindhoven, Netherlands) or a Hitachi S-3000H SEM.

Table 2. Composition of morphotypes in field samples.

					Morphotype composition obtaine in this study (%)		
Sampling Station	Latitude	Longitude	Sampling date	Morphotype recognition in previous studies	Type A	Type B/C	Type O
KH-30	50˚00'N	155˚05W	1969.8.23	subarctic form (Okada and Honjo 1973)	0	0	100
KH-31	49˚12'N	154˚37'W	1969.8.27	subarctic form (Okada and Honjo 1973)	0	0	100
KH-32	48˚02'N	155˚44'W	1969.8.28	subarctic form (Okada and Honjo 1973)	0	0	100
KH-33	46˚49'N	154˚32'W	1969.8.28	subarctic form (Okada and Honjo 1973)	0	0	100
KH-34	45˚04'N	154˚46'W	1969.8.28	subarctic form (Okada and Honjo 1973)	0	0	100
KT90-9, st. 11	42˚24'N	144˚22'E	1990.6.26	Type B (Hagino et al. 2005)	0	0	100
KT90-9, st. 35	37˚49'N	142˚07'E	1990.6.28	Types A and B (Hagino et al. 2005)	81	1	18
KT90-9, st. 38	35˚58'N	141˚10'E	1990.6.29	Types A and B/C (Hagino et al. 2005)	90	0	10
KH90-1, st. 9	33˚09'N	139˚50'E	1990.7.21	Types A and B/C (Hagino et al. 2005)	97	1	2
KH90-1, st. 18	32˚47'N	142˚47'E	1990.7.24	Types A (Hagino et al. 2005)	100	0	0

DNA preparation, PCR and sequencing: Thirty-nine clonal *E. huxleyi* and four clonal *G. oceanica* strains from various geographic origins were used for molecular studies (Table S1). Genomic DNA of each strain was extracted using benzyl chloride extraction (Zhu et al. 1993) or phenol-chloroform extraction (Sambrook et al. 1989) methods. The DNA extracts were then purified using Geneclean II ® Kits (Bio 101 Inc., Vista, California, USA). Purified DNA was used for PCR to amplify the region from cytochrome oxidase 1b (*cox1b*) through adenosine triphosphate synthase 4 (*atp4*) of the mitochondrial genome. Three sets of PCR and sequencing primers listed in Table 3 were designed based on the complete mitochondrial genome sequence of *E. huxleyi* reported by Sánchez Puerta et al. (2004) (GenBank accession number AY342361). The PCR conditions were: initial denaturation at 94°C for 60 s followed by 35 cycles of denaturation at 94°C for 30 s, annealing at 50°C for 30 s and extension at 72°C for 30 s. The temperature profile was completed by a final extension at 72°C for 4 min. The PCR products were sequenced directly using the ABI PRISM BigDye Terminator Cycle Sequencing Kit (Perkin-Elmer, Foster City, California, USA) by DNA auto sequencer ABI PRISM 310 and/or 3130 Genetic Analyzers (Perkin-Elmer). Both forward and reverse strands were sequenced. Genbank accession number of each sequence is listed in Table S1.

Table 3. Oligonucleotide primers used for amplification and sequencing

Code of Primer	Synthesis direction	Sequence (5'-3')	Anneals to [a]
EGcox1-F2	Forward	GCTCATTCAGGAGGTTCTGT	15333-15352
EGcox1-R4	Reverse	GATAAAACAATACCTGTTAA	15978-15997
EGcox1-F3	Forward	ACTATGATTATTGCTGTTC	15846-15864
EGcox1-R5	Reverse	ACTAAGTAATCAGTTTCTGC	16401-16429
EGcox1-16274F	Forward	TGCAATTGCTTCATTTGGTAC	16274-16294
EGatp4-16959R	Reverse	TGCCGATTTCGCATCAATAAG	16959-16979

[a] Annealing site in the mtDNA of strain CCMP373 (Virginia Sáchez Puerta et al. 2004)

Phylogenetic analysis: Sequences were manually aligned and based on this alignment, rooted and unrooted phylogenetic trees were inferred by Maximum Likelihood (ML), Neighbor Joining (NJ), and Maximum Parsimony (MP) methods using PAUP version 4.0b10 (Swofford 2002). Furthermore, rooted and unrooted Bayesian trees were constructed by Mr. BAYES v3.1.2 (Ronquist and Huelsenbeck 2003). To decide which evolutionary model for ML best

fitted the data set, the program Modeltest V. 3.7 (Posada and Cradall 1998) was used. The model selected by the hierarchical likelihood ratio tests (hLRTs) and by the Akaike information criterion (AIC) for all data sets in rooted and unrooted ML trees were K81uf + I + G model. Base frequencies and substitution parameters were estimated by Modeltest. ML analysis was performed using the heuristic search option with a branch-swapping algorithm (Tree bisection-reconnection; TBR). Starting trees were obtained by stepwise random addition of sequences (10 replicates). The distance matrix was calculated using Kimura two parameter distances (Kimura 1980), and the distance tree was constructed using the NJ method (Saitou and Nei 1987). MP was performed using the heuristic search option with random addition of sequences (1000 replicates) and a branch-swapping algorithm (TBR). All characters were weighted equally in both rooted and unrooted trees. Bootstrap analyses with 100 replicates for rooted and unrooted ML analyses, and 1000 replicates for rooted and unrooted NJ and MP analyses were applied to examine the robustness and statistical reliability of the topologies (Felsenstein 1985). For ML bootstrapping, the heuristic search option with a branch-swapping algorithm of nearest neighbor interchange (NNI) was employed. Bayesian analyses were conducted to construct rooted and unrooted trees with two runs of four Markov chains, for at least 2 million generations, sampling every 100th generation. The burn-in option was set discarding 25% from the 20,000 trees found.

Comparison of environmental parameters at the sites of culture strain isolation: Annual mean environmental values at the sampling location of each strain and monthly mean environmental parameters for the sampling month of each sampling location were obtained from the World Ocean Atlas 2005 (Antonov et al. 2006, Garcia et al. 2006a, 2006b, Locarnini et al. 2006). Welch's t-test (Welch 1947) with 5% rejection rate was applied to examine whether mean values of environmental parameters (temperature, salinity, concentrations of nitrate and phosphate) between the clades obtained by molecular phylogenetic analyses were significantly different from each other.

Results

Morphological studies of culture samples

Of the 39 *E. huxleyi* strains, five strains were non-calcifying and so could not be used for morphological studies of coccoliths, however, the morphotype of coccoliths in two of the five naked strains was known from previous studies (Table S1). Based on the morphology of the central area and of the distal shield of coccoliths, the 34 calcifying strains were classified

into morphotypes. Thirty of the calcifying strains could be assigned to the previously established morphotypes A, B/C, and R, of Young and Westbroek (1991) and Young et al. (2003). The remaining four calcifying strains were similar in shield characteristics and in size to Types B or B/C but different in central area morphology. These four strains have never calcified their central area (i.e. they have maintained an open central area) over >4 years under various laboratory culture conditions, whereas culture strains of other morphotypes have always had calcified central areas. It therefore seems clear that the morphology of the central area is stable and genetically controlled. Hereafter, we call the morphotype with an open central area 'Type O'. The definition of morphotypes used in this study is summarized in Table 1.

Type A was the most common morphotype; 26 out of the 34 calcifying strains were classified as Type A, based on the presence of a grill in the central area and small-medium (<4µm) distal shield length (Tables 1 and S1, Figs. 1, 2a and 3). The degree of calcification of the distal shield and central area was stable in each strain over several years in culture, but varied among strains. Variation in the degree of calcification within Type A strains, however, was not used for subdivision of this morphotype because a classification scheme related to intensity of calcification has not yet been established. Strain NS10Y, which is characterized by a solid/plated central area, delicate distal shield elements and medium size (3.5-4.0 µm in distal shield length), was the only Type B/C strain in this study. This Type B/C strain was isolated from the S.E. Atlantic Ocean off the coast of South Africa (Tables 1 and S1, Figs. 1, 2b, 3). Three Type R strains with heavily calcified *Reticulofenestra*-like distal shields came from the same water sample collected from the E. Tasman Sea, off South Island, New Zealand (Tables 1 and S1, Figs. 1, 2c and 3). Of the four Type O strains identified by having an open central area and delicate distal shield elements, two strains came from the E. Bering Sea, and two from the northern part of the Japan Sea (Tables 1 and S1, Figs. 1, 2d and 3). The central area of the Type O coccoliths was often covered by an organic membrane that can be mistaken for the central plate, but careful observation in high magnification revealed that Type O strains never possessed a calcified central area structure (Fig. 2d).

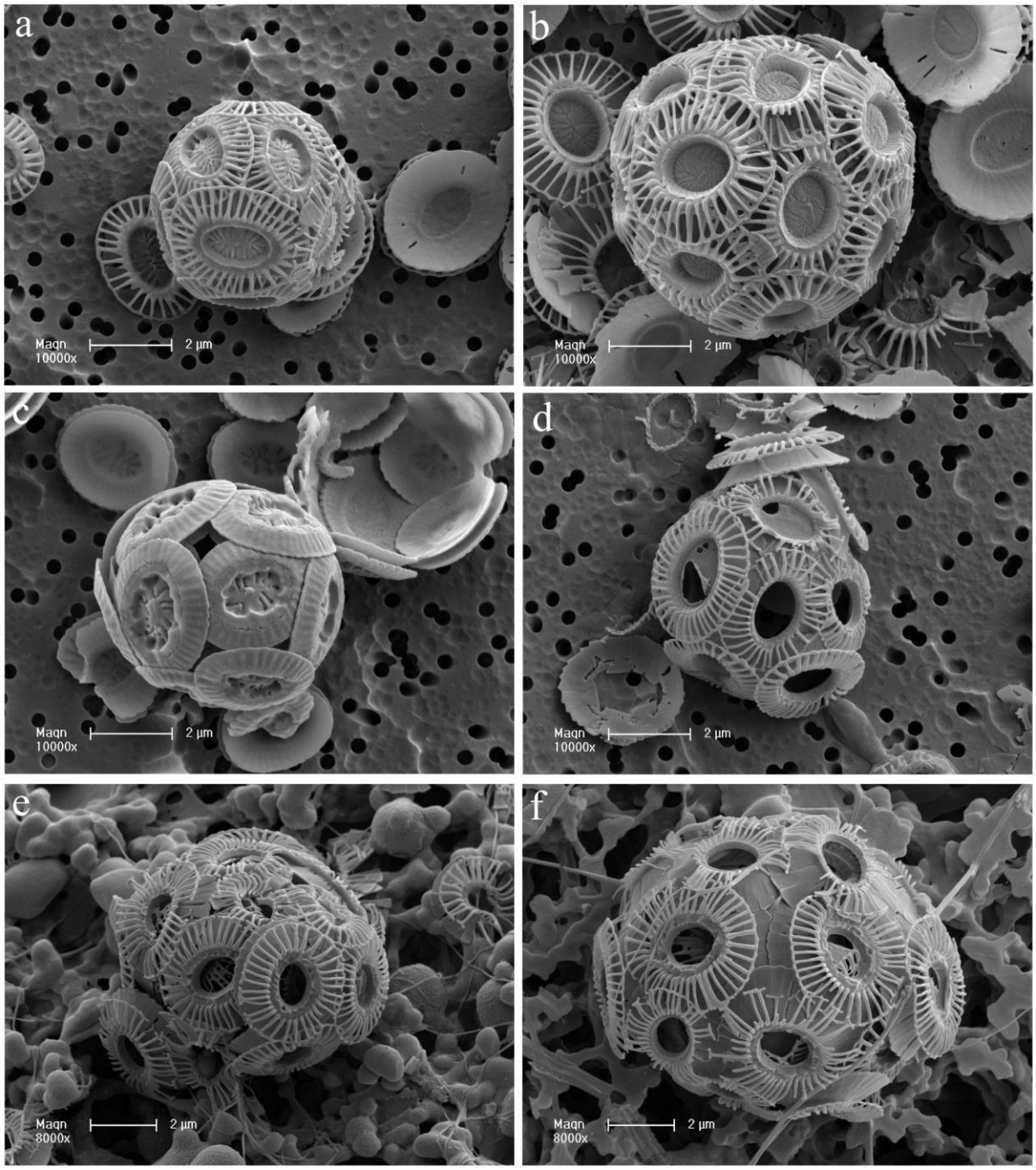

Figure. 2. SEM images of clonal culture strains and field specimens. (a) Type A strain NG-1, (b) Type B/C strain NS10Y, (c) Type R strain TQ22, (d) Type O strain NIES 1311, (e) Type O specimen from field sample KH69-4, sample KH-30, and (f) Type O specimen from field sample KT90-9, st. 11.

Morphological studies of field samples

All *E. huxleyi* specimens observed from samples KH-30 through KH-34, which were used by Okada and Honjo (1973) for description of their subarctic type, showed type O morphology (Table 2; Figs. 2e, and 3). The distal shield elements were occasionally disconnected from the neighboring elements, which resulted in the 'irregular distal shield elements' reported by Okada and Honjo (1973). Distal and proximal shields were almost the

same size, and varied from 2.5-4.0µm in length. Of the samples from the N.W. Pacific, sample KT90-9, station 11, which was recorded as dominated by Type B (Hagino et al. 2005), yielded exclusively specimens with an open central area and elevated delicate distal shield elements, i.e. Type O. The distal shield was usually smaller than the proximal shield. The coccolith length varied greatly, ranging from 2.5-5.0 µm. In the five N.W. Pacific samples re-examined, the composition of *E. huxleyi* morphotypes varied latitudinally. Type O dominated the northernmost station and decreased in abundance southwards (Table 2), whilst Type A increased in abundance southwards, and dominated the southernmost station (KH90-1 station 18). Type B/C with plated central area, delicate distal shield elements and relatively small coccoliths (< 4µm in distal shield length) occurred rarely at KT90-9 station 35 and KH90-1 station 9 (Table 2).

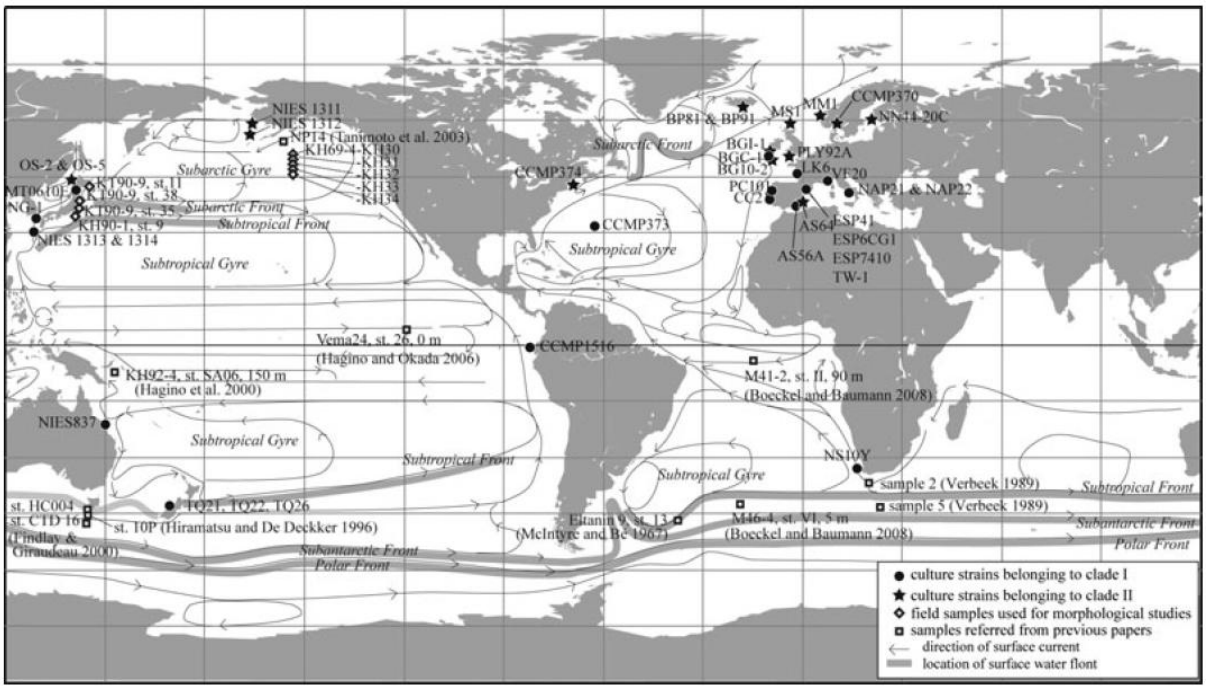

Figure. 3. Location of culture strains and field samples used or discussed in this study, and distribution of surface currents and water fronts (Tomczak and Godfrey, 1994).

Phylogenetic analysis of culture strains

The alignment of obtained sequences of the *cox*1b-*atp*4 region was 1517bp in length with no gaps. For construction of rooted ML, NJ, MP, and Bayesian trees, a total of 43 sequences, including sequences of four *G. oceanica* strains as an outgroup, were used. A likelihood score (-lnL) of 2491.6389 was obtained under the K81uf + I + G model with the following parameters: assumed nucleotide frequencies A=0.2682, C=0.1505, G=0.1691, and

T=0.4122; substitution-rate AC=1, AG=6.7470, AT=0.0717, CG=0.0717, CT=6.7470, GT=1; proportion of sites assumed to be invariable=0.7793; rates for variable sites assumed to follow a gamma distribution with shape parameter=0.7062, estimated by Modeltest 3.7. Parsimony analysis resulted in a single most parsimonious tree of 73 steps (CI=0.877, RI=0.965). ML, NJ, and MP analyses resulted in similar trees, while the topology of the Bayesian tree was different from that of ML, NJ, and MP trees. Fig. 4 shows only the ML tree with bootstrap values obtained by ML, NJ, and MP methods, and Fig. 5 shows the Bayesian tree with posterior probabilities.

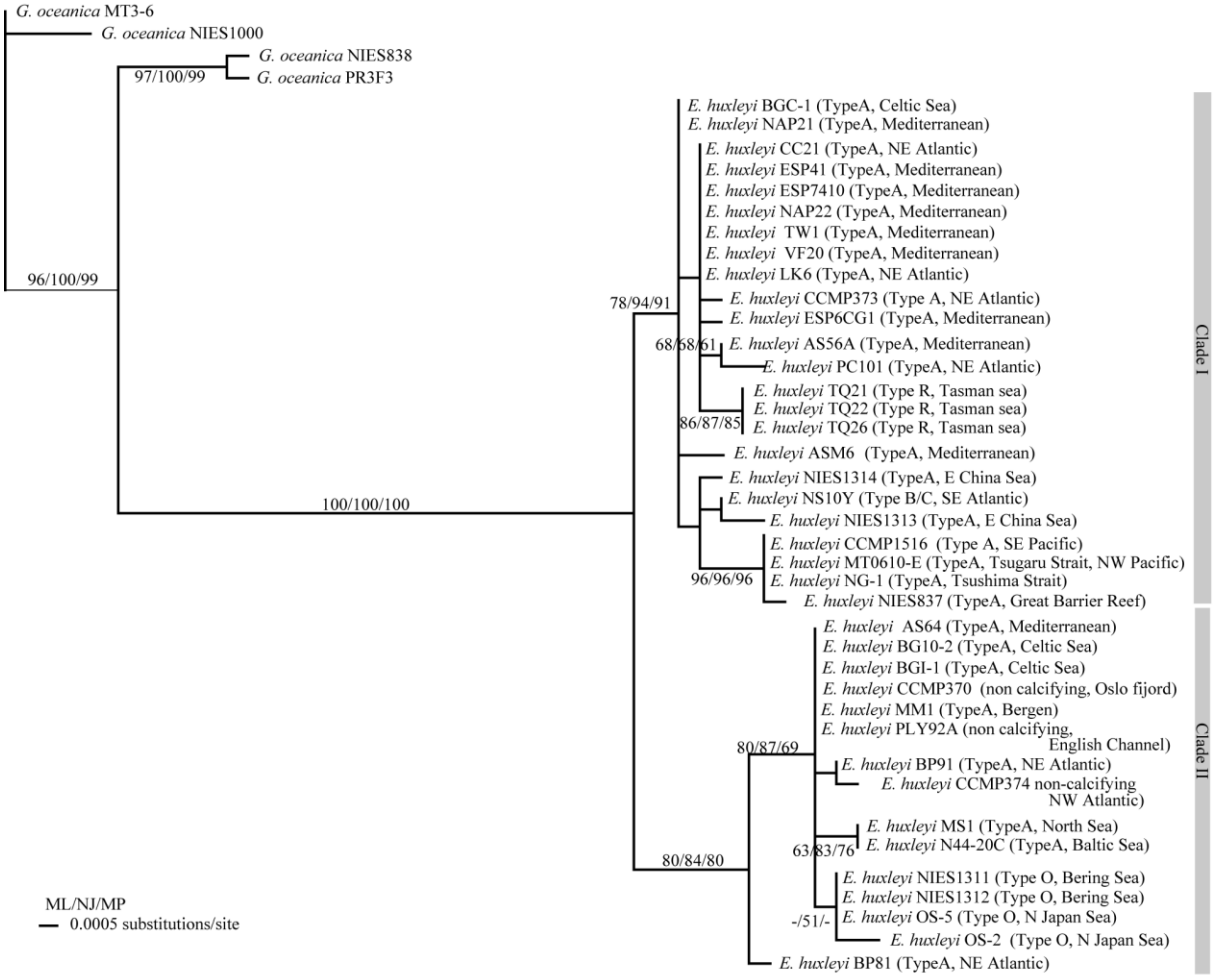

Figure. 4. Rooted ML tree (−lnL=2491.6389) based on *cox1-atp4* sequences. Four sequences of *Gephyrocapsa oceanica* were used as an outgroup. The numbers on each node indicate the bootstrap values from ML, NJ, and MP analyses.

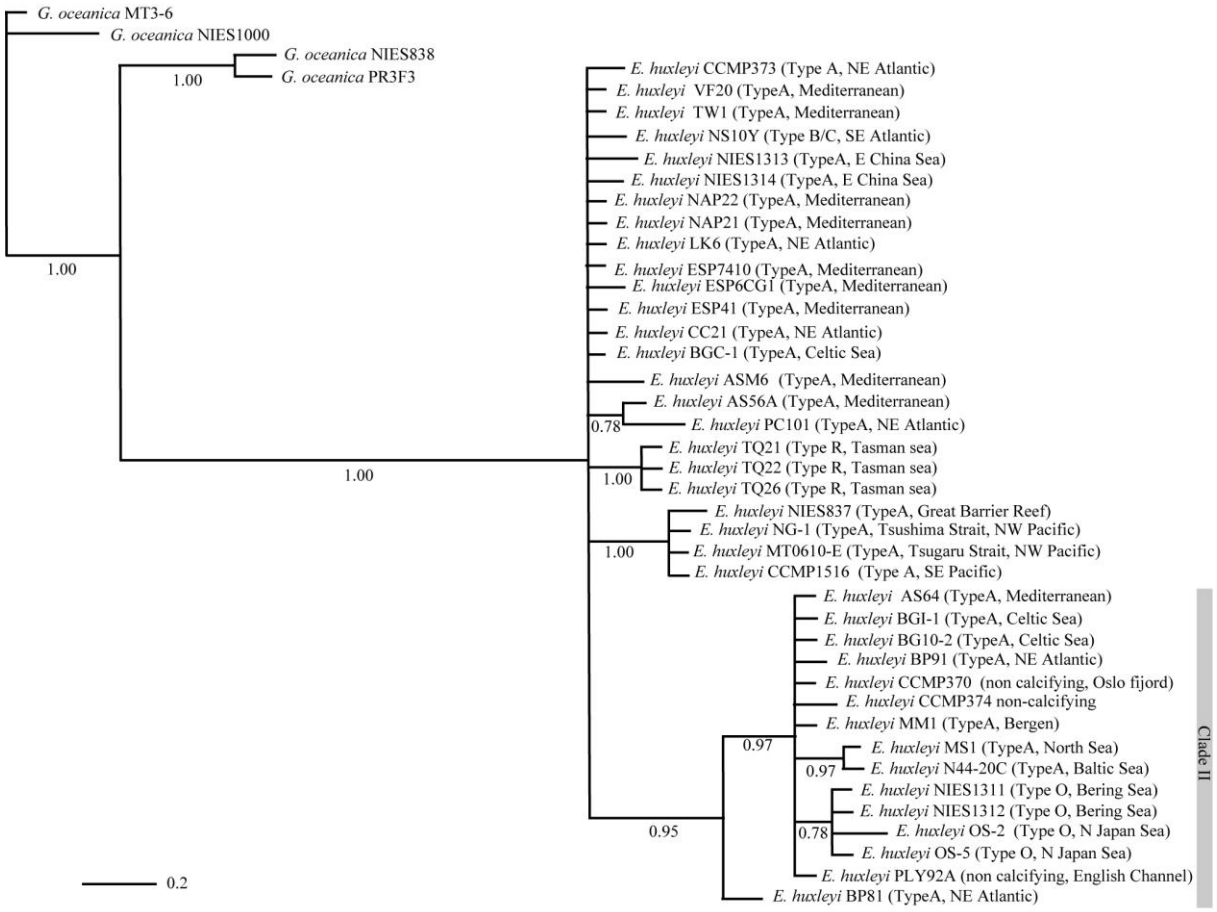

Figure 5. Rooted Bayesian tree based on *cox1-atp 4* sequences. Four sequences of *Gephyrocapsa oceanica* were used as an outgroup. The numbers on each node indicate the Bayesian posterior probabilities.

In the rooted ML, NJ, and MP trees, *E. huxleyi* made a clade with 100% bootstrap values (Fig. 4). *E. huxleyi* consisted of two major clades, I and II, which were separated from each other by eight common substitutions, and were supported by moderate to high bootstrap values (78-91%). Clade I consisted of 26 strains including 22 Type A, one Type B/C, and three Type R strains. Type A strains in clade I had diverse mitochondrial sequences which resulted in several small clusters with bootstrap values ≤70%, and one sub-clade with bootstrap values 96%. This well-supported sub-clade comprised four Type A strains (NG-1, MT0610E, NIES 837, and CCMP 1516) from the Pacific Ocean and adjacent seas. The sequences of the three Type R strains (TQ21, 22 and 26) were identical to each other, and different from other morphotypes. The only Type B/C strain, NS10Y from the S.E. Atlantic, formed a sub-clade with NIES1313 (Type A) from the N.W. Pacific with low bootstrap support in the ML and NJ trees, but no support in the MP analysis.

Clade II included eight Type A strains, four Type O strains, and three non-calcifying strains. Strain BP81 (Type A) from northern N.E. Atlantic (Iceland) occupied a well-separated basal position within clade II. The remaining strains branched into a cluster

supported by low to moderate bootstrap values of 69-87%. Within this cluster, the four Type O strains made a sub-clade with low bootstrap support (51%) in the NJ trees, but no support in the ML and MP analysis.

In the rooted Bayesian tree, all *E. huxleyi* strains made a clade with a posterior probability of 1.00 (Fig. 5). The *E. huxleyi* clade included three sub-clades supported by high posterior probabilities (0.95-1.0) and a sub-clade with low posterior probability (0.78) as well as 15 non-clustered strains. Of the sub-clades with high posterior probabilities, the largest consisted of eight Type A, four Type O and three non-calcifying strains corresponding to Clade II in the rooted ML, NJ, and MP trees (Figs. 4 and 5). Hereafter, we refer to this largest sub-clade as Clade II following the classification in the rooted ML, NJ, and MP trees. In Clade II, Type A strain BP81 occupied a basal position. The remaining strains formed an internal sub-clade with 0.97 posterior probability. Within this sub-clade, two Type A strains clustered together with 0.97 posterior probability, and four Type O strains clustered with low posterior probability (0.78). The *E. huxleyi* strains outside Clade II varied in sequences, and two Type A strains from N.E. Atlantic and Mediterranean Sea, four Type A strains from the Pacific and its adjacent seas, and three Type R strains from the Tasman Sea made subclades with 0.78, 1.0, 1.0 posterior probability, respectively.

A total of 39 *E. huxleyi* sequences were used for constructing unrooted ML, NJ, MP, and Bayesian trees. A likelihood score (-lnL) of 2491.6389 was obtained under the K81uf + I + G model with the following parameters: assumed nucleotide frequencies A=0.2682, C=0.1505, G=0.1691, and T=0.4122; substitution-rate AC=1, AG=6.7471, AT=0.0717, CG=0.0717, CT=6.7471, GT=1; proportion of sites assumed to be invariable=0.7793; rates for variable sites assumed to follow a gamma distribution with shape parameter=0.7062, estimated by Modeltest 3.7. Parsimony analysis resulted in a single most parsimonious tree of 73 steps (CI=0.877, RI=0.965). ML, NJ, MP, and Bayesian analyses without outgroup sequences resulted in similar trees, and here we show only the ML tree with bootstrap values obtained by ML, NJ, and MP methods and bayesian posterior probabilities (Fig. 6).

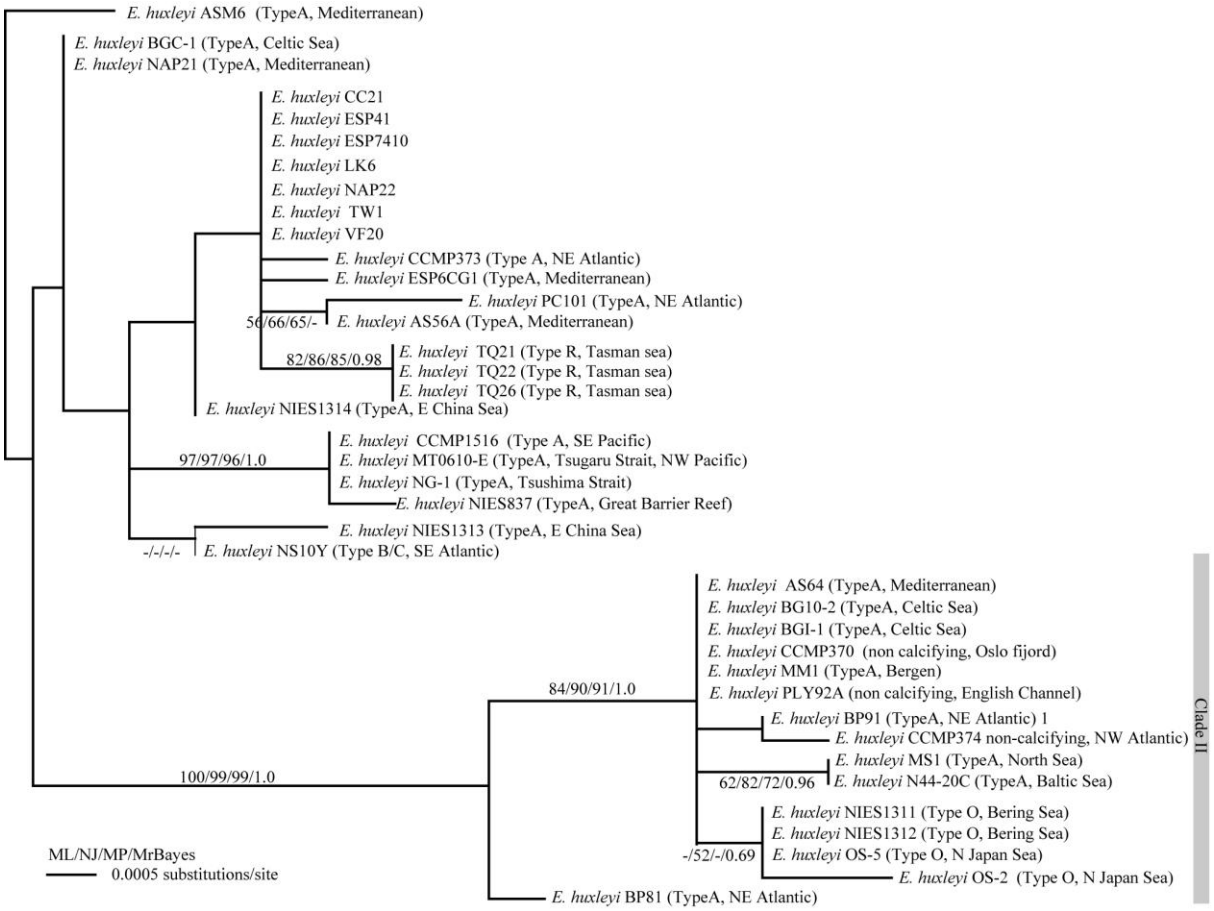

Figure 6. Unrooted ML tree (−lnL=2491.6389) based on *cox1-atp4* sequences. The numbers on each node indicate the bootstrap values from ML, NJ, and MP analyses and Bayesian posterior probabilities.

In unrooted ML, NJ, MP, and Bayesian trees, the 15 *E. huxleyi* strains that constituted Clade II in the rooted ML, NJ, and MP trees (Fig.4) made a clade with very high bootstrap values from 99-100% and 1.0 Bayesian posterior probability (Fig. 6). Hereafter, we refer to this clade as Clade II following the classification in the rooted trees. In this clade, strain BP81 occupied a well-separated basal position, and other strains formed an internal sub-clade with moderate to high bootstrap values (from 84-91%) and high Bayesian posterior probability (1.0). Type O strains formed a sub-clade within Clade II with very low bootstrap support (52%) in the NJ tree and with low posterior probability (0.69) in the Bayesian tree, but no support in the ML and MP analyses. Type A strains were distributed throughout the phylogenetic trees, although four Type A strains from the Pacific Ocean and adjacent seas (NG-1, MT0610E, NIES 837, and CCMP 1516) formed a clade with high bootstrap values (96-97%) and 1.0 posterior probability.

Geographic and hydrographic range of mitochondrial clades I and II

The culture strains included in clades I and II of rooted ML, NJ, and MP trees showed different biogeographic ditributions (Fig. 3). Clade I strains were isolated from tropical to temperate waters on the equatorial side of subarctic fronts. By contrast, clade II strains were mainly collected from boreal subarctic waters, except for one clade II strain, AS64, from the western Mediterranean Sea (Fig. 3). Identical sequences were found between N. Atlantic and Mediterranean strains, but not between 'N Atlantic + Mediterranean' and Pacific strains. (Fig. 4).

The very different biogeographic distributions suggest that the culture strains of clades I and II have different environmental preferences.,This was tested by comparing environmental data from the locations at which the strains were isolated. Comparison of annual and monthly mean environmental parameters showed that the variation range of clades I and II differed in annual and monthly mean temperature, and annual mean nitrate and phosphate concentration, but overlapped greatly in annual and monthly mean salinity and in monthly mean nitrate and phosphate concentration (Fig. 7). Table 4 shows the results of the Welch's T-test. When P values are less than 0.05 or absolute t values are less than absolute t-Stat values, the two groups are significantly different. The results indicate that clades I and II are statistically different from each other in annual and monthly mean temperature and phosphate concentration and in annual mean nitrate concentration, but equal in variance in annual and monthly salinity and in monthly mean nitrate concentration (Table 4). These results suggest that the habitat separation of clades I and II strains is primarily related to differences in temperature and/or phosphate and not to salinity.

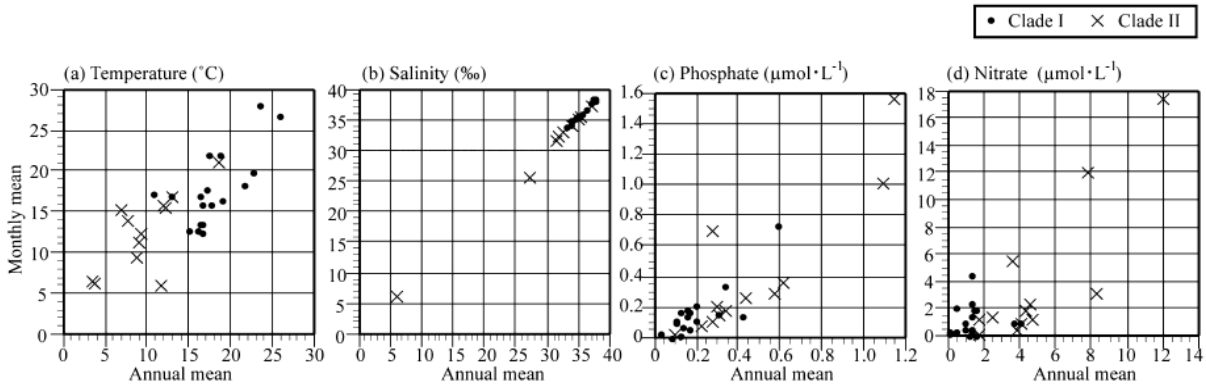

Figure 7. Plots showing the annual mean and monthly mean (for the month in which they were collected) of various environmental parameters for the sampling locations from which the strains were collected. These plots show the degree to which the two clades occur under different conditions.

Table 4. Results of Welch's t-test

	t-Stat	t Critical (two-tail)	P value (two-tail)	Assumption by Welch's t-test
temperature (annual mean)	6.962476846	1.699126996	0.0000001182	not equal variance
temperature (monthly mean)	3.576598296	1.701130908	0.0012909848	not equal variance
salinity (annual mean)	2.043838627	2.131449536	0.0589416046	equal variance
salinity (monthly mean)	2.058859027	2.144786681	0.0586170981	equal variance
phosphate (annual mean)	-2.766845052	2.09302405	0.0122778891	not equal variance
phosphate (monthly mean)	-2.136999339	2.131449536	0.0494780018	not equal variance
nitrate (annual mean)	-4.572295083	2.109815559	0.0002705760	not equal variance
nitrate (monthly mean)	-1.942597981	2.144786681	0.0724553362	equal variance

Discussion

Geographic distribution of morphotypes

Based on the morphological stability of the central area of the coccoliths reported here, we propose to distinguish coccoliths with an open central area as Type O from Types B, B/C and C that are characterized by the presence of a solid plate in the central area of coccoliths. This new subdivision means that the geographic distribution of Types B, B/C and C reported in previous studies could be biased by inclusion of Type O. Distribution of Types B, B/C, C and O, however, can be re-evaluated from SEM images shown in previous studies and from the geographic origin of culture strains.

Morphotypes B, B/C and C (with a central plate) were separated from each other based on the size of the distal shield (Table 1, Young et al. 2003). Van Bleijswijk et al. (1991) reported Type B with plated central area from the North Sea and English Channel, and the only three Type B strains reported to date (92D, Ch25 and MCH) were isolated from the North Sea and English Channel (Young and Westbroek 1991). Type B is evidently distributed in the N.E. Atlantic, especially in the seas surrounding the U.K., but it is currently not clear whether this type is restricted to this area.

In this study, Type B/C specimens (< 4µm in distal shield length) were found rarely from surface waters of the temperate N.W. Pacific (Table 2). In the literature, Types B/C and C have mainly been reported from temperate surface waters and from the lower photic zone of stratified tropical waters. McIntyre and Bé (1967) described the cold-water type (=Type C) with solid central plate from the S.W. Atlantic, close to Subtropical Front (Eltanin 9 station 13 of Fig. 3). Hagino and Okada (2006) reported the common occurrence of Type C in surface samples from the equatorial upwelling zone, and showed an image of an *E. huxleyi* specimen with a central plate as an example of their Type C (Vema24, station 26, 0m). Hagino et al. (2000) and Boeckel and Baumann (2008) showed SEM images of *E. huxleyi* with plated

central area as examples of Type C (KH92-4, SA06, 150m) and Type B/C (M41-2, station II, 90m) from the lower photic zone of stratified tropical water masses (Fig. 3). From these observations, it is thought that Types B/C and C with plated central area change their depth habitat depending on the intensity of stratification, temperature, and/or nutrient level (Hagino et al. 2000).

Re-observation of the samples used in previous studies revealed that the subarctic type of Okada and Honjo (1973) from the northern central N. Pacific and Type B of Hagino et al. (2005) from the N.W. Pacific correspond to our Type O. Tanimoto et al. (2003) displayed an SEM image of an *E. huxleyi* specimen with an open central area from the northern N.E. Pacific Ocean as an example of their *E. huxleyi* var. *kleijniae* (st. NP14 of Fig. 3). Furthermore, all four culture strains isolated from adjacent seas of the northern N. Pacific were Type O. Therefore, it appears that the *E. huxleyi* population of the North Pacific Subarctic Gyre and its adjacent seas is dominated by Type O.

Biogeographic studies from the Southern Ocean have also shown SEM images of *E. huxleyi* with an open central area (Type O). Verbeek (1989) showed SEM images of their cold-water and malformed forms with open central area from subtropical and polar stations of the Southern Ocean (samples 2 and 15 of Fig. 3). Hiramatsu and De Decker (1993) showed two *E. huxleyi* specimens with open central area as their Type K (station 10P, Fig. 2), and mentioned that the coccolithophore flora south of the Subtropical Front was dominated by Type K. Findlay and Giraudeau (2000) showed SEM images of their Types C and D with open central area, which were collected from transitional water between the Subtropical and Subantarctic Fronts (stations HC004 and CTD16 of Fig. 3). Boeckel and Baumann (2008) showed an SEM image of an *E. huxleyi* specimen with an open central area as an example of their Type B from south of the Subtropical Front of the S. Atlantic Ocean (M46-4, st. VI, 5m of Fig. 3). From these reports, it is evident that Type O is extensively distributed in the Southern Ocean. Type O is therefore a dominant morphotype in the northern North Pacific and in the Southern Ocean, but rare/absent in tropical surface waters of the Pacific Ocean. These results suggest that Type O is a cold water dweller with bi-polar geographic distribution.

Diversity of mitochondrial sequences of Emiliania huxleyi and relationships to environmental conditions and morphotypes

In the rooted phylogenetic trees, *E. huxleyi* strains were divided into two main clades with relatively minor but highly consistent differences in *cox*1b-*Atp*4 sequences. The

differences in nucleotide sequences do not affect amino acid sequences and at this stage it is unclear whether the two clades correspond to discrete biological entities (cryptic species) or intra-specific lineages. The topology of ML and Bayesian trees differed in the relationships of the two main groups; in the ML tree clades I and II are sister groups whereas in the Bayesian analysis clade II is derived from "clade" I, which is thus a paraphyletic group. Nonetheless, the separation of the strains into these two groups was a consistent feature of all the unrooted trees and was supported by high bootstrap values and posterior probability. In this context, it can be postulated that gene flow may well be limited between the two clades given the spatial separation (in surface/upper-subsurface waters at least), clade I strains originating from warm tropical/temperate water masses and clade II strains mainly from colder subarctic water masses (Figs. 3-5). The occurrence of a single clade II strain (AS64) in warmer water (Mediterranean Sea), however, may indicate that separation is not so clear-cut.

Similarity in mitochondrial sequences between the northern N. Atlantic and northern N. Pacific clade II populations indicates that these two boreal populations have the same genetic origin even though they are separated from each other by the polar ice cap in the north, and warm water masses in the south. How did the clade II population migrate between the northern N. Atlantic and N. Pacific Oceans? Reid et al. (2007) reported that a Pacific cold-water diatom *Neodenticula seminae* appeared in the N. Atlantic in May 1999 for the first time in the last 800ky, and concluded that it had probably migrated from the N. Pacific to N. Atlantic through the Arctic pathway opened by melting of Arctic ice in 1998/early1999. Surface water of the Arctic pathway flows from the Pacific to the Atlantic, so, migration of planktonic microalgae is likely to occur in this direction. The presence of strain PLY92A (Clade II), isolated from the English Channel in 1957, indicates that the Clade II population has been in the Atlantic before opening of the Arctic pathway in 1998/1999. Migration of *E. huxleyi* populations through the Arctic pathway might have occurred in the geological past, particularly during the last interglacial MIS5e. However, the absence of evidence for similar migration in other plankton groups at this time makes this unlikely. An alternative route for clade II migration is within the lower photic zone of equatorial waters. Morphological studies of *E. huxleyi* have reported that morphotype composition is different between the upper and lower photic zone in tropical waters, and Type C changes its depth habitat from warm oligotrophic surface water to relatively cool eutrophic lower photic zone water (below the thermocline from 50 to 150m) according to water stratification, as opposed to Type A that remains in the upper photic zone regardless of water stratification (Hagino et al. 2000). Therefore, there is a possibility that clade II populations cross the equator in the lower photic

zone. All culture strains used in this study were isolated from surface water or upper-subsurface water samples. To assess the possibility of clade II migration through the lower photic zone, mitochondrial DNA of *E. huxleyi* strains from the lower photic zone of tropical waters should be studied. A final possible cause of migration of the clade II population is mixing by human activity (e.g. transportation by ship ballast water). This possibility cannot be ruled out completely, but geological core studies have shown that *E. huxleyi* has been distributed in both the northern N. Atlantic and northern N. Pacific Oceans since about 250-260ka (e.g. Worslely 1973, Thierstein et al. 1977, Sato et al. 2002), so migration of cold-adapted populations into the subarctic was unlikely to have been a result of human activity.

The Celtic Sea and English Channel appear to be the boundary between the habitats of clade I and II strains in the eastern N.E. Atlantic. Three strains (BGC-1, BGI-1, and BG10-2) isolated from an *E. huxleyi* bloom in the Celtic Sea in 2007 varied in mitochondrial sequence (Figs. 3-4). Strain BGC-1 was genetically identical to strain NAP 21 (Mediterranean Sea) and belonged to clade I. Strains BGI-1 and BG10-2 were identical to four clade II strains CCMP370 (North Sea), MM1 (Bergen), PLY92A (English Channel), and AS64 (Mediterranean Sea) (Fig. 4). Previous studies reported that multiple GPA genotypes can be found in *E. huxleyi* blooms (Martínez-Martínez et al. 2007, Ripley et al. 2008). Genetic diversity in mitochondrial sequences in bloom-forming *E. huxleyi* strains suggests that *E. huxleyi* populations forming blooms can have diverse genetic origins, with similar environmental preferences.

Clades I and II were rather well separated by correlation with both monthly and annual mean temperature and annual nutrient concentrations, but were less well-separated by monthly nutrient levels, and were not separated by monthly or annual salinity (Table 4, Fig. 5). Weaker correlations of clades I and II with monthly mean nutrient concentration suggest that culture strains of clades I and II came from similar (overlapping) nutrient ranges, and the better correlation shown in annual mean nutrient values is probably a misleading result caused by including environmental data from winter which is an unsuitable period for growth of *E. huxleyi* in high latitudes. Differences in the range of sampling months between clades I and II also suggest that including winter environmental parameters is unsuitable for the discussion of environmental preferences of clade II strains, since the sampling month of clade II is limited from March-October (spring-autumn), whereas the clade I strains were collected from January-December. Therefore, it is thought that genetic separation between clades I and II likely stem from difference in temperature preference/tolerance rather than nutrient limitation. We have observed that culture strains collected from warm water masses usually do not grow

in low temperature culture conditions (<13˚C), although the temperature preference/tolerance of most culture strains has not yet been systematically studied. For better understanding of the relationship between geographic diversification in mitochondrial DNA of *E. huxleyi* and their range of temperature preference/tolerance, more culture studies using strains from various regions are required.

The phylogenetic diversification observed from mitochondrial sequences of *E. huxleyi* was not consistent with the genetic variation reported in the GPA gene in previous research. Schroeder et al. (2005) sequenced the GPA region of 13 clonal *E. huxleyi* strains and classified the strains into four coccolith morphology motif (CMM) groups. Our mitochondrial analysis included four strains (CCMP370, CCMP 373, CCMP 374 and CCMP1516) used by Schroeder et al. (2005). In our results, CCMP373 and CCMP1516 belonged to clade I, and CCMP370 and CCMP374 belonged to clade II (Fig. 4). In the CMM grouping of Schroeder et al. (2005), however, CCMP 370 and CCMP373 belonged to CMM group I. Schroeder et al. (2005) also showed that strains CCMP374 and CCMP 1516 exhibited inter-clonal variation in CMM sequences, with CCMP 374 having both CMM I and IV sequences, and CCMP 1516 having both CMM III and IV sequences. To clarify population structure of *E. huxleyi,* further studies based on multiple genetic regions are needed.

From our dataset we cannot draw strong conclusions as to potential relationships between mitochondrial genotypes and coccolith morphotypes since our molecular analyses included limited numbers of Types B/C, C, R and O strains relative to Type A strains (and no Type B strains). Type A strains occurred in both clades I and II and occupied basal positions in both clades. Type O and Type R strains formed discrete subclades within clades II and I, respectively. This may suggest that type A is the primitive morphology of *E. huxleyi,* and that other morphotypes have evolved from Type A within one or other of the clades. Type O may well be mitochondrial genotype specific, since in surface waters it is evidently restricted to higher latitudes like clade II. The known distributions of Types B, B/C, C and R, however, do not so clearly correspond with the biogeography of *cox*1b-*ATP*4 clades and the possibility clearly exists that morphotypes diversified before separation of the two clades, in which case morphotype would be an inherited polymorphism present in each clade.

Concluding Remarks

Variability in the *cox*1b-*ATP*4 region of the *E. huxleyi* mitochondrial genome appears to correspond to geographic origin and to some extent to environmental conditions at the site of origin of the strain and this genetic region is potentially a useful marker either for intra-

specific diversity within this taxon or for species-level diversity between cryptic taxa within the morphospecies. From the data currently available, however, the diversity revealed by this marker does not clearly relate to morphological diversity of coccoliths which itself seems to be a relatively stable, genetically controlled character. Further comparison of morphological and molecular characters of *E. huxleyi*, in environmental studies, may shed light on the biological, ecological and evolutionary implications of microdiversity of these important microalgae. However, ultimate proof of whether speciation has already occurred within this relatively young lineage and whether biological diversification has any link to coccolith morphology is likely to require either extensive comparative genomic information from multiple *E. huxleyi* strains and/or evidence from mating experiments between haploid culture strains. In either case, culture-based studies are likely to provide key information.

Acknowledgements

We are grateful to two anonymous reviewers for their valuable comments. This research was primarily supported by a 21st Century COE Program on 'Neo-Science of Natural History' at Hokkaido University financed by the Ministry of Education, Culture, Sports, Science and Technology, Japan, and by Grant-in Aid for Scientific Research from the Japan Society for the Promotion of Sciences (No. 20740296). The collaborative work of EB, JRY, IP, and CdV was supported by the EU FP7 "European Project on Ocean Acidification" (EPOCA) (FP7/2007-2013), the EU I3 project ASSEMBLE (FP7/227799) and the EU BiodivERsA EraNet project *BioMarKs* – Biodiversity of Marine euKaryotes.

References

Antonov, J. Locarnini, I., R. A., Boyer, T. P., Mishonov, A. V. and Garcia, H. E. 2006. *World Ocean Atlas 2005, Volume 2: Salinity. In* Levitus, S. [Ed.] *NOAA Atlas NESDIS 62*, U.S. Government Printing Office, Washington, D.C., 182 pp.

Boeckel, B. and Baumann, K-H. 2008. Vertical and lateral variations in coccolithophore community structure across the subtropical frontal zone in the South Atlantic Ocean. *Mar. Micropaleontol*. 67: 255–73.

Corbyn, Z. 2007. Atlantic invaders. *Nature.* 207:82-4.

Corstjens, P. L. A. M., van der Kooij, A., Linschooten, C., Brouwers, G.-J. Westbroek, P. and de Vrind-de Jong, E. W. 1998. GPA, a calcium-binding protein in the coccolithophorid *Emiliania huxleyi* (Prymnesiophyceae). *J. Phycol.* 34:622-30.

Felsenstein, J. 1985. Confidence limits on phylogenies: an approach using the bootstrap. *Evolution* 39:783–91.

Findlay, C. S. and Giraudeau J. 2000. Extant calcareous nannoplankton in the Australian Sector of the Southern Ocean (austral summers 1994 and 1995). *Mar. Micropaleontol.* 40:417-39.

Fujiwara, S., Tsuzuki, M., Kawachi, M., Minaka, N. and Inouye, I. 2001. Molecular phylogeny of the haptophyta based on the *rbc*L gene and sequence variation in the spacer region of the Rubisco operon. *J. Phycol.* 37: 121-9.

Gard, G. 1986. Calcareous Nannofossil Biostratigraphy of Late Quaternary Arctic Sediments. *Boreas*, 15:217-29.

Gard, G. 1989. Variations in coccolith assemblages during the Last Glacial Cycle in the High and Mid-Latitude Atlantic and Indian Oceans, *In* Crux, J. A. and van Heck, S. E. [Eds.] *Nannofossils and their applications*. Ellis Horwood, Chichester, pp. 108-21.

Garcia, H. E., Locarnini, R. A., Boyer, T. P., and Antonov, J. I. 2006a. *World Ocean Atlas 2005, Volume 3: Dissolved Oxygen, Apparent Oxygen Utilization, and Oxygen Saturation. In* Levitus, S. [Ed.] *NOAA Atlas NESDIS 63*, U.S. Government Printing Office, Washington, D.C., 342 pp.

Garcia, H. E., Locarnini, R. A., Boyer, T. P. and Antonov, J. I. 2006b. *World Ocean Atlas 2005, Volume 4: Nutrients (phosphate, nitrate, silicate). In* Levitus, S. [Ed.] *NOAA Atlas NESDIS 64*, U.S. Government Printing Office, Washington, D.C., 396 pp.

Hagino, K., Okada, H. and Matsuoka, H. 2000. Spatial dynamics of coccolithophore assemblages in the Equatorial Western-Central Pacific Ocean. *Mar. Micropaleontol.* 39:53-72.

Hagino, K., Okada, H. and Matsuoka, H. 2005. Coccolithophore assemblages and morphotypes of *Emiliania huxleyi* in the boundary zone between the cold Oyashio and warm Kuroshio currents off the coast of Japan. *Mar. Micropaleontol.* 55:19-47.

Hagino, K. and Okada, H. 2006. Intra- and infra-specific morphological variation in selected coccolithophore species in the equatorial and subequatorial Pacific Ocean. *Mar. Micropaleontol.* 58:184-206.

Hine N. and Weaver, P. P. E. 1998. Quaternary. *In* Bown, P. [Ed.] *Calcareous Nannofossil Biostratigraphy.* Chapman and Hall, Cambridge, UK, pp. 266-83.

Hiramatsu, C. and De Deckker, P. 1996. Distribution of calcareous nannoplankton near thte subtropical convergence, south of Tasmania, Australia. *Mar. Freshwater Res.* 47:707-13.

Iglesias-Rodríguez, M.D., Sáez, A., Groben, R., Edwards, K.J., Batley, J. Medlin, L. and Hayes, P.K. 2002. Polymorphic microsatellite loci in global populations of the marine coccolithophorid *Emiliania huxleyi. Molec. Ecol. Notes.* 2:495-7.

Iglesias-Rodríguez, M. D., Schfield, O. M., Batley, J. Medlin, L.K. and Hayes, P. K. 2006. Intraspecific genetic diversity in the marine coccolithophore *Emiliania huxleyi* (Prymnesiophyceae): the use of microsatellite analysis in Marine Phytoplankton Population Studies. *J. Phycol.* 42:526-36.

Jordan, R. W., Zhao, M., Eglinton, G. and Weaver, P. P. E. 1996. Coccolith and alkenone stratigraphy and palaeoceanography at an upwelling site off NW Africa (ODP 658C) during the last 130,000 years. *In*: Moguilevsky, A. and Whatley, R. [Eds.] *Microfossils and oceanic environments*. University of Wales, Aberystwyth - Press, Aberystwyth, pp. 111-30.

Kimura, M. 1980. A simple method for estimating rate of base substitutions through comparative studies of nucleotide sequences. *J. Mol. Evol*. 16:111–20.

Locarnini, R. A., Mishonov, A. V., Antonov, J. I., Boyer, T. P. and Garcia, H. E. 2006. *World Ocean Atlas 2005, Volume 1: Temperature.* S. Levitus, Ed. NOAA Atlas NESDIS 61, U.S. Government Printing Office, Washington, D.C., 182 pp.

Martínez-Martínez J., Schroeder, D. C., Larsen, A., Bratbak, G. and Wilson, W. H. 2007. Molecular Dynamics of *Emiliania huxleyi* and Cooccurring Viruses during Two Separate Mesocosm Studies. *Appl. Env. Microbiol*. 73:554-62.

McIntyre, A. and Bé, A. 1967. Modern coccolithophoridae of the Atlantic Ocean-I. Placoliths and cyrtoliths. *Deep-Sea Res.* 14:561-597.

Medlin, L. K., Barker, G. L. A., Campbell, L., Green, J. C., Hayes, P. K., Marie, D., Wrieden, S. and Vaulot, D. 1996. Genetic characterization of *Emiliania huxleyi* (Haptophyta). *J. Mar. System.* 9:13-31.

Noël M-H., Kawachi, M. and Inouye I. 2004. Induced dimorphic life cycle of a coccolithophorid, *Calyptrosphaera sphaeroidea* (Prymnesiophyceae, Haptophyta). *J. Phycol.* 40:112-29.

Okada, H. and Honjo, S. 1973. The distribution of oceanic coccolithophorids in the Pacific. *Deep-Sea Res.* 20:355-74.

Okada H. and McIntyre, A. 1977. Modern coccolithophores of the Pacific and North Atlantic Oceans. *Micropaleontology* 23(1):1-55.

Posada, M. A. and Crandali, K. A. 1998. Modeltest: testing the model of DNA substitution. *Bioinformatics* 14: 817–8.

Raffi, I., Backman, J., Fornaciari, E., Pälike, H., Rio, D., Lourens, L. and Hilgen, F. 2006. A review of calcareous nannofossil astrobiochronology encompassing the past 25 million years. *Quaternary Sci. Rev.* 25: 3113-37.

Reid, P. C., Johns, D. G., Edwards, M., Starr, M., Poulin, M. and Snoeijs, P. 2007. A biological consequence of reducing Arctic ice cover: arrival of the Pacific diatom

Neodenticula seminae in the North Atlantic for the first time in 800 000 years. *Global Ch. Biol*. 13: 1910-1921.

Ripley, S. J., Highfield, A. C., Miller, P. I., Walne, A. W. and Schroeder, D. C. 2008. Development and validation of a molecular technique for the analysis of archived formalin-preserved phytoplankton samples permits retrospective assessment of *Emiliania huxleyi* communities. *J. Microbiol. Method.* 73: 118-24.

Ronquist, F. and Huelsenbeck, J.P. 2003. MrBayes 3: Bayesian phylogenetic inference under mixed models. *Bioinformatics* 19: 1572-4.

Rost, B. and Riebesell, U. 2004. Coccolithophores and the biological pump: responses to environmental changes. *In* Thierstein, H. R. and Young, J. R. [Eds.] *Coccolithophores from molecular processes to global impact*. Springer-Verlag, Berlin Heidelberg, Germany, pp. 99-125.

Saitou, N. and Nei, M. 1987. The neighbor-joining method: a new method for reconstructing phylogenetic trees. *Mol. Biol. Evol*. 4: 406–25.

Sato, T., Saito, T., Yuguchi, S., Nakagawa, H., Kameo, K. and Takayama, T. 2002. Late Pliocene calcareous nannofossil palaeobiogeography of the Pacific Ocean: evidence for glaciation at 2.75 Ma. *Revista Mexicana de Ciencias Geológica.* 19:175-189.

Sambrook, J., Fritsch, E. F. and Maniatis, T., 1989. Molecular Cloning - A Laboratory Manual. Cold Spring Harbour Laboratory Press.

Sánchez Puerta V., Bachvaroff, T. R. and Delwiche, C.F. 2004. The complete Mitochondrial genome sequence of the Haptophyte *Emiliania huxleyi* and its Relation to Heterokonts. *DNA Res.* 11:1-10.

Schroeder, D. C., Biggi, G. F., Hall, M., Davy, J., Martínez-Martínez, J., Richardson, A. J., Malin, G. and Wilson, W. H. 2005. NOTE. A genetic marker to separate *Emiliania huxleyi* (Prymnesiophyceae) morphotypes. *J. Phycol.* 41:874-9.

Schwaninger, H. R. 2008. Global mitochondrial DNA phylogeography and biogeographic history of the antitropically and longitudinally disjunct marine bryozoan *Membranipora membranacea* L. (Cheilostomata): Another cryptic marine sibling species complex?. *Mol. Phylog. Evol*.. 49: 893–908.

Swofford, D. L. 2002. PAUP*—Phylogenetic Analysis Using Parsimony (* and Other Methods), Version 4. Sinaver Associates, Sunderland, Massachusetts

Tanimoto, M., Aizawa, C. and Jordan, R. W. 2003. Assemblages of living microplankton from the subarctic North Pacific and Bering Sea during July-August 1999. *Cour. Forsch.-Inst. Senckenberg.* 244:83-103.

Thierstein, H. R., Geitzenauer, K. R. and Molfino, B. 1977. Global synchroneity of Late Quaternary coccolith datum levels: validation by oxygen isotope. *Geology*. 5:400-4.

Tomczak M.and Godfrey, J. S. 1994. Regional Oceanography: An Introduction. Pergamon, London. 422 pp.

Van Bleijswijk, J. van der Wal, P., Kempers, R., Veldhuis, M., Young, J. R., Muyzer, G., de Vrind-de Jong, E. and Westbroek, P. 1991. Distribution of two types of *Emiliania huxleyi* (Prymnesiophyceae) in the northeast Atlantic region as determinded by immunofluorescence and coccolith morphology. *J. Phycol.* 27:566-70.

Verbeek, J. W. 1989. Recent calcareous nannoplankton in the southernmost Atlantic. *Polarforschung.* 59:45-60.

Welch, B. L. 1947. The generalization of "Student's" problem when several different population variances are involved. *Biometrika* 34: 28–35.

Winter, A. 1985. Distribution of living coccolithophore in the California Current system, southern California Borderland. *Mar. Micropaleontol.* 9:385-93.

Worsley, T.R. 1973. Calcareous nannofossils: Leg 19 of the Deep Sea Drilling Project. *In* Creager, J.S., Scholl, D.W., et al. [Eds.] *Init. Repts. DSDP,* 19: Washington, DC (U.S. Govt. Printing Office). 741-750.

Young, J.R. 1998, Neogene. *In* Bown, P. [Ed.] *Calcareous Nannofossil Biostratigraphy.* Champman and Hall, Cambridge, UK, pp. 225-65.

Young J. R. and Westbroek, P. 1991. Genotypic variation in the coccolithophorid species *Emiliania huxleyi. Mar. Micropaleontol.* 18:5-23.

Young, J. R. Geisen, M. Cros, L. Kleijne, A., Sprengel, C., Probert, I. and Ostergaard, J. 2003. A guide to extant coccolithophore taxonomy. *J. Nannoplankton Res.* Special Issue 1:1-125.

Zhu H., Qu, F., Zhu, L. H. 1993. Isolation of genomic DNAs from plants, fungi and bacteria using benzyl chloride. *Nucleic Acids Res.* 21(22):5279-80.

Table S1. List of clonal culture strains, with information of morphotype, sampling month and location, and GenBank accession number of their SSU rDNA sequences.

Strain name	Other name	Morphotype	Sampling month and year	Latitude (degree)	Longitude (degree)	Mitochondrial Clade	Accession number
MT3-6		*G. oceanica*	Sep-06	41.50N	141.25E	out group	AB563741
NIES 838		*G. oceanica*	Nov-90	41.00N [a]	141.00E [a]	out group	AB563743
NIES 1000	CCMP 2054, RCC1562	*G. oceanica*	Nov-99	34.08N	139.57E	out group	AB563742
PR3F3		*G. oceanica*	unknown	16.50N [a]	66.50W [a]	out group	AB563744
AS56A	RCC1254	Type A	Oct-99	37.10N	01.13W	I	AB563745
AS64	RCC1208	Type A	Oct-99	37.25N	00.53W	II	AB563750
ASM6	RCC1250	Type A	Oct-99	37.10N	01.13W	I	AB563746
BG10-2	RCC1262	Type A	Aug-07	49.30N	10.30W	II	AB563747
BGC1	RCC1277	Type A	Aug-07	49.30N	10.30W	I	AB563748
BGI1	RCC1263	Type A	Aug-07	51.20N	10.29W	II	AB563749
BP81	RCC1257	Type A	Jul-99	63.27N	20.14W	II	AB563751
BP91	RCC1256	Type A	Jul-99	63.27N	20.14W	II	AB563752
CC21	RCC1251	Type A	Jun-99	38.44N	09.37W	I	AB563753
CCMP 370	RCC1255	non calcifying	May-05	59.50N	10.60E	II	AB563754
CCMP 373	BT6, RCC1260	non calcifying (Type A) [b]	Apr-60	32.17N	64.50W	I	AY342361
CCMP 374	RCC1259	non calcifying	Sep-90	42.50N	69.00W	II	AB563755
CCMP 1516	RCC1242	non calcifying (Type A) [c]	unknown	02.67S	82.72W	I	AB563756
ESP41	RCC1249	Type A	Apr-98	41.28N	02.19E	I	AB563757
ESP 6CG1	RCC1261	Type A	Apr-99	42.16N	03.18E	I	AB563758
ESP 7410	RCC1247	Type A	May-99	41.28N	02.19E	I	AB563759
LK6	RCC1245	Type A	Feb-99	44.60N	01.15W	I	AB563760
MM1		Type A	unknown	60.50N [a]	4.50E [a]	II	AB563761
MS1	D2801-5, RCC1226	Type A	Jul-98	58.23N	03.30W	II	AB563762
MT0610-E	RCC1252	Type A	Oct-06	41.50N	141.25E	I	AB563763
N44-20C	RCC1210	Type A	Jul-98	59.77N	20.64E	II	AB563764
NAP21	RCC1214	Type A	Dec-00	40.90N	14.15E	I	AB563765
NAP22	RCC1213	Type A	Dec-00	40.90N	14.15E	I	AB563766
NG-1		Type A	Apr-07	32.40N	129.07E	I	AB563767
NIES 837	EH-2	Type A	Nov-90	19.50S [a]	148.50E [a]	I	AB563768
NIES 1311	MH27	Type O	Oct-02	58.30N	166.01W	II	AB563769
NIES 1312	MH28	Type O	Oct-02	56.00N	170.00W	II	AB563770
NIES 1313	MH74	Type A	Sep-03	29.59N	128.41E	I	AB563771
NIES 1314	YK3-87	Type A	Sep-03	29.59N	128.41E	I	AB563772
NS10Y	RCC1212	Type B/C	Sep-00	34.28S	17.18E	I	AB563773
OS-2	RCC1253	Type O	Apr-06	43.22N	141.02E	II	AB563774
OS-5	RCC1239	Type O	Apr-06	43.22N	141.02E	II	AB563775
PC101	RCC1258	Type A	Jun-98	40.35N	10.00W	I	AB563776
PLY92A		non calcifying	Jul-57	50.20N [a]	4.22W [a]	II	AB563777

TQ21	RCC1231	Type R	Sep-98	42.18S	169.50E	I	AB563778
TQ22	RCC1220	Type R	Sep-98	42.18S	169.50E	I	AB563779
TQ26	RCC1216	Type R	Sep-98	42.18S	169.50E	I	AB563780
TW1	RCC1215	Type A	Feb-01	41.40N	02.48E	I	AB563781
VF20	RCC1235	Type A	Sep-07	43.41N	07.19E	I	AB563782

[a] Latitude and longitude data are unavailable and were estimated from name of sampling locations.

[b] Currently naked strain and the morphotype was identified from SEM images of strain BT6 shown in Watabe and Wilber (1966).

[c] Currently naked strain but the morphotype was referred from Schroeder et al. (2005).

Note. RCC = Roscoff Culture Collection (http://www.sb-roscoff.fr/Phyto/RCC), NIES = Microbial Culture Collection at National Institute for Environmental Science of Japan (http://mcc.nies.go.jp/top.jsp), PLY = The Plymouth Culture Collection of Marine Algae (http://mcc.nies.go.jp/top.jsp)

Reference

Schroeder, D. C., Biggi, G. F., Hall, M., Davy, J., Martínez-Martínez, J., Richardson, A. J., Malin, G. and Wilson, W. H. 2005. NOTE. A genetic marker to separate *Emiliania huxleyi* (Prymnesiophyceae) morphotypes. *J. Phycol.* 41:874-9.

Watabe, N. and Wilbur, K. M. 1966. Effect on temperature on growth calcification, and coccolith form in *Coccolithus Huxleyi* (Coccolithtineae). *Limnol. Oceanogr*. 11:567-75.

CHAPITRE 4

SENSITIVITY OF COCCOLITHOPHORES TO CARBONATE CHEMISTRY AND OCEAN ACIDIFICATION

Luc Beaufort[1], Ian Probert[2], Thibaut de Garidel-Thoron[1], El Mahdi Bendif[2], Dominique Ruiz-Pino[3], Nicolas Metzl[3], Catherine Goyet[4], N. Buchet[1], Patrique Coupel[3], Matthieu Grelaud[1,5], Bjorn Rost[6], Ros Rickaby[7] et Colomban de Vargas[2]

[1] CEREGE, CNRS / Université Aix-Marseille, Aix-en-Provence, France

[2] Station Biologique de Roscoff, CNRS / Université P. and M. Curie, Roscoff, France

[3] LOCEAN-IPSL, CNRS / Université P. and M. Curie, Paris, France

[4] Université de Perpignan, Perpignan, France

[5] Present adress : ICTA, Universitat Autonoma de Barcelona, Bellaterra, Spain

[6] Alfred Wegener Institute, Bremerhaven, Germany

[7] Oxford University, Oxford, United Kingdom

Beaufort L, Probert I, de Garidel-Thoron T, Bendif EM, Ruiz-Pino D, Metzl N, Goyet C, Buchet N, Coupel P, Grelaud M, Rost B, Rickaby REM and de Vargas C. Sensitivity of coccolithophores to carbonate chemistry and response to ocean acidification. Nature 476: 80 – 84, 2011

Abstracts

About one third of the carbon dioxide (CO_2) released to the atmosphere as a result of human activity has been absorbed by the oceans[1], where it partitions into the constituent ions of carbonic acid. This leads to ocean acidification (OA), one of the major threats to marine ecosystems[2] and particularly to calcifying organisms such as corals[3,4], foraminifera[5-7] and coccolithophores[8]. Coccolithophores are abundant phytoplankton responsible for a large part of modern oceanic carbonate production. Culture experiments investigating the physiological response of coccolithophore calcification to increased CO_2 have yielded contradicting results between and even within species[8-11]. We quantified the calcite mass of dominant coccolithophores in the present ocean and over the last 40 kyr and found a significant pattern of decreasing calcification with increasing pCO_2 and concomitant decreasing [CO_3^{2-}]. Our analyses revealed that differentially calcified species and morphotypes are distributed in the ocean according to carbonate chemistry. A significant impact on the marine carbon cycle might be expected upon extrapolation of this correlation to predicted future OA scenarios. However, our discovery of a heavily calcified Emiliania huxleyi morphotype in modern waters with low pH highlights the complexity of assemblage-level responses to environmental forcing factors.

Keywords: Ocean carbonate chemistry, coccolithophores, ocean acidifcation, pCO_2**.**

In order to assess environmental influence on coccolithophore calcification, we investigated 180 surface water and 555 sediment core samples encompassing a wide spectrum of present and past oceanic conditions (Fig. 1). The family Noelaerhabdaceae (including the extant genera *Emiliania*, *Gephyrocapsa* and *Reticulofenestra*) has numerically dominated coccolithophore communities for more than 20 Myr. Although genetically closely related[12], noelaerhabdaceans exhibit variability in the morphology of the calcite scales (coccoliths) forming their composite skeletons (coccospheres) both between and within species[13]. An optical method to automatically analyze the size and mass of individual noelaerhabdacean coccospheres and detached coccoliths was applied, with an average of 700 coccoliths measured per sample. The mass of isolated coccoliths was strongly correlated with mass of coccospheres in modern samples (R^2=0.88), demonstrating the validity of coccolith mass as a proxy for calcification state of noelaerhabdaceans.

Temperature, salinity, alkalinity and dissolved inorganic carbon were recorded directly from modern water samples, allowing derivation of all carbonate chemistry parameters[14]. To reconstruct carbonate chemistry of past surface waters, published paleo-proxy records for sea-surface temperature and salinity from each core site were combined with Antarctic ice pCO_2 records. Uncertainties due to propagation of errors from temperature and salinity estimates and from our assumption that relationships linking alkalinity and salinity, $\delta^{18}O_{water}$ and salinity, and pCO_{2water} and pCO_{2atm} were stable over the last 40 kyr had only limited effect on the general trend (Supplementary Information). The resulting glacial-interglacial ranges of carbonate chemistry parameters are similar to those published elsewhere[5,15].

Temperature, salinity, light and nutrients have all been reported to affect coccolithophore calcification or coccolith size[13,16-20]. Analysis of our large dataset reveals that temperature and salinity are not strongly correlated with coccolith mass. The contrasting correlations between coccolith mass and temperature in modern (R=+0.59) and sediment samples (R between -0.12 and -0.71) reflect the differing relationship between temperature and $[CO_3^{2-}]$ in modern and past oceans (Table 1). No significant correlations were found between coccolith mass and productivity-related parameters (chlorophyll or cell abundance), where available.

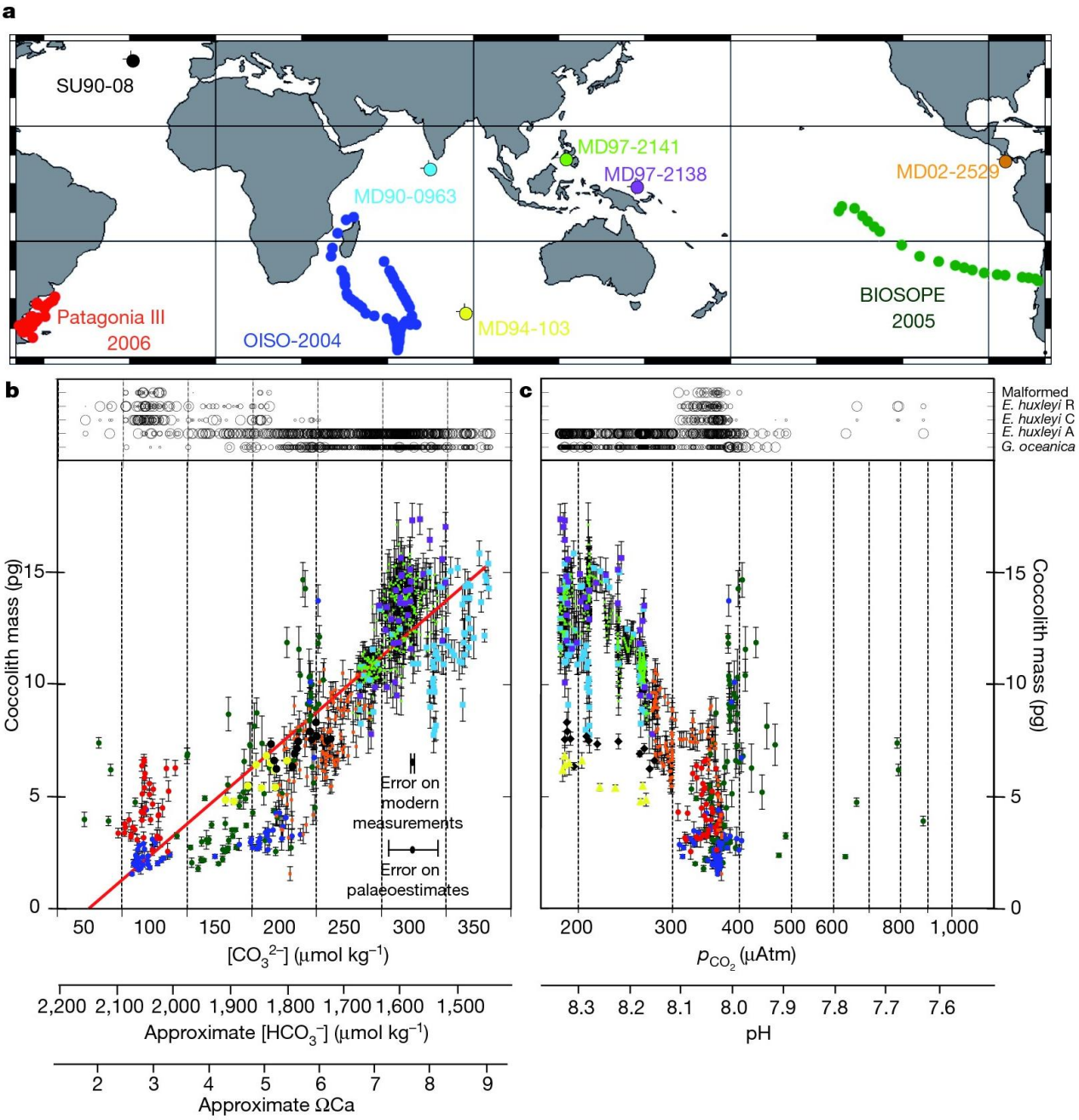

Figure 1. Relationships between coccolith mass and carbonate chemistry. a, Sample locations. b, Relationship between $[CO_3^{2-}]$ and coccolith mass (colours correspond to those of the map). Vertical bars are standard error on the mass distribution. For comparison, the corresponding scales for ΩCa, and $[HCO_3^-]$. Error bars for $[CO_3^{2-}]$ as estimated from modern and past data. c, Relationship between coccolith mass and pCO_{2water}. The corresponding pH scale is given. Upper panels in (b-c) show qualitative distribution of noelarhabdacean taxa: large circles for dominant taxa (>50%), medium circles for abundant taxa (30 to 50%), small circles for less abundant taxa (10-30%).

Table 1 | Correlation between coccolith mass and physicochemistry

Sample set	Temperature	Salinity	Alkalinity	DIC	pH	p_{CO_2}	HCO_3^-	CO_3^{2-}	ΩCa	*n*
All data	**0.68**	**0.27**	**0.13**	**−0.82**	**0.75**	**−0.69**	**−0.87**	**0.86**	**0.86**	712
BIOSOPE	**0.77**	**0.58**	**0.63**	−0.02	**−0.52**	**0.53**	**−0.57**	**0.71**	**0.72**	84
PATAGONIA	0.31	0.18	0.14	0.03	0.04	0.01	−0.11	0.26	0.26	39
OISO-11	**0.65**	0.32	0.19	**−0.68**	−0.31	0.29	**−0.65**	**0.60**	**0.61**	57
MD90-0963	−0.12	**0.62**	**0.63**	**0.60**	0.37	−0.33	−0.07	**0.53**	**0.52**	68
MD97-2141	**−0.71**	−0.15	−0.12	**−0.68**	**0.79**	**−0.80**	**−0.75**	**0.67**	**0.67**	305
MD97-2138	−0.34	0.11	0.13	−0.41	**0.59**	**−0.60**	**−0.60**	**0.65**	**0.65**	35
MD02-2529	**−0.48**	**0.45**	**0.48**	0.23	**0.62**	**−0.62**	−0.23	**0.61**	**0.61**	124
MD94-103	−0.80	0.00	0.12	−0.50	**0.88**	**−0.87**	−0.75	0.64	0.67	9
SU90-08	−0.40	0.60	0.59	0.02	0.64	−0.65	−0.41	**0.68**	**0.68**	18

Coccolith mass was related to carbonate chemistry. Significant overall correlations of coccolith mass with pH and pCO_2 were recorded, but with important regional variations (Fig. 1c), implying that these parameters are not solely responsible for the observed trend. The only correlations that were highly significant in all subsets of the data were those linking coccolith mass to carbonate ion concentration [CO_3^{2-}], bicarbonate ion concentration [HCO_3^-], and calcite saturation state (ΩCa) (R^2>0.74, Fig. 1b and Table 1). The influence of carbonate chemistry was striking in sediment records: during the Last Glacial Maximum (LGM), pCO_2 was low (=high [CO_3^{2-}]) and coccolith mass was high (Fig. 2).

During deglaciation and the Holocene, coccolith mass decreased with increasing pCO_2 at all latitudes in different ocean basins. This trend cannot have resulted from post-depositional corrosion since glacial-interglacial dissolution conditions evolved in opposite directions in the Atlantic and Pacific oceans[21]. Significant correlation was also found between [CO_3^{2-}] and amount of calcite per unit cell volume (R^2=0.76), indicating that the degree of calcification was not dependent on cell size. [HCO_3^-] was negatively correlated with calcite mass despite this anion being the primary carbon source for intracellular calcification in *E. huxleyi*[16,22,23]. [HCO_3^-] varied by ~20% in our dataset, but is the most abundant carbon species in seawater and therefore unlikely to limit biomineralization. [CO_3^{2-}], on the other hand, varied by 77%. Multiple physico-chemical parameters potentially synergistically affect calcification, but multiple regression does not markedly increase the significance of the correlation of coccolith mass with [CO_3^{2-}]. While various parameters clearly exert localized influence on coccolith mass, our data point to [CO_3^{2-}] and/or ΩCa being the key parameter(s) with regard to the global assemblage-scale response of noelaerhabdacean calcification to OA.

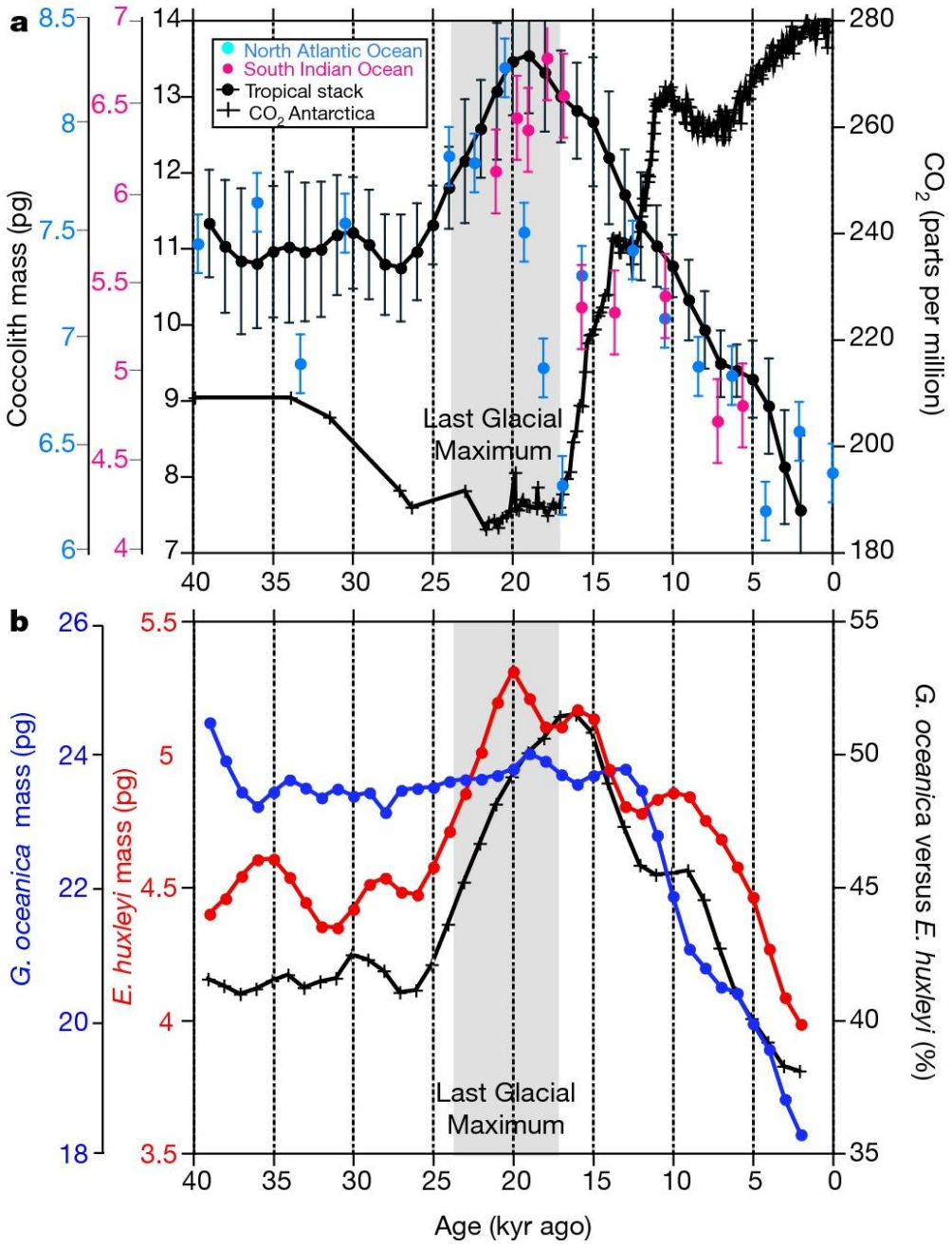

Figure 2. Variation of coccolith mass, species composition, and CO_2 concentration over the last 40 Kyrs. a, Coccolith mass (closed circles), low latitude stack (average of the four records) in black (error bars are standard error between records), MD94-103 in red and SU90-08 in blue (error bars are standard error in each sample). The CO_2 concentration in ice cores at EPICA[29] (0-22 Ka) and Vostok[30] (22-40 Ka) is represented by crosses. b, Low latitude stack of *G. oceanica* (blue) *E. huxleyi* (red), and relative abundance between the two taxa (black). Grey shading marks the period of the Last Glacial Maximum.

What drives this trend linking calcification and carbonate chemistry? The results of monoclonal culture experiments that show a decrease in noelaerhabdacean calcification (degree and rate) with OA[e.g.8,11] have focused attention on the existence of a direct environmentally-mediated physiological constraint on calcification. Coccoliths are secreted intracellularly in coccolith-producing vesicles where pH and ΩCa are maintained at levels that

stimulate calcite precipitation. Several explanations have been proposed to explain decreased calcification rates with OA[24], e.g. that the necessary outward transport of protons may become more costly in low pH and/or low [CO_3^{2-}] waters[25]. The environmental relevance of such a physiological mechanism cannot be resolved directly from our data, but in culture experiments the maximum mass decrease within a clone over carbonate chemistry ranges comparable to that of our dataset is on the order of 20%, i.e. only a fraction of the total response in our dataset. In addition, some culture strains (of noelaerhabdaceans and other coccolithophores) are capable of maintaining calcification (degree and/or rate) over certain carbonate chemistry ranges, a phenomenon that could contribute to localized within-sample deviations from the broad trend linking coccolith mass to carbonate chemistry.

A general physiological mechanism is evidently insufficient to explain the overall decline in coccolith mass in our dataset. The 3 noelaerhabdaceaen genera include several species, each harbouring a number of morphological variants (morphotypes)[26]. In our global sample set, the lightest *E. huxleyi* (morphotype C) was present in waters with [CO_3^{2-}] <200 μmol.kg^{-1}, while heavy *G. oceanica* (which includes several morphotypes[13]) only occurred above this concentration (Fig. 1b). *Emiliania huxleyi* with intermediate mass (morphotypes A and B) occupied wider and intermediate [CO_3^{2-}] ranges. Significant coccolith malformation occurred at low [CO_3^{2-}] in *E. huxleyi* morphotype C from the Patagonian shelf and Antarctic ocean. Changes in the relative abundance of taxa were therefore predominantly responsible for coccolith mass decrease with OA in modern samples. Both *Gephyrocapsa* and *Emiliania* displayed a coccolith mass decrease of ~25% from the LGM to near-present, paralleling a ~100 ppmv CO_2 increase (Fig. 2). In addition to a physiological response of individual morphotypes, this could have resulted from changes in the abundance of different morphotypes within the genera. Superimposed on this intra-generic response, a decrease in relative abundance of *Gephyrocapsa* vs *Emiliania* was the main factor underlying the overall mass variation over the last 40 kyr (Fig. 2b). Although the function of coccoliths is unknown, our data suggest that variability in calcite mass (or the associated energy expenditure) is subject to ecological selective pressure.

We observed a key exception to the global correlation between noelaerhabdacean calcification and [CO_3^{2-}]. In Patagonian shelf and Chilean upwelling waters with low [CO_3^{2-}], where the overall trend would predict low coccolith mass, we detected an unexpectedly highly calcified *E. huxleyi* morphotype (Fig. 1b) reminiscent of morphotype R[26]. The relative

abundance of this morphotype increased with decreasing pH along the Pacific transect towards Chile (Fig. 3). Many environmental gradients exist along this transect, leading to correlation of several factors with calcite mass, with mutual interactions[e.g.18] potentially masking the typical mass response to carbonate chemistry. Alternatively, since coccolith morphotype is thought to be subject to genetic regulation[11], this highly calcified *E. huxleyi* morphotype is potentially a genetic entity that exhibits an adaptation enabling it to calcify heavily in the relatively acidic upwelling waters. In this context, we note that the one culture study that reported an increase in *E. huxleyi* calcification with OA was conducted with a morphotype R strain[9].

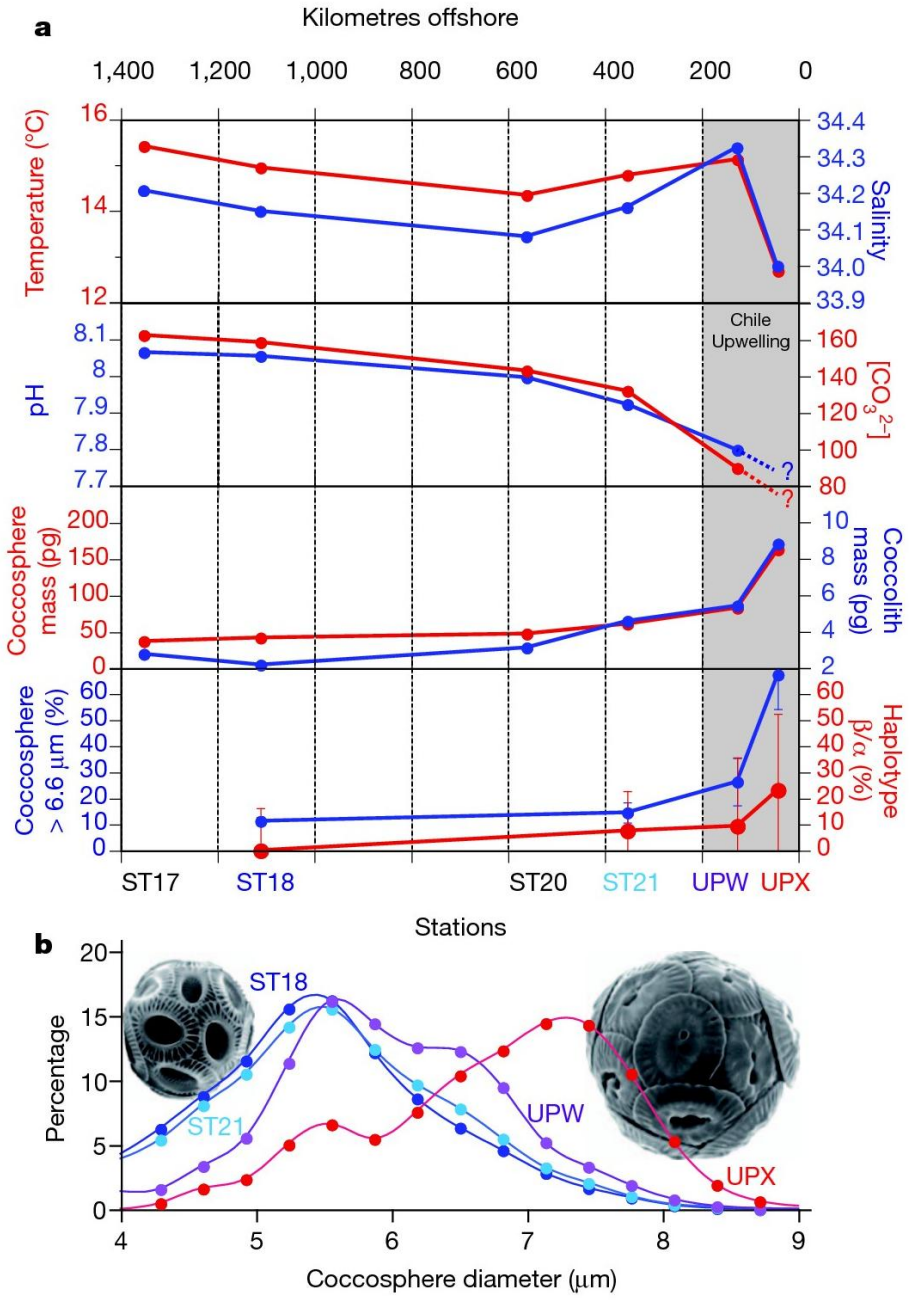

Figure 3: Physico-chemical and coccolithophore variability along an east-west acidity gradient in the south-east Pacific. BIOSOPE (station average of values given in Suppl. Table 2). **a**, (1) temperature and salinity; (2) $[CO_3^{2-}]$ and pH (water chemistry was not measured at station UPX); (3) mass of coccospheres and coccoliths; (4) percentages of large coccospheres (>6.6µm) and of haplotype α vs β. Error bars are confidence intervals at 95%. **b**, Distribution of coccosphere diameter: ST18 (n=1334); ST21 (n=578), UPW (n=210); UPX (n=203). Typical coccospheres of *E. huxleyi* Type A (Left from St18) and Type « R » (right from UPX) .

In order to probe the genetic diversity of *E. huxleyi*, we generated clone libraries from samples collected along the acidity gradient characterizing offshore Chilean water masses. We detected a shift in the relative abundance of two distinct mitochondrial haplotypes of *E. huxleyi* that coincided with the shift in relative abundance of morphotypes along the transect (Fig. 3). Each haplotype has wide oceanic distribution (Supplementary Information), indicating that the observed distribution is not the result of regional endemism. The relationship between mitochondrial haplotypes and morphotype is not, however, straightforward[27], and establishing a strict link between morphotypic and genotypic diversities requires further environmental morphogenetic studies and/or culture-based physio-genomic comparisons. The presence of highly calcified *E. huxleyi* in these samples does not mask the main pattern of decreasing calcification at low $[CO_3^{2-}]$, but highlights that coccolithophores can calcify heavily at low pH (7.62) and $[CO_3^{2-}]$ (71 μmol kg^{-1}).

Coccolithophore calcification may be influenced by multiple factors, but our environmental data reveal a spatio-temporally consistent decline of coccolith mass with decreasing $[CO_3^{2-}]$. Integrating this coccolithophore response with predicted decrease in calcification of planktonic foraminifera[6,7] and neritic corals[3,4] under elevated CO_2, means entire marine calcifying communities seem likely to be affected in the future. However, the presence of highly calcified *E. huxleyi* in CO_2-rich modern waters demonstrates that prediction of future responses is not likely to be straightforward. Such complexity could account for the lack of obvious overall direction in the response of coccolithophore calcification over a potentially analogous OA event ~55 Mya at the Paleocene-Eocene Thermal Maximum[28]. Attention should now focus not only on the physiological response of individual strains to changing carbonate chemistry, but also on characterizing responses in complex assemblages.

Methods summary

Image analyses were performed on 40 frames (240 x 180 µm² with a pixel area of 0.0225

µm²) per microscope slide grabbed using an automated microscope (Leica DMRBE). Coccoliths and coccospheres were detected, classified and morphometrically analyzed by the SYRACO software that performs pattern recognition using Artificial Neural Networks. Mass was estimated by measuring brightness in cross-polarized light (birefringence), brightness being converted into mass after calibration with calcite microspheres of known mass.

Water sampling and measurements of temperature and salinity on the 3 oceanographic cruises were conducted onboard. Total dissolved inorganic carbon (DIC) and total alkalinity (TA) were determined by the potentiometric acid titration method. To infer past changes in surface ocean carbonate system values, past salinity and TA values were estimated from geochemical proxies of past surface hydrography using published estimates of past sea surface temperature (SST) and measured δ18O. Surface ocean pCO2 was estimated using atmospheric pCO2 values measured in ice cores at Vostok29 and EPICA30 which are considered to represent global values throughout the temporal range of our records. Other carbonate chemistry parameters were calculated using the CO2sys software with temperature, salinity, TA and DIC as input.

For genetic analyses, 10-litre seawater samples were filtered onto nucleopore membranes (Millipore). Total DNA was extracted using the DNeasy Plant mini kit (Qiagen) and cox3 sequences amplified using the Phusion High-Fidelity PCR mix (New England Biolabs). PCR primers are given in the Supplementary Information. For construction of environmental clone libraries, amplifications were inserted into the TOPO-TA PCR 4 vector (Invitrogen) before transforming competent cells. PCR products were sequenced directly using the ABI PRISM BigDye Terminator Cycle Sequencing Kit on an ABI PRISM 3100 xl auto sequencer (Applied Biosystems). Maximum likelihood analysis was performed in TREEFINDER using manually aligned 812 b.p. cox3 sequences under the corrected Akaike information criterion model. The GenBank accession numbers are JN098138 to JN098158, JN098160 and JN098163 to JN098174 and their correspondance are given in the online Supplementary Information.

Acknowledgements

We thank crew from Puerto Deseado, Atalante, Suroit, and Marion-Dufresne, and D. Vaulot, L. Garczarek, M.-A. Sicre and H. Claustre for their help collecting materiel for this work. The long-term OISO observational program is supported by INSU (Institut National des Sciences de l'Univers), IPSL (Institut Pierre-Simon Laplace) and IPEV (Institut Paul-Emile

Victor). We thank F.C. Bassinot for discussion in estimating paleosalinities. The IMAGES program is acknowledged for collection and curation of the cores. Nucleotide sequences were deposited in GenBank and accession numbers are given in the online Supplementary Information. This work has been funded by the "Agence National de la Recherche" project PALEO-CTD (grant ANR-06-JCJC-0142)**,** by the European Research Council under grant agreement no. 205150, by the European Funding Agencies from the ERA-net program BiodivERsA, under the BioMarKs project and by the European Community's Seventh Framework Program EPOCA (European Project on OCean Acidification) under grant agreement no. 211384.

Author Contributions

Based on an original idea of L.B. the concept of this paper was developed in discussion between all authors. L.B., N.B., P.C and M.G. conducted coccolith measurements, D.R.-P., N.M and C.G. conducted modern ocean chemistry measurements, L.B. and T.d.G-T. computed past ocean chemistry, E.M.B., I.P. and C.d.V. performed genetic analyses, B.R., R.E.M.R. and I.P. conceptualized the physiological interpretation, L.B., I.P., D.R.-P., C.d.V. and R.E.M.R. interpreted the relationships between calcification and environment.

References

1 Sabine, C. L. *et al.* The Oceanic Sink for Anthropogenic CO2. *Science* **305**, 367-371 (2004).

2 Fabry, V. J., Seibel, B. A., Feely, R. A. and Orr, J. C. Impacts of ocean acidification on marine fauna and ecosystem processes. *ICES Journal of Marine Sciences* **65**, 414-432, doi:10.1093/icesjms/fsn048 (2008).

3 Gattuso, J.-P., Frankignoulle, M., Bourge, I., Romaine, S. and Buddemeier, R. W. Effect of calcium carbonate saturation of seawater on coral calcification. *Glob. Planet. Change* **18**, 37-46 (1998).

4 Kleypas, J. A. *et al.* Geochemical Consequences of Increased Atmospheric Carbon Dioxide on Coral Reefs. *Science* **284**, 118-120, doi:10.1126/science.284.5411.118 (1999).

5 Barker, S. and Elderfield, H. Foraminiferal Calcification Response to Glacial-Interglacial Changes in Atmospheric CO2. *Science* **297**, 833-836 (2002).

6 Moy, A. D., Howard, W. R., Bray, S. G. and Trull, T. W. Reduced calcification in

modern Southern Ocean planktonic foraminifera. *Nat. Geosci.* **2**, 276-280, doi:10.1038/ngeo460 (2009).

7 de Moel, H. *et al.* Planktic foraminiferal shell thinning in the Arabian Sea due to anthropogenic ocean acidification? *Biogeosciences* **6**, 1917-1925 (2009).

8 Riebesell, U. *et al.* Reduced calcification of marine plankton in response to increased atmospheric CO2. *Nature* **407**, 364-367 (2000).

9 Iglesias-Rodriguez, M. D. *et al.* Phytoplankton Calcification in a High-CO2 World. *Science*, 336-340, doi:DOI: 10.1126/science.1154122 (2008).

10 Langer, G., M. *et al.* Species-specific responses of calcifying algae to changing seawater carbonate chemistry. *Geochemistry, Geophysics, Geosystems* **7**, Q09006, doi:09010.01029/02005GC001227 (2006).

11 Langer, G., Nehrke, G., Probert, I., Ly, J. and Ziveri, P. Strain-specific responses of Emiliania huxleyi to changing seawater carbonate chemistry. *Biogeosciences Discussions* **6**, 4361-4383 (2009).

12 de Vargas, C., Aubry, M. P., Probert, I. and Young, J. in *Evolution of Aquatic Photoautotrophs* eds P.G. Falkowski and A.H. Knoll) 456 pp. (Academic Press, 2007).

13 Bollmann, J., Henderiks, J. and Brabec, B. Global calibration of Gephyrocapsa coccolith abundance in Holocene sediments for paleotemperature assessment. *Paleoceanogr.* **17**, 10.1029 (2002).

14 Lewis, E. and Wallace, D. W. R. Program Developed for CO2 System Calculations. *Oak Ridge National Laboratory* (1998).

15 Honisch, B. and Hemming, N. G. Surface ocean pH response to variations in pCO2 through two full glacial cycles. *Earth and Planetary Science Letters* **236**, 305-314 (2005).

16 Paasche, E. A review of the coccolithophorid Emiliania huxleyi(Prymnesiophyceae), with particular reference to growth, coccolith formation, and calcification–photosynthesis interactions. *Phycologia* **40**, 503-529 (2002).

17 Zondervan, I. The effects of light, macronutrients, trace metals and CO2 on the production of calcium carbonate and organic carbon in coccolithophores - A review. *Deep-Sea Research Part Ii-Topical Studies in Oceanography* **54**, 521-537, doi:10.1016/j.dsr2.2006.12.004 (2007).

18 Feng, Y. *et al.* Interactive effects of increased pCO(2), temperature and irradiance on the marine coccolithophore Emiliania huxleyi (Prymnesiophyceae). *Eur. J. Phycol.* **43**,

87-98 (2008).

19 Bollmann, J. and Herrle, J. O. Morphological variation of Emiliania huxleyi and sea surface salinity. *Earth and Planetary Science Letters* **255**, 273-288 (2007).

20 Colmenero-Hidalgo, E., Flores, J. A. and Sierro, F. J. Biometry of Emiliania huxleyi and its biostratigraphic significance in the Eastern North Atlantic Ocean and Western Mediterranean Sea in the last 20 000 years. *Marine Micropaleontology* **46**, 247-264 (2002).

21 Anderson, D. M. and Archer, D. Glacial interglacial stability of ocean pH inferred from foraminifer dissolution rates. *Nature* **416**, 70-73 (2002).

22 Buitenhuis, E. T., de Baar, H. J. W. and Veldhuis, M. J. W. Photosynthesis and calcification by Emiliania huxleyi (Prymnesiophyceae) as a function of inorganic carbon species. *J. Phycolog.* **35**, 949-959 (1999).

23 Berry, L., Taylor, A. R., Lucken, U., Ryan, K. P. and Brownlee, C. Calcification and inorganic carbon acquisition in coccolithophores. *Functional Plant Biology* **29**, 289-299, doi:10.1071/pp01218 (2002).

24 Mackinder, L., Wheeler, G., Schroeder, D., Riebesell, U. and Brownlee, C. Molecular Mechanisms Underlying Calcification in Coccolithophores. *Geomicrobiol. J.* **27**, 585-595, doi:10.1080/01490451003703014 (2010).

25 Zondervan, I., Rost, B. and Riebesell, U. Effect of CO2 concentration on the PIC/POC ratio in the coccolithophore Emiliania huxleyi grown under light-limiting conditions and different daylengths. *J. Exp. Mar. Biol. Ecol.* **272**, 55-70 (2002).

26 Young, J. *et al.* A guide to extant coccolithophore taxonomy. *Journal of Nannoplankton Research* **Special Issue 1**, 1-132 (2003).

27 Hagino, K. *et al.* New evidence for morphological and genetic variation in the cosmopolitan coccolithophore Emiliania huxleyi (Prymnesiophyseae) from the COX1b-ATP4 genes. *J. Phycol.* (2011 accepted).

28 Gibbs, S. J., Bown, P. R., Sessa, J. A., Bralower, T. J. and Wilson, P. A. Nannoplankton extinction and origination across the Paleocene-Eocene Thermal Maximum. *Science* **314**, 1770-1773, doi:10.1126/science.1133902 (2006).

29 Monnin, E. *et al.* Atmospheric CO2 concentrations over the last glacial termination. *Science* **291**, 112-114 (2001).

30 Petit, J. R. *et al.* Climate and atmospheric history of the past 420,000 years from the Vostok ice core, Antarctica. *Nature* **399**, 429-436 (1999).

.

SUPPLEMENTARY INFORMATION

doi:10.1038/nature10295

CONTENTS page

A. SAMPLING

Water samples were collected during 3 cruises: Southern Indian Ocean samples were collected during the CARAUS_OISO-11 cruise in 2004. Pacific samples were collected during the BIOSOPE cruise in 2004[31]. South Atlantic shelf samples were collected during the PATAGONIA III cruise in 2006.

Sediment samples were taken from six cores : Core MD90-0963 was retrieved in the central Indian Ocean (5°03.30'N - 73°53.60'E) at a water depth of 2446 m during the SEYMAMA cruise[32]. Cores MD97-2138 and MD97-2141 were retrieved respectively in the Western Pacific Warm Pool (1°25'S - 146°24'E, 1912m water depth) and in the Sulu Sea (8°47'N -121°17'E, 3633m water depth) during the IMAGES III cruise in 1997[33]. Core MD02-2529 was retrieved in the Eastern Pacific (8°12.33'N - 84°07.32'W, 1619 m water depth) during IMAGES VIII cruise in 2002[34]. Core SU90-08 was retrieved on the mid-Atlantic ridge (43°03'N - 30°02'W, 3080 m water depth) during the PALEOCINAT I cruise in 1990[35]. The choice of the four tropical cores was based on several criteria: (i) they were collected from relatively stable tropical, open oceanic regions, as upwelling and/or higher latitude zones may be affected by large surface ocean temperature and carbonate chemistry variations; (ii) published $\delta^{18}O$ and derived sea surface temperature (SST) estimates were available, allowing further assessment of salinity; (iii) the sedimentation rate over the analyzed period allowed accurate chronology, without detectable evolutionary change in coccolithophore species composition (E. huxleyi being the dominant species[36]). The two cores from higher latitudes were selected based on similar criteria. The Indian Ocean core was located close to the Kerguelen Plateau and hence in the vicinity of the OISO cruise. Due to low coccolith abundance in sediments of this area, 3 subsequent samples (e.g. 0, 10, 20 cm) were merged to obtain each data point. Coccoliths were not present in sufficient numbers in Stage 3 of this core to provide an estimate of their mass before 22-ka. In order to include a high latitude core far from this first location to identify possible effects of regionalism, the second high latitude core was selected from the centre of the North Atlantic ocean.

Influences of sedimentation bias and/or post-depositional dissolution on coccolith mass in these cores can be ruled out because (i) the cores are located well above the lysocline, (ii) mass variation estimates were very similar in two records from the same area but with a depth difference of 2km (Sulu Sea and Western Pacific Warm pool), (iii) mass records show little correlation to the published dissolution history of these cores[37,38], (iv) Atlantic and Pacific records of the coccolith mass vary in parallel despite the fact that these two oceans are known to have experienced opposite variations in the depth of their lysocline[20], and (v) recent laboratory acidification experiments on coccolithophore powder has shown that coccolith dissolution is a non-gradual, threshold process, either dissolving entirely the calcite plate, or having virtually no impact on the mass of surviving coccoliths[39].

B. MICROSCOPY AND IMAGE ANALYSIS

Water samples: 1 to 4 liters of seawater were filtered onto cellulosic membranes with a 0.45µm nominal porosity and air dried. A portion of each membrane was mounted with Canada balsam between microscope slide and cover slip. Sediment samples were prepared as standard smear slides.

Grabbing frames: A polarizing microscope (LEICA DMRBE) with a 50x oil immersion objective was used for automatic scanning of slides in cross-polarized light. For each sample, a 2 Megapixel Spot Insight camera grabbed forty fields of view. Each frame was 240 x 180 µm² with a pixel area of 0.0225 µm². The amount of light transmitted through the sample was held constant.

doi:10.1038/nature 10295

Automatic recognition: Coccoliths and coccospheres were automatically detected by the software SYRACO[40,41], which performs pattern recognition using Artificial Neural Networks (ANN). In this study we used two ANNs, one for oceanic samples[42], the other for core samples[40]. The specimen determination error was low (<5% for the Noelaerhabdaceae)[40,42]. Images of specimens recognized as Noelaerhabdaceae were saved for further analysis.

Morphometry: Image sets were analyzed by software developed in Labview that rapidly and accurately estimates the size and calcite mass of coccoliths and coccospheres. Mass was estimated by measuring the brightness of carbonate grains when viewed in cross-polarized light (birefringence)[43]. The brightness of calcite is proportional to its thickness in the range 0-1.5 µm. By measuring the total brightness of a coccolith as the sum of the Grey Level (GL) of every component pixel, brightness can be converted into weight after proper calibration. Taking into account the light tuning and the magnification of the microscope, the sum of the GL of every pixel multiplied by a given factor gives an accurate estimate of the weight (in picograms of calcite) of a coccolith. This method is highly reproducible (±0.13 pg). Error on the calibration is estimated to be about 12% (2 sigma of the distribution in the calibration), this being due to the sample preparation method. Different calibrations were used for fossil and modern samples because of the difference in preparation techniques[41]. The different series of samples were analyzed at different periods over a number of years. In order to check for possible bias in image collection linked to variation in light quality over time, we reran 6 samples per series in the same set. Small linear adjustments had to be made for measurements from core MD97-2141 and from the PATAGONIA cruise.
For mutilayered coccospheres (very rarely observed in SEM in our samples), the mass of coccospheres inferred by this method includes the mass of the external (visible in SEM) layer of coccoliths, and of all internal layers of coccoliths, since the brightness in cross polarized light is cumulative.

Statistics: On average 750 coccoliths per sample (a total of more than 550000 coccoliths) and 513 coccospheres per grouped sample (a total of almost 15000 coccospheres) were measured. The coccolithophore data from the BIOSOPE cruise have been presented elsewhere[42].

For the PATAGONIA cruise and the northern part of the OISO cruise, neighboring samples were grouped to increase the number of coccospheres in order to reach statistical significance. For the BIOSOPE cruise, samples were grouped by station (6 samples were collected per station at different depths). The list of grouped samples is presented in Table 3, and is exhibited in Suppl. Figure 1. The same procedure was used for measurements of isolated coccoliths in order to compare these two independent data sets. The mass of coccospheres and isolated coccoliths was highly correlated (R^2=0.94, Suppl. Figure 1). The mean coccosphere/coccolith mass ratio in our dataset implies that noelaerhabdaceaens build coccospheres composed of ~17 coccoliths, i.e. within the range described in the literature[17].

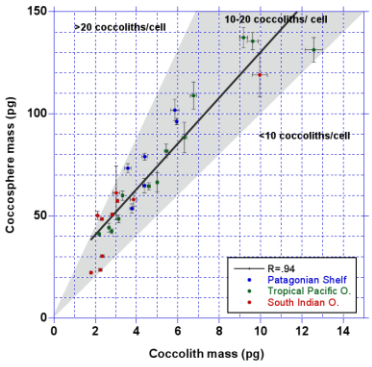

Supplementary Figure 1 : Comparison of the mass of coccoliths and coccospheres. The shaded area corresponds to coccospheres bearing 10 to 20 coccoliths (i.e. coccosphere mass divided by coccolith mass comprised between 10 and 20).

doi:10.1038/nature 10295

Coccosphere mass recorded in our dataset was comparable with that found in culture at similar concentration of CO_3 with morphotype R[9] or morphotype A[8] strains

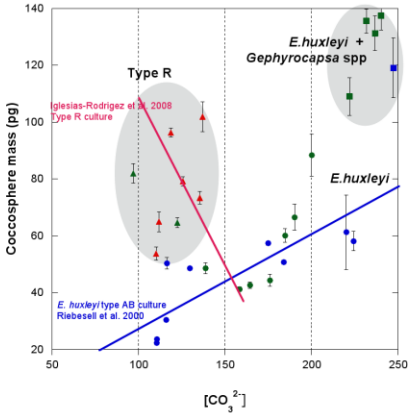

Supplementary Figure 2 : Relationship between coccosphere mass and carbonate ion concentration. The blue and red lines represent inorganic carbon per cell as a function of carbonate ion concentration from cultures assuming constant growth rate of 1 day-1 published in (8) and (9) Respectively.

It is possible to estimate the mass of calcite per cell volume from the size of coccoliths in order to assess whether calcification state may simply be a function of an increase in cell volume. A relationship has been reported between coccosphere diameter and coccolith size[42,44]. From BIOSOPE samples, coccosphere (=cell) volume can be estimated by multiplying the length of coccoliths by a factor of 1.5[42]. The number of coccoliths per coccosphere being about 17 coccoliths, the mass of coccospheres can be estimated by multiplying coccolith mass by 17. From these estimations, calcite mass per cell volume is linearly related to the concentration of CO_3 (R^2=0.87).

C. CHEMISTRY

Modern Samples: During the BIOSOPE cruise, water sampling and measurements of temperature and salinity were conducted using a SeaBird SBE 911plus CTD/Carousel system fitted with an SBE 43 oxygen sensor. Seawater was sampled in 500ml borosilicate bottles and poisoned with a saturated solution of mercuric chloride before being sealed. Samples were shipped back to the laboratory where measurements were performed within one month of the end of the cruise. Total dissolved inorganic carbon (DIC) and total alkalinity (TA) were determined by the potentiometric acid titration method[45]. From replicate analyses of a reference seawater sample of known TA concentration (Certified Referenced Materials (CRM) from Pr. Andrew Dickson of Scripps Institution of Oceanography, University of California), the precision of the analyses were determined to be within 1.5 µmol.kg^{-1} for DIC and 1.7 µmol.kg^{-1} for TA. These data are described elsewhere[45]. For the OISO cruise, details of the instruments and techniques for all analyses have been previously described[46,47]. For the PATAGONIA cruise, the same instruments and techniques were used than in OISO cruise, and precisions of TA and DIC measurements were comparable to those for BIOSOPE and OISO. Other carbon chemistry parameters were estimated using the CO2sys software[16] with temperature, salinity, TA and DIC as input. Precision levels were about +/-13 µmol.kg^{-1} for HCO_3, +/-10 µmol.kg^{-1} for CO_3 and +/- 0.03 for pH.

doi:10.1038/nature 10295

Fossil samples: To infer past changes in surface ocean carbonate system values, past TA values were estimated from geochemical proxies of past surface hydrography. A four-step approach was followed.

Firstly, using published estimates of past sea surface temperature (SST) and measured $\delta^{18}O$ in planktonic foraminifera, records of $\delta^{18}O$ seawater changes were derived using the isotopic equation of Bemis et al.[48]. For MD90-0963[49], MD02-2529[50] and SU90-08[51,52] cores, temperature estimates were based on the alkenone unsaturation index (UK'37), whereas for the MD97-2138[37] and MD97-2141 cores[53], SST was estimated using the Mg/Ca value measured in shells of the surface-dwelling planktonic foraminifera *Globigerinoides ruber*. For MD94-103, the alkenone data were not valid, and the foraminifera transfer function provided the best estimate of SST[54]. For the MD90-0963[49,55], MD02-2529[50] and MD97-2138 cores[38], past temperature estimates were available from both Mg/Ca and alkenones. For our reconstructions, we chose the proxy records with the highest available resolution. In these cores, the two proxies yielded slightly different temperature estimates, but comparison of mean Holocene (0-10 Ka) to glacial (26-18 ka BP) temperature estimates from each proxy revealed that the difference over these time intervals does not exceed 0.8°C (for Holocene temperatures in MD97-2138 and MD90-0963), within the range of error bars of temperature estimates.

Secondly, these records were corrected for the mean global sea-level effect[56] in order to assess the local $\Delta\delta^{18}O_{seawater}$ value.

Thirdly, using modern GEOSECS measurements of salinity and $\delta^{18}O_{seawater}$ from subsurface (depth >200 meters) in the Indo-Pacific subtropics, past salinity changes were derived using the equation $SSS=33.941+2.729*\Delta\delta^{18}O_{seawater}$ to which we added the global salinity changes[57]. Note that for MD90-0963, we used the published salinity estimates interpolated at the coccolith sample levels[49].

Lastly, the global relationships between TA and salinity and temperature in surface waters of the world's oceans[58] were used to reconstruct TA from SST and SSS. Surface ocean pCO_2 was estimated using the atmospheric pCO_2 measured in ice cores at Vostok[29] and EPICA[30] which are considered to represent the global value at all times of our records. Atmospheric CO_2 is near equilibrium with that of seawater for 3 cores (MD90-0963; MD97-2138; MD97-2141)[59,60]. Core MD02-2529 is from the Panama Basin, a location that represents a source of CO_2[59]. We therefore added 90 ppm to the ice core values to account for seasonal difference between water and atmospheric pCO_2 in this area in order to obtain more appropriate surface ocean values. The accuracy for paleosalinity estimates which includes the error on SST is +/-1.4[61].This propagated into an error of +/-40 µm ol.kg^{-1} for CO_3^{2-} concentration when incorporated into CO2sys. The decreases of CO_3^{2-} ion concentration and pH estimated during deglaciation in all 6 cores were ~50-100 µmol.kg^{-1} and 0.1, respectively, values that are comparable to other estimations including those obtained by boron isotopes studies[5,12,13,62].

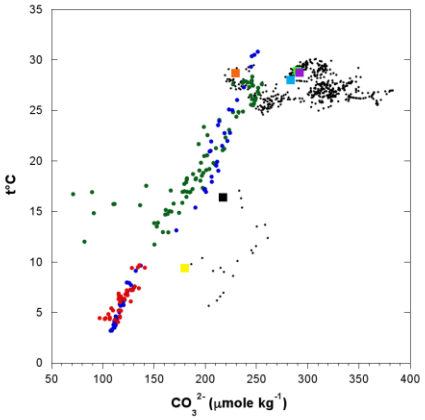

Supplementary Figure 3 : Relationship between carbonate ion concentration and temperature. Departure from the linear relationship in modern samples is in the Chilean upwelling and in paleodata toward the LGM. Modern data are represented by filled circles, core tops by squares, and paleoreconstruction by black dots.

doi:10.1038/nature 10295

To show graphically the absence of significant correlation between coccolith mass and temperature or salinity in the entire data set we present these 2 graphs (Supplementary Figure 4a,b).

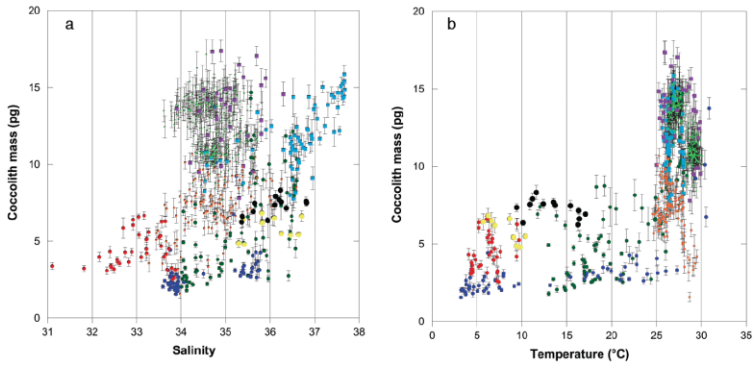

Supplementary Figure 4 : Relationship between coccolith mass and salinity (a) and temperature (b). Colour codes are those of the map in Fig. 1.

We performed simple sensibility tests in order to check the effect of past departures from the modern relationship between alkalinity and salinity. For each core, we estimated the CO_3 concentration at 18 Ky (low pCO_2) after having deducted or added 1 psu of salinity from the original value (alkalinity was calculated using the modern equations). Another test was to add or deduct 100 micromol.kg^{-1} of alkalinity without changing the salinity, and then estimate the CO_3 concentration. The values of ±1psu and ±100 micromol.kg^{-1} corresponded to the total glacial/interglacial range of salinity and alkalinity (Suppl. Fig. 5).

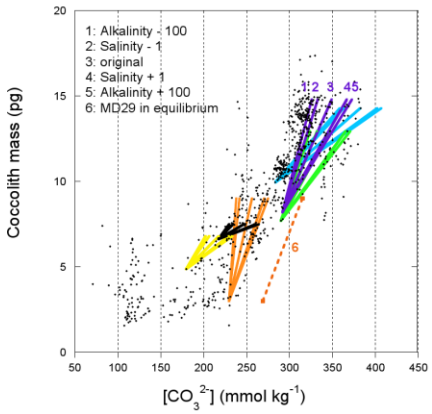

Supplementary Figure 5 : Effects of last glacial maximum difference in salinity and alkalinity estimates on a CO3/coccolith mass diagram. Black dots denote the original data. Cores are represented by the colour codes used elsewhere in the paper (Fig. 1). Lines with the same colour converge at present (core top) values. Their opposite ends are LGM values when alkalinity (1,5) or salinity (2,4) values are altered, or left unchanged (3). The orange dotted line (6) shows where values of MD02-2529 would lie without deduction of 90 ppm pCO2 to account for seasonal upwelling in this area (according to modern values61). All other cores where retrieved in areas where surface ocean pCO2 is in equilibrium with the atmosphere.

Records of temperature, salinity, CO_3^{2-} concentration and coccolith mass for each core are shown for comparison in Suppl. Fig. 6..

doi:10.1038/nature 10295

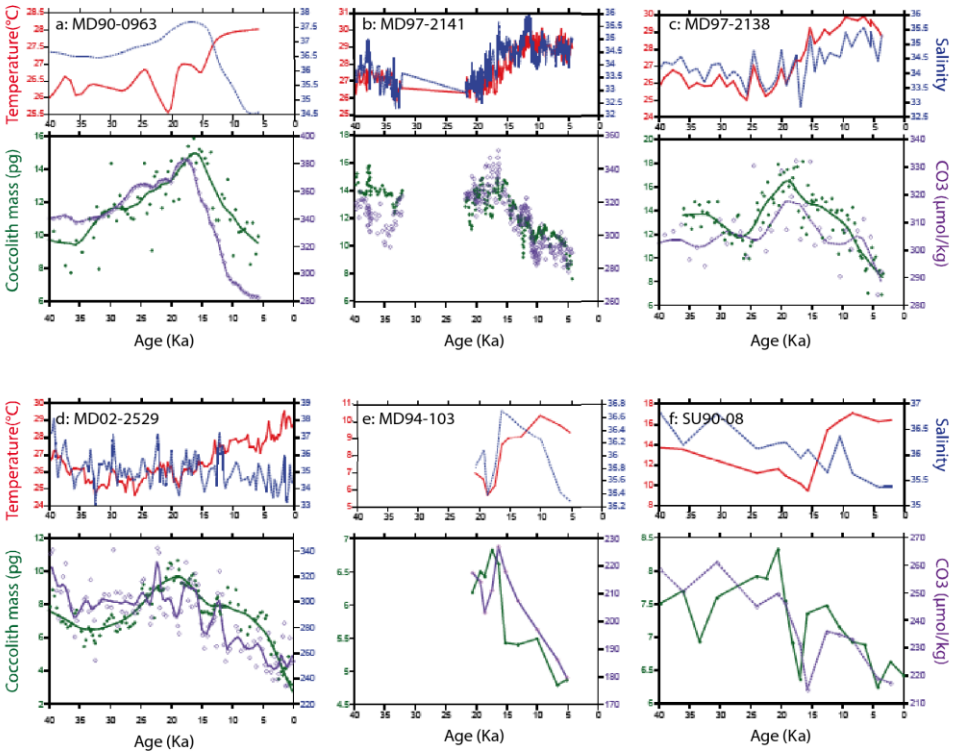

Supplementary Figure 6 : Records of salinity (solid lines on top diagrams - scales on the right), temperature (dotted line on top diagrams - scale on the left), coccolith mass (filled circles and solid lines on bottom diagrams - scales on the left) and carbonate ion concentration (open circles and dotted lines on bottom diagrams - scales on the right) in each core. Lines are smoothed data.

D. GENETICS

DNA sampling and extraction, PCR and clone library construction :

Samples for DNA extraction were collected at four stations along the BIOSOPE transect (UPX-2 (15m), UPW-1 (25m), STB21-4 (55m) and STB18-3 (75m)) using niskin bottles. 10L of seawater were filtered onto 3µm nucleopore membrane filters (Millipore) that were stored at -80°C until analysis. DNA was also sampled from 17 culture strains of different origin (see Suppl. Table 1). Total DNA was isolated using the DNeasy Plant mini kit (Qiagen). Cox3 sequences were amplified using the following primers: cox3-F1 5'-TCCTACACTTGGATATTTAG-3' as forward and cox3-R1 5'-TCGCATTTTTGGTTTGGAAGACC-3' as reverse. Amplification was performed in 25µL with the Phusion PCR Mix (Finnzyme) using an ABI thermal cycler with the following protocol: 30s initial denaturation at 98°C, followed by 35 cycles of 10s at 98°C, 30s annealing at 55°C, and 30s extension at 72°C, and a final 10 min extension step at 72°C.

For construction of the environmental clone libraries, amplifications were inserted after purification and a short elongation step into the TOPO-TA PCR 4 vector (Invitrogen) before transforming competent cells. Presence of the insert was tested by PCR on the colonies following the manufacturer's specifications using the primers M13for and M13rev from the cloning kit. PCR products were

doi:10.1038/nature 10295

sequenced directly using the ABI PRISM BigDye Terminator Cycle Sequencing Kit (Perkin-Elmer) on a DNA auto sequencer ABI PRISM 3100 xl Genetic Analyzer (Perkin-Elmer).

Sequence treatment, alignment and phylogeny

Cox3 sequences of 812 bp length including reference sequences from culture strains were manually aligned before phylogenetic inferences using a *Gephyrocapsa oceanica* sequence as an outgroup. Genbank accession numbers are provided for all sequences in the Supplementary Tables 1 and 2. The most appropriate model of DNA substitution and associated parameters was estimated based on the corrected Akaike information criterion (AICc)[64] using JModeltest[65]. The HKY[66] substitution model selected by taking into account a gamma-shaped distribution of the rates of substitution among sites was G=0.90187084 +I optimised with the following rate parameters: TC= 0.39497424, TA= 0.052512878, TG= 0.052512878, CA= 0.052512878, CG= 0.052512878, AG= 0.39497424 and the following nucleotide frequency parameters: T= 0.40214659, C= 0.16327712, A= 0.2523381, G= 0.18223819. This model was then used to perform phylogenetic analyses. The phylogenetic tree (Supplementary Figure 7) was determined by maximum likelihood (ML) using TREEFINDER[67]. The robustness of the branching in the tree was tested by bootstrapping on 1000 replicates.

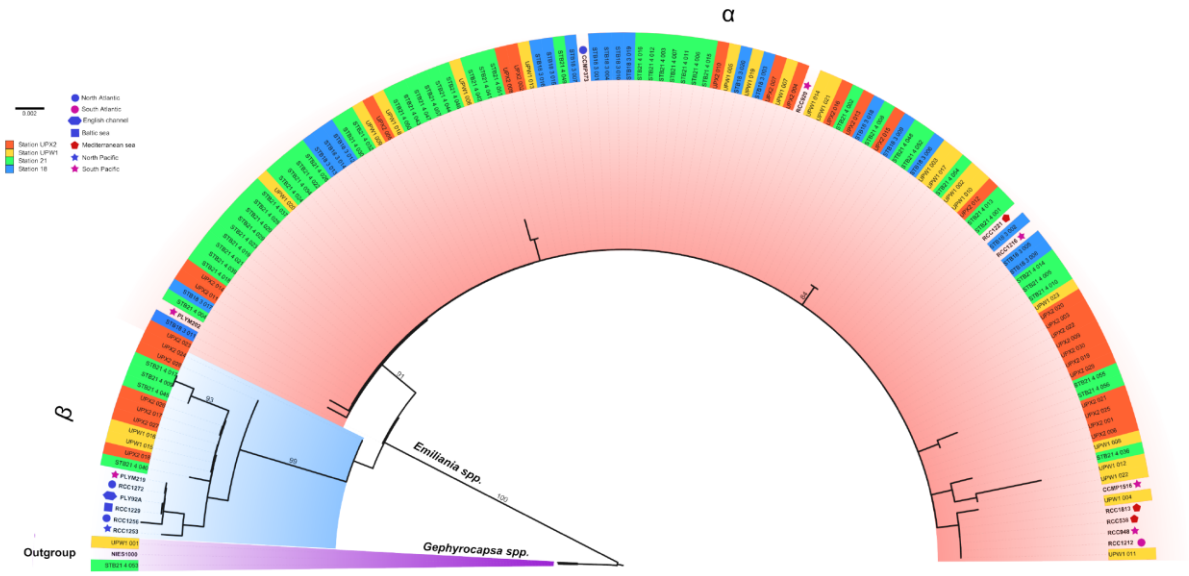

Supplementary Figure 7: Phylogenetic tree inferred by Maximum Likelihood under the HKY+G+I model with one *G. oceanica* sequence as an outgroup. Bootstrap support is shown for values up to 80. *Emiliania huxleyi* haplotype β is indicated in blue, *E. huxleyi* haplotype α in red, and *Gephyrocapsa* sequences in purple. The outside colour code represents the sample origin : blue is ST18, green is ST21, yellow is UPW and orange is UPX; the white with geometric symbols is for culture strains.

doi:10.1038/nature 10295

Supplementary Table 1 : Culture strains used for genetic analyses and accession numbers

	Strain designation[1]	other designation[1]	origin	morphotype	Cox3 haplotype	Genbank accession number
E.huxleyi	CCMP1516	RCC1242	Pacific Ocean	Naked	α	JN098163
E.huxleyi	CCMP373	RCC1270	Atlantic Ocean	Naked	α	JN098164
E.huxleyi	RCC1212	NS10Y	Atlantic Ocean	TypeB	α	JN098165
E.huxleyi	PLY92A		English Channel	TypeA	β	JN098167
E.huxleyi	PLYM202	EH2	South Pacific	Naked	α	JN098168
E.huxleyi	PLYM219	NZEH	South Pacific	TypeR	β	JN098169
E.huxleyi	RCC538	PROSOPE_140-4-1	Mediterranean Sea	not observed	α	JN098170
E.huxleyi	RCC920	Biosope_32B_HO8	Pacific Ocean	TypeA	α	JN098171
E.huxleyi	RCC948	Biosope_175_FL2-4	Pacific Ocean	TypeA	α	JN098172
E.huxleyi	RCC1216	TQ26	Pacific Ocean	TypeR	α	JN098173
E.huxleyi	RCC1253	OS2	Pacific Ocean	TypeC	β	JN098166
E.huxleyi	RCC1229	D1902-28A	North Sea	TypeA	β	JN098158
E.huxleyi	RCC1272	BG10-6	Atlantic Ocean	TypeA	β	JN098160
G.oceanica	NIES1000	RCC1526	Pacific Ocean	Gephyrocapsa	outgroup	JN098174

1 Culture collection designation: CCMP: Provasoli-Guilard National Center for Culture of Marine Phytoplankton; NIES: National Institut for Environmental Science culture collection; PLY: Plymouth culture collection; RCC: Roscoff Culture Collection.

Supplementary Table 2 : Environmental sequences and accession numbers

Environmental haplotypes	leaf name	Haplotype	Genbank accession number
GoCox3g	UPW1 001	*Gephyrocapsa*	JN098138
EhCox3a1	STB21-4 040	β	JN098139
EhCox3a2	UPW1 015, 016; UPX2 017, 018, 026, 027	β	JN098140
EhCox3a3	STB21-4 045	β	JN098141
EhCox3a4	STB21-4 009, 017	β	JN098142
EhCox3a5	UPX2 028	β	JN098143
EhCox3a6	UPX2 024	β	JN098144
EhCox3b1	UPX2 023	α	JN098145
EhCox3b2	STB18-3 011	α	JN098146
EhCox3b3	STB21-4 041	α	JN098147
EhCox3b4	STB21-4 051	α	JN098148
EhCox3b5	STB18 -3 001, 002, 003, 004, 005, 006, 007, 008, 009, 010, 012, 013, 014, 015, 016, 017, 018, 019, 020; STB21-4 001, 002, 003, 004, 005, 006, 007, 008, 010, 012, 013, 014, 018, 019, 020, 021 ,022, 023, 024, 025, 026, 027, 028, 029, 030, 031, 032, 033, 034, 035, 037, 038, 039, 040, 042, 043, 044, 046, 047, 049, 050, 051, 053, 054, 057; UPW1 002, 003, 005, 006, 007, 008, 009, 010, 013, 017, 018, 019, 020, 021, 022, 023; UPX2 001, 002, 003, 004, 005, 006, 007, 008, 009, 010, 011, 012, 013, 014, 015, 016, 019, 020, 021, 022, 025, 028, 029, 030	α	JN098149
EhCox3b6	STB21-4 048, 052	α	JN098150
EhCox3b7	STB21-4 055	α	JN098151
EhCox3b8	STB21-4 056	α	JN098152
EhCox3b9	UPW1 008	α	JN098153
EhCox3b10	STB21-4 036	α	JN098154
EhCox3b11	UPW1 012	α	JN098155
EhCox3b12	UPW1 022	α	JN098156
EhCox3b13	UPW1 004, 011	α	JN098157

doi:10.1038/nature 10295

REFERENCES

31. Claustre, H., Sciandra, A. & Vaulot., D. Introduction to the special section : bio-optical and biogeochemical conditions in the South East Pacific in late 2004 - the BIOSOPE cruise. *Biogeosciences Discussions* **5**, 605-640 (2008).
32. Bassinot, F. C. *et al.* Coarse fraction fluctuations in pelagic carbonate sediments from the tropical Indian Ocean : a 1500 kyr record of carbonate dissolution. *Paleoceanogr.* **9**, 579-600 (1994).
33. Beaufort, L. & party, S. s. *MD148/PECTEN*. (Institut Polaire Francais, 2005).
34. Beaufort, L. & the members of the scientific party. MD126 MONA (Marges Ouest Nord Americaines) IMAGES VIII. 453 pp (Insitut Polaire Francais Paul Emile Victor (IPEV), Brest, 2002).
35. Grousset, F. *et al.* Patterns of ice rafted detritus in the Glacial North Atlantic (40^55³N). *Paleoceanography* **8**, 175-192 (1993).
36. Thierstein, H. R., Geitzenauer, K. R., Molfino B. & Shackleton, N. J. Global synchroneity of late Quaternary coccolith datum levels : validation by oxygen isotopes. *Geology* **5**, 400-404 (1977).
37. Bassinot, F. C. *et al.* The astronomical theory of climate and the age of the Brunhes-Matuyama magnetic reversal. *Earth Planet. Sci. Let.* **126**, 91-108 (1994).
38. de Garidel-Thoron, T. *et al.* A multiproxy assessment of the western equatorial Pacific hydrography during the last 30 ky. *Paleoceanogr.* **22**, DOI PA3204 3210.1029/2006PA001269 (2007).
39. Beaufort, L., Probert, I. & Buchet, N. Effects of acidification and primary production on coccolith weight: implications for carbonate transfer from the surface to the deep ocean. *Geochemistry Geophysics Geosystems* **8**, DOI 2006GC001493 (2007).
40. Beaufort, L. & Dollfus, D. Automatic recognition of coccolith by dynamical neural network. *Mar. Micropaleont.* **51/1-2**, 57-73 (2004).
41. Dollfus, D. & Beaufort, L. Fat neural network for recognition of position-normalised objects. *Neural Networks* **12**, 553-560 (1999).
42. Beaufort, L., Couapel, M. J. J., Buchet, N., Claustre, H. & Goyet, C. Calcite production by Coccolithophores in the South East Pacific Ocean. *Biogeosciences* **5**, 1101-1117 (2008).
43. Beaufort, L. Weight estimates of coccoliths using the optical properties (birefringence) of calcite. *Micropaleontol.* **51**, 289-298 (2005).
44. Henderiks, J. Coccolithophore size rules - Reconstructing ancient cell geometry and cellular calcite quota from fossil coccoliths. *Marine Micropaleontology* **67**, 143-154, doi:10.1016/j.marmicro.2008.01.005 (2008).
45. Goyet, C., Ito Goncalves, R. & Touratier, F. Anthropogenic carbon distribution in the eastern South Pacific Ocean. *Biogeosciences* **6**, 149-156 (2009).
46. Metzl, N., Brunet, C., Jabaud-Jan, A., Poisson, A. & Schauer, B. Summer and winter air-sea CO2 fluxes in the Southern Ocean. *Deep Sea Res I* **53**, 1548-1563, doi:10.1016/j.dsr.2006.07.006 (2006).
47. Metzl, N. Decadal increase of oceanic carbon dioxide in the Southern Indian Ocean surface waters (1991-2007). *Deep-Sea Res II*, **56**, 607-639, doi:10.1016/j.dsr2.2008.12.007 (2009).
48. Bemis, B. E., Spero, H. J., Bijma, J. & Lea, D. W. Reevaluation of the oxygen isotopic composition of planktonic foraminifera: experimental results and revised paleotemperature equations. *Paleoceanography* **13**, 150-1660 (1998).
49. Rostek, F. *et al.* Reconstructing sea surface temperature and salinity using ð18O and alkenone records. *Nature* **364**, 319-321 (1993).
50. Leduc, G. *et al.* Moisture transport across Central America as a positive feedback on abrupt climatic changes. *Nature* **445**, 908-911 (2007).
51. Villanueva, J. *et al.* Precessional forcing of productivity in the North Atlantic Ocean. *Paleoceanography* **13**, 561-571 (1998).
52. Calvo, E., Villanueva, J., Grimalt, J. O., Boelaert, A. & Labeyrie, L. New insights into the glacial latitudinal temperature gradients in the North Atlantic. Results from UK37 sea surface temperatures and terrigenous inputs. *Earth Planetary Science Letters* **188**, 509-519 (2001).
53. Rosenthal, Y., Oppo, D. W. & Linsley, B. K. The amplitude and phasing of climate change during the last deglaciation in the Sulu Sea, western equatorial Pacific. *Geophysical Research Letters* **30**, 4, doi:1428-10.1029/2002gl016612 (2003).
54. Sicre, M.-A. *et al.* Mid-latitude Southern Indian Ocean response to Northern Hemisphere Heinrich évents, *Earth and Planetary Science Letters* **240**, 724–731 (2005).
55. Tachikawa, K., Sepulcre, S., Toyofuku, T. & Bard, E. Assessing influence of diagenetic carbonate dissolution on planktonic foraminiferal Mg/Ca in the southeastern Arabian Sea over the past 450 ka: Comparison between Globigerinoides ruber and Globigerinoides sacculifer. *Geochemistry Geophysics Geosystems* **9**, doi:Q04037 10.1029/2007gc001904 (2008).
56. Waelbroeck, C. *et al.* Sea-level and deep water temperature changes derived from benthic foraminifera isotopic records. *Quaternary Science Reviews* **21**, 295-305 (2002).
57. Duplessy, J. C. *et al.* Surface salinity reconstruction of the North-Atlantic ocean during the last glacial maximum. *Oceanologica Acta* **14**, 311-324 (1991).
58. Lee, K. *et al.* Global relationships of total alkalinity with salinity and temperature in surface waters of the world's oceans. *Geophysical Research Letters* **33**, 5, doi:L19605 10.1029/2006gl027207 (2006).
59. Metzl, N. *et al.* Spatio-temporal distributions of air-sea fluxes of CO2 in the Indian and Antarctic Oceans: a first step. *Tellus* **47B**, 56-69 (1995).
60. Takahashi, T. & al., e. Climatological Mean and Decadal Change in Surface Ocean pCO2, and Net Sea-air CO2 Flux over the Global Oceans. *Deep-Sea Res II,*, doi:doi:10.1016/j.dsr2.2008.12.009 (2009).
61. Schmidt, G. A. Error analysis of paleosalinity calculations. *Paleoceanography* **14**, 422-429 (1999).
62. Palmer, M. R. & Pearson, P. N. A 23,000-Year Record of Surface Water pH and PCO2 in the Western Equatorial Pacific Ocean. *Science* **300**, 480-482 (2003).
64 . Akaike H. 1974. A new look at the statistical model identification. IEEE Transactions on Automatic Control 19: 716–723
65 . Posada D. 2008. jModelTest: Phylogenetic Model Averaging. Molecular Biology and Evolution 25: 1253-1256.
66 . Hasegawa M. Kishino H. and Yano T.1985. Dating of the human–ape splitting by a molecular clock of mitochondrial DNA. Journal of Molecular Evolution 22: 160-174
67 . Jobb G, von Haeseler A, Strimmer K (2004) TREEFINDER: A powerful graphical analysis environment for molecular phylogenetics. BMC Evolutionary Biology.

CHAPITRE 5

LOSS OF SEX AND REDUCED ADAPTABILITY IN BIOGEOCHEMICALLY KEY OPEN OCEANIC EUKARYOTIC PHYTOPLANKTON

Peter von Dassow[1], Uwe John[2], Hiroyuki Ogata[3], Ian Probert[4], El Mahdi Bendif[5], Jessica Kegel[6], Stéphane Audic[5], Patrick Wincker[7], Corinne Da Silva[7], Jean-Michel Claverie[3] and Colomban de Vargas[5]

[3] CNRS-UPR2589 Information Génomique et Structurale, Institut de Microbiologie de la Méditerranée 13288, Marseille cedex 09, France

[4]CNRS-UPMC (Université Paris-06), FR2424, Station Biologique de Roscoff, 29682 Roscoff cedex, France

[5]CNRS-UPMC (Université Paris-06), UMR 7144, Groupe Plancton, Station Biologique de Roscoff, 29682 Roscoff cedex, France

[6]Marine Biological Association of the United Kingdom, Citadel Hill, Plymouth, Devon, PL1 2PB, UK

[7]Genoscope, 2 Rue Gaston Crémieux, 91057 Evry, France

Abstract

Sex is predicted to be maintained by moderate population sizes and fluctuating environmental pressures but lost in infinite populations in stable environments. Here we demonstrate strong genome content variation correlating with the apparent loss of the haploid phase and meiotic recombination in the globally important calcifying eukaryotic phytoplankton *Emiliania huxleyi*. The loss of sex in some *E. huxleyi* lineages occurred recently and independently within this relatively young (290 ka) morpho-species and associates with adaptation to open ocean conditions of lower biomass and ecological spatio-temporal variability, as predicted by theories. Asexuality might inhibit capacity for adaptation to environmental change, a factor that is particularly relevant for this ecologically and biogeochemically key species threatened by ocean acidification.

Key words: Adaptability, *Emiliania huxleyi*, EST, Haplo-diplobiontic life cycle,

Coccolithophores are calcifying phytoplankton that play a major role in global carbon cycling and may be negatively impacted by ocean acidification (*1*). The most abundant coccolithophore in today's oceans, *Emiliania huxleyi*, has a facultative sexual life cycle consisting of non-flagellated diploid (2N) cells that produce calcite plates (coccoliths), and haploid (1N) cells that are flagellated but not calcified (*2, 3*). Both cell types are capable of mitosis. *E. huxleyi* forms dense blooms (10^3-10^5 cells ml^{-1}) of calcified 2N cells in fjordal, coastal and open-oceanic temperate to subpolar surface waters of both hemispheres, as part of annual productivity cycles (*4*). 2N *E. huxleyi* cells are also a dominant component of coccolithophorid communities in more stable oligotrophic waters such as the Mediterranean Sea (*5*) or South Pacific gyre (*6*), despite rarely or never forming blooms in these regions and existing in populations 100-1000 fold more dilute.

We tested the hypothesis that the *E. huxleyi* life cycle has differentially adapted to bloom-promoting conditions or open-ocean conditions where blooms are not formed. 1N and 2N clonal axenic *E. huxleyi* cultures originating from the RCC1216 strain (isolated from temperate coastal waters near New Zealand) were grown under identical physiological conditions and their total DNA and mRNAs were extracted and analysed using a combination of Sanger sequenced normalized (*7*), and 454 sequenced non-normalized, cDNA libraries, as well as comparative genomic hybridization (CGH) by microarrays. 87% of Sanger ESTs and 90% of 454 cDNA sequences mapped onto the full genome assembly of *E. huxleyi* CCMP1516 (a strain from the Eastern Equatorial Pacific), suggesting an significant difference in genome content between these strains. Sequence divergence is unlikely to bias this mapping since average sequence identity between matching ESTs from three different *E. huxleyi* strains (RCC1216, CCMP1516, CCMP371) was >99.3%, which compares to that of ESTs from the same genetic background (99.7%) and thus represents a maximum estimate of allelic divergence. Varying the *BLAT* threshold between 90% and 97% did not significantly alter the percentage of RCC1216 reads that mapped to the CCMP1516 genome. CGH microarrays confirmed the gene content differences between *E. huxleyi* RCC1216 and CCMP1516 strains. 1344 genes (~5%) showed >5x lower hybridization signals in CCMP1516 relative to RCC1216 genomic DNA. At this threshold, 34% of genes had no *BLAST* hit in the CCMP1516 genome assembly and another 19% had only weak *BLAST* hits (*BLASTN* scores <200). In contrast, only 4% and 5% of genes showing <5x reduction in hybridization signal from CCMP1516 relative to RCC1216 genomic DNA had either no or weak *BLAST* hits in

the CCMP1516 genome. Genes showing weak *BLAST* hits may represent cases where a closely related gene sequence, such as a recent paralog or a remnant pseudo-gene, still exists in the CCMP1516 genome. Genes showing no *BLAST* hits and strongly reduced CGH signals likely represent genes that do not exist in the CCMP1516 genome, as confirmed by PCR tests for several target genes (Supplementary Materials).

Table 1. Mapping statistics of the ESTs (proportion/average percent identity) against CCMP1516 genome assembly

	RCC1216 (2N)	RCC1217 (1N)	CCMP1516	Total
Sanger ESTs	86.7%/???	81.7% /???	???/???	???/???
454 ESTs	???/???	???/???	???/???	???/???

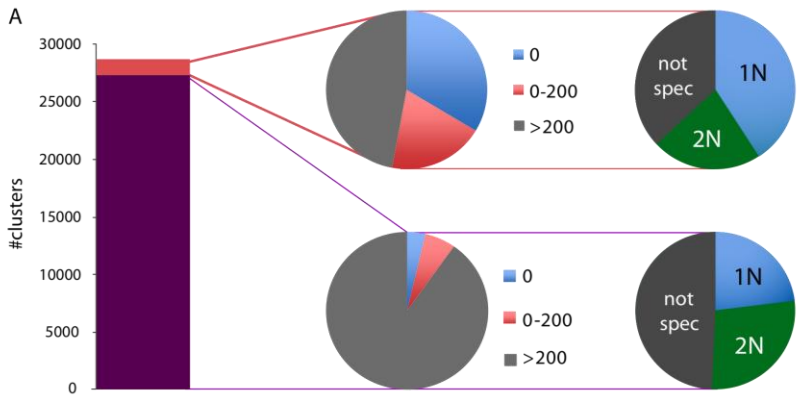

C

	DHC1b & cDHC amplify	DHC1b and/or cDHC fail to amplify
Cultures observed to form flagellated cells	17	0
Cultures not observed to form flagellated cells	22	38

Fishers exact test: p<0.0001

Figure 1. A. CGH correlates with absence or only weak homology in CCMP1516 genome assembly and with 1N-specific expression in RCC1216 genetic background. Left panel: 1344 (4.75%) of genes (EST clusters) tested exhibited >5x reduction in hybridization signal from CCMP1516 compared to RCC1216 gDNA by CGH on at least one probe. Middle panel: Proportions of genes showing no BLASTN hits (0) or weak BLASTN hits (0-200) in the CCMP1516 genome assembly among genes showing >5x reduction (top) or <5x reduction in CGH signal from CCMP1516 gDNA (difference in proportions judged to be highly significant by χ^2 test $p<0.0001$). Right panel: Ploidy-specific expression defined by microarray for the two categories of genes. B. Example PCR confirmation of gene loss from CCMP1516. Top gel: Primers for the control gene EF1a successfully amplified for all strains tested. Middle and bottom gel: Independent primer pairs for the cDHC homolog successfully amplified the expected product from the RCC1216 genetic background and several other strains. In contrast, no primer pair amplified this gene from any sub-strain of the CCMP1516 genetic background or from several other strains. Two other primer pairs yielded identical results (see Supplementary Materials). C. Failure to amplify key flagellar genes by PCR with multiple primer pairs successfully predicts lack of formation of 1N cells in culture. Genes tested included the flagellar inner arm DHC1b homolog (GJ10775) and the cytoplasmic cDHC homolog (GJ11760-GJ12389) required for maintenance of cilia and flagella). Two independent primer pairs were used to test GJ10775 and up to four independent primer pairs were used to test GJ11760-GJ12389. Control genes included the elongation factor 1a homolog GJ00953 and the t-SNARE homolog GJ03030, which were amplified from all strains. Correlation between PCR results and culture observation was judged to be highly significant (Fisher's Exact Test $p<0.0001$).

Furthermore, both 454-sequencing and CGH-microarray expression analyses showed that 1N-specific Sanger EST clusters were much less likely to map to the CCMP1516 assembly than 2N-specific or life-cycle non-specific clusters (Table 1). CGH (Fig. 1) and Illumina re-sequencing of CCMP1516 gDNA confirmed that genes displaying highly 1N-specific expression were more than twice as likely as 2N-specific or non-specific genes to show absence or reduced copy number in CCMP1516 gDNA. More detailed analyses of individual genes showing reduced CGH signals and weak or no matches in the CCMP1516 genome indicated that *E. huxleyi* CCMP1516 has likely lost the ability to form functional 1N cells. 82 EST clusters from the RCC1216 strain were identified as homologs of proteins highly specific to eukaryotic cilia or flagella (*7*), and this gene group showed expected 1N-restricted expression patterns. Strikingly, 22 (27%) of these flagellar-specific homologs did not map to the CCMP1516 genome assembly by *BLASTN* and a further 8 (10%) had weak *BLAST* scores (<200) (Table S6). Likewise 32 (39%) also appeared to be missing or under-represented in the genome of CCMP1516 by CGH (Table S6). A typical eukaryotic flagella contains >12 paralogous axonemal dynein heavy chains (DHCs) and a cytoplasmic DHC (cDHC). Absence of any DHC paralog can lead to flagellar defects (*8*). We identified 12 distinct axonemal DHC homologs and 1 cDHC homolog in EST clusters from RCC1216 1N

cells (*7*), 9 of which did map to the CCMP1516 genome assembly. Querying the CCMP1516 assembly with full length axonemal DHCs by tBLASTn revealed at least 19 loci encoding partial DHC homologs (Table 3), yet no locus had a length sufficient to encode a complete DHC protein, thus appearing to be pseudogenes. Similarly, remnants of the Outer-Arm(OA)-DHC gene were found to exist on homologous contigs of 2 scaffolds of the CCMP1516 genome. PCR (Fig. 2) and sequencing (Fig. S4) confirmed the presence of this apparent pseudogene in the CCMP1516 genome, and further showed that RCC1216 contains the full-length version of this gene specifically expressed in 1N cells.

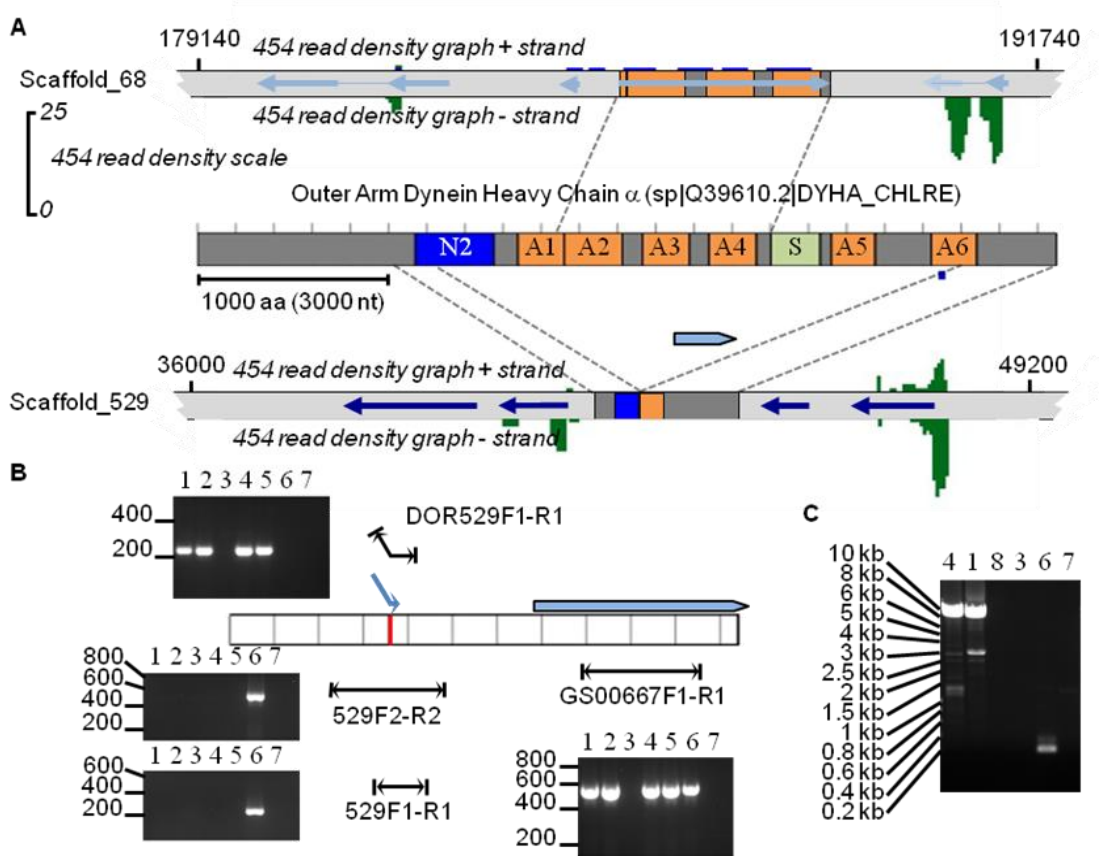

Figure 2. Independent loss-of-function rearrangments affect two alleles of OA- DHCain CCMP1516 genome. A) Scaffold_68 (top) and Scaffold_529 (bottom) contain homology to parts of *C. reinhardtii* OA- DHCa Q39610.2. Conserved DHC structure elements: AAA ATPase domains, A1-A6; N-terminal region, N2; Stalk, S. Nucleotide positions indicated above scaffolds. Arrows: gene model locations/directions of (dark blue= Sanger EST supported). Graphed 454 read mapping density: light blue, reads from RCC1217 1N cells; light green, reads from RCC1216 2N cells. Blue arrow bar: Sanger 1N EST cluster GS00667. B) PCRs confirmed predicted break of Scaffold_529 (red bar) where homology to Q39610.2 residues 1271-3957 (requiring 8074 coding nt) were deleted. PCR results displayed next to maps of primer pairs and predicted products (random-primed 1N cDNA ,1; oligo-dT-primed 1N cDNA, 2; RT- 1N RNA, 3; RCC1216 2N gDNA, 4; RCC1217 1N gDNA, 5; CCMP1516 gDNA, 6; H2O, 7; RCC1216 2N cDNA, 8). 1N 454 read FGFGJ1101DOR30 (blue arrow) matched to Q39610.2 residues 3898-3817 (E-value 3e-27). The last 46 bp were identical to Scaffold_529. Read portion

not matching to Scaffold_529 angled. C) Long-range PCR using primers 529F1-R1 and 529F2-R2 (not shown) amplified ≈8 kb fragments from RCC1217 1N cDNA and gDNA. End sequencing confirmed fragments' homology to Q39610.2 residues 1271-3957.

We thus multiplied the PCR tests on 73 additional cultured *E. huxleyi* strains from the world oceans. Using multiple primers for each target flagellar-related gene, it was confirmed that these could not be amplified from CCMP1516 and from many other strains. Whole genome Illumina sequencing of two other strains confirmed 1N-specific gene loss (in strain EH2) and retention (in strain 92F). Notably, the cDHC and the inner arm DHC1b homolog failed to amplify in 36 2N *E. huxleyi* strains, suggesting loss of the genomic potential for motility in their haploid stage, an observation corroborated by the fact that none of these cultured strains have ever been observed to produce flagellated 1N cells. In contrast, DHC genes were amplified in 37 other strains, 17 (45%) of which were observed to produce 1N flagellated cells typically within 1 year of isolation. This strongly supports that absence of these key flagellar genes is indeed linked to a loss of 1N cells from *E. huxleyi* life cycle.

The cilium/flagellum, an ancient and sophisticated eukaryotic structure, has been lost in certain extant eukaryotic lineages that nevertheless undergo sexual reproduction, such as terrestrial plants, red algae, pennate diatoms, certain fungi (*9*). In case of *E. huxleyi*, two factors suggest that the loss of the ability to form functional 1N cells correlates with the loss of capacity for sexual recombination. Firstly, syngamy is initiated by flagellar contact in haptophytes (REF), like in many other flagellated protists, ranging from green algae (*10*) to dinoflagellates (*11*). Secondly, the allelic structure of the CCMP1516 genome contains hints of long-term absence of meiotic recombination. 16 of the loci identified as containing remnant DHC-pseudogenes occurred as 9 pairs of largely homologous, likely allelic scaffolds. In 7 of these pairs, each scaffold contained pseudogenized DHC that had undergone independant loss-of-function rearrangements on otherwise homologous genomic contigs. In the 2 other pairs, a partial DHC homolog pseudogene were found on one member of the pair. Such diverging allele pairs can arise when sister chromosomes have not engaged in pairing and homologous recombination during meiosis, accumulating distinct mutations and rearrangements over thousands or millions of asexual generations (*12, 13*).

The correlated loss of flagellar genes in some but not all strains of *E. huxleyi*, a species that arose only 290 ka (*14*), shows that evolutionary loss of a highly conserved, ancestral

eukaryotic structure encoded by hundreds of genes can occur remarkably rapidly. Phylogenetic analysis of the examined *E. huxleyi* strains based on mitochondrial cytochrome c oxidase (*cox*) gene sequences shows that losses of 1N-specific genes have occurred recently and independently in separate sub-lineages of *E. huxleyi* (Fig. 3A).

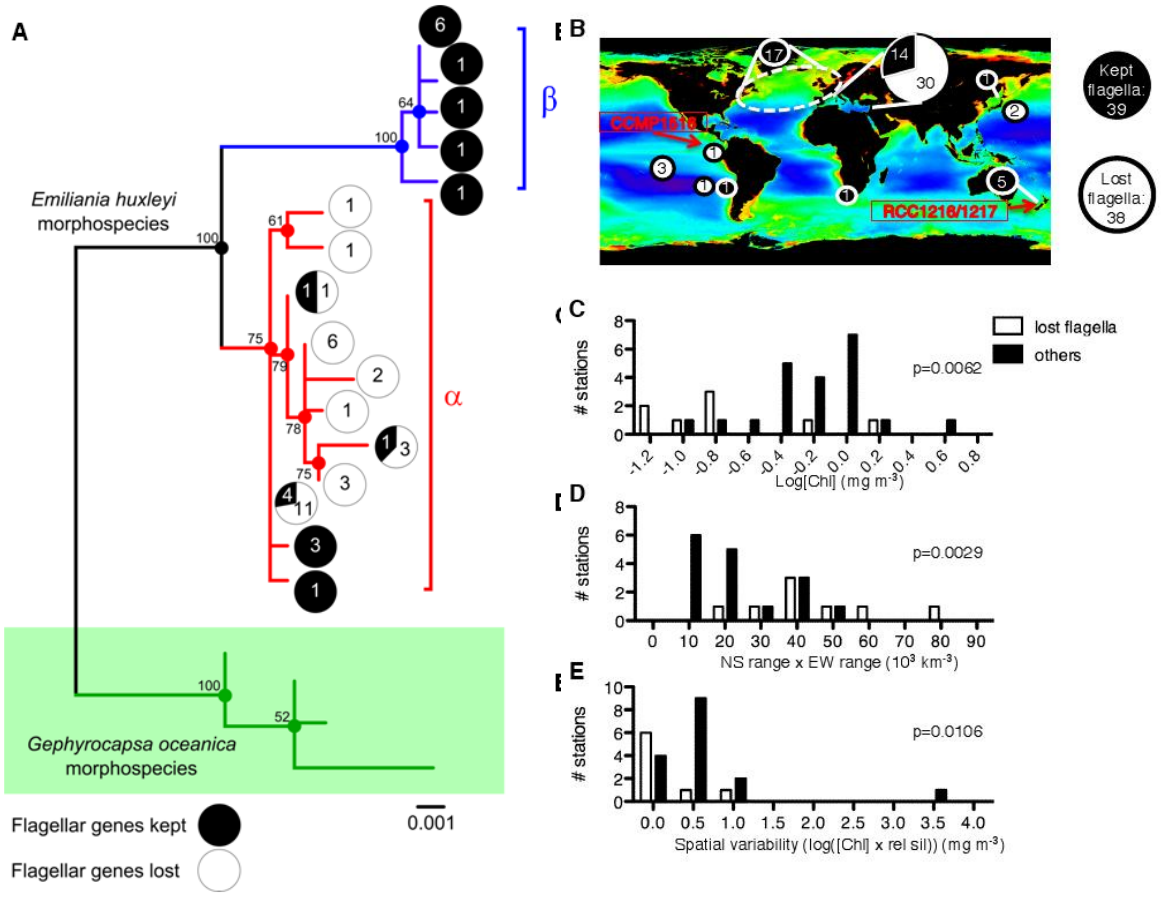

Figure 3. Loss-of-flagellar genes mapped against COX1-3 phylogeny (A) and strain origin (B), plotted on mission composite MODIS chlorophyll A, 9 km resolution (Level 3 product). C. Strains that lost flagellar genes originated from waters with lower average annual surface [Chl] (mission composite MODIS chlorophyll A, 9 km resolution, Level 3 product, averaged over 2˚x2˚ sections centered on strain origins). D. Product of spatial de-correlation scales (product of east-west range and north-south range in variogram analysis) determined from Donney *et al.* (2003) analysis of SeaWIFS ocean color data over 1998 as a measure of physical scale of environmental variability. E. Log_{10} of estimated spatial variability at strain origins (determined as $((\text{east-west relative sil})^2+(\text{north-south relative sil})^2)^{0.5}$x([Chl])).

Sexuality is the ancestral eukaryotic state, yet the evolutionary forces that maintain sex despite high inherent costs have long been debated. In terrestrial plant and animal species in which obligate asexuals and sexuals co-exist, asexuality predominates small populations inhabiting pole-ward and higher altitude marginal habitats. Competing explanations include better preservation of heterozygosity by asexuals in very small populations, higher colonizing potential of asexual reproduction, higher cost of sex in low density populations, and lower biotic stresses reducing the advantage of sex (Red Queen) (*15*).

Higher colonization potential is unlikely to select for asexuality in *E. huxleyi*, which, like other protists, is facultatively sexual. Lower abiotic pressure may play a role in the selection of asexuality in *E. huxleyi*: Arguably the major biological control on *E. huxleyi* population dynamics in productive North Atlantic and fjord systems are specific, lytic viruses (EhVs). 1N *E. huxleyi* cells are resistant to EhV infection, which might permit regular annual cycles of large-scale 2N blooms followed by viral-mediated demise (*16*). None of the *E. huxleyi* strains isolated from regions exhibiting annual EhV-controlled *E. huxleyi* blooms lost the genomic capacity to form 1N cells. In contrast, several *E. huxleyi* strains isolated from low productivity regions (Fig. 3C), where blooms are infrequently or never observed, have lost essential 1N genes. However, adaptation to oligotrophy cannot alone explain asexuality in *E. huxleyi* as some asexual strains came from relatively productive regions, such as the Equatorial Upwelling.

Higher physical variability and stronger seasonality of marginal environments has been invoked to explain patterns of terrestrial asexuality (*17*). The opposite pattern was seen in *E. huxleyi*. The strains from the North Atlantic and NW coastal Mediterranean Sea, areas exhibiting pronounced seasonality in water column hydrographic structure and productivity (*18-20*), retained flagellar genes. In contrast, 36 of 38 strains that lost genomic capacity for flagella originated from the Equatorial Pacific, South Pacific gyre, or open ocean Mediterranean, water bodies characterized by greater stability and lower seasonal variation. Likewise, strains that lost flagella - and most likely sex - tended to come from regions defined by lower spatial variability (*21*) (Fig. 3D-E).

Theoretical models indeed predict that sex is maintained in moderate-sized populations experiencing high and variable biotic pressure, but will be lost in very large populations in environments with low variability (*22*). This prediction has not previously been observed empirically, likely as well-studied terrestrial animal and plant population sizes do not reach the nearly infinite population sizes required. Marine microbes do exist in nearly infinite populations: A population of 10 cells ml^{-1} inhabiting an ocean gyre would consist of on the order of 10^{21} individuals. Asexuality might frequently be selected in marine plankton by life in huge dilute populations in relatively stable sub-tropical and tropical open ocean conditions.

The independent and significant gene content divergence between recently diverged lineages within the eukaryotic morpho-species described herein demonstrates that abrupt adaptations leading to radical physiological modification can occur in eukaryotic phytoplankton facing environmental change. This is particularly relevant to the ability to predict the response of coccolithophores to ocean acidification, where laboratory experiments yield highly variable responses between species and notably between *E. huxleyi* strains (*23-25*). Asexual populations are expected to adapt more slowly to changing environments (*26*) and cannot assimilate new adaptations from other populations. For *E. huxleyi*, for example, the productive Chilean upwelling system appears to contain populations that maintain calcification under naturally high pCO_2/low [CO_3^{2-}] conditions, whereas adjacent populations in the South Pacific gyre show decreased calcification as pCO_2 rises (*1*). Clonality in South Pacific gyre populations theoretically means they would have difficulty adapting as ocean acidification accelerates and be unlikely to obtain genetic adaptations from neighboring sexual populations. Loss of sexuality has been reported for some planktonic metazoans (*27*), and possibly one marine planktonic diatom (*28*). If the pattern of sex loss in oligotrophic open oceanic domains reported here in *E. huxleyi* is extended to other key marine planktonic biota, the inherent reduction in adaptability might have global biogeochemical implications in light of ongoing environmental changes.

Methods

Strains and growth conditions. Cultures were grown at 17˚ C, 50-80 µmol·photons·m^{-2} on a 14:10 light-dark cycle in a modified K-based medium (iK/5) containing 115 µM nitrate, 20 µM ammonium, 7.2 µM phosphate, trace metals at half the concentration of K/2, and full-strength K/2 vitamins. Cultures of CCMP1516R, B10-5, and B10-8 were made axenic following (*1*). Absence of bacteria in these strains and in RCC1216 and RCC1217 was confirmed by inoculation in bacterial test media (protocols available at ccmp.bigelow.org) and by extensive epifluorescence examination of samples fixed in 1% formaldehyde, 0.05% glutaraldehyde, stained with Sybr Green I (Invitrogen, Carlsbad, California, USA), and collected onto 0.2 µm pore-size filters (Millipore). These tests were repeated several times, always in comparison to non-axenic cultures as positive controls and sterile media as negative controls.

Cultures used for preparation of cDNA for Sanger and 454 sequencing were described previously (*1*). Briefly, after an acclimatization phase of >10 days, 10L cultures were grown in iK/5 media with ammonia at 17˚C, 100 µmol·photons·m^{-2} on a 14:10 light-dark cycle to a

density of 50000-100000 cells ml^{-1} and harvested at 8 time points equally spaced throughout the day-night cycle. For microarray expression experiments, cultures were acclimatized to iK/5 media without ammonium at 17˚C, 100 μmol·photons·m^{-2} on a 14:10 light-dark cycle for at least 10 days (including two changes of media to maintain cells in exponential growth) before inoculating 2.5L cultures. Cultures were grown to a density of 40000 to 60000 cells ml^{-1} and harvested at mid-day (6-7 hr into light) and mid-night (4-5 hr into light), at the time when the maximum number of cells was in the G2 phase of cell division as determined by flow cytometry (*1*).

DNA extraction. 25-50 ml of dense cultures (≈ 10^6 cells ml^{-1}) were harvested for DNA extraction using DNeasy Plant Mini-kit (Qiagen). DNA quantity and purity was checked by measuring A_{260}, A_{280}, and A_{230} using a Nanodrop spectrophotometer while DNA integrity was evidenced by presence of a single high molecular weight band in agarose gel electrophoresis.

RNA extraction and cDNA preparation. Cells were harvested by filtration onto 1.2 μm pore-size membrane filters (Millipore) and extracted following the Trizol protocol. Ethanol-washed total RNA pellets were resuspended in RNA-free H2O, treated with DNase I and further purified using an RNeasy Minikit following the manufacturer's recommendations (Qiagen, Valencia, California, USA). RNA quantity and quality was assessed using a Nanodrop spectrophotometer (Thermo Fisher Scientific, Waltham, Massachussets, USA) and a Bioanalyzer (Agilent Technologies, Inc., Santa Clara, California, USA). The 260:280 ratios were typically greater than 2.2 and absence of degradation was evidenced by sharp 18 s and 28 s bands. PCR tests were used to confirm absence of amplifiable DNA contamination.

454 sequencing. The same RNA samples used in construction of 1N and 2N *E. huxleyi* normalized cDNA libraries for Sanger sequencing (von Dassow *et al.* 2009) were used in Oct. 2008 for preparation of random-primed non-normalized cDNA Vertis Biotechnologies (Freising-Weihenstephan, Germany): First, poly(A^+) RNA was purified from total RNA and first-strand cDNA synthesis was performed with a N6 randomized primer. Then 454 adapters A (5'- GCCTCCCTCGCGCCATCAGCTACTAGACCTTGGCTGTCACTC) and B (TCGCAGTGAGTGACAGGCTAGTAGCTGAGCGGGCTGGCAAGGC-3') were ligated to the 5' and 3' ends of the cDNA. The cDNA was amplified with PCR using a proof reading enzyme (22 cycles). Amplified cDNA in the size range of 450 – 650 bp was eluted from a preparative agarose gel using the Macherey and Nagel NucleoSpin Extract II kit and sent to

Genoscope for 454 sequencing.

Sanger EST analysis. 38386 Sanger EST reads previously generated from RCC1216 (2N) and RCC1217 (1N) were assembled with 72513 Sanger EST reads from strain CCMP1516 (downloaded from www.jgi.doe.gov). Vector, adaptor, and poly-A sequences were removed using in-house software and the NCBI/UniVec database. Trimmed ESTs ≥ 50 nucleotides long were selected for further analysis. Single-linkage clustering was performed using BLAT version 34 with the criteria of ≥ 98% identity across the BLAT alignment and a length constraint (either the alignment was ≥ 150 nucleotides, or ≥ 90% of the length of the shortest trimmed read). The CAP_3 program was used to generate one or more 'mini-clusters' and a consensus sequence was simultaneously obtained for each of the total 38101 'mini-clusters'. Finally, a third round of clustering was performed based on the overlap of consensus sequences after BLAT mapping on the JGI draft genomic sequences of *E. huxleyi* strain CCMP1516. If the longest consensus sequence of the mini-clusters composing a cluster was shorter than 90 nucleotides, the corresponding cluster was discarded, leading to a final total of 28670 clusters.

Statistics of Sanger EST read mapping to CCMP1516 genome assembly and 454 read mapping to Sanger EST clusters. Ploidy-specific expression was determined from 454 reads from 1N and 2N cells matching to Sanger EST clusters by calculating the AudicandClaverie statistic (*2*).

Construction of microarrays. The longest mini-cluster consensus sequences in 28306 final clusters were represented by 84881 60-mer oligonucleotide probes in custom Agilent 105K microarrays (#022065), with oligonucleotide probes designed using Agilent's eArray online platform (28281 clusters were represented by 3 probes each, 12 clusters were represented by 2 probes each, 13 clusters were represented by 1 probe each, and 364 clusters could not be represented).

Microarray analysis of gene expression. Two-color competitive microarray hybridizations were conducted with each RNA sample compared against a reference RNA pool prepared by mixing equal quantities from all total RNA samples and processed in the same way. An RNA Spike-In Mix (Agilent, p/n 5188-5279) internal standard for labeling and hybridization performance was added to 4.15 µg of total RNA from each sample that was reverse-

transcribed into cDNA and then Cy3- and Cy5-labeled cRNA was *in vitro* transcribed using T7 RNA polymerase. All steps followed the Agilent QuickAmp Labeling Kit instructions with the modification that SuperScript III reverse transcriptase was added in addition to the MMLV reverse transcriptase during reverse transcription. Labeling efficiencies of cRNA were in the range 14.8-20.0 pmol dye (µg cRNA)$^{-1}$. Control arrays were prepared with the Cy3-labeled reference pool against Cy5-labeled reference pool RNA. Hybridizations were performed for 17 hr at 65˚ C in an Agilent Microarray Hybridization Chamber (Agilent #G2534A) at an agitation of 6 rpm following the manufacturer's protocol. After hybridization, arrays were disassembled in Wash Buffer 1 (Agilent, #5188-5325) and then washed 1 min in Wash Buffer 1, 1 min in 37˚ C Wash Buffer 2 (Agilent, #5188-5326), 10 s in acetonitrile, and 30 s in Stabilization and Drying Solution (Agilent, #5185-5979). Arrays were scanned in a G2565BA microarray scanner (Agilent). Raw data was extracted using Feature Extraction Software version 9.0 (Agilent) incorporating the GE2_105_Dec08 protocol. Spots flagged "outliers", "not known" or "bad" were excluded from further processing. Gene expression was analyzed using the GeneSpring software package (Agilent). Day and night time points were analyzed separately to determine probes showing expression differences between 1N and 2N using unpaired T-tests and analyzed together (by ANOVA) with a p-value cut-off of 0.05 (after Benjamini-Hochberg corrections for multiple testing). Then, genes were assigned to be 1N-specific or 2N-specific by combining data from all probes per gene and from day and night time points in the following manner: First, probes were only considered if 1N vs. 2N expression differences were not contradictory between day and night (e.g., a probe showing 1N-specific expression in day and 2N-specific expression in the night was not considered). Second, genes were assigned to be 1N-specific or 2N-specific based on the majority of probes showing significant differences. Finally, a threshold of 1.5x difference over all probes showing significant differences was selected.

Phylogenetic analysis. Cox1 and Cox3 sequences were amplified using the respective following primers set EGcox1F5 5'-GCTCACCGAACTCCTTTATTTG-3'/EGcox1R8 5'-GAAGCAATTGCATTTCATTGAG-3' and cox3F1 5’-TCCTACACTTGGATATTTAG-3’/cox3R1 5’-TCGCATTTTTGGTTTGGAAGACC-3’ as reverse. Amplification was performed in 25µL with the Mix Phusion (Finnzyme) following these PCR protocol on a ABI thermal cycler: 30s initial denaturation at 98°C, followed then by 35 cycles of 10s at 98°C, 30s annealing at 55°C, 30s extension at 72°C and a final 10 min extension step at 72°C was done to complete the amplification. Amplification products were controlled by electrophoresis

on a 1% agarose gel. The PCR products were sequenced directly on an ABI PRISM 3100 xl DNA auto sequencer (Perkin-Elmer, Foster City, CA, USA) using the ABI PRISM BigDye Terminator Cycle Sequencing Kit (Perkin-Elmer). The sequences determined in this study were deposited in GenBank.

The nucleotide sequence datasets of each gene were aligned using the online version of the multiple alignment program MAFFT (Katoh et al. 2007). Alignments were double-checked *de visu* in the sequence editor BIOEDIT (Hall 1999). Cox1 and cox3 sequences were concatenated using SequenceMatrix software. Maximum likelihood (ML) phylogenetic trees were inferred using the MEGA 5 for both genes and the concatenated dataset. Appropriate models of DNA substitution were detected with MEGA 5, using the three proposed statistics (AIC, AICc and BIC). The robustness of the branching of trees was tested by bootstrapping based on 1000 replicates for both methods. Phylogenetic trees in correspondence to fig. 3A are presented in the supplementary results (SFig. 5A-B).

References

1. L. Beaufort *et al.*, *Nature* **476**, 80 (2011).
2. J. C. Green, P. A. Course, G. A. Tarran, *J Marine Syst* **9**, 33 (Oct, 1996).
3. D. Klaveness, *British Phycological Journal* **7**, 309 (1972).
4. E. Paasche, *Phycologia* **40**, 503 (Nov, 2001).
5. I. Siokou-Frangou, U. Christaki, M. Mazzocchi, M. Montresor, D. Ribera, *Biogeosciences* **7**, 1543 (2010).
6. L. Beaufort, M. Couapel, N. Buchet, H. Claustre, C. Goyet, *Biogeosciences* **5**, 1101 (2008).
7. P. von Dassow *et al.*, *Genome Biol* **10**, R114 (2009).
8. R. Kamiya, *Int. Rev. Cytol.* **219**, 115 (2002).
9. M. L. Ginger, N. Portman, P. G. McKean, *Nat. Rev. Microbiol* **6**, 838‚Äì850 (2008).
10. E. H. Harris, *The Chlamydomonas sourcebook: A comprehensive guide to biology and laboratory use*. (Academic Press, Inc., San Diego, CA, USA, 1989), pp. 780.
11. R. Figueroa, I. Bravo, *J. Phycol.* **41**, 370 (2005).
12. D. B. Mark Welch, M. Meselson, *Science* **288**, 1211 (2000).
13. T. Schwander, L. Henry, B. J. Crespi, *Curr. Biol.*, (2011).
14. I. Raffi *et al.*, *Quaternary Sci Rev* **25**, 3113 (2006).

15. T. J. Kawecki, *Annu Rev Ecol Evol S* **39**, 321 (2008).
16. M. Frada, I. Probert, M. J. Allen, W. H. Wilson, C. de Vargas, *Proc. Natl. Acad. Sci. U. S. A.* **105**, 15944 (Oct 14, 2008).
17. J. R. Peck, J. M. Yearsley, D. Waxman, *Nature* **391**, 889 (Feb 26, 1998).
18. Y. Dandonneau, Y. Montel, J. Blanchot, J. Giraudeau, J. Neveux, *Deep Sea Research Part I: Oceanographic Research Papers* **53**, 689 (2006).
19. H. Sverdrup, *J. Cons. Int. Explor. Mer.* **18.**, 287 (1953).
20. J. Uitz, H. Claustre, B. Gentili, D. Stramski, *Global Biogeochemical Cycles* **24**, GB3016 (2010).
21. S. C. Doney, D. M. Glover, S. J. McCue, M. Fuentes, *J. Geophys. Res.* **108**, 3024 (2003).
22. S. P. Otto, *American Naturalist* **174**, S1 (Jul, 2009).
23. M. D. Iglesias-Rodriguez *et al.*, *Science* **320**, 336 (Apr 18, 2008).
24. G. Langer, G. Nehrke, I. Probert, J. Ly, P. Ziveri, *Biogeosciences* **6**, 2637 (2009).
25. U. Riebesell *et al.*, *Nature* **407**, 364 (Sep 21, 2000).
26. O. Kaltz, G. Bell, *Evolution* **56**, 1743 (Sep, 2002).
27. J. Simon, F. Delmotte, C. Rispe, T. Crease, *Journal of the Linnean Society* **79**, 151 (2003).
28. V. A. Chepurnov, D. G. Mann, K. Sabbe, W. Vyverman, *Int. Rev. Cytol.* **237**, 91 (2004).

Supplementary results

Expression differences between 1N and 2N cells.

Microarray analysis indicated potential 1N-specificity for 6327 genes (22.1%) and potential 2N-specificity for 7296 genes (25.4%). Microarray expression analysis was validated first by comparing matching 454 reads to each cluster from 1N and 2N libraries. We consider this a highly robust test for the validity of microarray data to predict expression differences as RNA for each approach was generated in completely separate experiments, involving different growth conditions, and both methods analyze the transcriptome globally. 454 EST reads overlapped 16883 (58.9%) of the 28670 Sanger EST clusters, with 454 reads from both 1N and 2N libraries matching to 8516 clusters. 454 reads overlapped 4534 clusters predicted to be 1N-specific and 4825 clusters predicted to be 2N-specific from microarray analysis.

The number of 454 read numbers per cluster for each library showed very significant correlations with the raw microarray fluorescence reads from corresponding probes on microarrays (Supplementary Figure S1 (in prep)). Likewise, the ratio of the total 454 reads that came from the 2N vs the 1N library also showed a highly significant correlation with the 1N:2N relative fluorescence ratios from microarrays (averaging across all probes and both day and night time points). In spite of the statistically highly significant correlations, in all analyses (read numbers versus raw fluorescence within a library and ploidy state, and read ratios versus fluorescence ratios between ploidy states), there was strong scatter about the central tendency. This variation may result from the fact that 1) cells harvested for the libraries were grown under somewhat different conditions than cells harvested for microarray analysis, and 2) the 454 libraries were prepared from RNA collected at 8 different time points over the day-night cycle whereas microarray analysis was conducted just at mid-day and mid-night time points. Indeed, much of the discrepancy between 454 and microarray 1N vs. 2N expression ratios was accounted for by clusters which displayed opposite ploidy specificity between day and night time points according to microarray data.

We then examined the validity of microarray and 454 profiling of 1N- vs. 2N- specificity of gene expression at the individual gene level. We checked 23 genes (represented by 24 clusters) previously found to be highly 1N-specific and 10 genes (10 clusters) previously found to be highly 2N-specific (*1*). In both cases, there was strong agreement between microarray and 454 data (Table S3). Only 1 gene (GJ03005, a putative cGMP protein kinase previously found to have highly 1N-specific expression) showed disagreement between microarray expression data and previous expression findings, as microarray results assigned

the gene as 2N-specific. We also determined correlations between microarray results and previously published qRT-PCR analysis of the ploidy-specific expression of a further 15 genes (*3, 4*) (Table S3).

Finally, we examined whether the microarray and 454 profiling of 1N- vs. 2N- specificity of gene expression successfully predicted expected expression differences based on known structural differences between 1N and 2N *E. huxleyi* cells. We considered all 82 genes previously identified in the *E. huxleyi* Sanger EST databases encoding homologs of proteins with functions highly restricted to the eukaryotic flagellum/cilium (*1*) (Tables S3, S4). These genes are expected to be expressed only in 1N cells as only 1N cells are flagellated and no flagellar structures are found in 2N cells. 56 showed significant evidence for 1N-specific expression by microarrays. In all 82 genes, the average microarray fluorescence signal from 1N RNA (averaged over all probes per gene, all replicates, and both time points) was greater than the signal from 2N RNA. Likewise, 454 reads mapped to 72 clusters. In all cases, the number of 454 reads mapping from the 1N library was greater (in fact, in only one cluster, GJ22899, did any reads map from the 2N library) and this was judged to be significant ($p<0.05$, Audic and Claverie statistic) for 46 clusters.

Comparative genomic hybridization and EST cluster mapping to genome assembly.

There were strong correlations between microarray comparative genomic hybridization (CGH) results comparing genomic DNA of CCMP1516 and RCC1216 and the mapping results comparing EST clusters to the JGI full genome assembly of *E. huxleyi* CCMP1516. The proportion of clusters with an identifiable BLASTN hit in the CCMP1516 genome dropped and the average BLAST score of clusters with a hit dropped as the CGH signal ratio CCMP1516 to RCC1216 dropped below 0.5. The threshold of 5-fold lower CCMP1516 gDNA signal to RCC1216 gDNA signal was arbitrarily chosen for the main results presented because this threshold corresponded approximately to a 10-fold increase in the number of clusters that displayed no BLASTN hits in the CCMP1516 genome assembly: Clusters displaying differences of <0.2x in CCMP1516 than RCC1216 had a much higher probability (33.6% vs. 3.2%) of not mapping to the CCMP1516 genome assembly by BLAST, or showing only a weak BLAST score (BLAST score $\leq$ 200, 19.3% vs. 6.1%) when a hit was found, when compared to clusters where the CCMP1516 signal was >0.2x that of the RCC1216 signal (Fig. S3).

The BLASTN results show that genes showing reduced representation by CGH in CCMP1516 compared to RCC1216 include an important fraction of genes that appear to be

not present in the CCMP1516 genome, in addition to other genes which may show copy number variation. We chose to focus on conserved genes that may have been lost from CCMP1516 but retained in RCC1216, as these genes may more readily yield predictions of functional differentiation (i.e., loss-of-function from CCMP1516).

The CGH and mapping results were validated by PCR targeting 5 genes found to have low CGH signal and no BLASTN hit detected in the CCMP1516 genome assembly. None of these genes could be amplified from CCMP1516 gDNA arising from 3 different sub-strains of CCMP1516 even though up to three independent PCR primer pairs were tried for some genes (Table S8). In contrast, 8 genes which displayed >0.2x CGH signal from CCMP1516 compared to RCC1216 and had BLASTN hits in the CCMP1516 genome assembly were all easily amplified by PCR from both RCC1216 and CCMP1516 gDNA (Table S8). Thus, CGH and mapping results appeared to reflect the genome content of CCMP1516.

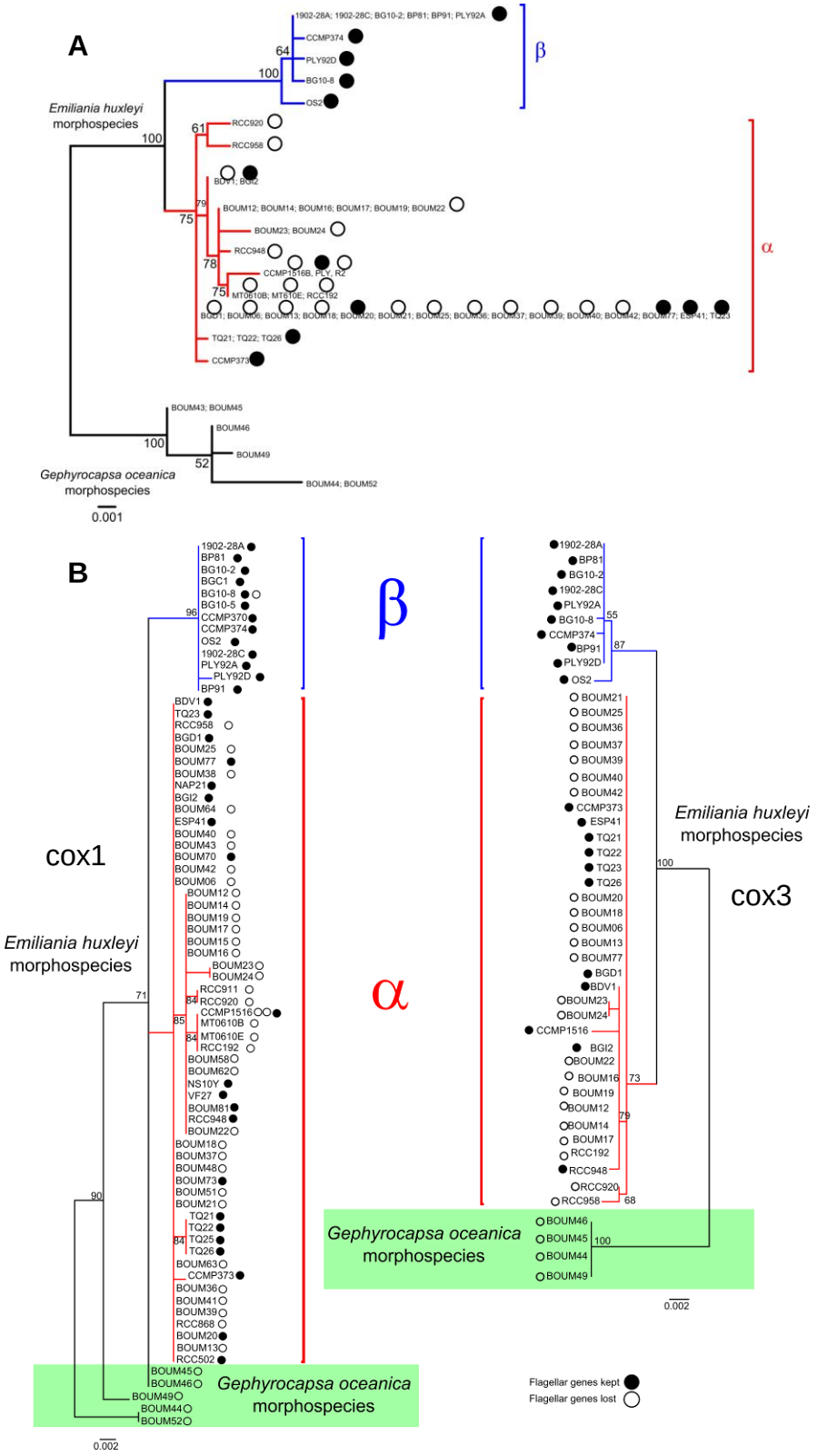

SFigure 5. Maximum likelihood phylogenetic trees of mtDNA cox1 and cox3. A. Tree obtained from concatenated cox1 and cox3, corresponding to Fig. 3A phylogenetic tree. B. Phylogenetic trees of cox1 and cox3 respectively (right to left).

References:

1. P. von Dassow *et al.*, *Genome Biol* **10**, R114 (2009).
2. S. Audic, J. M. Claverie, *Genome Res.* **7**, 986 (Oct, 1997).
3. L. Mackinder *et al.*, *Environmental Microbiology*, (in press).
4. S. D. Rokitta *et al.*, *J. Phycol.*, (in press).

CHAPITRE 6

A MORPHO-GENETIC ASSESSMENT OF MICRO-EVOLUTION IN THE COSMOPOLITAN COCCOLITHOPHORE *GEPHYROCAPSA HUXLEYI*

El Mahdi Bendif[1], Ian Probert[1], Andrea C. Highfield[2], Steven Ripley[2], Declan Schroeder[2], Kyoko Hagino-Tomioka[3], Sarah Romac[1], Margaux Carmichael[1], Jeremy Young[4], Masanobu Kawachi[5], Gustaaf Hallegraff[6] and Colomban de Vargas[1]

[1]CNRS, UMR 7144 & UPMC Univ Paris 06, Equipe *EPPO* - Evolution du Plancton et Paléo-Océans, Station Biologique de Roscoff, 29682, France

[2]The Marine Biological Association of United Kingdom, Plymouth, UK

[3]Division of Biological Sciences, Graduate School of Science, Hokkaido University, Sapporo 060-0810, Japan

[4]The Marine Biological Association of United Kingdom, Plymouth, UK

[5]Environmental Biology Division, National Institute for Environmental Studies, 16-2 Onogawa, Tsukuba, 305-8506, Japan

[6]Institute for Marine and Antarctic Studies, University of Tasmania, Private Bag 55, Hobart, Tasmania, Australia

Abstract

Gephyrocapsa huxleyi is a widely distributed bloom-forming coccolithophore that plays a key role in global marine carbon fluxes. Consequences of anthropogenically-induced increase in CO_2 such as global warming and ocean acidification likely impact such calcifying species. Like other coccolithophore species, *G. huxleyi* is defined by a morphological species concept according to the structure of the minute calcite platelets (coccoliths) covering the cell. Despite the fact that it is a relatively young taxon (first appearance in the fossil record ca. 300 ka), a number of fine-scale morphological variants (morphotypes) are recognized within the *G. huxleyi* morphospecies. Using sequences of several mitochondrial genes, we conducted multi-strain phylogenetic reconstructions of the microdiversity within this morphospecies, confirming the occurrence of two genetically and biogeographically (but not morphologically) distinct lineages within *G. huxleyi*. Comparison of inferred topologies with observed morphology and with 'coccolith morphology motifs' (CMMs) from the nuclear-encoded GPA gene, together with molecular clock dating of divergence times, gives an overview of this relatively recent radiation process. The ancestor of extant *G. huxleyi* lineages was likely morphotype A, which now contains at least two cryptic genetic entities. Other morphotypes evolved by independent diversification events in one or other of the *G. huxleyi* haplotype lineages. Diversification events in the history of the lineage mainly occurred during interglacial periods, potentially due to colonisation of newly available niches at high latitudes, but also during the last glacial period due to geographic isolation of North Atlantic and North Pacific populations. Implications of the proposed evolutionary history of *G. huxleyi* are discussed in the context of the conflicting results on coccolithophore responses to ocean acidification.

Keywords: Biomineralisation, Coccolithophore, Biogeography, *Gephyrocapsa*, Molecular-clock, Plankton evolution

Introduction

The coccolithophores are a monophyletic group of planktonic marine microalgae in the sub-class Calcihaptophycideae (Prymnesiophyceae) that produce a covering of minute calcite platelets (the coccoliths) and thereby have played extremely important roles in global biogeochemical cycles (Rost and Riebesell 2004) since their origin in the Triassic (Bown 2005). Of the ca. 250 described extant species, *Gephyrocapsa huxleyi* (Lohmann) Reinhardt (= *Emiliania huxleyi*, Bendif et al. submitted-a) is by far the most abundant and widespread, being present in all but polar oceans and regularly forming extensive "white water" blooms in high latitude coastal and shelf ecosystems. Coccolithophores have traditionally been distinguished according to a morphological species concept, with relatively gross differences in coccolith morphology (i.e. differences in arrangement and shape of the crystal units forming the coccolith) used to distinguish species, and minor differences (i.e. size of crystals (=degree of calcification)) used to distinguish "morphotypes" which are often inferred to be intra-specific variants. Comparison of gene sequences has provided evidence of pseudo-cryptic speciation within a number of well known extant coccolithophore morpho-species (Saez et al. 2003), but classical ribosomal and plastid gene markers provide little or no resolution between the two most ecologically important extant morpho-species, *G. huxleyi* and it's close relative *G. oceanica* Kamptner (Edvardsen et al, 2001; Fujiwara et al. 2001; Liu et al 2009; Bendif et al. submitted-b). These two members of the family Noëlaerhabdaceae are distinguished by their relative degree of calcification and above all by the elevation of two of the central tube crystals to form a disjunct bridge over the central area of coccoliths of *G. oceanica* (Figure 1). The fossil record suggests that *G. huxleyi* evolved from *G. oceanica*, possibly via *G. ericsonii* (= *G. protohuxleyi*, MacIntyre 1970), and the first appearance of *G. huxleyi* in the fossil record was relatively recent (291 ka, Raffi et al 2006), which explains the lack of resolution in classical ribosomal gene markers. Different morphotypes have been defined within the bridge-forming *Gephyrocapsa* complex (Bollmann 1997) and despite the fact that *G. huxleyi* has a relatively short evolutionary history, a number of different morphotypes are recognized (table 1 and see Hagino et al. 2011).

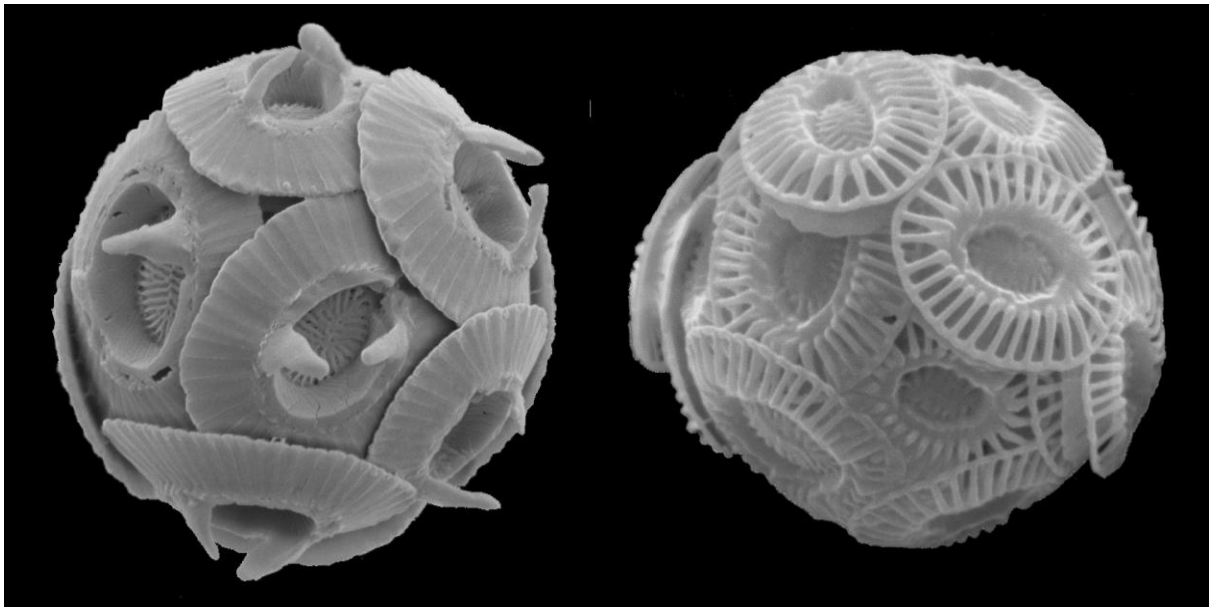

Figure 1. *Gephyrocpasa oceanica* and *Gephyrocapsa huxleyi*

Table 1. Classification of some commonly defined morphotypes

Ghux Morphotypes	Variants designation	Reference designation	Morphology of distal shield	Morphology of central area	Length of distal shield	Geographic distribution	Comparable morphotypes in literature
Type A	Var. *huxleyi*		moderate-heavily calcified elements	grill	< 4µm		Warm type (McIntyre and Bé, 1967) (Young and Westbroek, 1991)
Type R			*Reticulofenestra*-like heavily calcified distal shield elements	grill	< 4µm	South Pacific	Type R (Young et al. 2003; Cubillos et al 2007; Beaufort et al 2007; Beaufort et al 2011)
var. *corona*			moderately calcified elements with elevated central tube	grill	3.5-4.5 µm	Oligotrophic Atlantic and Pacific	var. *corona* (Okada and McIntyre, 1977)
Type B	Var. *pujosae*		lightly calcified elements	solid plate	≥ 4µm	N.Atlantic/sub artic	Type B (Young et al. 2003)
Type B/C	Var. *aurorae*	Cook et al 2011	lightly calcified elements	solid plate	< 4µm	temperate/sub polar South hemisphere	Type B/C (Young et al. 2003) Cubillos et al 2007 Cook et al 2011
Type C	Var. *kleijniae*		lightly calcified elements	solid plate	< 3.5µm	sub tropical (DCM), sub polar	Cold type (McIntyre and Bé, 1967) Type C (Findlay et Giraudeau 2000) Type C (Young et al. 2003)
Type O		Hagino et al 2011	lightly calcified elements	open	varied in size	Temperate/sub polar North and South hemisphere	Subarctic type (Okada and Honjo, 1975) Type C (Findlay et Giraudeau 2000) Type B (Young et al. 2003; Hagino et al 2005) Type C (Young et al. 2003) Type B/C (Mohan et al 2005; Cubillos et al 2007; Cook et al 2011) Type B (Hagino et al. 2005)

In terms of calcification, culture strains of different morphotypes of *G. huxleyi* have been reported to respond differently to acidification of the growth medium (Riebesell et al.

2000, Iglesias-Rodriguez et al. 2008), raising the question as to whether morphotypes are distinct genetic entities and potentially separate pseudo-cryptic species (Langer et al. 2009). Evidence from two genetic markers, the nuclear-encoded calcium-binding protein GPA gene and the plastid-encoded elongation factor *tufA* gene, provides some support for genetic separation of morphotypes. Schroeder et al (2005) demonstrated that variation (termed "coccolith morphology motifs" or CMMs) in a short non-coding region flanking the 3' end of the GPA gene correlates significantly with separation of the most widely recognized morphotypes A and B, and furthermore that morphotype A is composed of a number of distinct CMMs. Cook et al (2011) reported that *tufA* sequences distinguished morphotypes A, B/C (indistinguishable from B) and R, with little variation within morphotypes. Evidence from a mitochondrial marker spanning the cytochrome c oxidase 1 (cox1) and atp4 genes, however, indicates the occurrence of two distinct, biogeographically separated *G. huxleyi* haplotypes, with no obvious overall correlation with morphotype (Hagino et al, 2011). Bendif et al (submitted-b) determined that the use of *cox1* has certain drawbacks (the occasional presence of an intron, for example), but that a range of mitochondrial markers are suitable for phylogenetic reconstructions in this lineage, in contrast to plastid genes, the phylogenetic signals of which appear to be confused by incomplete lineage sorting.

In this study, we build on the previous studies of *G. huxleyi* microdiversity by sequencing several genetic markers from a collection of morphologically-defined, clonal cultures originating from locations throughout the world oceans. The aims of the study were to assess whether a coherent morpho-genetic classification of intra-morphospecies diversity could be achieved and to investigate the micro-evolutionary history of the lineage in an environmental context since the relatively recent appearance of this ecologically and biogeochemically important species. To this end, we undertook a molecular clock analysis of the multi-gene mitochondrial phylogeny and compared the estimated timing of diversification events with published paleo-climate records in order to reconstruct a hypothetical evolutionary scenario.

Materials and Methods

Origin and morphological characterisation of analysed strains. Clonal *Gephyrocapsa* strains (Supp Table 1) from the Roscoff Culture Collection (RCC), the Plymouth culture collection (PLY) and the Provasoli-Guillard Center for Culture of Marine Phytoplankton (CCMP) were maintained in K/2(-Si,-Tris,-Cu) medium (Keller et al. 1987) at 17°C with 50

µmol-photons.m^{-2}.s^{-1} illumination provided by daylight neon tubes with a 14:10h L:D cycle. *C*alcified cells were harvested at early exponential growth phase on 0.22 µm nucleopore filters, then dried in a 55°C oven for 2 hours. Following gold coating, filters were observed with a FEI Quanta scanning electron microscope.

DNA extraction, PCR and sequencing. Total DNA was isolated from all the strains using the DNeasy Plant mini kit (Quiagen). Gene sequences were amplified using the primers detailed in Supplementary Table 2. Amplifications were performed in a total reaction volume of 25 µL with the *GoTaq* Polymerase kit (Promega) using the following PCR protocol on a T1 thermal cycler (Biometra): 2 min initial denaturation at 95°C, followed by 35 cycles of 30s at 95°C, 30s annealing at 55°C and 1 min 30s extension at 72°C. A final 5 min extension step at 72°C was conducted to complete the amplification. PCR products were sequenced directly using the ABI PRISM BigDye Terminator Cycle Sequencing Kit (Perkin-Elmer, Foster City, CA, USA) by a ABI PRISM 3100 xl DNA auto-sequencer (Perkin-Elmer).

Phylogenetic analyses. CMMs were determined by alignment of the newly generated sequence set with sequences published by Schroeder et al. (2005). For mitochondrial genes, sequences of individual markers and sequences concatenated using the program SequenceMatrix (Vaidya et al. 2011) were manually aligned using BioEdit (Hall et al 1999). The most appropriate model of DNA substitution was estimated for each partition gene using three statistical criteria (AIC, AICc and BIC) using the partition-wise estimation option in TREEFINDER (Jobb et al 2008). Phylogenetic trees were inferred from the alignments by two phylogenetic methods, maximum likelihood (ML) using MEGA 5 (Tamura et al 2011) and Bayesian analysis (BS) with BEAST v1.4.6 (Drummond et Rambaut 2007; the branch length substitution tree was retrieved from the divergence time estimation). The robustness of ML tree branching was tested by bootstrapping based on 1000 replicates for the ML inference. For BS analyses, the Markov chain Monte Carlo analysis was run for 10 million generations, of which the last 5 million (time required for likelihood to converge on stationary value) were used for generating summary statistics and trees.

Molecular clock analyses. Molecular clock reconstructions were compared using ML and BS approaches. A prior test of clock-like behaviour between clades α and β was performed on our concatenated data set with a relative rate test (Tajima 1993) implemented in the MEGA 5 software, using a *G. oceanica* sequence as an outgroup (supp table 3). Divergence times were

estimated with constraints established from the first occurrence of *G. huxleyi* at 291 ka (Raffi et al. 2006) which is the only reliable fossil calibration for this lineage. ML reconstructions were performed in MEGA, testing the null hypothesis of a clock constrained topology against the inferred ML topology (supp tables 4, supp fig 1. and Hasegawa et al 1985). The Bayesian approach was conducted with the uncorrelated lognormal relaxed molecular clock model (Drummond et al 2006) implemented in BEAST.

Results and Discussion

Genetic vs morphological diversity

Evidence from phylogenetic reconstructions using concatenated mitochondrial markers (ca. 3500bp) supports the differentiation of *G. huxleyi* into two distinct haplotypes that potentially represent separate, reproductively isolated species. The geographical structuring of the distribution of these two haplotypes is correlated to temperature (Hagino et al. 2011), with a "warm" haplotype (α) corresponding to isolates from temperate, tropical and equatorial waters, and a "cold" haplotype (β) corresponding to isolates from temperate and sub-polar waters of both the northern and southern hemispheres (bipolar latitudinal discontinuity). Haplotype a is further characterized by 2 sub-lineages, α1 for isolates from neritic and certain open ocean provinces and α2 for isolates mainly from open ocean regions (horizontal discontinuity over a gradient from coast to open ocean). In *cox3* and *dam* phylogenies, haplotype bcomprises 3 sub-lineages with β1 assimilated to isolates from the North Atlantic, β2 to isolates from the North Pacific and β3 from the South Pacific (provincial discontinuity). While *cox1* exhibits more diversity in haplotype a than haplotype β, the other markers show the opposite trend.

The association of GPA (a gene known only from *G. huxleyi*) with coccoliths indicates a close relationship with calcification (Corstjens *et al*., 1998), but the recent finding that GPA is strongly down-regulated in calcifying cells suggests that either (i) at low levels, GPA plays a role in calcite nucleation and determining coccolith geometry, but increased cellular concentrations result in inhibition of calcite precipitation; (ii) GPA protein or *GPA* mRNA may play a role in gene regulation, or (iii) *GPA* transcripts may not be translated to protein resulting in accumulation of mRNA (McKinder et al. 2011). Conservation of the GPA gene in *G. huxleyi* suggests a strong selective constraint on the gene and probably on the mechanism of calcification. GPA cannot be directly used for evolutionary reconstructions due to lack of

phylogenetic signal (occurrence of deletions / insertions), but the genetic signal provided by CMMs (issuing from a non-coding portion adjacent to the GPA gene) provides a link between genotype and morphotype (Schroeder et al. 2005) that is further supported by our new data with the definition of a new CMM type (VI) specific to morphotype B/C and O strains.

The classification scheme of *G. huxleyi* morphotypes has not always been consistent between authors (table 1). From the "warm" and "cold" types of McIntyre and Bé (1967) to the A, B and C morphotypes of Young and Westbroek (1991), classifications based on morphometric criteria (degree of calcification, width of T-elements, coccolith length, etc.) are in some cases not easy to distinguish. All of these morphometric criteria can vary within an environmental sample and even within a clonal culture (e.g. Paasche 1998), likely reflecting environmentally-mediated cellular / gene expression influences on coccolithogenesis. Distinction of morphotypes can therefore be difficult even for an experienced observer, particularly when coccoliths are affected by dissolution. Whereas morphotypes A, R and *corona* are relatively clearly separated, morphotypes B, B/C and O are defined by empirical criteria that do not permit clear distinction (Figure 2).

One of the aims of this study was to evaluate whether a coherent combined morpho-genetic classification of microdiversity within *G. huxleyi* could be achieved. In light of the morphometric and genetic data available for our set of culture strains, we first propose the regrouping of morphotypes into 2 classes: class A which includes the previously defined morphotypes A, R and *corona*, and class B comprising the previously defined B, B/C, C and O morphotypes (Figure 2). In class A, morphotypes A and R possess CMMs I, III, IV or V, with CMMs I and III having longer sequences than CMMs IV and V (due either to deletions in the latter or insertions in the former). To our knowledge, the *corona* morphotype has never been cultured and is missing from our dataset, but morphometric characters are similar to those of morphotype A and it is therefore likely to have one of the same CMMs as class A morphotypes, or a similar, new CMM. In class B, all morphotypes have more lightly calcified coccolith T-elements. One of the criteria defined by Young and Westbroek (1991) was coccolith length, that has been defined as greater than or equal to 4 µm for morphotype B, less than or equal to 3.5 µm for morphotype C, less than 4 µm for morphotype B/C and variable for morphotype O. These distinctions are clearly inconsistent, morphotypes C and B/C, and A and O potentially overlapping. In addition, the attribution of these distinctions is based partly on the geographic region or the depth of occurrence of the morphotypes. The CMMs of these morphotypes are very similar, differing by a single substitution between morphotype B

(CMM II) and the tandem B/C and O (CMM VI), independent of the calcification state of the central area (that seems also to vary between morphotype A strains). The sequences of CMMs II and VI contain gaps similar to those of CMMs IV and V. In terms of biogeographical distribution, class A morphotypes are dominant in all but polar oceans, whereas class B morphotypes are found principally in temperate and sub-polar regions. Within class A, morphotype A is widely distributed in all oceans, whereas morphotype R is found particularly in southern hemisphere temperate waters and *corona* in oligotrophic regions. In class B, morphotypes B and C are found in the North Atlantic, and morphotypes B/C, C and O in southern sub-polar zones and the North Pacific. It is likely that the corresponding CMMs follow the same distribution patterns.

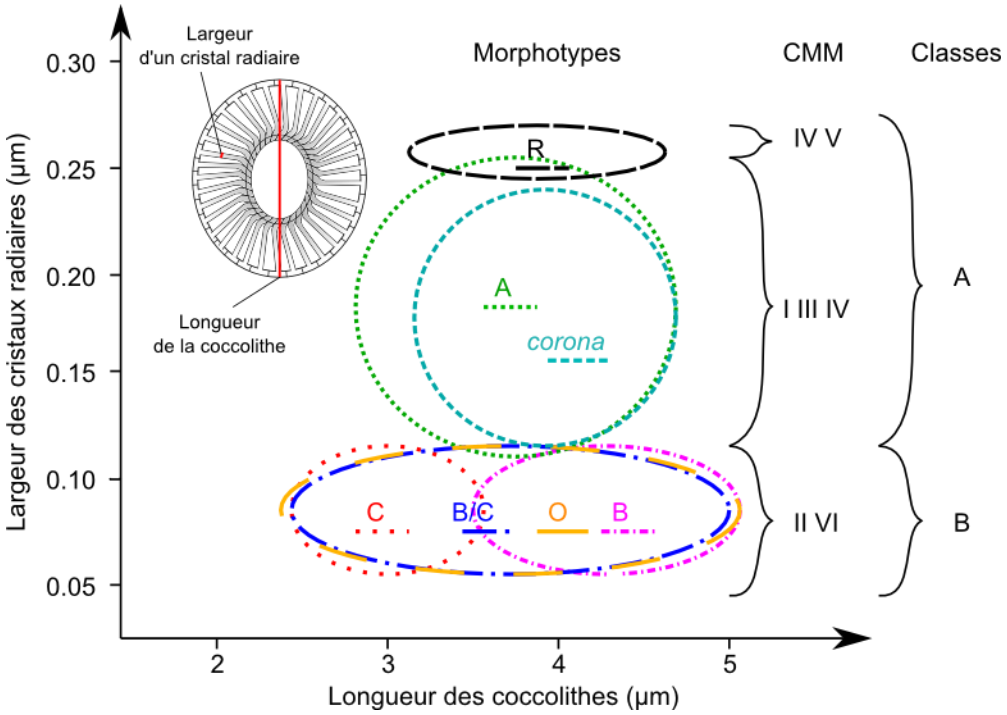

Figure 2. Characterization of the morphotypes.

Two patterns of bipolar distribution are thus found, on the one hand for morphotypes / CMMs (class A temperate and tropical, class B temperate and polar), and on the other hand for mitochondrial haplotypes (α in temperate and tropical zones, β in temperate and polar regions). However, the concordance between distribution of morphotypes/CMMs and haplotypes is not complete: *G. huxleyi* haplotype α consists only of class A morphotypes, but haplotype β includes morphotypes from the 2 classes. Mapping of morphotype/CMM distribution onto the mitochondrial phylogeny (Figure 3) provides the basis for proposing an evolutionary scenario that can account for putative biological and observed morphological

diversification within this lineage. The present distribution of morphotype A (CMMs I, III or IV) in both haplotype lineages suggests that this was the ancestral morphological state. Morphotype A is the most widely distributed and one of the most highly calcified *G. huxleyi* morphotypes, and the morphological similarity between coccoliths of *G. huxleyi* morphotype A and *G. ericsonii* provides support for this hypothesis. Of morphotype A CMMs, IV might be considered to be more recent than I and III given the occurrence of a putative deletion in the sequence of CMM IV. After divergence of the two haplotypes, morphotype R (CMM IV or V) evolved within the haplotype α_1 lineage (CMM V potentially evolving from CMM IV given sequence similarity) and morphotypes B (CMM II) and B/C / O (CMM VI) within the haplotype $\beta 3$ and $\beta 2/\beta 1$ lineages respectively (with CMMs again potentially evolving from CMM IV due to sequence similarity). The implication of this hypothesis is that morphotype A contains at least 2 cryptic lineages, whereas other morphotypes may distinguish pseudo-cryptic entities. All relatively lightly calcified morphotypes (B, B/C / O) fall within the β haplotype, distributed in colder high-latitude waters. The marked bipolarity indicates that either haplotype β populations can transit between hemispheres (perhaps at depth, as suggested by Hagino et al. 2011) or that isolated populations evolved by convergence in the different hemispheres.

Reconstruction of micro-evolution within *G. huxleyi*

The use of molecular clocks allows estimation of divergence dates of genes, and of species when the history of the gene accurately reflects that of the species. When this is the case, assuming stable evolutionary rates between lineages, estimated divergence dates allow inference of evolutionary scenarios covering the origin of species/lineages and their colonisation of different environments. In addition to the assumption on evolutionary rates, fossil calibrations (in this case the first appearance of *G. huxleyi*) are another source of potential bias. Whilst it is not possible to affirm that the calibration date used (291 ka) corresponds to the divergence date of the genes used for the molecular clock, given the quality and continuity of the coccolith fossil record, this potential bias is likely minimal (even in relative terms) compared to most molecular clock reconstructions undertaken for terrestrial organisms for which the fossil record frequently has gaps in the succession of species through time. According to the different tests applied (Supplementary Table 1), molecular clock hypotheses from mitochondrial genes are not excluded, affording a degree of confidence in

the inferences. Addition of a sequence of *G. ericsonii* to the dataset was particularly useful for strengthening confidence in the molecular clock reconstruction.

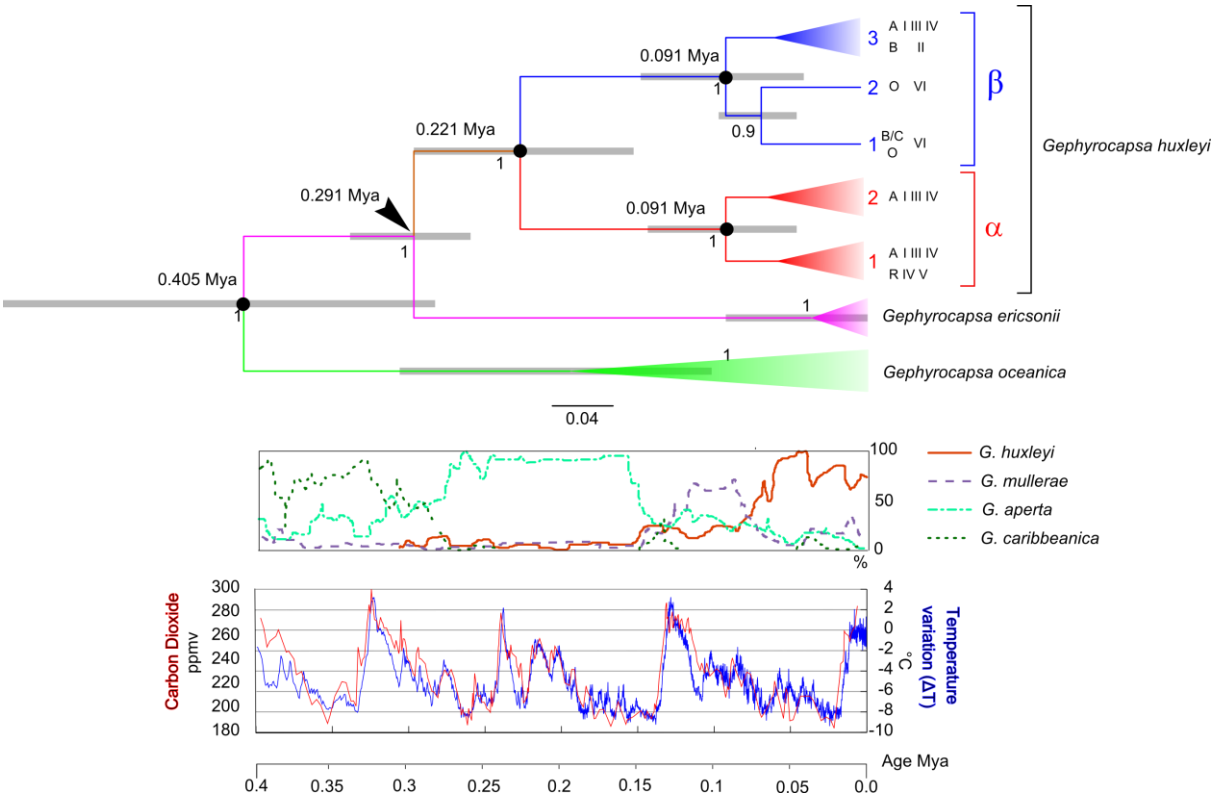

Figure 2. Divergence time estimates (Mya) among Noelaerhbdaceans based on a Bayesian relaxed molecular clock applied to a concatenated alignment of cox1, cox2, cox3, rpl16 and dam sequences, and calibrated based on the first occurrence of *G. huxleyi* (Raffi et al 2006). Uncertainty of divergence times are indicated by gray bars on internal nodes, corresponding to the 95% highest posterior density of node ages. Concordance with the fossil record is based on Hine and Weaver (1998). Carbon dioxide and temperature variation are estimated from the Vostock core (Petit et al 1999).

The definition of *G. ericsonii* varies between authors, resulting in certain discordances in terms of stratigraphic dating. Often confounded with *G. aperta* and *G. protohuxleyi*, the coccoliths of *G. ericsonii* are morphologically intermediate between *G. oceanica* and *G. huxleyi*, due to the presence of a bridge and the lightly calcified nature of T-elements. Pujo-Lamy (1977) did not give a first appearance date for this species, but inferred appearance soon before that of *G. huxleyi* according to its presence in Atlantic sediments, and Samtleben (1980) integrated this hypothesis into his phylogenetic reconstructions. Hine and Weaver (1998) put the first appearance date of this species at 370 ka following analysis of worldwide sediments. In our molecular clock reconstruction, calibrated with the first appearance of *G. huxleyi* at 291 ka, the appearance of *G. ericsonii* was estimated close to this fossil date, at 405 ka. *G. ericsonii* and *G. huxleyi* appear therefore to both have their origins in interglacial periods (between 375 and 450 ka for *G. ercisonii* and between 280 and 340 ka for *G. huxleyi*).

The little information available on *G. ericsonii* indicates that it is a species with a large biogeographic distribution, limited in the north by the transition between tropical and temperate waters and particularly present in the southern hemisphere to a latitude of around 55°. Given this distribution, the ancestor of extant *G. huxleyi* can be concluded to have had a haplotype related to the current αclade if its emergence was due to a sympatric speciation event, or related to βif its emergence was due to allopatric speciation. Biostratigraphic data on *G. huxleyi* first appearance dates in different geographical provinces tend to support the former hypothesis, but are not sufficiently numerous to conclusively answer this question.

The relative abundance of *G. huxleyi* not exceeding 20% between its first appearance and the divergence of the two haplotypes, *G. huxleyi* populations were evidently limited and relatively discrete during the first phase of its existence, perhaps constrained by niche occupation by other coccolithophores that already existed in large populations. The divergence within *G. huxleyi* between the α and β haplotypes is estimated to have occurred around 221 (150-250) ka during the end of the interglacial episode that occurred between 200 and 250 ka. The separation of haplotypes could thus correlate with the opening of new niches linked to restructuring of ocean circulation. Populations may have experienced a bottleneck during the ensuing glacial period prior to the initial diversification within each haplotype lineage that occurred consecutively in the two lineages ca. 95ka, again towards the end of an interglacial period (estimated between 90 and 140 ka), and was soon followed (90ka to present) by maximal relative abundance of *G. huxleyi* and decrease of relative abundance of *G. mullerae* and *G. aperta*. Subsequent divergence within haplotype β , estimated to have occurred ca. 70 ka during the last glacial period, could correspond to geographical separation between Atlantic and Pacific populations by limitation of exchange at the North Pole and by modification of ocean circulation in the southern oceans (Stocker et al 1991), as well as by lowering sea level. Diversification events within each lineage therefore correspond to separate isolation episodes, potentially by occupation of new niches or by geographic separation. It is not possible with the information at our disposal to deduce whether reproductive isolation within haplotypes is effective and hence whether these diversifications reflect population structuring or speciation. Genetic exchanges may well therefore be possible between lineages within haplotypes.

Concluding remarks

Conflicting results from laboratory experiments on the response of different culture strains of *G. huxleyi* to acidification have focussed attention on the potential genetic variability within this morphologically defined species and the implications of this variability in terms of future adaptability to rapid environmental change. While much has still to be learnt about the biochemical pathways and genetic basis of coccolithophore calcification, the scenario proposed here to define the nature and account for the evolution of microdiversity within this taxon provides insights into links between biology and environment as concerns coccolithophores, as well as a robust framework within which to plan and interpret future inter-strain physiological and/or genomic comparisons aimed at understanding environmental influence on the biogeochemically key process of pelagic calcification.

References

Bendif EM (a), Probert I, Young J, Schroeder D, and de Vargas, C. Species concept in the Haptophytes order Isochrysidales. *(in prep*)

Bendif EM (b), Probert I, Schroeder D and de Vargas, C. Evaluation of DNA barcodes for the cosmopolitan coccolithophores *Emiliania huxleyi* and *Gephyrocapsa oceanica* (Haptophyta) (in prep)

Bown PR (2005) Calcareous nannoplankton evolution: a tale of two oceans. *Micropaleontology*, 51(4): 299-308.

Cook, S.S., Whittock, L., Wright, S.W. & Hallegraeff, G.M. (2011). Photosynthetic pigment and genetic differences between two Southern Ocean morphotypes of *Emiliania huxleyi* (Haptophyta). *Journal of Phycology* 47(3): 615-626.

Corstjens, P. L. A. M., van der Kooij, A., Linschooten, C., Brouwers, G.-J. Westbroek, P. and de Vrind-de Jong, E. W. 1998. GPA, a calcium-binding protein in the coccolithophorid *Emiliania huxleyi* (Prymnesiophyceae). *J. Phycol.* 34:622-30.

Drummond AJ & Rambaut A (2007) "BEAST: Bayesian evolutionary analysis by sampling trees." *BMC Evolutionary Biology* 7, 214

Drummond AJ, Ho SYW, Phillips MJ, Rambaut A (2006) Relaxed Phylogenetics and Dating with Confidence. PLoS Biol 4(5): e88. doi:10.1371/journal.pbio.0040088

Edvardsen B, Eikrem W, Green JC, Andersen RA, Moon-van der Staay SY, Medlin LK (2000) Phylogenetic reconstructions of the Haptophytes inferred from 18S ribosomal DNA sequences and available morphological data. *Phycologia* 39: 19-35.

Fujiwara S, Tsuzuki M, Kawachi M, Minaka N and Inouye I (2001). Molecular phylogeny of the Haptophyta based on the *rbcL* gene and sequence variation in the spacer region of the RUBISCO operon. *Phycologia* 37: 121-129.

Hagino-Tomioka K, Bendif EM, Probert I, Young J, Kogame K, Takano Y, Horiguchi T, de Vargas C and Okada, H. (2000) New evidence for morphological and genetic variation in a cosmopolitan coccolithophore *Emiliania huxleyi* (Prymnesiophyceae) from the cox1b-ATP4 genes. Journal of Phycology 47:1164-1176

Hall TA (1999). BioEdit: a user-friendly biological sequence alignment editor and analysis program for Windows 95/98/NT. *Nucleic Acids Sym* 41: 95-98.

Hasegawa M., Kishino H., and Yano T. (1985). Dating the human-ape split by a molecular clock of mitochondrial DNA. Journal of Molecular Evolution 22:160-174.

Hine N. and Weaver, P. P. E. (1998). Quaternary. *In* Bown, P. [Ed.] *Calcareous Nannofossil Biostratigraphy.* Chapman and Hall, Cambridge, UK, pp. 266-83.

Iglesias-Rodriguez MD, Halloran PR, Rickaby REM, Hall IR, Colmenero-Hidalgo E, Gittins JR, Green DRH, Tyrrell T, Gibbs SJ, von Dassow P, Rehm E, Armbrust EV et Boessenkool KP (2008) Phytoplankton calcification in a high-CO2 world. *Science* 320: 336-340

Jobb G, von Haeseler A and Strimmer K (2004). TREEFINDER: A powerful graphical analysis environment for molecular phylogenetics. *BMC Evol Biol* 28: 4-18.

Kamptner E (1943). Zur Revision der Coccolithineen-Spezies *Pontosphaera huxleyi* Lohmann. *Anz Akad Wiss Wien Math -Naturw K* 80: 43-49.

Keller MD, Selvin RC, Claus W and Guillard RRL (1987). Media for the culture of oceanic ultraphytoplankton. *J Phycol* 23: 633-638.

Langer G, Nehrke G, Probert I, Ly J and Ziveri P (2009). Strain-specific responses of *Emiliania huxleyi* to changing seawater carbonate chemistry. *Biogeosciences* 6: 2637-2646.

Liu H, Aris-Brosou S, Probert I and de Vargas C (2010). A timeline of the environmental genetics of the haptophytes. *Mol Biol Evol* 27: 171-176.

Lohmann H (1902). Die Coccolithophoridae, eine monographie der Coccolithen bildenden flagellaten, zugleich ein Beitag zur Kenntnis des Mittelmeerauftriebs. *Arch Protistenkde* 1: 89-165

McIntyre A and Bé AWH (1967). Modern coccolithophorids of the Atlantic Ocean - I. Placoliths and cyrtoliths. *Deep Sea Res* 14: 561-597.

Mackinder L, Wheeler L, Schroeder D, von Dassow P, Riebesell U and Brownlee C (2011) Expression of biomineralization-related ion transport genes in *Emiliania huxleyi*. *Environnemental Microbiology* doi:10.1111/j.1462-2920.2011.02561.x

Paasche E (2002). A review of the coccolithophorid *Emiliania huxleyi* (Prymnesiophyceae), with particular reference to growth, coccolith formation, and calcification-photosynthesis interactions. *Phycologia* 40: 503-529.

Petit, J. R. *et al.* (1999) Climate and atmospheric history of the past 420,000 years from the Vostok ice core, Antarctica. *Nature* 399, 429-436.

Raffi, I., Backman, J., Fornaciari, E., Pälike, H., Rio, D., Lourens, L. and Hilgen, F. (2006). A review of calcareous nannofossil astrobiochronology encompassing the past 25 million years. *Quaternary Sci. Rev.* 25: 3113-37.

Rost B and Riebesell U (2004). Coccolithophores and the biological pump responses to environmental changes. In Thierstein, H. R. and Young, J. R. [Eds.] Coccolithophores – From Molecular Processes to Global Impact. Springer, Berlin. pp. 99-125.

Saez AG, Probert I, Young JR, Edvardsen B, Eikrem W et Medlin LK (2004) A review of the phylogeny of the Haptophytes. *In*: Thierstein HR, Young JR (eds) *Coccolithophores: From the molecular processes to global impact.* Springer Verlag, pp. 251-270.

Samtleben C (1980) Die evolution der coccolithophoriden-Gattung Gephyrocapsa nach Befunden im Atlantik. *PaläontologischeZeitschrift* 54, 91– 127.

Schroeder DC, Biggi GF, Hall M, Davy J, Martínez JM, Richardson AJ, Malin G and Wilson WH (2005) A genetic marker to separate *Emiliania huxleyi* (Prymnesiophyceae) morphotypes. *J Phycol* 41: 874-879.

Tajima F. (1993). Simple methods for testing molecular clock hypothesis. Genetics 135:599-607.

Young JR and Westbroek P (1991). Genotypic variation in the coccolithophorid species *Emiliania huxleyi*. *Mar Micropal* 18: 5-23.

Supplementary table 1. List of strains used in this study.

Genus	*Species*	RCC #	Strain name	Other names	Ocean Origin	Morphotype	CMM	*cox1 short*	*cox1 long*	*cox2*	*cox3*	*rpl16*	*dam*
Emiliania	*huxleyi*	174	PLY92D	92 D	English Channel	TypeB	II	Beta1	Beta1		Beta1		
Emiliania	*huxleyi*	192	RCC192	CCMP625, H3-14			III	Alpha2			Alpha2		
Emiliania	*huxleyi*	912	RCC912	Biosope_34B_HO17	Pacific Ocean	TypeA	I, IV	Alpha1		Alpha1		Alpha1	
Emiliania	*huxleyi*	920	RCC920	Biosope_32B_HO3	Pacific Ocean		III, IV	Alpha2			Alpha2	Alpha2	
Emiliania	*huxleyi*	921	RCC921	Biosope_32B_HO8	Pacific Ocean	TypeA	III, IV	Alpha2			Alpha2	Alpha2	
Emiliania	*huxleyi*	948	RCC948	Biosope_175_FL2-4	Pacific Ocean	TypeA		Alpha2			Alpha2	Alpha2	
Emiliania	*huxleyi*	1208	AS64	AC451	Mediterranean Sea	TypeA		Alpha1			Alpha1	Alpha1	Alpha1
Emiliania	*huxleyi*	1213	NAP22	AC476	Mediterranean Sea	TypeA		Alpha1	Alpha1				
Emiliania	*huxleyi*	1215	TW1	AC474	Mediterranean Sea	TypeA		Alpha1	Alpha1			Alpha1	Alpha1
Emiliania	*huxleyi*	1216	TQ26	AC472	Pacific Ocean	TypeR	IV	Alpha1			Alpha1		
Emiliania	*huxleyi*	1218	TQ25	AC471	Pacific Ocean	TypeR	IV	Alpha1	Alpha1				
Emiliania	*huxleyi*	1219	TQ23	AC469	Pacific Ocean	TypeR	IV	Alpha1	Alpha1		Alpha1		
Emiliania	*huxleyi*	1220	TQ22	AC468	Pacific Ocean	TypeR	IV	Alpha1	Alpha1	Alpha1	Alpha1		
Emiliania	*huxleyi*	1221	ASM4-3	AC456	Mediterranean Sea	TypeA		Alpha1			Alpha1	Alpha1	
Emiliania	*huxleyi*	1222	N44-20D	AC466	Baltic Sea	TypeA	IV	Beta1	Beta1				
Emiliania	*huxleyi*	1225	D2303-15	AC461	North Sea	TypeA		Beta1			Beta1	Beta1	
Emiliania	*huxleyi*	1226	D2301-5, MS1	AC460	North Sea	TypeA		Beta1	Beta1				
Emiliania	*huxleyi*	1227	D1902-28C	AC459	North Sea	TypeA		Beta1	Beta1	Beta1	Beta1		
Emiliania	*huxleyi*	1228	BDV1	AC481	English Channel	TypeA		Alpha1		Alpha2	Alpha2		
Emiliania	*huxleyi*	1229	D1902-28A	AC457	North Sea	TypeA	I	Beta1	Beta1	Beta1	Beta1		
Emiliania	*huxleyi*	1231	TQ21	AC467	Pacific Ocean	TypeR	V	Alpha1			Alpha		
Emiliania	*huxleyi*	1233	VF18	AC667	Mediterranean Sea	TypeA		Alpha1			Alpha1		
Emiliania	*huxleyi*	1235	VF20	AC669	Mediterranean Sea	TypeA		Alpha1	Alpha1	Alpha1	Alpha1		
Emiliania	*huxleyi*	1237	VF22	AC671	Mediterranean Sea	TypeA		Alpha1	Alpha1			Alpha1	
Emiliania	*huxleyi*	1238	EHJG	AC672	Pacific Ocean	TypeA		Alpha1	Alpha1				
Emiliania	*huxleyi*	1239	OS5	AC674	Pacific Ocean	TypeO	II	Beta2	Beta2	Beta2	Beta2		
Emiliania	*huxleyi*	1240	MT0610A	AC676	Pacific Ocean		III	Alpha2			Alpha2		
Emiliania	*huxleyi*	1241	MT0610B	AC677	Pacific Ocean		III	Alpha2			Alpha2		
Emiliania	*huxleyi*	1242	CCMP1516	AC665	Pacific Ocean	Naked	IV	Alpha2	Alpha2	Alpha2	Alpha2		Alpha2
Emiliania	*huxleyi*	1243	S-13	AC619	Atlantic Ocean			Alpha1			Alpha1		
Emiliania	*huxleyi*	1245	LK6	AC298	Atlantic Ocean	TypeA	I, III	Alpha1	Alpha1	Alpha1	Alpha1		
Emiliania	*huxleyi*	1246	ESP6CL2	AC304	Mediterranean Sea	TypeA	I, III						
Emiliania	*huxleyi*	1247	ESP7410	AC313	Mediterranean Sea	TypeA		Alpha1	Alpha1	Alpha1	Alpha1		
Emiliania	*huxleyi*	1249	ESP41	AC439	Mediterranean Sea	TypeA		Alpha1	Alpha1	Alpha1	Alpha1	Alpha	Alpha
Emiliania	*huxleyi*	1250	ASM6	AC453	Mediterranean Sea	TypeA		Alpha1	Alpha1				
Emiliania	*huxleyi*	1251	CC21	AC320	Atlantic Ocean	TypeA		Alpha1	Alpha	Alpha1	Alpha1		
Emiliania	*huxleyi*	1252	MT0610E	AC678	Pacific Ocean	TypeA	III	Alpha2	Alpha2		Alpha2		

Emiliania	*huxleyi*	1253	OS2	AC675	Pacific Ocean	TypeO	II	Beta2	Beta2	Beta2	Beta2		Beta2
Emiliania	*huxleyi*	1254	AS56A	AC449	Mediterranean Sea	TypeA		Alpha1	Alpha1				
Emiliania	*huxleyi*	1255	CCMP370	AC664	Atlantic Ocean	Naked	I	Beta1			Beta1		
Emiliania	*huxleyi*	1256	BP91	AC448	Atlantic Ocean	TypeA	I, IV	Beta1	Beta1	Beta1	Beta1	Beta1	
Emiliania	*huxleyi*	1257	BP81	AC447	Atlantic Ocean	TypeA		Beta1			Beta1		
Emiliania	*huxleyi*	1258	PC101	AC441	Atlantic Ocean	TypeA		Alpha1	Alpha1		Alpha1		
Emiliania	*huxleyi*	1259	CCMP374	AC663	Atlantic Ocean	Naked	I, IV	Beta1	Beta1	Beta1	Beta1		Beta1
Emiliania	*huxleyi*	1260	CCMP373	AC662	Atlantic Ocean	Naked	I	Alpha1	Alpha1	Alpha1	Alpha1	Alpha	Alpha
Emiliania	*huxleyi*	1261	ESP6CG1	AC442	Mediterranean Sea	TypeA		Alpha1	Alpha1	Alpha1	Alpha1	Alpha	Alpha
Emiliania	*huxleyi*	1262	BG10-2	BG10-2	Atlantic Ocean	TypeA		Beta1	Beta1				
Emiliania	*huxleyi*	1266	BG10-5	BG10-5	Atlantic Ocean		IV	Beta1	Beta1				
Emiliania	*huxleyi*	1268	BG10-8	BG10-8	Atlantic Ocean			Beta1	Beta1		Beta1		
Emiliania	*huxleyi*	1270	BG10-9	BG10-9	Atlantic Ocean			Beta1	Beta1				
Emiliania	*huxleyi*	1271	BGI2	BGI2	Atlantic Ocean						Alpha2		
Emiliania	*huxleyi*	1272	BG10-6	BG10-6	Atlantic Ocean	TypeA		Beta1	Beta1	Beta1	Beta1	Beta1	
Emiliania	*huxleyi*	1275	BG10-1	AC709	Atlantic Ocean			Beta1					
Emiliania	*huxleyi*	1276	BGD1	BGD1	Atlantic Ocean	TypeA	IV				Alpha1		
Emiliania	*huxleyi*	1277	BGC1	BGC1	Atlantic Ocean	TypeA		Beta1	Beta1				
Emiliania	*huxleyi*	1322	JS12	AC438	Mediterranean Sea	TypeA		Alpha1			Alpha1		
Emiliania	*huxleyi*	1710	NG1	NG1	Pacific Ocean	TypeA		Alpha2	Alpha2				
Emiliania	*huxleyi*	1731	CCMP2090	CCMP1516	Pacific Ocean	Naked	IV	Alpha2	Alpha2	Alpha2	Alpha2		
Emiliania	*huxleyi*	1812	BOUM06	BOUM6	Mediterranean Sea	TypeA	III, IV	Alpha1			Alpha1	Alpha1	Alpha1
Emiliania	*huxleyi*	1813	BOUM12	BOUM12	Mediterranean Sea	TypeA	III	Alpha2		Alpha2	Alpha2	Alpha2	Alpha2
Emiliania	*huxleyi*	1814	BOUM13	BOUM13	Mediterranean Sea	TypeA		Alpha1		Alpha1	Alpha1	Alpha1	Alpha1
Emiliania	*huxleyi*	1815	BOUM14	BOUM14	Mediterranean Sea	TypeA		Alpha1			Alpha2		
Emiliania	*huxleyi*	1817	BOUM16	BOUM16	Mediterranean Sea	TypeA		Alpha2			Alpha2		
Emiliania	*huxleyi*	1818	BOUM17	BOUM17	Mediterranean Sea	TypeA		Alpha2		Alpha2	Alpha2	Alpha2	Alpha2
Emiliania	*huxleyi*	1819	BOUM18	BOUM18	Mediterranean Sea	TypeA		Alpha1		Alpha1	Alpha1	Alpha1	Alpha1
Emiliania	*huxleyi*	1820	BOUM19	BOUM19	Mediterranean Sea	TypeA		Alpha2			Alpha2		
Emiliania	*huxleyi*	1821	BOUM20	BOUM20	Mediterranean Sea	TypeA		Alpha1			Alpha1	Alpha1	Alpha1
Emiliania	*huxleyi*	1822	BOUM21	BOUM21	Mediterranean Sea	TypeA		Alpha1			Alpha1		
Emiliania	*huxleyi*	1823	BOUM22	BOUM22	Mediterranean Sea			Alpha2			Alpha2		
Emiliania	*huxleyi*	1824	BOUM23	BOUM23	Mediterranean Sea	TypeA		Alpha2			Alpha2		
Emiliania	*huxleyi*	1825	BOUM24	BOUM24	Mediterranean Sea	TypeA		Alpha2			Alpha2		
Emiliania	*huxleyi*	1826	BOUM25	BOUM25	Mediterranean Sea			Alpha1			Alpha1		
Emiliania	*huxleyi*	1827	BOUM36	BOUM36	Mediterranean Sea	TypeA		Alpha1			Alpha1		
Emiliania	*huxleyi*	1828	BOUM37	BOUM37	Mediterranean Sea	TypeA		Alpha1			Alpha1		
Emiliania	*huxleyi*	1830	BOUM39	BOUM39	Mediterranean Sea	TypeA		Alpha1			Alpha1		
Emiliania	*huxleyi*	1831	BOUM40	BOUM40	Mediterranean Sea	TypeA		Alpha1			Alpha1		

Emiliania	*huxleyi*	1833	BOUM42	BOUM42	Mediterranean Sea	TypeA		Alpha1			Alpha1			
Emiliania	*huxleyi*	1857	BOUM77	BOUM77	Mediterranean Sea	TypeA		Alpha1			Alpha1			
Emiliania	*huxleyi*		C2		South Pacific						Beta3		Beta3	
Emiliania	*huxleyi*		C4		South Pacific						Beta3		Beta3	
Emiliania	*huxleyi*		C6		South Pacific						Beta3		Beta3	
Emiliania	*huxleyi*		C7		South Pacific	Type B/C?					Beta3		Beta3	
Emiliania	*huxleyi*		C8		South Pacific						Beta3		Beta3	
Emiliania	*huxleyi*		C9		South Pacific						Beta3		Beta3	
Emiliania	*huxleyi*		ESP7414	ESP7414	Mediterranean Sea	TypeA	I, III	Alpha1						
Emiliania	*huxleyi*		J26		Irish sea???						Beta1		Alpha	
Emiliania	*huxleyi*		J7		Irish sea???						Beta1		Alpha	
Emiliania	*huxleyi*		J9		Irish sea???						Beta1		Alpha	
Emiliania	*huxleyi*		MM1	MM1	Pacific Ocean	TypeA		Beta1	Beta1		Beta1	Beta1		
Emiliania	*huxleyi*		PLY573	PLY573				Alpha1			Alpha1	Alpha		
Emiliania	*huxleyi*		PLY92A	PLY92A	English Channel	TypeA		Beta1	Beta1		Beta			
Emiliania	*huxleyi*		PLYM202	PLYM202	South Pacific			Alpha1			Alpha			
Emiliania	*huxleyi*		PLYM218	PLYM218	South Indian ocean		IV	Beta1			Alpha			
Emiliania	*huxleyi*		PLYM219	NZEH	South Pacific	TypeA	IV	Beta1	Beta1		Beta1			
Gephyrocapsa	*oceanica*	1223	ASM9	AC454	Mediterranean Sea	Gephy		Alpha1						
Gephyrocapsa	*oceanica*	1224	ASM9(N)	ASM9(N)	Mediterranean Sea	naked		Alpha1						
Gephyrocapsa	*oceanica*	1244	MM4-3	AC673	Pacific Ocean	Gephy		Gephy						
Gephyrocapsa	*oceanica*	1279	ESP755	AC315	Mediterranean Sea	Gephy		Gephy						
Gephyrocapsa	*oceanica*	1280	ESP752	AC314	Mediterranean Sea	Gephy		Gephy						
Gephyrocapsa	*oceanica*	1281	THAU1	AC338	Indian Ocean	Gephy		Alpha1	Gephy		Gephy	Gephy	Gephy	
Gephyrocapsa	*oceanica*	1282	ESP6M11	AC311	Mediterranean Sea	Gephy		Alpha1		Gephy	Gephy	Gephy		
Gephyrocapsa	*oceanica*	1284	ESP6M3	AC309	Mediterranean Sea	Gephy		Gephy		Gephy	Gephy	Gephy	Gephy	
Gephyrocapsa	*oceanica*	1285	ESP6M2	AC308	Mediterranean Sea	Gephy		Alpha1				Gephy		
Gephyrocapsa	*oceanica*	1286	AS62E	AC332	Mediterranean Sea	Gephy		Alpha1			Gephy	Gephy		
Gephyrocapsa	*oceanica*	1287	AS62A	AC328	Mediterranean Sea	Gephy		Alpha1			Gephy	Gephy		
Gephyrocapsa	*oceanica*	1288	JS8	AC287	Mediterranean Sea	Gephy		Alpha1	Gephy		Gephy			
Gephyrocapsa	*oceanica*	1289	ASM10	AC325	Mediterranean Sea	Gephy		Alpha1				Gephy	Gephy	
Gephyrocapsa	*oceanica*	1292	PR3F1	AC638	Atlantic Ocean	Gephy		Gephy	Gephy		Gephy	Gephy	Gephy	
Gephyrocapsa	*oceanica*	1293	NS10Z	AC337	Atlantic Ocean	Gephy		Alpha1			Gephy			
Gephyrocapsa	*oceanica*	1295	PZ1-3	AC642	Pacific Ocean	Gephy					Gephy			
Gephyrocapsa	*oceanica*	1296	ESP56	AC277	Mediterranean Sea	Gephy		Alpha1						
Gephyrocapsa	*oceanica*	1297	PZ3-14	AC648	Pacific Ocean	Gephy		Alpha1	Gephy		Gephy			
Gephyrocapsa	*oceanica*	1300	PZ3-1	AC645	Pacific Ocean	Gephy		Alpha1	Gephy		Gephy	Gephy	Gephy	
Gephyrocapsa	*oceanica*	1302	JS7	AC286	Mediterranean Sea	Gephy		Alpha1			Gephy			
Gephyrocapsa	*oceanica*	1303	LK7	AC300	Atlantic Ocean	Gephy		Gephy	GephyII		Gephy	Gephy	Gephy	

Gephyrocapsa	*oceanica*	1305	PC65	AC295	Atlantic Ocean	Gephy	Alpha1	Alpha1		Gephy	Gephy		
Gephyrocapsa	*oceanica*	1306	PC64	AC294	Atlantic Ocean	Gephy	Alpha1			Gephy			
Gephyrocapsa	*oceanica*	1307	PC51	AC293	Atlantic Ocean	Gephy	Alpha1						
Gephyrocapsa	*oceanica*	1308	JS15	AC291	Mediterranean Sea	Gephy	Alpha1		Gephy	Gephy	Gephy	Gephy	
Gephyrocapsa	*oceanica*	1309	JS14	AC290	Mediterranean Sea	Gephy							
Gephyrocapsa	*oceanica*	1310	PR3S4	AC637	Atlantic Ocean	Gephy	Gephy			GephyI			
Gephyrocapsa	*oceanica*	1316	LK9	AC302	Atlantic Ocean	Gephy	Gephy	Gephy			Gephy		
Gephyrocapsa	*oceanica*	1317	JS10	AC288	Mediterranean Sea	Gephy	Alpha1		Gephy	Gephy	Gephy	Gephy	
Gephyrocapsa	*oceanica*	1318	THAU4	AC480	Indian Ocean	Gephy	Gephy		Gephy	Gephy			
Gephyrocapsa	*oceanica*	1319	NS6-2	AC335	Atlantic Ocean	Gephy	Alpha2			Gephy			
Gephyrocapsa	*oceanica*	1320	ESP6M6	AC479	Mediterranean Sea	Gephy			Gephy	Gephy			
Gephyrocapsa	*oceanica*	1562	NIES1000	CCMP 2054	Pacific Ocean	Gephy	Gephy	Gephy	GephyI	Gephy			
Gephyrocapsa	*oceanica*	1709	MT0610G	MT0610G	Pacific Ocean	Gephy	Alpha1			Gephy	Gephy		
Gephyrocapsa	*oceanica*	1796	DS7	DS7	South China Sea	Gephy	Gephy			Gephy			
Gephyrocapsa	*oceanica*	1834	BOUM43	BOUM43	Mediterranean Sea	Gephy	Alpha1			Gephy			
Gephyrocapsa	*oceanica*	1835	BOUM44	BOUM44	Mediterranean Sea	Gephy	Gephy			Gephy			
Gephyrocapsa	*oceanica*	1836	BOUM46	BOUM46	Mediterranean Sea	Gephy	Gephy			Gephy			
Gephyrocapsa	*oceanica*	1839	BOUM50	BOUM50	Mediterranean Sea	Gephy	Gephy	Gephy		Gephy			
Gephyrocapsa	*oceanica*	1841	BOUM53	BOUM53	Mediterranean Sea	Gephy	Gephy			Gephy			
Gephyrocapsa	*oceanica*	1842	BOUM54	BOUM54	Mediterranean Sea	Gephy	Gephy	Gephy					
Gephyrocapsa	*oceanica*		BOUM45	BOUM45	Mediterranean Sea	Gephy	Gephy			Gephy			
Gephyrocapsa	*oceanica*		LK7	LK7	Atlantic Ocean	naked	Alpha1	Gephy			Gephy		
Gephyrocapsa	*oceanica*		MM4_6	MM4_6	Pacific ocean	Gephy	Alpha1			Gephy			
Gephyrocapsa	*oceanica*		MT3-6	MT3-6		Gephy	Gephy	Gephy			Gephy	Gephy	
Gephyrocapsa	*oceanica*		PR3F3	PR3F3	Atlantic Ocean		Gephy	Gephy					

Supplementary table 2. Results from Tajima's Relative Rate Test for 3 sequences

Configuration	Count
Identical sites in all three sequences	2431
Divergent sites in all three sequences	0
Unique differences in Sequence A	14
Unique differences in Sequence B	13
Unique differences in Sequence C	35

NOTE.-- The equality of evolutionary rate between sequences **A** (*CCMP374 3614 bases*) and **B** (*CCMP373 3614 bases*), with sequence **C** (*LK7 254 3614 bases*) used as an outgroup in Tajima's relative rate test [1]. The χ^2 test statistic was 0.04 (P = 0.84739 with 1 degree[s] of freedom) . P-value less than 0.05 is often used to reject the null hypothesis of equal rates between lineages. The analysis involved 3 nucleotide sequences from concatenated *cox1*, *cox2*, *cox3*, *rpl16* and *dam*. All positions containing gaps and missing data were eliminated. There were a total of 2493 positions in the final dataset.

Supplementary table 3. Results from a test of molecular clocks using the Maximum Likelihood method

	ln*L*	Parameters	(+*G*)	(+*I*)
With Clock	-1586.295	24	n/a	n/a
Without Clock	-1574.364	43	n/a	n/a

NOTE.-- The molecular clock test was performed by comparing the ML value for the given topology with and without the molecular clock constraints under Hasegawa-Kishino-Yano (1985) model [1]. The null hypothesis of equal evolutionary rate throughout the tree was not rejected at a 5% significance level (P < 0.201499007361498). The analysis involved 21 nucleotide sequences. All positions containing gaps and missing data were eliminated. There were a total of 918 positions in the final dataset.

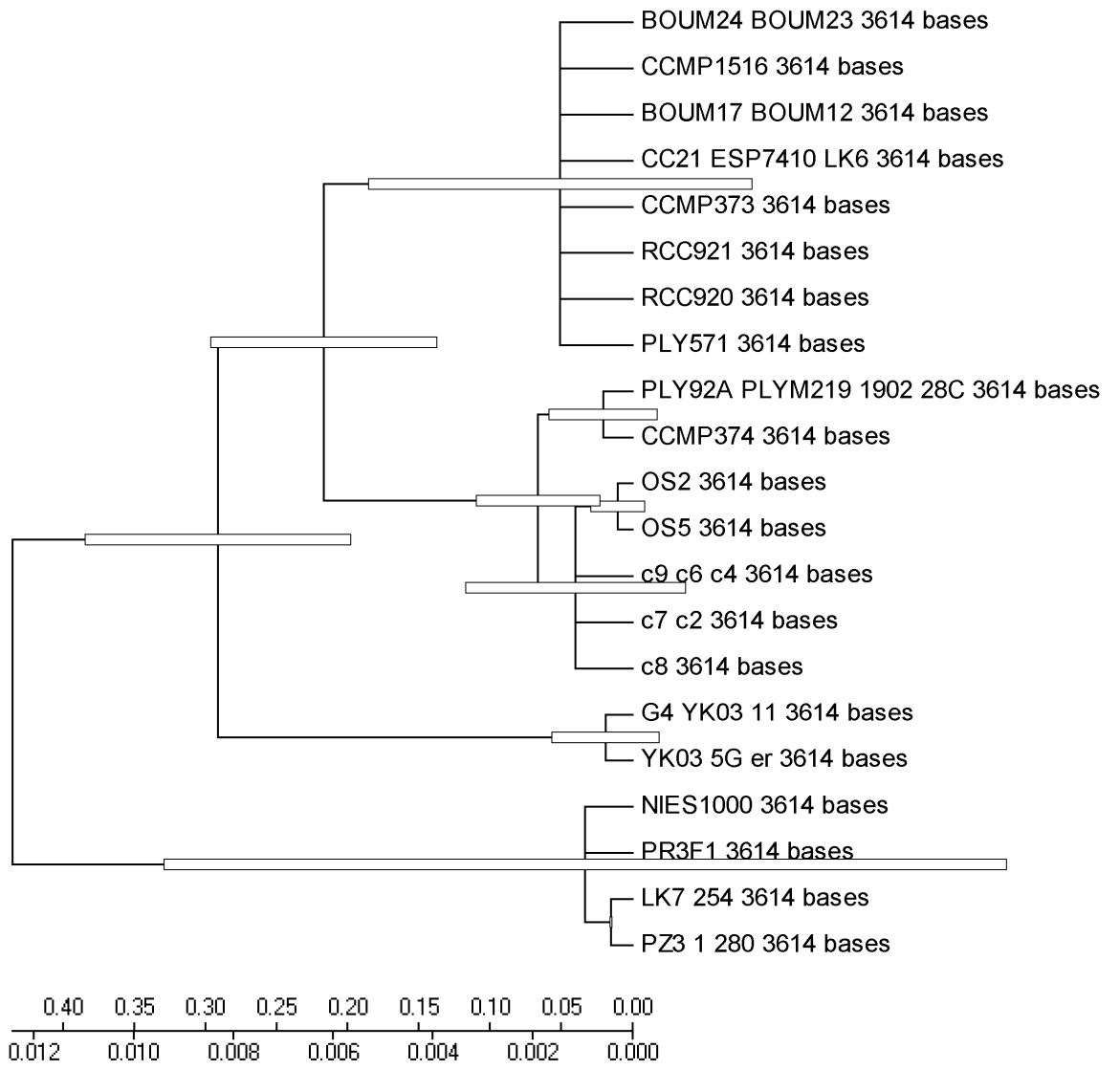

Supplementary figure 1. Chronogram obtained from the Maximum likelihood approach.

DISCUSSION

E. huxleyi, sa famille et ses « sœurs », un problème de définition des espèces

La révision du contexte phylogénétique des Isochrysidales a mis en évidence une différence fondamentale dans les approches taxinomiques utilisées pour chacune des familles,. La primeur du concept d'espèce basé sur la morphologie et l'ultrastructure est en partie dûe à l'histoire des méthodologies appliquées à l'ensemble des protistes et en particulier aux flagellés. Chez les Noëlaerhabdaceae, la présence évidente des coccolithes a certainement influencé le choix d'un concept d'espèce basé sur l'exosquelette calcitique et sa morphométrie, également exploitable en micropaléontologie et stratigraphie. Chez les Isochrysidaceae, l'absence des coccolithes a contribué au choix d'un concept d'espèce basé sur la morphologie cellulaire et son organisation ultrastructural. Malgré de nombreuses similitudes ultrastructurales et métaboliques, telle que la production des alcénones, de nombreux auteurs ont souvent maintenus une séparation des deux familles dans des ordres différents (Chretiennet-Dinot 1990 et 1993; Green et Jordan 1994). Un concept phylétique basé sur l'analyse des séquences ADN (Edvardsen et al 2000) a finalement permis d'opter pour la réunification des deux familles au sein d'un seul et même ordre. Les distances génétiques des trois marqueurs génétiques analyses au cours du présent travail confirment la distinction des deux familles. Les Isochrysidaceae présentent de plus grandes divergences génétiques que les Noëlaerhabdaceae, cependant l'ultrastructure et la morphologie des Isochrysidaceae sont étonnamment conservées, notamment entre les genres *Isochrysis* et *Tisochrysis*. Chez les Noëlaerhabdaceae, les ultrastructures cellulaires sont également très conservées, alors que les caractères morphologiques de la coccosphère sont singulièrement plastiques, comme par exemple le pont de calcite qui distingue les coccolithes du genre *Gephyrocapsa* de celui d'*Emiliania*. Ainsi, si l'on garde une cohérence dans les critères taxinomiques au niveau de l'ordre, le transfert de l'espèce *E. huxleyi* dans le genre *Gephyrocapsa*, déjà proposé en 1972 par Reinhardt, semble tout a fait logique, soutenu par la très faible distance génétique entre les deux espèces et l'unique caractère que represent ce crystal surnuméraire.

Chez les Noëlaerhabdaceae, les séquences de l'ADN ribosomique ne permettent pas d'analyse phylogénétique. Une seule et unique substitution sépare *Gephyrocapsa huxleyi* de *G. oceanica*. L'immense taille des populations effectives chez les protistes (Piganneau et al. 2010) pourrait expliquer la conservation particulièrement forte des séquences d'ARN

ribosomiques. Mais avant tout, l'implication de ces molécules dans le mécanisme génétique fondamental et moléculairement complexe de la traduction des ARNm en proteines est à l'origine d'une forte pression de sélection stabilisatrice. Plus un gène est sollicité dans un réseau fonctionnel complexe, plus sa séquence est conservée. Les ARN ribosomiques sont de loin les molécules les plus exprimées dans toutes cellules et ils interagissent avec de nombreux partenaires moléculaires lors de la synthèse protéique. Finalement, le mécanisme encore mal compris de l'évolution concertée qui uniformise les multiples copies des gènes ribosomaux présent dans chaque génome pourrait avoir un impact négatif sur le taux de fixation des mutations.

D'une singulière ubiquité …

Théoriquement, les gènes cytoplasmiques évolueraient plus rapidement que les gènes nucléaires (Birky et al 2006). Cependant les gènes chloroplastiques étudiés jusqu'à présent chez les Noëlaerhabdaceae ne présentent pas de variations, ou alors des phylogénies discordantes avec l'histoire des espèces pour *tufA* (voir prochain paragraphe; Medlin et al 2008; Cook et al, 2011)). Les gènes mitochondriaux n'avaient jamais été testés au sein des Gephyrocapsids avant nos travaux.

Ainsi nous avons teste une série de gènes d'origine génomique cytoplasmique chez les Noëlaerhabdaceae: *tufA* et *petA* pour le plaste et *cox1*, *cox2*, *cox3*, *rpl16* et *dam* pour la mitochondrie. Les gènes *16S*, *rbcl*, *rbcs* et *tufA* font parties des gènes fondamentaux des génomes plastidiaux à l'instar de *petA* bien que présents dans la plupart des grandes lignées photosynthétique (Sanchez Puerta et al 2005). De même, *cox1*, *cox2*, *cox3* et *rpl16* sont communs a tous les génomes mitochondriaux, alors que le gène *dam*, codant pour une N6 adénine méthylase, ne trouve d'homologues que chez les procaryotes, les virus et *Anophelia gambia*[1] (Sanchez Puerta et al. 2004).

Les marqueurs plastidiaux analyses démontrent des taux substitutions et des distances relativement élevés sans pour autant permettre de distinguer les espèces *G. oceanica* et *G.*

[1] Cette famille fonctionnelle de gène est impliquée dans les mécanismes de défense contre les pathogènes (souvent les virus bactériophages) chez les procaryotes ce qui en suggère une évolution liée à la « course aux armes ». L'état de méthylation de l'ADN en modifierait la conformation rendant le contenu génique potentiellement inaccessible et/ou inhiberait l'expression de gènes. Cette présence au sein d'une mitochondrie eucaryote est assez rare et en suppose soit une origine par transfert latéral par une bactérie ou un virus, soit un gène reliquat provenant de l'ancêtre mitochondrial ou alors une origine par un transfert latéral provenant d'un autre compartiment génomique.

huxleyi. Les phylogénies moléculaires basées sur les gènes *petA* et *tufA* sont incongruentes et polyphyletiques, suggérant une ségrégation incomplète des lignées génétiques décalant l'histoire des gènes de celle des espèces. La discordance entre l'histoire d'un gène et l'histoire des espèces dépend du rapport entre le temps de spéciation et le temps de coalescence. L'histoire des gènes répond de phénomènes aléatoires, variant suivant les forces relatives de la sélection et de la dérive génétique, qui en détermine le temps rétrospectif de ségrégation (coalescence). L'apparente polyphylie des reconstructions chloroplastiques pourrait aussi etre due à des phénomènes d'introgression entre les différentes lignées évolutives de *Gephyrocapsa*, voir aussi à une transmission monoparentale non exclusive du plaste. Cependant le manque de connaissance sur la transmission –verticale et/ou horizontale- du plaste ne nous permet pas de nous prononcer.

Dans le cas du gène *petA*, de nombreuses branches non soutenues (bootstraps inferieurs à 70%) amènent à certaines irresolutions de la reconstruction phylogénétique (polytomies), indiquant un signal phylogénétique douteux, potentiellement du à une évolution rapide du gène. De plus, la relative absence des substitutions non-synonymes témoigne potentiellement d'une pression de sélection purifiante malgré la proportion relativement élevée de substitutions par rapport aux autres gènes étudiés. Le gène *tufA*, lui, présente un taux de substitution relativement plus faible, mais plus de substitutions non-synonymes. Nous pouvons supposer que la pression de sélection est plus faible permettant la fixation de plus de substitutions affectant la séquence protéique alors que l'évolution du gène est plus lente. Le niveau de saturation en substitution nucleotidique de la troisième position des codons est généralement estimé afin de vérifier la validité du signal phylogénétique des gènes codants mais les faibles distances entre nos lignées n'en permettent pas une estimation adéquate.

Les phylogénies des gènes mitochondriaux, quant a elles, ne concordent que peu (*tufA*) ou pas avec celles des marqueurs plastidiaux, mais concordent avec la phylogenie du *28SrDNA*[1] et avec les donnes strato-phénétiques des Noëlaerhabdaceae. La séparation entre *G. oceanica* et *huxleyi* est marquée par une distance génétique variable selon le taux de substitution des marqueurs et une variabilité intraspécifique est détectée a l'intérieur des deux lignées principales, avec notamment la distinction claire de deux haplotypes pour la morpho-

[1] Une phylogénie préliminaire basée sur le gène nucléaire *eif1* (facteur d'élongation 1) sépare distinctement *G. oceanica* et *huxleyi* deux espèces mais deux formes alléliques semblent coexister au sein de nombreuses souches de *G. huxleyi*. Le fragment ciblé inclut deux zones introniques hautement variables non alignables lorsque les deux copies allèliques du gène sont présentes. L'étude de ce gène encore en cours nécessite une attention particulière de séquençage et de clonage pour une analyse approfondie.

espèce *G. huxelyi*. Cette monophylie réciproque est confirmée par toutes les phylogénies mitochondriales, à part *cox1* qui présente un patron paraphylétique.

Le gène *cox1* montre des caractéristiques structurales particulières. Il est séparé en deux fragments distants dans le génome mitochondrial, ce qui suggère un épisode de recombinaison antérieur à l'apparition de *G. oceanica* et surtout une structure du génome en opéron où l'ensemble des gènes seraient transcrits puis exprimés après un processus d'épissage dont un épissage alternatif spécifique pour le gène *cox1* (Sanchez Puerta et al 2004). Chez certaines souches, *cox1* est pourvu d'un intron long de ~2,500pb, spécifique pour chacune des deux morpho-espèces. Ces introns seraient assimilables a ceux trouvés dans les genes mitochondriaux de *Pavlova lutheri* et *Thalassosira pseudonana* (Ehara et al, 2000), et correspondraient à des introns de type 2 qui ont la caractéristique de s'auto-épisser lors de la maturation de l'ARNm. L'expression du gène cox1 présente donc un degré potentiel de régulation accentué par sa disposition dans le génome mitochondrial, ce qui peut sembler paradoxal etant donne son importance métabolique fondamentale. *Cox1* est aussi le gène qui présente le moins de substitutions non-synonymes parmi les gènes mitochondriaux étudiés, la seule substitution non-synonyme caractérisant la région 3' terminale d'un type d'haplotypes de *G. oceanica*. Cette substitution affecte la séquence protéique sans en changer l'encombrement stérique. Ainsi la conformation de la protéine serait conservée, soulignant son importance vitale. De plus, cox1 possède le taux de substitutions le plus bas de notre jeu de données bien qu'il soit le plus polymorphique parmi les souches de *G. oceanica*, générant le patron morphospecifique paraphylétique susmentionné. Les autres gènes mitochondriaux présentent plus de substitutions et sont moins polymorphiques. Leurs phylogénies génèrent des patrons monophyletiques pour les espèces. L'ensemble des marqueurs mitochondriaux définissent deux espèces phylogénétiques au sein de *G. huxleyi*, correspondant à une distribution géographique sans recouvrement évident des morphotypes.

… à la bipolarité pseudocryptique

Biogéographie mitochondriale

La structuration géographique des deux haplotypes mitochondriaux principaux de *G. huxleyi* définit une distribution bipolaire. La biogéographie des deux populations distinctes

semble corréler à des différences de température (chapitre 3), avec un haplotype « chaud » (α) qui correspond à des isolats issus d'eaux tempérées, tropicales et équatoriales, et un haplotype « froid » (β) qui correspond à des isolats provenant d'eaux tempérées et subpolaires des hémisphères nord et sud (discontinuité latitudinal apparente). L'haplotype α est caractérisé par deux sous-haplotypes, l'haplotype α1 pour des isolats en provenance de provinces néritiques et partiellement oligotrophes (voir annexe 1, OTU39, fig. 8) et l'haplotype α2 pour des isolats majoritairement issus de régions oligotrophes pélagiques. Ces deux groupes sont donc définis par une discontinuité horizontale, definissant un gradient océanique. Selon les genes *cox3* et *dam,* l'haplotype β comprend aussi trois sous-haplotypes.β1 est assimilé aux isolats de l'Atlantique Nord, β2 a ceux du Pacifique Nord, et β3 au Pacifique Sud, ces deux derniers groupes sont définis par une réelle discontinuité provinciale. Alors que *cox1* presente plus de diversité dans l'haplotype α que dans l'haplotype β, les autres marqueurs mitochondriaux distinguent un patron opposé.

Vers une révision des morphotypes chez *G. huxleyi*.

La définition des morphotypes de *G. huxleyi* est variable selon les auteurs. Des « warm type » et « cold type » de McIntyre et Bé (1967) aux morphotypes A, B et C de Young et Westbroek (1991), les morphotypes définis avant tout sur des critères de la morphométrie des coccolithes (degré de calcification, largeurs des cristaux radiaires (Cook et al. 2011) et longueurs) ne se distinguent pas toujours facilement. L'élargissement du spectre de l'observation dévoile souvent une grande variabilité au sein des échantillons environnementaux voire même au niveau des cultures, difficile à interpréter selon les schémas existant. Les variations observées au sein d'une même culture indiquent que les coccolithes ne sont pas produits à l'identique et que différentes modulations peuvent s'exercer durant la coccolithogénèse, telles que des modifications de l'activité cellulaire ou de l'expression de gènes impliques dans la biomineralisation. La distinction n'est donc pas évidente même pour un observateur exercé et peut être d'autant plus difficile suivant l'état de dissolution des coccolithes. Autant les morphotypes A, R et *corona* se distinguent très clairement, les morphotypes B, B/C, C et O sont définis sur des critères empiriques à mi chemin entre la biogéographie et la morphométrie qui ne permettent pas une distinction sans équivoque. Ce manque de clarté mène a des redéfinitions fréquentes de cette typologie A/B/C/R/O par les auteurs (voir tableau 1).

Les séquences ADN CMM (Coccolith Morphotype Motif) du gène *gpa* permettent d'établir un lien partiel entre morphotypes et génotypes (Schroeder et al 2006). Le gène *gpa*, présent exclusivement chez *G. huxleyi* (communication du Dr. Peter von Dassow, déduite par la comparaison de banques d'EST et l'échec d'essais d'amplifications chez *G. oceanica*), pourrait être impliqué dans la calcification (Cortjens et al 1998), bien que sa fonction reste encore inconnue. Le haut degré de conservation du gène *GPA* au sein des *G. huxleyi* suggère une forte contrainte sélective sur la séquence nucléotidique et donc sur les mécanismes de calcification, et empêche toute reconstruction phylogénétique. Néanmoins, quelques mutations fixées et délétions sont presentes sur deux régions précises du gène, chacune d'~100pb, qui co-varient avec les morphotypes. La région définissant les CMMs correspond à une région non codante à l'extrémité 3' du gène. L'autre région variable se trouve plus en amont du gène en région codante.

Tableau 1. Correspondance entre les morphotypes, les CMM et les haplotypes

Morphotypes	CMM	Haplotypes mitochondriaux	Désignation taxonomique et référence	Morphologie du bouclier distal	Morphologie de l'aire centrale	Longueur du bouclier distal	Distribution géographique	Morphotypes comparables dans la littérature
Type A	I, III, IV	alpha, beta	var. *huxleyi* Medlin et al. 1996	éléments modérément à extrêmement calcifiés	grille	< 4µm	Partout excepté les fronts subpolaires	Warm type (McIntyre and Bé, 1967) Type A (Young and Westbroek, 1991)
Type R	IV, V	alpha	Young et al. 2003	Ressemblance avec *Reticulofenestra, éléments* extrêmement calcifiés	grille	< 4µm	Pacifique sud	Type R (Young et al. 2003; Cubillos et al. 2007; Beaufort et al. 2007; Beaufort et al. 2011)
var. *corona*	?	alpha?	var. *corona* Okada et McIntyre 1977	éléments modérément calcifiés avec un tube central élevé	grille	3.5-4.5 µm	Gyre oligotrophe Atlantique et Pacifique	var. *corona* (Okada and McIntyre, 1977)
Type B	II	beta	var. *pujosae* Medlin et al. 1996	éléments légèrement calcifiés	plaque solide	≥ 4µm	Nord Atlantique/sub arctique	Type B (Young and Westbroek, 1991; Young et al. 2003; Beaufort et al. 2011)
Type B/C	VI	beta?	var. *aurorae* Cook et al. 2011	éléments légèrement calcifiés	plaque solide ou ouverte	< 4µm	Hémisphère sud tempéré/sub australe	Type B/C (Young et al.. 2003; Cubillos et al. 2007; Cook et al. 2011) Type C (Beaufort et al 2011)
Type C	?	beta?	var. *kleijniae* Medlin et al. 1996	éléments légèrement calcifiés	plaque solide	< 3.5µm	Sub tropical au niveau de la DCM des upwellings, sub polaire	Cold type (McIntyre and Bé, 1967) Type C (Findlay et Giraudeau 2000; Young et al.. 2003) Type C (Beaufort et al 2011)
Type O	VI	beta	Hagino et al. 2011	éléments légèrement calcifiés	ouverte	Taille variable	Tempéré/sub polaire, sub tropical au niveau de la DCM des upwellings	Subarctic type (Okada and Honjo, 1975) Type B (Young et al. 2003; Hagino et al. 2005; Beaufort et al 2011) Type B/C (Young et al. 2003; Mohan et al. 2005; Cubillos et al. 2007; Cook et al. 2011) Type C (Findlay et Giraudeau 2000; Young et al. 2003; Beaufort et al 2011)

Notre analyse permet une révision de la classification des morphotypes, intégrant les données morphométriques et génétiques (Fig. 1). Nous proposons le regroupement des morphotypes dans deux classes, **A** qui comprendrait A, R et « *corona* », et **B** qui comprendrait les ex-morphotypes B, B/C, C et O. Pour la classe A, les morphotypes A et R comprennent les CMMs I, III, IV et V, le morphotype « corona » étant absent de nos études. Néanmoins, sa ressemblance au morphotype A nous permet de suspecter que les CMMs A et « *corona* » sont identiques ou similaires. Dans la classe B, les morphotypes sont tous caractérisés par une calcification plus faible des cristaux radiaires. Un des critères définis par Young et Westbroeck était la longueur, supérieure ou égale à 4µm pour le morphotype B, inférieure ou égale à 3,5µm pour le morphotype C, inférieur à 4µm pour le morphotype B/C, et de taille variable pour le morphotype O. D'un point de vue morphométrique, ces distinctions morphotypiques sont inconsistantes. Par exemple, le morphotype C serait inclus dans la définition du morphotype B/C. Aussi, le caractère morphologique caractérisant le morphotype O est l'absence d'une aire centrale, or les caractères de l'aire centrale ne font par partie de la définition des autres morphotypes ; on pourrait donc potentiellement trouver des morphotypes O parmi les morphotypes B, C et B/C. De plus, l'attribution des distinctions morphologiques dépend parfois de la région géographique ou de la profondeur d'occurrence de ces morphotypes. En ce qui concerne les CMMs, une seule et unique substitution sépare le type B du tandem B/C et O, indifféremment de l'état de l'aire centrale des coccolithes (critères de distinction arbitraire qui semble varier aussi entre les souches du morphotype A) [1].

[1] Cette correspondance entre l'état de calcification des cristaux radiaires des coccolithes et le gène *gpa* semble indiquer que le gène serait lié à une fonction de régulation de la calcification. Peu de données existe mise à part un potentiel role inhibiteur de la calcification (communication du Dr. Declan Schroeder).

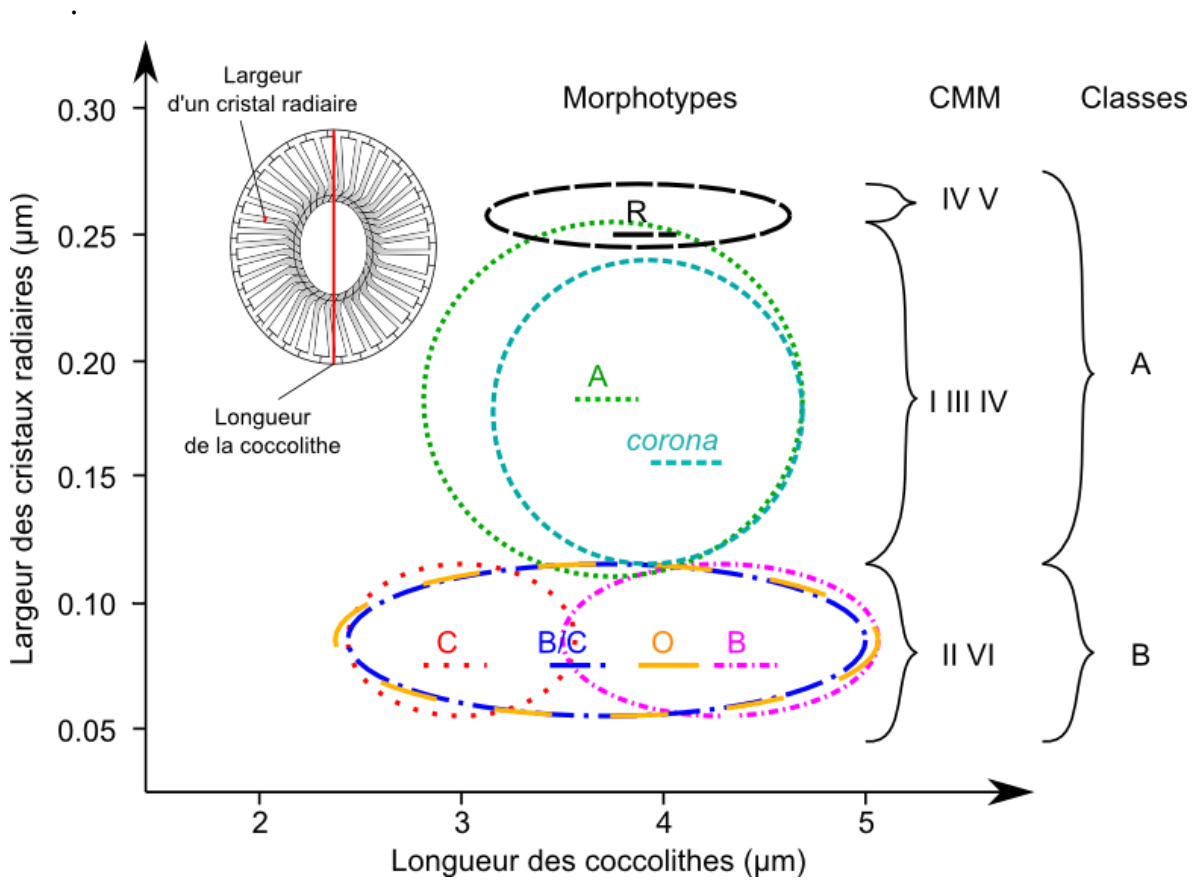

Figure 1. Révision de la classification des morphotypes chez la morpho-espèce *Gephyrocapsa huxleyi*.

Par ailleurs, nous constatons que les morphotypes ont une distribution bipolaire, un patron biogéographique assez classique du plancton océanique. La classe A est la plus dominante avec une large distribution océanique cependant limitée aux niveaux des océans tropicaux, subtropicaux et tempérés, alors que la classe B se retrouve principalement dans les régions tempérées et subpolaires, jusqu'à de hautes latitudes. Le morphotype A est largement distribué, présent dans tous les océans planétaires, alors que le type R est essentiellement présent dans les eaux tempérées australes et le morphotype *corona* semble être restreint aux masses d'eaux oligotrophes. Dans la classe B, les morphotypes B et C sont observés dans l'Atlantique nord, et les B/C, C et O dans les régions australes et du Pacifique nord. Nous pouvons dès lors supposer que les CMMs suivent la même distribution.

Haplotypes et morphotypes, concordance ou parallélisme ?

Nous retrouvons donc deux patrons de bipolarité partiellement recouvrant pour les morphotypes/CMMs d'une part, et les génotypes mitochondriaux (haplotypes) d'autre part

(fig. 2). Les classes A et B (morphotypes/CMMs), et les haplotypes α et β occupent les oceans tropicaux/tempérés, et tempérés/subpolaires, respectivement. Cependant la concordance biogéographique entre les morphotypes/CMM et les haplotypes n'est pas complète., La morpho-classe A correspond au type génétique α, tandis que le type genetique β inclut les deux morpho-classes A et B. Ainsi les haplotypes représenteraient des espèces pseudocryptiques par rapport aux morphotypes et les morphotypes et haplotypes ne répondraient pas des mêmes processus évolutifs. Le patron de bipolarité pose une question classique de biogéographie planctonique : les populations β ont soit transite entre les deux hémisphères, soit évolué par convergence a chaque pole. La première hypothèse implique un échange des masses d'eaux entre les deux hémisphères alors que la deuxième implique un isolement de populations monopolaires. La courantologie et l'hydrographie, influençant fortement la structuration des populations planctoniques, sont des phénomènes physico-chimiques hautement dynamiques.

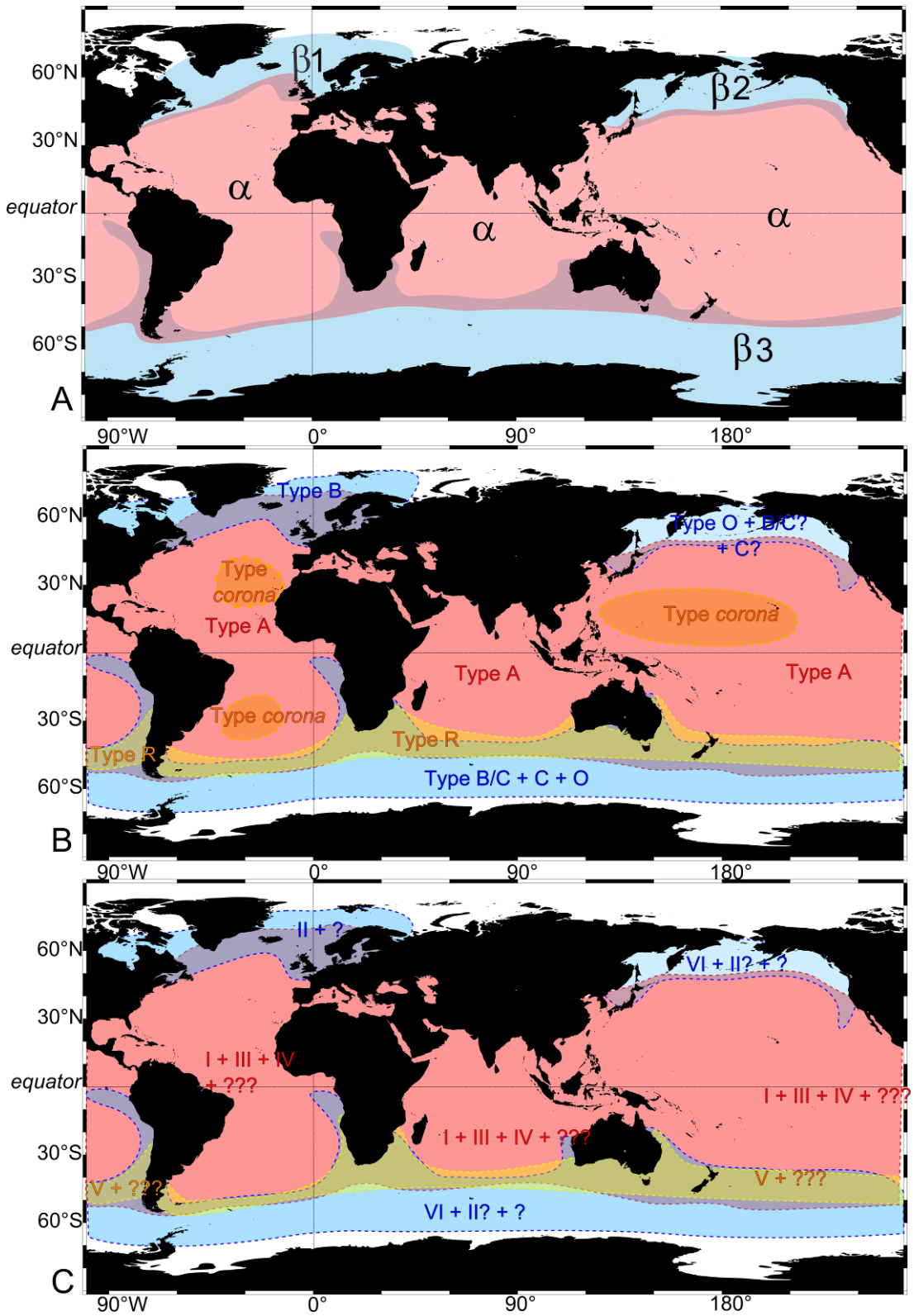

Figure 2. Cartes prédictives de la distribution des haplotypes (A), des morphotypes (B) et des CMM (C).

Des stratégies adaptatives en jeu dans la spéciation de *G. huxleyi*…

Peut-on parler d'un environnement marin planctonique structuré ? Le milieu marin est souvent caractérisé par de constants changements dynamiques, façonnés par les processus physiques, chimiques et biologiques qui s'y opèrent. Les gradients édaphiques et la topologie des océans amènent à une succession continue de zones, littorale, néritique et océanique. Les principaux paramètres influant les stratégies adaptatives et la distribution du phytoplancton dans le milieu marin sont (i) la turbulence dont l'origine est le mouvement des masses d'eau et les ondes de marées, le mélange des eaux amenant à (ii) la modulation de la luminosité et (iii) la distribution des nutriments (Margalef 1978). Ces paramètres suivent généralement différents gradients, allant de forts contrastes dans la zone littorale à de plus faibles dans la zone océanique et sont aussi modulés, sur des échelles temporelles plus longues, par la latitude, le climat et l'activité biologique. Ces paramètres définissent des habitats qui vont contraindre le développement des organismes phytoplanctoniques, qui par diverses réponses des processus d'acclimatation et d'adaptation y trouveront ou non leur adéquation dans l'environnement et dans le temps..

Adaptations à l'acidification ?

L'accroissement de la concentration de CO_2 atmospherique lié à l'activité humaine module les paramètres précédemment décrit et d'autres paramètres essentiels comme la température et le pH des masses d'eaux océaniques (cf introduction). Pour *G. huxleyi*, nous avons pu étudier les morphologies des coccolithes échantillonnés de part le monde mais aussi sur divers transects incluant des gradients côtiers/oligotrophes, nous permettant d'aborder la question essentielle et mal comprise de l'adaptation des espèces de protistes en milieu marin planctonique. Clairement les haplotypes α et β ont des préférences climatiques differentielles, pouvant etre liees, entre autre, à la température, a l'irradiance (latitudes), ou aux apports nutritifs (différence entre l'haplotype $\alpha 2$ qui semble lies aux milieux oligotrophes et les autres haplotypes).

Dans les figures 1b et 1c du chapitre 5, les morphotypes A et B de *G. huxleyi* sont mélangés sous la dénomination A, ce qui ne nous permet pas de nous prononcer pleinement sur notre nouvelle morpho-classe B. Néanmoins nous baserons nos prédictions adaptatives de la classe B au morphotype C de l'étude. Ainsi, la présence des morphotypes peut être

assimilée à des patrons de sélections correspondant à la concentration en ions carbonates (figure 1b du chapitre 5) ou a la pression partielle en CO_2 (figure 1c). Ces patrons sont les suivant :

a. Morphoclasse A dominante (α et β; CMM I, III, IV et V) : présente entre 50 et 400 µmol.kg-1 de [CO_3^{2-}] et présente pour toutes les valeurs de pCO_2 du spectre d'étude mais extrêmement limité au dessus de 400 µatm de pCO_2
b. Morphoclasse A surcalcifiée (morphotype R ; α; CMM IV et V): présente essentiellement entre 50 et 250 µmol.kg-1 de [CO_3^{2-}] et entre 300 et 400 µatm pCO_2 (pH8.0 et pH8.1), quelques individus peuvent être retrouvés jusqu'à une pCO_2 de 900 µatm (pH 7,6).
c. Morphoclasse B (morphotype C), tempérée et polaire (β; CMM II et VI): présence notable entre 50 et 250 µmol.kg-1 de [CO_3^{2-}] et entre 300 et 400 µatm pCO_2 (pH8.0 et pH8.1), quelques individus peuvent être retrouvés jusqu'à une pCO_2 de 900 µatm (pH 7,6)
d. Malformation = individus mal-adaptés ?

Les classes A surcalcifiée et B seraient positivement sélectionnées dans les eaux de pH 8-8.1, et présentes en condition encore plus corrosives. Dans la morpho-classe A dominante, les individus présentant des coccolithes malformés seraient mal adaptés. Cette sélection des morphotypes par les variations du système carbonate agit probablement sur les patrons de calcifications sans complète correlation avec les haplotypes. Malgré cette apparente adaptation, la tendance de la calcification est à la baisse depuis le dernier maximum glaciaire, ce qui laisse suggérer que l'acidification aurait un impact négatif sur la calcification des *G. huxleyi*, si l'on suit la loi de correlation (chapitre 4) entre les ions carbonates et la masse estimée des coccolithes.

Si les patrons hydro-geographiques observés correspondent à des adaptations genetiques, le gène *gpa* apporterait-il un début d'explication des mécanismes moléculaires impliqués dans ces supposées adaptations? Il aurait été particulièrement intéressant de séquencer la zone codante du gène qui montre des délétions similaires entre les CMMs II, III, IV, V et VI. Suivant cette idée, le CMM I, qui correspond aux souches pour qui la zone codante sera la plus complète, correspondrait soit aux morphotypes A mal adaptés, soit serait absent des zones où les valeurs de pCO_2 sont >300 µatm. Cette présomption est renforcée par

l'étude de Riebesell et al (2000) qui utilise la souche B92-11, isolée dans un fjord en Norvège, répondant negativement l'expérience de fort pCO_2. Cette souche présente une séquence complète du gène *gpa* pour un morphotype A (communication personnelle de Declan Schroeder). Le séquençage de cette portion devrait donc être effectué pour tester cette hypothèse de correspondance entre l'adaptation de la calcification à l'acidification et les génotypes.

Le gène *gpa* n'étant surement pas le seul acteur de la coccolithogénèse, la détermination des réseaux métaboliques en jeu dans la fonction de calcification permettra de mieux comprendre les adaptations a la chimie marine des carbonates. Nous nous attachons là à une correspondance génotype/phénotype basée sur un seul gène dont la fonction est à peine suspectée, notre connaissance limitée ne nous permet pas non plus d'exclure la possibilité d'une plasticité phénotypique chez certaines souches.

De la stabilité de l'environnement et du maintien de la sexualité chez *G. huxleyi*

Les régions océaniques néritiques et côtières sont caractérisées par une instabilité physico-chimique évidente, avec des turbulences causées par l'effet d'onde sur les masses d'eau, la topologie des fonds et potentiellement les différences de salinités par les apports fluviaux. Les régions océaniques tempérées à polaires subissent des perturbations physiques dues au régime des vents et à l'action de leur friction sur les eaux de surfaces. Ces régions sont aussi caractérisées par de fortes variations saisonnières se traduisant par de fortes flutuations de temperatures mais aussi de l'état de stratification de la colonne d'eau qui régule la disponibilité des nutriments. Finalement, les pressions biotiques liées à la compétition, la prédation et les pathogènes sont aussi sont aussi d'importants facteurs sélectifs. Ces fortes variations abiotiques ou biotiques de l'environnement favoriseraient le maintien de la reproduction sexuée, qui accroit le potentiel adaptatif par le partage de mutations bénéfiques et régule de manière subtile les populations à travers le cycle de vie. Chez *G. huxleyi*, de larges efflorescences de cellules diploïdes font suite à la stratification de la colonne d'eau printanière, liée à l'augmentation de la température. Ces efflorescences sont fortement régulées par l'infection des cellules diploïdes par le virus *Ehv*, un phénomène qui donne naissance à des populations de cellules haploïdes, insensibles au virus (Frada, 2009). Le modèle de coévolution proposé pour ce phénomène suit deux hypothèses de stratégies adaptatives, celle dite du « Chat de Chechire », qui suppose que l'entité infectée devient invisible à son pathogène par une transformation diplo-haploide, en référence et opposition à

la deuxième dite de la « Reine rouge », basé sur la course aux armes hôtes/pathogènes ; Van Valen 1973; Frada 2009). L'infection virale induirait donc chez *G. huxleyi* le passage de la phase diploïde à la phase haploïde et un recours à la reproduction sexuée. Cela peut être conçu comme une réponse à l'infection, impliquant la fuite physique par invisibilité et dispersion (« Chat de Chechire ») et la fuite moléculaire par recombinaison et brassage des informations génétiques: phénomènes qui sélectionnent fortement la fonction reproductrice. Dans le cas de la course aux armes, un tri sélectif des nouveaux individus résistants au virus permettrait à un pool génétique retour l'installation de nouvelles populations de *G. huxleyi*, jusqu'à une prochaine infection après sélection de nouvelles formes virale. La première force mettant en jeu un épisode méïotique/syngamique exemple illustre particulièrement la sélection et le nécessaire maintien de la reproduction sexuée pour la survie de l'espèce.

Nous pouvons supposer que l'entrée des *G. huxleyi* dans les eaux océaniques impose une régulation de la reproduction par le coût énergétique et adaptatif qu'elle implique. Dans le vaste domaine océanique oligotrophe, les conditions physico chimiques sont bien plus stables que dans les milieux côtiers/néritiques, la disponibilité des nutriments étant le principal facteur limitant. Les conséquences successives et rétroactives sur la reproduction et les populations seraient donc les suivantes :(i) Une reproduction biaisée vers un mode asexué probablement ralentie ; (ii) une réduction des probabilités de rencontres des individus haploïdes ; (iii) une réduction des brassages génétiques ; (iv) un ralentissement du taux de croissance des populations.

Ces phénomènes auraient pour conséquence une baisse de la sélection positive sur la reproduction sexuée et notamment sur la fonction flagellée des cellules haploïdes, impliquée dans la dispersion et la rencontre cellulaire. En accord avec ce modèle, nous observons, chez plusieurs souches océaniques de *G. huxleyi*, l'accumulation de mutations amenant à la perte de fonctions des gènes spécifiquement exprimés dans la phase haploïde, suivie parfois de l'élimination complète de ces gènes sous sélection négative (Chapitre 5). La corrélation avec l'absence de formes flagellées en culture confirme le constat de l'érosion du « génome haploïde ». Ce phénomène est étonnamment rapide, comme le montre l'exemple de la souche CCMP1516 ayant été cultivée indépendamment dans différentes collections de cultures. Le processus d'érosion du génome haploïde est polyphyletique, tout en étant particulièrement lié à l'haplotype α2 –qui contient la plupart des souches en provenance de régions oligotrophes.

En contraste, les souches de l'haplotype β et les isolats α des régions côtières ont préservé leurs gènes flagellaires fonctionnels, et produisent régulièrement des cellules flagellées en culture. L'absence conséquente d'épisodes méiotiques est suggérée par l'absence de signes de recombinaison dans les génomes de la souche CCMP1516 qui a perdu les gènes flagellaires par rapport aux souches RCC1216 et CCMP371. La possibilité d'une reproduction sexuée chez ces souches oligotrophes est donc largement compromise, confirmant la théorie selon laquelle le coût de la reproduction sexuée (accroissement moins rapide des populations, cout énergétique de la nécessite de rencontre des gamètes Maynard-Smith, 1978), serait plus élevé dans ces milieux que l'avantage qu'il procure.

Au regard des avantages que procurent la reproduction sexuée, à savoir la mise en place de nouveaux génotypes par la recombinaison méiotique (« crossing over ») et la recombinaison syngamique (combinaison d'allèles avantageux et leur transmission plus rapide comparée aux populations exclusivement asexuées ; Burt 2000), la résistance aux pathogènes (hypothèse de la reine rouge, Van Valen 1973, du Chechire Cat, Frada et al. 2009), on peut supposer une réduction de l'adaptabilité a moyen et long termes des individus qui ne maintiennent pas la reproduction sexuée. D'autres mécanismes inhérents à la reproduction sexuée joueraient à la défaveur de la capacité adaptative de ces formes asexuées, comme le balayage des mutations délétères (Kondrashov 1988) mais aussi la réparation des dommages à l'ADN (Bernstein et al 1985).

L'effet démographique de cette modification des traits reproductifs serait la sélection d'une stratégie R lorsque la reproduction sexuée est adéquatement sélectionnée et inclut les haplotypes β et certains α1. En effet, ces populations démontrent de forts taux d'accroissement (efflorescences). L'éloignement vers les contrées océaniques qui entrainerait un relâchement de la sélection conservatrice sur la reproduction sexuée suggère la sélection d'une stratégie K ou l'accroissement des populations serait plus limité.

Les crises biologiques et les stratégies de survies des coccolithophores

Considéré comme un trait indéniable de la lignée des Noëlaerhabdaceae, la stratégie R serait la stratégie écologique lié au succés évolutif des espèces actuelles. L'opportunisme de *G. huxleyi* en est le meilleur exemple parmi les coccolithophores modernes, ce trait semble partagé par les plus anciens ancetres de cette famille, comme chez les Biscutaceae, famille

décrite comme ancestrale des Isochrysidales. Cette famille serait l'une des rares familles de coccolithophores à avoir survécu à la crise K/T, il y a 65 millions d'années. Lors de cette crise où plus de 80% de la diversité des coccolithophores aurait disparu, seules les espèces supposées côtières ou à large spectre biogéographique auraient survécu, ces dernières auraient justement été réduites à la vie côtière. La description du bilan fossile d'espèces survivantes a mis en évidence une large dominance dans les assemblages sédimentaires supposés océanique ainsi que la possibilité d'espèces formant de larges efflorescences dans les zones néritiques. Cela soutient l'idée selon laquelle ces espèces étaient potentiellement opportunistes (des strateges R) comme l'est actuellement *G. huxley,*. La survie des Biscutaceae est probablement liée à un contexte de refuge côtier, avec spécialisation des traits de vie.

La capacité de vie benthique des stades haploïdes de *G. huxleyi*, qui peuvent être maintenus en culture sur substrat solide, suggère que ces espèces n'ont pas nécessairement une vie exclusivement pélagique. Cette capacité rappelle le cycle bentho-pélagique des Isochrysidaceae, mais aussi celui des Pleurochrysidaceae qui présenteraient aussi des stades haploïdes non calcifiants souvent benthiques qui, après quelque cycle mitotiques, produisent des cellules flagellées. Le maintien à travers les temps géologiques de telles stratégies démontre le succès de ces espèces, notamment par leur survie lors d'une crise majeure telle que la crise K/T.

Considérations écologiques et similarité entre Isochrysidaceae et phases haploïdes des Noëlaerhabdaceae

Les caractères morphologiques et ultrastructuraux hautement similaires entre les espèces d'Isochrysidaceae (Chapitre 1) suggèrent une forte conservation du caractère mobile et du développement de la valence écologique. Ces caractères morphologiques sont aussi très proches de ceux des cellules haploïdes de Noëlaerhabdaceae qui ne semblent se différencier que par une plus grande taille des écailles organiques et une réduction des composants du corps basal des flagelles. Les valences écologiques des Isochrysidaceae sont larges, notamment dans le genre *Chrysotila* qui peut être euryhalin, voire cultivé dans l'eau de mer sans milieux de culture. Il se trouve que le stade haploïde de *G. huxleyi* présente aussi une valence écologique plus grande que le stade diploïde. L'affinité des cultures haploïdes de Noëlaerhabdaceae pour des milieux riches en nutriments suggère aussi quelques similitudes physiologiques avec les Isochrysidaceae. Ces exigences trophiques expliquent la présence des Isochrysidaceae dans les habitats néritiques et littoraux, voir dulcicole et terrestre. Ainsi la

sélection de la mobilité et d'une sexualité semble être fondamentale à la vie dans ces environnements en constant changement. Les taux de croissances pour ces lignées sont plus élevés que pour le stade diploïde des Noëlaerhabdaceae. Si l'on considère donc que les Isochrysidaceae sont bloqués en stade haploïde, leur adaptation aux environnements est avant tout misée sur l'exploitation de leurs capacités écologiques telle le déplacement et la plasticité phénotypique.

Avec la capacité des souches haploïdes des Noëlaerhabdaceae à pouvoir se multiplier clonalement en culture, nous pouvons aisément imaginer que si les Isochrysidaceae ne possèdent pas de stade diploïde un évènement majeur d'isolement reproductif à l'origine de la famille a pu se produire, comme un isolement hétérothallique due à l'absence prolongée de formes compatibles à la syngamie. Cet événement expliquerait la perte de la calcification au sein de cette famille, avec l'hypothèse d'un ancêtre commun Isochrysidales ne calcifiant que lors de la phase diploïde. Si l'on considère une homologie entre les Isochrysidaceae et les formes haploïdes des Noelaerhabdaceae, il est possible que cet événement ait été promu par une crise océanique forçant un refuge côtier. La spécialisation à l'environnement côtier chez les haptophytes est lié à la sélection du pigment *Chlc1*. Considérant la large palette pigmentaire des *Phaeocystis*, à la base des Prymnesiophyceae, on peut supposer un ancêtre commun possédant la même palette pigmentaire. La réduction des pigments accessoires serait potentiellement le signe d'un retour évolutif à l'habitat côtier. Cette réduction se retrouverait donc aussi chez les Pleurochrysidaceae, chez qui les stades haploïdes présentent les mêmes types structuraux et comportementaux que les Isochrysidaceae et les stades haploïdes des Noëlaerhabdaceae, ainsi que chez certaines espèces du genre *Prymnesium* et de la classe des Pavlovophyceae. Les données stratigraphiques confirment d'autant plus cette assomption d'un retour à une vie côtière chez les Pleurochrysidaceae. Nous pouvons suggérer que le même processus ait été à l'origine des Isochrysidaceae (ainsi que des *Prymnesium* et les Pavlovophyceae).

La perte de la phase diploïde serait le processus inverse de celui que nous constatons chez *G. huxleyi*. Chez ce dernier, les formes diploïdes calcifiantes ne produisent plus de phase haploïde en milieux océaniques. Chez les Isochrysidaceae, la spécialisation a l'environnement côtier serait une sélection de la forme haploïde adéquate dans cet habitat, induisant la perte de la phase diploïde calcifiante. Nous pouvons supposer que les deux familles d'Isochrysidales montrent deux cas opposés d'évolutions de leur stratégie reproductive en adéquations avec leurs habitats.

… à l'origine des espèces (Conclusion)

Hypothèse d'un scénario évolutif des espèces de *Gephyrocapsa huxleyi*

L'utilisation des horloges moléculaires permet d'estimer les dates de divergences des séquences génétiques et de celles des espèces lorsque l'histoire des gènes reflète celle des espèces (chapitre 6). Dans ce cas, tout est question de taux d'évolution et les dates de diversifications nous permettraient d'inférer un ou des scenarios évolutifs sur l'origine des espèces et leur colonisation des différents milieux. Nous partons donc d'une très forte assomption pour proposer le scénario que nous avons décrit, à cela s'ajoute le biais de la calibration fossile de notre horloge moléculaire qui correspond à la date de première occurrence de l'espèce *G. huxleyi*. Nous ne pouvons affirmer que cette date soit la date de divergence des gènes utilisés pour la reconstruction phylogénétique. Cependant, ce biais est moindre par rapport aux reconstitutions moléculaires effectuées sur les organismes terrestres pour lesquels le bilan fossile est souvent très incomplet. Les différents tests effectués montrent que les gènes mitochondriaux satisfont l'hypothèse d'une horloge moléculaire. L'ajout dans la phylogénie d'autres espèces de *Gephyrocapsa* est essentiel pour une estimation de l'horloge plus précise. L'accès aux séquences mitochondriales de *G. ericsoni* est tout à fait providentiel, cette espèce étant absente de nos collections de culture de par sa difficulté à être isolée[1].

La définition de l'espèce *G. ericsonii*, différente selon les auteurs, est à l'origine de certaines discordances aux niveaux des datations stratigraphiques, elle est souvent confondue avec *G. aperta* ou *G. protohuxleyi*. Au niveau morphologique, ses coccolithes présentent une morphologie intermédiaire entre *G. oceanica* et *G. huxleyi*, par la présence d'un pont et l'aspect peu calcifié des éléments radiaires. Pujo-Lamy (1977) ne donne pas de première date d'apparition pour cette espèce, mais en suppose une apparition relativement récente parmi les gephyrocapsids, proche de celle de *G. huxleyi* et Samtleben (1980) intègre cette hypothèse dans ses reconstructions phylogénétiques. Hine et Weaver (1998), font remonter l'apparition de *G. ericsonii* dans les sédiments globaux aux alentours de 370 000 ans. Si l'on calibre notre moléculaire sur la date d'apparition de *G. huxleyi* (291,000 ans), cette date de 370Ka pour la premiere occurrence de *G. ericsonii* est proche de la date de 405Ka inférée par l'horloge

[1] Le Pr. Masanobu Kawashi possède quelques isolats de cette espèce. Nous lui sommes particulièrement reconnaissant du partage de séquences mitochondriales de ces espèces.

moléculaire. Ainsi les deux espèces trouveraient leur origine dans la succession de deux épisodes interglaciaires. Le peu d'informations sur l'écologie de *G. ericsonii* indique qu'il s'agit d'une espèce restreintes a la zone de transition entre les eaux tempérés et les eaux tropicales dans l'hémisphère Nord, et ubiquiste dans l'hémisphère sud jusqu'à 55° de latitude. *G. ericsonii* serait particulièrement adaptées aux eaux relativement froides et riches en nutriments.

Selon notre horloge moléculaire, la divergence entre les haplotypes α et β remonterait à ~221 000 ans (entre 150 et 250 000 ans) lors d'un épisode interglaciaire. L'abondance en fossile de *G. huxleyi* n'excédant pas les 20% entre la première apparition et la séparation des deux haplotypes, nous pouvons supposer que les populations de *G. huxleyi* étaient relativement discrètes et réduites, peut être contraintes par le contexte climatique d'augmentation interglaciaire du CO_2. Les autres espèces de coccolithophores déjà présentes en large population et plus adaptées auraient occupé la plupart des niches. La séparation des haplotypes α et β pourrait corréler avec la fin d'une période interglaciaire, et correspondre a l'ouverture de nouvelles niches écologiques, notamment liees a la restructuration de la circulation océanique mais aussi au déclin de l'abondance de certaines formes qui potentiellement les occupaient. La fin de cette période glaciaire (~150 000 ans) se retrouve suivie d'une augmentation de l'abondance fossile des *G. huxleyi* à ~25 %, qui précède légèrement la diminution d'autres formes ainsi que de l'augmentation brutale de la température et du CO_2 corrélative a l'entrée dans une période interglaciaire d'environ 50 000 ans. Nous pouvons supposer que ces événements auraient influencé la spéciation en haplotypes α et β car, l'augmentation brutale des températures et la chute qui suivent corrèlent avec une légère baisse de l'abondance en fossile des *G. huxleyi* à ~15% et l'entrée dans la dernière ère glaciaire avant notre époque. Les populations auraient pu subir un goulot d'étranglement à cette période, avant de se diversifier en plusieurs haplotypes.

La diversification au sein des haplotypes α et β semble concurrente et bien établie dès 95 000 ans. Cette diversification des lignées de G. huxleyi semble corréler avec l'abondance maximale de *G. huxleyi* fossiles dans les océans, débutant à environ 90 000 ans jusqu'à nos jours et la baisse des abondances des autres formes de gephyrocapsids comme *G. mullerae* et *G. aperta*. La divergence au sein de l'haplotype α serait liée à la colonisation de provinces oligotrophes, lié à la baisse du niveau des océans. La divergence au sein de l'haplotype β correspond à une séparation géographique entre les populations Pacifique et Atlantiques par la limitation des échanges entre le Pacifique et l'Atlantique au niveau du pole nord, et par les

modifications de la circulation marine au niveau de l'océan austral (Stocker et al 1991) et la diminution du niveau des océans. Ces deux événements parallèles pourraient correspondre à deux épisodes d'isolements, le premier par l'occupation d'une nouvelle niche (bien que l'on en puisse pas vraiment savoir si elle n'était pas déjà occupée) et le deuxième par une séparation géographique. Cependant nous ne savons pas encore si les haplotypes de *G. huxleyi* correspondent vraiment à des espèces reproductivement isolées, et donc si la diversification au sein des haplotypes pourraient plutôt correspondre a des structuration microevolutives qui n'excluent pas l'échange de matériel génétique entre lignées. L'abondance maximale pendant la dernière glaciation pourrait être attribuée aux morphotypes dit « cold » de McIntyre et Bé (1967) retrouvés en forte abondance dans le relevé stratigraphique de Pujos-Lamy en (1977). Ce morphotype correspondrait aux morphotypes C, B/C ou O et donc à notre classe morphologique B. Nous pouvons potentiellement lui attribuer l'haplotype β. L'existence de ces morphotypes et donc des CMMs associés seraient antérieure à cette événement de diversification. Le dernier maximal glaciaire à environ 20 000 ans est suivi de températures et d'un taux de CO_2 en augmentation, en corrélation avec une baisse tendancielle du poids des coccolithes (chapitre 4).

Ce scenario évolutif mettrait en relation une évolution des haplotypes parrallèle à celle de la calcification où la fluctuation des abondances fossiles peut être associée à des episodes de reductions ou d'expansions de populations. Bien que la diversification des morphotypes ne puissent pas être caractèrisée, la diversification des haplotypes semble être liée à la colonisation de nouvelles niches sachant que les populations pouvant s'adapter sur le long terme correspondent aux populations favorisée par la reproduction sexuée. Ces populations assureraient le renouvellement génétique potentiellement à l'origine des pools retour des populations de *G. huxleyi* après épisodes de réduction de populations (goulot d'étranglement) et donc le maintien. Ces populations trouvent par les regions à forte instabilité environnementale et notamment par la succession des épisodes saisonniers de réductions de populations par efflorescences (la succession de ces episodes etant relativement rapide). Nous pouvons supposer que la diversité de la forme *G. huxleyi*, telle que nous l'avons décrite au cours de cette étude en serait un resultat sur le long terme, les forces sélectives étant garant de la structuration des populations dans le temps. Nous pouvons fortement suggérer que ce que nous caractèrisions de succès évolutif de l'espèce *G. huxleyi* serait à voir comme le succès de

la radiation adaptative au sein des populations, le découplage espèce/fonction (calcification) representant un de ces signes d'adaptations.

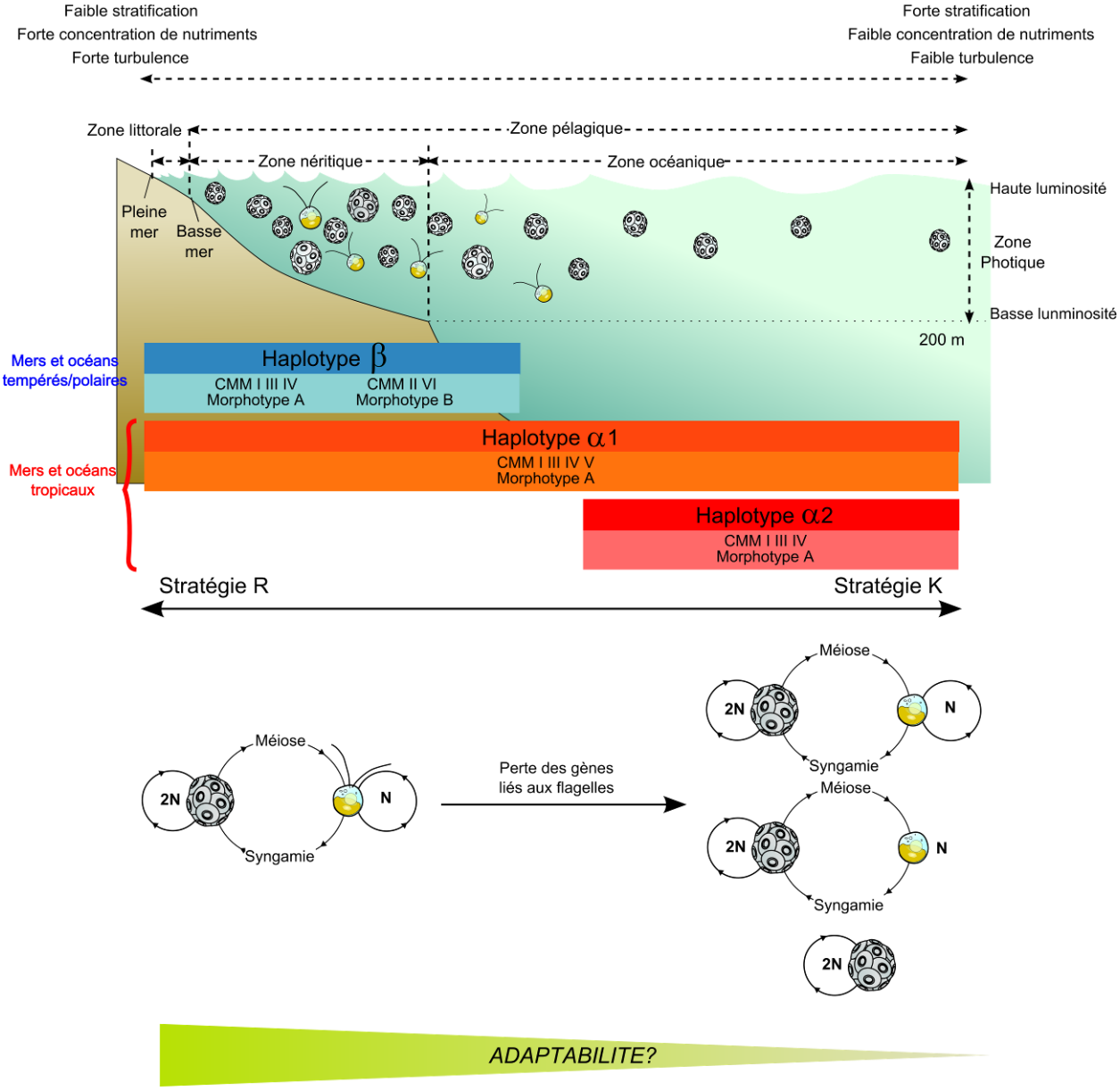

Figure 3. Succession et stratégies adaptatives des différents génotypes et morphotypes de *G. huxleyi* en relation avec les principaux gradients environnementaux des écosystèmes planctoniques marins.

BIBLIOGRAPHIE

Anand PL (1936). Seven new Chrysophyceae from the south-east of England. *Proceedings of the Tweny Third Indian Science Congress, Indore*. 282-283.

Anand PL (1937). A taxonomic study of the algae of British chalk-cliffs. *J Bot* 75: 1-51.

Anderson, D. M. and Archer, D. (2002) Glacial interglacial stability of ocean pH inferred from foraminifer dissolution rates. *Nature* 416, 70-73.

Andersson, S. G. E. *et al.* (1998). The genome sequence of *Rickettsia prowazekii* and the origin of mitochondria. *Nature* 396, 133–143

Andrews JT and Giraudeau J (2003) Multi-proxy records showing significant Holocene environmental variability: the inner N. Iceland shelf (Húnaflói). *Quaternary Science Reviews*, 22: 175-193

Andruleit H, Rogalla U et Stager S (2004) From living communities to fossil assemblages: origin and fate of coccolithophores in the northern Arabian Sea. *Micropaleontology* 50: 5-21.

Antonov, J. Locarnini, I., R. A., Boyer, T. P., Mishonov, A. V. and Garcia, H. E. (2006). *World Ocean Atlas 2005, Volume 2: Salinity. In* Levitus, S. [Ed.] *NOAA Atlas NESDIS 62*, U.S. Government Printing Office, Washington, D.C., 182 pp.

Avise JC (2000) *Phylogeography: The History and Formation of Species.* Harvard University Press, Cambridge.

Barker, S. and Elderfield, H. (2002) Foraminiferal Calcification Response to Glacial-Interglacial Changes in Atmospheric CO2. *Science* 297, 833-836.

Berney C et Pawlowski J (2006) A molecular time-scale for eukaryote evolution recalibrated with the continuous microfossil record. *Proc Biol Sci*. 273:1867–1872.

Bernstein H, Byerly HC, Hopf FA, Michod RE (1985). "Genetic damage, mutation, and the evolution of sex". *Science* 229 (4719): 1277–81.

Berry, L., Taylor, A. R., Lucken, U., Ryan, K. P. and Brownlee, C. (2002) Calcification and inorganic carbon acquisition in coccolithophores. *Functional Plant Biology* 29, 289-299,

Biekart JW (1989). The distribution of calcareous nannoplankton in late Quaternary sediments collected by the Snellius II Expedition in some southeast Indonesian basins. *Proc K Ned Akad Wet* 92: 77-141.

Billard C (1994) Life cycles. In: Green JC, Leadbeater BSC (eds) The Haptophyta Algae, Vol

Billard C and Gayral P (1972). Two new species of *Isochrysis* with remarks on the genus *Ruttnera*. *Br Phycol J*: 289-297.

Billard C and Inouye I (2004) What's new in coccolithophore biology? In: Thierstein HR, Young JR (eds) *Coccolithophores: From the molecular processes to global impact*. Springer

Birky, CW (2008), Uniparental inheritance of organelle genes, *Current Biology* 18 (16): R692–R695

Boeckel, B. and Baumann, K-H. 2008. Vertical and lateral variations in coccolithophore community structure across the subtropical frontal zone in the South Atlantic Ocean. *Mar. Micropaleontol*. 67: 255–73.

Bollmann J and Herrle JO (2007) Morphological variation of Emiliania huxleyi and sea surface salinity. *Earth and Planetary Science Letters* 255: 273-288

Bollmann J (1997) Morphology and biogeography of *Gephyrocapsa* coccolithes in Holocene sediments. *Mar Micropal* 29:319–350

Bollmann J, Henderiks J and Brabec B (2002) Global calibration of Gephyrocapsa coccolith abundance in Holocene sediments for paleotemperature assessment. *Paleoceanogr*. 17: 1010-1029.

Bougaran G, Le Déan L, Lukomska E, Kaas R and Baron R (2003). Transient initial phase in continuous culture of *Isochrysis galbana* affinis *Tahiti*. *Aquat Living Res* 16: 389-394.

Bourrelly P (1957). Recherches sur les Chrysophycées. Morphologie, Phylogénie, Systématique. *Rev Algo*, mémoire hors-série 1. 414 pp.

Bourrelly P and Magne F (1953). Deux nouvelles espèces de Chrysophycées marines. *Rev Gen Bot* 60: 684-687.

Bown PR (1998). *Calcareous Nannofossil Biostratigraphy*. British *Micropalaeontological* Society Publication Series, Chapman and Hall (London). 315 pp.

Bown PR (2005) Calcareous nannoplankton evolution: a tale of two oceans. *Micropaleontology*, 51(4): 299-308.

Bown PR, Lees JA et Young JR (2004) Calcareous nannoplankton evolution and diversity through time. In: Thierstein, H.R. and Young, J.R. (Editors), *Coccolithophores - From molecular processes to global impact.* Springer.

Bowring SA, Erwin DH, Jin YG, Martin MW, Davidek K, Wang, W (1998) U/Pb zircon geochronology and tempo of the end-Permian mass extinction. *Science* 280: 1039-1045

Brassell SC and Dumitrescu M (2004). Recognition of alkenones in a lower Aptian porcellanite from the west-central Pacific. *Org Geochem* 35: 181-188.

Brassell SC, Eglinton G, Marlowe IT, Plaufmann U and Sarnthein M (1986). Molecular stratigraphy: a new tool for climatic assessment. *Nature* 320: 129-133.

Bréhéret J (1978). Formes nouvelles quaternaires et actuelles de la famille des Gephyrocapsaceae (Coccolithophorides). *C R Acad Sc Paris* 287: 447-449.

Brown CW and Yoder JA (1994). Coccolithophorid Blooms In The Global Ocean. *J Geo Res-Ocean* 99: 7467-7482.

Brown MR, Garland CD, Jeffrey SW, Jameson ID and Leroi JM (1993). The gross and amino acid compositions of batch and semi-continuous cultures of *Isochrysis* sp. (clone T.ISO), *Pavlova lutheri* and *Nannochloropsis oculata*. *J Appl Phycol* 5: 285-296.

Brown RM, Franke WW, Kleinig H, Sitte P (1969) Cellulosic wall component produced by the Golgi apparatus of *Pleurochrysis scherffelii* Pringshelm. *Science* 166: 894-896

Buitenhuis, E. T., de Baar, H. J. W. and Veldhuis, M. J. W. (1999) Photosynthesis and calcification by Emiliania huxleyi (Prymnesiophyceae) as a function of inorganic carbon species. *J. Phycolog.* 35, 949-959.

Burki F, Shalchian-Tabrizi K, Minge M, Skjaveland A, Nikolaev SI, Jakobsen KS, Pawlowski J (2007) Phylogenomics Reshuffles the Eukaryotic Supergroups. *PLoS ONE* 2:e790

Burt, A. (2000). "Perspective: sex, recombination, and the efficacy of selection—was Castresana J (2000). Selection of conserved blocks from multiple alignments for their use in phylogenetic analysis. *Mol Biol Evol* 17: 540-552.

Cavalier-Smith T (1994) Origin and relationship of Haptophyta. In: Green JC, Leadbeater BSC (eds) *The Haptophyta Algae*, Vol Special volume No. 51. The Systematics Association, Oxford, p 413-435.

Cavalier-Smith,T *(*2000) The phagotrophic origin of eukaryotes and phylogenetic classification of Protozoa. *Int. J. Syst. Evol. Microbiol*., 52*:* 297–354.

Christensen T (1962). Alger. In Botanik Bd. 2, Systematisk Botanik, Nr. 2, (ed. Böscher TW, Lange M and Sorensen T), Munksgaard (Copenhagen). pp 1-178.

Clocchiatti M (1971). Sur l'éxistence de coccosphères portant coccolithes de *Gephyrocapsa oceanica* et de *Emiliania huxleyi* (Coccolithophoridés). *C R Acad Sc Paris* 273: 318-321.

Colmenero-Hidalgo, E., Flores, J. A. and Sierro, F. J. (2002) Biometry of Emiliania huxleyi and its biostratigraphic significance in the Eastern North Atlantic Ocean and Western Mediterranean Sea in the last 20 000 years. *Marine Micropaleontology* 46, 247-264.

Conte MH, Volkman JK and Eglington G (1994). Lipid biomarkers of the Haptophyta. In Green JC and Leadbeater BSC (eds) The Haptophyte algae. The Systematics Association special volume 51, Oxford University Press (Oxford, UK). pp 265-85.

Coolen MJL, Muyzer G, Rijpstra, WIC, Schouten S, Volkman JK and Damste JSS (2004). Combined DNA and lipid analyses of sediments reveal changes in Holocene haptophyte and diatom populations in an Antarctic lake. *Earth Planet Sci Lett* 223: 225-239.

Corbyn, Z. 2007. Atlantic invaders. *Nature.* 207:82-4.

Corstjens, P. L. A. M., van der Kooij, A., Linschooten, C., Brouwers, G.-J. Westbroek, P. and de Vrind-de Jong, E. W. 1998. GPA, a calcium-binding protein in the coccolithophorid *Emiliania huxleyi* (Prymnesiophyceae). *J. Phycol.* 34:622-30.

Cros L and Fortuno JM (2002). Atlas of Northwestern Mediterranean Coccolithophores. *Scientia Marina*, 66 (supplement 1). 186 pp.

Edvardsen B, Eikrem W, Green JC, Andersen RA, Moon-van der Staay SY, Medlin LK (2000) Phylogenetic reconstructions of the Haptophytes inferred from 18S ribosomal DNA sequences and available morphological data. *Phycologia* 39: 19-35.

Edvardsen B, Vaulot D (1996) Ploidy analysis of the two motile forms of *Chrysochromulina polylepsis* (Prymnesiophyceae). *Journal of Phycology* 32:94-102.

Ehrenberg CG, (1836) Über mikroskopische neue Charaktere der erdigen und derben Mineralien: Ann. Phys. u. Chem. (Poggendorff),. 39: 101-106.

Epstein BL, D'Hondt S and Hargraves PE (2001). The possible metabolic role of C37 alkenones in *Emiliania huxleyi. Org Geochem* 32: 867-875.

Ernst Haeckel, (1866) *Generelle Morphologie der Organismen*, Berlin, Reimer,

Fabry, V. J., Seibel, B. A., Feely, R. A. and Orr, J. C. (2008) Impacts of ocean acidification on marine fauna and ecosystem processes. *ICES Journal of Marine Sciences* 65, 414-432,

Falkowski P, Scholes RJ, Boyle E, Canadell J, Canfield D, Elser J, Gruber N, Hibbard K, Hogberg P, Linder S, Mackenzie FT, Moore B, Pedersen T, Rosenthal Y, Seitzinger S, Smetacek V et Steffen W (2000). The global carbon cycle: A test of our knowledge of earth as a system. *Science* 290: 291-296.

Farmer C (1993). Steroidal-diols and long-chain ketones as biomarkers of Prymnesiophyte algae. *Honours Thesis, University of Tasmania, Australia.*

Felsenstein, J. (1985). Confidence limits on phylogenies: an approach using the bootstrap. *Evolution* 39:783–91.

Feng, Y. *et al.* (2008) Interactive effects of increased pCO(2), temperature and irradiance on the marine coccolithophore Emiliania huxleyi (Prymnesiophyceae). *Eur.*

J. Phycol. 43, 87-98.

Findlay, C. S. and Giraudeau J. (2000). Extant calcareous nannoplankton in the Australian Sector of the Southern Ocean (austral summers 1994 and 1995). *Mar. Micropaleontol.* 40:417-39.

Frada M (2009) "The haplo-diplontic life cycles of the Haptophytes, with emphasis on the eco-physiology of *Emiliania huxleyi*." Université Pierre et Marie Curie (Paris VI), Paris.

Fujiwara S, Tsuzuki M, Kawachi M, Minaka N and Inouye I (2001). Molecular phylogeny of the Haptophyta based on the *rbcL* gene and sequence variation in the spacer region of the RUBISCO operon. *Phycologia* 37: 121-129.

Fujiwara, S., Tsuzuki, M., Kawachi, M., Minaka, N. and Inouye, I. (2001). Molecular phylogeny of the haptophyta based on the *rbc*L gene and sequence variation in the spacer region of the Rubisco operon. *J. Phycol.* 37: 121-9.

Garcia, H. E., Locarnini, R. A., Boyer, T. P. and Antonov, J. I. (2006b). *World Ocean Atlas 2005, Volume 4: Nutrients (phosphate, nitrate, silicate). In* Levitus, S. [Ed.] *NOAA Atlas NESDIS 64*, U.S. Government Printing Office, Washington, D.C., 396 pp.

Garcia, H. E., Locarnini, R. A., Boyer, T. P., and Antonov, J. I. (2006a). *World Ocean Atlas 2005, Volume 3: Dissolved Oxygen, Apparent Oxygen Utilization, and Oxygen Saturation. In* Levitus, S. [Ed.] *NOAA Atlas NESDIS 63*, U.S. Government Printing Office, Washington, D.C., 342 pp.

Gard, G. (1986). Calcareous Nannofossil Biostratigraphy of Late Quaternary Arctic Sediments. *Boreas*, 15:217-29.

Gard, G. (1989). Variations in coccolith assemblages during the Last Glacial Cycle in the High and Mid-Latitude Atlantic and Indian Oceans, *In* Crux, J. A. and van Heck, S. E. [Eds.] *Nannofossils and their applications*. Ellis Horwood, Chichester, pp. 108-

21.

Gattuso, J.-P., Frankignoulle, M., Bourge, I., Romaine, S. and Buddemeier, R. W. (1998) Effect of calcium carbonate saturation of seawater on coral calcification. *Glob. Planet. Change* 18, 37-46.

Geitler L (1943). Eine neue atmophytische Chrysophycee, *Ruttnera spectabilis* nov. gen., nov. spec.. *Int Rev Gesamten Hydrobiol Hydrogr* 43: 100-109.

Gibbs, S. J., Bown, P. R., Sessa, J. A., Bralower, T. J. and Wilson, P. A. (2006) Nannoplankton extinction and origination across the Paleocene-Eocene Thermal Maximum. *Science* 314, 1770-1773.

Goddéris Y, Donnadieu Y, de Vargas C, Pierrehumbert R, Dromart G et van de Schootbrugge B (2008) Causal or casual link between the rise of nannoplankton calcification and a tectonically-driven massive decrease in late triassic atmospheric CO2? *Earth Planet. Sc. Lett.*, 267: 247–255

Gould SB, Waller RF, McFadden GI (2008). "Plastid evolution". *Annu Rev Plant Biol* 59: 491–517.

Gray, M. W., Burger, G. and Lang, B. F. (2001) The origin and early evolution of mitochondria. Genome Biol. 2, 1–5.

Green JC and Course PA (1983) Extracellular calcification in *Chrysotila lamellosa* (Prymnesiophyceae). *Br Phycol J* 18: 367-382.

Green JC and Parke M (1974). A reinvestigation by light and electron microscopy of *Ruttnera spectabilis* Geitler (Haptophyceae), with special reference to the fine structure of the zooids. *J mar biol Ass UK* 54: 539-550.

Green JC and Parke M (1975). New observations upon members of the genus *Chrysotila* Anand, with remarks upon their relationships within the Haptophyceae. *J*

mar biol Ass UK 55: 109-121.

Green JC and Pienaar RN (1977). The taxonomy of the order Isochrysidales (Prymnesiophyceae) with special reference to the genera *Isochrysis* Parke, *Dicrateria* Parke and *Imantonia* Reynolds. *J mar biol Ass UK* 57: 7-17.

Green JC, Course PA and Tarran GA. (1996). The life cycle of *Emiliania huxleyi*: A brief review and a study of relative ploidy levels analysed by flow cytometry. *J Marin Sys* 9: 33-44.

Green JC, Leadbeater BSC (1994) The Haptophyta Algae, Vol Special volume No. 51. The Systematics Association, Oxford

Hackett J, Yoon H, Li S, Reyes-Prieto A, Rümmele SE, Bhattacharya D (2007) Phylogenomic analysis supports the monophyly of cryptophytes and haptophytes and the association of rhizaria with chromalveolates. *Molecular Biology and Evolution* 24: 1702-1713.

Hagino, K. and Okada, H. (2006). Intra- and infra-specific morphological variation in selected coccolithophore species in the equatorial and subequatorial Pacific Ocean. *Mar. Micropaleontol.* 58:184-206.

Hagino, K., Okada, H. and Matsuoka, H. (2000). Spatial dynamics of coccolithophore assemblages in the Equatorial Western-Central Pacific Ocean. *Mar. Micropaleontol.* 39:53-72.

Hagino, K., Okada, H. and Matsuoka, H. (2005). Coccolithophore assemblages and morphotypes of *Emiliania huxleyi* in the boundary zone between the cold Oyashio and warm Kuroshio currents off the coast of Japan. *Mar. Micropaleontol.* 55:19-47.

Hall TA (1999). BioEdit: a user-friendly biological sequence alignment editor and analysis program for Windows 95/98/NT. *Nucleic Acids Sym* 41: 95-98.

Hardt M et Safina (2010) Threatening Ocean Life from the Inside Out. *Scientific*

American 303: 66–73.

Hay WW (2004) Carbonate fluxes and calcareous nannoplankton. *In: Coccolithophores: from molecular processes to global impact*" (H. Thierstein, and J. R. Young, Eds.), pp. 509–527. Springer.

Hay WW, Mohler HP and Wade ME (1966). Calcareous nannofossils from Nal'Chik (Northwest Caucasus). *Eclog Geol Helvet* 59: 379-399.

Hay WW, Mohler HP, Roth PH, Schmidt RR and Boudreaux JE (1967). Calcareous nannoplankton zonation of the Cenozoic of the Gulf Coast and Caribbean-Antillean area, and transoceanic correlation. *Trans Gulf Coast Asso Geol Soc* 17: 428-480.

Hayashi-Ishimaru Y, Ehara M, Inagaki Y and Ohama T (1997) A deviant genetic code in prymnesiophytes (yellow-algae): UGA codon for tryptophan. Curr Genet 32: 296-299.

Heimdal BR (1973). Two new taxa of recent coccolithophorids. *Met ForErge* 13: 70-75.

Hibberd DJ (1976) The ultrastructure and taxonomy of the Chrysophyceae and Prymnesiophyceae (Haptophyceae): a survey with some new observations on the ultrastructure of the Chrysophyceae. *Journal of the Linnean Society of London, Botany* 72: 55-80.

Hine N. and Weaver, P. P. E. (1998). Quaternary. *In* Bown, P. [Ed.] *Calcareous Nannofossil Biostratigraphy.* Chapman and Hall, Cambridge, UK, pp. 266-83.

Hiramatsu, C. and De Deckker, P. (1996). Distribution of calcareous nannoplankton near thte subtropical convergence, south of Tasmania, Australia. *Mar. Freshwater Res.* 47:707-13.

Honisch, B. and Hemming, N. G. (2005) Surface ocean pH response to variations in

pCO2 through two full glacial cycles. *Earth and Planetary Science Letters* 236, 305-314.

Houdan A, Billard C, Marie D, Not F, Saez A, Young G, Probert I (2004) Holococcolithophores-heterococcolithophores (Haptophyta) life cycles: flow cytometry analysis of relative ploidy levels. *Systematics and Biodiversity* 1: 453-465.

Huxley TH (1858) Appendix A. *In* "*Deep Sea Soundings in the North Atlantic Ocean between Irelandd and Newfoundland*" (J. Dayman, Ed.), pp. 63-68. H. M. Stationary Office, London.

Iglesias-Rodriguez MD, Brown CW, Doney SC, Kleypas J, Kolber D, Kolber Z, Hayes PK et Falkowski PG (2002) Representing key phytoplankton functional groups in ocean carbon cycle models: Coccolithophorids. *Global Biogeochem. Cycles*, 16.

Iglesias-Rodriguez MD, Halloran PR, Rickaby REM, Hall IR, Colmenero-Hidalgo E, Gittins JR, Green DRH, Tyrrell T, Gibbs SJ, von Dassow P, Rehm E, Armbrust EV et Boessenkool KP (2008) Phytoplankton calcification in a high-CO2 world. *Science* 320: 336-340.

Iglesias-Rodriguez MD, Schofield OM, Batley J, Medlin LK and Hayes PK (2006). Intraspecific genetic diversity in the marine coccolithophore *Emiliania huxleyi* (Prymnesiophyceae): the use of microsatellite analysis in marine phytoplankton population studies. *J Phycol* 42: 526-536.

Iglesias-Rodríguez, M.D., Sáez, A., Groben, R., Edwards, K.J., Batley, J. Medlin, L. and Hayes, P.K. (2002). Polymorphic microsatellite loci in global populations of the marine coccolithophorid *Emiliania huxleyi. Molec. Ecol. Notes.* 2:495-7.

Jeffrey SW and Wright SW (1994). Photosyntheitic pigments in the Haptophyta. In Green JC and Leadbeater BSC (eds) The Haptophyte algae. The Systematics Association special volume 51, Oxford University Press (Oxford, UK). pp 113-132.

Jeffrey SW, Brown MR and Volkman JK (1994). Haptophytes as feedstocks in mariculture. In Green JC and Leadbeater BSC (eds) The Haptophyte algae. The Systematics Association special volume 51, Oxford University Press (Oxford, UK). pp 265-85.

Jerkovic L (1970). *Noelaerhabdus* nov. gen. Type d'une nouvelle famille de coccolithophoridés fossiles : Noëlaerhabdaceae du Miocène supérieur de Yougoslavie. *C R Acad Sc Paris* 270: 468-470.

Jobb G, von Haeseler A and Strimmer K (2004). TREEFINDER: A powerful graphical analysis environment for molecular phylogenetics. *BMC Evol Biol* 28: 4-18.

Jordan RW and Young JR (1990). Proposed changes to the classification system of living coccolithophorids. *INA Newsletter* 12: 15-18.

Jordan RW, Cros L and Young JR (2005). A revised classification scheme for living haptophytes. *Micropaleontology* 50 (Suppl. 1): 55-79.

Jordan, R. W., Zhao, M., Eglinton, G. and Weaver, P. P. E. (1996). Coccolith and alkenone stratigraphy and palaeoceanography at an upwelling site off NW Africa (ODP 658C) during the last 130,000 years. *In*: Moguilevsky, A. and Whatley, R. [Eds.] *Microfossils and oceanic environments*. University of Wales, Aberystwyth - Press, Aberystwyth, pp. 111-30.

Kamptner E (1930). Die Kalkflagellaten des Süsswassers und ihre Beziehungen zu jenen der Brackwassers und des Meeres. *Int Rev Gesamten Hydrobiol Hydrogr* 24: 147-163.

Kamptner E (1941). Die Coccolithineen der Südwestküste von Istrien. *Ann Naturhistor Mus Wien* 51: 54-149.

Kamptner E (1943). Zur Revision der Coccolithineen-Spezies *Pontosphaera huxleyi* Lohmann. *Anz Akad Wiss Wien Math -Naturw K* 80: 43-49.

Kamptner E (1956). Das Kalkskelett von *Coccolithus huxleyi* (Lohmann) Kamptner und *Gephyrocapsa oceanica* Kamptner (Coccolithineae). *Arch Protistenkde* 101: 171-202.

Katoh K, Kuma K, Toh H and Miyata T (2007). MAFFT version 5 : improvement in accuracy of multiple sequence alignment. *Nucleic Acids Res* 33: 511-518.

Keller MD, Selvin RC, Claus W and Guillard RRL (1987). Media for the culture of oceanic ultraphytoplankton. *J Phycol* 23: 633-638.

Kimura, M. (1980). A simple method for estimating rate of base substitutions through comparative studies of nucleotide sequences. *J. Mol. Evol*. 16:111–20.

Kishino H and Hasegawa M (1989). Evaluation of the maximum-likelihood estimate of the evolutionary tree topologies from DNA sequence data, and the branching order in Hominoidea. *J Mol Evol* 29: 170-179.

Klaveness D (1972a). *Coccolithus huxleyi* (Lohmann) Kamptner I. Morphological investigations on the vegetative cell and the process of coccolith formation. *Protistologica* 8: 335-346.

Klaveness D (1972b). *Coccolithus huxleyi* (Lohmann) Kamptner. II. The flagellate cell, aberrant cell types, vegetative propagation and life cycles. *Br Phycol J* 7: 309-318.

Kleypas, J. A. *et al.* Geochemical Consequences of Increased Atmospheric Carbon Dioxide on Coral Reefs. *Science* 284, 118-120, doi:10.1126/science.284.5411.118 (1999).

Kondrashov, A. S. (1988). "Deleterious mutations and the evolution of sexual reproduction". *Nature* 336 (6198): 435–440.

Lackey JB (1939). Notes on plankton flagellates from the Scioto River (with

descriptions of new forms). *Llyodia* 2: 128-143

Langer G, Nehrke G, Probert I, Ly J and Ziveri P (2009). Strain-specific responses of *Emiliania huxleyi* to changing seawater carbonate chemistry. *Biogeosciences* 6: 2637-2646.

Langer, G., M. *et al.* (2006) Species-specific responses of calcifying algae to changing seawater carbonate chemistry. *Geochemistry, Geophysics, Geosystems* 7,

Lewis, E. and Wallace, D. W. R. (1998) Program Developed for CO2 System Calculations. *Oak Ridge National Laboratory*.

Liu H, Aris-Brosou S, Probert I and de Vargas C (2010). A timeline of the environmental genetics of the haptophytes. *Mol Biol Evol* 27: 171-176.

Liu H, Probert I, Uitz J, Claustre H, Aris-Brossou S, Frada M, Not F and de Vargas C (2009) Extreme oceanic biodiversity in noncalcifying haptophytes explains a major pigment paradox. *Proc Natl Acad Sci USA* 106: 12803-12808.

Locarnini, R. A., Mishonov, A. V., Antonov, J. I., Boyer, T. P. and Garcia, H. E. (2006). *World Ocean Atlas 2005, Volume 1: Temperature.* S. Levitus, Ed. NOAA Atlas NESDIS 61, U.S. Government Printing Office, Washington, D.C., 182 pp.

Lohmann H (1902). Die Coccolithophoridae, eine monographie der Coccolithen bildenden flagellaten, zugleich ein Beitag zur Kenntnis des Mittelmeerauftriebs. *Arch Protistenkde* 1: 89-165.

Lohmann H (1912) Untersuchungen über das Pflanzen- und Tierleben der Hochsee. *Veroff Inst Meereskd Univ Berlin NF, Georg-Naturw Reihe* 1: 1-92.

Mackinder, L., Wheeler, G., Schroeder, D., Riebesell, U. and Brownlee, C. (2010) Molecular Mechanisms Underlying Calcification in Coccolithophores. *Geomicrobiol. J.* 27, 585-595.

Marlowe IT, Green JC, Neal AC, Brassell SC, Eglington G and Course PA (1984). Long chain (n-C_{37}-C_{39}) Alkenones in the Prymnesiophyceae. Distribution of Alkenones and other Lipids and their Taxonomic Significance. *Br Phycol J* 19: 203-216.

Martínez-Martínez J., Schroeder, D. C., Larsen, A., Bratbak, G. and Wilson, W. H. (2007). Molecular Dynamics of *Emiliania huxleyi* and Cooccurring Viruses during Two Separate Mesocosm Studies. *Appl. Env. Microbiol*. 73:554-62.

Massart J (1920) Recherches sur les organismes inférieurs. VIII. Sur la motilité des flagellées. *Bull. Acad. r. Belg. Cl. Sci. Sér*. 5, 6: 116-141.

Maynard Smith J 1978 *The Evolution of Sex.*

McFadden GI (2001). "Primary and secondary endosymbiosis and the origin of plastids". *J Phycology* 37 (6): 951–9.

McIntyre A (1970). *Gephyrocapsa protohuxleyi* sp. n. a possible phyletic link and index fossil for the Pleistocene. *Deep Sea Res* 17: 187-190.

McIntyre A and Bé AWH (1967). Modern coccolithophorids of the Atlantic Ocean - I. Placoliths and cyrtoliths. *Deep Sea Res* 14: 561-597.

Medlin LK, Barker GLA, Campbell L, Green JC, Hayes PK, Marie D, Wrieden S and Vaulot D (1996). Genetic characterisation of *Emiliania huxleyi* (Haptophyta). *J Marin Sys* 9: 13-31.

Medlin LK, Sàez AG and Young JR (2008). A molecular clock for coccolithophores and implications for selectivity of phytoplankton extinctions across the K / T boundary. *Mar Mic* 67: 69-86.

Milliman JD, Troy PJ, Balch WM, Adams AK, Li YH et Mackenzie FT (1999)

Biologically mediated dissolution of calcium carbonate above the chemical lysocline? *Deep-Sea Research I* 46: 1653-1669.

de Moel, H. *et al.* (2009) Planktic foraminiferal shell thinning in the Arabian Sea due to anthropogenic ocean acidification? *Biogeosciences* 6, 1917-1925.

Monnin, E. *et al.* (2001) Atmospheric CO2 concentrations over the last glacial termination. *Science* 291, 112-114

Moy, A. D., Howard, W. R., Bray, S. G. and Trull, T. W. (2009) Reduced calcification in modern Southern Ocean planktonic foraminifera. *Nat. Geosci.* 2, 276-280,.

Müller PJ, Kirst G, Ruhland G, von Storch I and Rosell-Mele A (1998). Calibration of the alkenone paleotemperature index $U^{K'}37$ based on core-tops from the eastern South Atlantic and the global ocean (60°N-60°S). *Geochim. Cosmochim. Acta* 62: 1757-1772.

Noël M-H., Kawachi, M. and Inouye I. (2004). Induced dimorphic life cycle of a coccolithophorid, *Calyptrosphaera sphaeroidea* (Prymnesiophyceae, Haptophyta). *J. Phycol.* 40:112-29.

Okada H and McIntyre A (1977). Modern coccolithophores of the Pacific and North Atlantic Oceans. *Micropal* 23: 1-55.

Okada, H. and Honjo, S. (1973). The distribution of oceanic coccolithophorids in the Pacific. *Deep-Sea Res.* 20:355-74.

O'Shea SK, Holland F and Bilodeau A (2010). Modeling the Effects of Salinity and pH on the Cadmium Bioabsorptive Properties of the Microalgae *Isochrysis galbana* (T-Iso) in Coastal Waters. *J Coast Res* 26: 56-66.

Paasche E (2002). A review of the coccolithophorid *Emiliania huxleyi* (Prymnesiophyceae), with particular reference to growth, coccolith formation, and

calcification-photosynthesis interactions. *Phycologia* 40: 503-529.

Parke M (1949). Studies on marine flagellates. *J mar biol Ass UK* 28: 255-286.

Parke M and Dixon PS (1964). A revised check-list of British marine algae. *J mar biol Ass UK* 44: 499-542.

Parke M et Adams I (1960) The motile (*Crystallolithus hyalinus* Gaarder and Markali) and nonmotile phases in the life-history of *Coccolithus pelagicus* (Wallich). *Journal of the Marine Biological Association of the United Kingdom* 39:263-274.

Pascher A (1910). Chrysomonaden aus dem Hirschberger Grossteiche. *Int Rev Gesamten Hydrobiol Hydrogr* 1: 1-66.

Pawlowski J, Bolivar I, Fahrni J F, de Vargas C, Gouy M and Zaninetti L (1997) Extreme differences in rates of molecular evolution of foraminifera revealed by comparison of ribosomal DNA sequences and the fossil record. *Mol Biol Evol* 14: 498-505

Pennick NC (1977). Studies on the external morphology of *Pyramimonas*. 4. *Pyramimonas virginica* sp.. *Archr Protistenkd* 119: 239-246.

Petit, J. R. *et al.* (1999) Climate and atmospheric history of the past 420,000 years from the Vostok ice core, Antarctica. *Nature* 399, 429-436.

Posada, M. A. and Crandali, K. A. (1998). Modeltest: testing the model of DNA substitution. *Bioinformatics* 14: 817–8.

Raffi, I., Backman, J., Fornaciari, E., Pälike, H., Rio, D., Lourens, L. and Hilgen, F. (2006). A review of calcareous nannofossil astrobiochronology encompassing the past 25 million years. *Quaternary Sci. Rev.* 25: 3113-37.

Ratnasingham, S. and Hebert, P. D. N. (2007). BOLD : The Barcode of Life Data

System(www.barcodinglife.org). Molecular Ecology Notes 7, 355–364.

Reid, P. C., Johns, D. G., Edwards, M., Starr, M., Poulin, M. and Snoeijs, P. (2007). A biological consequence of reducing Arctic ice cover: arrival of the Pacific diatom *Neodenticula seminae* in the North Atlantic for the first time in 800 000 years. *Global Ch. Biol*. 13: 1910-1921.

Reinhardt P (1972). Coccolithen. Kalkiges Plankton seit Jahrmillionen. *Die neue Brehm Bücheri* 453: 1-99.

Reynolds ES (1963). The use of lead citrate at high pH as an electron-opaque stain in electron microscopy. *J Cell Biol* 17: 208-212.

Reynolds N (1974). *Imantonia rotunda* gen. et sp. nov., a new member of the Haptophyceae. *Br Phycol J* 9: 429-434.

Riebesell U, Zondervan I, Rost B, Tortell PD, Zeebe RE and Morel FMM (2000). Reduced calcification of marine plankton in response to increased atmospheric CO_2. *Nature* 407: 364-367.

Ripley, S. J., Highfield, A. C., Miller, P. I., Walne, A. W. and Schroeder, D. C. (2008). Development and validation of a molecular technique for the analysis of archived formalin-preserved phytoplankton samples permits retrospective assessment of *Emiliania huxleyi* communities. *J. Microbiol. Method.* 73: 118-24.

Ronquist F and Huelsenbeck JP (2003). MRBAYES 3: Bayesian phylogenetic inference under mixed models. *Bioinformatics* 19: 1572-1574.

Rost B and Riebesell U (2004). Coccolithophores and the biological pump responses to environmental changes. In Thierstein, H. R. and Young, J. R. [Eds.] Coccolithophores – From Molecular Processes to Global Impact. Springer, Berlin. pp. 99-125.

Sabine, C. L. *et al.* (2004) The Oceanic Sink for Anthropogenic CO_2. *Science* 305, 367-371.

Saez AG, Probert I, Young JR, Edvardsen B, Eikrem W et Medlin LK (2004) A review of the phylogeny of the Haptophytes. *In*: Thierstein HR, Young JR (eds) *Coccolithophores: From the molecular processes to global impact.* Springer Verlag, pp. 251-270.

Saitou, N. and Nei, M. (1987). The neighbor-joining method: a new method for reconstructing phylogenetic trees. *Mol. Biol. Evol*. 4: 406–25.

Sambrook, J., Fritsch, E. F. and Maniatis, T., (1989). Molecular Cloning - A Laboratory Manual. Cold Spring Harbour Laboratory Press.

Samtleben C (1980) Die evolution der coccolithophoriden-Gattung Gephyrocapsa nach Befunden im Atlantik. *PaläontologischeZeitschrift* 54, 91– 127.

Sánchez Puerta V., Bachvaroff, T. R. and Delwiche, C.F. (2004). The complete Mitochondrial genome sequence of the Haptophyte *Emiliania huxleyi* and its Relation to Heterokonts. *DNA Res.* 11:1-10.

Sato, T., Saito, T., Yuguchi, S., Nakagawa, H., Kameo, K. and Takayama, T. (2002). Late Pliocene calcareous nannofossil palaeobiogeography of the Pacific Ocean: evidence for glaciation at 2.75 Ma. *Revista Mexicana de Ciencias Geológica.* 19:175-189.

Sawada K and Shiraiwa Y (2004). Alkenone and alkenoic acid compositions of the membrane fractions of *Emiliania huxleyi*. *Phytochemistry* 65: 1299-1307.

Scherffel A (1900) *Phaeocystis globosa* nov. spec. nebst einigen Betrachtungen über die Phylogenie niederer, insbesondere brauner Organismen. *Wiss. Meeresuntersuchungen Abt. Helgoland N.F.*, 4: 1-29

Schroeder DC, Biggi GF, Hall M, Davy J, Martínez JM, Richardson AJ, Malin G and Wilson WH (2005) A genetic marker to separate *Emiliania huxleyi* (Prymnesiophyceae) morphotypes. *J Phycol* 41: 874-879.

Schwaninger, H. R. (2008). Global mitochondrial DNA phylogeography and biogeographic history of the antitropically and longitudinally disjunct marine bryozoan *Membranipora membranacea* L. (Cheilostomata): Another cryptic marine sibling species complex?. *Mol. Phylog. Evol*.. 49: 893–908.

Shimodaira H (2002). An approximately unbiased test of phylogenetic tree selection. *Syst Biol* 51: 492-508.

Shimodaira H and Hasegawa M (1999). Multiple comparisons of log-likelihoods with applications to phylogenetic inference. *Mol Biol Evol* 16: 1114-1116.

Sogin ML (1990) Amplification of ribosomal RNA genes for molecular evolution studies. In Innes MA, Gelfand DH, Sninsky JJ, White TJ (eds) PCR protocols. Academic Press, San Diego. pp. 307-320.

Sorby HC (1861) On the organic origin of the so-called 'Crystalloids' of the Chalk. *Ann. Mag. Nat. History*, s. 3, v. 8: 193-200.

Stocker T. F. et Wright D. G., (1991). Rapid transitionsof the ocean's deep circulation induced by changes in surface water fluxes. *Nature*, 351, pp. 729-732.

Subrahmanyan R (1962). On *Ruttnera pringsheimii* sp. nov. (Chrysophyceae) from the coastal waters of India. *Arch Microbiol* 42: 219-225.

Swofford, D. L. (2002). PAUP*—Phylogenetic Analysis Using Parsimony (* and Other Methods), Version 4. Sinaver Associates, Sunderland, Massachusetts

Tamura K and Nei M (1993). Estimation of the number of nucleotide substitutions in the control region of mitochondrial DNA in humans and chimpanzees. *Mol Biol Evol* 10: 512-526.

Tanimoto, M., Aizawa, C. and Jordan, R. W. (2003). Assemblages of living microplankton from the subarctic North Pacific and Bering Sea during July-August 1999. *Cour. Forsch.-Inst. Senckenberg.* 244:83-103.

Thierstein HR, Geitzenauer KR, Molfino B and Shackleton NJ (1977). Global synchroneity of late Quarternary coccolith datum levels: Validation by oxygen isotopes. *Geology* 5: 400-404.

Tomczak M.and Godfrey, J. S. (1994). Regional Oceanography: An Introduction. Pergamon, London. 422 pp.

Van Bleijswijk, J. van der Wal, P., Kempers, R., Veldhuis, M., Young, J. R., Muyzer, G., de Vrind-de Jong, E. and Westbroek, P. (1991). Distribution of two types of *Emiliania huxleyi* (Prymnesiophyceae) in the northeast Atlantic region as determinded by immunofluorescence and coccolith morphology. *J. Phycol.* 27:566-70.

de Vargas C et Probert I (2004) New keys to the past: Current and future DNA studies in coccolithophores. *Micropaleontology* 50: 45-54.

de Vargas C, Aubry MP, Prober, I, Young J, Falkowski P et Knoll A (2007) Origin and evolution of Coccolithophores: from coastal hunters to oceanic farmers. *In* "*Evolution of primary producers in the sea*" (P. Falkowski, and A. Knoll, Eds.), pp. 251-285.

Van Valen, L. (1973). "A New Evolutionary Law". *Evolutionary Theory* 1: 1–30.

Volk T et Hoffert MI (1985) Ocean carbon pumps: Analysis of relative strengths and efficiencies in ocean-driven atmospheric CO_2 changes. *In* Sundquist ET et Broecker WS (eds) *The Carbon Cycle and Atmospheric CO_2: Natural Variations Archean to Present*. *Geophys. Monogr. Ser.* 32, pp. 99-110.

von Dassow P, Ogata H, Probert I, Wincker P, Da Silva C, Audic S, Claverie J-M and de Vargas C (2009). Transcriptome analysis of functional differentiation between haploid and diploid cells of *Emiliania huxleyi*, a globally significant photosynthetic calcifying cell. *Genome Biol* 10: R114.

von Stosch HA (1958) Der Geisselapparat einer Coccolithophoride. *Naturwissenschaften,* 45: 140-141.

Wahlund TM, Hadaegh AR, Clark R, Nguyen B, Fanelli M and Read BA (2004). Analysis of expressed sequence tags from calcifying cells of marine coccolithophorid (*Emiliania huxleyi*). *Mar Biotech* 6: 278-290.

Wallich GC (1861) Remarks on some novel phases of organic life, and on the boring powers of minute annelids, at great depths in the sea. *Ann. Mag. nat. Hist.*, 8: 52-58.

Wallich GC. (1877). Observations on the coccosphere. *Ann Magazine Natural History* 4, 342-350.

Watabe, N. and Wilbur, K. M. (1966). Effect on temperature on growth calcification, and coccolith form in *Coccolithus Huxleyi* (Coccolithtineae). *Limnol. Oceanogr*. 11:567-75.

Weismann right?". *Evolution* 54 (2): 337–351.

Welch, B. L. (1947). The generalization of "Student's" problem when several different population variances are involved. *Biometrika* 34: 28–35.

Westbroek P, Brown CW, van Bleijswijk J, Brownlee C, Brummer GJ, Conte M, Egge J, Fernandez E, Jordan R, Knappertsbusch M, Stefels J, Veldhuis M, van der Wal P and Young J (1993). A model system approach to biological climate forcing. An example of *Emiliania huxleyi*. *Global Planetary Change* 8: 27-46.

Winter A, Jordan R, Roth P (1994) Biogeography of living coccolithophores in ocean

waters. In: Winter A and Siesser WG (editors) "Coccolithophores". Cambridge University Press, Cambridge, UK.

Winter, A. (1985). Distribution of living coccolithophore in the California Current system, southern California Borderland. *Mar. Micropaleontol.* 9:385-93.

Worsley, T.R. (1973). Calcareous nannofossils: Leg 19 of the Deep Sea Drilling Project. *In* Creager, J.S., Scholl, D.W., et al. [Eds.] *Init. Repts. DSDP*, 19: Washington, DC (U.S. Govt. Printing Office). 741-750.

Yoon HS, Hackett JD, Pinto G et Bhattacharya D (2004) A molecular timeline for the origin of photosynthetic eukaryotes. *Mol. Biol. Evol*. 21: 809–818.

Young J. R. and Westbroek, P. (1991). Genotypic variation in the coccolithophorid species *Emiliania huxleyi. Mar. Micropaleontol.* 18:5-23.

Young JR (1992). The description and analysis of coccolith structure. In: Harmsmid B and Young JR, *Nannoplankton Research*. ZPZ. pp 35-71.

Young JR and Bown PR (1997). Higher classification of calcareous nannofossils. *J Nanno Res* 19: 15-20.

Young JR and Geisen M (2002). Xenospheres-associations of coccoliths resembling coccospheres. *J Nanno Res* 24: 127-135.

Young JR and Westbroek P (1991). Genotypic variation in the coccolithophorid species *Emiliania huxleyi*. *Mar Micropal* 18: 5-23.

Young JR, Davis SA, Bown PR and Mann S (1999). Coccolith ultrastructure and biomineralisation. *J Struct Biol* 126: 195-215.

Young JR, Geisen M et Probert I (2005) A review of selected aspects of coccolithophore biology with implications for paleobiodiversity estimation.

Micropaleontology 51:267-288.

Young JR, Geisen M, Cros L, Kleijne A, Probert I, Sprengel C and Østergaard JB (2003). A guide to extant coccolithophore taxonomy. *J Nanno Res* Special Issue 1. 124 pp.

Young JR, Henriksen K and Probert I (2004). Structure and morphogenesis of the coccoliths of the CODENET species. In Thierstein, H. R. and Young, J. R. [Eds.] Coccolithophores – From Molecular Processes to Global Impact. Springer, Berlin. pp.191-216.

Young, J.R. (1998), Neogene. *In* Bown, P. [Ed.] *Calcareous Nannofossil Biostratigraphy*. Champman and Hall, Cambridge, UK, pp. 225-65.

Zapata M, Jeffrey SW, Wright SW, Rodriguez F, Garrido JL and Clementson L(2004). Photosynthetic pigmentsin 37 species (65 strains) of Haptophyta: Implications for oceanography and chemotaxonomy. *Mar Eco Prog Ser* 270: 83-102.

Zhu H., Qu, F., Zhu, L. H. (1993). Isolation of genomic DNAs from plants, fungi and bacteria using benzyl chloride. *Nucleic Acids Res.* 21(22):5279-80.

Zondervan, I. (2007) The effects of light, macronutrients, trace metals and CO2 on the production of calcium carbonate and organic carbon in coccolithophores - A review. *Deep-Sea Research Part Ii-Topical Studies in Oceanography* 54, 521-537

Zondervan, I., Rost, B. and Riebesell, U. (2002) Effect of CO2 concentration on the PIC/POC ratio in the coccolithophore Emiliania huxleyi grown under light-limiting conditions and different daylengths. *J. Exp. Mar. Biol. Ecol.* 272, 55-70.

ANNEXE 1

Diversité moléculaire et environnementale de la famille des Noëlaerhabdaceae (ordre des Isochrysidales) en Méditerranée

Mémoire de Master

« Mention Sciences de l'Univers, Environnement, Ecologie »

« Spécialité Océanographie et Environnements Marins » Année 2

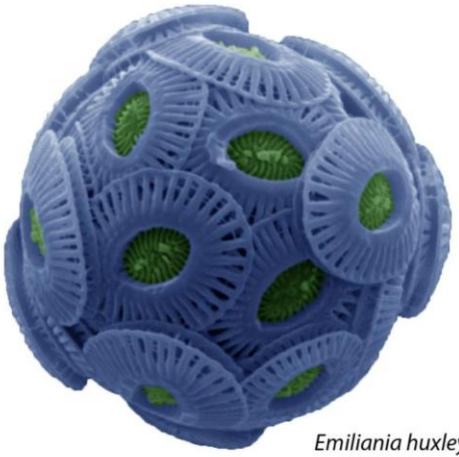

Emiliania huxleyi

Sous la co-direction de Colomban de Vargas et de El Mahdi Bendif
UMR 7144, Equipe EPPO (Evolution du Plancton et PaleoOcéans)

LAURENT Julien

Année universitaire
2009/2010

Index

Introduction

Les études de phylogénie moléculaire ont conduit à des modifications importantes des schémas de classification traditionnelle des Eucaryotes (Figure 1). Des changements fondamentaux sont apparus avec les protistes qui présentent une grande diversité. En dépit du fait qu'ils restent assez difficiles à classer, Adl et al. (2005) ont réussi à établir une nouvelle classification qui reflète le consensus général actuel. Ils définissent les protistes comme des organismes eucaryotes avec une organisation pouvant être unicellulaire, en colonie, filamenteuse ou parenchymateuse et qui ne possèdent pas de tissus végétatifs différentiés, excepté pour la reproduction. Des travaux de Slapeta et al. (2005) montrent que le taux de découverte des protistes dans la plupart des échantillons environnementaux est considérable. L'utilisation conjointe du microscope et de l'analyse des séquences d'ADN pour étudier la biodiversité des échantillons provenant du sol, de l'eau douce ou du milieu marin a permis de mettre en évidence la présence d'une multitude d'espèces non décrites. De plus, l'analyse des données moléculaires soulignent la présence et l'importance d'espèces cryptiques que l'observation seule des caractères morphologiques ne permet pas de distinguer (Adl et Gupta 2006., Foissner, 2006). Epstein et López-García (2008) ont mis en évidence l'importance des perspectives moléculaires pour étudier l'étendue, la dynamique spatiale et temporelle et le rôle écologique d'une diversité des protistes insoupçonnée. Nos connaissances actuelles de ces organismes restent encore fragmentaires en raison d'une très vaste biodiversité et de nombreuses relations phylogénétiques dans ce groupe n'ont pas encore été élucidées.

L'étude présentée ici concerne la biodiversité environnementale d'une famille de protistes photosynthétiques, les Noëlaerhabdaceae. Ces organismes appartiennent à l'embranchement des Haptophytes, à la classe des Prymnesiophyceae et à l'ordre des Isochrysidales (Figure 2). Le travail que nous avons réalisé aborde la biodiversité générale de cette famille dans la Méditerranée s'appuyant sur des données de phylogénie moléculaire obtenues à partir d'échantillons provenant de la campagne BOUM (Biogéochimie de l'Oligotrophie à l'Ultra-oligotrophie Méditerranéenne) réalisée entre le 16 juin et le 20 juillet 2008 (Figure 5).

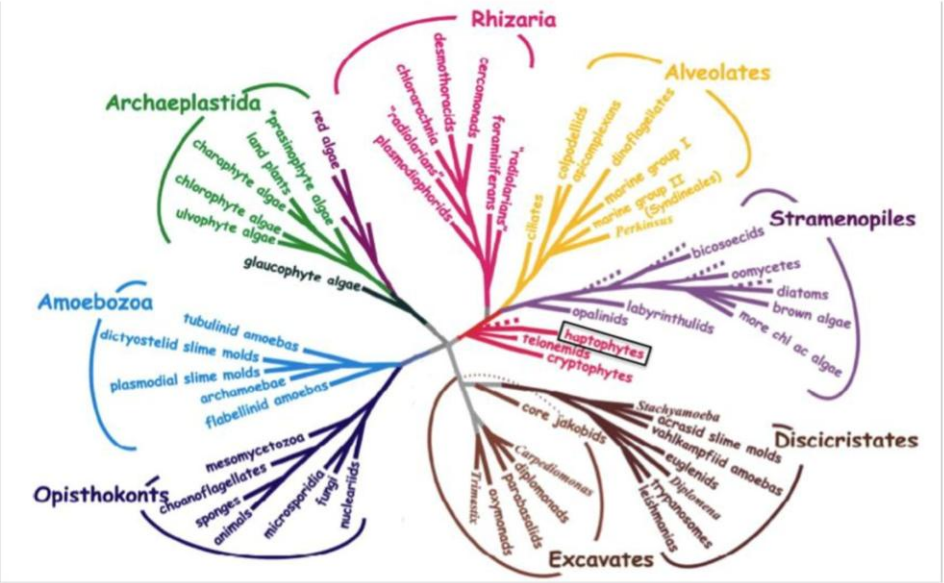

Figure 1: Arbre phylogénétique synthétiques des grands domaines eucaryotiques, basé sur les données publiées d'ultrastructure et de phylogénie moléculaire (adapté de Baldauf, 2008). Le groupe des haptophytes est encadré en noir.

L'embranchement des Haptophytes (figure 1) constitue un groupe de protistes très répandu dans les océans dont le nombre d'espèces actuelles est estimé à environ 300 (Reviers, 2002b). De nombreuses espèces sont tropicales, d'autres vivent en eau douce et de nombreux groupes fossiles existent. Ce sont des algues unicellulaires de la lignée rouge contenant de la chlorophylle a et c (Jordan et al., 2004). Ce groupe eucaryotique unicellulaire est caractérisé par la présence d'un appendice inséré entre deux flagelles : l'haptonème. Cet appendice filiforme constitué de microtubules dont la taille varie selon l'espèce permettrait l'adhésion à un substrat, le déplacement de particules, voire la capture de proies (Inouye et Kawashi, 1994).

Les corrélations établies entre d'une part les caractéristiques morphologiques (Green, 1980; Cavalier-Smith 1994; Green et Jordan, 1994), et d'autre part les récentes données moléculaires (Edvardsen et al., 2000 ; Fujiwara et al., 2001) ont permis de confirmer que la division des Haptophytes est composée de deux classes bien distinctes (Figure 2): les Pavlovophyceae Green et Medlin (Edvardsen et al., 2000) et les Prymnesiophyceae Hibberd (Hibberd, 1976).

5

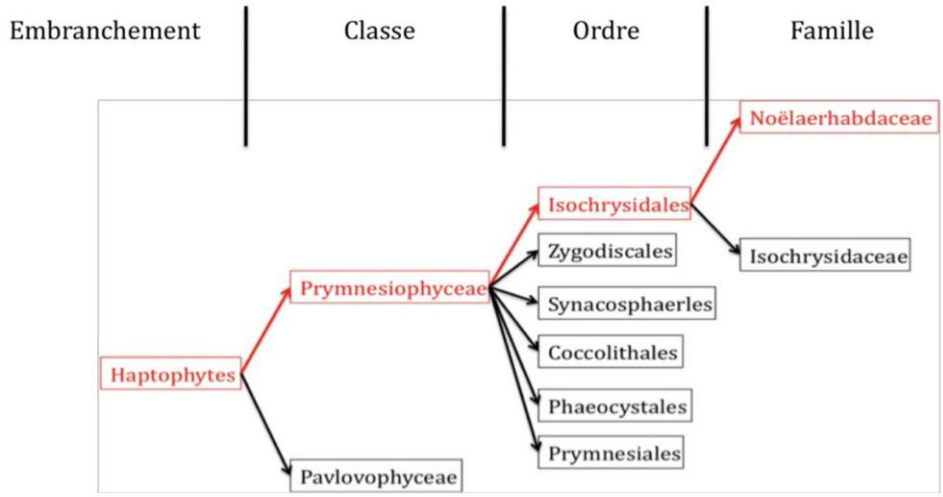

Figure 2 : Schéma taxonomique au sein de de l'embranchement des Haptophytes

Certaines espèces des Prymnesiophyceae comme Prymnesium parvum sont toxiques (hémolytiques), mais leurs toxines sont encore peu connues (Moestrup, 1994). D'autres espèces de cette classe sont réputées pour les « blooms » très importants qu'elles constituent à la fin du printemps ou au début de l'été : c'est par exemple le cas de Phaeocystis globosa dont les efflorescences sont connues pour provoquer une importante mortalité animale. Cette espèce produit un mucus dont la dégradation génère une écume qui peut provoquer le colmatage des filets de pêche ou des canalisations d'eau de mer, mais aussi contrarier la nutrition des bivalves et porter atteinte à l'attrait touristique lorsque l'écume nauséabonde s'accumule sur les plages (Sournia et al., 1991). Ces blooms massifs de Phaeocystis provoquent également des rejets de DMS (dimethylsulfide) ce qui a suggéré une implication de ces algues dans le cycle du soufre et les changements climatiques globaux (Reviers, 2002b).

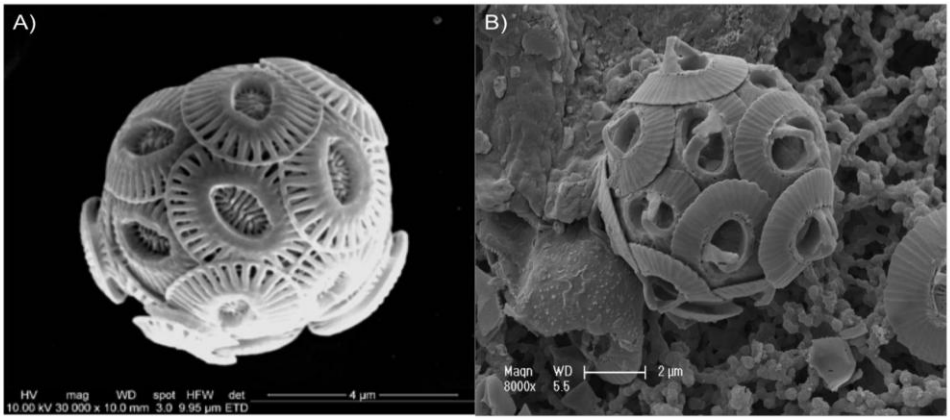

Figure 3: Deux espèces emblématiques de coccolithophore, vues en microscopie électronique à balayage: A) Emiliana huxleyi et B) Gephyrocapsa oceanica (photographie : © EPPO/SB Roscoff)

L'ordre des Isochrysidales Pascher (Edvardsen et al., 2000 ; Pascher, 1910) appartenant à la classe des Prymnesiophyceae est caractérisé par sa production exclusive de longues chaines alkenones (Marlowe et al., 1984). Ces lipides sont assez résistants pour être retenus dans les anciens sédiments et sont utilisés pour estimer la température de la surface de l'eau dans les paléoocéans (Brassel et al., 1986). L'ordre des Isochrysidales est composé de deux familles (Annexe 1). La première nommée Isochrysidaceae Bourelly (Bourelly, 1953 ; Edvardsen et al., 2000) est composée d'organismes non calcifiants. La seconde appelée Noëlaerhabdaceae Jerkovic (Jerkovic, 1970 ; Young and Bown, 1997) est formée d'organismes calcifiants. Elle est notamment représentée par les espèces Emiliana huxleyi Lohmann (Lohmann, 1902) et Gephyrocapsa oceanica Kamptner (Kamptner, 1943) (Figure 3). La première apparition de G. oceanica dans les assemblages fossiles a été estimée à 3,5 Ma (Samtleben, 1980 ; Rio, 1982). Cette espèce a dominé les océans avant l'émergence quasi-invasive de l' «espèce morphologique » E. huxleyi il y a environ 270Ka (Thierstein et al., 1977). Emiliania huxleyi est aujourd'hui un des eucaryotes marins les plus abondants à l'échelle de la planète.

Figure 4: « Bloom » de coccolithophores sur plusieurs centaines de kilomètres carrés au large de la Bretagne française (www.nasa.org). Ces populations apparaissent à la fin du printemps, après les efflorescences de diatomées.

Les espèces appartenant à l'ordre des Isochrysidales sont des organismes potentiellement calcifiants appelés coccolithophores (De Vargas et al., 2007). Ils sont à l'origine de larges traînées laiteuses dans l'océan, visibles par satellite depuis l'espace (Figure 4). Ces microalgues possèdent des écailles de carbonate de calcium appelées coccolithes. Elles attestent de leur capacité à fixer le carbone et seraient responsables de la moitié de la précipitation du $CaCO_3$ vers le fond des océans (Milliman, 1993). Les propriétés calcifiantes de ces organismes associées à leur caractère ubiquiste leur confère un statut tout particulier pour construire des modèles d'écologie et d'évolution du phytoplancton. Cette position est renforcée par l'impact biogéochimique associé au bloom massif et au cycle du carbone dans les océans (Van Cappellen, 2003). L'étude de la famille des Noëlaerhabdaceae apparait fondamentale pour comprendre l'impact de la physiologie et de l'écologie des coccolitophores et plus largement des protistes sur la chimie global du carbone dans les océans.

8

La connaissance de la biodiversité existante des Isochrysidales est limitée et basée exclusivement sur les caractères morphologiques et parfois ultrastructuraux de la cellule. Dans le cas des Noëlaerhabdaceae, elle se base sur la forme des coccolithes recouvrant la cellule (Young et al., 2003). Les séquences d'ADN les plus fréquemment utilisées pour la reconstruction phylogénétique des groupes eucaryotes correspondent à celles des sous-unités de l'ADN ribosomal 18S et 28S. Les gènes 18S, 28S, ITS, 16S, TufA, Rbc-1 ont été utilisés pour plusieurs études s'intéressant à la phylogénie des haptophytes (Edvardsen et al, 2000 ; Liu et al., 2010). Chez les Noëlaerhabdaceae, les séquences obtenues pour ces gènes chez E. huxleyi et G. oceanica sont identiques (de Vargas et al. 2007). Géneralement, l'utilisation des sous-unités d'ADN ribosomaux dans le cadre des études phylogénétiques a tendance à sous-estimer la diversité intragénétique et le taux d'évolution de certains clades (Keeling et al., 2005 ; Simpson et Roger, 2004).

L'étude présentée ici cherche à apporter une nouvelle vision phylogénétique de la famille des Noëlaerhabdaceae en utilisant des séquences correspondant à des fragments du gène mitochondrial cox I codant pour la première sous-unité de la cytochrome c oxydase (Annexe 2). Bendif et al. (en préparation) ont récemment constitué une collection de séquences du gène cox I à partir de souches de la famille des Noëlaerhabdaceae en culture. Ces souches proviennent de différents endroits de la planète. Leurs morphotypes ont pu être identifiés par microscopie en laboratoire. Il est donc possible d'assigner des séquences du gène cox I à des morphotypes donnés. La transmission du génome mitochondrial est supposée monoparentale. Il échapperait à la reproduction et de ce fait ne serait pas soumis à la recombinaison (Day et al., 2004). De ce fait les taux de mutation du gène cox I sont souvent plus élevés, permettant d'augmenter la résolution phylogénétique entre les différents organismes. Ainsi le gène cox I est un marqueur très utilisé pour des études de phytogéographie au niveau intraspécifique. Les échantillons environnementaux de la campagne BOUM (Figure 5) ont permis de déterminer la distribution spatiale de clades définis au sein de la jeune famille des Noëlaerhabdaceae en Méditerranée pour mieux en apprécier la biodiversité.

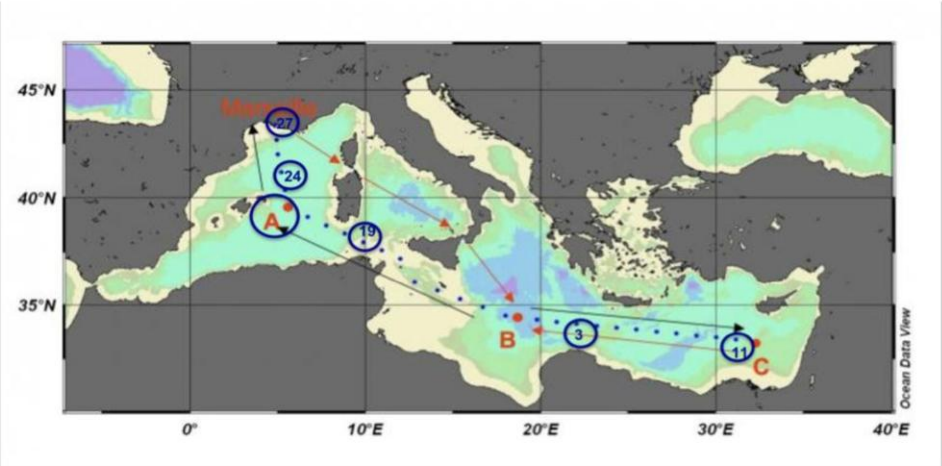

Figure 5: Transect de la campagne BOUM. Les stations analysées dans le présent travail sont entourées en bleu.

10

Matériel et Méthodes

Echantillonnage

Les prélèvements d'eau de mer dans les différentes stations d'échantillonnage ont été réalisés en utilisant des bouteilles Niskin de 12l. Des filtres Sterivex avec une porosité de 0,22 µm (Millipore) ont été utilisés pour filtrer 10l d'eau de mer pour chaque station étudiée lors de la campagne BOUM (Figure 5). Les échantillons ont ensuite été stockés à -80 °C jusqu'à la réalisation de l'extraction de l'ADN génomique. Dans cette étude, nous nous sommes intéressés à la surface et à la DCM (Deep Chlorophyll Maximum ; pic maximum profond de chlorophylle) pour les stations 27, 24, A, 19, 3 et 11 (Figure 5).

Extraction d'ADN

Nous avons utilisé un protocole d'extraction (Annexe 3) qui a été adapté du manuel pratique BIO 14825 de l'université de Biologie cellulaire et moléculaire de Laval (communiqué par le Dr. Ramon Massana, CMIMA, Barcelona). Après avoir décongelé les Sterivex à température ambiante une première étape de dénaturation des protéines a été réalisée en incubant 1 h à 55 °C les filtres avec de la protéinase K à 0,8 % (Sigma) préparée de façon extemporanée dans du tampon de lyse (40 mM d'EDTA ; 50 mM de Tris pH = 8,3 ; 0,75 M de sucrose (Sigma) et du SDS à 10 % (Biorad). Une seconde lyse de 15 min à 55°C a été réalisée afin de dégrader les cellules potentiellement résiduelles dans le filtre Sterivex. L'ADN a ensuite été extrait par ajout de NaCl 6 M (SIGMA) puis précipité à l'éthanol 70% (SIGMA). Les culots obtenus ont alors été séchés et solubilisés dans 100 µl d'eau milliQ stérile. L'intégrité de l'ADN a été vérifiée par migration sur un gel à 1% d'agarose coloré au BET. La pureté et la quantité d'ADN ont été mesurées en utilisant le spectrophotomètre Nanodrop ND-1000 (Thermo scientific) en calculant le rapport d'absorbance 260nm/280nm. Les échantillons d'ADN ont ensuite été conservés à -20 °C.

Amplification du gène coxI et purification des produits de PCR

Un fragment de 830pb appartenant au gène coxI (provenant des organismes appartenant à la famille Noëlaerhabdaceae) a été amplifié par PCR (Polymerase chain reaction). Ces séquences d'ADN présentes dans les extractions environnementales ont été obtenues en utilisant les amorces forward et reverse spécifiques aux Noelaerhabdaceae F5 (5'-GCTCACCGAACTCCTTTATTTG-3') et R8 (5'-GAAGCAATTGCATTTCATTGAG-3') (Bendif et al., en préparation). Les réactions ont été effectuées dans des volumes de 25 µl à l'aide d'un Kit GoTaq®Flexi DNA Polymerase (Promega) contenant une solution tampon à 5 X, 1,5 mM de MgCl2 et une unité de GoTaq Flexi polymérase auxquels il a été ajouté 0,4 mM de dNTP, 0,2 µM de chacune des amorces, et de l'ADN. Les amplifications ont été réalisées en utilisant le thermocycleur Gene Amp® PCR system 9700 (Applied Biosystems) avec le programme suivant : 95 °C pendant 30 s, 55 °C pendant 30 s, 72 °C pendant 60 s sur 35 cycles, avec une dénaturation initiale de 2 min à 95 °C et une étape d'extension finale de 5 min à 72 °C. Cette dernière étape permet d'utiliser la propriété d'adénylation de la polymérase GoTaq capable de rajouter une Adénine surnuméraire à l'extrémité 3' des brins amplifiés. Les produits de PCR ont été visualisés sur un gel d'agarose à 1% contenant du BET avant d'être purifiés à l'aide du Kit NucleoSpin®Extract II (MACHEREY-NAGEL) pour éliminer les sels, les dNTP qui n'ont pas été incorporés lors de la PCR ainsi que les amorces et les dimères d'amorces.

Clonage et séquençage

Les produits de PCR ont été clonés en utilisant le kit « Topo TA cloning Kit for Sequencing » (Invitrogen). Une première étape de ligation a permis d'intégrer les fragments d'ADN amplifiés au vecteur pCR®4-TOPO® (Annexe 4) présentant aux extrémités 5' du site de clonage des Thymines complémentaires des Adénines 3' terminal des inserts. Des bactéries compétentes ont ensuite été transformées avec les produits de ligation puis cultivées sur milieu solide LB-agar (Sigma) sélectif (Ampicilline) pendant une nuit à 37 °C. La présence de l'insert a été vérifiée dans les colonies obtenues par une PCR utilisant les amorces M13 forward et M13 reverse complémentaires de séquences flanquantes du site de clonage. Les conditions de

réaction et d'amplification ont été strictement les mêmes que celles utilisées lors de l'amplification initiale du gène coxI.

Les produits PCR ont été purifiés à l'aide de Kit Montage™ PCR96 (Millipore). Son principe repose sur l'utilisation d'une membrane retenant les produits PCR supérieurs à 100 pb. Les amplicons purifiés ont ensuite été séquencés. La réaction de séquençage a été réalisée selon la méthode de Sanger avec l'amorce R8 en utilisant le Kit BigDye® Terminator v3.1. Ces étapes de purification et de séquençage ont été réalisées sur la plate-forme de séquençage génotypage « Biogenouest ». La visualisation des chromatogrammes de séquençage à l'aide du logiciel FinchTV nous a permis de vérifier la qualité des séquences obtenues.

Analyse phylogénétique

Les séquences obtenues ont ensuite été comparées par le programme Blast aux banques de données génétiques GenBank (www.ncbi.nlm.nih.gov) afin de s'assurer de leur affiliation à l'ordre des Isochrysidales. Cela a également permis de placer chaque séquence dans le cadre de lecture protéique du gène.

Nos séquences environnementales ont été alignées avec les séquences acquises précédemment par Bendif et al. (en préparation) grâce l'application d'alignement multiple Clustal W implémentée dans l'éditeur de séquences BioEdit (Hall, 1999). Pour les analyses de diversité moléculaire présentées dans ce travail, les mutations unique à une seule séquence –pouvant être dues aux erreurs de séquençage- n'ont pas été prises en considération. Toute substitution répétée dans au moins deux séquences a été inclue dans les calculs de diversité génétique.

Dans le but d'étudier la limite de la biodiversité des Noëlaerhabdaceae en Méditerranée nous avons réalisé une analyse de raréfaction de la diversité des séquences obtenues lors de notre étude à l'aide du logiciel DOTUR (Schloss et Handelsman, 2005). Cette analyse consiste à calculer la richesse d'OTU (operational taxonomic units, unité opérationnelle taxonomique) pour un nombre donné de séquence.

Deux méthodes de construction d'arbres phylogénétiques s'intéressant à la famille des Noëlaerhabdaceae ont été utilisées. Il s'agit de la méthode « BioNJ» en se basant sur le modèle simple de substitutions (Kimura 2 paramètres) et de la méthode du

« maximum de vraisemblance » (méthode générant des algorithmes probabilistes) à partir du logiciel Treefinder et des programmes en ligne du site internet « phylogeny.fr ». Par la suite le logiciel MEGA a été utilisé pour dessiner les arbres phylogénétiques.

Dans le but de donner une direction évolutive à l'arbre phylogénétique, nous avons du définir un Outgroup. Celui-ci, devant apporter une racine à l'arbre, est déterminé par la séquence d'une espèce voisine proche du groupe étudié. Dans notre cas les séquences du gène cox I du genre voisin Isochrysis et présentes dans GenBank ont permis de positionner le Clade1 a la racine de l'arbre.

Résultats

Les séquences environnementales de la campagne BOUM.

Au cours de cette étude, nous avons obtenu 685 séquences du gène cox I provenant des échantillons environnementaux de 6 stations de la campagne BOUM (Tableau I). Pour 4 stations (27, 24, A et 19) plus de 100 séquences ont été obtenues. Dans le bassin Est (station 27, 24 et A), une moyenne de 147 séquences par station a été obtenue. Dans le bassin Est (station 3 et 11) cette moyenne est de 58 séquences. Il a également été plus difficile d'obtenir des séquences à partir des échantillons de surface avec une moyenne de 52 séquences. Cela a notamment été le cas avec la station A (23 séquences), la station 3 (28 séquences) et la station 11 (24 séquences). A la DCM on a obtenu en moyenne 63 séquences par échantillons.

Table I : 685 séquences ont été obtenues en utilisant des échantillons environnementaux de la campagne BOUM à partir de la DCM et de la surface de 6 stations d'échantillonnages.

Stations	Profondeur	nombre de séquences obtenues/ profondeur	nombre de séquences obtenues/ station
27	DCM	79	174
	Surface	95	
24	DCM	71	131
	Surface	60	
A	DCM	112	135
	Surface	23	
19	DCM	45	125
	Surface	80	
3	DCM	35	63
	Surface	28	
11	DCM	33	57
	Surface	24	
TOTAL		685	

15

Limites de la biodiversité des Noëlaerhabdaceae en Méditerranée.

La divergence maximale observée entre deux séquences pour l'ensemble des séquences ayant servies à cette étude (échantillons environnementaux et souches) est de 2,8%. Il est également intéressant de constater que 16% des couples de séquences ont entre eux une distance nulle (Annexe 5).

Nous avons réalisé une analyse de la raréfaction (Figure 6) à partir de l'ensemble des séquences provenant des stations du transect BOUM (685 issues des échantillons environnementaux et 46 issues de souches cultivées en laboratoire provenant d'échantillons des stations A, B, C et 19 de la campagne BOUM). Cette analyse des limites de la biodiversité des Noëlaerhabdaceae montre la présence de seulement 4 OTUs en se basant sur un indice d'identité de 99% entre les séquences. En revanche, en considérant un indice d'identité de 100%, soit la modification d'au moins une paire de base, il apparait 24 OTUs différentes. Dans ce cas de figure, 50% des OTUs ont été observées sur 115 séquences étudiées.

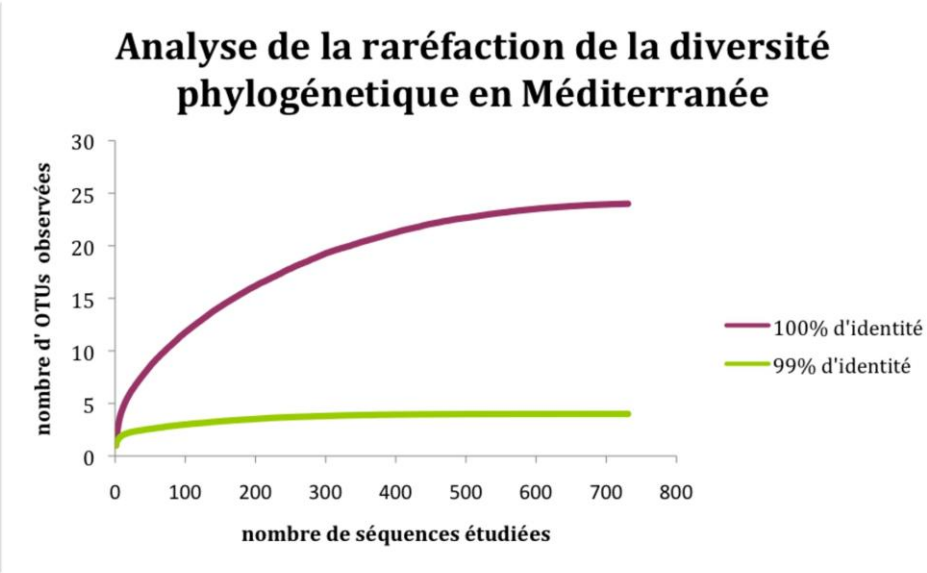

Figure 6 : Courbe montrant l'évolution du nombre d'OTUs observées (ordonnée) en fonction du nombre de séquences étudiées (abscisse). La courbe en violet illustre la diversité en se basant sur une identité de 100%, elle définit 24 OTUs. La courbe en vert illustre la diversité en se basant sur une identité de 99%, elle définit 4 OTUs.

Arbre phylogénétique des Noëlaerhabdaceae.

Au regard de l'analyse de raréfaction il a été choisi de considérer une identité de 100% entre les séquences pour définir les OTUs. En conséquence, la modification d'1 paire de base conduit à l'apparition d'une nouvelle OTU. L'ensemble des séquences analysées montre la présence de 50 OTUs (Figure 7), mais les séquences spécifiques de la famille des Noëlaerhabdaceae obtenues à partir de la campagne BOUM ne font ressortir que 24 OTUs différentes. Les souches issues de la campagne BOUM qui ont été cultivées en laboratoire ont permis de définir 4 OTUs (OTU 1, OTU 22, OTU 24, OTU 39), tandis que les échantillons environnementaux définissent 22 OTUs. Les OTU 24 et 39 ont été retrouvées à la fois dans les séquences provenant des souches et dans des séquences provenant de l'environnement. En revanche les OTUs 1 et 22 qui proviennent également de la campagne BOUM correspondent à des séquences issues uniquement des souches en culture et n'ont pas été retrouvées dans les échantillons environnementaux.

La base de données de Bendif et al. est constituée de 30 OTUs obtenues en laboratoire à partir de souches d'Emiliana huxleyi et de Gephyrocapsa oceanica provenant de différents endroits de la planète. En l'associant aux séquences environnementales de la campagne BOUM, il apparaît 20 nouvelles séquences non référencées définissant 20 nouvelles OTUs (Annexe 6).

La souche CCMP 373 (Figure 7) dont le génome mitochondrial et le génome plastidial ainsi que des ESTs ont été séquencés est la souche à partir de laquelle les amorces spécifiques de la famille des Noëlaerhabdaceae ont été dessinées pour obtenir les séquences qui ont fourni l'arbre phylogénétique. Elle s'inscrit dans l'OTU 33. Pour les souches TQ 26 (OTU 34) et CCMP 1516 (OTU44), le génome nucléaire et des ESTs (Expressed Sequence Tags, étiquettes de séquences exprimées) ont également été séquencés.

L'arbre phylogénétique (Figure 7), nous a permis de définir 6 clades, basés sur une analyse empirique de la structure de l'arbre et des caractéristiques morphologiques et écologiques associées aux différents groupes génétiques. Les valeurs de bootstraps relativement faibles définissant ces clades et la plupart des structures topologiques de notre phylogénie en général, sont attendues dans un tel cas d'évolution très récente.

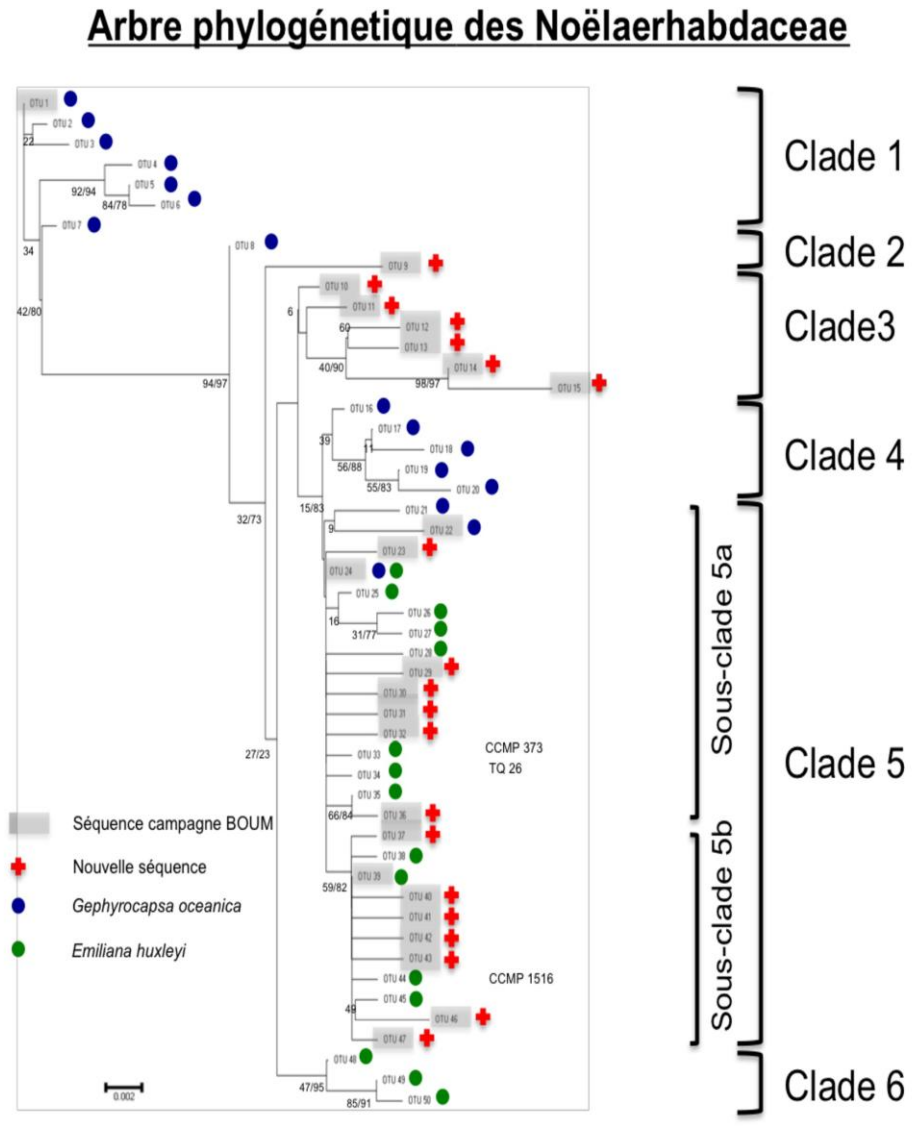

Figure 7: Arbre phylogénétique (NJ) de la famille des Noëlaerhabdaceae obtenu à partir des séquences issues de souches en culture au laboratoire de Roscoff et des séquences provenant des échantillons environnementaux collectés au niveau de plusieurs stations d'échantillonnages de la campagne BOUM. Les valeurs des bootstraps (neighbour joining /maximum de vraisemblance) sont indiquées aux nœuds de l'arbre. Les OTUs avec des séquences provenant de la campagne BOUM sont surlignées en gris. Les séquences obtenues à partir des souches cultivées en laboratoire permettent d'associer un morphotype à certaines OTUs. Les souches TQ 26, CCMP 1516 et CCMP 370 sont présentes sur l'arbre en regard de leur OTUs respectives. Les ronds bleus correspondent au morphotype connu de Gephyrocapsa oceanica et les ronds verts à celui d'Emiliana huxleyi. Les croix rouges correspondent aux nouvelles séquences obtenues à partir des échantillons de la campagne BOUM et pas retrouvées chez les souches en culture. Les clades et les sous clades ont été définis de manière semi-empirique.

Le clade 1 est constitué de 7 OTUs (OTU 1 à 7). Il est exclusivement composé de séquences provenant de souches en culture. 4 de ces souches proviennent de la campagne BOUM et appartiennent à l'OTU 1. Toutes les OTUs de ce clade sont associées au morphotype de Gephyrocapsa oceanica.

Le clade 2, qui ne mérite peut-être pas son statut de clade, comporte deux OTUs orphelines. L'OTU 8 qui correspond à des souches de Gephyrocapsa oceanica et l'OTU 9 qui est associée à 3 nouvelles séquences environnementales.

Le clade 3 regroupe 5 OTUs (OTUs 10 à 15) non référencées à partir des séquences issues de souches en culture. Ces 5 OTUs définissent un nouveau clade bien isolé dont la présence est non négligeable, puisqu'ils représentent 23,8% de la biodiversité totale.

Le clade 4 est constitué de 5 OTUs issues uniquement des souches en culture dont le morphotype correspond à celui Gephyrocapsa oceanica.

Le cinquième clade est proche du clade 4 sur l'arbre phylogénétique. Il est le plus grand et regroupe 27 OTUs provenant des souches en culture et des échantillons de la campagne BOUM. Les OTUs 24 et 39 qui appartiennent à ce clade sont les 2 OTUs qui ont été les plus séquencées à partir des échantillons environnementaux de la campagne BOUM (Figure 8B). Ce clade peut être divisé en deux sous clades. Le sous clade 5a qui englobe 16 OTUs et le sous clade 5b qui en réunit 11. Le sous clade 5a comporte des morphotypes d'Emiliana huxleyi et de Gephyrocapsa oceanica. De plus l'OTU 24 a la particularité d'être associée à la fois au morphotype d'Emiliana huxleyi et à celui de Gephyrocapsa oceanica. En revanche le sous clade 5b est exclusivement associé au morphotype d'Emiliana huxleyi.

Le dernier clade (clade 6) est composé de 3 OTUs associées exclusivement à Emiliana huxleyi et provenant uniquement de souches en culture issues de hautes latitudes avec des eaux froides ou tempérées.

Structure phylogéographique des Noëlaerhabdaceae

L'emplacement des stations étudiées au cours de cette étude permet d'avoir une idée claire de la distribution de la biodiversité du groupe des Noëlaerhabdaceae en Méditerranée (Figure 8). Sur l'ensemble du bassin méditerranéen, les OTUs 24 et 39 représentent à elles seules 66,35% de la diversité totale avec respectivement 38,85% et 27,5%. Les nouvelles OTUs 14 (14,3%) et 10 (7,8%) tiennent également une place non négligeable dans cette diversité globale. Seules 3 autres OTUs sont présentes à hauteur de plus de 0,6%, la 13 (3%), la 40 (1,78%) et la 20 (0,68%). Toutes les autres OTUs identifiées pendant la campagne BOUM sont représentées à hauteur de moins de 0,6%.

Le bassin Est est beaucoup plus oligotrophe que le bassin Ouest avec des valeurs proches de 0,05 $mg.m^{-3}$ de chlorophylle-a pour les stations 3 et 11, contre des valeurs comprises entre 1,89 et 0,12 $mg.m^{-3}$ au niveau du bassin Ouest. Les deux bassins méditerranéens ne présentent pas la même biodiversité. Alors que dans le bassin Ouest on trouve des organismes appartenant à 4 clades (clade 1, 2, 3 et 5), dans le bassin Est les organismes appartiennent tous au clade 5. La station 19 intermédiaire a des organismes dans les clades 3 et 5. Ainsi l'OTU 24 est plus abondante dans le bassin ouest où elle est présente à 43% de la biodiversité, tandis que dans le bassin Est, elle ne représente que 24% de la biodiversité. Cette OTU est retrouvée à toutes les stations et à toutes les profondeurs, excepté en surface de la station A. En revanche pour l'OTU 39, la tendance est inversée car elle constitue seulement 15% de la biodiversité du bassin ouest alors qu'elle est présente à 58% dans le bassin Est avec un maximum de 80% pour la station 3. L'OTU 14 est elle plus abondante dans le bassin Ouest où elle représente 23% de la biodiversité alors qu'elle ne représente uniquement que 0,3% de la biodiversité dans le bassin Est. La station 19 située entre les deux bassins montre des valeurs intermédiaires avec 33% de la biodiversité pour l'OTU 24 et 42% de la biodiversité pour l'OTU 39 et seulement 0,4% pour l'OTU 14. L'OTU 10 n'est elle présente que dans le bassin ouest à hauteur de 11% et à la station intermédiaire 19 (0,6%) alors qu'elle est absente du bassin Est. L'OTU 13 est plus représentée dans le bassin Est avec 0,83% que dans le bassin Ouest avec 0,14% et 0,48 % à la station 19.

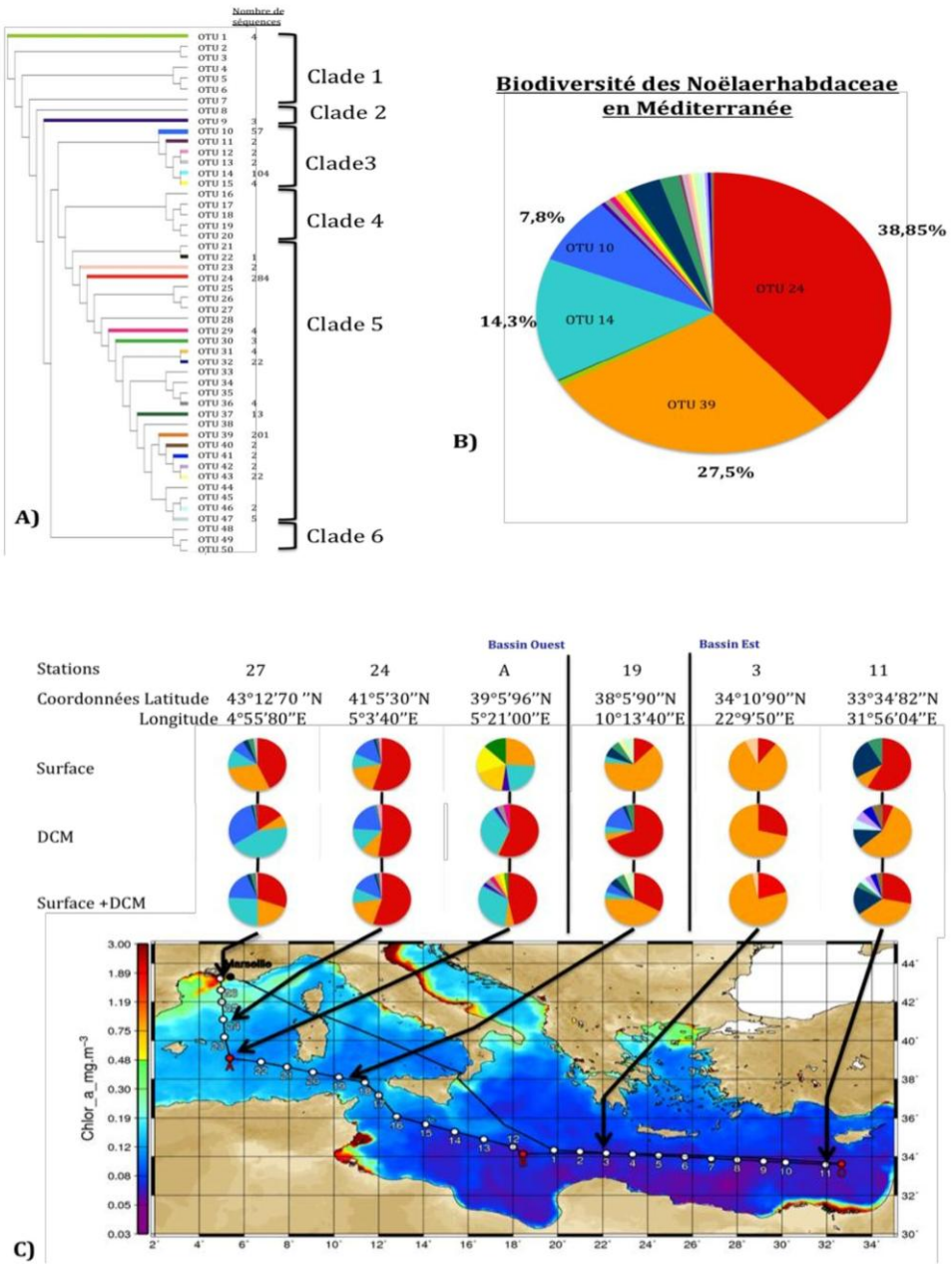

Figure 8: En (A), l'arbre phylogénétique de la famille des Noëlaerhabdaceae présente des couleurs distinctes pour chacune des différentes OTUs trouvées dans les échantillons de la campagne BOUM, ainsi que le nombre de séquences observées pour chaque OTU. La diversité de l'ensemble des OTUs séquencées est représentée sous forme de diagramme circulaire (même code couleur qu'en A) pour l'ensemble du bassin méditerranéen (B), et pour chaque station étudiée, en surface et au maximum de chlorophylle en profondeur (voir Annexe 7 pour la position exacte des échantillons dans la colonne d'eau). Le gradient de couleur du bassin méditerranéen traduit la concentration de l'eau de mer en chlorophylle a (mg.m^{-3}) pour la période considérée.

Par ailleurs il y a en moyenne 9 OTUs différentes par station dans le bassin Ouest alors qu'il n'y en a en moyenne que 5 dans le bassin Est. A la station 19, 8 OTUs différentes ont été observées. De plus pour les 3 stations les plus à l'Est (19, 3 et 11) il est intéressant de constater qu'à toutes les profondeurs une OTU domine largement l'ensemble des autres OTUs avec une abondance supérieure à 50%. La station 3 qui est très oligotrophe se démarque des autres stations par le fait qu'elle ne présente que 3 OTUs largement représentées et seulement 2 en profondeur (OTUs 24 et 39).

On trouve en moyenne moins d'OTUs en surface qu'en profondeur. La station 24 est la seule à montrer une distribution identique de la biodiversité en surface et en profondeur. Elle est dominée par l'OTU 24 (54,9% de la diversité). Pour la station 27, les OTUs 24 et 39 sont très largement représentées en surface (43,1% et 29,5%) alors que ce sont les OTUs 10 et 14 qui sont les plus présentes à la DCM (43% et 30,4%). A la station A, les OTU 24 et 14 sont majoritaires à la DCM avec 56,5% et 33% respectivement, mais en surface on observe une distribution homogène des OTUs 14, 15, 30, 31 et 39. A la station 19 l'OTU 39 représente 63,8 % et écrase le reste de la biodiversité alors qu'à la DCM c'est l'OTU 24 qui joue ce rôle avec 68,9% de la biodiversité.A la station 3, l'OTU 39 domine largement la diversité en surface et à la DCM, avec respectivement 82,1% et 71,4% des séquences, mais à la DCM, l'OTU 24 occupe également une place importante avec 28,5%. La station 11 montre un profil un peu à l'opposé de celui de la station 19 avec 57,6% de la diversité à la DCM pour l'OTU 39 et 58,3% de la diversité pour l'OTU 24 à la surface. La station 11 fait exception avec l'OTU 39 qui est plus présente à la DCM (35,4%) qu'en surface (18,6%). Inversement, l'OTU 24 est plus abondante en surface (41,3%) qu'à la DCM (35,3%).

Discussion

La méthode que nous avons utilisée a plusieurs avantages. Tout d'abord, elle a permis de découvrir et d'étoffer plusieurs nouveaux sous-groupes génétiques qui n'avaient pas été identifiés à partir des souches mises en culture. Elle a aussi permis d'augmenter de manière significative la base d'information regroupant les séquences mitochondriales de ce groupe clef du phytoplancton océanique. Ce type de données est particulièrement important pour les groupes d'organismes difficiles à initier et préserver en milieux de culture au laboratoire (López-García et al., 2001). Enfin, cette étude apporte une nouvelle vision de la distribution géographique de la famille des Noëlaerhabdaceae en Méditerranée.

Diversité

Nous avons effectué une approche moléculaire (le clonage de la séquence nucléotidique codant pour le gène cox I chez la famille des Noëlaerhabdaceae) pour caractériser des souches en culture au laboratoire ou des populations prélevées dans l'environnement afin d'observer une plus grande diversité. En effet, Shi et al. (2009) montrent qu'une très large partie des organismes eucaryotes phytoplanctoniques présents dans l'environnement ne sont pas cultivables en laboratoire. Nos résultats montrent que la diversité des séquences des Noëlaerhabdaceae est relativement limitée. Néanmoins, l'ensemble des 850 séquences analysées a finalement conduit à l'apparition de 50 OTUs différentes peu divergentes (Figure 7).

La diversité environnementale estimée à partir de cette méthode peut comporter des biais. Par exemple, certains groupes sont plus facilement amplifiés que d'autres. Plusieurs études montrent que les groupes photosynthétiques sont souvent sous représentés dans les librairies de clones (Not et al., 2004 ; Romari & Vaulot, 2004). Ce type de biais peut-être évité en utilisant des amorces qui sont spécifiques de certains groupes phylogénétiques (Bass & Cavalier-Smith, 2004). Les amorces F5 et R8 dessinées par Bendif et al. (en préparation) pour le gène cox I sont spécifiques de la famille des Noëlaerhabdaceae. Nos résultats ont confirmé cette spécificité puisque l'ensemble des séquences obtenues à partir des échantillons environnementaux s'intègre dans l'arbre phylogénétique de la famille des Noëlaerhabdaceae dessiné par Bendif et al. (en préparation).

Originalité phylogénétique et nouveaux clades

L'arbre phylogénétique traduit la présence d'un certain degré de biodiversité cryptique au sein des Noëlaerhabdaceae. En effet, il démontre l'existence de groupe de séquences divergentes au sein des espèces morphologiques E. huxleyi et G. oceanica, ces groupes génétiques étant associés a des structures morphologiques, écologiques, ou géographiques spécifiques (Figures 7 et 8). La question de savoir si les clades ou les OTUs, ou encore un degré de divergence intermédiaire, correspond à des espèces biologiques différentes reste ouverte. Le clade 1, associé au morphotype de Gephyrocapsa oceanica est constitué uniquement de séquences de souches en culture dont 4 proviennent de la campagne BOUM. Les amorces dessinées pour amplifier le fragment du gène cox I chez les Noëlaerhabdaceae n'ont pas permis d'obtenir des séquences à partir des échantillons environnementaux. Afin d'essayer d'obtenir des séquences environnementales pour ce clade, nous avons réalisé une expérience avec l'échantillon de la DCM à la station A. Nous avons obtenu 50 séquences en diminuant la température d'hybridation de la PCR de 55°C à 50°C. Aucune des séquences obtenues, malgré ce changement dans le protocole, n'appartient au clade 1. Ainsi, soit les amorces ne sont pas capables de s'hybrider au gène cox I des cellules appartenant à ce clade, soit les individus du clade 1 sont extrêmement rare, mais particulièrement aptes à pousser en milieu de culture. On peut dès lors se demander si l'abondance de certaines OTUs ne masque pas la présence des OTUs du clade 1. Les amorces dessinées, malgré un travail préalable d'optimisation, sont peut être également trop spécifiques de certains groupes.

Le clade 2 constitue un clade intermédiaire entre les clades 1 et 3. L'OTU 8 qui est issue de séquences de souches en culture soutient l'idée que ce clade peut-être associé au groupe Gephyrocapsa.

Les séquences environnementales ont fait apparaître le nouveau clade 3, constitué de 174 séquences. Aucune souche en culture du laboratoire ne possède de séquence similaire du gène coxI pour ce clade. On ne peut donc pas déterminer si ce clade est apparenté au groupe Emiliania ou au groupe Gephyrocapsa. Cependant, sur l'arbre phylogénétique, ce clade semble être apparu avant l'émergence du groupe Emiliania. Il est donc plus judicieux de penser que le clade 3 puisse être rattaché au groupe Gephyrocapsa.

Le clade 4, tout comme le clade 1, est constitué exclusivement de souches qui peuvent

être reliées au morphotype de Gephyrocapsa oceanica. L'arbre phylogénétique montre qu'aucune des OTUs de ce clade ne provient de la Méditerranée. Deux explications peuvent permettre d'expliquer ce phénomène : soit ce clade est totalement absent en Méditerranée, soit, comme pour le clade 1, les amorces utilisées pour amplifier le gène cox I ne se sont pas hybridées à l'ADN des organismes présents.

Le clade suivant (clade 5) est composé des deux sous-clades 5a et 5b que l'arbre phylogénétique présente sous forme de râteau. Dans ces regroupements, de nombreuses OTUs sont très proches et les analyses des séquences montrent que pour la plupart d'entre elles, cette divergence est due à la modification de la troisième base constitutive d'un codon. De nombreuses études réalisent des analyses phylogénétiques parcimonieuses en évitant d'utiliser la troisième base des codons pour obtenir des données plus robustes (Christianson., 2005). En effet, en raison de la redondance du code génétique, une modification de la troisième base d'un codon conduit moins souvent à une modification d'un acide aminé. La modification de cette troisième base d'un codon est donc moins significative quant à l'apparition d'une nouvelle OTU. Il est de ce fait raisonnable de regrouper les nombreuses OTUs (OTU 21 à 47) dans des sous-clades.

Le sous-clade 5a, d'un point de vu évolutif, réalise la transition entre les morphotypes Gephyrocapsa et Emiliana. Ce phénomène est mis en évidence au niveau de l'OTU 24 constitué de 284 séquences environnementales et de séquences de souches en culture. Dans cette OTU, les séquences issues des souches en culture révèlent deux morphotypes, celui de G.oceanica et celui d'E. huxleyi. Le sous-clade 5b, directement issu du clade 5a, est lui uniquement associé au groupe Emiliana. Il est très présent dans l'environnement puisqu'il réunit 254 séquences provenant de la campagne BOUM.

Le clade 6 est exclusivement composé de séquences provenant de souches en culture d'E. huxleyi qui ont été isolées dans les eaux froides ou tempérées de l'Atlantique nord. Il est intéressant de constater que pour les autres clades, les séquences proviennent de régions au climat méditerranéen ou tropical. Aucune séquence de la campagne BOUM n'appartient au clade 6. Il semble donc que ce clade soit isolé et adapté aux eaux froides. Pour confirmer cette hypothèse, il serait intéressant d'obtenir des séquences de la famille des Noëlaerhabdaceae provenant des eaux froides situées dans l'hémisphère sud.

Les Noëlaerhabdaceae en Méditerranée

La structure phylogéographique des Noëlaerhabdaceae met en évidence une dichotomie entre le bassin ouest et le bassin Est de la Méditerranée. La diversité des organismes de la famille des Noëlaerhabdaceae apparaît plus importante dans le bassin Ouest que dans le bassin Est. Plusieurs explications se posent : la proximité du détroit de Gibraltar, qui constitue le point de renouvellement des eaux méditerranéennes avec l'océan Atlantique pourrait contribuer à augmenter la diversité des organismes. D'autre part, les paramètres environnementaux ne sont pas les mêmes entre le bassin Ouest et le bassin Est (Annexe 7). Le bassin Est a une structure hydrologique particulière qui diffère du bassin Ouest. Il est plus salé, la température y est plus élevée et les concentrations en PO_4, $N0_2$ et NH_4 sont moins importantes. Seul le clade 5 constitué essentiellement *d'Emiliana huxleyi* est associé aux conditions oligotrophes de ce bassin. Les autres clades n'ont pas colonisé ce milieu. La station 19 située entre les deux bassins a fourni une diversité de séquences intermédiaire. Il apparaît donc un gradient de richesse spécifique décroissant du bassin Ouest vers le bassin Est. Les paramètres physico-chimiques (Figure 8C, Annexe 6) montrent que ce gradient évolue en parallèle d'un gradient dans le statut trophique des eaux du bassin méditerranéen. Néanmoins, la différence de biodiversité entre les deux bassins peut-être biaisée du fait que moins de séquences ont été obtenues dans le bassin Est que dans le bassin Ouest (Tableau I). Cet argument s'illustre particulièrement pour la station 3 pour laquelle seulement 3 OTUs ont été retrouvées.

Un nombre inférieur d'OTUs a été observé en surface par rapport à la DCM, mais là encore, ces résultats peuvent être biaisés du fait que moins de séquences ont été obtenues en surface qu'à la DCM (Tableau I). Par ailleurs, la répartition des taxons n'est pas très significative entre la surface et la DCM. Alors que pour certaines stations, des taxons sont beaucoup plus représentés en surface qu'à la DCM, c'est l'inverse pour d'autres stations avec le même taxon. La profondeur ne semble donc pas avoir un rôle majeur quant à la distribution des organismes et leurs abondances relatives.

Perspectives

Afin de mieux quantifier combien les séquences provenant d'échantillons environnementaux représentent la diversité naturelle, l'approche de clonage utilisée au cours de ce travail pourrait être appliquée à des mélanges connus de cultures de plusieurs souches de la familles des Noëlaerhabdaceae. Il serait alors possible d'établir une corrélation entre la diversité des séquences obtenues et la diversité des organismes présents dans le mélange de souches cultivées.

Les techniques consistant à construire des librairies de clones ne fournissent que des informations semi-quantitatives, permettent une évaluation de la diversité et de la composition de la communauté globale (Vaulot et al., 2008). D'autres techniques telles que le FISH (Fluorescent In Situ Hybridization) ou la PCRq (PCR quantitative) pourront être utilisées pour quantifier de façon plus précise l'abondance de groupes spécifiques dans la Méditerranée (Vaulot et al., 2008). Pour l'intégration des données génétiques dans un cadre environnemental, une analyse multifactorielle comparant les OTUs définis à différents degrés de distance génétique à l'ensemble des paramètres environnementaux mesurés au cours de la campagne BOUM permettrait de mieux comprendre la distribution de la famille des Noëlaerhabdaceae en Méditerranée.

Dans le cadre des études liées à la campagne BOUM et dans la continuité du présent travail, de nouvelles recherches vont être effectuées. Il s'agit notamment de déterminer les morphologies pouvant être associées aux OTUs inconnues. Une analyse détaillée en Microscopie Electronique à Balayage (MEB) des morphotypes de Noëlaerhabdaceae présents a chaque profondeur permettra une première comparaison des diversités génétique et morphologiques. Cette démarche pourra être suivie par l'application de la méthode CODFISH (Frada et al. 2006). Le CODFISH consiste à cibler les Noëlaerhabdaceae (ou tout autre groupe de cellules calcifiantes du plancton) avec une sonde ADNr spécifique, tout en préservant leur coccosphère calcitique. Les structures calcaires des organismes marqués sont ensuite observées soit en microscopie optique en lumière polarisée, soit en MEB. Enfin, ce travail s'intégrera dans l'étude plus générale des interactions entre la diversité et l'écologie des coccolithophores et la chimie des carbonates en milieu océanique. En particulier, il sera intéressant de comparer nos résultats aux données générées par la méthode SYRACO (Système de Reconnaissance Automatique de Coccolithes, Beaufort et

Dollfus, 2004), qui permet de reconnaitre automatiquement et quantifier la masse calcitique de groupe clefs de coccolithophore, dont les Noëlaerhabdaceae. Dans le contexte actuel d'acidification globale des océans, il semble urgent de comprendre la biodiversité des principaux organismes calcifiant du plancton océanique, et les réponses de cette biodiversité aux changements de pH de l'eau de mer.

Références

Adl, M. S., Simpson, A. G. B., Farmer, M. A., Andersen, R. A., Anderson, O. R., Barta, J., Bowser, S. S., Brugerolle, G., Fensome, R. A., Fredericq, S., James, T. Y., Karpov, S., Kugrens, P., Krug, J., Lane, C., Lewis, L. A., Lodge, J., Lynn, D. H., Mann, D. G., McCourt, R. M., Mendoza, L., Moestrup, Ø., Mozley-Standridge, S. E., Nerad, T. A., Shearer, C. A., Smirnov, A. V., Spiegel, F., Taylor, F. J. R., 2005. The new higher level classification of eukaryotes with emphasis on the taxonomy of protists. J. Euk. Microbiol. 52, 399–451.

Adl, S.M., and Gupta, V.V.S.R., 2006. Protists in soil ecology and forest nutrient cycling. J Can Forest Res. 36, 1805-1817.

Beaufort, L., and Dollfus, D., 2004. Automatic recognition of coccolith by dynamical neural network.Mar. Micropaleont, 51(1–2), 57–73.

Baldauf, S.L., 2008. An overview of the phylogeny and diversity of eukaryotes. J Systemat Evol. 46 (3), 263–273.

Bass, D., & Cavalier-Smith, T., 2004. Phylum-specific environmental DNA analysis reveals remarkably high global biodiversity of Cercozoa (Protozoa). Int J Syst Evol Microbiol. 54, 2393–2404.

Bourrelly P. and Magne F.,1953. Deux nouvelles espèces de Chrysophycées marines. Revue générale de Botanique. 60, 684–687.

Brassell, S.C., Eglinton, G., Marlowe, I.T., Plaufmann, U. and Sarnthein, M., 1986. Molecular stratigraphy: a new tool for climatic assessment. Nature. 320, 129-133.

Cavalier-Smith, T., 1994. Origin and relationships of Haptophyta. . In Green, J. C. & Leadbeater, B. S. C. The Haptophyte Algae. The Systematics Association special volume, n° 51, Oxford University Press, pp. 413-436.

Christianson, M.L, 2005. Codon usage patterns distort phylogenies from or DNA sequences. Am J Bot. 92, 1221-1233.

Day, D., Harvey Millar, A., Whelan, J., 2004. Plant Mitochondria: From Genome to Function. Editon Kempken, Frank. 325 p.

De Vargas, C., Aubry, M.P., Propert, I., Young, J., 2007 Origin and Evolution of Coccolithophores: From Coastal Hunters to Oceanic Farmers, in: Falkowski, P. (Eds.) Evolution of primary producers in the sea. Rutgers University, Institute of Marine and Coastal Science, New Brunswick, New Jersey, U.S.A. Andrew Knoll, Harvard

University, Cambridge, MA, USA. Chapter 12

Edvardsen, B., Eikrem, W., Green, J. C., Andersen, R. A., Moon-Van-Der-Staay, S. Y. & Medlin, L. K., 2000. Phylogenetic reconstructions of the Haptophyta inferred from 18S ribosomal DNA sequences and available morpholgical data. Phycologia. 39, 19-35.

Epstein, S., López-García, P., 2008. « Missing» protists: a molecular prospective. Biodivers Conserv. 17, 261-276.

Foissner, W., 2006. Biogeography and dispersal of micro-organisms: A review emphasizing protists. Acta Protozool. 45, 111-136.

Frada, M., Not, F., Probert, I. & de Vargas, C, 2006. CaCO3 optical detection with fluorescent in situ hybridization: a new method to identify and quantify calcifying microorganisms from the oceans. J Phycol. 42.

Fujiwara, S., Tsuzuki, M., Kawachi, M., Minaka, N., and Inouye, I., 2001. Molecular phylogeny of the Haptophyta based on the rbcL gene and sequence variation in the spacer region of RUBISCO operon. J Phycol. 37, 121–129.

Green, J. C., 1980. The fine structure of Pavlova pinguis Green and a preliminary survey of the order Pavovales (Prymenesiophyceae). British Phycological Journal. 15, 151-191.

Green, J. C. & Jordan, R. W., 1994. Systematic history and taxonomy. In Green, J. C. & Leadbeater, B. S. C. The Haptophyte Algae. The Systematics Association Special Volume, n° 51, Oxford University Press, pp. 1-21.

Hall, T.A. 1999. BioEdit: a user-friendly biological sequence alignment editor and analysis program for Windows 95/98/NT. Nucl. Acids. Symp. Ser. 41, 95-98.

Inouye, I. & Kawashi, M., 1994. The haptonema. In Green, J. C. & Leadbeater, B. S. C. The Haptophyte Algae. The Systematics Association special volume, n° 51, Oxford University Press, pp. 73-89.

Jerkovic, L., 1970. Noelaerhabdus nov. gen. Type d'une nouvelle famille de coccolithophoridés fossiles : Noëlaerhabdaceae du Miocène supérieur de Yougoslavie. Comptes Rendus Hebdomadaires des Séances de l'Académie des Sciences. série D, 270, 468-470.

Jordan, R.W., Cros, L., and Young, J.R., 2004. A revised classification schème for living haptophytes. Micropaleontology 50, 55-79.

Hibberd, D.J., 1976. The ultrastructure and taxonomy of the Chrysophyceae and Prymnesiophyceae (Haptophyceae): a survey with some new observations on the ultrastructure of the Chrysophyceae. Botanical Journal of the Linnaen Society. 72, 55-80.

Kamptner, E., 1943. Zur Revision der Coccolithineen-Spezies Pontosphaera huxleyi Lohm. Anzeiger der Akademie der Wissenschaften. 80, 43-49.

Keeling, P. J., Burger, G., Durnford, D. G., Lang, B. F., Lee, R. W., Pearlman, R. E., Roger, A. J., and Gray, M.W. , 2005. The tree of eukaryotes. Trends Ecol. Evol. 20, 670–676.

Liu, H., Aris-Brosou, S., Probert, I., de Vargas, C., 2010. A timeline of the environmental genetics of the haptophytes. Mol Biol Evol. 27, 171-176.

Lohmann, H., 1902. Die Coccolithophoridae, eine monographie der Coccolithen bildenden flagellaten, zugleich ein Beitag zur Kenntnis des Mittelmeerauftriebs. Archiv für Protistenkunde. 1, 89-165.

López-García, P., Rodriguez-Valera, F., Pedrós-Alío, C & Moreira, D., 2001. Unexpected diversity of small eukaryotes in deep-sea Antarctic plankton. Nature. 409, 603–607.

Marlowe I. T., Green J. C., Neal A. C., Brassell S. C., Eglington G. and Course P. A.,1984. Long chain (//-C37-C39) Alkenones in the Prymnesiophyceae. Distribution of Alkenones and other Lipids and their Taxonomic Significance. British phycological Journal. 19, 203-216.

Milliman, J.D., 1993. Production and accumulation of calcium carbonate in the ocean budget of a nonsteady state. Global Biogeochemi Cy. 7, 927-957.

Moestrup, Ø., 1994. Economic aspects: « blooms », nuisance species, and toxins. In Green, J. C. & Leadbeater, B. S. C. The Haptophyte Algae. The Systematics Association Special Volume, n°51, Oxford University Press, pp. 265-285.

Not. F., Latasa, M., Marie. D., Cariou. T., Vaulot, D. & Simon, N., 2004. A single species Micromonas pusilla (Prasinophyceae) dominates the eukaryotic picoplankton in the western English Channel. Appl Environ Microbiol. 70, 4064–4072.

Pascher A., 1910. Chrysomonaden aus dem Hirschberger Grossteiche. Monographien und Abhandlungen zur Intemationale Revue der gesamten. Hydrobiologie und Hydrographie. 1, 1-66.

Rio, D., 1982. The fossil distribution of coccolithophore genus Gephyrocapsa Kamptner and related Plio-Pleistocene chronostratigraphic problems. In: Prell, W. L., Gardner, J. V. et al. (Editors), Init. Rep. DSDP, 68, 325-343.

Reviers, B. de., 2002b. Biologie et phylogénie des algues, Tome 2. Edition Belin, 255p.

Romari, K. & Vaulot, D. 2004. Composition and temporal variability of picoeukaryote communities at a coastal site of the English Channel from 18S rDNA sequences. Limnol Oceanogr. 49, 784–798.

Samtleben, C., 1980. Die evolution der coccolithophoriden-Gatung Gephyrocapsa mach befunden im Atlantik. Paleontol. Z., 54, 91-127.

Schloss, P.D. & Handelsman, J., 2005. Introducing DOTUR, a computer program for defining operational taxonomic units and estimating species richness. Appl Environ Microbiol. 71(3), 1501-1506.

Shi, X. L., Marie, D., Jardillier, L., Scanlan, D. J. & Vaulot, D, 2009. Groups without cultured representatives dominate eukaryotic picophytoplankton in the oligotrophic South East Pacific Ocean. PLoS ONE. 4, e7657.

Simpson, A. G. B. and Roger, A., 2004. The real kingdoms of eukaryotes. Curr. Biol. 14, R693–R696.

Slapeta, J., Moreira, D., and Lopez-Garcia, P., 2005. The extent of protist diversity: insights from molecular ecology of freshwater eukaryotes. Proc. Royal Soc. B Biol. Sci. 272, 2073-2081.

Sournia, A., Erard-Le Denn, E., Berland, B. Grzebyk, D., 1991. Le phytoplancton nuisible des côtes de France ; de la biologie à la prévention. Ifremer/CNRS, 154p. ISBN 2-905434-30- 9.

Thierstein, H. R., Geitzenauer, K. R., Molfinoand, B. N., Shackleton, J., 1977. Global synchroneity of late Quarternary coccolith datum levels: Validation by oxygen isotopes. Geology. 5, 400-404.

Van Cappellen, P., 2003: Biomineralization and global biogeochemical cycles, in: Biomineralization, Mineralogical Reviews, edited by: Weiner, S., De Yoreo, J. J., and Dove, P., 54, 357–381.

Vaulot, D., Eikrem, W., Viprey, M. & Moreau, H., 2008. The diversity of small eukaryotic phytoplankton (≤3µm) in marine ecosystems. Microbiol Rev. 32, 795-820.

Young, J.R., Bown, P.R., 1997. Cenozoic calcareous nannoplankton classification. Journal of Nannoplankton Research. 19, 1, 15 – 47.

Young, J. R., Geisen, M., Cros, L., Kleijne, A., Sprengel, C., Probert, I., Ostergaard, J., 2003. A guide to extant coccolithophore taxonomy. Journal of nannoplankton Research. Special issue 1, P 125.

Annexes

Annexe 1: Taxonomie actuelle des l'ordre des Isochrysidales (Jordan., 2004)

Order ISOCHRYSIDALES Pascher, 1910, emend. Edvardsen et Eikrem
Family ISOCHRYSIDACEAE Bourrelly 1957 emend. Edvardsen et Eikrem
Genus *Chrysotila* Anand 1937
Chrysotila lamellosa Anand 1937
***Chrysotila stipitata* Anand 1937**
Genus *Dicrateria* Parke 1949
Dicrateria gilva Parke 1949
***Dicrateria inornata* Parke 1949**
Genus *Isochrysis* Parke 1949
***Isochrysis galbana* Parke 1949**
Isochrysis litoralis Billard et Gayral 1972
Family NOËLAERHABDACEAE Jerkovic 1970
Genus *Emiliania* Hay & Mohler 1967
***Emiliania huxleyi* (Lohmann) W.W. Hay & H.P. Mohler 1967**
Genus *Gephyrocapsa* Kamptner 1943
Gephyrocapsa caribbeanica Boudreaux & Hay 1967
Gephyrocapsa crassipons Okada & McIntyre 1977
Gephyrocapsa ericsonii McIntyre & Bé 1967
Gephyrocapsa kamptneri Deflandre & Fert 1954
Gephyrocapsa mullareae Bréhéret 1978
***Gephyrocapsa oceanica* Kamptner 1943**
Gephyrocapsa ornata Heimdal 1973
Gephyrocapsa protohuxleyi McIntyre 1970
Gephyrocapsa reticulata Nishida 1971
Gephyrocapsa undulata Lecal 1967
Genus *Reticulofenestra* Hay, Mohler et M. Wade, 1966
***Reticulofenestra caucasica* Hay et al. 1966**
Reticulofenestra maceira (Okada & McIntyre) Young 2003
Reticulofenestra parvula (Okada & McIntyre) Biekart 1989
Reticulofenestra punctata (Okada & McIntyre) Jordan & Young 1990
Reticulofenestra sessilis (Lohmann) Jordan & Young 1990

Annexe 2 : Organisation des gènes et carte physique du génome de l'ADN mitochondrial d'E. huxleyi. Les flèches grises représentent les gènes et les ORF_s (Open Reading Frame) qui sont tous transcrits dans le sens des aiguilles d'une montre.

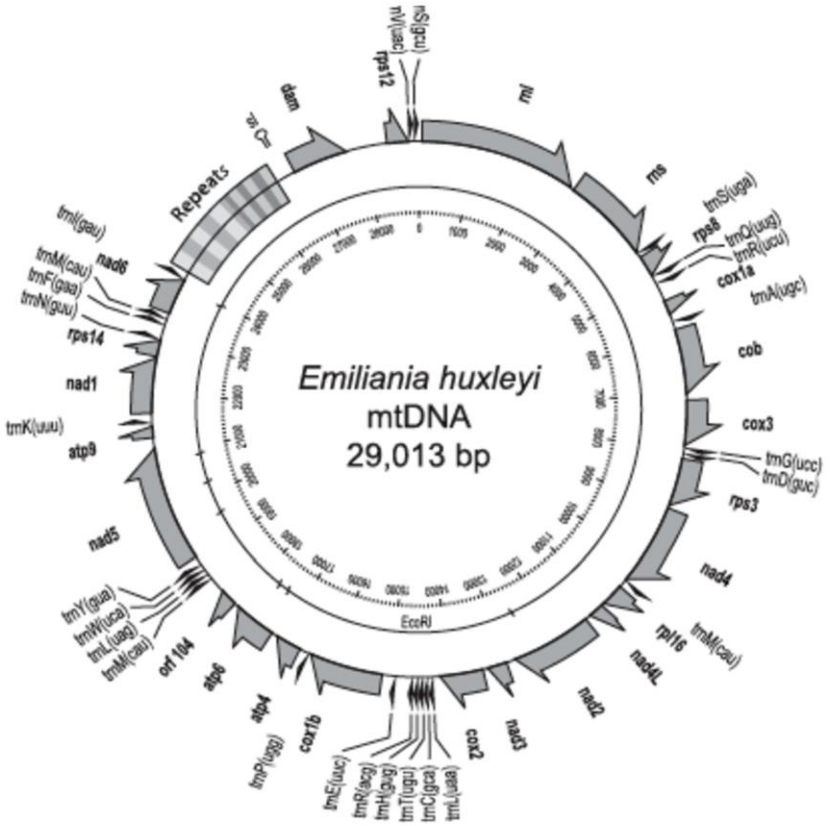

Annexe 3: Protocole d'extraction au sel.

1. Put the 70% ethanol in the freezer. You need +/- 6mL per sample.
2. Thaw your sample (RT or 37°C).
3. Add 50µL of protéinase K and 200 µL of SDS 10% in the sterivex and incubate 1h at 55°C, with rotation.
4. Transfer sterivex content in a 15mL tube (Falcon) and add 1mL of lysis buffer in the sterivex. Incubate for 15 min at 55°C with rotation.
5. Add 1,9mL of NaCl 6M. Vortex 1 min. Centrifuge at maximum speed (10000rpm) at 4°C for 20min.
6. Transfer flow through in a new 15mL tube (at this step you can often see a white fuzzy form, you can centrifuge longer. Be careful to not transfer too much of that in the new tube).
7. Add 5mL of cold 70% ethanol, mix by inverting the tubes and put at -20°C (or on the ice) for at least 10 min.
8. Transfer 2mL of this solution in 2mL tubes (you can use two 2 mL tubes per sample to go faster)
9. Spin 10 min at maximum speed (10000rpm) at 4°C and discard flow through
10. Using the same 2mL tube, repeat steps 8 and 9 until all the solution has been centrifuge.
11. Quick spin to remove remaining ethanol. Be careful not to remove the pellet, it can be invisible.
12. Add 200µL of cold ethanol. Spin 5 min at maximum speed (10000rpm) at 4°C. Remove ethanol. Let pellets dry (no alcohol trace, but do not let dry them for too long). 30 min at 40°C in bath dry by example.
13. Add 100µL of water milliQ stérile, stand for 1-5 min. Dissolve by up an down and vortex. Transfer in a clean tube.
14. DNA Observation on gel ; DNA quantification (nanodrop) and dilution if it is useful to make aliquots. Keep DNA samples at -20°C or at -20°C.

Materials :

-*ethanol 70%* : For 500ml 368,4ml of 95% ethanol with 131,6ml of milliQ water.
For 100ml 73,68ml of 95% ethanol with 26,32ml of milliQ water.
-*10% SDS*
-*Lysis Buffer* (40mM EDTA ; 50mM Tris ; ph=8,3 ; 0,75M sucrose)
For 10 ml: 0,8ml EDTA 0,5M; 0,5mL Tris 1M ; 7,5ml sucrose 1M; 1,2ml H20 milliQ)
-*Proteinase k* (prepare it in an eppendorf) 0,8%. 0,4mg of proteinase k in 50µL of lysis buffer. I prepared actually 500µL at 1 %.
-*6M NaCl*

Annexe 4: Organisation du vecteur de clonage pCR®4-Topo® (Invitrogen)

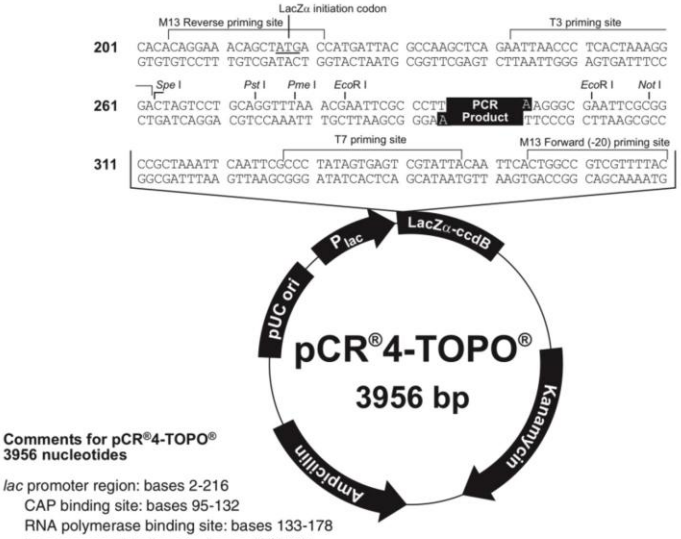

Comments for pCR®4-TOPO®
3956 nucleotides

lac promoter region: bases 2-216
CAP binding site: bases 95-132
RNA polymerase binding site: bases 133-178
Lac repressor binding site: bases 179-199
Start of transcription: base 179
M13 Reverse priming site: bases 205-221
LacZα-*ccdB* gene fusion: bases 217-810
LacZα portion of fusion: bases 217-497
*ccd*B portion of fusion: bases 508-810
T3 priming site: bases 243-262
TOPO® Cloning site: bases 294-295
T7 priming site: bases 328-347
M13 Forward (-20) priming site: bases 355-370
Kanamycin promoter: bases 1021-1070
Kanamycin resistance gene: bases 1159-1953
Ampicillin (*bla*) resistance gene: bases 2203-3063 (c)
Ampicillin (*bla*) promoter: bases 3064-3160 (c)
pUC origin: bases 3161-3834
(c) = complementary strand

Annexe 5: Evaluation de la divergence par paires de base des séquences ayant été utilisées pour cette étude

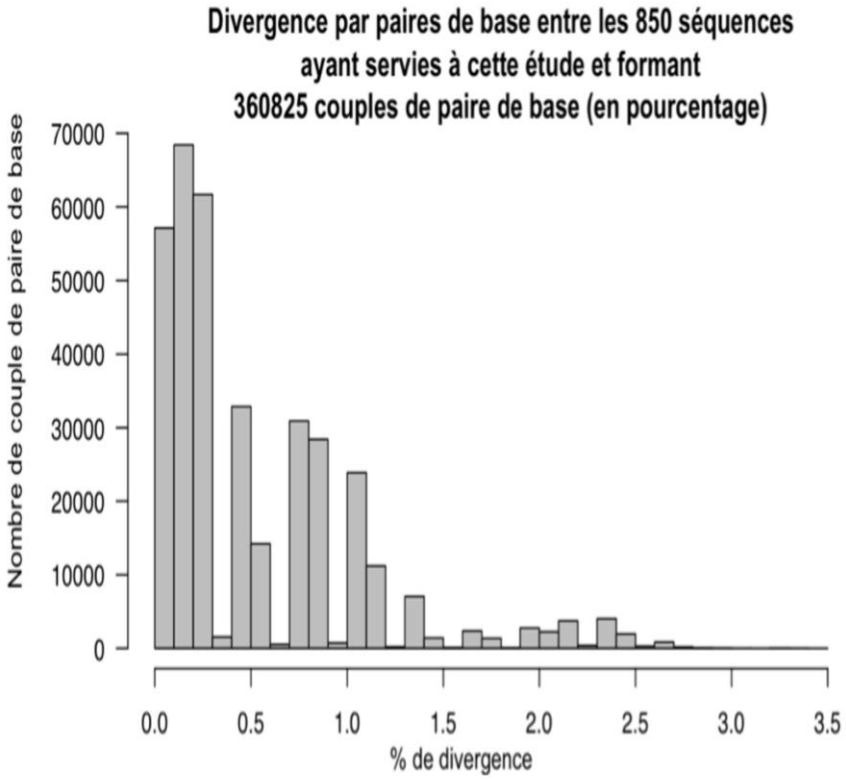

36

Annexe 7: Données physico-chimiques acquises au cours de la campagne BOUM. Les petits points représentent les profondeurs d'acquisition des métadonnées pour chacune des stations (de 0 à >150m). Les stations sont ordonnées sur les Latitudes pour la dernière partie du transect (stations A à 27), et sur les Longitudes pour la premiere partie (stations C à 22). La position des 12 échantillons de plancton analysés dans ce travail est indiquée à chaque station par des points noirs plus volumineux.

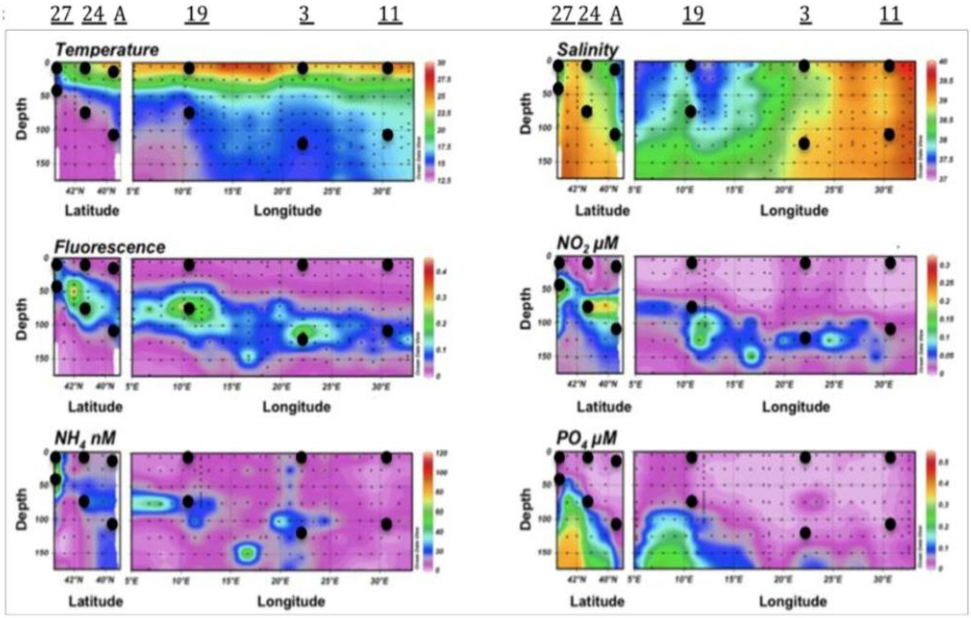

Diversité moléculaire et environnementale de la famille des Noëlaerhabdaceae (ordre des Isochrysidales) en Méditerranée

Mots clés : Biodiversité, cox I, Méditerranée, Noëlaerhabdaceae, Phylogénie.

Résumé : Les Noëlaerhabdaceae (ordre des Isochrysidales, embranchement des Haptophytes), dont les représentants les plus connus sont les espèces ubiquistes Emiliana huxleyi et Gephyrocapsa oceanica, constituent une famille de protistes photosynthétiques à l'origine d'efflorescences massives dans les océans. De part leur capacité à former des micro-plaques de carbonate de calcium (les coccolithes), les Noëlaerhabdaceae jouent un rôle prépondérant dans le cycle du carbone. Les marqueurs génétiques classiques utilisés pour comprendre la diversité du plancton océanique (18S, 28S, ITS, 16S, TufA, Rbc-1) ne permettent pas d'accéder aux structures génétiques à l'intérieur de la jeune famille des Noëlaerhabdaceae. Dans cette étude, nous avons développé une stratégie différente utilisant le gène mitochondrial à taux d'évolution rapide cox I comme outil phylogénétique et phytogéographique. 685 séquences cox I de Noëlaerhabdaceae ont été obtenues à partir d'échantillons environnementaux de la campagne BOUM (Biogéochimie de l'Oligotrophie à l'Ultra-oligotrophie Méditerranéenne). La découverte de 50 OTUs organisés en 6 clades montre une diversité génétique insoupçonnée parmi les genres Gephyrocapsa et Emiliania. Une analyse phylogéographique préliminaire de cette diversité génétique révélée montre que la répartition des OTUs et clades est non-aléatoire, réagissant aux contraintes hydrographiques.

Environmental and molecular diversity of the Noëlaerhabdaceae family (order Isochrysdales) in the Mediterranean sea.

Keywords : Biodiversity, cox I, Méditerranean, Noëlaerhabdaceae, Phylogeny.

Abstract : The Noëlaerhabdaceae (order Isochrysidales) are one of the most important family of photosynthetic unicellular eukaryotes in modern oceans, whose most famous representatives are the ubiquitous species Emiliana huxleyi and Gephyrocapsa oceanica. Species within the Noëlaerhabdaceae can generate massive blooms in the oceans, visible by satellites from the space. The cells secrete calcium carbonate scales (coccoliths) which are significant actors in global carbon cycling. Classical genetic markers to study the diversity and ecology of phytoplankton (18S, 28S, ITS, 16S, TufA, Rbc-1) are not able to discriminate within the Noëlaerhabdaceae. In this work, we used for the first time the fast-evolving mitochondrial gene cox-I to explore the phylogeny and phylogeography within this key family. 685 cox-I sequences were obtained from environmental samples collected along the BOUM (Biogéochimie de l'Oligotrophie à l'Ultra-oligotrophie Méditerranéenne) cruise. An unsuspected genetic diversity was unveiled within the genera Gephyrocapsa and Emiliania, which correspond to 50 distinct OTUs organized in 6 clades. Preliminary phylogeographic analysis shows that the distribution of the novel genetic diversity is not random, but seemingly constrained by hydrographic features.

ANNEXE 2

INTEGRATIVE TAXONOMY OF THE PAVLOVOPHYCEAE (HAPTOPHYTA): A REASSESSMENT

El Mahdi Bendif[1] , Ian Probert[2], Annie Hervé[3], Chantal Billard[4], Didier Goux[5], Christophe Lelong[4], Jean-Paul Cadoret[3] and Benoît Véron[4]

[1]CNRS-UPMC (Université Paris-06), UMR 7144, Groupe Plancton, Station Biologique de Roscoff, BP74, 29682 Roscoff cedex, France

[2]Roscoff Culture Collection, CNRS-UPMC (Université Paris-06), FR2424, Station Biologique de Roscoff, BP74, 29682 Roscoff cedex, France

[3]Laboratoire de Physiologie et Biotechnologie des Algues, IFREMER, rue de l'Ile d'Yeu, BP21105, 44311 Nantes cedex 3, France

[4]UMR 100 PE2M Université de Caen Basse-Normandie - IFREMER, Université de Caen Basse-Normandie, 14032 Caen cedex, France

[5]Centre de Microscopie Appliquée à la Biologie, IFR 146, Université de Caen Basse-Normandie, 14032 Caen cedex, France

Bendif EM, Probert I, Hervé A, Billard C, Goux D, Lelong C, Cadoret JP, and Véron B. A taxonomic reassessment of the Pavlovophyceae (Haptophyta). Protist 162: 738-761, 2011

Abstract

The Pavlovophyceae (Haptophyta) contains four genera (*Pavlova, Diacronema, Exanthemachrysis* and *Rebecca*) and only thirteen characterised species, several of which are important in ecological and economic contexts. We constructed molecular phylogenies inferred from sequencing of ribosomal gene markers with comprehensive coverage of the described diversity, using type strains when available, together with additional cultured strains. The morphology and ultrastructure of 12 of the described species was also re-examined and the pigment signatures of many culture strains were determined. The molecular analysis revealed that sequences of all described species differed, although those of *Pavlova gyrans* and *P. pinguis* were nearly identical, these potentially forming a single cryptic species complex. Four well-delineated genetic clades were identified, one of which included species of both *Pavlova* and *Diacronema*. Unique combinations of morphological/ultrastructural characters were identified for each of these clades. The ancestral pigment signature of the Pavlovophyceae consisted of a basic set of pigments plus MV chl cPAV, the latter being entirely absent in the *Pavlova* + *Diacronema* clade and supplemented by DV chl cPAV in part of the *Exanthemachrysis* clade. Based on this combination of characters, we propose a taxonomic revision of the class, with transfer of several *Pavlova* species to an emended *Diacronema* genus. The evolution of the class is discussed in the context of the phylogenetic reconstruction presented.

Key words: 18S rDNA; Haptophyta; Pavlovophyceae; phylogeny; taxonomy; ultrastructure

Introduction

The Haptophyta is a phylum of chlorophyll a + c containing unicellular algae characterised by the presence of a unique flagellum-like organelle, the haptonema, and comprising two distinct classes, the Prymnesiophyceae Hibberd emend. Cavalier-Smith and the Pavlovophyceae (Cavalier-Smith) Green et Medlin. The erection of a third class of haptophytes was recently proposed based exclusively on molecular data (Shi et al. 2009). The Prymnesiophyceae contains ca. 400 described species including many well known taxa such as *Phaeocystis*, *Chrysochromulina*, *Prymnesium* and the coccolithophores that can periodically form blooms in coastal and oceanic environments and thereby have a highly visible impact on marine ecosystem functioning, global biogeochemical cycles and global climate change (Moestrup 1994). By contrast, the Pavlovophyceae contains only 13 described species that inhabit littoral, brackish water and sometimes freshwater environments, and which have consequently not received a great deal of attention in the context of global issues.

The Pavlovophyceae is nevertheless a class of interest for a number of reasons, not least because it is seemingly a very common component of near coastal phytoplankton communities in widespread locations. The Pavlovophyceae synthesise long chain polyunsaturated fatty acids such as docosahexaenoic (DHA) and eicosapentaenoic (EPA) acids and certain species, notably *Pavlova lutheri* and *P. gyrans*, are extensively used as feedstocks in the aquaculture of bivalves, crustaceans and fish (Green 1975; Gayral 1980; Meireles et al. 2003; Ponis et al. 2006). The separation of the two known haptophyte classes is genetically well supported with 6% divergence in 18S rDNA phylogeny (Edvardsen et al. 2000). Using molecular clocks calibrated with the coccolithophore fossil record, the time of divergence of these two classes of the Haptophyta has been estimated at between 805 and 1000 million years ago (de Vargas et al. 2007, Medlin et al. 2008, Liu et al 2010). This deep divergence provides a model of key interest for evolutionary studies on the origin of the Haptophyta and the early radiation of eukaryotes.

In this context, the Pavlovophyceae are generally perceived to be representative of the primitive state, with characteristics likely to be related to those of the ancestral haptophyte. Structural features common to all or most members of the Pavlovophyceae that distinguish them from the Prymnesiophyceae include the markedly anisokont nature of the heterodynamic flagella and the relatively simple arrangement of microtubular and fibrous roots of the pavlovophyceaen flagellar-haptonematal basal complex (Green and Hori 1994). This flagellar arrangement results in pavlovophyceaen cells exhibiting a characteristic swimming movement. In addition, pavlovophyceaen scales, when present, consist of small dense bodies in contrast to the plate scales of the Prymnesiophyceae. These so-called 'knob scales', considered to be modified scales (Green 1980) or modified hairs (Cavalier-Smith 1994), often form a dense investment on the longer flagellum together with fine hairs. The process of mitosis in the Pavlovophyceae differs notably from that in the

Prymnesiophyceae (Green and Hori 1988, Hori and Green 1994). The Pavlovophyceae are also known to synthesise certain specific sterols and conjugates, the pavlovols (Véron et al. 1996; Volkmann et al. 1997) and a unique photosynthetic pigment (Van Lenning et al. 2003).

Due to their trophic, economic and phylogenetic importance, the Pavlovophyceae represent a highly relevant model for genomic studies. *Pavlova lutheri* was part of the protist EST program (http://megasun.bch.umontreal.ca/pepdb/pep.html, Tonon et al 2005) and the genome size and structure of two species, *P. gyrans* and *Diacronema sp.*, have been estimated using Pulse Field Gel Electrophoresis with a view to the possibility of initiating a full genome sequencing project (Nosenko et al 2007).

The 13 described species of Pavlovophyceae are classified in a single subclass, the Pavlovophycideae Cavalier-Smith, one order, the Pavlovales Green, and one family, the Pavlovaceae Green, that is composed of 4 genera: *Diacronema* (Prauser) Green et Hibberd, *Exanthemachrysis* Lepailleur, *Pavlova* (Butcher) Green and *Rebecca* Green (Table 1). Butcher (1952) erected the genus *Pavlova* with the description of *P. gyrans* as the type species. Based mostly on TEM ultrastructural studies of culture strains, new species were sporadically described until 1992. The last major taxonomic survey of the class was conducted over a quarter of a century ago (Green 1980), when a determination key was proposed for the three existing genera, *Diacronema*, *Pavlova* and *Exanthemachrysis*. More recently, the availability of 18S rDNA sequences for a sub-set of pavlovophyceaen taxa led to the transfer of two *Pavlova* species to the new genus *Rebecca* (Edvardsen et al. 2000). In addition, analysis of photosynthetic pigment profiles of a selection of species demonstrated that such profiles are phylogenetically informative (Van Lenning et al. 2003). In both of these latter studies, however, a complete reinvestigation of the class was not carried out. Undescribed species are frequently observed in miscellaneous samples (Gayral 1980) and the majority of the main microalgal culture collections hold several unidentified Pavlovophyceae strains that are likely to include new species.

Using type cultures when still available (11 of the 13 described species), we conducted a combined morphological and molecular genetic analysis in order to assess the validity of the current taxonomic scheme and to provide detailed information on phylogenetic relationships across the entire described diversity of the class. This led to a taxonomic revision of the class that will provide a framework for future description of the underestimated diversity within this lineage.

Table 1: Actual Pavlovophyceae taxonomy and authorities

Haptophyta Hibberd Cavalier-Smith ex Edvardsen et Eikrem in Edvardsen et al. 2000

Pavlovophyceae Cavalier-Smith ex Green et Medlin in Edvardsen et al. 2000

Pavlovales Green 1976

Pavlovaceae Green 1976

Diacronema (Prauser) Green et Hibberd 1977

Diacronema vlkianum (Prauser) Green et Hibberd 1977

Exanthemachrysis Lepailleur 1970

Exanthemachrysis gayraliae Lepailleur 1970

Pavlova Butcher 1952

Pavlova calceolata van der Veer 1976

Pavlova ennorea van der Veer et Leewis 1977

Pavlova granifera (Mack) Green 1973

Pavlova gyrans (Butcher) Green et Manton 1970

Pavlova lutheri (Droop) Green 1975

Pavlova noctivaga (Kalina 1970) van der Veer et Lewis 1970

Pavlova pinguis Green 1967

Pavlova virescens Billard 1976

Pavlova viridis Tseng, Chen et Zhang 1992

Rebecca Green 2000

Rebecca helicata (van der Veer) Green 2000

Rebecca salina (Carter) Green 2000

Results

Molecular phylogenies

The twenty-eight 18S and twenty seven 28S rDNA sequences of Pavlovophyceae generated in this study were added to 33 sequences from Genbank for the phylogenetic analyses. The accession numbers of these sequences are given in Table 2.

Table 2: Taxa with their original names and strains, genes and accession numbers used in the phylogenies (Fig 1, 2 and 3) (AC, Algobank-Caen; ACOI, Coimbra culture collection; ASIO, Algal culture collection; CCAP, Culture Collection of Algae and Protozoa; PLY, Plymouth Algal Culture Collection; SAG, SAG Culture collection)

Taxon	Strain Code	18S rDNA	28S rDNA	Pigment analysis
Diacronema vlkianum	AC67			x
Exanthemachrysis gayraliae *	AC15			x
Pavlova ennorea *	AC253			x
Pavlova granifera *	PLY552			x
Pavlova granifera	ACOI449			x
Pavlova gyrans *	CCAP940/1b			x
Pavlova lutheri *	PLY75			x
Pavlova noctivaga *	SAG 5.83	DQ207406		x
Pavlova pinguis *	CCAP940/2		EU502883	x
Pavlova virescens *	AC16		EU729477	x
Pavlova viridis *	ASIO3012	DQ075201		
Pavlova sp	AC19			x
Pavlova sp	AC28			x
Pavlova sp	AC33			x
Pavlova sp	AC35			x
Pavlova sp	AC37			x
Pavlova sp	AC54			x
Pavlova sp	AC245			x
Pavlova sp	AC246			x
Pavlova sp	AC247			x
Pavlova sp	AC248			x
Pavlova sp	AC249			x
Pavlova sp	AC250			x
Pavlova sp	AC251			x
Pavlova sp	AC252			x
Pavlova sp	AC537			x
Pavlova sp	AC538			x
Rebecca salina *	PLY465			
Rebecca salina	CCAP 940/3			x

* type strain

Phylogenetic trees generated for both genes and the concatenation using different methods (ML, Bayesian) recovered similar topologies, delineating four well-supported clades (fig 1, 2 and 3). The sequence of the type strain of *Exanthemachrysis gayraliae* together with sequences of undescribed strains forms a first clade with a bootstrap value of 77%, 98% and 100%. Support for this branch is reinforced by the Bayesian posterior probability of 0.99, 1.00 and 1.00 A second, strongly supported clade (bootstrap value 100% posterior probability 1.00 (in all inferred trees)) is composed of the sequence of the type strain of *Rebecca* together with sequences of undescribed strains. The third and fourth clades split the genus *Pavlova*. The third clade (bootstrap value 96%, 80% and 89%, and posterior probability 1.00, 0.90 and 0.99), including sequences of the type strains of *P. gyrans*, *P. pinguis* and *P. granifera* and other unidentified *Pavlova* strains, splits into two well-supported sub-clades. The type strains of *P. gyrans* and *P. pinguis* have identical sequences, falling in a sub-clade with closely related sequences from other strains (mostly previously identified as *P. gyrans*, but some identified as *P. lutheri* or *R. salina*). The other sub-clade includes sequences of the type strain of *P. granifera* and of several strains identified as *P. pinguis* as well as unidentified strains. The last clade, supported by an 87%, 58% and 97% bootstrap value with 1.00, 0.96 and 1.00 posterior probability, comprises a mix of distinct sequences of *Pavlova* and *Diacronema*.

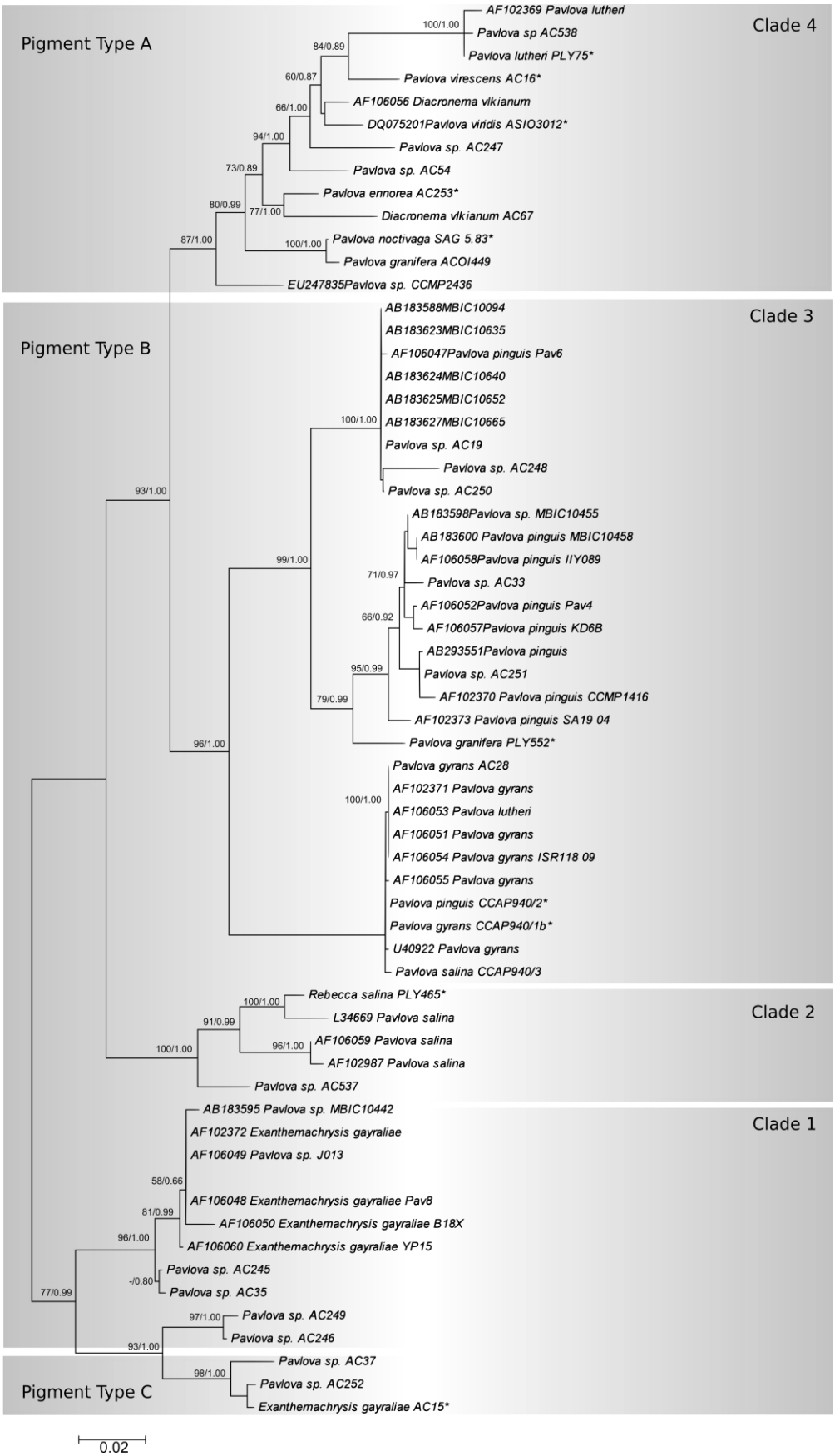

Figure 1: Molecular phylogeny of the Pavlovophyceae inferred from comparison of 18S rDNA sequences. The tree shown resulted from a maximum likelihood analysis using Prymnesiales sequences as an outgroup. Bootstrap percentage values determined for maximum likelihood (>50%) are shown on the left and posterior probability of the bayesian inference on the right. Type strains are marked with an asterisk.

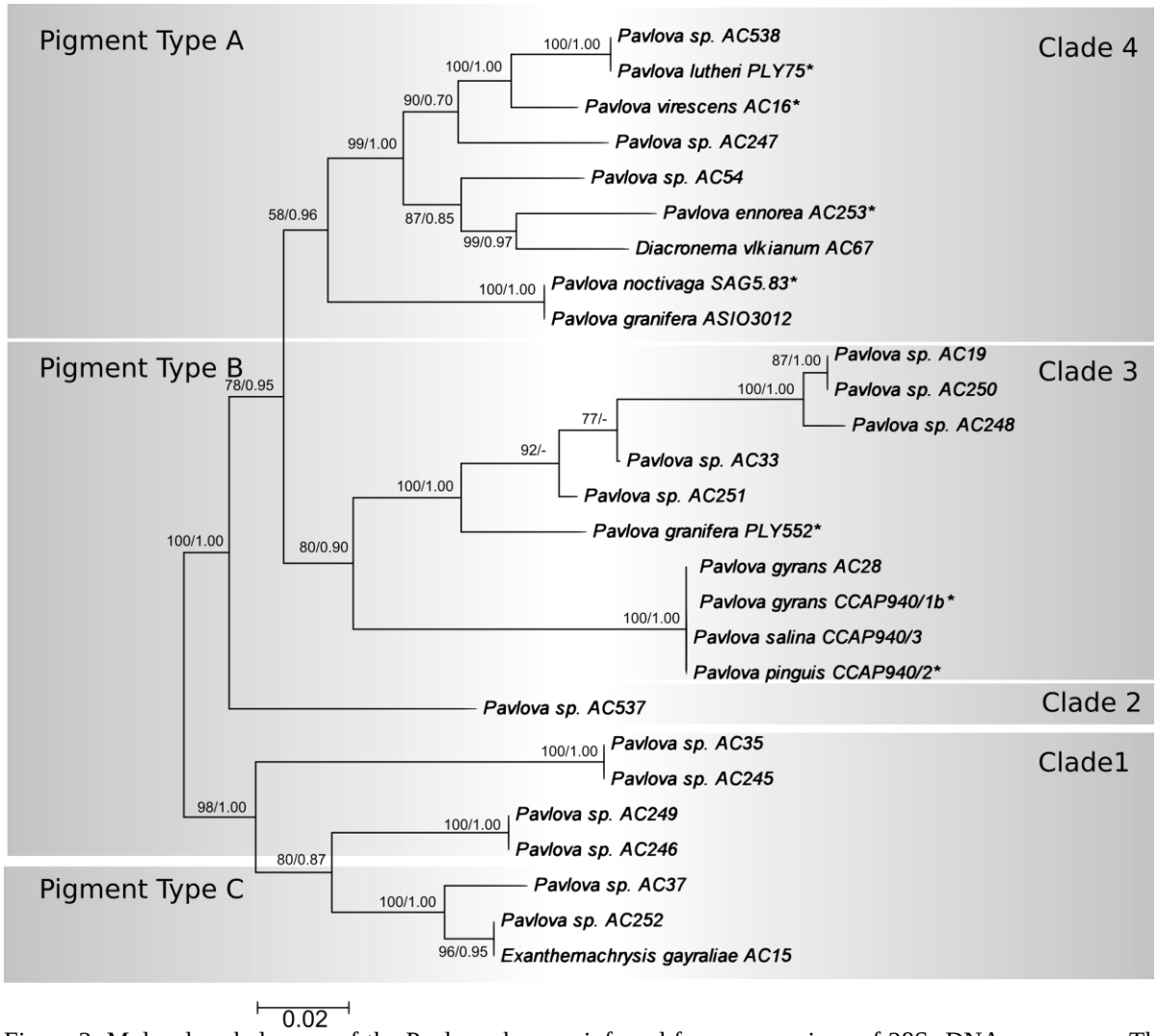

Figure 2: Molecular phylogeny of the Pavlovophyveae inferred from comparison of 28S rDNA sequences. The tree shown resulted from a maximum likelihood analysis using Prymnesiales sequences as an outgroup. Bootstrap percentage values determined for maximum likelihood (>50%) are shown on the left and posterior probability of the bayesian inference on the right. Type strains are marked with an asterisk.

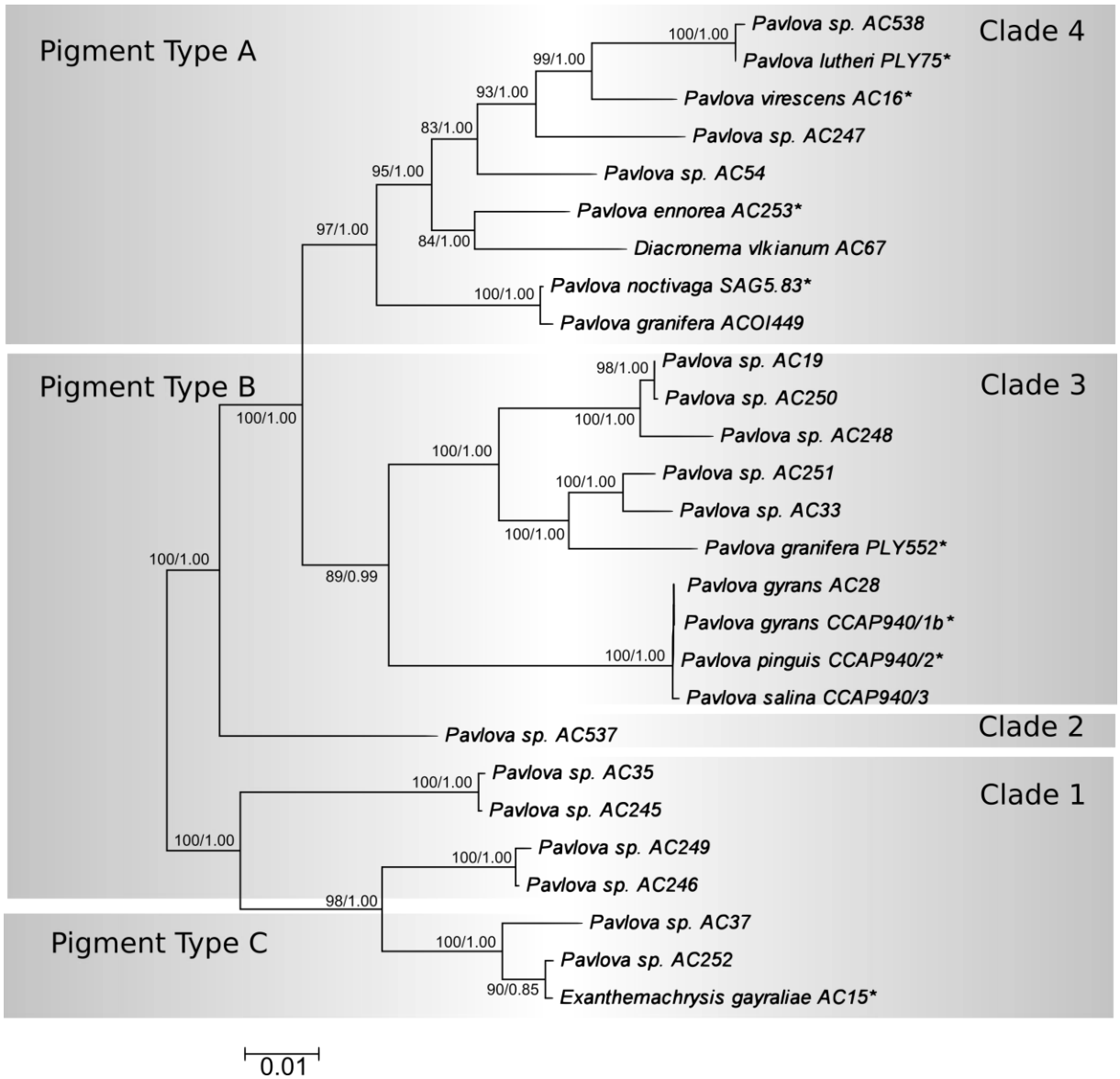

Figure 3: Molecular phylogeny of the Pavlovophyveae inferred from comparison of concatenated 18S rDNA and 28S rDNA sequences. The tree shown resulted from a maximum likelihood analysis using Prymnesiales sequences as an outgroup. Bootstrap percentage values determined for maximum likelihood (>50%) are shown on the left and posterior probability of the bayesian inference on the right. Type strains are marked with an asterisk.

Pigment analyses

The suite of photosynthetic pigments identified across the Pavlovophyceae was identical to that reported by Van Lenning et al. (2003). No trace of 19'-hexanoyloxyfucoxanthin (HFx), 4-keto-hexanoyloxyfucoxanthin (4-keto-HFx), 4-keto-fucoxanthin (4-keto-Fx), monovinyl (MV), and divinyl (DV) forms of chl c3 or nonpolar chl c2 types were found in the strains analysed, confirming the conclusion of Van Lenning et al. (2003) that these compounds can be classified within the Haptophyta as typical pigments of the class Prymnesiophyceae. In terms of pigment content, the profiles of all strains fell into the three pigment types (A, B and C) defined and detailed by Van Lenning et al. (2003). Type strains with pigment type A (the simplest pigment profile comprising Chls a, Mg-divinyl protochlorophyllide (MgDVP), c1, and c2 and the carotenoids fucoxanthin (Fx), diadinoxanthin (Ddx), diatoxanthin (Dtx), and ß, ß-carotene) included *P. lutheri, P. virescens, P. noctivaga, P. ennorea* and *D. vlkianum*. Pigment type B (type A pigments plus an unknown Ddx-like carotenoid - Unk-1- and an unidentified DV form of chl c - DV-chl cPAV) was found in the type strains of *P. gyrans, P. pinguis* and *P. granifera*. Pigment type C (type B pigments plus MV-chl cPAV, the most complex composition observed) was restricted to the type strain of *E. gayraliae* and 2 other strains (AC37 and AC252). The superposition of pigment groupings and molecular phylogeny is shown in Figure 1.

Morphology and ultrastructure

Pavlovophyceae cells are solitary or may form non-motile aggregations. Solitary cells are laterally flattened and typically highly metabolic. The anisokont flagella, when present, are inserted subapically or sometimes ventrally, and surround a non-coiling, often vestigial, haptonema. Flagellar movement is markedly heterodynamic. Intracellular storage bodies are present in some species, likely containing paramylon-like storage carbohydrates in crystalline microfibrillar units forming granules as described by Kiss and Triemer (1988). Crystalline inclusions rich in sulphur and barium and polyphosphate granules have been reported in some members of the class (van der Veer 1976; Fresnel et al. 1979). An eyespot is generally present in association with an invagination of the plasmalemma, but not associated with a flagellar swelling.

Based on a literature survey and our observations, a detailed synthesis of morphological and ultrastructural information for each of the 13 described species is presented in Table 4. A summary of the principal characters for each species is given below.

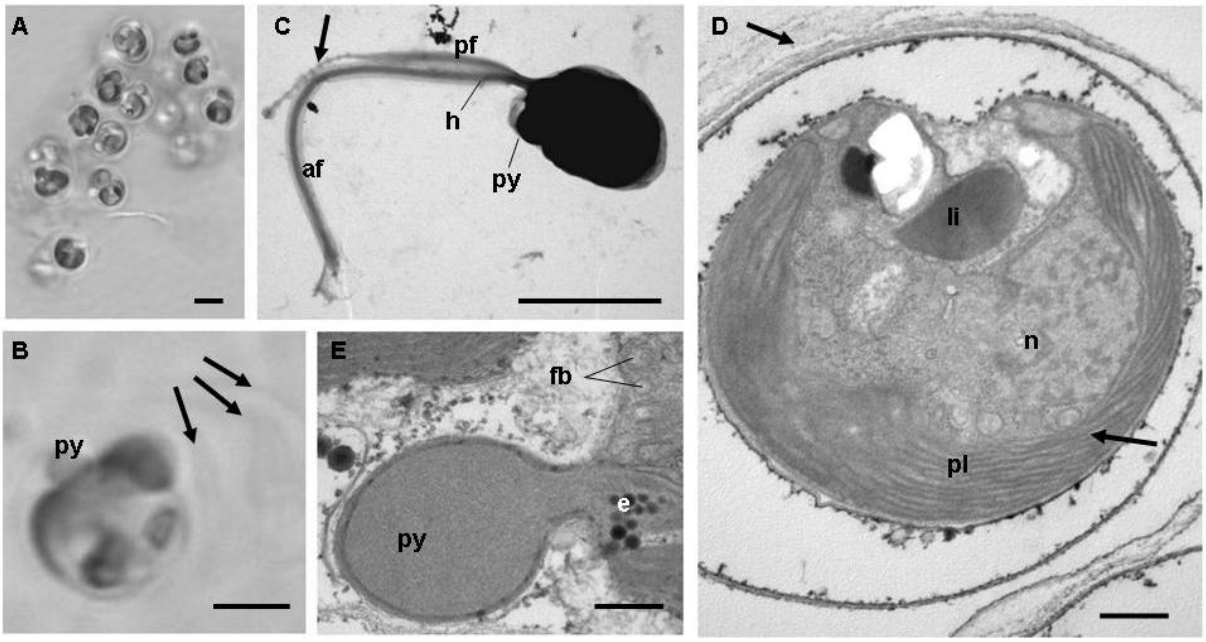

Figure 4: *Exanthemachrysis gayraliae*: A. Non-motile colony of cells embedded in mucilage; B. Non-motile cell with bulging pyrenoid in stratified mucilage (arrows); C. TEM. micrograph of motile cell (negative staining) showing three appendages and a bulging pyrenoid, with a string of pearl-like structures on the posterior flagellum (arrow); D. TEM micrograph of motile cell in transversal section showing the nucleus, one parietal plastid with helicoidal arrangement of the thylakoid lamellae (right arrow) and stratified mucilage (left arrow); E. TEM micrograph showing section of a pyrenoid and the eyespot; a section of the basal body visible on one side. Scale bar: A, B, C: 5 µm; D, E: 500 nm. Abbrev : af : anterior flagellum, e: eyespot, fb:flagellar base, h: haptomena, li: lipidic droplet, n: nucleus, pf : posterior flagellum, pl: plastid, py: pyrenoid.

Exanthemachrysis gayraliae **(fig 4):** The dominant stage consists of non-motile colonies of slightly ovate cells embedded in multiple layers of mucilage (fig 4A and 4B). The parietal plastid is brownish-green with a bulging pyrenoid that forms a visible protuberance on the cell body (fig 4B). The flagella of motile cells do not possess hairs and a haptonema is present (fig 4C). A distal string of pearl-like structures is present on the posterior flagellum (fig 4C), a feature that has never previously been described. Thylakoid lamellae exhibit a helicoidal arrangement (fig 4D) as noticed by van der Veer (1979) for R. salina and R. helicata, formerly Pavlova mesolychnon (van der Veer 1969) and Pavlova helicata (van der Veer 1972), respectively. The bulging pyrenoid is delimited from chloroplast stroma by osmiophilic vesicles forming an eyespot (fig 4E). The cell body is devoid of knob-scales.

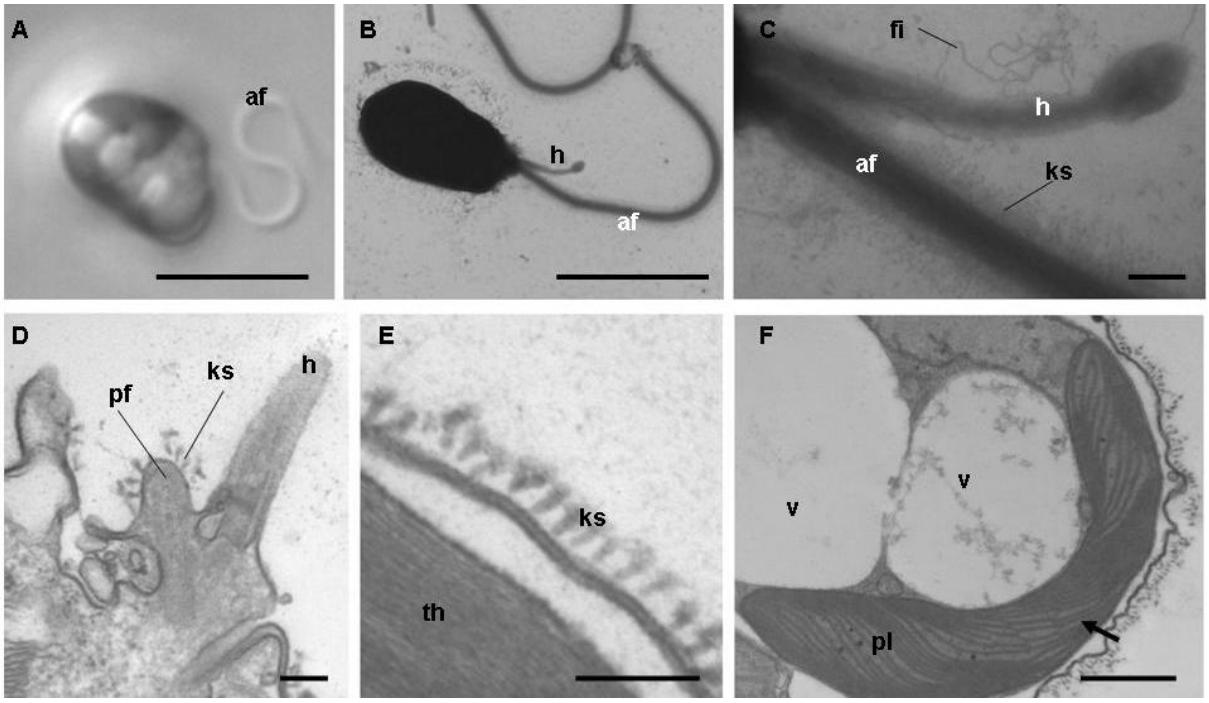

Figure 5: *Rebecca salina*; A. Motile cell with conspicuous anterior flagellum; B. TEM micrograph of a motile cell (negative staining) with anterior flagellum and haptonema; C. detail of the haptonema and the anterior flagellum bearing knob-scales; D. TEM micrograph of the haptonema and vestigial posterior flagellum covered with knob scales in longitudinal section ; E. TEM micrograph of detail of a section showing body knob-scales on the plasma membrane; F. TEM micrograph of the plastid in transversal section showing the thylakoid arrangement (arrow). Scale: A, B: 5 µm; C, D: 200 nm. Abbrev : af : anterior flagellum, fi: filipodium, h: haptomena, ks: knob-scales, pf : posterior flagellum, pl: plastid, th: thylakoids, v: vacuole.

***Rebecca salina* (fig 5) :** Motile cells are ovate to oblong and slightly metabolic with a golden-green parietal plastid (fig 5A). The anterior flagellum is visible and bears hairs and knob-scales (fig 5B). A well-developed haptonema emerges adjacent to the anterior flagellum, sometimes with fine filipodia (fig 5B and 6C). The vestigial posterior flagellum is reduced to the axoneme structure and is covered by small clavate knob scales (fig 5D), like the entire cell body external to the plasma membrane (fig 5E). A pyrenoid and an eyespot were not observed. One or two plastids are present with a parallel helicoidal arrangement of thylakoid lamellae (fig 5F) as in *E. gayraliae*.

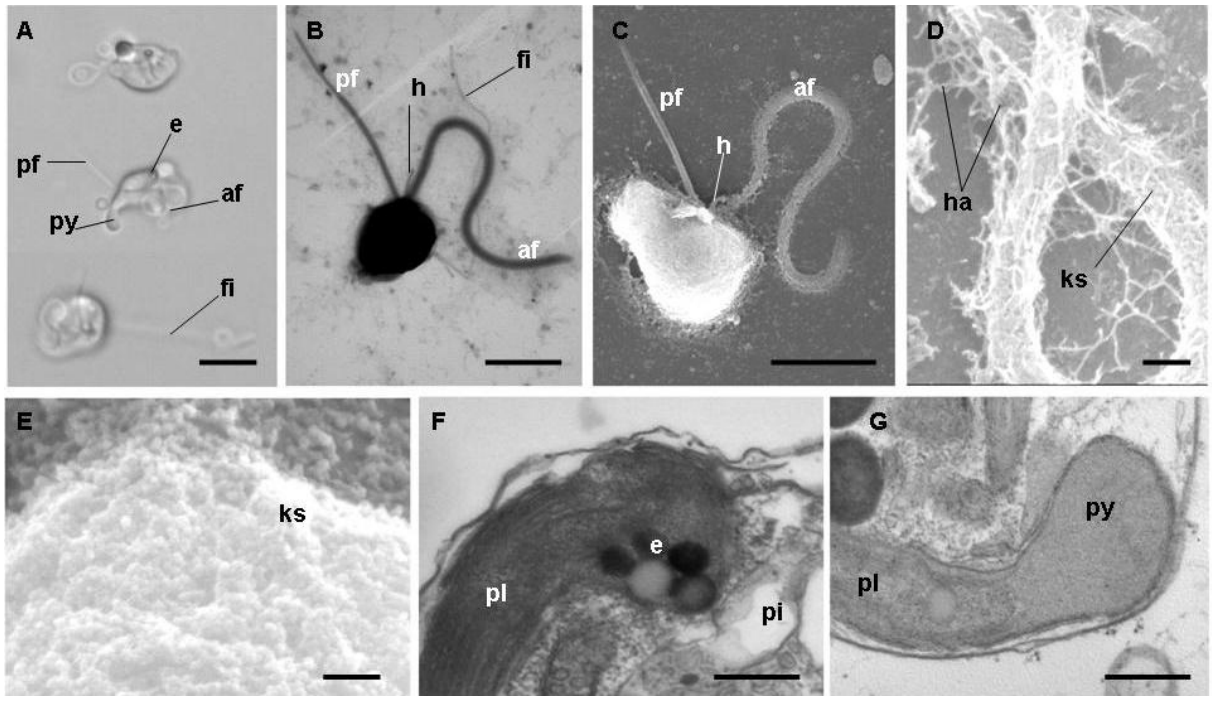

Figure 6: *Pavlova gyrans*; A. Highly metabolic motile cells showing 2 flagella, a conspicuous eyespot, a bulging pyrenoid and a filipodium B. TEM micrograph (negative staining) of a motile cell with three appendages and a filipodium; C. SEM micrograph of a motile cell with three appendages; D. SEM micrograph of hairs and knob-scales on the anterior flagellum; E. SEM micrograph of body knob-scales; F. TEM micrograph showing section of eyespot; G. TEM micrograph of the inner bulging pyrenoid in longitudinal section. Scale bar: A, B, C: 5µm; D: 200 nm; F, G: 500 nm. Abbrev : af: anterior flagellum, e: eyespot, fi: filipodium, h: haptomena, ha: hair, ks: knob-scales, pf: posterior flagellum, pi: flagellar pit, pl: plastid, py: pyrenoid.

***Pavlova gyrans* (fig 6):** The motile phase is dominant and the strongly metabolic cells have a yellow-green parietal plastid with a red-orange eyespot located near the flagellar insertion (fig 6A). Filipodia are sometimes observed extending from the cell surface (fig 6A and 6B). The hairy anterior flagellum is covered with knob scales, while the shorter posterior flagellum is naked (fig 6B, 6C and 6D). The haptonema is often visible (fig 6B and 6C). Smaller body knob scales surround the plasma membrane of the cell body (fig 6E). The plastid has parallel thylakoid lamellae, some osmiophilic globules forming an eyespot on the inner face and located near the flagellar pit (fig 6F), and a bulging pyrenoid (fig 6G).

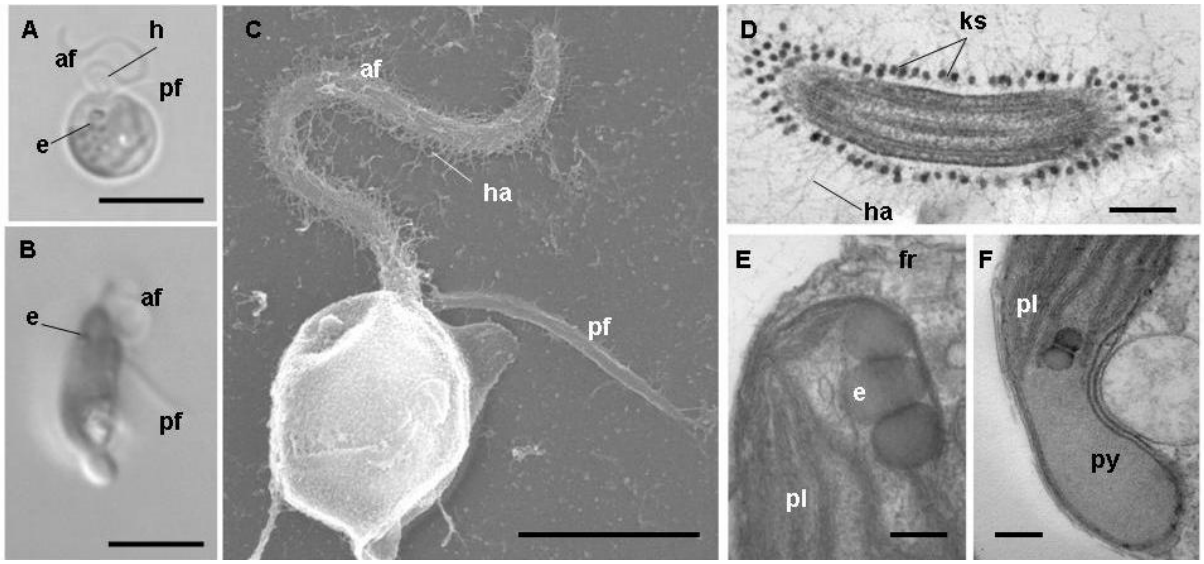

Figure 7: *Pavlova pinguis*; AB. Metabolic motile cells (A. round B. elongated) showing 2 flagella, a conspicious eyespot, a bulging pyrenoid; C. SEM micrograph of a round motile cell showing hairy anterior- and glabrous posterior flagella and a filipodium; D. TEM micrograph of anterior flagellum with knob scales and hairs in longitudinal section; E. TEM micrograph of inner plastid face eyespot at proximity of a flagellar root in longitudinal section; F. TEM micrograph of inner bulging pyrenoid in longitudinal section. Scale bar: A, B, C: 5µm; D, E, F: 200nm. Abbrev : af: anterior flagellum, e: eyespot, fr: flagellar root, h: haptomena, ha: hair, ks: knob-scales, pf: posterior flagellum, pl: plastid, py: pyrenoid.

***Pavlova pinguis* (fig 7):** This species has strongly metabolic motile cells with many filipodia and with a green-yellow parietal plastid (fig 7A and 7B). The three appendages are present: the posterior flagellum is naked (fig 7C) whereas the anterior flagellum possesses hairs and knob scales (fig 7C and 7D), with the haptonema inserted between them. Knob scales were not observed on the cell body. A red eyespot is located near the flagellar insertion on the inner face of the plastid (fig 7E). Like P. gyrans, the plastid has parallel thylakoid lamellae. A bulging pyrenoid is also present (fig 7F).

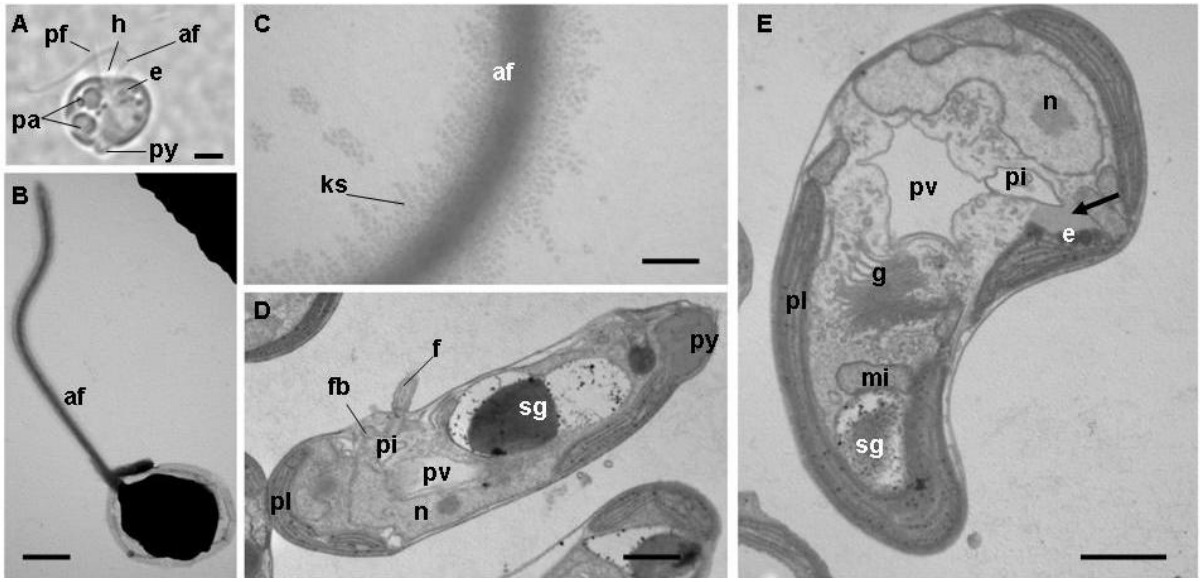

Figure 8: *Pavlova granifera*: A. Motile cell showing both flagella, the haptonema, the eyespot, storage (paramylon) granules and a pyrenoid; B. TEM micrograph (negative staining) of flagellate cell showing the anterior tomentose flagellum; C. TEM (negative staining) micrograph of knob-scales covering the anterior flagellum; DE. TEM sections of elongate motile cells showing proximity between pulsatile vacuole, flagellar pit and base; E. Unidentified contrasted area between flagellar pit and eyespot (arrow). Scale bar: A, B, E: 1 µm; C: 200 nm. Abbrev: af: anterior flagellum, e: eyespot, f: flagellum, fb:flagellar base, g: golgi apparatus, h: haptomena, ks: knob-scales, mi: mitochondrion, n: nucleus, pf: posterior flagellum, pi: flagellar pit, pl: plastid, pv: pulsatile vacuole, py: pyrenoid, sg: storage granule.

Pavlova granifera **(fig 8):** Motile cells are strongly metabolic and possess a brown plastid with a red-orange eyespot located near the flagellar insertion (fig 8A). The naked posterior flagellum is rigid (fig 8A), the anterior flagellum is flexible and covered by hairs and knob scales (fig 8A, 8B and 8C), and an emergent haptonema is present between the flagella (fig 8A). Sections of whole cells demonstrate the high degree of plasticity of cell shape, from compressed to long (fig 8D and 8E). There is also variability in nuclear shape. A pulsate vacuole is present at the centre of the cell, showing a relation with the flagellar pit (fig 8D and 8E). The plastid has parallel thylakoid lamellae, a bulging pyrenoid (fig 8D) and an eyespot on the inner face, adjacent to a less osmiophilic zone connected with the flagellar pit (fig 8E).

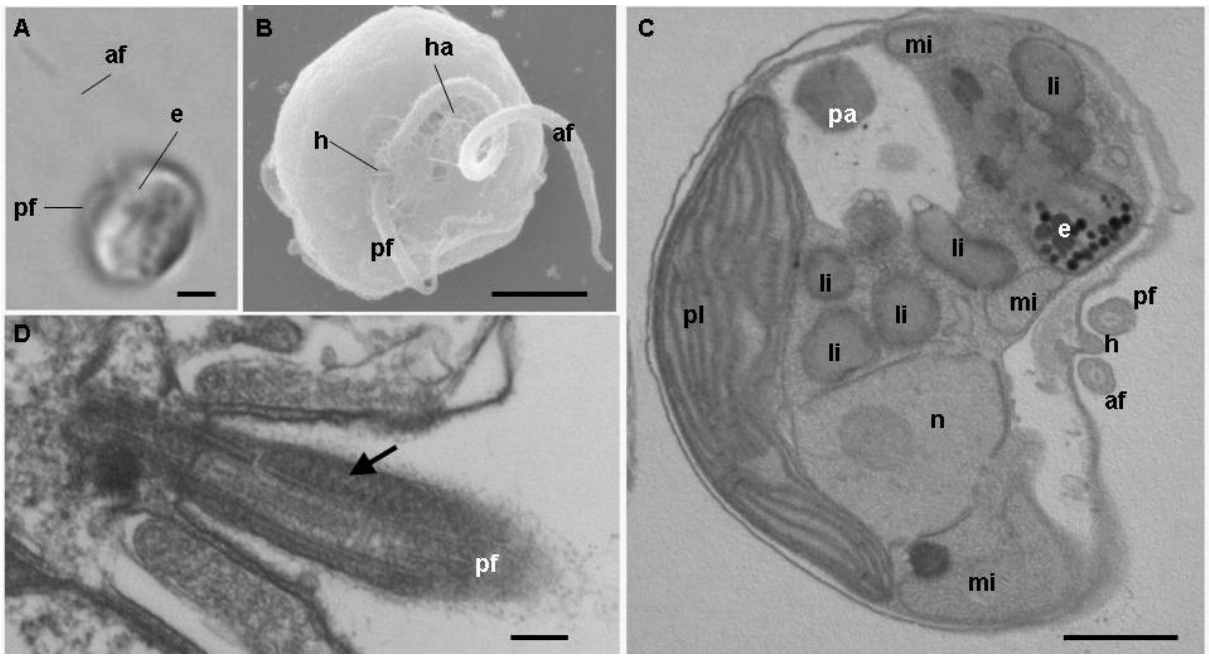

Figure 9: *Diacronema vlkianum*: A. Motile cell showing both flagella; B. SEM micrograph of the apex of a whole mounted motile cell showing hairy long anterior- and short posterior flagella; C. TEM section of a motile cell showing appendage insertion, with a hairy anterior flagellum, a posterior flagellum and the haptonema; D. TEM section of posterior flagellum longitudinal, with teeth-like structures (arrow) in the flagellar swelling. Scale bar: A, B, C: 1µm; D: 200nm. Abbrev: af: anterior flagellum, e: eyespot, h: haptomena, ha: hair, li: lipidic droplet, mi: mitochondrion, n: nucleus, pf: posterior flagellum, pl: plastid, sg: storage granule.

***Diacronema vlkianum* (fig 9):** The dominant stage consists of motile cells that are round to ovate in shape with a slight ventral compression (fig 9A, 9B and 9C). The brownish-green plastid is parietal and flagella are ventrally inserted near a red eyespot. The anterior flagellum possesses hairs but no knob-scales (fig 9B); the posterior flagellum is naked. Both flagella exhibit a small distal attenuation and the haptonema is not always visible, but is present (fig 9B and 9C). The eyespot is composed of osmiophilic globules on the external face of the plastid adjacent to the posterior flagellum (fig 9C), which has a swelling with a distinctive teeth-like structure (fig 9D) as described for the type strain of D. vlkianum. The plastid has parallel thylakoid lamellae and does not possess a pyrenoid.

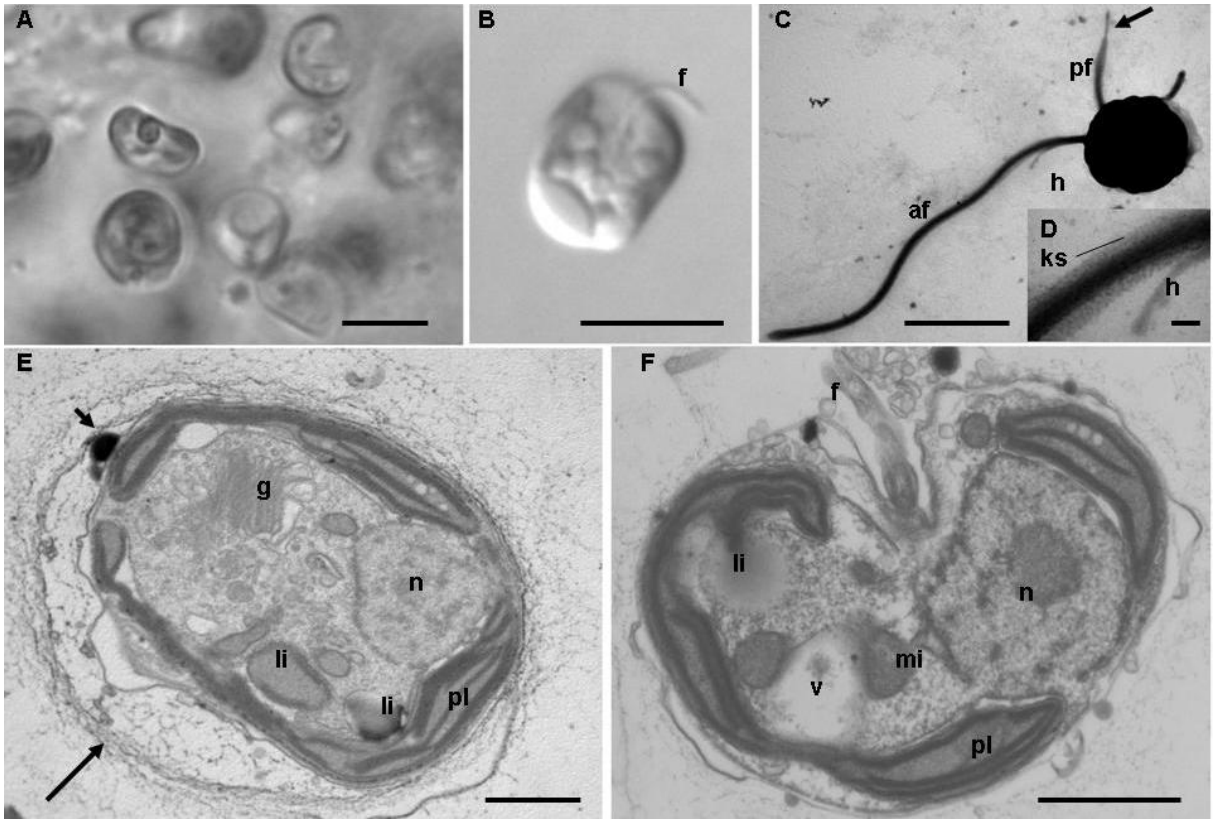

Figure 10: *Pavlova ennorea*: A. Colony of non-motile cells; B. Apical view of a motile cell with one visible flagellum; C. TEM micrograph (negative staining) of a motile cell showing the haptonema near the base of the tomentose anterior flagellum and the shorter attenuated (arrow) posterior flagellum ; D. Detail of the anterior flagellum covered by knob-scales; E. TEM section of a non-motile cell surrounded by mucilage (arrows); F. TEM section of a motile cell. Scale bar: A, B, C: 5µm; D: 200 nm; E, F: 1µm. Abbrev: af: anterior flagellum, f: flagellum, g: Golgi apparatus, h: haptomena, ks: knob-scales, li: lipidic droplet, mi: mitochondrion, n: nucleus, pf: posterior flagellum, pl: plastid, py: pyrenoid, v: vacuole.

Pavlova ennorea **(fig 10):** The dominant stage consists of non-motile colonies of slightly compressed cells embedded in mucilage (fig 10A). Parietal chloroplasts are golden-brown in colour (fig 10A and 10B). Appendages of motile cells are inserted ventrally (fig 10B). The anterior flagellum possesses hairs and is covered by round knob scales (a feature that has not previously been reported for this taxon) and the short posterior flagellum is distally reduced (fig 10C and 10D). Incomplete flagella with knob scales were observed in non-motile cells. Non-motile cells possess peripheral mucilage vesicles and are surrounded by a homogeneous mucilage layer (fig 10E). Cells may have two plastids with parallel thylakoid lamellae separated by a large stromatal space (fig 10E and 10F). Flagella are inserted in an invagination near the nucleus in motile cells (fig 10F). This species has no pyrenoid and no eyespot.

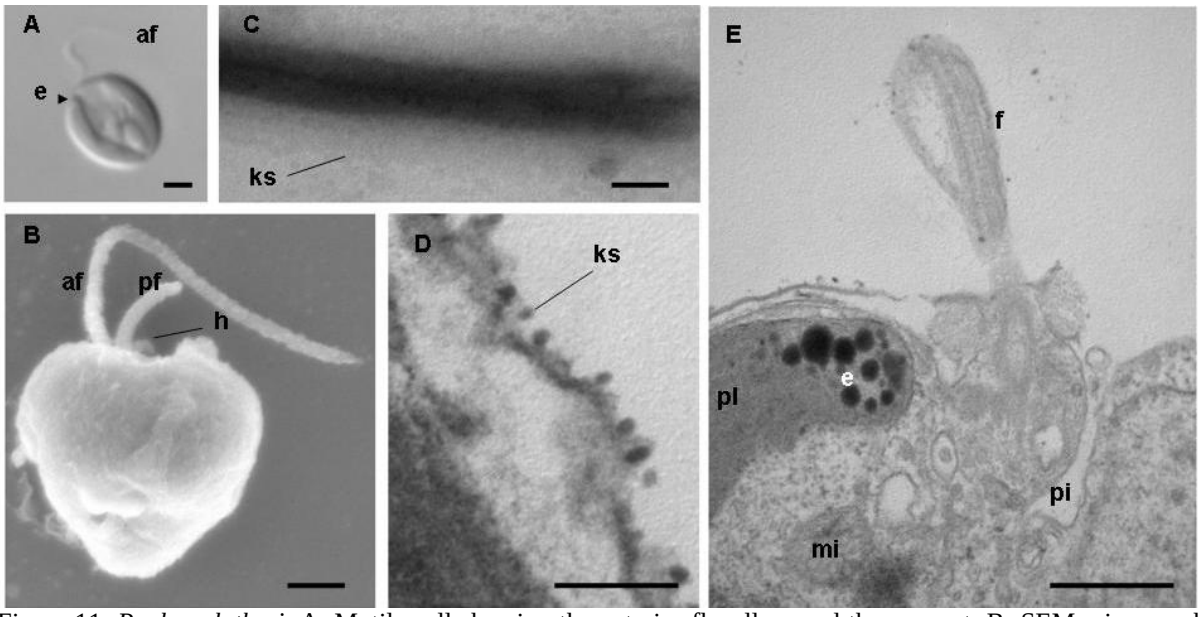

Figure 11: *Pavlova lutheri*; A. Motile cell showing the anterior flagellum and the eyespot; B. SEM micrograph of a motile cell showing anterior flagellum, posterior flagellum and haptonema; C. TEM micrograph (negative staining) of anterior flagellum covered by knob-scales; D. Details of a section (TEM micrograph) showing body knob-scales; E. Longitudinal section (TEM Micrograph) showing location of the eyespot and flagellar insertion near a pit. Scale bar: A, B: 1 µm; C: 200 nm; D; 100 nm; E: 500 nm. Abbrev: af: anterior flagellum, e: eyespot, h: haptomena, ks: knob-scales, mi: mitochondrion, pf: posterior flagellum, pi: flagellar pit, pl: plastid.

***Pavlova lutheri* (fig 11):** The dominant motile cells are mainly round with a yellow-green plastid and a red eyespot (fig 11A 11B and 11E). Vacuoles containing a regularly organised crystalline substance were sometimes observed (fig 11A). The haptonema is inserted between the hairy anterior flagellum that bears knob scales, unlike the naked posterior flagellum (fig 11B and 11C). The cell body is covered with small knob scales (fig 11D). The appendages are inserted near a pit and adjacent to the eyespot which is located on the external face of the plastid (fig 11E). Thylakoid lamellae are parallel. A pyrenoid was not observed.

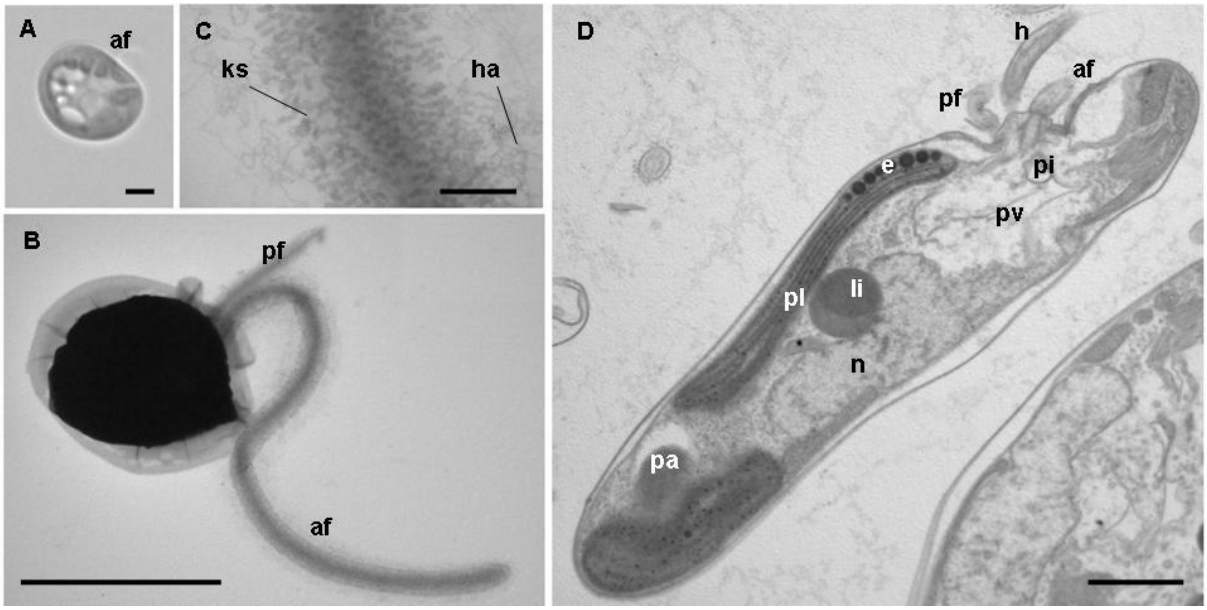

Figure 12: *Pavlova noctivaga*; A. Motile cell with an anterior flagellum; B. TEM micrograph (negative staining) of a motile cell showing the anterior long tomentose and flexible flagellum and the shorter posterior flagellum; C. TEM micrograph of hairy anterior flagellum covered by knob-scales (negative staining) D. TEM section of a motile cell showing eyespot on the outer face of the plastid and a pulsatile vacuole near the flagellar pit at the base of flagellar apparatus. Scale bar: A: 1 µm, B: 5 µm; C: 200 nm; D: 1 µm. Abbrev: af: anterior flagellum, e: eyespot, h: haptomena, ha: hair, ks: knob-scales, li: lipidic droplet, n: nucleus, pf: posterior flagellum, pi: flagellar pit, pl: plastid, pv : pulsatile vacuole , sg: storage granule.

***Pavlova noctivaga* (fig 12):** Motile cells are ovate with a parietal brown-green plastid (fig 12A). The anterior flagellum is hairy and is covered by clavate knob scales and the posterior flagellum with a slight distal attenuation is naked (fig 12B and 12C). Cells are sometimes elongate (fig 12D). A layer of eyespot globules is present on the external face of the plastid, near the flagellar insertion. A pyrenoid is not present. The plastid presents a simple parallel arrangement of thylakoid lamellae. A pulsate vacuole seems to be connected to the flagellar pit (fig 12D).

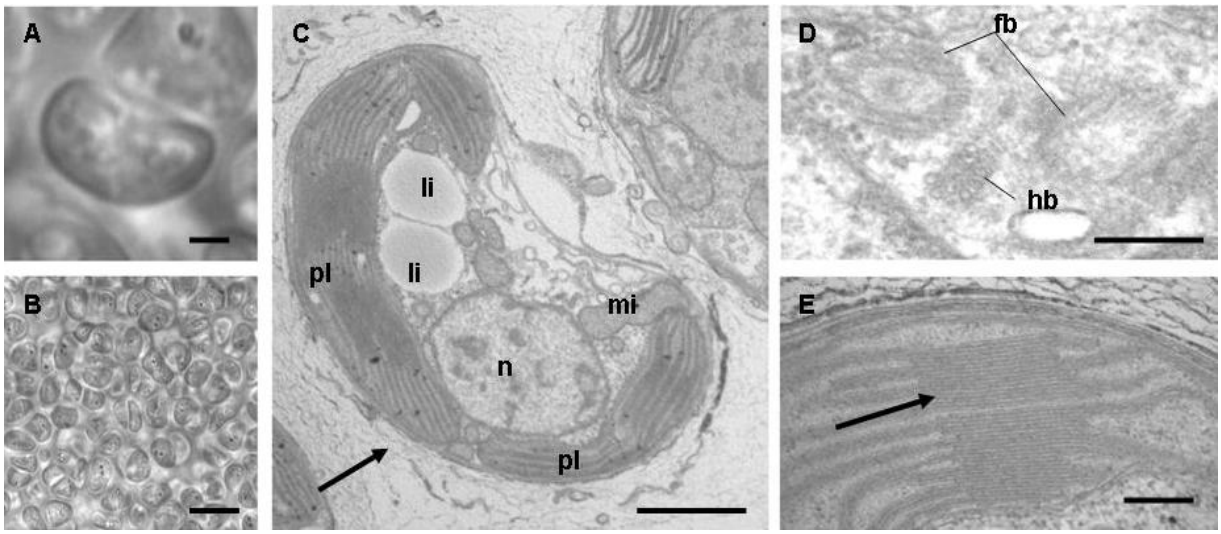

Figure 13: *Pavlova virescens*; A.B. Non-motile cells in colonies; C. TEM section of a motile cell showing two plastids, lipidic droplets and mitochondrium; D. TEM micrograph of flagellar and haptonematal bases; E. TEM section of plastid with granum-like thylakoid arrangement (arrow). Scale bar: A: 1 µm; B: 10 µm; C: 1 µm; D, E: 200 nm. Abbrev: fb:flagellar base, h: haptomena, hb: haptonema base, li: lipidic droplet, mi: mitochondrion: nucleus, pl: plastid.

***Pavlova virescens* (fig 13):** The dominant stage consists of compressed green non-motile cells embedded in mucilage (fig 13A) and this stage may form colonies (fig 13B). Cells are surrounded by a homogenous mucilage layer (fig 13C). Flagellar bases occur in the ventral depression, the haptonematal base consisting of eight microtubules being inserted between the two flagellar bases (fig 13D). Thylakoid lamellae are often stacked, giving a granum-like appearance (fig 13E). Absence of thylakoid exvagination indicates that these structures are not grana as in green plants. No stigma and no pyrenoid were observed.

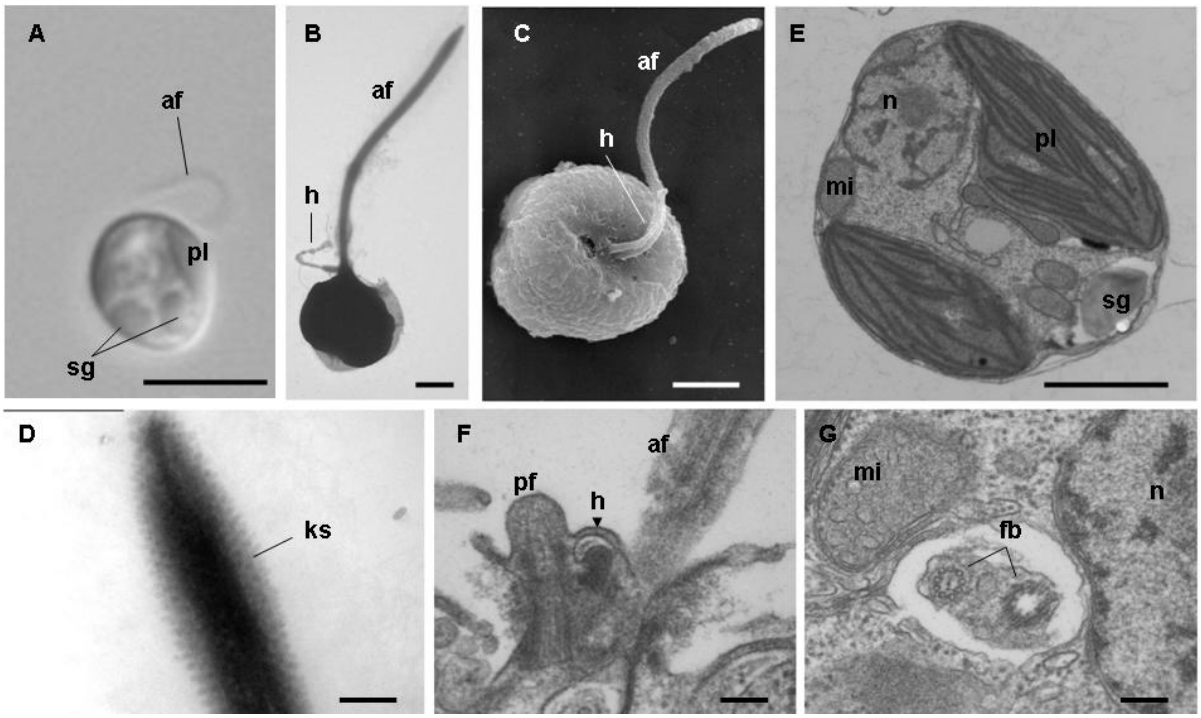

Figure 14: *Pavlova viridis*; A. Motile cell with anterior flagellum visible; B. TEM micrograph of motile cell with anterior flagellum and haptonema (negative staining); C. SEM micrograph of apical view of a motile cell with anterior flagellum and haptonema; D. TEM micrograph of anterior flagellum covered by knob scales (negative staining); E. TEM section of a motile cell; F. TEM micrograph of haptonema and vestigial posterior flagellum in longitudinal section; G. TEM micrograph of haptonema and vestigial posterior flagellum in transversal section. Scale bar: A: 5 µm; B, C: 1 µm; D: 200 nm; E, 1 µm; F, G: 200 nm. Abbrev.: af: anterior flagellum, fb:flagellar base, h: haptomena, ks: knob-scales, mi: mitochondrion, n: nucleus, pf: posterior flagellum, pi: flagellar pit, pl: plastid, pv : pulsatile vacuole, py: pyrenoid, sg : storage granule.

***Pavlova viridis* (fig 14):** Motile cells are spherical with a green parietal plastid (fig 14A). The anterior flagellum and the haptonema emerge from a ventral depression (fig 14B and 14C). The anterior flagellum is covered with knob scales (fig 14D). The plastid has parallel thylakoid lamellae, with no eyespot and no pyrenoid (fig 14E). The posterior flagellum is

reduced to the axoneme structure with only nine single structural microtubules rather than nine triplets (fig 14F and 14G).

Discussion

Based largely on the study of authentic cultures, we present the first full molecular phylogenetic reconstruction of described members of this ancient class of haptophyte algae. In parallel, an ultrastructural re-examination of all described taxa was conducted. This integrative morpho-molecular approach provides the basis for a revision of the taxonomy of the class and insights into the evolutionary ecology of the group.

At the genetic level all described species differ, even in sequences of the conservative 18S rDNA gene, although in some cases, notably *P. pinguis / P. gyrans*, differentiation is minor. Sequences from unidentified culture strains and from Genbank indicate the existence of significant microdiversity within the group, part or all of which very probably represents novel species. In this study, four distinct clades were distinguished within the Pavlovophyceae based on the molecular phylogenies. This provides a framework within which to assess the phylogenetic significance of morphological and ultrastructural features.

Clade 1: The only described species in this clade is *Exanthemachrysis gayraliae*. This is the only described member of the Pavlovophyceae that has a ventral bulging pyrenoid and an eyespot formed of osmiophilic vesicles located at the transition between the chloroplast stroma and thylakoids. The complete absence of knob scales is also a distinctive feature, albeit shared with *Diacronema vlkianum* and *Pavlova viridis* that fall in clade 4. The distal string of pearl-like structures on the posterior flagellum is a unique feature that was not reported in the original description of the species. Gayral and Fresnel (1979) transferred *P. ennorea* and *P. noctivaga* to the genus *Exanthemachrysis* based on the fact that motile cells lack flagellar knob scales and non-motile cells apparently lacked external flagellar apparatus. Green (1980) adopted a more conservative approach of retaining these species in *Pavlova* because the flagellar apparatus of *P. ennorea* was only described as “incomplete” with little detail given by van der Veer and Leewis (1977), whereas Kalina (1975) described and illustrated flagella and haptonema as present in both motile and non-motile cells of *P. noctivaga*. No non-motile cells were present in our culture strain of *P. noctivaga*, but in *P. ennorea* non-motile cells with external flagella covered with knob-scales were observed. Our results clearly indicate that *P. ennorea* and *P. noctivaga* do not belong to the genus *Exanthemachrysis*.

Clade 1 includes a number of non-identified strains, most of which are genetically distinct from the type strain, with at least 2 sub-clades likely representing new species (genetic distance equal to or greater than that separating related pairs of described species within the class). All strains we observed from this clade have a dominant non-motile phase. If members of the sub-clades prove to have the same type of pyrenoid and eyespot as *E. gayraliae*, these should logically be classified in the genus *Exanthemachrysis*. It is notable, however, that within this clade only 2 strains closely related to the type strain of *E. gayraliae* share the type C pigment profile (i.e. presence of MV-chl cPAV) with the type species. In Van Lenning et al. (2003), the type strain was the only strain from this clade included in the analysis, hence their conclusion that the presence of MV-chl cPAV is characteristic of the genus and potentially ancestral for the class. Our extended analysis indicates that either (1) the type C pigment profile is not indicative at the genus level, or (2) other sub-clades in clade 1 should be described as a new genus (in fact as at least 2 new genera in order to avoid paraphyly). Ultrastructural examination of other strains in the clade is required to resolve this taxonomic point. The analysis also clearly shows that pigment type C is derived from pigment type B, the latter being the ancestral pigment type for the class.

Clade 2: This clade is composed of five sequences and includes that of the type strain of the genus *Rebecca*, *R. salina* PLY465. The four other sequences, one from an undescribed strain (AC537) and three Genbank sequences labelled as *Rebecca salina* (or *Pavlova salina*), are all different. Based on a combination of ultrastructural features and molecular phylogeny, *P. salina* was transferred to the new genus *Rebecca* by Edvardsen et al. (2000). According to Edvardsen et al. (2000) a unique feature of this genus, which also includes *R. helicata*, is the vestigial nature of the posterior flagellum. However, this feature is also observed in *P. viridis* (which falls in clade 4). Another feature considered distinctive of *Rebecca* was the lack of an eyespot, but *P. ennorea* and *P. viridis* from clade 4 also lack an eyespot. Unlike *P. viridis*, Rebecca possesses knob scales, a feature that remains phylogenetically relevant for this clade. The unusual intra-plastidial structure consisting of thylakoid lamellae separated by large inter-stromatal spaces reported in both *R. salina* and *R. helicata* has been classed as a pyrenoid (Green 1976, van der Veer 1979), but there is doubt as to the exact nature of this structure. Green mentioned that *R. salina* (as *P. salina*) has 'no obvious pyrenoid' (Edvardsen et al 2000), and likewise we did not observe a structure that can be considered to be a pyrenoid in *R. salina*. The absence of a pyrenoid is a feature shared with clade 4 and notably with P. *ennorea* that possesses similar intra-stromatal spaces between thylakoid lamellae. To our

knowledge, the type strain of *R. helicata* no longer exists and it will therefore be difficult to prove that it belongs to *Rebecca*, although further study of strain AC537 and other cultures in this clade may help.

It should be noted that Edvardsen et al. (2000) based their taxonomic revision (creation of the genus *Rebecca*) on the sequence of the culture strain PLY468 (labelled as *Pavlova* aff. *salina*) that is not the type strain of *R. salina*. The 18S rDNA sequence of the type strain (PLY465) studied here is not identical to that of PLY468, the latter therefore likely to be a different species. However, the proximity of these two strains within clade 2 in our molecular phylogeny indicates that the revision proposed by Edvardsen et al. (2000) is indeed warranted. Comparison of ribosomal gene sequences clearly separates *Rebecca* from other members of the Pavlovales, but pigment profiles do not separate the *Rebecca* clade from clade 3 and most of clade 1, and there is no single unique ultrastructural feature that distinguishes the clade. The *Rebecca* clade (as represented by the type strain of *R. salina*) does, however, exhibit a unique combination of features, namely vestigial posterior flagellum, lack of eyespot, presence of knob scales, lack of pyrenoid and pigment type B.

Clade 3: This clade includes sequences of the type strains of *P. granifera*, *P. gyrans* and *P. pinguis*. Clade 3 is composed of two clear sub-clades.

Clade 3.1: This sub-clade contains the type strains of both *P. pinguis* (CCAP940/2) and *P. gyrans* (CCAP940/1b) that have identical 18S rDNA sequences, with 4 bp difference in ITS sequences and no difference in 28S rDNA sequences. Similarity in flagellar structure and in the arrangement of the pit, eyespot, chloroplast and pyrenoid between *P. pinguis* and *P. gyrans* prove clear affinities between them (Green 1980). Minor ultrastructural differences noticed by Green (1980) included less osmiophilic droplets in *P. pinguis* and the presence of hairs on the short flagellum of *P. gyrans* (that of *P. pinguis* being naked). We did not observe an obvious difference in the quantity of osmiophilic droplets and we did not observe hairs on the short flagellum of either species (or any other pavlovophyceaen taxon). The presence/absence of knob scales is the only differential feature between the two species noted by Green (1980) that was confirmed in our study. In the context of the extreme genetic similarity between the two type strains, the significance of this morphological difference is not clear. The presence/absence of knob scales and very minor genetic difference could be the result of a recent speciation event, but it is also possible that presence/absence of knob scales is a phenotypic difference within a single species (the name *P. gyrans* having priority). In this latter context, it is noteworthy that differences in scale morphology characterise haplo-diploid

life cycle stages in the Prymnesiophyceae (Billard 1994, Houdan et al. 2004). In most known cases in the Prymnesiophyceae, the two life cycle stages both possess body (plate-type) scales with different ornamentation between the stages, but there are examples (most notably the coccolithophore *Emiliania huxleyi*) where one phase possesses scales and the other phase does not (Klaveness, 1972; Green et al. 1996; Houdan et al. 2004). Digenetic and/or dimorphic life cycles have never been reported in the Pavlovophyceae, but the possibility that *P. gyrans* and *P. pinguis* could be different forms within a common life cycle should be considered.

Pavlova gyrans, described by Butcher (1952), is the type species of the genus, and this sub-clade thus retains the name *Pavlova*. A number of sequences from other culture strains (from our analysis and from Genbank) are identical or very similar to those of *P. gyrans* / *P. pinguis* and together these form a definite sub-clade, potentially representing recent radiation within a *P. gyrans* species complex.

A problem was encountered during examination of the strain CCAP940/3 that was labelled as being equivalent to PLY465, the type strain of *Rebecca salina*, but which exhibited an 18S rDNA sequence and morphological characters with close affinity to *Pavlova pinguis*. The original type strain, PLY465, which we confirmed to have the ultrastructural characters of *R. salina*, is in the Plymouth Culture Collection as *Pavlova salina*.

Clade 3.2: There is a clear genetic distinction between this second sub-clade and sub-clade 3.1. The type strain of *Pavlova granifera* (PLY552), a freshwater species with ultrastructural characters similar to *P. pinguis* and *P. gyrans*, is part of this sub-clade. The brackish strain AC33 has a sequence close to that of *P. granifera* and the ultrastructure of both strains is similar. *Pavlova granifera* does not possess knob scales (like *P. pinguis*), but there are no other obvious ultrastructural differences between *P. granifera* and *P. gyrans* /*P. pinguis* except the presence of a pulsatile vacuole in *P. granifera*, that is likely to be the consequence of being cultured in a freshwater medium (cf. the conclusion of Green and Hibberd (1977) for Diacronema). *Pavlova granifera* was described (as *Chrysocapsa granifera*) before *P. gyrans* (and P. pinguis), but only by light microscopy (Mack 1954). Green (1973) observed the type strain of *P. granifera* using electron microscopy only after the descriptions of *P. gyrans* and *P. pinguis* and it is clearly possible that strains of the latter two species could have been classified as *P. granifera* had this chronology been different. However, we consider that *P. granifera* and *P. gyrans/P. pinguis* should be maintained as separate species due to the genetic difference between them, and in this context habitat (freshwater/brackish vs marine)

could have resulted in speciation between the sub-clades. This sub-clade also contains Genbank sequences mostly labelled as *P. pinguis*, as well as AC19 (a marine strain) that had also been identified as P. pinguis by TEM. We propose maintenance of this sub-clade in the genus *Pavlova* in view of the evident morphological and ultrastructural affinity with clade 3.1. It seems clear, however, that this genus contains a number of cryptic entities.

Clade 4: This clade contains the type strains of *P. noctivaga* (SAG5.83), *P. lutheri* (PLY75), *P. ennorea* (AC253), *P. virescens* (AC16) and *P. viridis* (ASIO3012). The type strain of *D. vlkianum* is no longer available, but strain AC67 exhibits ultrastructural characters identical to the original description and thus is taken as being representative of *D. vlkianum*. This clade is distinguished by occurrence of pigment type A (lack of chl cPAV) in all examined strains. In terms of ultrastructure, however, this is the most diverse clade. Each species exhibits distinctive ultrastructural characters, but unifying features are the absence of a pyrenoid, the presence of scales (except *D. vlkianum*), the presence of an inconspicuous eyespot on the outer face of the chloroplast (except *P. viridis* and *P. ennorea*) and 'normal' anisokont flagella (except *P. viridis* and *D. vlkianum*).

Diacronema vlkianum is distinguished by the unique structure of the posterior flagellum, which has a proximal part swollen on the side adjacent to the cell, and the ventral position of the flagellar insertion (Green and Hibberd 1977). The absence of scales in *D. vlkianum* is also unique within this clade. *D. vlkianum* was basal to this clade in the phylogeny of Van Lenning et al. (2003), but falls within the clade in our extended phylogenies based on both 18S and 28S rDNA sequences. This provides a strong indication that these characters related to flagellar structure and positioning and lack of scales are not taxonomically relevant above the species level and that maintenance of this species in a separate genus from other members of this clade is not justified.

Four possibilities were proposed by Van Lenning et al. (2003) for the taxonomy of this clade: 1) *Diacronema vlkianum* could be transferred to *Pavlova* if certain morphological (presence/absence and structure of pyrenoid and eyespot) and pigment (presence/absence of DV-chl cPAV) features are not considered taxonomically relevant; 2) *Pavlova lutheri* and *P virescens* (and potentially *P. calceolata* and *P. noctivaga*) may be transferred to an emended genus *Diacronema* if the latter morphological and pigment groupings are considered relevant and the *D. vlkianum* flagellar morphology does not prove to be significant; 3) a new genus may be created to contain *P. lutheri* and *P virescens* (and potentially *P. calceolata* and *P. noctivaga*) if all of these features are considered relevant; and 4) the current taxonomy can be

retained, leaving *Pavlova* as a paraphyletic, but non-polyphyletic, genus. Based on the clear genetic differentiation of this clade from clade 3, together with the unifying features of the lack of a pyrenoid and lack of chl cPAV, we consider that option 2 is the most rational and we therefore propose the transfer of all species in this clade to an emended genus *Diacronema*. *Pavlova calceolata* was not studied here since the type strain no longer exists, but published ultrastructural characters clearly show that it belongs to this clade and therefore that it should also be transferred to *Diacronema*.

Table 4: Comparison of principal characters of the Pavlovales (inspired from Green 1980)

Evolutionary ecology

According to the molecular clock estimation of Liu et al. (2010) (and assuming that the evolutionary rate of the 28S rRNA gene is comparable across haptophytes), the divergences between the 4 extant clades of the Pavlovophyceae are very ancient. The *Exanthemachrysis* clade is estimated to have diverged around the time of the Permian/Triassic boundary ca. 250 Mya, the *Rebecca* clade diverged in the Jurassic ca. 170 Mya and the *Pavlova* and *Diacronema* clades diverged in the Cretaceous ca. 100 Mya. This provides strong additional support for taxonomic separation into 4 discrete genera following the delineation into clades presented here and indicates that the existing genera have traversed one or more major global extinction events. Medlin et al. (2008) suggested that the adaptation of certain non-calcifying prymnesiophytes to eutrophic coastal environments and their ability to switch modes of nutrition from autotrophy to mixotrophy are possible explanations for survival across the K/T boundary. Pavlovophytes are known mainly from culture strains isolated from near-shore coastal environments and the described species clearly thrive in rich culture media reminiscent of eutrophic environments. There is a general conception that all extant members of the Pavlovophyceae rely exclusively on photosynthesis as a source of nutrition (e.g. Cavalier-Smith 2002, de Vargas et al. 2007), but to our knowledge there have been no specific attempts to determine whether members of this class are capable of phagotrophy (and hence mixotrophy). Many chromalveolate algae with comparable body plans are capable of bacteriovory and this may yet be proved to be the case in the Pavlovophyceae.

Given the ancientness of pavlovophyte lineages and their apparent robustness to major global change events, it is perhaps surprising that diversity within this group is apparently

relatively limited (13 described species vs ca. 400 in the Prymesiophyceae). We provide molecular genetic evidence that the group is more diverse than previously thought, but diversity remains low compared to that known in the Prymnesiophyceae (particularly in light of the recent results of Liu et al. 2009) and to that of most other microalgal classes. This is probably in part due to the fact that pavlovophytes are relatively difficult to identify in natural samples using classical microscopy techniques and we therefore predict that future culture-based studies and particularly culture-independent metagenomic analyses will reveal more new diversity within this class, as pointed out by Shi et al. (2009). If, however, diversity in this group does prove to remain low, the question of why this should be the case links into the debate on the origins of the class: are the Pavlovophyceae living fossil relics of simple ancestral haptophytes or are they derived forms highly specialised for a particular type of ecological niche?

Certain predictions can be made as to the likely nature of the cenancestor of the known Pavlovophyceae based on the topology of our molecular phylogenetic reconstruction. It was probably an estuarine/marine organism with anisokont, subapically inserted flagella (with non-tubular hairs on the long anterior flagellum), a non-coiling haptonema, simple flagellar roots (associated only with the base of the mature short posterior flagellum), a primitive eyespot and a simple pigment profile with MV chl cPAV. It is not clear whether this ancestral pavlovophyte would have possessed knob-scales (due to absence in the *Exanthemachrysis* clade) or a pyrenoid (absence in the *Rebecca* and *Diacronema* clades). This picture for the ancestral pavlovophyte differs rather radically from the likely nature of the ancestral prymnesiophyte, which is likely to have possessed isokont, smooth, apically inserted flagella and a forward pointing, non-coiling haptonema with several microtubules in the emergent part, relatively complex flagellar roots, plate scales, and a pyrenoid (Edvardsen et al. 2000, de Vargas et al. 2007). The pigment profile of early prymnesiophytes is likely to have been the same as that of pavlovophyte pigment type A, meaning that chl cPAV evolved early in the Pavlovophyceae lineage after divergence from the Prymnesiophyceae. Stigmata have never been observed in the Prymnesiophyceae and were presumably absent in the cenancestor of this group. Cavalier-Smith (1994) proposed that it is likely that anisokonty with asymmetrical cell shape is the ancestral state for all Haptophyta due to the predominance of this body plan in chromist algae. However, the same author (Cavalier-Smith 2002) later considered that the loss of tubular flagellar hairs in haptophytes was essential for the evolution of a functionally correlated forward-pointing haptonema and homodynamic isokont cilia and that predatory prymnesiophytes retain this condition, whereas the purely photosynthetic Pavlovophyceae

became secondarily anisokont, moving the kinetid to the cell apex and therefore losing the roots associated with the anterior flagellum.

Although it has not been satisfactorily proved that pavlovophytes are purely photosynthetic, and despite the fact that the asymmetrical body plan with anisokont flagella is widespread in chromalveolate algae, it does seem that a number of the apparently simple characters of the pavlovophytes are derived. These include the reduction in the number of microtubules in the emergent part of the haptonema (most prymnesiophytes have at least 6 microtubules in the emergent part of the haptonema, when present), the loss of roots associated with the anterior flagellum (most chromalveolates have microtubular roots associated with both flagellar bases), the presence of simple non-tubular hairs on the anterior flagellum (these not being structurally comparable with bi- or tripartite mastigonemes in heterokonts), and the eyespot (the pavlovophyte stigmata do not have obvious homologies within the chromalveolates and in fact most closely resemble certain structures present in the green lineage). The fact that there is not a very high level of morphological diversity amongst known pavlovophytes despite divergence times of as much as a quarter of a billion years could be interpreted as indicating that the lineage has adopted a structure that is particularly well suited for a specific niche (near-shore coastal environments), but that this structure is fundamentally not very plastic in evolutionary terms. The existence of two phylogenetically distant extant freshwater pavlovophyte species, together with the occurrence of euryhaline species like *D. vlkianum*, indicates multiple invasions of freshwater, but there is little evidence that members of this class have managed to become established in more oligotrophic ecosystems. It will be particularly interesting to see from future metagenomic studies whether pavlovophytes are present (and diverse) in open ocean environments. Shi et al. (2009) provide the first evidence that this may be the case.

Concluding remarks

The combination of morphological, molecular genetic and biochemical analyses employed here is shown to be a powerful tool for phylogenetic reconstructions and verification of the taxonomic validity of species described using classical techniques only. In this context, the accuracy of classical techniques for distinguishing species is noteworthy. Our analysis confirms that most of the described species are discrete taxonomic entities, with one possible cryptic exception involving *P. gyrans* and *P. pinguis*. The existence of type strains as reference material is invaluable for this type of revaluation. Access to type strains allowed verification of certain contentious points, discovery of new features in some species, and

detection of the accidental mislabelling of a supposed type strain. This latter experience highlights the importance of independently verifying the identity of strains obtained from culture collections, a fact that most service collections are aware of and are addressing notably through the implementation of genetic barcoding of culture holdings.

We have highlighted the need for complementary studies on known pavlovophyte species, notably in terms of nutritional capacities and life cycle strategy. The class Pavlovophyceae contains a significant amount of undescribed diversity already in culture. The taxonomic scheme proposed in this study will provide a framework for describing this new diversity and for interpreting imminent environmental gene sequencing efforts.

Taxonomic summary

REVISED DIAGNOSES OF *DIACRONEMA* Prauser emend. Bendif et Véron

Motile cells with two unequal flagella and a short haptonema. Longer anterior flagellum with fine non-tubular hairs and with or without of minute dense bodies; posterior flagellum sometimes with a basal swelling and vestigial. Occasionally dense bodies on cell surface. A pit or canal penetrating the cell near the long anterior flagellum. Chloroplast single or double without a pyrenoid, sometimes with an eyespot located on the external face of the plastid. Non-motile cells with or without incomplete appendages.

Mobiles cellulae duobus inaequalibus flagellis et brevi haptonema instructae. Longum flagellum anterius cum tenuibus non tubularibus pilis atque cum aut sine minutis densisque corporibus, posterius autem flagellum interdum vestigiale et interdum cum basali tumore. Aliquando densa corpora in summa cellula. Fovea vel canalis penetrat cellulam prope longum flagellum. Chloroplastus unicus vel geminus sine pyrenoide, interdum cum stigmate in externa facie plastidi sito. Immobiles cellulae imperfecto appendice praesente aut deficiente.

TYPE SPECIES: *Diacronema vlkianum* Prauser

BASIONYM: *Diacronema vlkianum* Prauser 1958 Arch Protistenk 103: 117-128

Diacronema ennorea (Veer et Leewis) Bendif et Véron comb. nov.

BASIONYM: *Pavlova ennorea* Veer et Leewis 1977 Acta Bot Neerl 26: 159-176

SYNONYM: *Exanthemachrysis ennorea* (Veer et Leewis) Gayral et Fresnel 1979 Protistologica XV: 271-282

REVISED DIAGNOSIS of *Diacronema ennorea* Veer et Leewis 1977 emend. Bendif et Véron

Sedentary cells forming non-motile colonies, slightly compressed or often flattened if touching each other. Homogenous mucilage excretion with osmiophilic muciferous vesicles. Plastid single, yellow green, without eyespot or pyrenoid and thylakoid lamellae parallel with large stromatal space. Motile cells elongate with two unequal flagella and a haptonema. Anterior flagellum with fine hairs and circular knob-scales. Flagellar insertion in a slight ventral depression. Absence of body scales.

Sedentariae cellulae colonias immobiles formantes, leviter compressae vel saepius complanatae, si inter se contingentes. Homogenae mucilagini excretio cum muciferis vesiculis homogeneis. Unicus chloroplastus, flavovirens, nec stigmate nec pyrenoide instructus, ac thylacoides et parallelae lamellae cum magno stromatico spatio. Mobiles cellulae elongatae duobus flagellis inaequalibus et haptonema instructae. Anterius flagellum cum tenuibus pilis ac punctiformibus circularibusque squamis. Insertio flagellorum in levi depressione ventrali. Absentia squamarum cellularium.

DIAGNOSTIC FIGURE : fig 10

Diacronema lutheri (Droop) Bendif et Véron comb. nov.
BASIONYM: *Monochrysis lutheri* Droop 1953 Acta Bot Fenn 51: 3-52
SYNONYM: *Pavlova lutheri* (Droop) Green 1975 J mar biol Ass U.K. 55: 785-793

Diacronema noctivaga (Kalina) Bendif et Véron comb. nov.
BASIONYM: *Corcontochrysis noctivaga* Kalina 1970 Preslia 42: 297-302
SYNONYMS: *Pavlova noctivaga* (Kalina) Veer et Leewis 1977 Acta Bot Neerl 26: 159-176, Green 1980 Br Phycol J 15: 151-191, *Exanthemachrysis noctivaga* (Kalina) Gayral et Fresnel 1979 Protistologica XV: 271-282,
REVISED DIAGNOSIS of *Diacronema noctivaga* Kalina 1970 emend. Bendif et Véron
Free living cells mainly ovate or elongate with appendages inserted near a red eyespot. Three remarkably unequal appendages with a hairy anterior flagellum covered by knob-scales and a naked posterior flagellum with slight distal attenuation. Absence of body scales. Brown plastid with a layer of eyespot globules present on the external face near the appendage

insertion, without a pyrenoid. A pulsate vacuole connected to the flagellar pit. Occurrence of non-motiles colonies with stratified mucilage.

Cellulae solutae saepissime ovatae vel elongatae cum appendicibus prope rubro stigmate insertis. Tres appendices notabiliter inaequales, ex quibus anterius flagellum pilosum punctiformibus squamis coopertum et posterius flagellum nudum cum levi attenuatione distali. Absentia squamarum cellularium. Spadiceus chloroplastus, globulis stigmaticis adlineatis in externa facie prope insertionem appendicum praesentibus, sine pyrenoide. Pulsans vacuola puteo flagillari iuncta. Praesentia coloniarum immobilium cum mucilagine stratificata.

DIAGNOSTIC FIGURE : fig 12

Diacronema virescens (Billard) Bendif et Véron, comb. nov..

BASIONYM: *Pavlova virescens* Billard 1974 Soc Phycol de France Bull 21: 18-27

Diacronema viridis (Tseng, Chen et Zhang) Bendif et Véron, comb. nov.

BASIONYM: *Pavlova viridis* Tseng, Chen et Zhang 1992 Chin J Oceanol Limnol 10: 23-28

REVISED DIAGNOSIS of the genus *Pavlova* Butcher ex Green, emended Bendif et Véron

Motile cells, free swimming, strongly metabolic, with two unequal flagella and a short haptonema. Longer anterior flagellum with fine non tubular hairs and minute dense bodies, present or absent on the cell body. A pit or canal penetrating the cell near the long anterior flagellum. Plastid with posterior bulging pyrenoid and eyespot conspicuous on inner surface near the flagellar pit. Non-motile cells with incomplete appendages.

Mobiles cellulae, solute natantes, vehementer metabolicae, duobus inaequalibus flagellis et brevi haptonema instructae. Longum flagellum anterius cum tenuibus non tubularibus pilis ac minutis densisque corporibus, praesentibus aut absentibus in cellulari corpore. Fovea vel canalis cellulam prope longum flagellum anterius penetrans. Chloroplastus cum protuberante pyrenoide et visibili stigmate in interna facie prope puteum flagellarem. Immobiles cellulae imperfectis appendicibus praesentibus.

TYPE SPECIES: *Pavlova gyrans* Butcher

BASIONYM*: Pavlova gyrans* Butcher 1952 **J mar biol Ass U.K. 31: 175-191**

REVISED DIAGNOSIS of *Exanthemachrysis gayraliae* Lepailleur 1970, emend. Bendif et Véron

Dominant stage of non-motile cells slightly ovate, embedded in a multilayered mucilage. Brownish-green parietal plastid with a bulging pyrenoid forming a protuberance on the cell body. Motile metabolic cells with three naked appendages and a distal string of pearl-like structures on the posterior flagellum attenuation. Bulging pyrenoid delimited from chloroplast stroma by globules forming an eyespot near the insertion of the appendages.

Status dominans immobilium et leviter ovotarum cellularum pluristratificata mucilagine stipatarum. Parietalis chloroplastus olivaceus cum protuberante pyrenoide formante protubertionem in summo cellulari corpore. Mobiles et metabolicae cellulae cum tribus appendicibus et distali catena, margaritis similis structurae, in attenuatione posterioris flagelli sita. Protuberans pyrenoides globulis stigma prope insertionem appendicum formantibus a stromate chloroplasti delimitatus.

DIAGNOSTIC FIGURE: fig 4

Methods

Algal cultures. Twenty-nine strains of Pavlovophyceae were used in this study, including 10 authentic cultures (Table 2). Cultures were obtained from either Algobank-Caen or other listed culture collections. Marine species were grown in ES-Tris medium (Cosson 1987) and the freshwater species in modified Lefevre-Czarda medium (PavED) with peat extract prepared like the soil extract in ES-Tris and added at 1%. Temperature was 20 °C and illumination provided by day light fluorescent tubes at a photon flux of 30 µmol of photons.m^{-2}.s^{-1} and a light/dark cycle 12/12h.

Microscopy. Light microscope observations were conducted with an Olympus BX51 (Olympus Corporation, Tokyo, Japan) equipped with differential interference contrast (DIC) optics. Whole mounts were prepared for TEM from a drop of culture fixed with 1% osmium vapour on a Formvar-coated grid and negative stained with 1% uranyl acetate diluted in water/ethanol (1:1). The samples were analysed with a Jeol 1011 transmission electron microscope (JEOL Ltd, Tokyo, Japan). For SEM, cells were mounted by sedimentation on thermanox cover slides treated with L-polylysine and then fixed with 4% glutaraldehyde in 0.1 M cacodylate buffer (pH 7.4) and 0.25M sucrose. After stepwise dehydration in a graded alcohol series, the cells were critical point dried (Jeol Ltd, Tokyo, Japan) and finally coated with a thin layer of gold/palladium (Leica Microsystems GmbH, Wetzalr, Germany). Observations were made with a Jeol JSM 6400F SEM. TEM preparations for ultrastructural study were performed with a 2 hour 4% glutaraldehyde fixation in 0.1M cacodylate buffer (pH 7,4) and 0.25M sucrose at 4°C. The fixed cells were washed with decreasing sucrose concentrations and then post fixed in 2% osmium tetroxide for 2 hours at 4°C. After washing, the cells were embedded in 1% low melting point agar, dehydrated in a graded alcohol series and then impregnated in 1:1 epon /ethanol for 30 min, 100 % epon for 30 min and 100 % epon overnight. Then cells were embedded in epon resin (Epon 812, EMS, Hatfield, United Kingdom) and polymerised for 24 h at 60 °C. Thin sections were cut with a diamond knife (Diatome) on a Leica microtome (Leica Microsystems GmbH, Wetzlar, Germany) and stained with 1% uranyl acetate for 15 min followed with Reynolds lead citrate for 5 min (Reynolds 1963). The sections were observed with a Jeol 1011 transmission electron microscope.

DNA extraction. Cultures of cells were harvested by centrifugation (4500g, 15 min), washed twice with TE buffer, and suspended in 10 ml of lysis buffer (Tris, 0.1 M; EDTA, 0.05 M; NaCl, 0.1 M; 1% SDS; 2% N-lauroylsarcosine, proteinase K 200 mg/mL, pH 8.0) and incubated at 55°C for 2h for total DNA extraction. DNA was then extracted with equal volumes of phenol and chloroform and precipitated with ethanol (Maniatis et al. 1982).

Amplification of the SSU and LSU rDNA and intergenic regions. Primers used in this study for the PCR amplification are listed in Table 3. Due to difficulties to amplify the SSU in one step two additional internal primers were designed allowing the deduction of the complete SSU rDNA sequences. Standard PCR cycles were performed for the PCR amplification of the SSU and LSU rDNA and the intergenic regions as follow: a first denaturing step at 95 °C for 5 min followed by 30 cycles: 1 min. at 95 °C, 1 min. at 50 °C and 1 min. at 72 °C with a final extension at 72°C for 5 min. Most of the amplification products were cloned in the commercial cloning vector pCR 4-TOPO (TOPO TA Cloning Kit; Invitrogen Corporation, Carlsbad, USA). Plasmids from positive colonies were purified with the QIAprep Spin Miniprep Kit (QIAGEN, Hilden, Germany). The cloned PCR products included in the plasmids were sequenced with the M13 primers in both directions.

Phylogenetic analysis. For SSU rDNA analyses, sequences obtained in this study were aligned together. Alignment was first obtained using the online version of the multiple alignment program MAFFT (http://align.bmr.kyushu-u.ac.jp/mafft/software, Katoh et al. 2007), and were then improved by hand using the sequence editor BIOEDIT (Hall 1999). Very variable regions were automatically removed using the Gblocks software (http://www1.imim.es/~castresa/Gblocks/Gblocks.html), with optimised parameters for rRNA alignments (minimum length of a block, 5; allowing gaps in half of positions). The Gblock software retained 1711 positions for phylogenetic analyses from the initial 1820 positions for the SSU rDNA and retained 729 positions from the initial 890 positions for the LSU rDNA. The most appropriate model of DNA substitution and associated parameters were estimated by three statistics based on the Akaike information criterion (AIC, Akaike 1974), AIC, AICc and BIC using MrAIC (Nylander 2004). A GTR distribution model was selected by taking into account a gamma-shaped distribution of the rates of substitution among sites (G) with the proportion of invariable sites (I) for both SSU and LSU rDNA gene analyses (GTR+G+I). The selected model and parameters were used to perform phylogenetics analyses.

Phylogenetic trees were determined from both rDNA sequences (single and concatenated) by two phylogenetic methods: maximum likelihood (ML) using TREEFINDER (Jobb et al., 2004) and Bayesian analysis with Mr. BAYES v3.1.2 (Ronquist and Huelsenbeck 2003). The robustness of the branching of trees was tested by bootstrapping for the maximum likelihood inference and bootstrap values were based on 1000 replicates. Bayesian analysis was conducted with two runs of four Markov chains, for at least 5 000 000 generations, sampling every 100th generation. From the 50 000 trees found, 25% were discarded (time required for likelihood to converge on stationary value) by setting the burn-in option.

Table 3: List of primers used in this study

Primer name	Sequence (5'-3')	Target gene	References
A18 DIR (Forward)	AACCTGGTTGATCCTGCCAGT	SSU rDNA	Medlin et al. 1988
A18 REV (Reverse)	TCCTTCTGCAGGTTCACCTAC	SSU rDNA	Medlin et al. 1988
18S ISE (Internal primer)	CTGACACAGGGAGGTAGTGAC	SSU rDNA	Lab use
18S IAS (Internal primer)	TCCTCACTATGTCTGGACCTG	SSU rDNA	Lab use
LEUK2 (Forward)	ACCCGCTGAACTTAAGCATATCACT	LSU rDNA	Liu et al. 2009
EUK_34R (Reverse)	GCATCGCCAGTTCTGCTTACC	LSU rDNA	Liu et al. 2009

Pigment analyses. Cells of the strains indicated in table 1 were harvested during the logarithmic phase of growth by gentle vacuum filtration onto 25-mm GF/F Whatman (Kent, UK) glass fibre filters and stored frozen (-80°C) until analysis. Extraction and HPLC analysis of pigments was performed as described in Van Lenning et al. (2003) Pigment analyses were performed with a Thermo Separation Products chromatograph (currently Thermo Finnigan, San Jose, CA, USA), comprising a model P2000 solvent module, a UV3000 absorbance detector, an FL2000 fluorescence detector, an SN4000 controller, and a refrigerated (5°C) A/S-3000 autosampler.

Acknowledgements

We are deeply indebted to all persons who collected samples, isolated strains and maintained cultures for several decades in laboratories. Without them this type of work could not have been possible. Bertrand Le Roy, as well as his predecessors are sincerely thanked for their meticulous care in the maintenance of Algobank-Caen. Jacqueline Fresnel is thanked for her precious expertise in electron microscopy techniques. Professor Marie-Agnès Avenel of the Institut du Latin at the Université de Caen Basse-Normandie is warmly thanked for his critical

assistance in the drafting of the diagnosis in Latin. We thank Yoann Canon, who attended the first work of this job in 2000. The ASSEMBLE project (FP7-227799) funded some aspects of this work.

References

Akaike H (1974). A new look at the statistical model identification. IEEE Transactions on Automatic Control 19: 716–723

Antoine E, Fleurence J (2003) Species identification of red and brown seaweeds using ITS ribosomal DNA amplification and RFLP patterns. J Sci Food Agri 83: 709-713

Billard C (1976) Sur une nouvelle espèce de Pavlova, P. virescens nov. sp. (Haptophycées). Soc Phycol de France Bull 21: 18-27

Billard C (1994) Life cycles. In Green JC & Leadbeater BSC (eds) The Haptophyte algae. The Systematics Association special volume 51, Oxford University Press, Oxford, **pp 167-186**

Butcher RW (1952) Contributions to our knowledge of the smaller marine algae. J mar biol Ass U.K. 31: 175-191

Carter N (1937) New or interesting algae from brackish water. Arch Protistenk 90: 1-68

Cavalier-Smith T (1994) Origin and relationships of Haptophyta. **In Green JC & Leadbeater BSC (eds) The Haptophyte algae.** The Systematics Association special volume 51, Oxford University Press, Oxford, pp 413-436

Cavalier-Smith T (2002). The phagotrophic origin of eukaryotes and phylogenetic classification of Protozoa. Int J Syst Evol Microbiol 52: 297-354.

Cosson J (1987) Croissance des sporophytes résultants d'hybridations interspécifiques et intergénériques chez les laminaires. Crypto Algol 8: 61-72

De Vargas C, Aubry MP, Probert I, Young J (2007) Origin and evolution of Coccolithophores: from coastal hunters to oceanic farmers. In Falkowski PG, Knoll A, (eds.), Evolution of Primary Producers in the Sea. Academic Press, pp 251-285

Droop MR (1953) On the ecology of flagellates from some brackish and fresh-water pools of Finland. Acta Bot fenn 51: 3-52

Edvardsen B, Eikrem W, Green JC, Andersen RA, Moon-van der Staay ST, Medlin LK (2000) Phylogenetic reconstructions of the Haptophyta inferred from 18S ribosomal DNA sequences and available morphological data. Phycologia 39: 19-35

Fresnel J, Galle P, Gayral P (1979) Résultats de la microanalyse des cristaux vacuolaires chez deux Chromophytes unicellulaires marines : Exanthemachrysis gayraliae, Pavlova sp. (Prymnésiophycées, Pavlovacées). C R Acad Sc Paris 288: 823-825

Gayral P (1980) Particularités et intérêt subséquent de la famille des Pavlovophycées (Chrysophycophytes, Prymnesiophycées). 105e Congrès national des Sociétés savantes III: 201-212

Gayral P, Fresnel J (1979) Exanthemachrysis gayraliae Lepailleur (Prymnesiophyceae, Pavlovales) : Ultrastructure et discussion taxinomique. Protistologica XV: 271-282

Green JC (1967) A new species of Pavlova from Madeira. Br phycol Bull 3: 299-303

Green JC (1973) Studies in the fine structure and taxonomy of flagellates in the genus Pavlova. II. A freshwater representative, Pavlova granifera (Mack) comb. nov. Br Phycol J 8: 1-12

Green JC (1975) The fine structure and taxonomy of haptophycean fagellate Pavlova lutheri (Droop) comb. nov. (= Monochrysis lutheri Droop). J mar biol Ass U.K. 55: 785-793

Green JC (1976) Notes on the flagellar apparatus and taxonomy of Pavlova mesolychnon van der Veer, and on the status of Pavlova Butcher and related genera within the Haptophyceae. J mar biol Ass U.K. 56: 595-602

Green JC (1980) The fine structure of Pavlova pinguis Green and a preliminary survey of the order Pavlovales (Prymnesiophyceae). Br Phycol J 15: 151-191

Green JC, Hibberd DJ (1977) The ultrastructure and taxonomy of Diacronema vlkianum (Prymnesiophyceae) with special reference to the haptonema and flagellar apparatus. J mar biol Ass U.K. 57: 1125-1136

Green JC, Hori T (1988) The fine structure of mitosis in Pavlova (Prymnesiophyceae). Can J Bot 60: 1497-1509

Green JC, Hori T (1994) Flagellar and flagellar roots. In Green JC, Leadbeater BSC (eds) The Haptophyte Algae. The Systematics Association special volume 51, Oxford University Press, Oxford, pp 47-71

Green JC, Jordan RW (1994) Systematic history and taxonomy. **In Green JC & Leadbeater BSC (eds) The Haptophyte algae.** The Systematics Association special volume 51, Oxford University Press, Oxford, pp 1-21

Green JC, Leadbeater BSC, eds (1994) The Haptophyte Algae. The Systematics Association special volume 51, Oxford University Press, Oxford

Green JC, Manton I (1970) Studies in the fine structure and taxonomy of flagellates in the genus Pavlova. I. A revision of Pavlova gyrans, the type species. J mar biol Ass U.K. 50: 1113-1130

Green JC, Perch-Nielsen K, Westbroek P (1990) Phylum Prymnesiophyta. In Margulis L, Corliss JO, Melkonian M, Chapman DJ (eds) Handbook of Protoctista. Jones and Bartlett Publishers, Boston, pp 293–317

Hall TA (1999) BioEdit: a user-friendly biological sequence alignment editor and analysis program for Windows 95/98/NT. Nucl Acids Symp Ser 41, 95-98

Hibberd DJ (1976) The ultrastructure and taxonomy of the Chrysophyceae and Prymnesiophyceae (Haptophyceae): a survey with some new observations on the ultrastructure of the Chrysophyceae. Bot J Linn Soc 72: 55-80

Hori T, Green JC (1994) Mitosis and cell division. In Green JC & Leadbeater BSC (eds) The Haptophyte algae. The Systematics Association special volume 51, Oxford University Press, Oxford, pp 91- 109

Houdan A, Billard C, Marie D, Not F, Sáez AG, Young JR, Probert I (2004) Holococcolithophore-heterococcolithophore (Haptophyta) life cycles: flow cytometric analysis of relative ploidy levels. Syst Biodivers 1: 453-465

Jobb G, von Haeseler A, Strimmer K (2004) TREEFINDER: A powerful graphical analysis environment for molecular phylogenetics. BMC Evolutionary Biology 28: 4-18

Kalina T (1970) Corcontochrysis noctivaga gen et sp. n. (Chrysophyceae). Preslia 42: 297-302

Kalina T (1975) Taxonomie und ultrastruktur der art Corcontochrysis noctivaga (Haptophyceae). Preslia 47: 1-13

Katoh K, Kuma K, Toh H, Miyata T (2007) MAFFT version 5 : improvement in accuracy of multiple sequence alignment. Nucleic Acids Res 33: 511-518

Kiss JZ, Triemer RE (1988) A comparative study of storage carbohydrate granules from Euglena (Euglenida) and Pavlova (Prymnesiida). J Protozool 35: 237-21

Klaveness D (1972) Coccolithus huxleyi (Iohmann) Kamptner. II. The flagellate cell, aberrant cell types, vegetative propagation and life cycles. Br Phycol J 7: 309-318.

Lepailleur H (1970) Sur un nouveau genre de Chrysophycées: Exanthemachrysis nov. gen. (E. gayralii nov. sp.). C R Acad Sci, 270: 928-931

Liu H, Aris-Brosou S, Probert I, de Vargas C (2010) A timeline of the environmental genetics of the haptophytes. Mol Biol Evol 27:171-176

Liu H, Probert I, Uitz J, Claustre H, Aris-Brossou S, Frada M, Not F, de Vargas C (2009) Haptophyta rule the waves: Extreme oceanic biodiversity in non-calcifying haptophytes explains the 19-Hex paradox. Proc Natl Acad Sci USA 106:12803-12808

Mack B (1954) Untersuchungen an Chrysophyceen V. –VIII. Oesterr Bot Z 101: 64-73

Medlin L, Elwood HJ, Stickel S, Sogin ML (1988) The characterization of enzymatically amplified eukaryotic 16S-like rRNA-coding regions. Gene 71: 491-499

Medlin L, Kooistra W, Potter D, Saunders GW, Anderson RA (1997) Phylogenetic relationships of the 'golden algae' and their plastids. Plant Syst Evol 11: 187-210

Medlin LK, Sáez AG Young JR (2008) A molecular clock for coccolithophores and implications for selectivity of phytoplankton extinctions across the K/T boundary, Mar Micropaleontol 67: 69-86

Meireles LA, Guedes AC, Malcata FX (2003) Lipid class composition of the microalga Pavlova lutheri: eicosapentaenoic and docosahexaenoic acids. J. Agric. Food Chem 51: 2237–41

Moestrup Ø (1994) Economic aspects: "blooms", nuisance species, and toxins. **In Green JC & Leadbeater BSC (eds) The Haptophyte algae.** The Systematics Association special volume 51, Oxford University Press, Oxford, pp 265-85

Nosenko T, Boese B, Bhattacharya D (2007) Pulsed field gel electrophoresis analysis of genome size and structure in Pavlova gyrans and Diacronema sp. (Haptophyta). J Phycol 43: 763-767

Nylander JAA (2004) MrAIC.pl. Program distributed by the author. Evolutionary Biology Centre, Uppsala University

Ponis E, Probert I, Véron B, Le Coz J-R, Mathieu M, Robert R (2006) Nutritional value of six Pavlovophyceae for Crassostrea gigas and Pecten maximus larvae. Aquaculture 254: 544-553

Prauser H (1958) Diacronema vlkianum, eine neue Chrysomonade. Arch Protistenk 103: 117-128

Reynolds ES (1963) The use of lead citrate at high pH as an electron-opaque stain in electron microscopy. J Cell Biol 17: 208-12

Ronquist F, Huelsenbeck JP (2003) MRBAYES 3: Bayesian phylogenetic inference under mixed models. Bioinformatics 19: 1572-1574

Shi XL, Marie D, Jardillier L, Scanlan DJ, Vaulot D (2009) Groups without Cultured Representatives Dominate Eukaryotic Picophytoplankton in the Oligotrophic South East Pacific Ocean. PLoS ONE 4(10): e7657. doi:10.1371/journal.pone0007657

Tonon T, Harvey D, Larson TR, Yi L, Graham IA (2005) Acyl-CoA elongase activity and gene from the marine microalga Pavlova lutheri (Haptophyceae). J appl phycol 17: 111-118

Tseng CK, Chen J, Zhang Z (1992) On a new species of Pavlova (Prymnesiophyceae) from China. Chin J Oceanol Limnol 10: 23-28

Veer J van der (1969) Pavlova mesolychnon (Chrysophyta) a new species from the Tamar Estuary, Cornwall. Acta Bot Neerl 18: 496-510

Veer J van der (1972) Pavlova helicata (Haptophyceae), a new species from the Frisian Island Schiermonnikoog, the Netherlands. Nova Hedw XXIII: 131-159

Veer J van der (1976) Pavlova calceolata (Haptophyceae) a new species from the Tamar Estuary, Cornwall. J mar biol Ass U.K. 56: 21-30

Veer J van der (1979) Pavlova and the taxonomy of flagellates especially the Chrysomonads. Thesis, Rijks-universiteit, Groningen

Veer J van der, Leewis RJ (1977) Pavlova ennorea sp. nov. a haptophycean alga with a dominant non-motile phase from England. Acta Bot Neerl 26: 159-176

Van Lenning K, Estrada M, Latasa M, Medlin L, Probert I, Véron B, Sáez AG, Young J (2003) Pigment signatures and phylogenetic relationships of the Pavlovophyceae (Haptophyta). J Phycol 39: 379-389

Véron B, Dauguet J-C, Billard C (1996) Sterolic biomarkers in marine phytoplankton. I. Free and conjugated sterols of Pavlova lutheri (Haptophyta). Eur J Phycol 31: 211-215

Volkman JK, Farmer CM, Barrett SM, Sikes EL (1997) Unusual dihydroxysterols as chemotaxonomic markers for microalgae from the order Pavlovales (Haptophyceae). J Phycol 33: 1016-1023

Table 4: Comparison of principals characters of Pavlovales (inspired from Green 1980)

Phylogenetic clade		1	2		3			4						
Pigment profile		C	B?	B?	B	B	B	A?	A	A	A	A	A	A
Genus		***Exanthemachrysis***	***Rebecca***		***Pavlova***			***Diacrnema***						
Species		***gayraliae***	***helicata***	***salina***	***granifera***	***gyrans***	***pinguis***	***calceolata***	***ennorea***	***lutheri***	***noctivaga***	***virescens***	***viridis***	***vlkianum***
Habitat		estuarine	brackish	brackish	freshwater	brackish	marine	brackish	brackish	brackish	peat pools	littoral epilithic	brackich	marine and freshwater
Motile stage		strongly metabolic	ovate, compressed, with ventrale depression, not metabolic	ovate-pyriform; slightly compressed	irregular, elongate, compressed strongly metabolic	irregular, elongate, compressed strongly metabolic	irregular, elongate, compressed strongly metabolic	irregularly broadly lobed elongate; slightly compressed; metabolic	elongate	compressed with ventrale depression; not metabolic	elongate; not metabolic	elongate; somewhat metabolic	compressed with strong ventrale depression	compressed with ventrale depression
Non-motile stage		dominant stage, thick and striated mucilage, flagella bases only present	not recorded	non motile cells recorded apparently having lost flagella	dominant stage, homogenous mucilage, appendages not abbreviated	non motile cells recorded	homogenous mucilage, appendages not abbreviated	recorded (no details published)	dominant stage, homogenous mucilage, appendages incomplet	not recorded	dominant stage, stratified mucilage, appendages not abbreviated	homogenous mucilage, appendages not abbreviated	not recorded	not recorded
cell-size (µm)		5-6 x 3-4	(4,5-)6,5(-10) x (5-)6,5(-9) x 2	5-9(-13) x 4-5 x 2-3	6-(8-9) x 4,5 x 3,5-4	4-10 x 3-6 x 2-2,5	5-8 x 3-4	5-6(-9) x 3,5-6 x 2,5-3	6-9 x 3-4,5	7-9 x 5-7 x 3-4	5-8-12 x 6-8 x 4-5	7-8 x 2-3	6 x 4.8 x 4	3,5-7,5 x 4-5 x 1,5-3
Filipodia		-	+	+	+	+	+	+	-	-	-	-	-	+
Body-scales size (µm) and form		-	approx. 0,1 clavate	0,04 x 0,02 clavate	0,015 spherical	0,01 spherical	-	-	-	0,015-0,02 spherical	-	-	-	-
Insertion of appendages		ventral in a depression	ventral in a depression	ventral in a depression	sub-apical in a depression	sub-apical	sub-apical	ventral in a depression	semi-ventral	semi-ventral	sub-apical	sub-apical	semi-ventral in a depression	ventral in a depression
Short (posterior) flagellum (µm)		5-7, distal necklace of pearl is present	vestigial	approx. 0,2 , vestigial	approx. 6	approx. 3	approx. 4 ,	1-2	5	2-4	2,5-6	5	vestigial	4, accessory axoneme structures present
Long (anterior) flagellum	**Length (µm)**	7-12	17-20	12-17	10-20	6-20	8-11	6-10	10-13	5-11	6-18	13	9-12	7-10
	Hairs	long and fine	?	long and fine	long and fine	long and fine	long and fine	long and fine	long and fine	long and fine	long and fine	long and fine	long and fine	long and fine
	"Knob-scales" size (µm) and form	-	0,08 x 0,02 double constriction	0,05 x 0,02 double constriction	0,03 x 0,025, constricted	0,03 x 0,02, constricted	0,03 x 0,02 constricted	approx. 0,02 stellate	0,4 spherical	0,02 spherical	0,05 x 0,03 clavate	0,025 x 0,03 muriform	0.02 x 0,03 spherical	-
	Arrangement of scales	-	?	regular	regular	regular	regular	?	regular	irregular	irregular	irregular	?	-

Haptonema length (µm)		1-2	4-5(-6)	2-4,5	2.5	1.5	approx. 2	approx 1	2	approx. 1	1,5-2,5	2-4	0.75	1
Plastid	**Characteristics**	1 yellow-brown parietal, ventral	1(-2) brown/yellow markedly lobed	1-2 yellow-green	1 golden brown	1 golden brown	1 golden brown	1 pale yellow-green 4 lobes from dorsal isthmus	1 yellow-green parietal	1 yellow-green	1-2 brown	2 yellow-green	1 green	1 yellow/green
	Arrangement of thylakoïds	parallel and helicoïds	parallel and helicoïds	parallel and helicoïds	simply parallel	simply parallel	simply parallel	simply parallel	parallel with large intrastromatal space	simply parallel	simply parallel	parallel with ponctual thylakoid stacks	simply parallel	simply parallel
	Pyrenoid	ventral, near flagellar insertion, bulging	1 per plastid on the inner face	-	posterior-bulging	posterior-bulging	posterior-bulging	-	-	-	-	-	-	-
	Stigma	osmiophilic vesicles present at transition between chloroplast stoma and pyrenoid	-	-	apparent on the inner face of the plastid, associated with a pit	apparent on the inner face of the plastid, associated with a pit	apparent on the inner face of the plastid, associated with a pit	on the external face of the plastid	-	on the external face of the plastid	on the external face of the plastid	-	-	on the external face of the plastid

(- = absence, ? = no data)

LISTE DES PUBLICATIONS

Siano R, Alves-de-Souza C, Foulon E, **Bendif EM**, Simon N, Guillou L and Not F. Distribution and host diversity of Amoebophryidae parasites across oligotrophic waters of the Mediterranean Sea. *Biogeosciences* 7: 7391-7419, 2010

Jeanthon C, Boeuf D, Dahan O, Le Gall F, Garczarek L, **Bendif EM** and Lehours AL. Diversity of cultivated and metabolically active aerobic anoxygenic phototrophic bacteria along an oligotrophic gradient in the Mediterranean Sea. *Biogeosciences*, 8: 1955–1970, 2011

Beaufort L, Probert I, de Garidel-Thoron T, **Bendif EM**, Ruiz-Pino D, Metzl N, Goyet C, Buchet N, Coupel P, Grelaud M, Rost B, Rickaby REM and de Vargas C. Sensitivity of coccolithophores to carbonate chemistry and response to ocean acidification. *Nature* 476: 80 – 84, 2011

Mella-Flores D, Mazard S, Humily S, Partensky F, Mahe F, Bariat L, Courties C, Marie D, Ras J, Mauriac R, Jeanthon C, **Bendif EM**, Ostrowski M, Scanlan DJ and Garczarek L Is the distribution of Prochlorococcus and Synechococcus ecotypes in the Mediterranean Sea affected by global warming? *Biogeosciences* 8: 2785-2804, 2011

Bendif EM, Probert I, Hervé A, Billard C, Goux D, Lelong C, Cadoret JP, and Véron B. A taxonomic reassessment of the Pavlovophyceae (Haptophyta). *Protist* 162: 738-761, 2011

Hagino-Tomioka K, **Bendif EM**, Probert I, Young J, Kogame K, Takano Y, Horiguchi T, de Vargas C and Okada, H. New evidence for morphological and genetic variation in a cosmopolitan coccolithophore *Emiliania huxleyi* (Prymnesiophyceae) from the cox1b-ATP4 genes. *Journal of Phycology* 47:1164-1176, 2011

von Dassow P, John U, Ogata H, Probert I, **Bendif EM**, Kegel J, Audic S, Wincker P, Da Silva C, Claverie JM and Colomban de Vargas. Loss of sex and reduced adaptability in biogeochemically key open oceanic eukaryotic phytoplankton (submitted)

Bendif EM, Probert I, Young J, Schroeder D, and de Vargas, C. Species concept in the Haptophytes order Isochrysidales. *Protist* (submitted)

Bendif EM, Probert I, Hagino-Tomioka K, Romac S, Schroeder D, Young J, and de Vargas, C. A morpho-genetic assessment of micro-evolution in the cosmopolitan coccolithophore *Gephyrocapsa hhuxleyi* (in prep)

Bendif EM, Probert I, Schroeder D and de Vargas, C. Evaluation of DNA barcodes for the cosmopolitan coccolithophores *Emiliania huxleyi* and *Gephyrocapsa oceanica* (Haptophyta) (in prep)

LISTE DES PRESENTATIONS ORALES

"Resolving the phylogeny of the *Emiliana huxleyi*/*Gephyrocapsa oceanica* (Haptophyta) species complex" **El Mahdi Bendif**, Ian Probert, Kyoko Hagino-Tomioka, Sarah Romac, Peter von Dassow, Jeremy Young, Declan Schroeder and Colomban de Vargas MARINEXUS Meeting, Plymouth UK Juin 2011

"Resolving the phylogeny of the *Emiliana huxleyi*/*Gephyrocapsa oceanica* (Haptophyta) species complex" **El Mahdi Bendif**, Ian Probert, Kyoko Hagino-Tomioka, Sarah Romac, Peter von Dassow, Jeremy Young, Declan Schroeder and Colomban de Vargas Colloque de la Société Phycologique de France, Villefranche France Avril 2011

"Species Concept and Evolutionary Rates in the Noelaerhabdaceae" **El Mahdi Bendif**, Ian Probert, Kyoko Hagino-Tomioka, Sarah Romac, Peter von Dassow, Jeremy Young, Declan Schroeder and Colomban de Vargas. INA13, 13th International Nannoplankton Association Meeting, Yamagata Japan September 2010

"A morpho-genetic assessment of micro-evolution in extant Noelaerhabdacean coccolithophores" **El Mahdi Bendif**, Ian Probert, Kyoko Hagino-Tomioka, Sarah Romac, Jeremy Young and Colomban de Vargas. ECBOL2, European Consortium for Barcoding of Life II, Braga Portugal June 2010

"Species-concept in the Isochrysidales order". **El Mahdi Bendif**, Ian Probert, Hui Liu and Colomban de Vargas IPC9, International Phycological Congress IX Tokyo Japan August 2009

"Taxonomical reassessment of the Pavlovophyceae". **El Mahdi Bendif**, Annie Hervé, Chantal Billard, Didier Goux, Christophe Lelong, Jean Paul Cadoret and Benoit Veron "Resolving species in marine protists" Marplan (Marbef)/Aquaparadox workshop, Observatoire Océanologique de Villefranche-sur-mer, France, December 2008

LISTE DES POSTERS

"Assessing the microdiversity of the *Emiliana huxleyi*/*Gephyrocapsa oceanica* (Haptophyta) species complex". **El Mahdi Bendif**, Ian Probert, Kyoko Hagino-Tomioka, Sarah Romac, Jeremy Young and Colomban de Vargas. EPOCA Meeting, Bruxelles Belgique Mai 2011

"A taxonomical reassessment of the Isochrysidales order" **El Mahdi Bendif**, Ian Probert, Hui Liu, Kyoko Hagino-Tomioka and Colomban de Vargas. INA13, 13th International Nannoplankton Association Meeting, Yamagata Japan September 2010

"Species Concept and Evolutionary Rates in the Isochrysidales (Haptophyta)" **El Mahdi Bendif**, Ian Probert, Peter von Dassow, Kyoko Hagino-Tomioka, Sarah Romac, Jeremy Young, Declan Schroeder and Colomban de Vargas. SMBE 2010, Annual meeting of the society for molecular biology and evolution Lyon France July 2010

RESUMES

From macroevolution to microevolution in marine phytoplankton: the case of the Isochrysidales (Haptophyta)

The haptophyte order Isochrysidales contains several ecologically and/or economically key taxa, including the bloom forming coccolithophore *Gephyrocapsa (=Emiliania) huxleyi*. Having originated less than 300,000 years ago, *G. huxleyi* is a relatively very young coccolithophore morphospecies that displays remarkable adaptive potential, having colonized most of the world's oceans to become the most abundant extant coccolithophore. This thesis focusses on investigating the biocomplexity and adaptability of *G. huxleyi*, with approaches ranging from definition of its macro-evolutionary phylogenetic context to finer scale study of intraspecific morpho-genetic variability and biogeographic structuring. A phylogenetic analysis including most described isochrysidalean morpho-species led to reevaluation of the major phenotypic characters and evolutionary trajectories within the order, and confirmation of the very tight evolutionary links between *G. huxleyi* and a sister species, *G. oceanica*, hence the proposal that this organism should be classified within *Gephyrocapsa* rather than the seperate genus *Emiliania*. Of the multiple nuclear and organellar genetic markers tested, only mitochondrial genes provided both sufficient resolution and suitable phylogenetic signal for reconstructing the micro-evolutionary history within the *G. huxleyi* morphospecies. Phylogenetic analyses of multiple mitochondrial genes from a large set of clonal culture strains of *G. huxleyi* isolated from diverse locations allowed distinction of two major haplotypes, termed α and β, displaying distinct biogeographic distributions. Further combined morpho-genetic analyses within the α and β genotypes, including analysis of ultrastructural characters of the coccoliths and genetic variations within the *GPA* marker, a gene known to be involved in biomineralization, allowed proposition of an evolutionary scenario that reconciles biological and morphological diversity and highlights cryptic morphological entities within the morphospecies. Furthermore, a molecular clock analysis of the mitochondrial phylogeny allowed correlation of diversification events to past environmental conditions. Automated microscopy analyses of gephyrocapsid coccolith mass in the world oceans over the last 40 ky indicate a global calcification decrease with increasing ocean acidification. However, the presence of hypercalcified forms in the most corrosive modern waters offshore Chile suggests that certain *G. huxleyi* genotypes are able to adapt to low pH conditions. Exploring intra-specific evolution at the genomic level, significant variations in gene content related to both ploidy level and environmental conditions were detected. *G. huxleyi* strains from relatively stable, oligotrophic water-masses appear to have a tendency to have lost genes specifically expressed in the haploid phase of the haplo-diplontic life cycle. Seen as a dynamic process, the suggested loss of sex in open oceanic waters implies reduced long-term adaptability to environmental changes.

Keywords: Coccolithophores, *Emiliania huxleyi*, *Gephyrocapsa*, Adaptation, Ocean Acidification, Plankton Evolution

De la macroévolution à la microévolution dans le phytoplancton marin: le cas des Isoschrysidales (Haptophyta)

L'ordre phytoplanctonique des Isochrysidales comporte plusieurs taxa ayant une importance écologique et/ou économique remarquable, tel que le coccolithophore *Gephyrocapsa (=Emiliania) huxleyi*, connu pour ses larges efflorescences. Apparu il y a environ 300 000 ans, *G. huxleyi* est la plus jeune morpho-espèce de coccolithophore. *G. huxleyi* démontre un potentiel adaptatif remarquable et a colonisé tous les océans tout en étant aujourd'hui le plus abondant des coccolithophores. Au cours de ce travail de thèse, nous nous sommes interrogés sur la biocomplexité et l'adaptabilité de *G. huxleyi*, en partant de son contexte phylogénétique macroévolutif vers les échelles plus fines de sa variabilité morphogénétique intraspécifique et de sa structuration biogéographique. L'analyse phylogénétique de sept espèces d'Isochrysidales a permis de revisiter les caractères phénotypiques majeurs et les trajectoires évolutives au sein de l'ordre et de confirmer la relation étroite entre *G. huxleyi* et son espèce sœur *Gephyrocapsa oceanica*. Parmi les différents marqueurs nucléaires et cytoplasmiques testés, les gènes mitochondriaux sont les seuls qui ont un pouvoir de résolution suffisant pour reconstruire l'histoire évolutive récente au sein des lignées de *G. huxleyi*. Les analyses phylogénétiques des gènes *cox1*, *cox2*, *cox3*, *rpl16* et *dam* sur 150 souches isolées des océans mondiaux ont permis de distinguer deux haplotypes majeurs, α et β, qui présentent une distribution biogéographique bipolaire. En complément, des analyses morpho-génétiques combinant les caractères morphométriques des coccolithes et les variations génétiques du gène *gpa*, impliqué dans la biominéralisation, ont mené a une nouvelle définition des morphotypes de *G. huxleyi* au sein des deux haplotypes α et β. En particulier, des analyses en microscopie automatisée de la masse des coccolithes de gephyrocapsids dans les océans mondiaux sur les derniers 40 000 ans indiquent une baisse générale de la calcification avec l'augmentation de l'acidification de l'océan. Cependant, la présence de formes hypercalcifiées dans les eaux les plus corrosives au large du Chili suggère que certains génotypes de *G. huxleyi* seraient adaptés à ces conditions de faible pH. En explorant l'évolution des génomes au niveau intraspécifique, nous avons pu détecter de fortes variations du contenu génique liées au niveau de ploïdie et aux conditions environnementales. En effet, les souches de *G. huxleyi* provenant des masses d'eau oligotrophes relativement stables ont manifestement perdu des gènes exprimés spécifiquement durant la phase haploïde du cycle de vie. Perçue comme un processus dynamique, cette perte putative de la sexualité dans le domaine océanique implique une réduction de la capacité de *G. huxleyi* à s'adapter sur le long terme aux changements environnementaux.

Mots-clefs: Coccolithophores, *Emiliania huxleyi*, *Gephyrocapsa*, Adaptation, Acidification des oceans, Evolution du plancton